

# Abiotic stress mechanisms and enhancement in crops: Physiological and biochemical approaches

**Edited by**

Arpna Kumari, Milan Skalicky, Ibrahim Al-Ashkar  
and Hirofumi Saneoka

**Published in**

Frontiers in Plant Science



## FRONTIERS EBOOK COPYRIGHT STATEMENT

The copyright in the text of individual articles in this ebook is the property of their respective authors or their respective institutions or funders. The copyright in graphics and images within each article may be subject to copyright of other parties. In both cases this is subject to a license granted to Frontiers.

The compilation of articles constituting this ebook is the property of Frontiers.

Each article within this ebook, and the ebook itself, are published under the most recent version of the Creative Commons CC-BY licence. The version current at the date of publication of this ebook is CC-BY 4.0. If the CC-BY licence is updated, the licence granted by Frontiers is automatically updated to the new version.

When exercising any right under the CC-BY licence, Frontiers must be attributed as the original publisher of the article or ebook, as applicable.

Authors have the responsibility of ensuring that any graphics or other materials which are the property of others may be included in the CC-BY licence, but this should be checked before relying on the CC-BY licence to reproduce those materials. Any copyright notices relating to those materials must be complied with.

Copyright and source acknowledgement notices may not be removed and must be displayed in any copy, derivative work or partial copy which includes the elements in question.

All copyright, and all rights therein, are protected by national and international copyright laws. The above represents a summary only. For further information please read Frontiers' Conditions for Website Use and Copyright Statement, and the applicable CC-BY licence.

ISSN 1664-8714  
ISBN 978-2-8325-5224-7  
DOI 10.3389/978-2-8325-5224-7

## About Frontiers

Frontiers is more than just an open access publisher of scholarly articles: it is a pioneering approach to the world of academia, radically improving the way scholarly research is managed. The grand vision of Frontiers is a world where all people have an equal opportunity to seek, share and generate knowledge. Frontiers provides immediate and permanent online open access to all its publications, but this alone is not enough to realize our grand goals.

## Frontiers journal series

The Frontiers journal series is a multi-tier and interdisciplinary set of open-access, online journals, promising a paradigm shift from the current review, selection and dissemination processes in academic publishing. All Frontiers journals are driven by researchers for researchers; therefore, they constitute a service to the scholarly community. At the same time, the *Frontiers journal series* operates on a revolutionary invention, the tiered publishing system, initially addressing specific communities of scholars, and gradually climbing up to broader public understanding, thus serving the interests of the lay society, too.

## Dedication to quality

Each Frontiers article is a landmark of the highest quality, thanks to genuinely collaborative interactions between authors and review editors, who include some of the world's best academicians. Research must be certified by peers before entering a stream of knowledge that may eventually reach the public - and shape society; therefore, Frontiers only applies the most rigorous and unbiased reviews. Frontiers revolutionizes research publishing by freely delivering the most outstanding research, evaluated with no bias from both the academic and social point of view. By applying the most advanced information technologies, Frontiers is catapulting scholarly publishing into a new generation.

## What are Frontiers Research Topics?

Frontiers Research Topics are very popular trademarks of the *Frontiers journals series*: they are collections of at least ten articles, all centered on a particular subject. With their unique mix of varied contributions from Original Research to Review Articles, Frontiers Research Topics unify the most influential researchers, the latest key findings and historical advances in a hot research area.

Find out more on how to host your own Frontiers Research Topic or contribute to one as an author by contacting the Frontiers editorial office: [frontiersin.org/about/contact](https://frontiersin.org/about/contact)



# Abiotic stress mechanisms and enhancement in crops: Physiological and biochemical approaches

## Topic editors

Arpna Kumari — The University of Tokyo, Japan

Milan Skalicky — Czech University of Life Sciences Prague, Czechia

Ibrahim Al-Ashkar — Al-Azhar University, Egypt

Hirofumi Saneoka — Hiroshima University, Japan

## Citation

Kumari, A., Skalicky, M., Al-Ashkar, I., Saneoka, H., eds. (2024). *Abiotic stress mechanisms and enhancement in crops: Physiological and biochemical approaches*. Lausanne: Frontiers Media SA. doi: 10.3389/978-2-8325-5224-7

# Table of contents

- 05 ***DgCspC* gene overexpression improves cotton yield and tolerance to drought and salt stress comparison with wild-type plants**  
Wenwen Xia, Jiahang Zong, Kai Zheng, Yuan Wang, Dongling Zhang, Sandui Guo and Guoqing Sun
- 18 **ZmLBD2 a maize (*Zea mays* L.) lateral organ boundaries domain (LBD) transcription factor enhances drought tolerance in transgenic *Arabidopsis thaliana***  
Peng Jiao, Xiaotong Wei, Zhenzhong Jiang, Siyan Liu, Shuyan Guan and Yiyong Ma
- 34 **Mapping QTLs for anaerobic tolerance at germination and bud stages using new high density genetic map of rice**  
Jing Yang, Ji Wei, Jifen Xu, Yumeng Xiong, Gang Deng, Jing Liu, Shah Fahad and Hongyang Wang
- 49 **Comparison of lauric acid and 12-hydroxylauric acid in the alleviation of drought stress in peach (*Prunus persica* (L.) Batsch)**  
Binbin Zhang, Hao Du, Maoxiang Sun, Xuelian Wu, Yanyan Li, Zhe Wang, Yuansong Xiao and Futian Peng
- 64 **The redox status of salinity-stressed *Chenopodium quinoa* under salicylic acid and sodium nitroprusside treatments**  
Shokoofeh Hajihashemi, Omolbanin Jahantigh and Sahira Alboghobeish
- 76 **Cotton proteomics: Dissecting the stress response mechanisms in cotton**  
George Bawa, Zhixin Liu, Yaping Zhou, Shuli Fan, Qifeng Ma, David T. Tissue and Xuwu Sun
- 88 ***PHD-finger* family genes in wheat (*Triticum aestivum* L.): Evolutionary conservatism, functional diversification, and active expression in abiotic stress**  
Fei Pang, Junqi Niu, Manoj Kumar Solanki, Shaista Nosheen, Zhaoliang Liu and Zhen Wang
- 109 **Grafting promoted antioxidant capacity and carbon and nitrogen metabolism of bitter melon seedlings under heat stress**  
Le Liang, Wen Tang, Huashan Lian, Bo Sun, Zhi Huang, Guochao Sun, Xiaomei Li, Lihua Tu, Huanxiu Li and Yi Tang
- 123 **9-*cis*-epoxycarotenoid dioxygenase 1 confers heat stress tolerance in rice seedling plants**  
Yijin Zhang, Xiong Liu, Rui Su, Yunhua Xiao, Huabing Deng, Xuedan Lu, Feng Wang, Guihua Chen, Wenbang Tang and Guilian Zhang
- 135 **Combating ozone stress through N fertilization: A case study of Indian bean (*Dolichos lablab* L.)**  
Ansuman Sahoo, Parvati Madheshiya, Ashish Kumar Mishra and Supriya Tiwari

- 149 ***ZmG6PDH1* in glucose-6-phosphate dehydrogenase family enhances cold stress tolerance in maize**  
Xin Li, Quan Cai, Tao Yu, Shujun Li, Sinan Li, Yunlong Li, Yan Sun, Honglei Ren, Jiajia Zhang, Ying Zhao, Jianguo Zhang and Yuhu Zuo
- 164 **Sterile line Dexiang074A enhances drought tolerance in hybrid rice**  
Gengmi Li, Tao Zhang, Li Yang, Jian Qin, Qianhua Yang, Yingjiang Cao, Jing Luo, Xiangzhao Li, Lei Gao, Qian Chen, Xingping He, Yong Huang, Chuantao Liu, Ling He, Jiakui Zheng and Kaifeng Jiang
- 174 **Exogenous zinc mitigates salinity stress by stimulating proline metabolism in proso millet (*Panicum miliaceum* L.)**  
Naveed Ul Mushtaq, Khalid M. Alghamdi, Seerat Saleem, Inayatullah Tahir, Ahmad Bahieldin, Bernard Henrissat, Mohammed Khalid Alghamdi, Reiaz Ul Rehman and Khalid Rehman Hakeem
- 191 **Impact of dehydration on the physiochemical properties of *Nostoc calcicola* BOT1 and its untargeted metabolic profiling through UHPLC-HRMS**  
Priya Yadav, Rahul Prasad Singh, Hissah Abdulrahman Alodaini, Ashraf Atef Hatamleh, Gustavo Santoyo, Ajay Kumar and Rajan Kumar Gupta
- 213 **Exogenous phthalanilic acid induces resistance to drought stress in pepper seedlings (*Capsicum annuum* L.)**  
Xiaopeng Lu, Qiong Wu, Keyi Nie, Hua Wu, Guangyou Chen, Jun Wang and Zhiqing Ma



## OPEN ACCESS

## EDITED BY

Arpna Kumari,  
Southern Federal University,  
Russia

## REVIEWED BY

Ramazan Beyaz,  
Ahi Evran University,  
Turkey  
Sonia Mbarki,  
Center of Biotechnology of Borj Cedria  
(CBBC), Tunisia

## \*CORRESPONDENCE

Guoqing Sun  
Sunguoqing02@caas.cn

<sup>†</sup>These authors have contributed equally to this work and share first authorship

## SPECIALTY SECTION

This article was submitted to  
Plant Abiotic Stress,  
a section of the journal  
Frontiers in Plant Science

RECEIVED 04 July 2022

ACCEPTED 18 August 2022

PUBLISHED 06 September 2022

## CITATION

Xia W, Zong J, Zheng K, Wang Y, Zhang D,  
Guo S and Sun G (2022) *DgCspC* gene  
overexpression improves cotton yield and  
tolerance to drought and salt stress  
comparison with wild-type plants.  
*Front. Plant Sci.* 13:985900.  
doi: 10.3389/fpls.2022.985900

## COPYRIGHT

© 2022 Xia, Zong, Zheng, Wang, Zhang,  
Guo and Sun. This is an open-access  
article distributed under the terms of the  
[Creative Commons Attribution License \(CC  
BY\)](#). The use, distribution or reproduction in  
other forums is permitted, provided the  
original author(s) and the copyright  
owner(s) are credited and that the original  
publication in this journal is cited, in  
accordance with accepted academic  
practice. No use, distribution or  
reproduction is permitted which does not  
comply with these terms.

# *DgCspC* gene overexpression improves cotton yield and tolerance to drought and salt stress comparison with wild-type plants

Wenwen Xia<sup>1,2†</sup>, Jiahang Zong<sup>1,3†</sup>, Kai Zheng<sup>3†</sup>, Yuan Wang<sup>1</sup>,  
Dongling Zhang<sup>1</sup>, Sandui Guo<sup>1</sup> and Guoqing Sun<sup>1\*</sup>

<sup>1</sup>Biotechnology Research Institute, Chinese Academy of Agricultural Sciences, Beijing, China,

<sup>2</sup>Hainan Yazhou Bay Seed Lab, Sanya, China, <sup>3</sup>College of Agriculture, Xinjiang Agricultural University, Urumqi, China

Drought and high salinity are key limiting factors for cotton quality and yield. Therefore, research is increasingly focused on mining effective genes to improve the stress resistance of cotton. Few studies have demonstrated that bacterial *Cold shock proteins* (*Csps*) overexpression can enhance plants stress tolerance. Here, we first identified and cloned a gene *DgCspC* encoding 88 amino acids (aa) with an open reading frame (ORF) of 264 base pairs (bp) from a *Deinococcus gobiensis* I-0 with high resistance to strong radiation, drought, and high temperature. In this study, heterologous expression of *DgCspC* promoted cotton growth, as exhibited by larger leaf size and higher plant height than the wild-type plants. Moreover, transgenic cotton lines showed higher tolerance to drought and salts stresses than wild-type plants, as revealed by susceptibility phenotype and physiological indexes. Furthermore, the enhanced stresses tolerance was attributed to high capacity of cellular osmotic regulation and ROS scavenging resulted from *DgCspC* expression modulating relative genes upregulated to cause proline and betaine accumulation. Meanwhile, photosynthetic efficiency and yield were significantly higher in the transgenic cotton than in the wild-type control under field conditions. This study provides a newly effective gene resource to cultivate new cotton varieties with high stresses resistance and yield.

## KEYWORDS

*Deinococcus gobiensis*, cold shock proteins C (*DgCspC*), cotton, abiotic stress resistance, molecular breeding

## Introduction

Drought and salt significantly threaten plant growth, thus causing serious damage to crops and limiting yield and quality (Basu et al., 2016). Salt damage affects about 20% of the world's cultivated land and nearly half of the irrigated land (Zhu, 2001). Cotton is an important economic crop and is mainly grown in arid and semi-arid areas in China



(Fradin and Thomma, 2006; Shaban et al., 2018). Xinjiang, the main cotton-producing region in China, has a saline-alkali land area of 110,000 km<sup>2</sup>, accounting for about one-third of the country's saline-alkali land area. Therefore, effective drought- or salinity-resistant genes should be identified and incorporated in genetic engineering programs to generate drought- or salinity-resistant cotton genotypes.

Desert microbes are exposed to intense solar radiation, cycles of extreme temperatures and drought. The extreme environment can cause DNA and protein damage, which is fatal to most organisms. Desert bacteria evolve with time to protect their DNA and proteins from damage or effectively repair them (Heinemann and Roske, 2021). The Institute of Biotechnology, Chinese Academy of Agricultural Sciences published the genome of *D. gobiensis I-0* in 2012. The genome of *D. gobiensis I-0* contains seven replicons: a 3.1 Mb main chromosome and six plasmids from 433 to 53 kb. GenBank accession numbers for the main chromosome and plasmids P1–P6 are from CP002191 to CP002197 (Yuan et al., 2012). About half of the genes in the genome encode proteins with unknown functions. However, *D. gobiensis I-0* plays a crucial role in resisting extreme environment of the Gobi Desert and may provide genetic resources for stress resistance. A previous study cloned *CspC* from *D. gobiensis I-0*. Csps are widely found in various organisms, including animals, plants, and microorganisms, except archaea (Weinberg et al., 2004).

Cold shock proteins (Csps) are RNA molecular chaperones in bacteria, containing primitive cold-shock domains that bind to nucleic acids, prevent RNase degradation of mRNA, and correct the misfolding of mRNA (Kentaro and Ryoze, 2012). Nine members of the *Csp* gene family (*CspA*–*CspI*) have been identified in *Escherichia coli* (Yamanaka et al., 1994). The *Csp* gene of *E. coli* and *Bacillus subtilis* can significantly improve the resistance of transgenic plants to abiotic stresses, such as drought (Castiglioni et al., 2008; Kim et al., 2009; Pingli et al., 2013; Choi et al., 2015; Yu et al., 2017). The Csps involved in various physiological stress responses of cells, including antioxidant protection, DNA damage repair and pigment synthesis through direct or indirect regulation (Faßhauer et al., 2021). Genomic sequence analysis has revealed that *D. gobiensis I-0* contains an only *Csp* homologous protein-coding gene (*CspC*) that is 69% similar to the amino acid sequence of *B. subtilis CspB* (Yuan et al., 2009).

Sequence structure analysis revealed that the amino acid sequence of *CspC* from *D. gobiensis I-0* is similar to that of *Csp* from other bacteria, all of which consist of five reverse-parallel  $\beta$  chains. The expression of *CspC* and *CspE* in *E. coli* is induced by temperature changes. However, *CspD* is expressed only under nutrient deficiency or steady-state stress (Yamanaka and Inouye, 1997; Yamanaka et al., 1998). *Csp* of *Listeria monocytogenes* participates in stress response after salt shock (Schmid et al., 2009). *CspA* of *Brucella* is involved in response to stress and virulent infestation (De La Garza-García et al., 2021). *Enterococcus* contains four cold-excited proteins, of which *CspR* is involved in bacterial virulence infestation and

bacterial growth (Michaux et al., 2012). Csps in most bacteria are present in multiple copies and are induced in different ways. In contrast, *D. gobiensis I-0* contains only one *Csp*, implying that *DgCspC* may be induced by many different conditions, and potentially regulates multiple pathways. Previous study showed that the *CspC* expression can significantly improve the growth of *E. coli* cells under nutrient deficiency (Mingkun, 2011). In that study, a *CspC* gene expression vector driven by CaMV 35S promoter was constructed and was transformed into tobacco by *Agrobacterium*-mediated method. Transgenic tobacco lines grew normally under drought stress, while wild-type tobacco growth was retarded, indicating that this gene potentially enhances plant drought stress resistance (Mingkun, 2011). Studies on *Csp* gene in bacteria have mainly focused on *E. coli* and model plants, such as *Arabidopsis thaliana* and tobacco. However, no study has reported on the stress-resistant function of *Csp* gene in transgenic crops.

As an important oil and fiber crop, cotton is classified as moderately drought and salt tolerant crop (Zhang et al., 2013). To overcome salt and drought stresses, maintenance of cellular ion and osmotic pressure balance is the main adaptive mechanism in cotton (Naidoo and Naidoo, 2001; Rontein et al., 2002; Quan et al., 2004; Ding et al., 2010; Dai et al., 2014). Many osmoprotectants, such as amino acids, sugars, glycine betaine, polyols, and polyamines have been identified for positive involving drought and salt tolerance. It has been observed high glycine betaine and proline in response to salinity tolerance in transgenic Choline monooxygenase (CAM) gene cotton lines or wild cotton plants (Meloni et al., 2001; Zhang et al., 2009). Furthermore, high betaine could maintain the integrity of membranes against stresses and scavenging ROS (Annunziata et al., 2019). Therefore, both *GhABF3* and *GhMPK3* overexpression increases cotton tolerance to salt and drought through improving antioxidant activities (Sadau et al., 2021; Zhang et al., 2022). As an RNA molecular chaperones, Csps could maintain these RNA and improve these proteins content to enhance cotton resistant to extensive stresses.

In this study, genetic engineering technology was used to transfer the *DgCspC* gene into cotton. Subsequently, the transgenic cotton lines were self-bred to T4 generation to obtain stable lines for subsequent experiments. The *DgCspC* expression could promote growth of cotton with larger leaf size and higher plant height through improving the photosynthesis rate. The characteristic resulted in the cotton yield being significantly increased. Moreover, the transgenic cotton lines showed higher tolerant to drought and salinity stresses. Proline is key in plant response to stress (Brauc et al., 2012). *Csp* participates in osmotic stress, pigment regulation and nutritional stress regulation. Betaine is a key osmotic regulatory substance (Pukale et al., 2021). The enhanced tolerance was attributed to the proline and betaine synthesis promoted by the *DgCspC* expression. This study aimed to explore whether heterologous expression of *DgCspC* gene can improve drought and other abiotic stress resistance in cotton.

## Materials and methods

### Generation and molecular characterization of transgenic cotton expressing *DgCspC* gene

Binary expression vector pCambia2300-*DgCspC* containing *CspC* gene under the control of CaMV 35S promoter was transformed into *G. hirsutum* R15 via *Agrobacterium*-mediated method. CTAB method was used to extract DNA from the leaves of the transgenic lines. The transformants were screened via PCR to confirm the presence of *DgCspC* gene. Transgenic cotton lines expressing *DgCspC* gene (T1) were acclimatized and then transferred to the field. Kanamycin (mass/volume ratio: 7,000 ppm) was sprayed on the transgenic cotton plants at the seedling stage. DNA was extracted from the leaves of the T2 progenies to confirm the presence of the *DgCspC* gene. Until the stably expressed T4 transgenic *DgCspC* line was harvested. The T4 generation cotton plants were planted in the field and indoor greenhouse, and the PCR positive lines were used for follow-up experiments.

Total RNA was extracted from cotton leaves using an RNAPrep Pure Plant kit (Tiangen, Beijing, China), according to the manufacturer's instructions. The RNA was then used for cDNA synthesis using a cDNA conversion kit obtained from Transgene, Beijing, China (EasyScript First-strand cDNA Synthesis SuperMix). Real-time quantitative forward and reverse primers specific for *DgCspC* were designed using Beacon Designer software. Real-time quantitative PCR analyses were performed on the LightCycler® 96 System (Roche Diagnostics Corporation) using SYBR Premix Ex Taq II (TAKARA). The *G. hirsutum* UBQ7 gene were used as internal controls. The primers used are listed in [Supplementary Table S2](#). Relative expression level was calculated using the  $2^{-\Delta\Delta CT}$  method (Livak and Schmittgen, 2001).

### Cotton phenotype observation and stress treatment under laboratory conditions

Experiments were performed on the seedlings of T4 generation. Seeds of transgenic and wild-type cotton plants were simultaneously planted in pots before moving them to the greenhouse with conditions of a 16-h light/8-h dark photo period, constant temperature 30°C, 12,000 lux of light intensity and 30% of relative humidity. When the eighth leaf of cotton appears, measure the plant height and the surface area of all leaves with a ruler and a leaf area meter. We evaluated the expression level of cotton growth and development response genes *CYCA3;1* (Gh\_D06G022400.1), *CYCB1;1* (Gh\_D05G255500.1), *EOD* (Gh\_D11G228700.1), *AN3* (Gh\_D12G061800.1), *EBP1* (Gh\_A09G186000.1), and *GRF5* (Gh\_D13G220900.1) through RT-qPCR in the control and overexpressed plants, using the *G. hirsutum* UBQ7 gene as the internal control. The primers used are listed in [Supplementary Table S2](#).

Plump seeds of *DgCspC* transgenic T4 generation and control R15 were selected, and the nutrient soil and vermiculite were mixed evenly with tap water in the ratio of 3:1, and placed in flowerpots with the same specifications. During the growth of cotton plants, MS nutrient solution was watered every other week until 4 leaves grew. *DgCspC* transgenic cotton and control cotton lines with the same development status were selected for experimental grouping. Each group contained 1 control cotton plant and 2 transgenic cotton lines. After the nutrient soil in the pot was fully soaked with tap water, drought stress treatment was carried out. The stress experiment was carried out for a total of 25 days. During the drought stress experiment, each group of cotton leaves were taken and placed in -80°C refrigerator at the same time in each period to determine the corresponding physiological indicators.

Salt stress was initiated by watering the plants with 250 mM of sodium chloride (NaCl) for 12 days (Magwanga et al., 2018a). Cotton leaves of each group were placed in a -80°C refrigerator after treatment for physiological indicator analysis. The phenotypic changes of cotton under stress were continuously observed, recorded, and photographed.

### Measurement of physiological and biochemical indexes

All samples were collected with three biological replicates before treatment, and post stress treatment. We analyzed the physiological and morphological traits of the plants. Malondialdehyde content, relative water content and relative electrical conductivity of leaf extracts were measured as described by previous researchers (Xia et al., 2021). Betaine and proline contents in cotton leaves were determined using HPLC-MS (Shimadzu LC20AD-API 3200MD TRAP). Sample pretreatment was conducted as follows: Pure water was added to the samples, then vortexed for 10 min, followed by ultrasound for 10 min and centrifugation at 13,200 r/min for 4 min. The arginine and proline samples were precipitated with 50  $\mu$ l and 150  $\mu$ l acetonitrile, then vortexed for 2 min, centrifuged at 13,200 r/min for 4 min to obtain supernatant.

### Expression profile of genes related to betaine and proline synthesis

We evaluated the expression level of genes related to betaine and proline synthesis-responsive, such as HMT-2 (Gh\_D08G068000.1), At4g29890 (Gh\_A05G415500.1), ALDH10A8 (Gh\_A11G044900.1), ALDH10A8 (Gh\_D11G045100.1), ALDH10A8 (Gh\_A07G068600.1), HMT-2 (Gh\_A08G073000.1), At4g29890 (Gh\_D04G006200.1), HMT3 (Gh\_A02G039800.1), HMT3 (Gh\_D02G045900.1), At4g29890 (Gh\_A08G188100.1), Gh\_D11G286600 (Gh\_D11G286600.1), Gh\_A11G286400 (Gh\_A11G286400.1), ODC (Gh\_D11G286700.1), AIH (Gh\_D07G063100.1),

ALDH2B4(Gh\_A07G245500.1), Gh\_D07G028100(Gh\_D07G028100.1), Gh\_A03G228600(Gh\_A03G228600.1), Gh\_D02G245200(Gh\_D02G245200.1), ASP3(Gh\_A07G027000.1), Gh\_A13G098000(Gh\_A13G098000.1), POX2(Gh\_A07G195200.1), ALDH3H1(Gh\_D06G049900.1), AIH(Gh\_A07G062700.1), SPMS(Gh\_A12G275700.2), Gh\_D13G104800(Gh\_D13G104800.1), ASP3(Gh\_D07G028200.1), PAO5(Gh\_A05G023200.1), ARB\_02965(Gh\_D01G183300.1), ALDH2B4(Gh\_A12G299800.1), ALDH3F1(Gh\_D05G071600.1), PAO5(Gh\_D05G031600.1), ALDH2B4(Gh\_D12G293500.1), P4H4(Gh\_D09G248800.1), PAO1(Gh\_A08G165800.1), POX2(Gh\_D07G193100.1) and P4H7(Gh\_D06G014100.1) through RT-qPCR in the tissues of control and overexpressed plants, using the *G. hirsutum* UBQ7 gene as the internal control. The primers used are listed in [Supplementary Table S2](#). As demonstrated by previous researchers, these genes are highly upregulated in various cotton and *Arabidopsis* plants' tissues and enhance the synthesis of betaine and proline.

## Determination of agronomic traits and photosynthetic rate in the field

The field sowing experiment was carried out between *DgCspC* transgenic cotton and the control (43°335' N, 84°976' E) in Shawan County, Xinjiang based on the random distribution principle (plot area; 2.25 m \* 5 m). Each plot was replicated three times. Photosynthetic parameters including net photosynthetic rate, intercellular CO<sub>2</sub> concentration, stomatal conductance, transpiration rate, vapor pressure deficiency, and net water use efficiency were measured during full flowering using a portable gas exchange photosynthetic GFS-3000 (WLAZ, Germany) following the system instructions. In addition, the related agronomic traits including plant height, number-of fruit branches, bell number, and bell weight were assessed at the full bolling stage, while the yield was quantified during the harvest stage.

## Statistical analysis

SPSS 18.0 statistical software (SPSS Inc. Chicago, IL, United States) was used to analyze and process the data. Origin9.0 software was used to plot the data. Data in the charts are expressed as mean ± standard error. Asterisks (\*) and \*\*) represent  $p \leq 0.05$  and  $p \leq 0.01$ , respectively.

## Results

### Identification and expression analysis of transgenic cotton expressing *DgCspC* gene

Tissue culture transgenic cotton seedlings expressing *DgCspC* gene were grafted to the stock and cultivated in a greenhouse to

obtain cotton plants with *DgCspC* overexpression in the T1 generation. Cotton seeds of the T1 generation were successively self-bred in Hainan and Xinjiang provinces to obtain T4 stable lines. The presence and expression of the *DgCspC* gene in the T4 stable lines were confirmed by kanamycin selection and PCR identification ([Figure 1A](#)). Lines 1 and 2, whose samples exhibited the right band size after gel electrophoresis were selected and named OE-C-1 and OE-C-2, respectively, for subsequent analysis. The *DgCspC* gene was stable and highly expressed in OE-C-1/OE-C-2 lines based on real-time fluorescence quantitative analysis ([Figure 1B](#)). These results suggest that *DgCspC* gene was stably expressed in T4 transgenic cotton.

### *DgCspC* gene promote cotton growth

The harvested T4 generation OE-C-1/OE-C-2 cotton seeds and wild-type R15 seeds were simultaneously planted in the greenhouse and cultured for 30 days. The transgenic cotton plants exhibited significantly higher growth rate compared with the wild-type, while their leaves gradually increased based on the area of the 1st–8th leaves ([Table 1](#)). The area of the third leaf of OE-C-1/OE-C-2 lines was significantly larger than that of the wild type ([Table 1](#); [Figure 2A](#)). The average plant height of OE-C-1/OE-C-2 lines was significantly higher than that of the wild type ([Figures 2B,D](#)). The taproot length of OE-C-1/OE-C-2 lines was slightly longer than that of the wild type, but the number of lateral roots was significantly higher than that of the wild type ([Figures 2C,E,F](#)). Cotton lines expressing *CspC* gene showed significantly higher nutritional growth relative to their wild-type counterparts. The fresh weight and dry weight of OE-C-1/OE-C-2 lines were significantly higher than those of the wild type ([Figures 2G–I](#)). These data suggest that *DgCspC* expression promotes the growth and leaf development of cotton.

In order to further study the reasons for the vigorous growth of cotton, we selected six genes related to cotton cell development for real-time quantitative expression analysis. Quantitative analysis revealed that the Type A and type B cyclins *CYCA3;1* and *CYCB1;1* were upregulated in the transgenic lines and regulated cell growth ([Figures 3D,E](#)). Growth and development regulatory genes, including *EOD*, *AN3*, *EBP1*, and *GRF5* were further selected for quantitative analysis. The results showed that *EOD* and *GRF5* genes were significantly upregulated in the transgenic cotton lines, suggesting that they facilitated the rapid growth of the transgenic cotton lines ([Figures 3A–C,F](#)). These data suggest that the rapid growth and leaf cell development of cotton were closely related to the upregulated expression of *CYCA3;1*, *CYCB1;1*, *EOD*, *AN3*, *EBP1*, and *GRF5*.

### *DgCspC* gene improves cotton tolerance to drought and salt stress

The transgenic cotton seedlings that grew naturally for 15 days were treated with drought to further identify the stress resistance

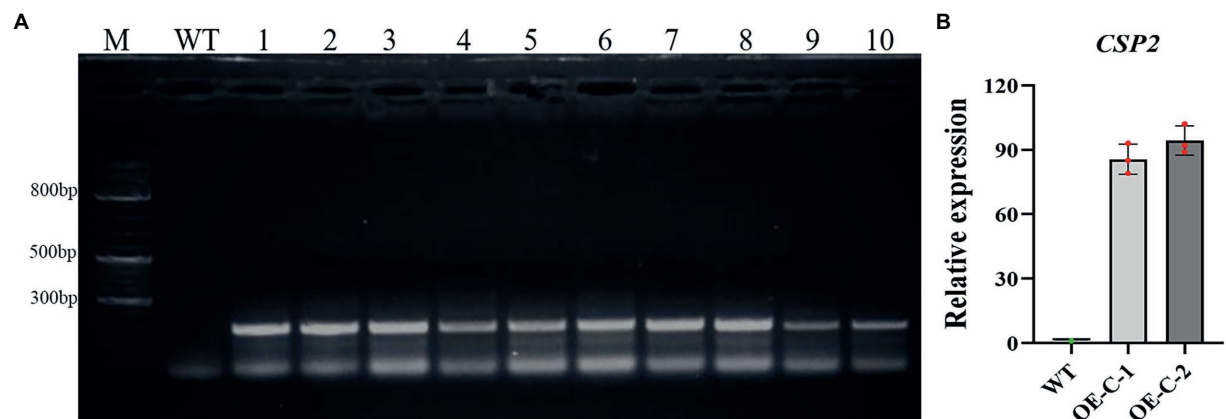


**FIGURE 1** Polymerase chain reaction (PCR) and quantitative RT-PCR (qRT-PCR) analysis of *CspC* transgenic cotton. **(A)** Gel image showing PCR identification of *CspC* T4 transgenic cotton; **(B)** *CspC* gene expression profile in OE-C-1/OE-C-2 lines.

**TABLE 1** Cotton leaf area (cm<sup>2</sup>).

|        | First leaf                 | Second leaf                | Third leaf                  | Fourth leaf                 | Fifth leaf                  | Sixth leaf                   | Seventh leaf                 | Eighth leaf                  |
|--------|----------------------------|----------------------------|-----------------------------|-----------------------------|-----------------------------|------------------------------|------------------------------|------------------------------|
| WT     | 28.2 ± 0.57                | 29.3 ± 0.20                | 35.73 ± 0.50                | 59.13 ± 0.40                | 81.37 ± 1.15                | 105.6 ± 0.96                 | 121.97 ± 1.55                | 123.97 ± 0.42                |
| OE-C-1 | 28.63 ± 0.42 <sup>ns</sup> | 29.67 ± 0.38 <sup>ns</sup> | 56.97 ± 1.31 <sup>**</sup>  | 69.3 ± 0.95 <sup>***</sup>  | 109.2 ± 0.70 <sup>***</sup> | 130.67 ± 0.85 <sup>***</sup> | 139.77 ± 0.45 <sup>***</sup> | 142.73 ± 0.40 <sup>***</sup> |
| OE-C-2 | 28.33 ± 0.32 <sup>ns</sup> | 30.23 ± 0.15 <sup>*</sup>  | 61.47 ± 1.15 <sup>***</sup> | 73.73 ± 1.40 <sup>***</sup> | 111.5 ± 0.82 <sup>***</sup> | 133.73 ± 0.80 <sup>***</sup> | 143.23 ± 1.03 <sup>***</sup> | 145.37 ± 0.49 <sup>***</sup> |

Asterisks indicate significant differences between WT and the OE-C-1/OE-C-2 transgenic lines (Student's *t*-test, <sup>\*\*</sup>*p* < 0.01). WT, wild type; OE, overexpression; *CspC*, cold shock protein C.

<sup>\*</sup>*p* < 0.05, <sup>\*\*</sup>*p* < 0.01, <sup>\*\*\*</sup>*p* < 0.001 comparisons between the transgenic lines and wild-type plants by Student's *t*-tests.

function of *DgCspC* gene. The wild-type cotton leaves showed serious wilting and shriveled together when the natural drought lasted for 25 days (Figure 4A). However, the leaves of OE-C-1/OE-C-2 cotton lines were slightly dehydrated and grew normally. For instance, the cotton lines OE-C-1/OE-C-2 grew well and had a larger leaf size and higher plant height than the control group. *DgCspC* transgenic cotton showed a strong drought resistance phenotype. Similar results were obtained at the cellular physiological level in *DgCspC* transgenic cotton. The relative water content, MDA content, POD activity, and relative conductivity were measured using cotton leaves under normal growth versus those under drought treatment for 25 days. Relative water content and POD activity were significantly higher in OE-C-1/OE-C-2 lines than in the wild type after drought stress (Figures 4B–E). In contrast, the MDA content and relative conductivity were significantly lower in OE-C-1/OE-C-2 lines than in the wild type, indicating that cell damage was significantly lower in *DgCspC* transgenic cotton than in R15 wild type after drought stress.

The leaves of wild-type cotton turned yellow and withered after treatment with 250 mM NaCl for 12 days. However, the leaves of the transgenic cotton were slightly yellow after the treatment (Figure 4F). The damage to the membrane system was significantly lower in transgenic cotton than in the wild-type cotton under salt stress based on physiological indexes. The relative water content of cotton leaves decreased significantly after salt treatment, but the relative water

content of OE-C-1/OE-C-2 lines was still significantly higher than that of wild type (Figure 4G). The MDA content of *DgCspC* overexpression lines was significantly higher than that of wild type before and after salt treatment (Figure 4H). After 200 mM NaCl treatment, the POD activity of the OE-C-1/OE-C-2 lines was significantly higher than that of the wild type, and the relative conductivity was significantly lower than that of the wild type (Figures 4I,J). Overall, these results indicate that overexpression of *DgCspC* gene can improve drought and salt stress tolerance in cotton.

## Analysis of proline and betaine contents and gene expression level

To understand the reason that *DgCspC* expression enhance cotton tolerance to drought and salinity stresses, the proline and betaine contents of both transgenic cotton lines and WT lines were measured under the normal and stresses conditions. In this study, the proline content was significantly higher in OE-C-1/OE-C-2 lines than in wild type after drought and salt stress treatments (Figures 5A,B). Herein, betaine content in cotton leaves was determined using high-performance liquid chromatography mass spectrometry. The results showed that betaine content was significantly higher in OE-C-1/OE-C-2 cotton lines than in the control group after drought and salt treatments.



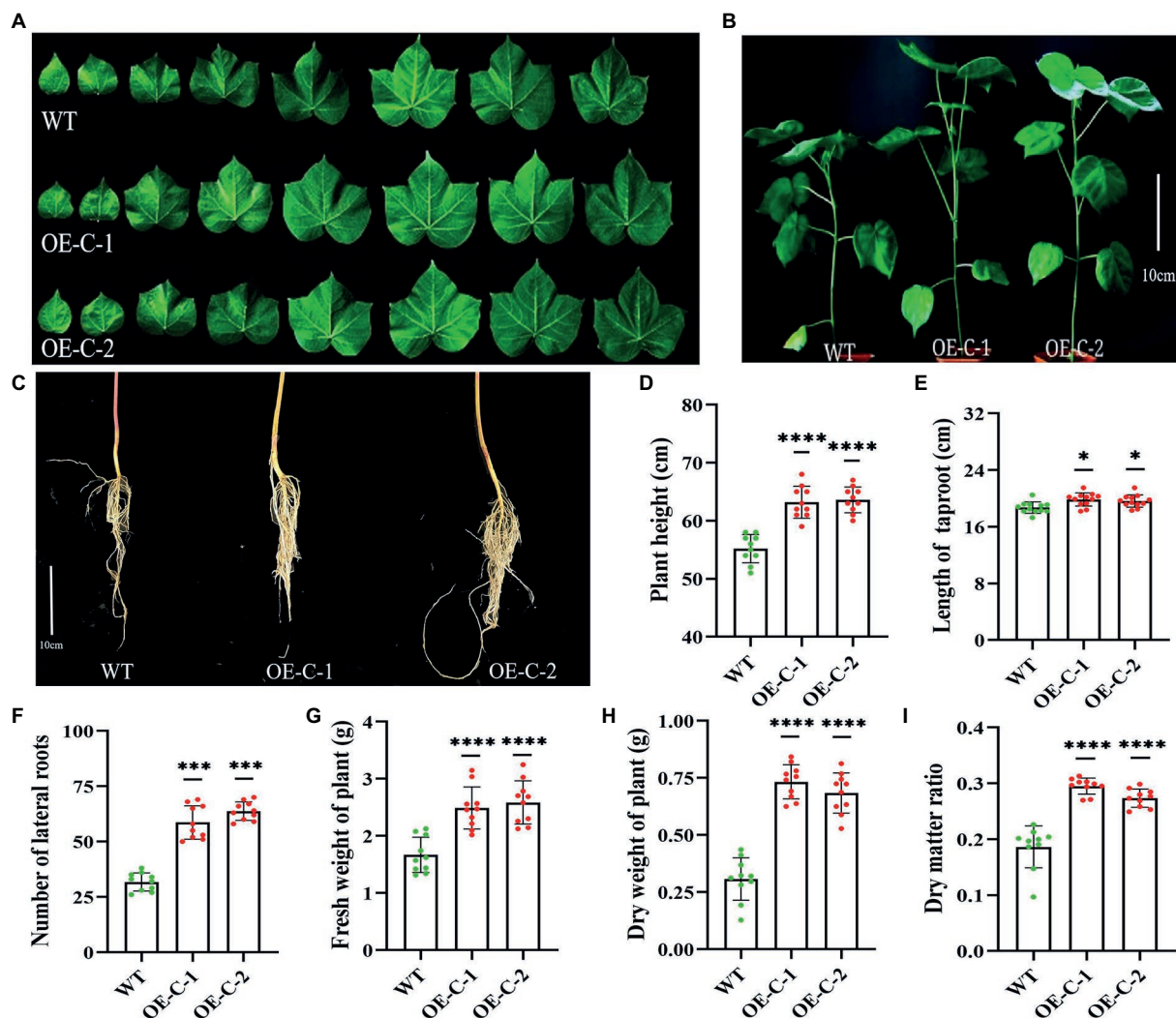


FIGURE 2

Growth analysis of *DgCspC* transgenic cotton lines. (A) Comparison of leaf size between transgenic and wild-type cotton lines; (B) growth phenotype of wild type and transgenic cotton lines; (C) root morphology between wild type and transgenic cotton lines; (D) height comparison between wild type and transgenic cotton lines; (E) length of taproot; (F) number of lateral roots; (G) fresh weight of plant; (H) dry weight of plant; (I) dry matter ratio. Asterisks indicate significant differences between WT and the OE-C-1/ OE-C-2 transgenic lines. (\* $p < 0.05$ , \*\*\* $p < 0.001$ , \*\*\*\* $p < 0.0001$  for comparisons between the transgenic lines and wild-type plants by Student's *t*-tests).

Under normal conditions, the betaine content of transgenic lines was slightly higher than that of wild-type lines, but not significantly (Figures 5C,D). Increased betaine content in cells can enhance osmotic regulation and drought and salt tolerance of plants.

Quantitative analysis revealed that several genes related to proline and betaine synthesis were upregulated in *DgCspC* transgenic cotton. Specifically, 26 proline synthesis-related genes were screened from the transgenic cotton lines, of which 18 genes were significantly upregulated (Figure 5E). Similarly, proline content was higher in the transgenic cotton leaves than in the wild type. Secondly, 10 betaine synthesis-related genes were screened from *DgCspC* overexpression cotton of which eight genes were upregulated. The upregulation range was slightly small (Figure 5F). Betaine content was not significantly different between transgenic cotton and wild type under normal conditions. However, betaine

content was significantly higher in transgenic cotton than in wild type after drought and salt stress treatments (Figures 5C,D). These data showed that the upregulated expression of most genes in the proline and betaine synthesis pathway led to the increase in proline and betaine contents in transgenic cotton leaves.

### *DgCspC* transgenic cotton exhibits strong photosynthetic rate under field conditions

In order to further observe the characters and yield of transgenic cotton in the field, the field sowing experiment was carried out between *DgCspC* transgenic cotton and the control. Photosynthesis represents the biomass and yield of the plant. For

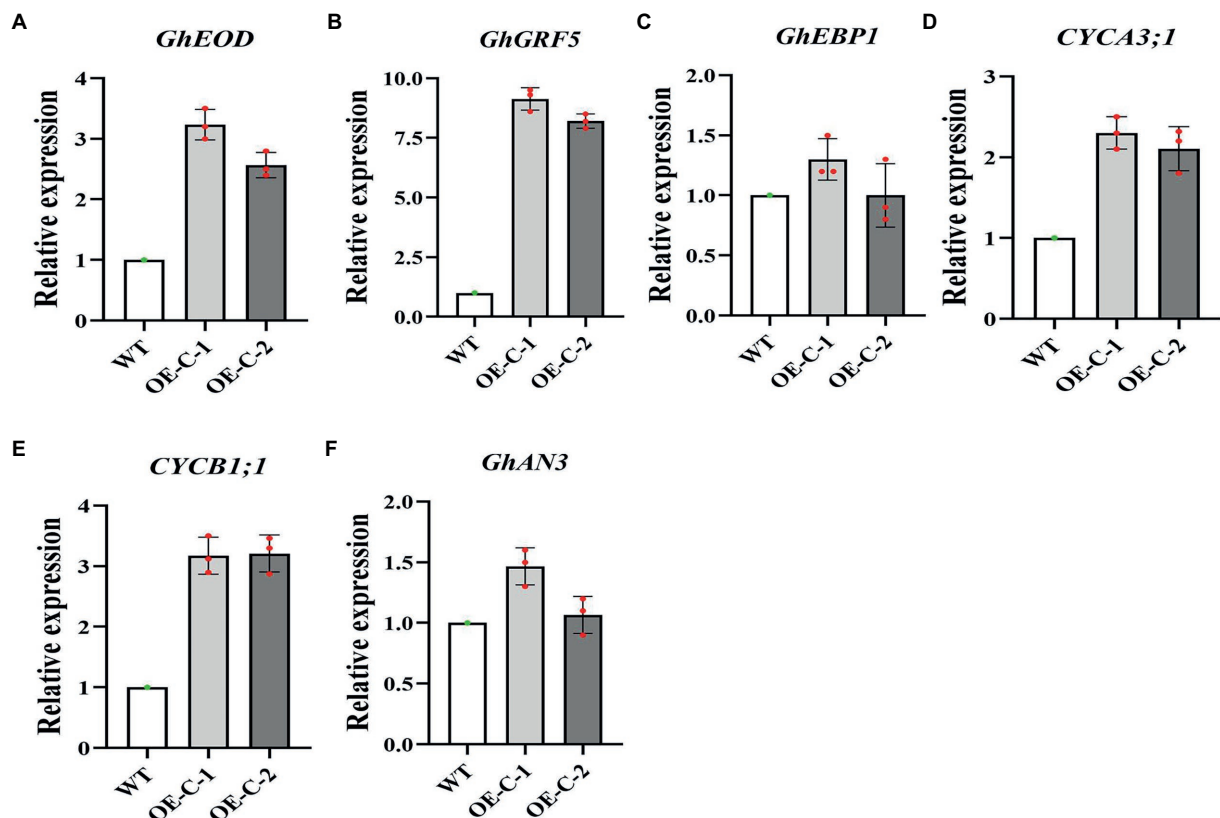


**FIGURE 3**  
Expression analysis of genes related to growth and development in the transgenic cotton lines. (A) *GhEOD* Relative expression. (B) *GhGRF5* Relative expression. (C) *GhEBP1* Relative expression. (D) *CYCA3;1* Relative expression. (E) *CYCB1;1* Relative expression. (F) *GhAN3* Relative expression.

the photosynthetic assay, penultimate leaves from transgenic cotton plants were obtained from 10 plants per line (*DgCspC*-transgenic lines and control recipient plants). The photosynthetic parameters, including net photosynthetic rate, intercellular CO<sub>2</sub> concentration, stomatal conductance, transpiration rate, and net water use efficiency were significantly higher in the *DgCspC*-transformed cotton than in control when grown normally in the field (Figure 6) except for vapor pressure deficiency (VPD). As a result, the transgenic cotton plants had better growth conditions and agronomic trait performance than the control.

The related agronomic traits were investigated at the full bolling stage, while yield was investigated at the harvest stage. Transgenic cotton lines exhibited higher plant height, more fruit branches, more bolls, and higher yield (which increased by 9.8%, 37%, and 30.08%, respectively) under field conditions than the wild type (Table 2). These data showed that the overexpression of *DgCspC* gene significantly increased cotton yield.

## Discussion

*Csps* are found in various bacteria. All *Csps* share common features that play a critical role in the survival of bacteria in

extreme environments (Amir et al., 2018). Efficient use of carbon sources in a competitive environment is essential for bacterial survival. As a result, bacteria have evolved a complex control system for efficient energy use (Chen, 2013). *Csp* genes act as molecular chaperones that maintain mRNA stability under abiotic stresses, such as drought and low temperature (Keto-Timonen et al., 2016). *Csp* genes can regulate transcription and translation efficiency by binding to DNA or RNA, improve freezing resistance of biofilms by encoding new proteins, and participate in signal transduction (Ermolenko and Makhatadze, 2002). Our study revealed that *CYCA3;1*, *CYCB1;1*, *EOD* and *GRF5* were significantly upregulated in the *DgCspC* transgenic lines and regulated cell growth. Cell cycle plays an important role in the growth and development of multicellular organisms (Dewitte and Murray, 2003). Type A and type B cyclins (*CYCA*s/*CYCB*s) are mitotic cyclins. Studies have shown that overexpression of *CYCA3* in tobacco can induce cell division in shoot tip meristem and leaf primordium (Wyrzykowska et al., 2002). Growth-Regulating Factors (*GRFs*) belong to a small plant specific transcription factor (TF) family. *GRFs* function in regulating leaf (Kim et al., 2003) and stem development, shoot apical meristem development (Kim and Lee, 2006), leaf primordia formation (Horiguchi et al., 2005),

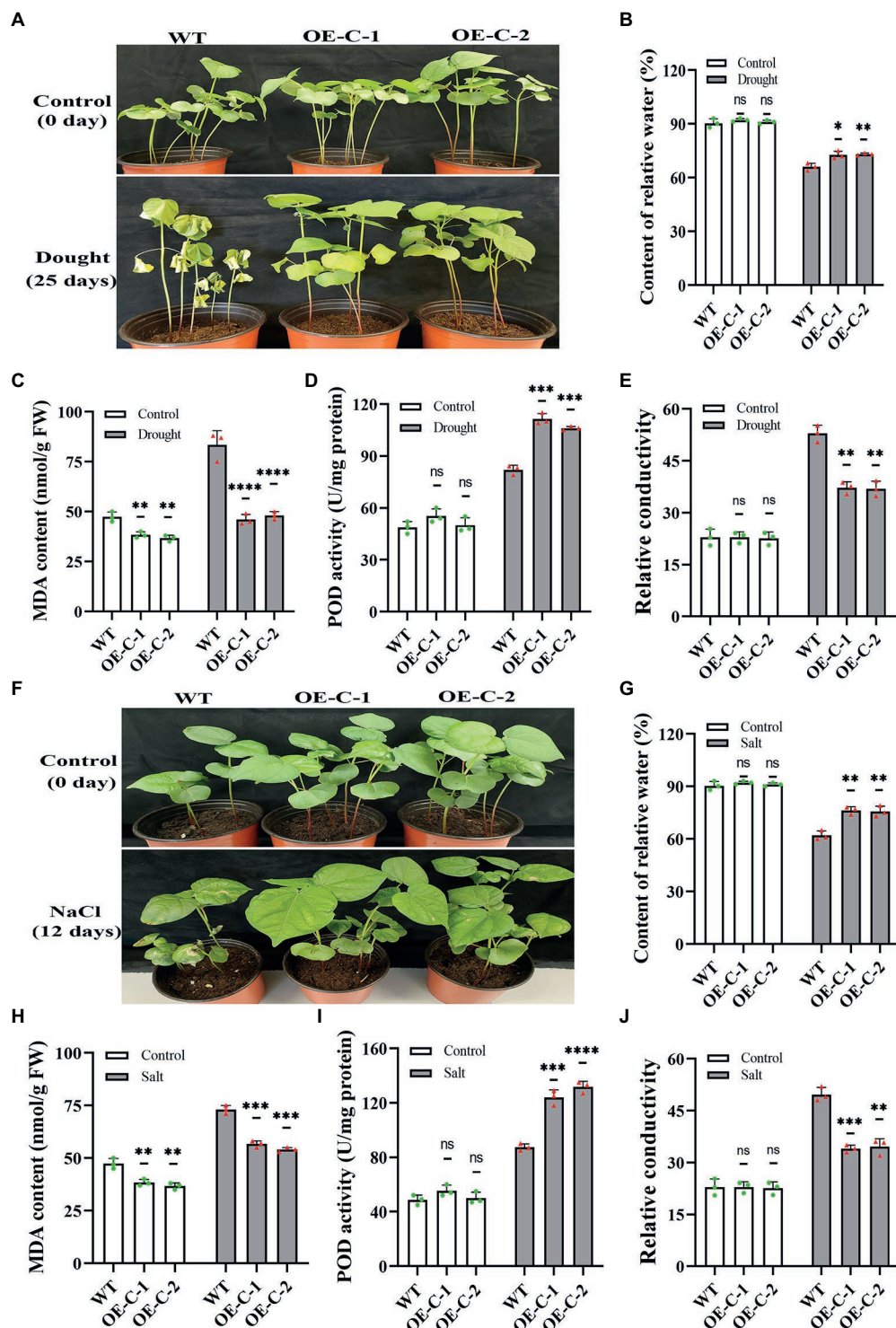


FIGURE 4

Phenotype and physiological indexes of *DgCspC* transgenic cotton under drought and salt stress. (A) Phenotype of transgenic and wild-type cotton line under natural drought and rehydration; (B) relative water content; (C) MDA content; (D) POD content; (E) relative conductivity; (F) phenotype of transgenic and wild-type cotton lines under salt treatment; (G) relative water content under salt stress; (H) MDA content under salt stress; (I) POD content under salt stress; (J) relative conductivity under salt stress; Asterisks indicate significant differences between WT and the OE-C-1/ OE-C-2 transgenic lines. (\* $p < 0.05$ , \*\* $p < 0.01$ , \*\*\* $p < 0.001$ , \*\*\*\* $p < 0.0001$  for comparisons between the transgenic lines and wild-type plants by Student's *t*-tests).



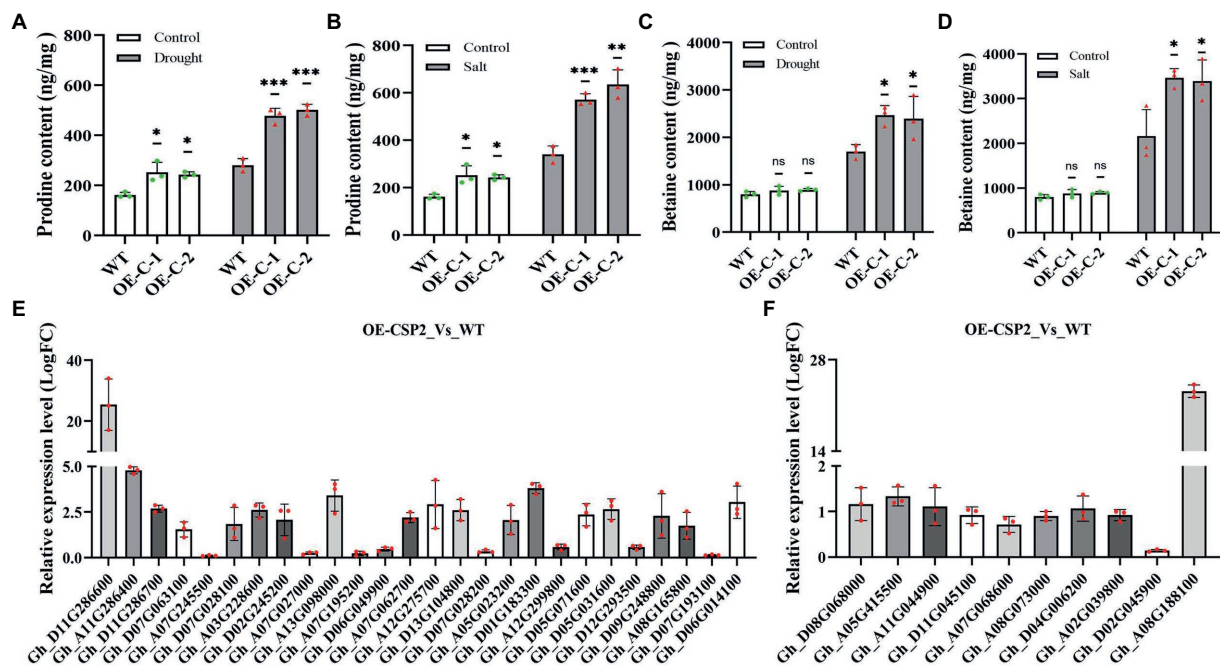


FIGURE 5

Analysis of proline and betaine contents and expression of related genes in transgenic cotton overexpressing *DgCspC* gene under drought or salt stress. (A) Proline content under drought stress; (B) proline content under salt stress; (C) betaine content under drought stress; (D) betaine content under salt stress; (E) expression of proline synthesis-related genes; (F) expression of betaine synthesis-related genes. (\* $p < 0.05$ , \*\* $p < 0.01$ , \*\*\* $p < 0.001$  for comparisons between the transgenic lines and wild-type plants by Student's *t*-tests.)

and leaf size and longevity (Debernardi et al., 2014). Growth-Regulating Factors (GRFs) plays an important role in regulating leaf and stem development, shoot tip meristem development, leaf primordium formation, and leaf size (Kim et al., 2003; Horiguchi et al., 2005; Kim and Lee, 2006; Debernardi et al., 2014). Overexpression of GRFs promotes the expression of cell cycle genes and auxin response genes, resulting in increased cell numbers and expansion of leaves (Omidbakhshfard et al., 2015; Piya et al., 2020). The *CspC* expression could cause these genes upregulated to increase expansion of cotton leaves. It was inferred that upregulated of these genes might be resulted from *DgCspC* function in transcription and translation efficiency or activating a signal pathway to induce these gene expression.

Csps in most bacteria are present in multiple copies and are induced in different ways. In contrast, *D. gobiensis I-0* contains only one *Csp*, implying that it may be induced by many different conditions, and potentially regulates multiple pathways. A study found that cold-excited proteins are involved in the survival of cells during the stable phase (Michaux et al., 2012). *Csp* participates in osmotic stress, pigment regulation, nutritional stress regulation, and other cellular processes, effectively enhancing resistance to cold and osmotic stresses.

Drought and salt significantly affect the normal growth and development of plants, causing a huge loss of cotton yield (Cai et al., 2021). Plant phenotype is the most visual response to drought and salt stresses. The relative leaf water content measure water status in the plant, and reflects the metabolic activity of

the tissues (Nayyar et al., 2006). In this study, transgenic cotton lines overexpressing *DgCspC* gene exhibited higher water content after stress, indicating that *DgCspC* gene can enhance the water retention of leaves under stress and improve the drought and salt resistance of the plants. Stresses, such as drought and salt can induce oxidative stress, leading to membrane peroxidation, thus damaging cells. MDA and the relative conductivity are effective indexes used to measure the degree of lipid peroxidation. The MDA content and the relative conductivity increase in plants under drought and salt stresses. In this study, the MDA content and relative conductivity were lower in the transgenic cotton than in the control plants under stress, indicating that overexpression of the *DgCspC* gene can reduce oxidative damage, consistent with the findings reported previously (Yu et al., 2017).

Excessive reactive oxygen species (ROS) in plants can cause membrane lipid peroxidation, resulting in oxidative damage to the membrane system (Zhang et al., 2005; Basu et al., 2017). Plants have various mechanisms of adapting to abiotic stress, such as accumulating some soluble sugars, amino acids, organic acids, proline, polyols, betaine, and other soluble substances (Giri, 2011; Kumar et al., 2017). Betaine resists adverse stress through osmotic regulation, scavenging ROS, maintaining biofilm stability, protecting photosynthetic mechanism, and maintaining the structure and function of macromolecular protein complexes and some enzymes (Chen and Murata, 2011). Betaine and proline are key osmoregulatory substances in plants. They enhance plant adaptation to water stress caused by



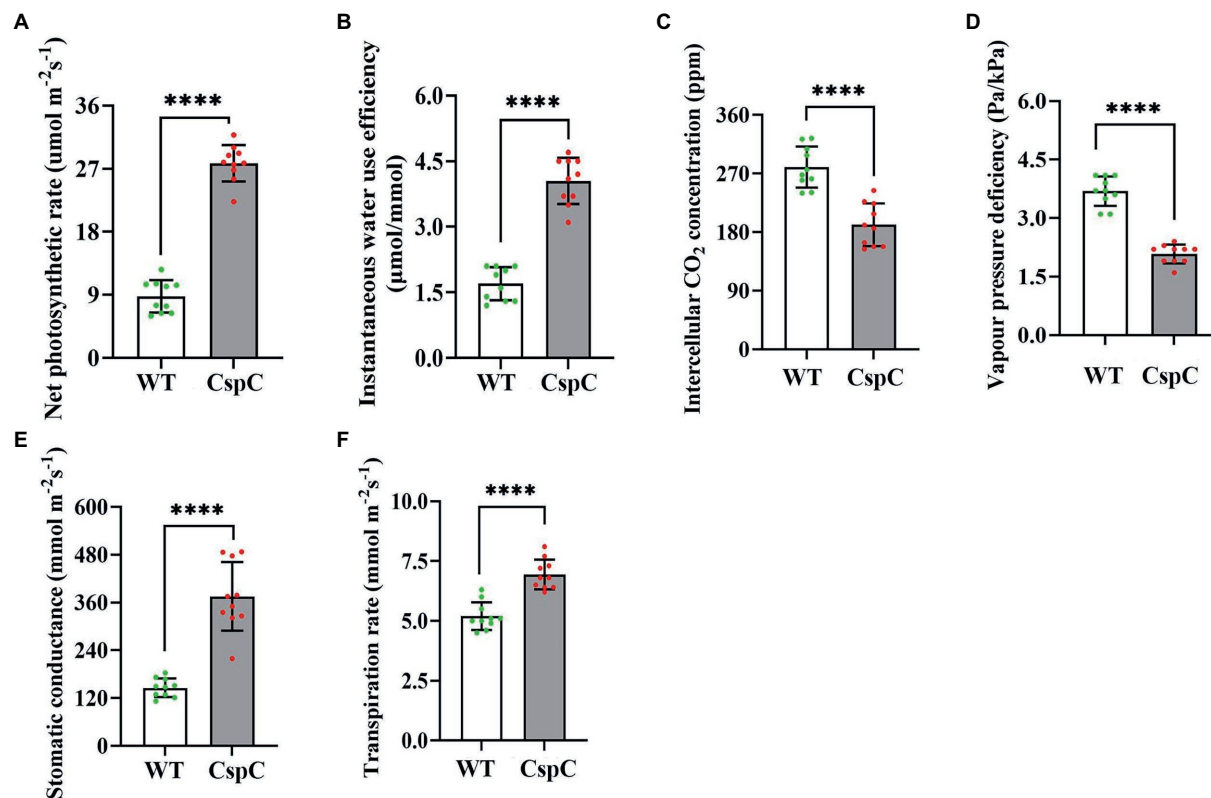


**FIGURE 6**  
Photosynthetic efficiency of *DgCspC* overexpression cotton. (A) Net photosynthetic rate; (B) instantaneous water use efficiency; (C) intercellular CO<sub>2</sub> concentration; (D) vapor pressure deficiency; (E) stomatal conductance; (F) transpiration rate. Asterisks indicate significant differences between WT and the OE-C-1/ OE-C-2 transgenic lines. (\*\*\*\**p* < 0.0001 for comparisons between the transgenic lines and wild-type plants by Student's *t*-tests).

**TABLE 2** Agronomic traits and yield of cotton in the field.

| Strain  | Plant height (cm) | Number-of fruit branches (/plant) | Bell number (/ plant) | Bell weight (g)  | Seed-cotton weight (g) |
|---------|-------------------|-----------------------------------|-----------------------|------------------|------------------------|
| WT      | 66.75 ± 4.96      | 6.75 ± 1.09                       | 4.92 ± 0.86           | 78.12 ± 18.84    | 90.79 ± 4.65           |
| OE-CspC | 73.33 ± 2.96***   | 9.25 ± 1.01****                   | 6.4 ± 1.34**          | 102.27 ± 21.45** | 113.82 ± 8.14****      |

Asterisks indicate significant differences between WT and the OE-C-1/OE-C-2 transgenic lines (Student's *t*-test, \*\**p* < 0.01). WT, wild type; OE, overexpression; CspC, Cold shock protein C.

\*\**p* < 0.01, \*\*\**p* < 0.001, \*\*\*\**p* < 0.0001 for comparisons between the transgenic lines and wild-type plants by Student's *t*-tests.

drought, salinity, and other stresses. High proline content can maintain the osmotic balance of cytosol and reduce the damage to cells (Yang and Gao, 2007; Chen and Murata, 2008; Ahmad et al., 2010; Zhang et al., 2014). In this study, overexpression of *DgCspC* gene significantly increased betaine and proline contents in cotton leaves, thus enhancing the cell osmotic regulation function under drought and salt stresses. Betaine can also improve salt tolerance by strengthening CO<sub>2</sub> assimilation ability of plant cells. A study showed that betaine significantly improves the photosynthetic capacity, stomatal conductance, transpiration rate, and the activity of related antioxidant enzymes in wheat plants under salt stress (Ashraf et al., 2008). Herein, the net photosynthetic efficiency was significantly higher in transgenic cotton than in wild-type, possibly due to

increased betaine content under salt and drought stresses. Increased photosynthetic efficiency increased cotton yield. Therefore, *DgCspC* expression could promote transcription and translation of genes of Betaine and proline metabolisms under adverse conditions, and contributed accumulated of Betaine and proline in cotton. It was consistent with the *DgCspC* expression induced by many ways and regulating various pathways. A previous study showed that *CspC* gene of *D. gobiensis I-0* can significantly improve the resistance of *E. coli* to low temperature, high salt, drought, and other adversities (Chen, 2013). In this study, heterologous expression of *CspC* gene from *D. gobiensis I-0* in cotton accelerated the growth, yield, and resistance to drought and salt stresses. This is the first study to demonstrate the functional application of *DgCspC* gene

in genetic engineering, thus is of theoretical and practical significance. Additionally, the genome of *D. gobiensis I-0* contains several functional genes and species genes. Therefore, this genome harbors important genetic resources, especially stress-related genes and damage repair genes. However, further studies should explore these genes and their practical application by clarifying their mechanism of action. Moreover, the stress-resistant genes can be used to generate new varieties of transgenic crops with stress resistance. Recent studies have shown that Csps can significantly enhance the salt tolerance of *E. coli* and *Brassica rapa* and globally regulate the expression of genes, including stress-reactive proteins and growth-related proteins (Pan et al., 2009). Therefore, Csps may provide candidate resources for developing superior transgenic plant varieties.

## Conclusion

These research findings have shown that *DgCspC* gene plays a role in enhancing drought and salt tolerance of cotton. In this study, heterologous expression of *DgCspC* promoted cotton growth, as exhibited by larger leaf size and plant height, compared with the wild-type plants. Furthermore, Proline and betaine content assays confirmed that the enhanced stress tolerance of *DgCspC* transgenic cotton was related to its osmotic regulation. In addition, comparative transcriptome analysis showed that the expression of genes related to the synthesis of betaine and proline was upregulated. Also, photosynthetic efficiency and yield were significantly higher in the transgenic cotton overexpressing *DgCspC* than in the wild-type control under field conditions. This is the first report that microbial *Csp* gene improves the stress resistance of cotton. This study provides insights into the molecular breeding of new cotton varieties with high stress resistance.

## Data availability statement

The original contributions presented in the study are included in the article/Supplementary material, further inquiries can be directed to the corresponding author.

## References

- Ahmad, R., Kim, Y. H., Kim, M. D., Kwon, S. Y., Cho, K., Lee, H. S., et al. (2010). Simultaneous expression of choline oxidase, superoxide dismutase and ascorbate peroxidase in potato plant chloroplasts provides synergistically enhanced protection against various abiotic stresses. *Physiol. Plant.* 138, 520–533. doi: 10.1111/j.1399-3054.2010.01348.x
- Amir, M., Kumar, V., Dohare, R., Islam, A., Ahmad, F., and Hassan, M. I. (2018). Sequence, structure and evolutionary analysis of cold shock domain proteins, a member of OB fold family. *J. Evol. Biol.* 31, 1903–1917. doi: 10.1111/jeb.13382
- Annunziata, M. G., Ciarmiello, L. F., Woodrow, P., Dell'Aversana, E., and Carillo, P. (2019). Spatial and temporal profile of glycine Betaine accumulation in plants Under abiotic stresses. *Front. Plant Sci.* 10:230. doi: 10.3389/fpls.2019.00230
- Ashraf, M., Nawaz, K., Athar, H. R., and Raza, S. H. (2008). *Growth enhancement in two potential cereal crops, Maize and Wheat, by Exogenous Application of Glycinebetaine*. Switzerland: Birkhäuser Basel.
- Basu, S., Giri, R. K., Benazir, I., Kumar, S., Rajwanshi, R., Dwivedi, S. K., et al. (2017). Comprehensive physiological analyses and reactive oxygen species profiling in drought tolerant rice genotypes under salinity stress. *Physiol. Mol. Biol. Plants* 23, 837–850. doi: 10.1007/s12298-017-0477-0
- Basu, S., Ramegowda, V., Kumar, A., and Pereira, A. (2016). Plant adaptation to drought stress. *F1000Res* 5:1554. doi: 10.12688/f1000research.7678.1
- Brauc, S., De Vooght, E., Claeys, M., Geuns, J. M. C., Höfte, M., and Angenon, G. (2012). Overexpression of arginase in *Arabidopsis thaliana* influences defence

## Author contributions

WX and SuG conceived and designed the study. JZ and KZ performed the experiments. YW and DZ prepared the figures and analyzed the data. WX wrote the manuscript. SaG and SuG performed a critical review for intellectual content. All authors contributed to the article and approved the submitted version.

## Funding

This research was funded by Hainan Yazhou Bay Seed Lab (grant nos. B21HJ8201 and B21Y10213).

## Acknowledgments

We are grateful for the support of the research group during this research work.

## Conflict of interest

The authors declare that the research was conducted in the absence of any commercial or financial relationships that could be construed as a potential conflict of interest.

## Publisher's note

All claims expressed in this article are solely those of the authors and do not necessarily represent those of their affiliated organizations, or those of the publisher, the editors and the reviewers. Any product that may be evaluated in this article, or claim that may be made by its manufacturer, is not guaranteed or endorsed by the publisher.

## Supplementary material

The Supplementary material for this article can be found online at: <https://www.frontiersin.org/articles/10.3389/fpls.2022.985900/full#supplementary-material>

- responses against Botrytis cinerea. *Plant Biol.* 14, 39–45. doi: 10.1111/j.1438-8677.2011.00520.x
- Cai, X., Jiang, Z., Tang, L., Zhang, S., Li, X., Wang, H., et al. (2021). Genome-wide characterization of carotenoid oxygenase gene family in three cotton species and functional identification of GaNCED3 in drought and salt stress. *J. Appl. Genet.* 62, 527–543. doi: 10.1007/s13353-021-00634-3
- Castiglioni, P., Warner, D., and Bensen, R. J. (2008). Bacterial RNA chaperones confer abiotic stress tolerance in plants and improved grain yield in maize under water limited conditions. *Plant Physiol.* 147, 446–455. doi: 10.1104/pp.108.118828
- Chen, J. (2013). Molecular mechanism of the *Escherichia coli* maltose transporter. *Curr. Opin. Struct. Biol.* 23, 492–498. doi: 10.1016/j.sbi.2013.03.011
- Chen, T. H. H., and Murata, N. (2008). Glycinebetaine: an effective protectant against abiotic stress in plants. *Trends Plant Sci.* 13, 499–505. doi: 10.1016/j.tplants.2008.06.007
- Chen, T. H. H., and Murata, N. (2011). Glycinebetaine protects plants against abiotic stress: mechanisms and biotechnological applications. *Plant Cell Environ.* 34, 1–20. doi: 10.1111/j.1365-3040.2010.02232
- Choi, M. J., Park, Y. R., Park, S. J., and Heung, K. (2015). Stress-responsive expression patterns and functional characterization of cold shock domain proteins in cabbage (*Brassica rapa*) under abiotic stress conditions. *Plant Physiol. Biochem.* 96, 132–140. doi: 10.1016/j.plaphy.2015.07.027
- Dai, J., Duan, L., and Dong, H. (2014). Improved nutrient uptake enhances cotton growth and salinity tolerance in saline media. *J. Plant Nutr.* 37, 1269–1286. doi: 10.1080/01904167.2014.881869
- De La Garza-García, J. A., Bettache, S. O., Lyonais, S., Eusebio, E. O., Freddi, L., Dahouk, S. A. I., et al. (2021). Comparative genome-wide Transcriptome analysis of *Brucella suis* and *Brucella microti* Under acid stress at pH 4.5: cold shock protein CspA and Dps are associated With acid resistance of *B. microti*. *Front. Microbiol.* 12:794535. doi: 10.3389/fmicb.2021.794535
- Debernardi, J. M., Mecchia, M. A., Vercruyssen, L., Smaczniak, C., Kaufmann, K., Inze, D., et al. (2014). Post-transcriptional control of GRF transcription factors by microRNA miR396 and G1F co-activator affects leaf size and longevity. *Plant J.* 79, 413–426. doi: 10.1111/tj.12567
- Dewitte, W., and Murray, J. A. H. (2003). The plant cell cycle. *Annu. Rev. Plant Biol.* 54, 235–264. doi: 10.1146/annurev.arplant.54.031902.134836
- Ding, M., Peichen, H., Xin, S., Meijuan, W., Shurong, D., Jian, S., et al. (2010). Salt-induced expression of genes related to Na<sup>+</sup>/K<sup>+</sup> and ROS homeostasis in leaves of salt-resistant and salt-sensitive poplar species. *Plant Mol. Biol.* 73, 251–269. doi: 10.1007/s11103-010-9612-9
- Ermolenko, D. N., and Makhatazde, G. I. (2002). Bacterial cold-shock proteins. *Cell. Mol. Life Sci.* 59, 1902–1913. doi: 10.1007/pl00012513
- Faßhauer, P., Busche, T., Kalinowski, J., Mäder, U., Poehlein, A., Daniel, R., et al. (2021). Functional redundancy and specialization of the conserved cold shock proteins in *Bacillus subtilis*. *Microorganisms* 9:1434. doi: 10.3390/microorganisms9071434
- Fradin, E. F., and Thomma, B. P. H. J. (2006). Physiology and molecular aspects of Verticillium wilt diseases caused by *V. dahliae* and *V. albo-atrum*. *Mol. Plant Pathol.* 7, 71–86. doi: 10.1111/j.1364-3703.2006.00323.x
- Giri, J. (2011). Glycinebetaine and abiotic stress tolerance in plants. *Plant Signal. Behav.* 6, 1746–1751. doi: 10.4161/psb.6.11.17801
- Heinemann, U., and Roske, Y. (2021). Cold-shock domains—abundance, structure, properties, and nucleic-acid binding. *Cancers* 13:190. doi: 10.3390/cancers13020190
- Horiguchi, G., Kim, G. T., and Tsukaya, H. (2005). The transcription factor AtGRF5 and the transcription coactivator AN3 regulate cell proliferation in leaf primordia of *Arabidopsis thaliana*. *Plant J.* 43, 68–78. doi: 10.1111/j.1365-3113X.2005.02429.x
- Kentaro, E., and Ryozyo, E. (2012). Pleiotropic roles of cold shock domain proteins in plants. *Front. Plant Sci.* 2:116. doi: 10.3389/fpls.2011.00116
- Keto-Timonen, R., Hietala, N., Palonen, E., Hakakorpi, A., Lindström, M., and Korkeala, H. (2016). Cold shock proteins: A Minireview with special emphasis on Csp-family of Enteropathogenic *Yersinia*. *Front. Microbiol.* 7:1151. doi: 10.3389/fmicb.2016.01151
- Kim, J. H., Choi, D., and Kende, H. (2003). The AtGRF family of putative transcription factors is involved in leaf and cotyledon growth in *Arabidopsis*. *Plant J.* 36, 94–104. doi: 10.1046/j.1365-3113X.2003.01862.x
- Kim, J. H., and Lee, B. H. (2006). Growth-Regulating Factor4 of *Arabidopsis thaliana* is required for development of leaves, cotyledons, and shoot apical meristem. *J. Plant Biol.* 49, 463–468. doi: 10.1007/BF03031127
- Kim, M. H., Sasaki, K., and Imai, R. (2009). Cold shock domain protein 3 regulates freezing tolerance in *Arabidopsis thaliana*. *J. Biol. Chem.* 284, 23454–23460. doi: 10.1074/jbc.M109.025791
- Kumar, V., Shriram, V., Hoque, T. S., Hasan, M. M., Burritt, D. J., and Hossain, M. A. (2017). Glycinebetaine-mediated abiotic oxidative-stress tolerance in plants: physiological and biochemical mechanisms. Switzerland: Springer, Cham.
- Livak, K. J., and Schmittgen, T. D. (2001). Analysis of relative gene expression data using real-time quantitative PCR and the 2<sup>-ΔΔCT</sup> method. *Methods* 25, 402–408. doi: 10.1006/meth.2001.1262
- Magwanga, R. O., Lu, P., Kirungu, J. N., Cai, X., Zhou, Z., and Wang, X. (2018a). Whole genome analysis of cyclin dependent kinase (CDK) gene family in cotton and functional evaluation of the role of CDKF4 gene in drought and salt stress tolerance in plants. *Int. J. Mol. Sci.* 19. doi: 10.3390/ijms19092625
- Meloni, D. A., Oliva, M. A., Ruiz, H. A., and Martinez, C. A. (2001). Contribution of proline and inorganic solutes to osmotic adjustment in cotton under salt stress. *J. Plant Nutr.* 24, 599–612. doi: 10.1081/PLN-100104983
- Michaux, C., Martini, C., Shioya, K., Lecheheb, S. A., Budin-Verneuil, A., Cosette, P., et al. (2012). CspR, a cold shock RNA-binding protein involved in the long-term survival and the virulence of enterococcus faecalis. *J. Bacteriol.* 194, 6900–6908. doi: 10.1128/JB.01673-12
- Mingkun, Y. (2011). Functional Identification and Heterologous Expression of cold shock Proteins in *Deinococcus gobiensis* I-0. dissertation/master's thesis. China (IL): Chinese Academy of Agricultural Sciences.
- Naidoo, G., and Naidoo, Y. (2001). Effects of salinity and nitrogen on growth, ion relations and proline accumulation in Triglochin bulbosa. *Wel. Ecol. Manag.* 9, 491–497. doi: 10.1023/A:1012284712636
- Nayyar, H., Kaur, S., Singh, S., and Upadhyaya, H. D. (2006). Differential sensitivity of Desi (small-seeded) and Kabuli (large-seeded) chickpea genotypes to water stress during seed filling: effects on accumulation of seed reserves and yield. *J. Sci. Food Agric.* 86, 2076–2082. doi: 10.1002/jsfa.2574
- Omidbakhshfar, M. A., Proost, S., Fujikura, U., and Mueller-Roeber, B. (2015). Growth-regulating factors (GRFs): a small transcription factor family with important functions in plant biology. *Mol. Plant* 8, 998–1010. doi: 10.1016/j.molp.2015.01.013
- Pan, J., Wang, J., Zhou, Z., Yan, Y., Zhang, W., Lu, W., et al. (2009). IrrE, a global regulator of extreme radiation resistance in *Deinococcus radiodurans*, enhances salt tolerance in *Escherichia coli* and *Brassica napus*. *PLoS One* 4:e4422. doi: 10.1371/journal.pone.0004422
- Pingli, X. U., Chen, L., Zhou, X., and Daoyi, H. E. (2013). The study of Tobacco transformation with cspB gene from *Bacillus subtilis*. *Acta Laser Biology Sinica.* 22, 343–353. doi: 10.3969/j.issn.1007-7146.2013.04.010
- Piya, S., Liu, J., Burch-Smith, T., Baum, T. J., and Hewezi, T. (2020). A role for Arabidopsis growth-regulating factors 1 and 3 in growth-stress antagonism. *J. Exp. Bot.* 71, 1402–1417. doi: 10.1093/jxb/erz502
- Pukale, D. D., Farrag, M., Gudneppanavar, R., Baumann, H. J., Konopka, M., Shriver, L. P., et al. (2021). Osmoregulatory role of Betaine and Betaine/γ-Aminobutyric acid transporter 1 in post-traumatic Syringomyelia. *ACS Chem. Neurosci.* 12, 3567–3578. doi: 10.1021/acscchemneuro.1c00056
- Quan, R. D., Shang, M., Zhang, H., and Zhao, Z. J. (2004). Engineering of enhanced glycine betaine synthesis improves drought tolerance in maize. *Plant Biotechnol. J.* 2, 477–486. doi: 10.1111/j.1467-7652.2004.00093.x
- Rontein, D., Basset, G., and Hanson, A. D. (2002). Metabolic engineering of osmoprotectant accumulation in plants. *Metab. Eng.* 4, 49–56. doi: 10.1006/mben.2001.0208
- Sadau, S. B., Ahmad, A., Tajo, S. M., Ibrahim, S., Kazeem, B. B., Wei, H., et al. (2021). Overexpression of GhMPK3 from cotton enhances cold, drought, and salt stress in *Arabidopsis*. *Agronomy* 11:1049. doi: 10.3390/agronomy11061049
- Schmid, B., Klumpp, J., Raimann, E., Loessner, M. J., Stephan, R., and Tasara, T. (2009). Role of cold shock proteins in growth of listeria monocytogenes under cold and osmotic stress conditions. *Appl. Environ. Microbiol.* 75, 1621–1627. doi: 10.1128/AEM.02154-08
- Shaban, M., Miao, Y., Ullah, A., Khan, A. Q., Menghwar, H., Khan, A. H., et al. (2018). Physiological and molecular mechanism of defense in cotton against *Verticillium dahliae*. *Plant Physiol. Biochem.* 125, 193–204. doi: 10.1016/j.plaphy.2018.02.011
- Weinberg, M. V., Schut, G. J., Brehm, S., Datta, S., and Adams, M. W. W. (2004). Cold shock of a Hyperthermophilic Archaeon: *Pyrococcus furiosus* exhibits multiple responses to a suboptimal growth temperature with a key role for membrane-bound glycoproteins. *J. Bacteriol.* 187, 336–348. doi: 10.1128/jb.187.1.336-348.2005
- Wyrzykowska, J., Pien, S., Shen, W. H., and Fleming, A. J. (2002). Manipulation of leaf shape by modulation of cell division. *Development* 129, 957–964. doi: 10.1242/dev.129.4.957
- Xia, W., Liu, X., Xin, H., Wu, X., Liu, R., Li, J., et al. (2021). *Saussurea involucreata* PIP2;7 Improves Photosynthesis and Drought Resistance by Decreasing the Stomatal

Density and increasing intracellular osmotic pressure. *Environmental and Experimental Botany*.

Yamanaka, K., Fang, L., and Inouye, M. (1998). The CspA family in *Escherichia coli*: multiple gene duplication for stress adaptation. *Mol. Microbiol.* 27, 247–255. doi: 10.1046/j.1365-2958.1998.00683.x

Yamanaka, K., and Inouye, M. (1997). Growth-phase-dependent expression of CspD, encoding a member of the CspA family in *Escherichia coli*. *J. Bacteriol.* 179, 5126–5130. doi: 10.1128/jb.179.16.5126-5130.1997

Yamanaka, K., Mitani, T., Ogura, T., Niki, H., and Hiraga, S. (1994). Cloning, sequencing, and characterization of multicopy suppressors of a mukB mutation in *Escherichia coli*. *Mol. Microbiol.* 13, 301–312. doi: 10.1111/j.1365-2958.1994.tb00424.x

Yang, H. Q., and Gao, H. J. (2007). Physiological function of arginine and its metabolites in plants, Zhiwu Shengli yu Fenzi Shengwuxue Xuebao. *J. Physiol. Mol. Biol. Plants* 33, 1–8. doi: 10.1360/aps07042

Yu, T. F., Xu, Z. S., Guo, J. K., Wang, Y. X., Abernathy, B., Fu, J. D., et al. (2017). Improved drought tolerance in wheat plants overexpressing a synthetic bacterial cold shock protein gene ScCspA. *Sci. Rep.* 7. doi: 10.1038/srep44050

Yuan, M., Chen, M., Zhang, W., Lu, W., Wang, J., Yang, M., et al. (2012). Genome sequence and Transcriptome analysis of the Radioresistant bacterium *Deinococcus gobiensis*: insights into the extreme environmental adaptations. *PLoS One* 7:e34458. doi: 10.1371/journal.pone.0034458

Yuan, M., Wei, Z., Dai, S., Jing, W., Wang, Y., Tao, T., et al. (2009). *Deinococcus gobiensis* sp nov., an extremely radiation-resistant bacterium. *Int. J. Syst. Evol. Microbiol.* 59, 1513–1517. doi: 10.1099/ijss.0.004523-0

Zhang, H., Dong, H., Li, W., Sun, Y., Chen, S., and Kong, X. (2009). Increased glycine betaine synthesis and salinity tolerance in AhCMO transgenic cotton lines. *Mol. Breed.* 23, 289–298. doi: 10.1007/s11032-008-9233-z

Zhang, J. H., Huang, W. D., Liu, Y. P., and Pan, Q. H. (2005). Effects of temperature acclimation pretreatment on the ultrastructure of mesophyll cells in young grape plants (*Vitis vinifera* L. cv. Jingxiu) Under cross-temperature stresses. *J. Integr. Plant Biol.* 47, 959–970. doi: 10.1111/j.1744-7909.2005.00109.x

Zhang, H., Mao, L., Xin, M., Xing, H., Zhang, Y., Wu, J., et al. (2022). Overexpression of GhABF3 increases cotton (*Gossypium hirsutum* L.) tolerance to salt and drought. *BMC Plant Biol.* 22:313. doi: 10.1186/s12870-022-03705-7

Zhang, D. Y., Yang, H. L., Li, X. S., Li, H. Y., and Wang, Y. C. (2014). Overexpression of *Tamarix albiflora* TaMnSOD increases drought tolerance in transgenic cotton. *Mol. Breed.* 34, 1–11. doi: 10.1007/s11032-014-0015-5

Zhang, L., Zhang, G., Wang, Y., Zhou, Z., Meng, Y., and Chen, B. (2013). Effect of soil salinity on physiological characteristics of functional leaves of cotton plants. *J. Plant Res.* 126, 293–304. doi: 10.1007/s10265-012-0533-3

Zhu, J. K. (2001). Plant salt tolerance. *Trends Plant Sci.* 6, 66–71. doi: 10.1016/S1360-1385(00)01838-0





## OPEN ACCESS

EDITED BY  
Ibrahim Al-Ashkar,  
Al-Azhar University, Egypt

REVIEWED BY  
Hayssam M. Ali,  
King Saud University, Saudi Arabia  
Zongliang Xia,  
Henan Agricultural University, China

\*CORRESPONDENCE  
Shuyan Guan  
guanshuyan@jlu.edu.cn  
Yiyong Ma  
m18404319202\_1@126.com

SPECIALTY SECTION  
This article was submitted to  
Plant Abiotic Stress,  
a section of the journal  
Frontiers in Plant Science

RECEIVED 21 July 2022  
ACCEPTED 26 September 2022  
PUBLISHED 13 October 2022

CITATION  
Jiao P, Wei X, Jiang Z, Liu S, Guan S  
and Ma Y (2022) ZmLBD2 a maize (*Zea mays* L.) lateral organ boundaries domain (LBD) transcription factor enhances drought tolerance in transgenic *Arabidopsis thaliana*.  
*Front. Plant Sci.* 13:1000149.  
doi: 10.3389/fpls.2022.1000149

COPYRIGHT  
© 2022 Jiao, Wei, Jiang, Liu, Guan and Ma. This is an open-access article distributed under the terms of the Creative Commons Attribution License (CC BY). The use, distribution or reproduction in other forums is permitted, provided the original author(s) and the copyright owner(s) are credited and that the original publication in this journal is cited, in accordance with accepted academic practice. No use, distribution or reproduction is permitted which does not comply with these terms.

# ZmLBD2 a maize (*Zea mays* L.) lateral organ boundaries domain (LBD) transcription factor enhances drought tolerance in transgenic *Arabidopsis thaliana*

Peng Jiao<sup>1,2</sup>, Xiaotong Wei<sup>2,3</sup>, Zhenzhong Jiang<sup>1,2</sup>, Siyan Liu<sup>2,3</sup>, Shuyan Guan<sup>2,3\*</sup> and Yiyong Ma<sup>2,3\*</sup>

<sup>1</sup>College of Life Sciences, Jilin Agricultural University, Changchun, China, <sup>2</sup>Joint International Research Laboratory of Modern Agricultural Technology, Ministry of Education, Changchun, China, <sup>3</sup>College of Agronomy, Jilin Agricultural University, Changchun, China

Maize (*Zea mays* L.) is an annual gramineous herb and is among the world's most important crop species. Drought is the main factor contributing to maize yield reduction. The lateral organ boundaries domain (LBD) proteins belong to a class of higher-plant-specific transcription factors. LBD proteins usually include the highly conserved lateral organ boundaries (LOB) domains that play essential roles in plant growth and response to biotic stresses. However, few studies have addressed the biological functions of LBD genes associated with maize response to drought. Here we cloned the *ZmLBD2* gene from maize and described its role in combating drought. Investigating *ZmLBD2* subcellular localization, we show that it localizes to the cell nucleus and can specifically bind with inverted repeats of "GCGGCG". Under drought stress, *Arabidopsis thaliana* overexpressing *ZmLBD2* performed better than the wild-type plants in terms of seed germination rates, root length, relative water content, fresh weight, chlorophyll content, proline content, and antioxidant enzyme content. *Arabidopsis* overexpressing *ZmLBD2* contained less MDA, H<sub>2</sub>O<sub>2</sub>, and O<sub>2</sub><sup>-</sup> than the wild-type plants. Our protein-protein interaction results indicate an interaction between the *ZmLBD2* and *ZmIAA5* genes. In conclusion, the *ZmLBD2* gene positively regulates H<sub>2</sub>O<sub>2</sub> homeostasis in plants, strengthening drought resistance.

## KEYWORDS

lateral organ boundaries domain, LBD2, transcription factor, drought tolerance, maize

## Introduction

Maize (*Zea mays* L.) is the world's number one food crop, with strong adaptability and wide cultivation areas across the globe. Drought stress is one of the common factors reducing crop yield. Agricultural economic losses increase year on year as drought rages worldwide. In recent years, a series of genes crucial to combat drought stress has been described in plants (Sahebi et al., 2018; Liu et al., 2020; Wei et al., 2021; Chen et al., 2021; Wang B. et al., 2022). Reactive oxygen species (ROS), mainly including superoxide anion radicals ( $O_2^-$ ), hydroxyl ions ( $OH^-$ ), hydroxyl radicals ( $\cdot OH$ ), and hydrogen peroxide ( $H_2O_2$ ), accumulate under drought stress and work in various ways to influence the growth of plants and their responses to environmental stresses (Wang et al., 2018; Xiong et al., 2022). Yuan et al. (2019) found that the overexpression of the *NAC066* gene could significantly enhance the tolerance of rice (*Oryza sativa* L.) against drought and oxidative stress by reducing the accumulation of ROS. Hu et al. (2020) reported that TaCDPK13 could be considered the upstream regulatory factor of TaNOX7 to regulate the generation of ROS in wheat (*Triticum aestivum* L.). Xiong et al. (2018) reported that the natural mutation of the *OsLG3* gene strengthened the resistance of rice against drought by inducing the removal of ROS.

The lateral organ boundaries domain (LBD) proteins belong to a class of plant-specific transcription factors, including the conserved lateral organ boundaries (LOB) domain. This domain consists of the highly conserved C motif (C-block), Gly-Ala-Ser motif (GAS-block), and leucine zipper-like motif (leucine zipper-like block). Most LBD family members attribute to the class I, which is mainly responsible for several biological reactions in higher plants, such as growth and responses to adversities (drought, salt, cold, etc.). There are still many unanswered questions about the LBD gene. For example, does the LBD gene function in other species of plants, and what function(s) does it play? Xiong et al. (2022) found that the *ZmLBD5* of maize could increase the tolerance of *Arabidopsis thaliana* against drought by inhibiting the accumulation of ROS. Liu et al. (2020) discovered that the knockout of the *SLBD40* gene could promote the drought tolerance of tomatoes (*Solanum lycopersicum* L.). Liu et al. (2019) illustrated that the overexpression of *StLBD2-6* and *StLBD3-5* genes might help maintain a normal metabolism for potato (*Solanum tuberosum* L.) to improve its ability to resist drought. Research published by Guo et al. (2020) stated that drought stress induced the ABA (abscisic acid) signal to promote the expression of the *LBD15* gene in *A. thaliana*, which enhanced its tolerance against water stress. Ariel et al. (2010) found that overexpression of *Mt LBD1* could control the structure of *Medicago truncatula* roots under salt stress. Wang Z. et al. (2021) found that the lateral organ boundaries domain (LBD) genes, a plant-specific transcription factor family, play crucial roles in controlling plant architecture

and stress tolerance. Wang J. et al. (2021) found that *RrLBD12c*, *RrLBD25*, *RrLBD39*, and *RrLBD40* of *Rosa* may be potential regulators of salt stress signaling. Ba et al. (2016) reported that *MaLBD5* and *MaJAZ1* might act antagonistically concerning MeJA-induced cold tolerance of banana fruit.

In previous studies, 44 LBD transcription factors have been identified in the maize genome (Zhang et al., 2014). However, only the *ZmLBD5* gene (Zm00001d032286) has been functionally verified regarding the response to drought. The functions of other *ZmLBD* genes remain unclear. In this study, we analyzed how the *ZmLBD2* gene responded to drought. The overexpression of *ZmLBD2* in the transgenic *A. thaliana* could improve its drought tolerance by reducing the accumulation of ROS. Our results show that *ZmLBD2* can mediate the response of maize seedlings to drought by regulating the homeostasis of hydrogen peroxide, which may positively affect plants' drought tolerance.

## Materials and methods

### Plant materials and growth conditions

The wild-type (ecotype: Col-0) and transgenic *A. thaliana* (OE2 and OE3) seeds were disinfected with 75% alcohol for 1 min. After surface sterilization with 1%  $NaClO_3$  for 10 min, they were washed four times with sterile water. Following the disinfection treatment, all seeds were cultivated in 1/2 Murashige and Skoog (MS) media at 4°C in the dark for 3 days. Next, the culture media were moved to a plant incubator (at 22°C with a 16 h light/8 h dark cycle) for the seeds to grow. Two weeks later, the seedlings were transplanted into the soil and grown in a phytotron (at 22°C with a 16 h light/8 h dark cycle). They were treated with 8% PEG6000 (polyethylene glycol 6000) at the three-leaf stage, and the physiological data were measured. We collected their leaves at 0, 6, 12, 24, and 48 h and froze them in liquid nitrogen immediately after the collection to extract their RNA.

### Gene isolation and sequence analysis

The maize *LBD2* gene was obtained from MaizeGDB (<https://www.maizegdb.org/>) (accessed on 2 June 2022). Homologous sequences of *ZmLBD2* were retrieved from the Phytozome database (<https://phytozome-next.jgi.doe.gov/>) (accessed on 2 June 2022). Amino and multiple sequence alignments were constructed with ClustalX. Our laboratory completed the transcriptome data of maize under different drought treatment times, and the transcriptome data has been uploaded to the NCBI (National Center for Biotechnology Information) database (PRJNA793522).

## The subcellular localization of ZmLBD2

To explore the possible subcellular location of ZmLBD2, the full-length gene coding region of ZmLBD2 was obtained from the TA cloning vector containing the *ZmLBD2* gene fragment. The amplified product was then fused to the CaMV35S promoter and inserted upstream of the coding region of the pCambia1302-eGFP subcellular localization vector. The constructed vector pCambia1302-ZmLBD2-eGFP was introduced into tobacco leaves using agrobacterium-mediated methods. The leaves were then examined at 45 h after infiltration using an Olympus confocal laser scanning microscope (DAPY Olympus, Tokyo, Japan). The primers used here are listed in [Supplementary Table S1](#).

## Induced expression of ZmLBD2 protein and detection by Western blotting

Full-length cDNA of ZmLBD2 was amplified and inserted into a pET28a vector driven by a Cauliflower Mosaic Virus 35S (CaMV35S) promoter. The constructed vector pET28a-ZmLBD2-His was transformed into BL21 *E. coli* competent cells. Then, the protein expression of the positive recombinant plasmid was performed under isopropyl  $\beta$ -D-thiogalactoside (IPTG) induction conditions, and finally, the protein content was detected by SDS-PAGE (polyacrylamide gel electrophoresis) electrophoresis and Western blotting.

## Analysis of DNA binding characteristics of ZmLBD2

First, the cDNA of the target gene (*ZmLBD2*) was constructed on the pGADT7 empty vector to form the recombinant vector pGAD-ZmLBD2. Three tandem repeats of GCGGCG were synthesized by artificial synthesis to construct the yeast monohybrid reporter vector pHIS2-TCS. To verify the specificity of ZmLBD2 for this target recognition, we synthesized three tandem repeated mutant targets, GAGGAG. *EcoR* I and *Sac* I restriction sites was added at both ends to construct the yeast monohybrid reporter vector pHIS2-mTCS. Finally, the binding site of the *ZmLBD2* gene was verified by yeast one-hybrid (the yeast one-hybrid strain used in this study was Y187).

## Analysis of the drought resistance of the *ZmLBD2* gene in yeast

We designed the yeast plasmid vectors pYES2-ZmLBD2 and transformed them into competent INVSc1 yeast strains by the yeast transformation method. We cultivated the transformed

strain in YPD (Yeast Extract Peptone Dextrose) liquid media. When the OD<sub>600</sub> (optical density 600) concentration reached 0.8 after shake culture, we collected the strain bodies by centrifugation and dissolved them with physiological saline. After diluting the solution into six gradients, we added 5  $\mu$ L of each gradient into YPD culture media with and without mannitol.

## RNA extraction and quantitative RT-qPCR analysis

TRIzol reagent (TAKARA BIO INC. Dalian, China) was used to extract total RNA from the maize (maize inbred lines H8186) treated under different stresses and from the *A. thaliana* seedlings. After being identified, the RNA was used to generate cDNA with TaKaRa reverse transcription kit. And SYBR GreenFastqPCRMix kit (ABclonal Biotechnology Co., Ltd, RM21203) was used for qPCR amplification. The reaction procedure was as follows: denaturation at 95°C for 10 min, followed by 40 cycles of denaturation at 95°C for 10s, at 55°C for the 40s, at 72°C for 20s, and 72°C for 4 min. Zm18S and AtACTIN8 were selected as the internal reference genes for maize and *A. thaliana*, respectively. The  $2^{-\Delta\Delta CT}$  method was used to analyze the relative expression levels of relevant genes (Jiao et al., 2022; Wang C. et al., 2022). All primers used in this study are listed in [Supplementary Table S1](#).

## The genetic transformation of *A. thaliana* and phenotypic analysis

In this study, we constructed the plant overexpression vectors pCambia3301-ZmLBD2-bar and transformed the recombinant plasmids into *Agrobacterium tumefaciens* strain GV3101; and then we infected *A. thaliana* with the strain by floral dip method (Noman et al., 2019). We cultivated the *A. thaliana* in 1/2 Murashige and Skoog (MS) media, screened out the transgenic plants of T0 generation and collected their leaves for PCR and test strip assay. Our research used the seeds of representative homozygous *A. thaliana* OE2 and OE3 of T3 generation (Transgenic generation 3).

To examine the responses of the transgenic and wild *A. thaliana* to drought, we disinfected both the seeds of the wild type and the transgenic one with the *ZmLBD2* gene (OE2 and OE3) with 75% alcohol for 1 min. After conducting surface sterilization with 1% NaClO<sub>3</sub> for 10 min, we washed the seeds four times with sterile water. We cultivated the seeds in 1/2MS media and performed drought experiments by adding 200 and 300 mM mannitol. After cultivation at 4°C for 3 days, they were moved to another environment and grew at 24°C and 80% relative humidity with a 16 h light/8 h dark cycle for 5 days.

Then, we determined their germination rates and root length. The main root length was measured using the DJ-GXG02 root image analysis system (DianJiang Technology; <http://www.dianjiangtech.com/>). Each sample contains three biological replicates. One-way ANOVA method was used for statistical analysis. To identify the survival rates, we transplanted the *A. thaliana* seedlings, which sprouted in the 1/2MS media into the soil, and cultivated them at 22°C and 50% relative humidity with a 16 h light/8 h dark cycle for 3 weeks. After that, we stopped watering them for 14 days and took some pictures. Fourteen days later, we re-watered them for 3 days and calculated their survival rates (Ju et al., 2020).

### Tetranitroblue tetrazolium chloride (NBT) staining, diaminobenzidine (DAB) staining, and oxidative stress analyses

Tetranitroblue tetrazolium chloride (NBT) and diaminobenzidine (DAB) were used to stain the seedling leaves of the wild-type and transgenic *A. thaliana* (OE2 and OE3) after drought treatment to examine the accumulation of superoxide anion ( $O_2^-$ ) and Hydrogen peroxide ( $H_2O_2$ ) (Zhao J. Y. et al., 2020). The spectrophotography was used to test the activity of catalase (CAT), superoxide dismutase (SOD), malondialdehyde (MDA), and peroxidase (POD) (Zhao Q. et al., 2020; Ju et al., 2020; Liu et al., 2021; Li et al., 2021). The weighing method was used to determine relative water content (Sapes and Sala, 2021). The methods mentioned above were used to evaluate the concentration of hydrogen peroxide and the amount of  $O_2^-$ .

### Yeast two-hybrid system

The CDS of the *ZmLBD2* gene was cloned into the c-terminus of the GAL4 DNA-binding domain of the pGBKT7 vector. We used the recombinant plasmid *ZmLBD2*-BD as a decoy to search for every potential interaction between the encoded proteins on the STRING database (<https://string-db.org/>), and we cloned the CDS of interactive candidate gene *ZmIAA5* into the pGADT7 vector. The recombinant plasmids *ZmLBD2*-BD and *ZmIAA5*-AD were then transformed into yeast cells AH109 using the lithium acetate method (Xu et al., 2007). The transformation efficiency was examined on DDO culture medium SD (synthetic-defined)/-Trp/-Leu, and the protein-protein interaction was verified on QDO medium SD/-Leu/-Trp/-His/-Ade. pGADT7-T and pGBKT7-53 were used as positive controls, and pGADT7-T and pGBKT7-lam were used as negative controls. The yeast transformation procedure was completed concerning the yeast transformation system produced by Beijing Kulaibo Technology Co., Ltd.

### Bimolecular fluorescence complementation

The ORFs (Open Reading Frames) of *ZmLBD2* and *ZmIAA5* were cloned to the n-terminus and c-terminus of the coding regions of yellow fluorescent proteins (YFP) to construct plasmids nYFP-*ZmLBD2* and cYFP-*ZmIAA5*. Five microliters of each of the two recombinant plasmids were co-transformed into tobacco mesophyll cells by agroinfiltration (Yu et al., 2021). The leaves were then examined at 45 h after infiltration using an Olympus confocal laser scanning microscope (DAPY Olympus, Tokyo, Japan).

### Pull-down assay

We constructed Flag-*ZmIAA5* and Myc-*ZmLBD2* vectors and purified the fusion proteins by immunoprecipitation using Anti-Flag M1 Affinity Gel. And we purified the Myc-*ZmLBD2* recombinant proteins using amylose resin (Park et al., 1998). Flag or Flag-*ZmIAA5* was added with equal amounts of Myc-*ZmLBD2* protein beads into the buffer (50 mmol/L Tris-HCl, pH 8.0, 100 mmol/L sodium chloride, 0.2% glycerol and 0.5% TritonX-100) and incubated at 4°C for 6 h. The protein complexes were eluted by boiling the beads with electrophoresis loading buffer. Ultimately, the crude extracts and eluted products were determined on 10% SDS-PAGE, and the chemiluminescence signal was detected by Western Blot using Flag-tagged antibodies.

### Statistical analysis

Data were tested by analysis of variance using SPSS software (SPSS USA). The data are the mean  $\pm$  standard deviation (SD) of three biological replicates. The significance was analyzed using Student's t-tests. The \* and \*\* represents  $p < 0.05$  and  $p < 0.01$ , respectively. The figures were prepared with GraphPad Prism 7.

## Results

### Analysis of *ZmLBD2* sequence and expression pattern

In this study, we cloned the *ZmLBD2* gene from maize from the H8186 selfing line. *ZmLBD2* has a full-length CDS of 831bp, which encodes a polypeptide consisting of 244 amino acid residues with a predicted molecular weight of 25.47kD and a pI value of 5.66 (Table 1). The results of sequence alignment show that the *ZmLBD2* contains CX2CX6CX3C, a typical



TABLE 1 The physiochemical characteristics of maize ZmLBD2 proteins.

| Gene name | Gene ID        | CDS length (bp) | Protein length (aa) | MW (KDa) | pI   |
|-----------|----------------|-----------------|---------------------|----------|------|
| ZmLBD2    | Zm00001d027679 | 831             | 244                 | 25.47    | 5.66 |

conserved DNA-binding domain. GAS and leucine zipper-like motifs (LX6LX3LX6L) are primarily used to distinguish the members of the maize LBD family into class I and class II (Figure 1A).

We drew a heatmap (Figure 1B) based on the transcriptome data of maize roots (PRJNA793522) with different drought treatment processing times. The response of ZmLBD2 to drought stress was studied by RT-qPCR using maize plants under 8% PEG6000 drought treatment. The expression of the ZmLBD2 gene was highly induced as the time of suffering

drought stress increased (Figure 1C), indicating that the ZmLBD2 gene plays a crucial role in responding to drought.

### Subcellular localization of ZmLBD2 protein in tobacco

We designed subcellular localization vectors for the ZmLBD2 gene and transformed them into tobacco mesophyll cells via *Agrobacterium tumefaciens*. By confocal microscope

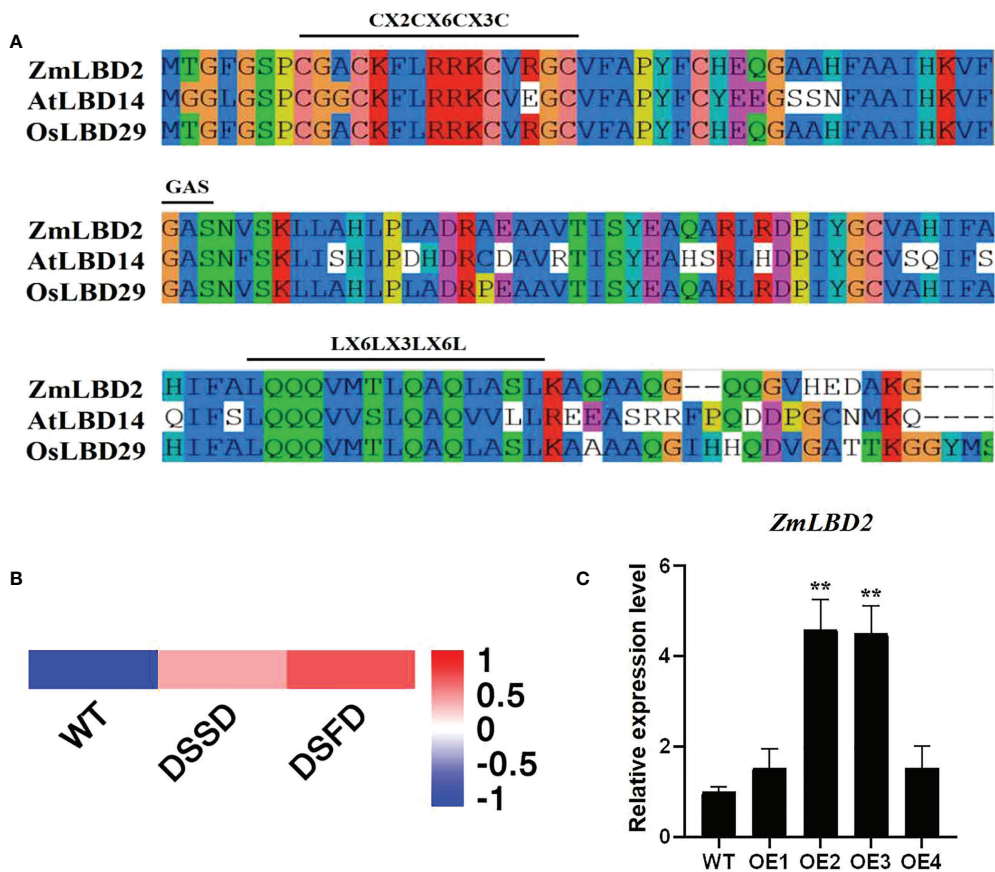


FIGURE 1  
Sequence and expression pattern analysis of ZmLBD2. (A) LOB domain sequence alignment of ZmLBD2 and LBD members from Arabidopsis and *Oryza sativa*. The class-I LBD members had typical CX2CX6CX3C, GAS, and LX6LX3LX6L domains. The alignment was performed using DNAMAN software. (B, C) The expression of ZmLBD2 upon drought treatment in maize. Total RNA was isolated from 3-leaf seedlings grown without (0 h) or with 8% PEG6000 treatment. Transcript levels of ZmLBD2 were determined by qPCR, using Zm18S as reference genes. The \*\* represents  $p < 0.01$ .



(Olympus, Japan), we observed that the proteins transcribed from the *ZmLBD2* gene localized to the cell nucleus (Figure 2).

## Efficient expression of ZmLBD2 in a prokaryotic system

BL21 strain with pET28a-ZmLBD2 recombinant plasmids was selected for single-colony shake cultivation. When the OD<sub>600</sub> concentration of the cultures was between 0.6 and 1.0, IPTG with a final concentration of 0.1 mM was added to induce protein expression. After that, BL21 strain with transformed pET28a-ZmLBD2 recombinant plasmids was obtained. We induced the expression at 26°C for 4 h and observed the changes in protein expression. The SDS-PAGE results showed that a clear band around 25.47 kDa was spotted for the recombinant protein of the ZmLBD2, which indicated that the ZmLBD2 recombinant protein could be expressed stably and effectively in the BL21 strain with the induction of IPTG (Figure 3A). The Western blot results showed that a specific band could be seen clear between 25 kDa and 35 kDa (Figure 3B), indicating that the ZmLBD2 protein of maize was successfully induced and expressed *in vitro*.

## The DNA binding characteristics of ZmLBD2

On the 20 mM 3-AT SD/Trp-/Leu-/His triple deficiency culture plate, only the yeast strains co-transformed with pGADT7-ZmLBD2 and pHIS2-TCS and the positive control p53HIS2+pGAD-Rec2-p53 can grow normally (Figure 4),

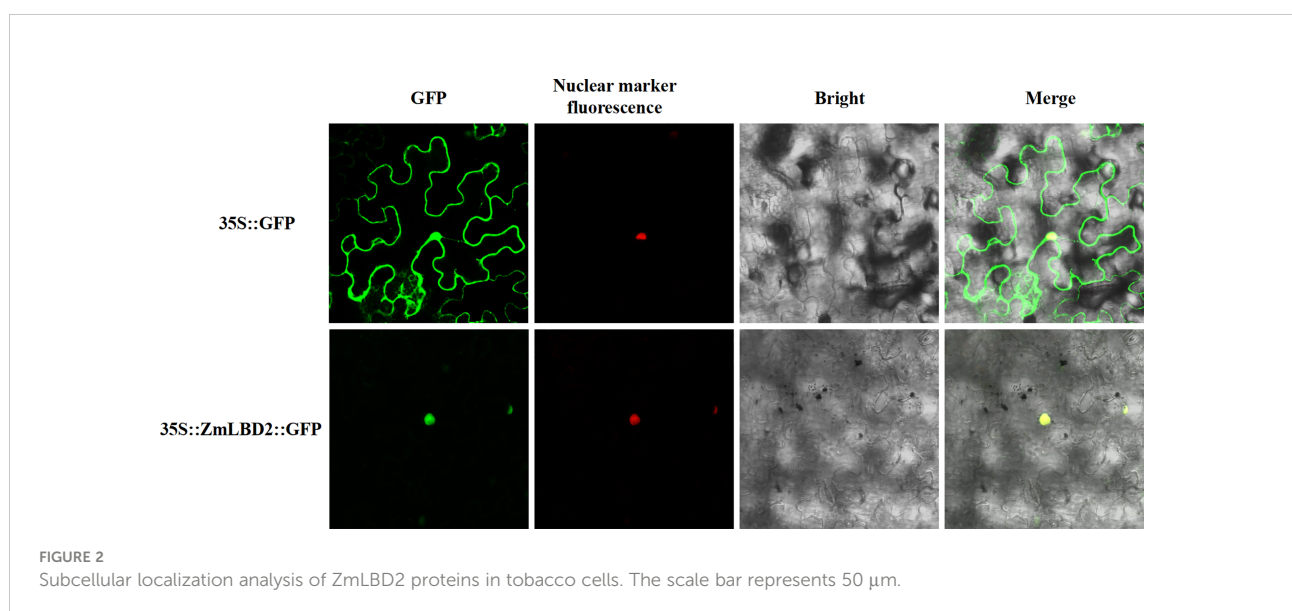
indicating that ZmLBD2 can activate the expression of the reporter gene HIS by binding to the “GCGGCG” inverted repeat sequence. To verify the specificity of the DNA binding method, the pGADT7-ZmLBD2 and pHIS2-mTCS vectors were co-transformed into yeast cells on the SD/Trp-/Leu-/His- triple lack culture plate containing 20 mM 3-AT. Only the positive control could grow normally. The binding of the *ZmLBD2* gene to the “GCGGCG” inverted repeat is specific.

## Dimer-forming ability of ZmLBD2

To test the dimerization ability of ZmLBD2, six truncated peptide fragments (a, b, c, ab, bc, and abc) of ZmLBD2 were tested for interaction with ZmLBD2. Fragments A, B, and C represent the N-terminal CX<sub>2</sub>CX<sub>6</sub>CX<sub>3</sub>C, the GAS and LX<sub>6</sub>LX<sub>3</sub>LX<sub>6</sub>L coiled-coil motifs, and the C-terminal domain, respectively (Figure 5A). To further define the necessary regions for ZmLBD2 interaction, we screened for homo- and heterodimerization by yeast two-hybridization (Figure 5B).

## Identification of the drought tolerance of transgenic yeast with ZmLBD2

We detected no differences between transgenic yeast with pYES2 empty vector and that with *ZmLBD2* gene in regular YPD culture media (Figure 6). But, in the YPD culture media containing 1M of mannitol, the transgenic yeast with ZmLBD2 grew better than that the pYES2 empty vector. This tentatively indicates that the *ZmLBD2* gene has the power to resist drought.



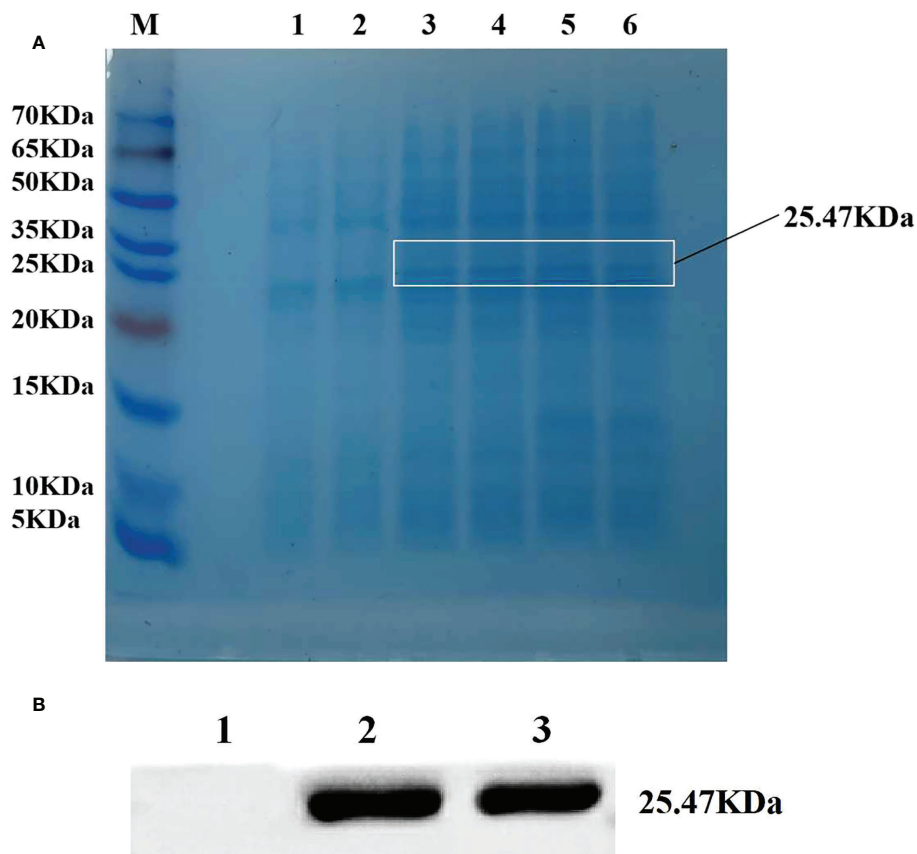


FIGURE 3

Efficient expression of ZmLBD2 in a prokaryotic system. (A) SDS-PAGE electrophoretic analysis of ZmLBD2 recombinant protein. M: Protein marker; 1: pET22b empty vector was not induced by IPTG; 2: pET22b-ZmLBD2 non-induced bacteria; 3-6: pET22b-ZmLBD2 was produced by IPTG for 4 h. (B) Western blotting detection of ZmLBD2 protein; 1: pET22b empty vector; 2-3: pET22b-ZmLBD2 after inducing.

## Genetic transformation and molecular identification of the *ZmLBD2* gene in *A. thaliana*

In this study, we transformed the plasmid DNA of constructed plant overexpression vector pCAMBIA3301-ZmLBD2-bar (Figure 7A) into the EHA105 chemically competent cells and finally, obtained four transgenic positive *A. thaliana* plants of T3 generation by using floral dip method (Figures 7B-D). By qRT-PCR, we found that the *ZmLBD2* gene was expressed in all transgenic plants, but a higher expression was observed in OE2 and OE3 (Figure 7E). In conclusion, the transgenic plants OE2 and OE3 could be used to further identify the ability of ZmLBD2 to combat drought.

## Overexpression of ZmLBD2 enhanced drought tolerance in transgenic *A. thaliana*

To investigate its biological function, we generated ZmLBD2 overexpressing *A. thaliana*. The seeds of the transgenic plants

OE2 and OE3 of T3 generation were cultivated in 1/2 MS media with 0, 200, or 300 mM of mannitol. After cultivation for 5 days, the results of comparing their germination status showed no differences between the wild type and the transgenic *A. thaliana* in the 1/2 MS media with 0 mannitol in terms of germination. As the concentration of mannitol increased, however, the OE2 and OE3 grew better than the wild type did (Figure 8A). Moreover, the germination rates (Figure 8B) and fresh weight (Figure 8C) and root length (Figure 8D) of the OE2 and OE3 were much higher than that of the wild type as the concentration of mannitol increased.

To further study the functions of ZmLBD2 in response to drought stress, we transplanted the 5-day-old cultivated plants into the soil. Then, we conducted drought treatment on 30-day-old *A. thaliana* for 10 days. After re-watering for 5 days, we found that the OE2 and OE3 performed much better than the wild type in terms of survival rates (Figures 9A, B), fresh weight (Figure 9C), relative water content (Figure 9D), chlorophyll content (Figures 9E, F), and proline content (Figure 9G). OE2 and OE3 also had less MDA than the wild-type plants

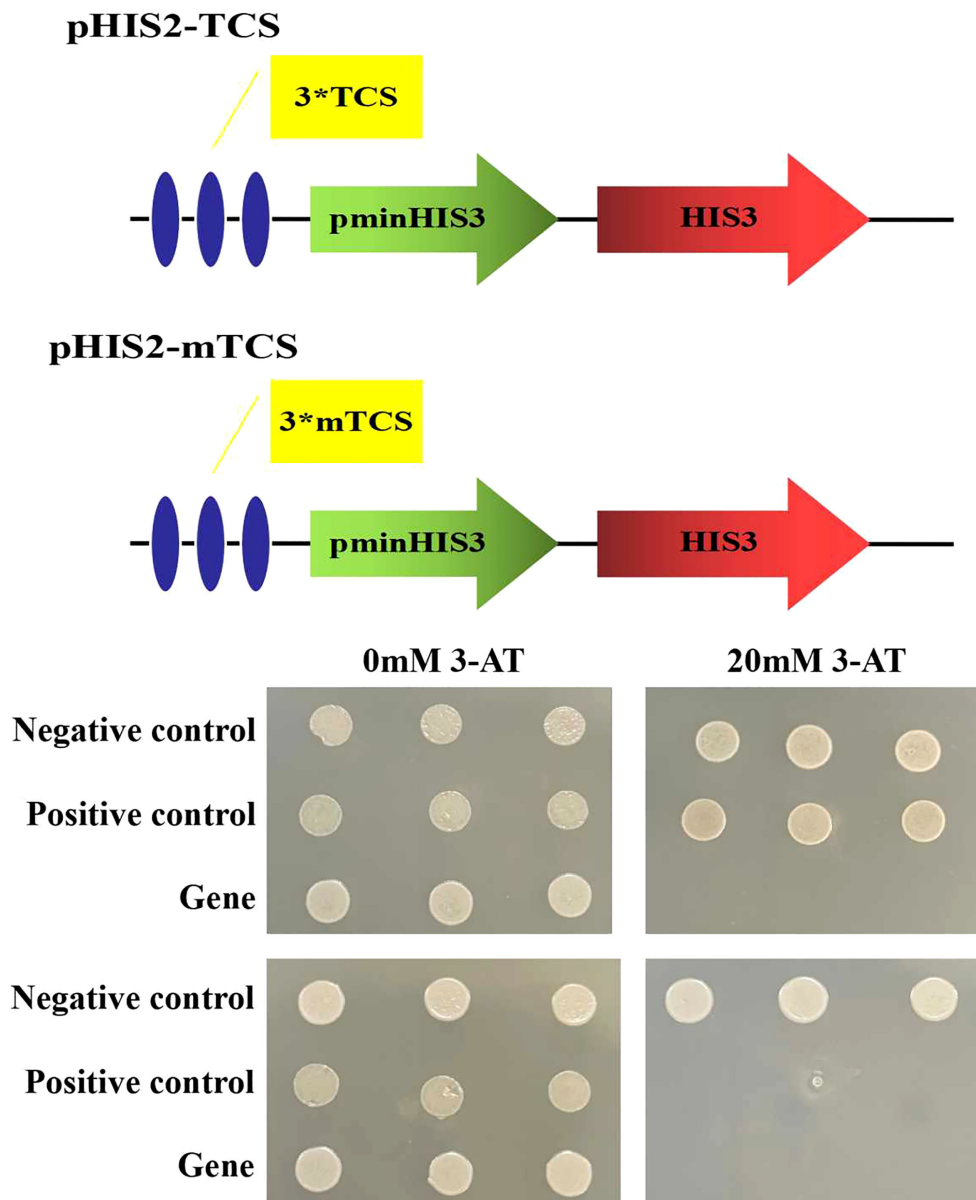


FIGURE 4

DNA-binding assays of ZmLBD2 in Y1HGold yeast cells. Yeast cells were assayed on SD/Trp-/Leu-/His- medium; Negative control: p53HIS2+pGAD-ZmLBD2; Positive control: p53HIS2+pGAD-Rec2-53p53; Gene: different positive colonies; TCS: GCGGCG; mTCS: GAGGAG; 3\*: The sequence was repeated three times; 3-AT: 3-amino-1,2,4-triazole.

(Figure 9H). These results indicate that the overexpression of ZmLBD2 can significantly boost the drought resistance of *A. thaliana*.

### Reducing the accumulation of reactive oxygen species by the overexpression of the *ZmLBD2* gene under drought stress

Reactive oxygen species (ROS) are essential signaling molecules for plant growth, which play a crucial role in adapting to

environments. Therefore, we analyzed the ROS levels of wild and transgenic plants by evaluating the accumulated amount of hydrogen peroxide and superoxide under drought stress. After staining with Nitroterazolium Blue chloride (NBT) and Diaminobenzidine (DAB), we found that the accumulation of hydrogen peroxide and superoxide of the wild type was more than that of the OE2 and OE3 (Figures 10A, B). Meanwhile, we compared the accumulation and production of hydrogen peroxide and  $O_2^{2-}$  in the leaves of the wide type OE2 and OE3 maize seedlings. Hydrogen peroxide and superoxide anion accumulated

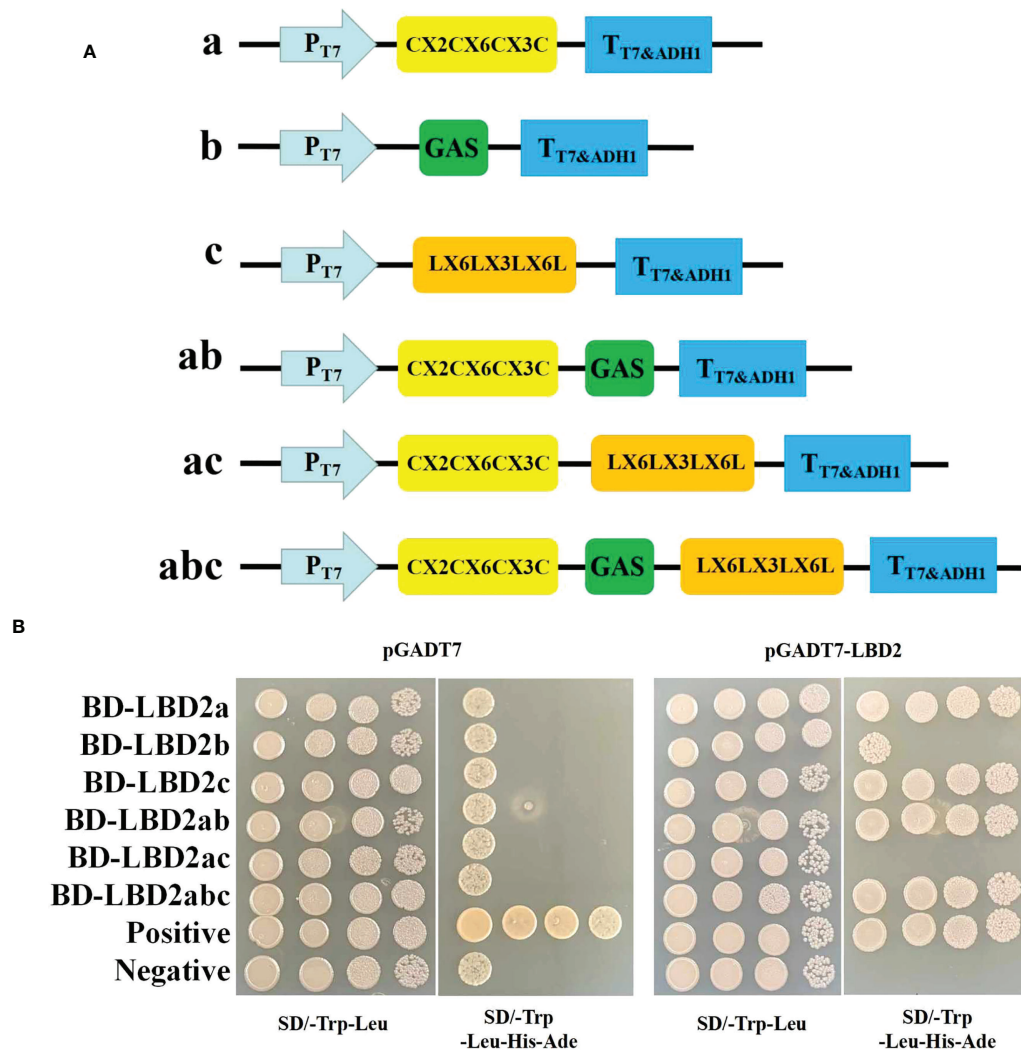


**FIGURE 5**  
Analysis of the dimer-forming ability of ZmLBD2. **(A)** Strategy for yeast two-hybrid vector construction of the maize ZmLBD2 sequence. **(B)** The ability of ZmLBD2 to form dimers in the yeast strain Y2H Gold. The Y2H Gold strains containing target plasmids were diluted and cultured on SD/-Trp-Leu media or SD/-Trp-Leu-His-Ade media. Fragments a, b, and c represent CX2CX6CX3C, GAS, and LX6LX3LX6L.

less in the leaves of seedlings with the overexpression of ZmLBD2 than in wild-type seedlings (Figures 10C, D). SOD, CAT, and POD enzymes directly eliminate ROS to regulate ROS levels in plant cells. They turn the ROS into less active and less toxic hazardous substances. We found that, with the threat of drought, SOD, CAT, and POD enzymes were more active in the *A. thaliana* with the overexpression of ZmLBD2 than those in the wild type (Figures 10E–G).

### The effects of ZmLBD2 on the expression of drought-stress-responsive genes

To investigate the molecular mechanism of ZmLBD2 regulation under drought conditions, we performed a quantitative expression analysis of six stress-related genes in transgenic Arabidopsis and wild-type plants. Under normal growth

conditions, the transcript expression levels of P5CS1, RD29A, COR15A, NCED3, DREB2A, and ABI4 were not significantly different between wild-type control and overexpressing lines. However, under drought conditions, the expression of these genes was rapidly induced and at higher levels, and the expression levels of these genes in ZmLBD2-overexpressing seedlings were lower than in wild-type controls (Figure 11). Therefore, ZmLBD2 may positively regulate the expression of drought stress-related genes in plants under drought stress.

### ZmIAA5, a candidate ZmLBD2 interacting gene

To study how the ZmLBD2 gene influences the drought resistance of the transgenic *A. thaliana*, we screened a cDNA

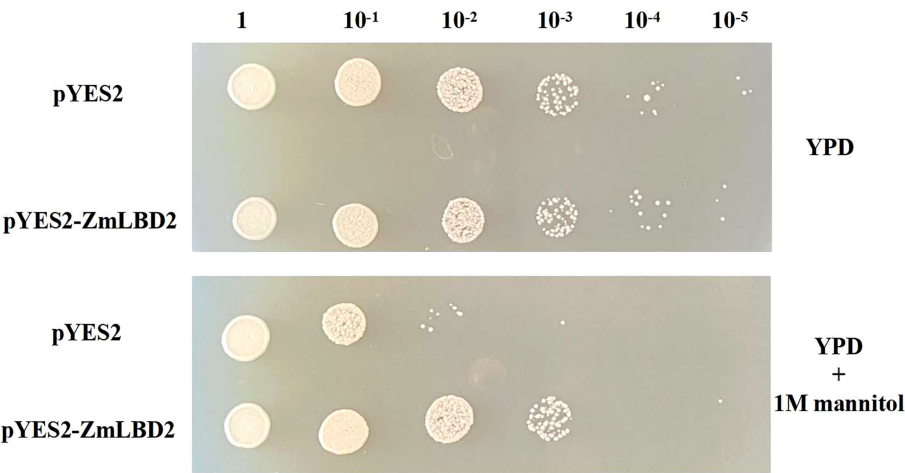


FIGURE 6  
Phenotypic analysis of ZmLBD2 transgenic yeast strains under mannitol stress.

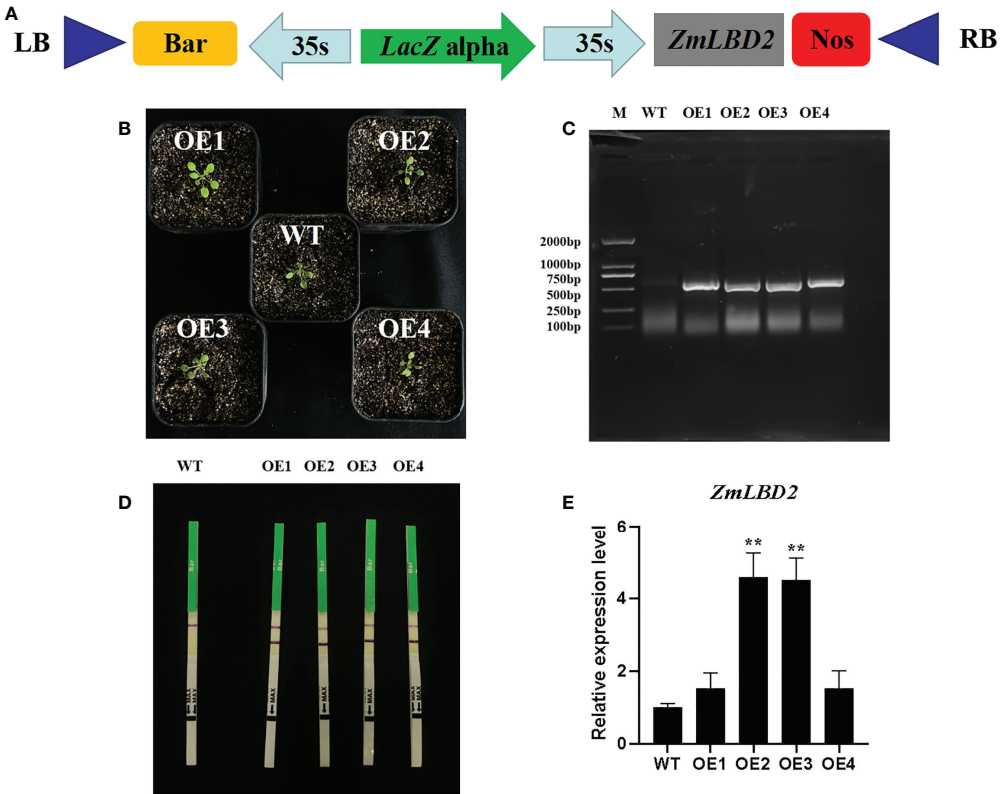


FIGURE 7  
Identification of Arabidopsis overexpressing the *ZmLBD2* gene. **(A)** Schematic of expression vectors pCAMBIA3301-*ZmLBD2*-*Bar*. **(B)** Transgenic Arabidopsis lines. **(C)** The PCR detection of the *Bar* gene in leaves of wild type (WT) and transgenic lines. **(D)** Rapid test strip analysis of the *Bar* gene in wild-type (WT) leaves and transgenic lines. **(E)** qRT-PCR analysis of the *ZmLBD2* gene in leaves of wild type (WT) and transgenic lines. The expression level was normalized to that of Arabidopsis *AtACTIN8*. Data were expressed as the mean of triplicate values, and error represented the SD. The \* and \*\* represents  $p < 0.05$  and  $p < 0.01$ , respectively.



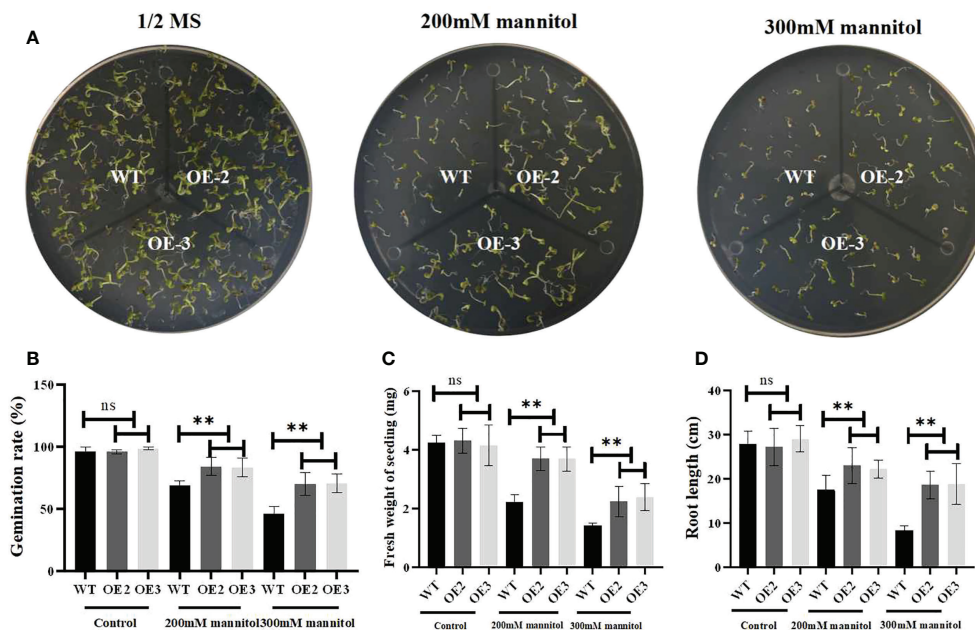


FIGURE 8

Drought stress responses of ZmLBD2-overexpressing transgenic Arabidopsis and wild-type plants. (A) Seedling growth by wild-type and ZmLBD2-overexpressing transgenic Arabidopsis plants under treatment with 0, 200, and 300 mM of mannitol for 5 days. (B) Statistical analysis of ZmLBD2-overexpressing transgenic lines and wild-type seed germination rates under 0, 200, and 300 mM mannitol, respectively. (C) Statistical analysis of ZmLBD2-overexpressing transgenic lines' and wild-type's fresh weight under 0, 200, and 300 mM mannitol, respectively. (D) Statistical analysis of ZmLBD2-overexpressing transgenic lines' and wild-type's root length under 0, 200, and 300 mM mannitol, respectively. Data were expressed as the mean of triplicate values, and error represented the SD. The \*\* represents  $p < 0.01$ , respectively. Non-significant (ns).

library for maize in a yeast two-hybrid system (with ZmLBD2 as a decoy) and identified an interactive candidate gene ZmIAA5 (Zm00001d043878). Figure 12A shows that all yeast grew normally in DDD culture media (SD/-Trp/-Leu), whereas only that with the coexpression of AD-ZmIAA5 and BD-ZmLBD2 grew well in QDO selective media (SD/-Trp/-Leu/-His/-Ade). We also conducted a BiFC assay to corroborate the interaction between ZmLBD2 and ZmIAA5. When nYFP-ZmLBD2 and cYFP-ZmIAA5 were coexpressed, we detected the fluorescence from yellow fluorescent proteins (YFP) in the nuclei of tobacco mesophyll cells. However, no fluorescence was detected in terms of the coexpression of nYFP-ZmLBD2 and cYFP, or nYFP and cYFP-ZmIAA5 (Figure 12B). Pull-down assay was performed to test the purified recombinants Myc-ZmLBD2 and Flag-ZmIAA5 *in vitro*. The Myc-ZmLBD2 protein interacted with Flag-ZmIAA5 protein, but it did not bind to Myc (Figure 12C). These results indicate a direct gene interaction between ZmLBD2 and ZmIAA5.

## Discussion

LBD genes are specific plant transcription factors. They are divided into class I and class II following the differences in the

LOB domain. LBD transcription factors from the class I contain the complete LOB domain, and they are mainly responsible for plant growth, such as developing lateral organs, extending leaves, and regeneration (Bell et al., 2012; Liu et al., 2018; Zhang et al., 2020; Huang et al., 2020). Class II LBD proteins hold an incomplete leucine zipper-like domain, so they cannot form the coiled-coil structure. They are primarily responsible for secondary metabolite production in plants, such as the synthesis of anthocyanidin and the growth of roots. They also play an active role in responding to pathogenesis, osmotic stress, salt stress, and drought stress (Lim et al., 2015; Liu et al., 2016; Zhang et al., 2017; Fernando Gil et al., 2018; Liu et al., 2019; Liu et al., 2020; Guo et al., 2020). Our study found that the ZmLBD2 gene was significantly induced to express under drought.

The growth of plants is not only regulated by internal hormones and transcription factors but also influenced by external environments. When the living environment changes or hazardous factors occur, plants need to respond to the environmental signals from the outside to better adapt to the environment. Liu et al. (2020) reported that the *SILBD40* gene in tomato (*Solanum lycopersicum* L.) was overexpressed under drought stress, which caused the plant to wither. In addition, the expression of this gene was affected by the signal transmission pathway of jasmonic acid. Huang et al. (2020) found that most

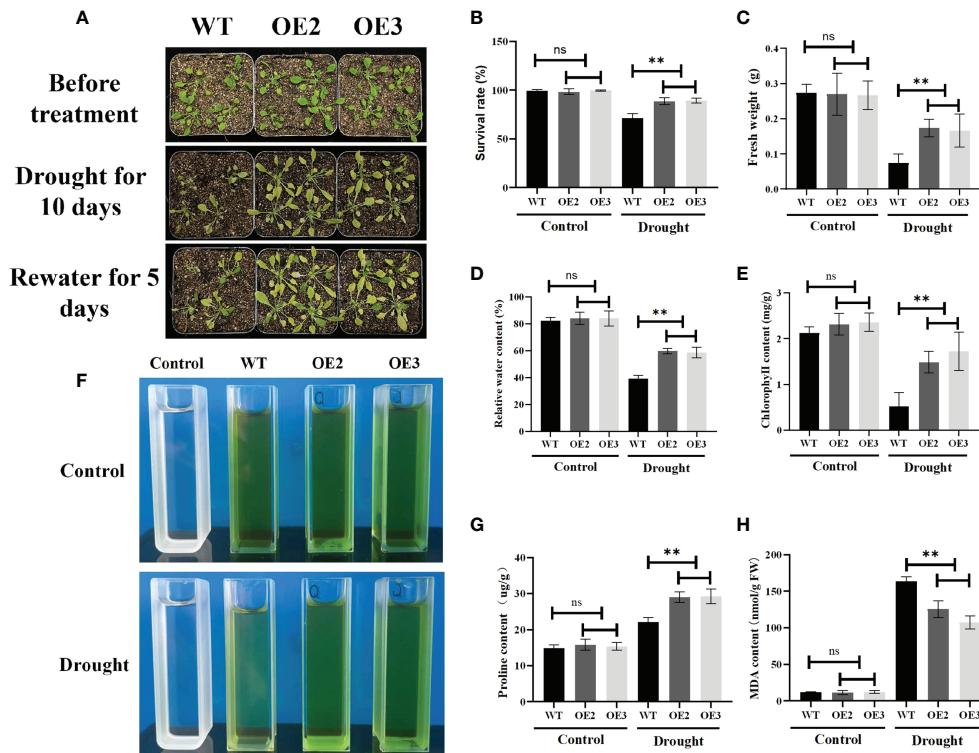


**FIGURE 9**  
Phenotypes of the ZmLBD2-overexpressing transgenic plants and wild-type controls in *A. thaliana* under drought conditions. (A) Drought treatment using 30 days plants. The wild-type controls and transgenic plants were grown in pots for 30 days and then subjected to drought treatment for 10 days. The plants were watered again 5 days after the treatment. Survival rate (B), fresh weight (C), relative water content (D), chlorophyll content (E, F), proline content (G), and MDA content (H) in transgenic Arabidopsis plants and wild-type controls under normal conditions and drought stress. Data were expressed as the mean of triplicate values, and error represented the SD. The \*\* represents  $p < 0.01$ , respectively. Non-significant (ns).

*Physcomitrium patens* mosses increased the expression of the *PpLBDs* gene after they were processed by mannitol. They extrapolated that the expression of *PpLBDs* might strengthen the drought resistance of the mosses. The expression of the *VvLBD1* gene in grape (*Vitis vinifera* L.) increased considerably under the threats of mannitol, salt stress, and heat stress, indicating the significance of *VvLBD1* in the responses to environmental signals (Cao et al., 2016). Liu et al. (2019) adopted qRT-PCR assay to potato (*Solanum tuberosum* L.) with drought treatment and found that the expression of *StLBD1-5* decreased while that of the *StLBD2-6* and *StLBD3-5* increased. This finding reveals the connection between these three genes and the response of potatoes to drought stress. The research published by Guo et al. (2020) showed that the *A. thaliana AtLBD15* gene could directly bind to the abscisic acid signaling pathway factor *ABI14*'s promoter to close the stomas and enhance drought resistance. Our study shows that the overexpression of the maize *ZmLBD2* gene can promote *A. thaliana* seeds to burgeon and grow roots under drought, showing that the *ZmLBD2* can strengthen the drought tolerance of plants.

Drought stress is to blame for the production of ROS. To protect cells from oxidative damage caused by oxidative stress when accumulating too much ROS, plants have developed various antioxidant mechanisms to remove toxins caused by excess ROS (McGrann et al., 2015). Xiong et al. (2022) found that the ROS content in Arabidopsis overexpressing *zmLBD5* was reduced, and the SOD and POD activities were higher than those in wild-type Arabidopsis. Xing et al. (2020) found that *A. thaliana* overexpressing the *CmLOX10* gene under drought conditions had lower MDA and hydrogen peroxide content than the wild type and had strong drought resistance. In our research, the activity of CAT, SOD, and POD increased in the *A. thaliana* overexpressing *ZmLBD2*, and the levels of  $H_2O_2$  and  $O_2^-$  were higher in the wild type. This finding indicates that the *ZmLBD2* can enhance drought resistance by reducing ROS accumulation.

Protein interaction has become a necessary link to further explore the role of maize LBD transcription factor genes in plant growth and development and abiotic stress response. Xu et al. (2018) found that Arabidopsis *LBD16* interacted with *bZIP59* protein to jointly initiate the expression of the downstream gene

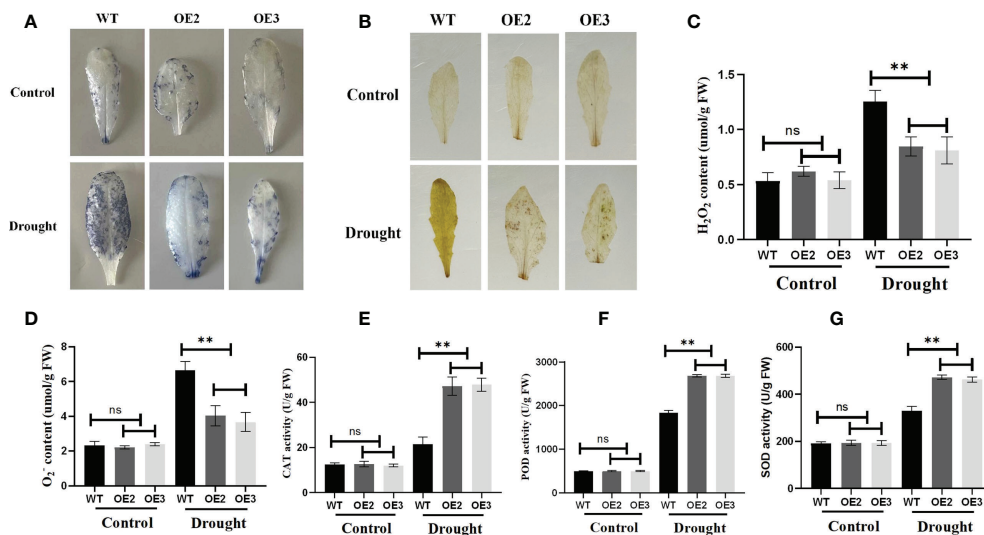


FIGURE 10

Reactive oxygen species staining and physiological indices in ZmLBD2 transgenic Arabidopsis. (A) NBT staining of leaves for H<sub>2</sub>O<sub>2</sub> from ZmLBD2 transgenic seedlings and wild-type plants under normal conditions and drought stress (30 days seedlings were subjected to drought for 10 days). (B) DAB staining of leaves for H<sub>2</sub>O<sub>2</sub> from ZmLBD2 transgenic seedlings and wild-type plants under normal conditions and drought stress (30 days seedlings were subjected to drought for 10 days). (C, D) H<sub>2</sub>O<sub>2</sub> and O<sub>2</sub><sup>-</sup> content in leaves from ZmLBD2 transgenic seedlings and wild-type plants under normal conditions and drought stress. CAT activity (E), POD activity (F), and SOD activity (G) in leaves from ZmLBD2 transgenic seedlings and wild-type plants under normal and drought conditions. Data were expressed as the mean of triplicate values, and error represented the SD. The \*\* represents  $p < 0.01$ , respectively. Non-significant (ns).

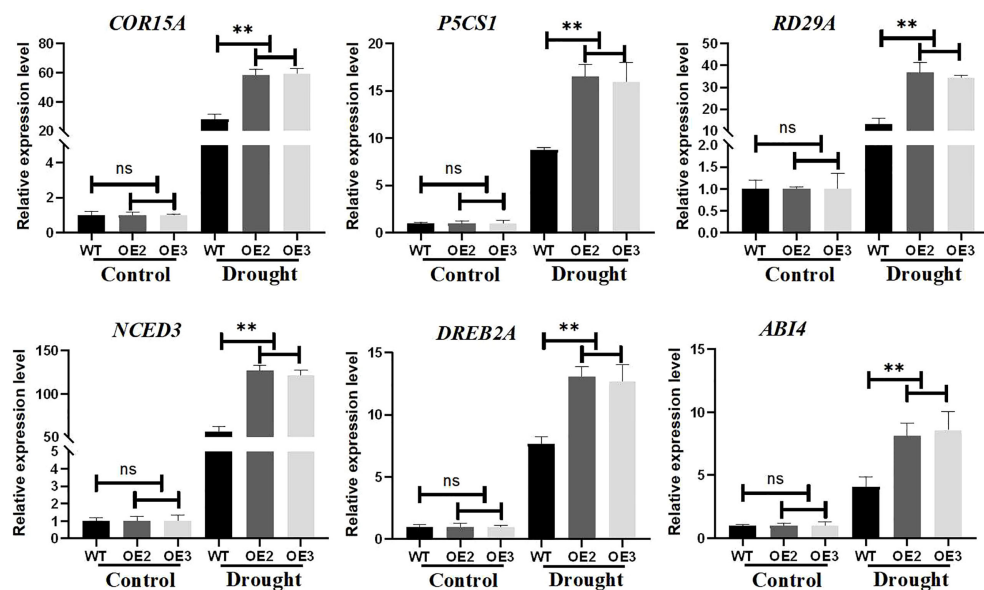


FIGURE 11

Expression levels of drought-stress-related genes in ZmLBD2 transgenic Arabidopsis. Total RNA was isolated from 15-day-old seedlings grown without (CK) or drought treatment for 10 days. Transcript levels of COR15A, P5CS1, RD29A, NCED3, DREB2A, and ABI4 in the transgenic lines and wild type were determined by qPCR AtACTIN8 as reference genes. Fold change was calculated by  $2^{-\Delta\Delta CT}$ . The \*\* represents  $p < 0.01$ , respectively. Non-significant (ns).

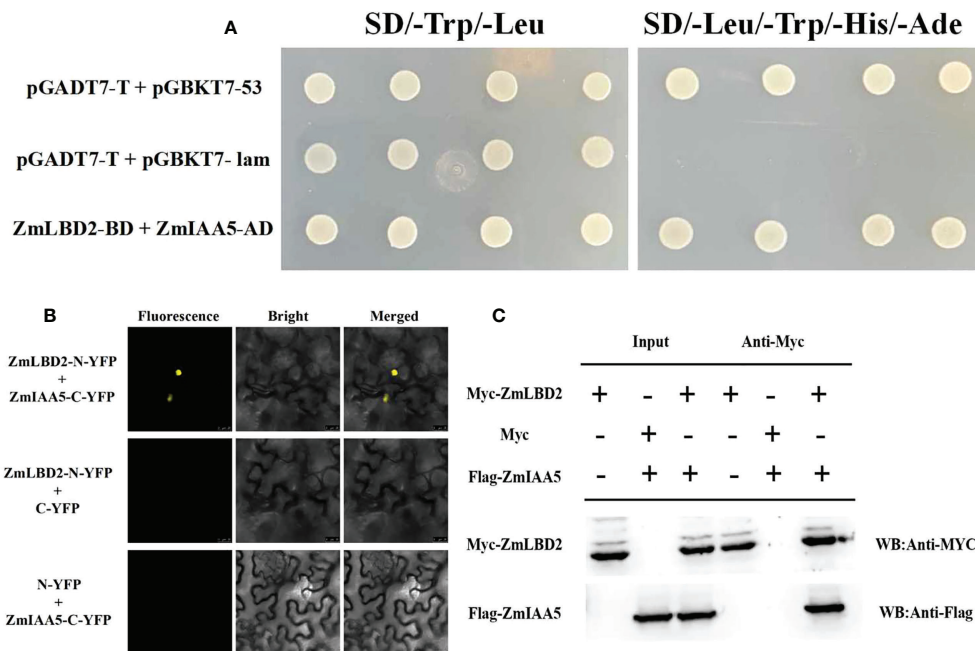


FIGURE 12

Interaction between ZmLBD2 and ZmIAA5. (A) Interaction analysis of ZmLBD2 and ZmIAA5 using a yeast two-hybrid system. (B) Interaction of ZmLBD2 and ZmIAA5 as determined with a BiFC assay. (C) Pull-down assay of ZmLBD2 and ZmIAA5.

FAD-BD, thereby promoting callus formation. Their study found that the AtbZIP59-LBD complex is an auxin-induced callus. Key regulators of cell fate change during wound tissue formation, which may open the door to further exploration of the relationship between the remarkable regenerative capacity of plants and developmental plasticity. In this study, through yeast two-hybrid, BiFC, and Pull-down assays, we identified IAA5 as an interacting protein of ZmLBD2. The Aux/IAA proteins are a large family of auxin coreceptors and transcriptional repressors, which are involved in auxin signaling. Aux/IAA proteins also play an important role in plant responses to abiotic stresses (Cheol Park et al., 2013; Wang F. et al., 2021). We found that the auxin content decreased under drought conditions, and the transcriptional expression levels of IAA-related genes were also affected. Jung et al. (2015) found that the rice Aux/IAA gene *OsIAA6* was highly induced by drought stress, thereby improving drought tolerance through the regulation of auxin biosynthesis genes. Therefore, we speculate that ZmLBD2 interacts with ZmIAA5 to regulate the expression of downstream auxin synthesis-related genes to improve the drought resistance of plants. We plan to further verify our hypothesis in future work.

## Conclusion

In conclusion, we show that the ZmLBD2 gene is a positive regulatory factor for drought response. Subcellular localization

results showed that the ZmLBD2 transcriptional protein was located in the nucleus. The ZmLBD2 gene specifically binds with the inverted repeats of “GCGGCG”. Under drought stress, overexpression of ZmLBD2 improved drought resistance by increasing plant germination rate, root length, fresh weight, relative water content, chlorophyll, and proline content. In addition, it can also be overexpressed to promote the activity of CAT, SOD, and POD in *A. thaliana* to strengthen drought resistance by lowering ROS levels. Meanwhile, we also screened out the ZmIAA5 gene interaction with ZmLBD2. This study provides a theoretical basis for the future analysis of the biological function of the interaction between maize LBD2 and IAA5 in auxin-regulated plant responses to drought stress.

## Data availability statement

The datasets presented in this study can be found in online repositories. The names of the repository/repositories and accession number(s) can be found in the article/Supplementary Material.

## Author contributions

SYG and YYM conceived research plans and designed experiments. PJ, XTW and ZZJ conducted experiments. PJ wrote the draft. SYL and ZZJ analyzed the data. PJ, SYG and



YYM reviewed and edited this article and provided helpful comments and discussions. All authors contributed to the article and approved the submitted version.

## Funding

This work was supported by Jilin Province Science and Technology Development Plan Project [20220202008NC].

## Conflict of interest

The authors declare that the research was conducted in the absence of any commercial or financial relationships that could be construed as a potential conflict of interest.

## References

- Ariel, F. D., Diet, A., Crespi, M., and Chan, R. L. (2010). The LOB-like transcription factor Mt LBD1 controls medicago truncatula root architecture under salt stress. *Plant Signaling Behav.* 5 (12), 1666–1668. doi: 10.4161/psb.5.12.14020
- Ba, L. J., Kuang, J. F., Chen, J. Y., and Lu, W. J. (2016). MaJAZ1 attenuates the MaLBD5-mediated transcriptional activation of jasmonate biosynthesis gene MaAOC2 in regulating cold tolerance of banana fruit. *J. Agric. Food Chem.* 64 (4), 738–745. doi: 10.1021/acs.jafc.5b05005
- Bell, E. M., Lin, W. C., Husbands, A. Y., Yu, L. F., Jaganatha, V., Jablonska, B., et al. (2012). Arabidopsis LATERAL ORGAN BOUNDARIES negatively regulates brassinosteroid accumulation to limit growth in organ boundaries. *proc. Natl. Acad. Sci. U.S.A.* 109 (51), 21146–21151. doi: 10.1073/pnas.1210789109
- Cao, H., Liu, C. Y., Liu, C. X., Zhao, Y. L., and Xu, R. R. (2016). Genomewide analysis of the lateral organ boundaries domain gene family in vitis vinifera. *J. Genet.* 95 (3), 515–526. doi: 10.1007/s12041-016-0660-z
- Chen, K., Su, C., Tang, W., Zhou, Y., Xu, Z., Chen, J., et al. (2021). Nuclear transport factor GmNTF2B-1 enhances soybean drought tolerance by interacting with oxidoreductase GmOXR17 to reduce reactive oxygen species content. *Plant J. Cell Mol. Biol.* 107 (3), 740–759. doi: 10.1111/tpj.15319
- Cheol Park, H., Cha, J. Y., and Yun, D. J. (2013). Roles of YUCCAs in auxin biosynthesis and drought stress responses in plants. *Plant Signaling Behav.* 8 (6), e24495. doi: 10.4161/psb.24495
- Fernando Gil, J., Liebe, S., Thiel, H., Lennfors, B. L., Kraft, T., Gilmer, D., et al. (2018). Massive up-regulation of LBD transcription factors and EXPANSINS highlights the regulatory programs of rhizomania disease. *Mol. Plant Pathol.* 19 (10), 2333–2348. doi: 10.1111/mpp.12702
- Guo, Z., Xu, H., Lei, Q., Du, J., Li, C., Wang, C., et al. (2020). The arabidopsis transcription factor LBD15 mediates ABA signaling and tolerance of water-deficit stress by regulating ABI4 expression. *Plant J. Cell Mol. Biol.* 104 (2), 510–521. doi: 10.1111/tpj.14942
- Huang, X. L., Yan, H. Q., Liu, Y. J., and Yi, Y. (2020). Genome-wide analysis of LATERAL ORGAN BOUNDARIES DOMAIN-in physcomitrella patens and stress responses. *Genes Genomics* 42 (6), 651–662. doi: 10.1007/s13258-020-00931-x
- Hu, C. H., Zeng, Q. D., Tai, L., Li, B. B., Zhang, P. P., Nie, X. M., et al. (2020). Interaction between TaNOX7 and TaCDPK13 contributes to plant fertility and drought tolerance by regulating ROS production. *J. Agric. Food Chem.* 68 (28), 7333–7347. doi: 10.1021/acs.jafc.0c02146
- Jiao, P., Jiang, Z., Wei, X., Liu, S., Qu, J., Guan, S., et al. (2022). Overexpression of the homeobox-leucine zipper protein ATHB-6 improves the drought tolerance of maize (*Zea mays* L.). *Plant Sci. an Int. J. Exp. Plant Biol.* 316, 111159. doi: 10.1016/j.plantsci.2021.111159
- Jung, H., Lee, D. K., Choi, Y. D., and Kim, J. K. (2015). OsIAA6, a member of the rice Aux/IAA gene family, is involved in drought tolerance and tiller outgrowth. *Plant Sci. an Int. J. Exp. Plant Biol.* 236, 304–312. doi: 10.1016/j.plantsci.2015.04.018
- Ju, Y. L., Yue, X. F., Min, Z., Wang, X. H., Fang, Y. L., and Zhang, J. X. (2020). VvNAC17, a novel stress-responsive grapevine (*Vitis vinifera* L.) NAC transcription factor, increases sensitivity to abscisic acid and enhances salinity, freezing, and drought tolerance in transgenic arabidopsis. *Plant Physiol. Biochem. PPB* 146, 98–111. doi: 10.1016/j.plaphy.2019.11.002
- Lim, C. W., Han, S. W., Hwang, I. S., Kim, D. S., Hwang, B. K., Lee, S. C., et al. (2015). Te Pepper lipoxygenase CaLOX1 plays a role in osmotic, drought and high salinity stress response. *Plant Cell Physiol.* 56(5), 930–942. doi: 10.1093/pcp/pcv020
- Liu, H., Cao, M., Chen, X., Ye, M., Zhao, P., Nan, Y., et al. (2019). Genome-wide analysis of the lateral organ boundaries domain (LBD) gene family in solanum tuberosum. *Int. J. Mol. Sci.* 20 (21), 5360. doi: 10.3390/ijms20215360
- Liu, J., Hu, X. M., Qin, P., Prasad, K., Hu, Y. X., and Xu, L. (2018). The WOX11-LBD16 pathway promotes pluripotency acquisition in callus cells during *de novo* shoot regeneration in tissue culture. *Plant Cell Physiol.* 59 (4), 739–748. doi: 10.1093/pcp/pcy010
- Liu, J., Xu, L., Shang, J., Hu, X., Yu, H., Wu, H., et al. (2021). Genome-wide analysis of the maize superoxide dismutase (SOD) gene family reveals important roles in drought and salt responses. *Genet. Mol. Biol.* 44 (3), e20210035. doi: 10.1590/1678-4685-gmb-2021-0035
- Liu, J. Y., Zhang, C., Shao, Q., Tang, Y. F., Cao, S. X., Guo, X. O., et al. (2016). Effects of abiotic stress and hormones on the expressions of five 13-CmLOXs and enzyme activity in oriental melon (*Cucumis melo* var. *makuwa* makino). *J. Integr. Agric.* 15, 326–338. doi: 10.1016/S2095-3119(15)61135-2
- Liu, L., Zhang, J., Xu, J., Li, Y., Guo, L., Wang, Z., et al. (2020). CRISPR/Cas9 targeted mutagenesis of SLBD40, a lateral organ boundaries domain transcription factor, enhances drought tolerance in tomato. *Plant Sci. an Int. J. Exp. Plant Biol.* 301, 110683. doi: 10.1016/j.plantsci.2020.110683
- Li, L. H., Yi, H. L., Liu, X.-P., and Qi, H. X. (2021). Sulfur dioxide enhance drought tolerance of wheat seedlings through H2S signaling. *Ecotoxicol. Environ. Saf.* 207, 111248. doi: 10.1016/j.ecoenv.2020.111248
- McGrann, G. R., Steed, A., Burt, C., Goddard, R., Lachaux, C., Bansal, A., et al. (2015). Contribution of the drought tolerance-related stress-responsive NAC1 transcription factor to resistance of barley to ramularia leaf spot. *Mol. Plant Pathol.* 16 (2), 201–209. doi: 10.1111/mpp.12173
- Noman, M., Jameel, A., Qiang, W. D., Ahmad, N., Liu, W. C., Wang, F. W., et al. (2019). Overexpression of GmCAMTA12 enhanced drought tolerance in arabidopsis and soybean. *Int. J. Mol. Sci.* 20 (19), 4849. doi: 10.3390/ijms20194849
- Park, J. H., Choi, E. A., Cho, E. W., Hahm, K. S., and Kim, K. L. (1998). Maltose binding protein (MBP) fusion proteins with low or no affinity to amylose resins can be single-step purified using a novel anti-MBP monoclonal antibody. *Molecules Cells* 8 (6), 709–716. doi: 10.1016/S0022-0981(98)00091-4

## Publisher's note

All claims expressed in this article are solely those of the authors and do not necessarily represent those of their affiliated organizations, or those of the publisher, the editors and the reviewers. Any product that may be evaluated in this article, or claim that may be made by its manufacturer, is not guaranteed or endorsed by the publisher.

## Supplementary material

The Supplementary Material for this article can be found online at: <https://www.frontiersin.org/articles/10.3389/fpls.2022.1000149/full#supplementary-material>



- Sahebi, M., Hanafi, M. M., Rafii, M. Y., Mahmud, T., Azizi, P., Osman, M., et al. (2018). Improvement of drought tolerance in rice (*Oryza sativa* L.): Genetics, genomic tools, and the WRKY gene family. *BioMed. Res. Int.* 2018, 3158474. doi: 10.1155/2018/3158474
- Sapes, G., and Sala, A. (2021). Relative water content consistently predicts drought mortality risk in seedling populations with different morphology, physiology and times to death. *Plant Cell Environ.* 44 (10), 3322–3335. doi: 10.1111/pce.14149
- Wang, C., Chen, N., Liu, J., Jiao, P., Liu, S., Qu, J., et al. (2022). Overexpression of ZmSAG39 in maize accelerates leaf senescence in arabidopsis thaliana. *Plant Growth Regul.* doi: 10.1007/s10725-022-00874-1
- Wang, F., Niu, H., Xin, D., Long, Y., Wang, G., Liu, Z., et al. (2021). OsIAA18, an Aux/IAA transcription factor gene, is involved in salt and drought tolerance in rice. *Front. Plant Sci.* 12, 738660. doi: 10.3389/fpls.2021.738660
- Wang, C. T., Ru, J. N., Liu, Y. W., Li, M., Zhao, D., Yang, J. F., et al. (2018). Maize WRKY transcription factor ZmWRKY106 confers drought and heat tolerance in transgenic plants. *Int. J. Mol. Sci.* 19 (10), 3046. doi: 10.3390/ijms19103046
- Wang, Y., Yu, Y., Wan, H., Tang, J., and Ni, Z. (2022). The sea-island cotton GbTCP4 transcription factor positively regulates drought and salt stress responses. *Plant Sci. an Int. J. Exp. Plant Biol.* 322, 111329. doi: 10.1016/j.plantsci.2022.111329
- Wang, J., Zhang, W., Cheng, Y., and Feng, L. (2021). Genome-wide identification of LATERAL ORGAN BOUNDARIES DOMAIN (LBD) transcription factors and screening of salt stress candidates of *Rosa rugosa* thunb. *Biology* 10 (10), 992. doi: 10.3390/biology10100992
- Wang, Z., Zhang, R., Cheng, Y., Lei, P., Song, W., Zheng, W., et al. (2021). Genome-wide identification, evolution, and expression analysis of LBD transcription factor family in bread wheat (*Triticum aestivum* L.). *Front. Plant Sci.* 12, 721253. doi: 10.3389/fpls.2021.721253
- Wei, S., Xia, R., Chen, C., Shang, X., Ge, F., Wei, H., et al. (2021). ZmBHLH124 identified in maize recombinant inbred lines contributes to drought tolerance in crops. *Plant Biotechnol. J.* 19 (10), 2069–2081. doi: 10.1111/pbi.13637
- Xing, Q., Liao, J., Cao, S., Li, M., Lv, T., and Qi, H. (2020). CmLOX10 positively regulates drought tolerance through jasmonic acid-mediated stomatal closure in oriental melon (*Cucumis melo* var. *makuwa makino*). *Sci. Rep.* 10 (1), 17452. doi: 10.1038/s41598-020-74550-7
- Xiong, H., Yu, J., Miao, J., Li, J., Zhang, H., Wang, X., et al. (2018). Natural variation in OsLG3 increases drought tolerance in rice by inducing ROS scavenging. *Plant Physiol.* 178 (1), 451–467. doi: 10.1104/pp.17.01492
- Xiong, J., Zhang, W., Zheng, D., Xiong, H., Feng, X., Zhang, X., et al. (2022). ZmLBD5 increases drought sensitivity by suppressing ROS accumulation in arabidopsis. *Plants (Basel Switzerland)* 11 (10), 1382. doi: 10.3390/plants11101382
- Xu, C., Cao, H., Zhang, Q., Wang, H., Xin, W., Xu, E., et al. (2018). Control of auxin-induced callus formation by bZIP59-LBD complex in arabidopsis regeneration. *Nat. Plants* 4 (2), 108–115. doi: 10.1038/s41477-017-0095-4
- Xu, Z. S., Xia, L. Q., Chen, M., Cheng, X. G., Zhang, R. Y., Li, L. C., et al. (2007). Isolation and molecular characterization of the triticum aestivum L. ethylene-responsive factor 1 (TaERF1) that increases multiple stress tolerance. *Plant Mol. Biol.* 65 (6), 719–732. doi: 10.1007/s11103-007-9237-9
- Yuan, X., Wang, H., Cai, J., Bi, Y., Li, D., and Song, F. (2019). Rice NAC transcription factor ONAC066 functions as a positive regulator of drought and oxidative stress response. *BMC Plant Biol.* 19 (1), 278. doi: 10.1186/s12870-019-1883-y
- Yu, T. F., Liu, Y., Fu, J. D., Ma, J., Fang, Z. W., Chen, J., et al. (2021). The NF-Y-PYR module integrates the abscisic acid signal pathway to regulate plant stress tolerance. *Plant Biotechnol. J.* 19 (12), 2589–2605. doi: 10.1111/pbi.13684
- Zhang, J., Huguet-Tapia, J. C., Hu, Y., Jones, J., Wang, N., Liu, S., et al. (2017). Homologues of CsLOB1 in citrus function as disease susceptibility genes in citrus canker. *Mol. Plant Pathol.* 18 (6), 798–810. doi: 10.1111/mpp.12441
- Zhang, Y. W., Li, Z. W., Ma, B., Hou, Q. C., and Wan, X. Y. (2020). Phylogeny and functions of LOB domain proteins in plants. *Int. J. Mol. Sci.* 21 (7), 2278. doi: 10.3390/ijms21072278
- Zhang, Y. M., Zhang, S. Z., and Zheng, C. C. (2014). Genomewide analysis of LATERAL ORGAN BOUNDARIES domain gene family in *zea mays*. *J. Genet.* 93 (1), 79–91. doi: 10.1007/s12041-014-0342-7
- Zhao, Q., Hu, R. S., Liu, D., Liu, X., Wang, J., Xiang, X. H., et al. (2020). The AP2 transcription factor NtERF172 confers drought resistance by modifying NtCAT. *Plant Biotechnol. J.* 18 (12), 2444–2455. doi: 10.1111/pbi.13419
- Zhao, J. Y., Lu, Z. W., Sun, Y., Fang, Z. W., Chen, J., Zhou, Y. B., et al. (2020). The ankyrin-repeat gene GmANK114 confers drought and salt tolerance in arabidopsis and soybean. *Front. Plant Sci.* 11, 584167. doi: 10.3389/fpls.2020.584167



## OPEN ACCESS

## EDITED BY

Hirofumi Saneoka,  
Hiroshima University, Japan

## REVIEWED BY

Mahender Anumalla,  
International Rice Research Institute  
(IRRI), Philippines  
Shailesh Yadav,  
Africa Rice Center (CGIAR), Côte  
d'Ivoire

## \*CORRESPONDENCE

Jing Liu  
liujing@ynnu.edu.cn  
Shah Fahad  
shah\_fahad80@yahoo.com  
Hongyang Wang  
hongyang8318@ynnu.edu.cn

## SPECIALTY SECTION

This article was submitted to  
Plant Abiotic Stress,  
a section of the journal  
Frontiers in Plant Science

RECEIVED 03 July 2022

ACCEPTED 26 September 2022

PUBLISHED 17 October 2022

## CITATION

Yang J, Wei J, Xu J, Xiong Y, Deng G,  
Liu J, Fahad S and Wang H (2022)  
Mapping QTLs for anaerobic tolerance  
at germination and bud stages using  
new high density genetic map of rice.  
*Front. Plant Sci.* 13:985080.  
doi: 10.3389/fpls.2022.985080

## COPYRIGHT

© 2022 Yang, Wei, Xu, Xiong, Deng, Liu,  
Fahad and Wang. This is an open-  
access article distributed under the  
terms of the [Creative Commons  
Attribution License \(CC BY\)](#). The use,  
distribution or reproduction in other  
forums is permitted, provided the  
original author(s) and the copyright  
owner(s) are credited and that the  
original publication in this journal is  
cited, in accordance with accepted  
academic practice. No use,  
distribution or reproduction is  
permitted which does not comply with  
these terms.

# Mapping QTLs for anaerobic tolerance at germination and bud stages using new high density genetic map of rice

Jing Yang<sup>1</sup>, Ji Wei<sup>1</sup>, Jifen Xu<sup>1</sup>, Yumeng Xiong<sup>1</sup>, Gang Deng<sup>2</sup>,  
Jing Liu<sup>1\*</sup>, Shah Fahad<sup>3,4\*</sup> and Hongyang Wang<sup>1\*</sup>

<sup>1</sup>Yunnan Key Laboratory of Potato Biology, Yunnan Normal University, Kunming, China, <sup>2</sup>School of Agriculture, Yunnan University, Kunming, China, <sup>3</sup>Department of Agriculture, Abdul Wali Khan University Mardan, Khyber Pakhtunkhwa, Pakistan, <sup>4</sup>Department of Agronomy, The University of Haripur, Haripur, Pakistan

Due to its low cost and convenience, direct seeding is an efficient technique for the production of rice in different rice growing areas. However, anaerobic conditions are a major obstacle to the direct seeding of rice and result in poor seedling establishment, which leads to yield losses. We constructed a collection of recombinant inbred lines (RIL) comprising 275 lines derived from the H335 and CHA-1 cross by the method of single seed descent. Via a genotyping-by-sequencing (GBS) strategy, a high-density genetic map containing 2498 recombination bin markers was constructed, the average physical distance between the markers was only 149.38 Kb. After anaerobic treatment, 12 phenotypes related to both the coleoptile at germination and seedling quality at budding were evaluated. There were no significant correlations between seedling and bud traits. Genetic mapping of quantitative traits was performed for these traits across two cropping seasons. A total of 20 loci were detected, named locus 1~20. Three of them were repeatedly detected across both seasons. Six loci overlapped with those in previous reports, and nine loci were associated with multiple traits at both stages. Notably, locus 3, which is located on chromosome 2 (26,713,837 to 27,333,897 bp), was detected for both the germination and bud traits. By focusing on the locus 3 interval and by combining gene annotation and expression analyses, we identified a promising candidate gene, trehalose-6-phosphate phosphatase (*OsTPP1*, LOC\_Os02g44230). Furthermore, RILs (G289, G379, G403, G430 and G454) that have superior phenotypes and that pyramid elite alleles were recognized. The findings of present study provide new genetic resources for direct-seeding rice (DSR) varieties for molecular breeding strategies and expand our knowledge of genetic regulation of seedling establishment under anaerobic conditions.

## KEYWORDS

direct-seeding rice, anaerobic seedling establishment, GBS, RIL, QTL mapping

## Introduction

Direct seeding is an energy-efficient and climate-resilient establishment technique for rice crops (Rao et al., 2007; Chauhan and Johnson, 2010). Compared with traditional transplanted-puddled rice system, direct-seeding rice (DSR) omitted transplanting process, thus saving a lot of water resources, labor and energy. Mahender et al. (2015) reported that dry DSR can save 35–57% of water. Flooding the field following direct seeding can help restrict weed growth and prevent damage from mice and birds (Manigbas et al., 2008). However, flooding also creates anaerobic conditions that affects on germination, seedling survival and morphogenesis (Yamauchi et al., 1993; Ismail et al., 2009). So, anaerobic stress has also become a limiting factor for adoption of DSR at commercial level.

In rice different strategies have been evolved to adapt the flooding stress; these strategies involve mainly two different mechanisms: the “quiescence strategy” and the “escape strategy” (Jackson, 2008; Loreti et al., 2016). A large amount of research clearly showed that, compared with those of susceptible cultivars, coleoptiles of tolerant cultivars showed higher and rapid growth under submergence during the germination phase and this adaptation in morphology allow them to arrive at surface rapidly, permitting oxygen to diffuse primary leaves and roots, to hold up seedling growth (Atwell et al., 1982; Yamauchi et al., 1993; Yamauchi and Biswas, 1997; Ismail et al., 2009). Indeed, this phenomenon is considered an “escape strategy” used to tolerate submergence during the germination phase. Therefore, these mechanisms also provide a good theoretical basis for breeding rice varieties that have enhanced capabilities for anaerobic germination (AG).

Unlike most cereal crop species, under  $O_2$  deficiency, rice can mobilize starchy endosperm as easily fermentable sugars to produce ATP; the phenomenon is important for supporting AG (Guglielminetti et al., 1995; Hwang et al., 1999). When the seeds germinate under submerged conditions, mitochondria release  $Ca^{2+}$  as secondary messenger in response of  $O_2$  deficiency and sugar starvation. Calcineurin B-like (CBL) is a  $Ca^{2+}$  sensor which binds and activated by  $Ca^{2+}$ . Activated CBL/ $Ca^{2+}$  activates SnRK1A by interacting with protein kinase CIPK15 which results in activation of the promoter of the transcription factor MYBS1 and phosphorylates the MYBS1 protein. Moreover, gibberellic acid (GA) synthesized by the embryo diffuses to aleurone cells and

induces expression of the transcription factor MYBGA. Sugar response elements (SREs) and GA response element (GAREs) are two important control elements. MYBGA binds to GAREs while, MYBS1 binds to SREs, developing a bipartite MYB-DNA complex that considerably activates  $\alpha$ -amylase gene promoters (Hong et al., 2012). The hydrolysis of starch stored within the rice seeds then provides energy for germination, *OsTPP7* encoding trehalose-6-phosphate (T6P) phosphatase, has been involved in T6P metabolic processes and functions to enhance starch mobilization for higher tolerance of AG (Kretzschmar et al., 2015). However, *OsTPP7* signaling pathway is still unclear and additional research is needed.

To date, genetic research on the germination of rice under  $O_2$  deficient conditions have focused majorly on mining functional genes and exploring their mechanisms of function. Some QTLs are identified by genetic mapping populations. Several studies have considered coleoptile elongation an indicator trait of tolerant phenotypes for QTL mapping. Seven QTLs associated with seed anoxia germinability were mapped onto chromosomes 1, 2, 5, and 7 via QTL mapping of two populations (Jiang et al., 2004; Jiang et al., 2006). Using the seedling survival rate as an indicator of tolerant phenotypes, Angaji. (2008); Anganji et al., (2010) investigated two different backcross inbred line populations, both of which were derived from the backcrossed offspring of IR64 as a recurrent parent, to map a total of 13 QTLs throughout the chromosomes. Septiningsih et al. (2013) identified six QTLs that were significantly associated with survival rate on chromosomes 2, 5, 6, and 7. Baltazar et al. (2014) identified four QTLs that contributed to anaerobic tolerance via improved survival rates. Kim and Reinke (2018) reported four QTLs responsible for survival rate to a certain extent on chromosomes 1, 8, and 11. Four QTLs derived from Kharsu 80A giving enhanced tolerance in the absence of free oxygen germination were identified by Baltazar et al. (2019): three on chromosome number 7 and one on chromosome number 3, phenotypic variance clarified from 8.1% to 12.6%. When two biparental mapping populations were used for QTL analyses, this identified four QTLs on chromosomes 1, 3 and 7 for seedling height and five QTLs on chromosomes 3, 5, 6, 7, and 8 for survival rate (Ghosal et al., 2019). Recently, Kong et al. (2022) identified two QTLs on chromosomes 1 (*qCL-1.1*) and 3 (*qCL-3.1*) using for coleoptile length as an indicator. Genome-wide association studies (GWASs) represent an efficient approach for complex traits dissection, however, little literature on excavation of loci linked with AG tolerance via GWASs is available. Hsu and Tung (2015) performed GWAS by 36901 single nucleotide polymorphisms (SNPs) in addition to find 88 genetic loci linked to AG tolerance. Via GWAS of the 5291 SNP markers in the 432 *indica* varieties, 15 genetic loci linked with AG tolerance were detected (Zhang et al., 2017). Fifty genes for submergence stress were identified when Gao et al. (2020) combined information of GWAS, transcriptomic analysis, and reported QTL locations. Su et al. (2021) conducted genome resequencing on 209 rice varieties, and a dynamic GWAS of coleoptile length and diameter was adopted, with 26 loci were detected.

**Abbreviations:** RIL, recombinant inbred line; CL, coleoptile length; CSA, coleoptile surface area; CD, coleoptile diameter; CV, coleoptile volume; SSD, shoot stem diameter; SH, shoot height; SFW, shoot fresh weight; RL, root length; RSA, root surface area; RV, root volume; RD, root diameter; RFW, root fresh weight; AG, anaerobic germination; QTL, quantitative trait loci; GWAS, genome-wide sequencing analysis; DSR, direct seeding rice; WS, wet season; DS, wet season; GBS, genotyping-by-sequencing; LOD, Logarithm of odds; PVE, Phenotypic variation explained.

Although some progress has been made in QTL analyses for AG tolerance, relatively few genetic loci associated with AG tolerance compared with other important rice traits have been identified. To date, due to a low density of markers, only *qAG-9-2* finely mapped and then cloned as the *OsTPP7* (Kretschmar et al., 2015). This has occurred because most of these genetic loci were recognized based on traditional markers, which are sparsely distributed across 12 rice chromosomes; in addition, only two main indicators have been used for mapping. These two reasons lead to the low efficiency of the excavation of genetic loci associated with AG tolerance and limit our knowledge of genetic regulatory mechanisms of AG tolerance in the seeds of rice. Therefore, the development of new types of high-density markers and additional high-efficiency phenotypic indicators are essential to assist fine mapping and cloning of QTLs.

In our previous study, we based on the protocol of Septiningsih et al. (2013), investigated the seedling survival rate of rice seeds after twenty one days of germination in water 10 cm deep of 200 conventional *indica* rice varieties mainly from Guangdong province, China. The average seedling survival rate of 200 materials was 42.67%, the maximum was 83.00%, and the minimum was 8.13%. Interestingly, the seedling survival rate of our donor parent H335 was 78.12%, while another parent CHA-1 was only 8.85% (unpublished data). Therefore, we created RIL population included 275 RILs derived *via* the single seed descent from CHA-1 and H335. The GBS approach was applied to sequence 275 recombinant inbred lines (RILs), generating a set of high-density SNP markers. To create linkage map of high density depending on the technique of parent independent genotyping constructing linkage map (Xie et al., 2010) and validate it using genes from the reference genome. We evaluated 12 traits of rice seeds after 6 days anaerobic treatment at the germination and bud stages; these 12 traits can be used for the comprehensive evaluation of the anaerobic seedling establishment ability of rice. QTL mapping was performed based on these 12 traits to identify additional genetic loci to enrich the genotypes of genetic pool associated with anaerobic seeding tolerance. These results broaden the knowledge of the anaerobic tolerance genetic mechanisms of rice seeds at germination and bud stages. Specifically some QTLs are promising targets for the marker assisted breeding of DSR varieties.

## Materials and methods

### Plant materials

In present study, National Engineering Research Center for Plant Space Breeding bred two parents H335 and CHA-1. RIL population of 275 lines were constructed using single seed descent method. Both the parents and RILs were grown in rice field during wet (WS) and dry season (DS) of 2017 at the South China Agricultural University, Province Guangzhou, China (113°E

longitude, 23°N latitude approximately). Block design was used to grown each RIL or parent, comprising 6 columns × 6 rows, with 20 cm space between the plants. Keeping in view the issues related to seed maturity, 6 plants were harvested independently from the center of each block on 35<sup>th</sup> and 40<sup>th</sup> day after heading during WS and DS respectively. Seeds obtained after harvest were then dried at 42°C in dryer using heated air for five days then finally stored at low temperature (-20°C).

### Evaluation of anaerobic tolerance at germination and bud stages

After harvesting 3 out of 6 plants per line per season with healthy seeds were chosen. Their seeds were kept in an oven at 50°C for the period of one week to break their dormancy, then sterilized with a 20% diluted bleach solution (6-7% NaClO) for 20 minutes and finally sterile water was used to rinse the seeds. For the germination stage, five seeds were added to each centrifuge tube of 10 cm and filled with the distilled water to develop anaerobic conditions. Four replicates (centrifuge tubes) were included per individual, and twelve replicates were included per line. For the bud stage, three individuals were selected per line, approximately 100 seeds per individual were placed in a petri dish (9 cm) randomly, and 10 ml of distilled water was poured. These petri dishes were positioned in a chamber of 8 hour light (200  $\mu\text{mol m}^{-2} \text{s}^{-1}$ ) and 16 h dark cycle at 30°C. Germinated seeds with approximately 3-mm-long buds were selected, and five seeds were positioned to the bottom of 1 tissue culture bottle (75 mm diameter, 108 mm height) that was filled with distilled water. Two replicates (tissue culture bottles) were included per individual, and a total of six replicates were included per line. All the centrifuge tubes and tissue culture bottles were placed immediately in a chamber where a shift of light 8 h (200  $\mu\text{mol m}^{-2} \text{s}^{-1}$ ) and dark 16 hour cycle was maintained at the temperature of 30°C. Coleoptile volume (CV), coleoptile surface area (CSA), coleoptile length (CL) and the coleoptile diameter (CD) of germination stage, shoot height (SH), shoot stem diameter (SSD), root length (RL), root volume (RV), root surface area (RSA), and root diameter (RD) of bud stage were determined after six days using WinRHIZO root image analysis system. Shoot fresh biomass (SFW) and root fresh biomass (RFW) were calculated using sensitive balance. For the statistical analysis Statistical Analysis System and Microsoft Excel were used. The statistical significance of the difference between two parents was evaluated by One-way ANOVA. The correlations of traits were computed using PROC CORR by SAS software.

### DNA extraction, library construction and illumina sequencing

Leaf samples were collected from the 275 RILs in the F<sub>7</sub> generation. Leaf tissues were used to extract total genomic DNA



using the CTAB method. The quantity and quality of genomic DNA was determined by NanoDrop ND-1000 Spectrophotometer and 1% agarose gel electrophoresis, respectively (Thermo Scientific, Wilmington, USA).

For 275 RILs, the genomic DNA was incubated with ATP (NEB), T4 DNA ligase (NEB), *MseI* (New England Biolabs, NEB), and *MseI* Y adapter N containing barcode at 37°C. Temperature at 65°C was used to inactivate restriction ligation reactions and digested at 37°C by the additional restriction enzyme (*NlaIII*). Agencourt AMPure XP (Beckman) was utilized to purify samples of the restriction ligation. Finally PCR was done with these purified samples, universal primers of Phusion Master Mix (NEB), index primers to add index, as well as entire i5 and i7 sequences. Purification of products of PCR was carried out by Agencourt AMPure XP (Beckman) then pooled and run on an agarose gel (2%). Gel extraction kit (Qiagen) was utilized to separate fragments of 375–400 bp (with indexes and adaptors) in size. The fragment products were subsequently purified by using Agencourt AMPure XP (Beckman) and diluted to further sequencing. After that paired-end sequencing was done on the selected tags with Illumina HiSeq PE150 platform (Novogene Bioinformatics Technology Co., Ltd, P.R. China).

## SNP identification and bin marker production

Sequencing give original image data which were converted into sequence data (raw data) in fastq format *via* base calling (Illumina pipeline CASAVA version 1.8.2). Firstly raw data were processed by a chain of quality control (QC) methods: (1) removing reads with  $\geq 10\%$  unidentified nucleotides (N), (2) removing reads with  $> 50\%$  bases having a phred quality  $< 5$ , and (3) removing reads with  $> 10$  nt aligned to adapter, allowing  $\leq 10\%$  mismatches. Burrows-Wheeler Aligner version 0.7.8 was utilized to align clean reads of every sample against reference genome (MSU Rice Genome Annotation Project database v.7; <http://rice.plantbiology.msu.edu/>); command line was 'BWA mem -t 4 -k 32 -M'. After alignment, by means of a Bayesian approach implemented in package SAMtools, we performed SNP calling on population scale (Li et al., 2009). According to the methods Xie et al. (2010), filtered abnormalities, identified biallelic homozygous SNPs. I.e. all potential SNPs were identified in the entire population to obtain drafts of parental genotypes using a maximum parsimonious inference of recombination. Then, filtering out low-quality SNPs by Bayesian inference. Finally, RILs were genotyped using high quality SNPs assisted by a hidden Markov model.

In accordance with the methods of Huang et al. (2009), with some modifications, RILs genotypic maps were aligned and split in recombination bins following breakpoints, with a window size parameter of 15 SNPs. In addition, their genotypes were compared for a 100-kb interval. Adjacent 100-kb intervals with similar genotype across all RILs were combined into a

recombination bin marker. Networks were visualized by Cytoscape version.3.6.1. (Smoot et al., 2011).

## Linkage map construction and QTL analyses

Bin markers utilized to construct genetic linkage map by the R/qtl package (Broman et al., 2003) with Kosambi map method, and genetic distances of markers were determined. QTL analyses were carried out using QTL IciMapping v4.1 (Meng et al., 2015) software. Significance threshold value of logarithm of odd (LOD) scores was 2.5 for the QTL detection, and QTL additive effect and contribution rate to trait were determined.

## Validation of the candidate genes by the real-time quantitative RT-PCR

According to the method of Yang et al. (2019). Total RNA of every RILs were homogenized by mortar and pestle using the liquid nitrogen and after that purified with a Purification Kit of Plant Total RNA (ComWin Biotech Company) following the manufacturer's instructions. Samples of RNA undergo reverse transcription process to develop cDNA by means of high capacity cDNA archive kit (Applied Biosystems, USA). AceQ qPCR SYBR Green Master Mix Kit (Vazyme Biotech) was utilized to conduct qRT-PCR following standard protocol. Furthermore, StepOnePlus System (Applied Biosystems, USA) was utilized to estimate genes expression levels. Each treatment has three replications. Being endogenous control, the Actin was utilized in normalization of cycle threshold (Ct) value achieved, and  $\Delta\Delta C_t$  method was applied to determine values for relative expression NCBI primer BLAST (<http://www.ncbi.nlm.nih.gov/tools/primer-blast/>) were utilized to design gene-specific primers and primer sequences of four candidate genes listed in Table S1.

## Results

### Sequencing and genotyping

Sequencing of the GBS libraries yielded approximately 110.95 Gb of raw data for the 275 RILs, with an average of 0.40 Gb for each line. The Q30 ratio for the entire samples ranged from 86.89 to 96.12%, with a mean of 92.14%; thus, data quality is high and meets the necessities for further analysis. After the raw data were filtered strictly, a total of 770,428,068 clean paired-end reads were obtained. Approximately 96.79% of reads were mapped to Nipponbare reference genome. The mapped regions were covered by the captured fragments totaled approximately 12.16% of genome sequence with coverage depth of 14.14 $\times$  on average for captured regions (Table S2).



To identify potential SNP sites by the use of sequences of RILs. Genotype calling was performed for each RIL, the detected SNPs are merged into a set, which contains 805,088 SNPs. According to the methods and criteria described in detail by Xie et al. (2010), after filtering for abnormalities, 100,307 biallelic homozygous SNPs were validated for the estimation of the recombinant event.

## Bin map construction and characteristics

For the RIL population, adjacent 100-kb intervals with same genotype across all 275 RILs were identified as single recombination bin marker (Huang et al., 2009). Finally, 2,498 recombination bin throughout 12 chromosomes adopted to develop genetic map for RIL population (Figure 1A). Map spanned a total of 2371.84 cM, with a mean interval of 0.95 cM between adjacent markers (Table 1 and Figure 1). Among the 12 chromosomes, chromosome 2 was highly saturated; it include 316 markers, with 0.62 cM average marker density. In contrast, chromosome 10 was the least dense with 1.77 cM average marker density. Approximately 197.65 cM was an average genetic size for 12 chromosomes while, 149.38 kb was an average physical distance between the markers.

## Bin map construction and characteristics

Collinearity analysis was performed by genetic map and physical location of the 2,498 bin markers. The spearman correlation coefficient was calculated for all the linkage groups. Its

value near to 1 showed an improved collinearity among physical and genetic map. Order of most markers on every chromosome of the project is consistent with genome, indicating that collinearity is good and calculation accuracy of genetic recombination rate is high (Figure S1). To evaluate the accuracy and power of present genetic map for traits, a QTL mapping of heading date was carried out. The QTL *qHD-8*, for which peak encompassed a cloned gene involved in heading date (*Hd18*) (Shibaya et al., 2016), was detected on chromosome 8, and this QTL had a high LOD value of 11.98 (Figure S2). *qHD-8*, which is located within the genetic interval from block12804~block12814, can explain 15.57% of the phenotypic variation. The physical distance between the *Hd18* gene and block12814 on chromosome 8 is only 77 kb.

## Phenotypic performance of RIL population for anaerobic tolerance

We investigated 4 traits (CL, CV, CD, CSA), at the germination stage and 8 traits (SH, SSD, RL, SFW, RV, RSA, RFW, RD) at the bud stage in the RIL population under anaerobic conditions. Variations in both the parents are obvious (Table 2). As for RILs population, single peak pattern distributions have examined for 12 investigated traits, and these distributions widely varied (Figure 2; Tables 2, S3).

The correlations among the 12 traits in RIL population were examined (Figure 2). Results revealed no strong correlations exist among traits at germination and bud stages and that the correlation coefficient between CD and SSD was the greatest 0.50 and 0.44 during WS and DS, respectively. For four traits at the germination stage, there were significant correlations between

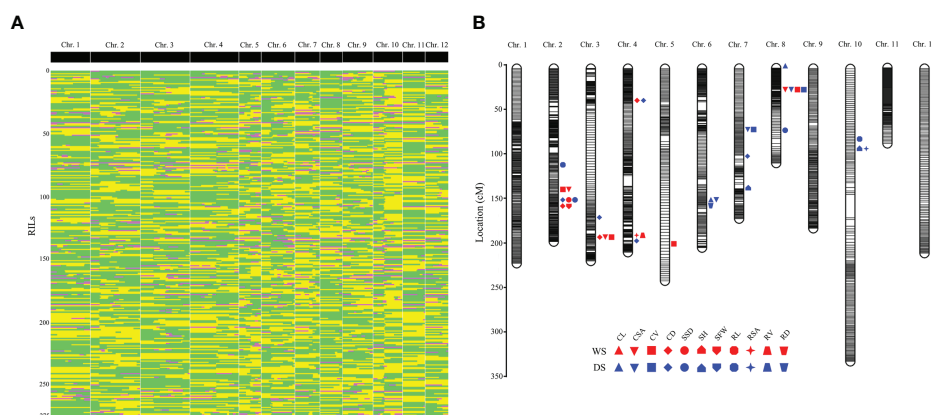


FIGURE 1

Genetic linkage map constructed with bin markers and the locations of QTLs associated with traits related to anaerobic seedling establishment. (A) Recombination bin map consisting of 2,498 bin markers. Green: CHA-1 genotype; yellow: H335 genotype; pink: heterozygote. (B) All of the QTL positions on the high-density map. The red patterns represent the QTLs detected during the wet season (WS); the blue patterns represent the QTLs detected during the dry season (DS). The words associated with different shapes are abbreviations of different phenotypes: CL, coleoptile length; CSA, coleoptile surface area; CV, coleoptile volume; CD, coleoptile diameter; SSD, shoot stem diameter; SH, shoot height; SFW, shoot fresh weight; RL, root length; RSA, root surface area; RV, root volume; RD, root diameter.

TABLE 1 Distribution of genetic markers across the 12 chromosomes in rice.

| Chromosome | Number of markers | Total Distance (cM) | Average Genetic Distance between Markers (cM) | Gap < 5 cM | Average Physical Distance between Markers (kb) |
|------------|-------------------|---------------------|---|------------|--|
| Chr. 1     | 251               | 219.89              | 0.88  | 100.00%    | 172.38   |
| Chr. 2     | 316               | 196.26              | 0.62  | 99.37%     | 113.70   |
| Chr. 3     | 313               | 217.4               | 0.70  | 99.68%     | 116.33   |
| Chr. 4     | 309               | 207.84              | 0.67  | 99.68%     | 114.77   |
| Chr. 5     | 138               | 238.62              | 1.74  | 99.27%     | 217.08   |
| Chr. 6     | 212               | 202.72              | 0.96  | 99.05%     | 147.38   |
| Chr. 7     | 156               | 171.16              | 1.10  | 99.35%     | 190.26   |
| Chr. 8     | 141               | 111.26              | 0.79  | 99.29%     | 201.70   |
| Chr. 9     | 192               | 181.65              | 0.95  | 100.00%    | 119.85   |
| Chr. 10    | 185               | 326.27              | 1.77  | 98.37%     | 125.44   |
| Chr. 11    | 140               | 89.95               | 0.65  | 100.00%    | 207.25   |
| Chr. 12    | 145               | 208.82              | 1.45  | 100.00%    | 189.86   |
| Overall    | 2,498             | 2,371.84            | 0.95  | 99.51%     | 149.38   |

the four traits, except the correlation between CL and CD was not strong. For the eight traits at bud stage, no strong correlation exist between the eight traits, except RSA was strongly correlated with RL and RV.

## QTL mapping in the RIL population

Via method of inclusive composite interval mapping (ICIM), 34 QTLs (14 and 20 for the WS and DS, respectively) by IciMapping v4.1 software. Phenotypic difference explained (PVE) via the QTLs were ranged 3.34–12.17%. Among them, 22 and 12 were detected at germination and bud stages, respectively, and they are distributed on chromosomes 2, 3, 4, 5, 6, 7, 8, and 10 (Figure 1B). QTLs were detected for all traits except RFW. The most QTLs (eight) were associated with CD. However, there was only one QTL each associated with SFW, RV and RD (Table 3). The average PVE of different traits was calculated, in which the CL was the lowest (3.78%) and the RL was the highest (9.90%) (Figure 3A). Both the parents contributed favorable alleles at different loci, while, among the 34 QTLs, 22 were from H335, and only 12 were from CHA-1 (Figure 3B). This observation is consistent with phenotypic differences observed between two parents.

QTLs which overlapped due to physical position were categorized as same locus. Eventually, a total of 20 loci were found (Table 3). Remarkably, 3 out of 20 loci were repetitively identified across the two seasons: locus 3 (*qCD-2-1*, DS; *qSSD-2*, WS and DS), locus 7 (*qCD-4-1*, WS and DS), and locus 17 (*qCSA-8*, WS and DS; *qCV-8*, WS and DS). To further authenticate the correctness these results, loci of present study were compared with reported QTLs previously identified by linkage or association mapping approach. We discovered that up to six loci have previously been reported. Locus 2 associated with

CV and CSA, was detected within genomic interval of *qAG-2*, was shown to be related to the length of shoots, including the coleoptile (Jiang et al., 2004). Multiple reported QTLs were clustered at the end of chromosome 2 (approximately 27 Mb). Specifically, *qAG-2* (Jiang et al., 2004), *qSAT-2-B* (Wang, 2009) and *qAG2* (Septiningsih et al., 2013) were shown to be associated with shoot length, the anaerobic response index and survival rate, respectively. We found two loci within this interval: locus 3, which is associated with SSD and CD, and locus 4, which is associated with SFW and CD. On the chromosome 7, locus 13, which is associated with CSA and CV, mapped to genomic region of *qAG7-1*. Another locus, locus 14, which is associated with CD, colocalized with a reported locus detected by the use of both linkage mapping as well as association mapping approaches (Septiningsih et al., 2013; Baltazar et al., 2014; Hsu and Tung, 2015). In addition, locus 17 on chromosome 7 overlapped with a reported locus that was also detected by the use both linkage mapping and GWAS approaches (Wang, 2009; Chen et al., 2012; Hsu and Tung, 2015).

## Genetic loci pleiotropy

Gene pleiotropy is a common phenomenon in plant genetics. A matrix summarizing of all the QTLs associated with 11 traits associated to anaerobic tolerance at the germination and budding is shown in Figure 3C. In our study, nine of the 20 loci were associated with multiple traits at both stages. Among these nine loci, five associated with multiple traits only at the germination stage. Specifically, locus 2, 13 and 17 were associated with both CSA and CV; locus 6 was associated with CSA, CV and CD; and locus 11 was linked with CL and CSA. Two loci associated with multiple traits only at the bud stage. Specifically, locus 8 was associated with both RV and RSA,

TABLE 2 Phenotypic performance during the germination and the bud stage under anaerobic stress across two cropping seasons.

| Trait <sup>a</sup>     | Env <sup>b</sup> | Parents <sup>c</sup> |                      | RIL population     |              |          |          |                     |
|------------------------|------------------|----------------------|----------------------|--------------------|--------------|----------|----------|---------------------|
|                        |                  | CHA-1                | H335                 | Mean $\pm$ SD      | Range        | Skewness | Kurtosis | CV <sup>d</sup> (%) |
| CL (cm)                | WS               | 1.770 $\pm$ 0.146    | 2.825 $\pm$ 0.216**  | 2.737 $\pm$ 0.254  | 1.776-3.400  | 0.006    | 0.311    | 9.266               |
|                        | DS               | 2.102 $\pm$ 0.193    | 2.657 $\pm$ 0.512    | 2.562 $\pm$ 0.349  | 1.421-3.608  | -0.189   | 0.265    | 13.604              |
| CSA (cm <sup>2</sup> ) | WS               | 0.303 $\pm$ 0.007    | 0.556 $\pm$ 0.042**  | 0.507 $\pm$ 0.062  | 0.297-0.652  | -0.006   | 0.151    | 12.238              |
|                        | DS               | 0.330 $\pm$ 0.034    | 0.542 $\pm$ 0.036**  | 0.462 $\pm$ 0.075  | 0.269-0.710  | 0.123    | 0.033    | 16.271              |
| CV (mm <sup>3</sup> )  | WS               | 4.200 $\pm$ 0.557    | 7.644 $\pm$ 0.840**  | 7.509 $\pm$ 1.220  | 4.000-10.668 | 0.063    | 0.047    | 16.245              |
|                        | DS               | 4.640 $\pm$ 0.289    | 7.381 $\pm$ 0.863**  | 6.658 $\pm$ 1.353  | 3.359-11.142 | 0.268    | -0.078   | 20.222              |
| CD (mm)                | WS               | 0.540 $\pm$ 0.030    | 0.620 $\pm$ 0.030*   | 0.588 $\pm$ 0.031  | 0.494-0.670  | -0.188   | 0.211    | 5.198               |
|                        | DS               | 0.500 $\pm$ 0.007    | 0.577 $\pm$ 0.021*   | 0.572 $\pm$ 0.034  | 0.482-0.662  | -0.238   | -0.277   | 5.939               |
| SSD (mm)               | WS               | 0.614 $\pm$ 0.075    | 0.713 $\pm$ 0.026*   | 0.699 $\pm$ 0.050  | 0.560-0.844  | -0.018   | 0.115    | 7.119               |
|                        | DS               | 0.580 $\pm$ 0.058    | 0.785 $\pm$ 0.008**  | 0.668 $\pm$ 0.049  | 0.511-0.818  | -0.161   | 0.130    | 7.307               |
| SH (cm)                | WS               | 4.400 $\pm$ 0.265    | 5.340 $\pm$ 0.560    | 4.930 $\pm$ 1.014  | 2.289-7.763  | -0.053   | -0.241   | 20.562              |
|                        | DS               | 3.730 $\pm$ .0680    | 5.285 $\pm$ 0.390*   | 4.687 $\pm$ 0.770  | 2.773-7.812  | 0.313    | 0.690    | 16.420              |
| SFW (mg)               | WS               | 10.871 $\pm$ 1.813   | 6.862 $\pm$ 2.415**  | 15.867 $\pm$ 2.815 | 9.243-29.390 | 0.386    | 1.251    | 17.754              |
|                        | DS               | 11.108 $\pm$ 1.062   | 18.313 $\pm$ 1.429** | 14.904 $\pm$ 3.399 | 8.300-53.798 | 5.646    | 61.418   | 22.808              |
| RL (cm)                | WS               | 2.347 $\pm$ 0.095    | 3.590 $\pm$ 0.152**  | 3.114 $\pm$ 1.212  | 1.316-9.357  | 1.852    | 4.462    | 38.919              |
|                        | DS               | 2.160 $\pm$ 0.321    | 3.244 $\pm$ 0.276*   | 2.425 $\pm$ 0.604  | 1.522-6.391  | 2.450    | 10.858   | 24.948              |
| RSA (cm <sup>2</sup> ) | WS               | 0.332 $\pm$ 0.031    | 0.424 $\pm$ 0.088    | 0.415 $\pm$ 0.107  | 0.222-0.874  | 1.259    | 2.348    | 25.742              |
|                        | DS               | 0.350 $\pm$ 0.040    | 0.558 $\pm$ 0.030**  | 0.407 $\pm$ 0.091  | 0.267-1.079  | 2.484    | 12.156   | 22.248              |
| RV (mm <sup>3</sup> )  | WS               | 3.560 $\pm$ 0.288    | 4.541 $\pm$ 0.186**  | 4.415 $\pm$ 0.903  | 2.710-9.083  | 0.953    | 2.484    | 20.464              |
|                        | DS               | 4.930 $\pm$ 0.030    | 6.916 $\pm$ 0.440**  | 5.497 $\pm$ 1.334  | 3.583-14.833 | 2.564    | 11.083   | 24.254              |
| RD (mm)                | WS               | 0.423 $\pm$ 0.199    | 0.477 $\pm$ 0.020    | 0.454 $\pm$ 0.043  | 0.299-0.568  | -0.266   | 0.505    | 9.389               |
|                        | DS               | 0.510 $\pm$ 0.048    | 0.568 $\pm$ 0.122    | 0.541 $\pm$ 0.045  | 0.429-0.735  | 0.752    | 2.073    | 8.344               |
| RFW (mg)               | WS               | 4.802 $\pm$ 0.040    | 7.225 $\pm$ 0.030**  | 6.548 $\pm$ 2.651  | 3.125-28.427 | 4.631    | 29.623   | 40.487              |
|                        | DS               | 5.548 $\pm$ 0.100    | 8.241 $\pm$ 0.120**  | 6.855 $\pm$ 3.184  | 4.495-36.327 | 6.531    | 47.883   | 46.447              |

<sup>a</sup>Trait: CL, coleoptile length; CSA, coleoptile surface area; CV, coleoptile volume; CD, coleoptile diameter; SSD, shoot stem diameter; SH, shoot height; SFW, shoot fresh weight; RL, root length; RSA, root surface area; RV, root volume; RD, root diameter; RFW, root fresh weight.

<sup>b</sup>Environment: WS is the wet season in 2017; DS is the dry season in 2017.

<sup>c</sup>Parent refers to the mean  $\pm$  standard deviation (SD) of the parents, \* and \*\* indicates significance at the levels of 0.05 and 0.01, respectively.

<sup>d</sup>CV (%), coefficient of variation.

and locus 20 was associated with both SH and RSA, indicating that locus 20 affects both the aboveground and the belowground traits of seedlings at the bud stage. In addition, there are two loci affecting traits at both the germination and budding; i.e., locus 3 was linked with CD at germination and SSD at bud stage. Locus 4 was associated with CD and SFW at the germination and bud stage, respectively. Notably, these results were also supported by Pearson correlation analyses based on traits measured at both stages in the two environments (Figure 2). Moreover, to further recognize the action relationship between these genetic loci as well as different traits, we constructed the action network between QTLs and traits (Figure 3D). The locus 3, 6 and 17 had higher connectivity, which were the ideal gene donor for direct seeding rice breeding. In summary, these QTLs will help us efficiently select rice varieties suitable for direct seeding.

## Screening materials that pyramid elite alleles

In general, some degree of transgressive segregation may occur in progeny due to elite parental alleles that sufficiently recombined in offspring. We determined the source of the elite alleles according to their additive effect value. The distribution of these 20 loci in individual RILs was analyzed in detail (Table S4 and Figure S3). Most individuals harbored six to ten elite alleles. The fewest harbored only one elite allele, and the most harbored up to 16 favorable alleles. Combined with the phenotypes across both seasons, we selected five RILs (G289, G379, G403, G430 and G454) that exhibited excellent phenotypes and that can serve as favorable alleles donor parents during breeding process.

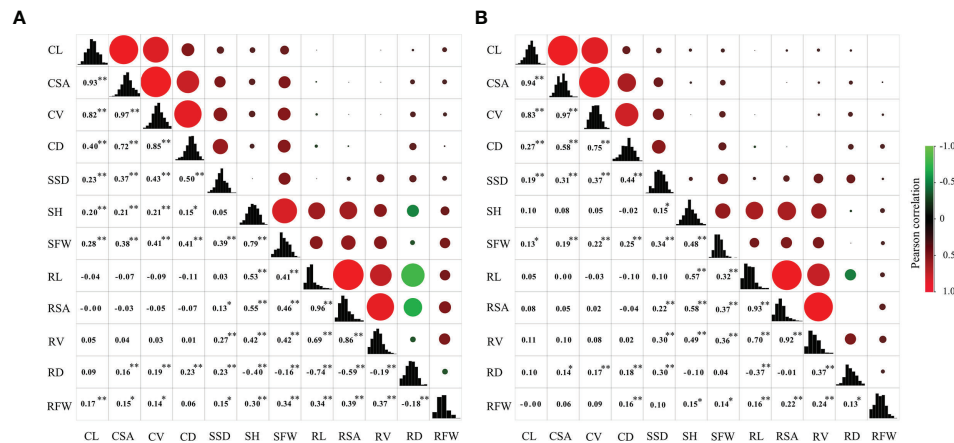


FIGURE 2

Correlation coefficients among 12 traits at the germination and bud stages under anaerobic stress in the RIL population. In the upper panel, the size of circle and depth of shading indicate magnitude of correlations. Negative correlations are colored green, and positive correlations are colored red. Lower panel contains correlation coefficients, and \* and \*\* represent significance at 0.05 and 0.01, respectively. The diagonal represents frequency distribution of 12 traits. (A) wet season; (B) dry season.

## Identification of the candidate genes from reliable locus

Among 20 loci we detected, locus 3 was implicated by multiple traits in both environments. In addition, locus 3 affects traits at both the germination and bud stages (Figure 4A). Notably, although it overlapped with previous reports (Jiang et al., 2004; Wang, 2009; Septiningsih et al., 2013), but no candidate genes were identified. To confirm the contributions of locus 3, present study summarize the phenotypic differences among two alleles of every QTL, and results illustrated that the phenotypic variations between two alleles were extremely significant within population ( $p \leq 0.01$ ) (Figures 4C-E). Therefore, we believe that locus 3 is very reliable and is valuable for further research and utilization.

Within the locus 3 interval (26,713,837 to 27,333,897 bp) on chromosome 2 (Figure 4B), 103 genes (Table S5) were identified from MSU Rice Genome Annotation Project database of version 7. To reduce number of candidate genes, we take benefit of three earlier expression profiles reported that were obtained from cultivars with respect to the aerobic and an anoxic germination (Lasanthi-Kudahettige et al., 2007; Narsai et al., 2009; Hsu and Tung, 2017). Based on gene differential expression multiples and the gene annotation, we focused on four candidate genes: *expansin precursor* (LOC\_Os02g44108), *trehalose-6-phosphate phosphatase* (*OsTPP1*, LOC\_Os02g44230), and two *LTPL113-Protease inhibitor/seed storage/LTP family protein precursor* (LOC\_Os02g44310 and LOC\_Os02g44320).

To examine the expression patterns of these four candidate genes in our materials, we chose eight RILs with contrasting phenotypic performances on SSD and CD (tolerant lines

carrying H335 marker type alleles: G406, G484, G510, and G544; sensitive lines carrying CHA-1 marker type alleles: G323, G338, G407, and G494). The qRT-PCR was carried out using total RNA isolated from the tissues (seeds + seedlings) of treated four-day-old seeds at the germination stage and bud stage, respectively (Figure 5). Notably, the expression level of LOC\_Os02g44230 (*OsTPP1*) was sharply upregulated in submerged plants for four tolerant RILs at both the germination and bud stage. However, the expression level of *OsTPP1* was almost unchanged in the four sensitive RILs and was not induced by anaerobic conditions.

## Discussion

### Using a RIL population to develop a high-density bin map could enhance the efficiency of genetic analyses of quantitative traits in rice

Mapping populations can be divided into temporary populations and permanent populations depending on the homozygosity. Temporary populations, for example,  $F_2$  population, is highly genetically diverse, but they cannot produce repeated observations. In addition, due to the complexity of the genetic background, the positioning of the QTL effect and location accuracy were low, which was suitable for the positioning of only major genes. Permanent populations, for example, RIL population, can produce repeated observations and can reduce the complexity of the genetic background. The location and effects of QTLs can be well estimated (Yin, 2015).

TABLE 3 QTLs that are associated with anaerobic tolerance at the germination and bud stages and that were detected in the RIL population.

| Locus    | QTL            | Env <sup>a</sup> | Chr. <sup>b</sup> | Marker interval       | Physical interval (bp) | LOD <sup>c</sup> | PVE (%) <sup>d</sup> | ADD <sup>e</sup> | Known loci  |
|----------|----------------|------------------|-------------------|-----------------------|------------------------|------------------|----------------------|------------------|---|
| Locus 1  | <i>qRL-2</i>   | DS               | 2                 | Block3371-Block3403   | 19,434,165-20,120,087  | 5.48             | 8.63                 | -0.7003          |   |
| Locus 2  | <i>qCV-2</i>   | WS               | 2                 | Block3775-Block3787   | 25,220,799-25,376,516  | 4.74             | 7.40                 | 0.3058           | ( <i>qAG-2</i> , Jiang et al., 2004)  |
|          | <i>qCSA-2</i>  | WS               | 2                 | Block3780-Block3787   | 25,304,101-25,376,516  | 4.31             | 6.61                 | 0.0154           |   |
| Locus 3  | <i>qSSD-2</i>  | WS               | 2                 | Block3943-Block3970   | 26,713,837-27,333,897  | 6.58             | 10.89                | 0.0162           | ( <i>qAG-2</i> , Jiang et al., 2004; <i>qSAT-2-B</i> , Wang, 2009; <i>qAG2</i> , Septiningsih et al., 2013) |
|          | <i>qSSD-2</i>  | DS               | 2                 | Block3943-Block3970   | 26,713,837-27,333,897  | 3.86             | 6.77                 | 0.0121           |   |
|          | <i>qCD-2-1</i> | DS               | 2                 | Block3943-Block3968   | 26,713,837-27,298,326  | 6.73             | 9.35                 | 0.0094           |   |
| Locus 4  | <i>qCD-2-2</i> | WS               | 2                 | Block3988-Block3998   | 27,829,823-27,932,432  | 6.60             | 11.28                | 0.0092           | ( <i>qAG-2</i> , Jiang et al., 2004 <i>qSAT-2-B</i> , Wang, 2009; <i>qAG2</i> , Septiningsih et al., 2013)  |
|          | <i>qSFW-2</i>  | WS               | 2                 | Block3988-Block3998   | 27,829,823-27,932,432  | 4.07             | 7.46                 | 0.0007           |   |
| Locus 5  | <i>qCD-3-1</i> | DS               | 3                 | Block5779-Block5782   | 26,642,814-26,700,736  | 8.60             | 12.17                | 0.0108           |   |
| Locus 6  | <i>qCD-3-2</i> | WS               | 3                 | Block6004-Block6012   | 31,084,034-31,304,364  | 4.60             | 7.66                 | 0.0076           |   |
|          | <i>qCSA-3</i>  | WS               | 3                 | Block6009-Block6012   | 31,220,745-31,304,364  | 4.63             | 7.00                 | 0.0160           |   |
|          | <i>qCV-3</i>   | WS               | 3                 | Block6009-Block6012   | 31,220,745-31,304,364  | 5.81             | 9.14                 | 0.3425           |   |
| Locus 7  | <i>qCD-4-1</i> | WS               | 4                 | Block6696-Block6755   | 5,559,903-6,480,536    | 3.51             | 5.88                 | 0.0067           |   |
|          | <i>qCD-4-1</i> | DS               | 4                 | Block6696-Block6755   | 5,559,903-6,480,536    | 5.73             | 7.91                 | 0.0086           |   |
| Locus 8  | <i>qRSA-4</i>  | WS               | 4                 | Block8028-Block8047   | 29,345,642-29,819,706  | 2.75             | 4.63                 | -0.0231          |   |
|          | <i>qRV-4</i>   | WS               | 4                 | Block8028-Block8047   | 29,345,642-29,819,706  | 3.19             | 5.26                 | -0.2099          |   |
| Locus 9  | <i>qCD-4-2</i> | DS               | 4                 | Block8102-Block8143   | 30,576,597-31,111,423  | 2.51             | 3.36                 | 0.0056           |   |
| Locus 10 | <i>qCV-5</i>   | WS               | 5                 | Block9860-Block9980   | 23,685,519-27,654,405  | 2.50             | 4.21                 | 0.0068           |   |
| Locus 11 | <i>qCL-6</i>   | DS               | 6                 | Block11298-Block11400 | 25,197,786-26,333,712  | 2.55             | 3.34                 | 0.0683           |   |
|          | <i>qCSA-6</i>  | DS               | 6                 | Block11298-Block11400 | 25,197,786-26,333,712  | 2.85             | 4.37                 | 0.0154           |   |
| Locus 12 | <i>qRD-6</i>   | DS               | 6                 | Block11313-Block11557 | 25,541,908-28,811,647  | 3.18             | 5.65                 | 0.0104           |   |
| Locus 13 | <i>qCSA-7</i>  | DS               | 7                 | Block12037-Block12088 | 11,776,612-13,217,331  | 3.90             | 5.99                 | 0.0180           | ( <i>qAG7-1</i> , Angaji et al., 2010)  |
|          | <i>qCV-7</i>   | DS               | 7                 | Block12037-Block12088 | 11,776,612-13,217,331  | 4.12             | 6.68                 | 0.3275           |   |
| Locus 14 | <i>qCD-7</i>   | DS               | 7                 | Block12247-Block12295 | 16,999,393-17,785,826  | 3.32             | 4.49                 | 0.0065           | ( <i>qAG7.2</i> , Septiningsih et al., 2013; <i>qAG7</i> , Baltazar et al., 2014; Hsu and Tung, 2015)       |
| Locus 15 | <i>qSH-7</i>   | DS               | 7                 | Block12476-Block12480 | 22,965,779-23,064,070  | 2.99             | 4.08                 | 0.1625           |   |
| Locus 16 | <i>qCL-8</i>   | DS               | 8                 | Block12756-Block12814 | 714,151-2,466,683      | 3.22             | 4.23                 | -0.0776          |   |
| Locus 17 | <i>qCSA-8</i>  | WS               | 8                 | Block13087-Block13127 | 5,429,796-6,001,857    | 2.94             | 4.41                 | -0.0127          | ( <i>qSAT-8-B</i> , Wang, 2009; <i>qGS8</i> , Chen et al., 2012; Hsu and Tung, 2015)                        |

(Continued)



TABLE 3 Continued

| Locus    | QTL            | Env <sup>a</sup> | Chr. <sup>b</sup> | Marker interval       | Physical interval (bp) | LOD <sup>c</sup> | PVE (%) <sup>d</sup> | ADD <sup>e</sup> | Known loci |
|----------|----------------|------------------|-------------------|-----------------------|------------------------|------------------|----------------------|------------------|------------|
|          | <i>qCSA-8</i>  | DS               | 8                 | Block13087-Block13127 | 5,429,796-6,001,857    | 3.14             | 4.80                 | -0.0163          |            |
|          | <i>qCV-8</i>   | WS               | 8                 | Block13087-Block13127 | 5,429,796-6,001,857    | 2.67             | 4.09                 | -0.2291          |            |
|          | <i>qCV-8</i>   | DS               | 8                 | Block13087-Block13127 | 5,429,796-6,001,857    | 3.09             | 4.97                 | -0.2855          |            |
| Locus 18 | <i>qSSD-8</i>  | DS               | 8                 | Block13593-Block13899 | 15,856,708-18,183,642  | 2.54             | 4.41                 | -0.0097          |            |
| Locus 19 | <i>qRL-10</i>  | DS               | 10                | Block16606-Block16617 | 4,481,303-4,549,204    | 7.62             | 11.18                | -1.0452          |            |
| Locus 20 | <i>qSH-10</i>  | DS               | 10                | Block16658-Block16661 | 4,917,750-4,985,707    | 4.12             | 5.68                 | -0.1928          |            |
|          | <i>qRSA-10</i> | DS               | 10                | Block16658-Block16661 | 4,917,750-4,985,707    | 4.50             | 4.05                 | -0.0928          |            |

<sup>a</sup>Env., WS is wet season in 2017; DS is dry season in 2017.

<sup>b</sup>Chr., chromosome.

<sup>c</sup>LOD, logarithm of odds.

<sup>d</sup>PVE (%), phenotypic variation explained (%).

<sup>e</sup>ADD, additive effect; positive values indicate the superiority of H335.

The ability of rice seeds to develop into anaerobic seedlings is a quantitative trait. Therefore, a RIL population is an ideal mapping population. In our study, we constructed a RIL population, and this population will help us to identify more genetic loci effectively.

QTL mapping resolution depends on both density of marker and mapping population size (Da et al., 2000). Usually, the markers increasing density is an efficient approach to enhance the QTL mapping resolution (Liu et al., 2008). High-throughput resequencing strategies are currently being used to map QTLs accurately. In this experiment, map of high density for RIL population was constructed *via* the GBS strategy and was utilized for the QTL mapping in rice. Mean physical distance among two markers was 149.38 kb, and the smallest physical QTL interval was approximately 50 kb (Table 3). Compared with that in previous QTL mapping results concerning AG ability through restriction fragment length polymorphism (RFLP) or by the simple sequence repeat (SSR) markers, this distance has been narrowed significantly (Jiang et al., 2006; Angaji, 2008; Angaji et al., 2010; Septiningsih et al., 2013; Manangkil et al., 2013). The results confirmed that, compared with the use of traditional markers, GBS has significantly increased the QTL mapping resolution.

## Additional indicators should be developed for the estimation of anaerobic seedling establishment

Few studies have evaluated genetic loci known to be associated with anaerobic seedling establishment. One of the

main reasons for this is that researchers have focused only on two traits directly related to anaerobic seedling establishment. The first trait is the rate of seedling survival after twenty one days submerged under the 10 or 20 cm of water. This was a technique developed by the International Institute of Rice Research (Angaji et al., 2010). The second trait is coleoptile elongation under anaerobic conditions. In previous studies on QTL mapping with these two indicators, some of the genetic loci identified overlapped with each other (Hsu and Tung, 2015; Zhang et al., 2017). The results indicate that these two indicators are reasonable. In present research, traits of coleoptile were validated by QTL mapping (Table 3). While, two loci were detected for CL, 18 loci were detected for CV, CSA, and CD. Notably, some genetic loci obtained using CSA, CV, CD, SSD and SFW overlapped with the previously reported using survival rate (Table 3). These results indicate that our indicators are feasible and that more high-efficiency indicators are necessary.

The ability of rice seeds to develop into anaerobic seedlings is a complex trait. It is well known that, in the process of anaerobic seedling establishment, both survival rate and the quality of the surviving seedlings are traits that should receive attention. However, neither survival rate nor coleoptile elongation are indicators that have directly and effectively been used to evaluate the quality of the surviving seedlings. Notably, seeds whose shoot length was approximately 3 mm were treated with anaerobic conditions, can successfully grew roots and leaves. In addition, many farmers prefer pregermination before sowing, indicating that the ability to survive and grow under anaerobic conditions at the bud stage is also critical. Therefore, seeds whose shoots were approximately 3 mm in length were treated with anaerobic conditions, which can help us evaluate relatively

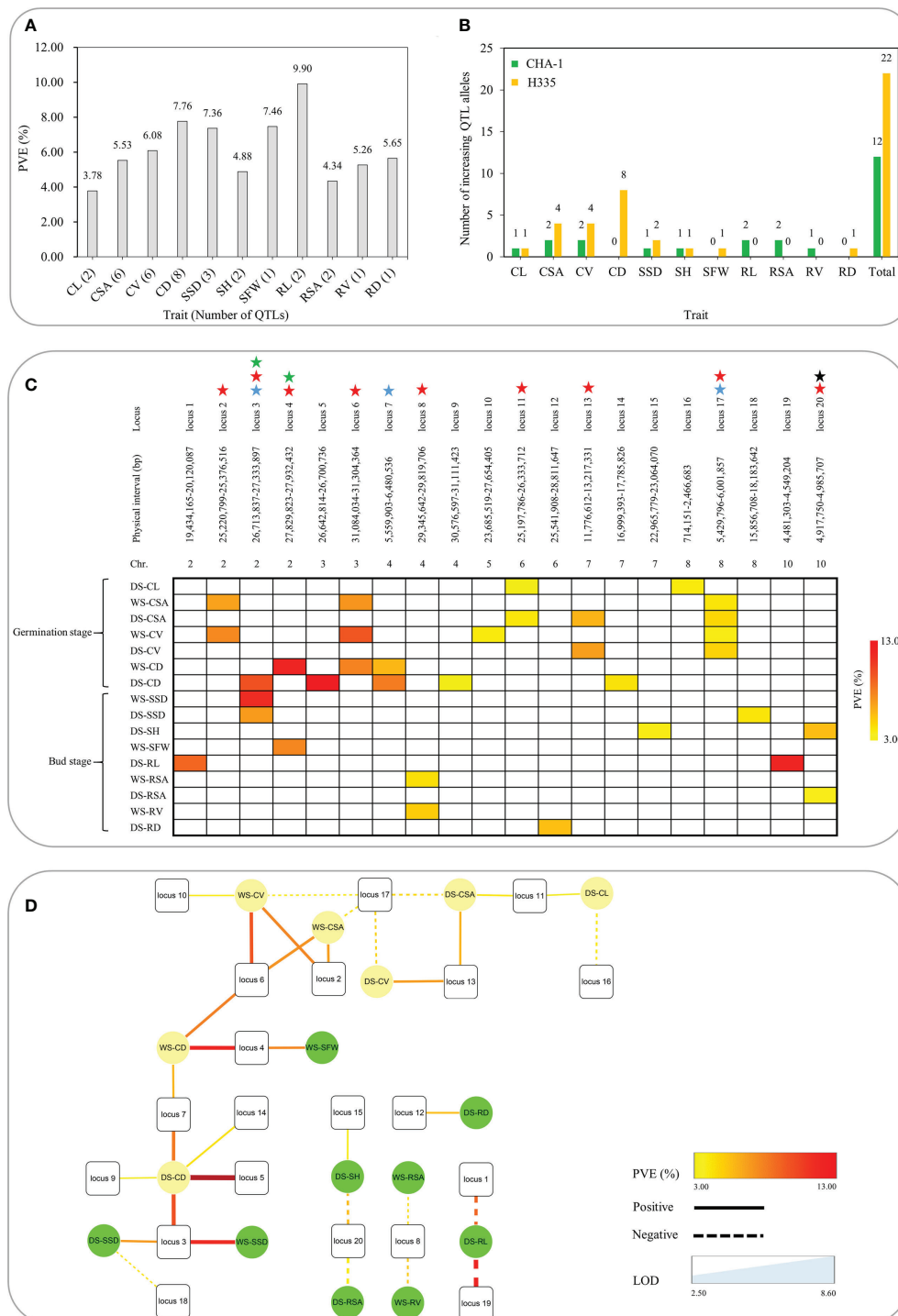
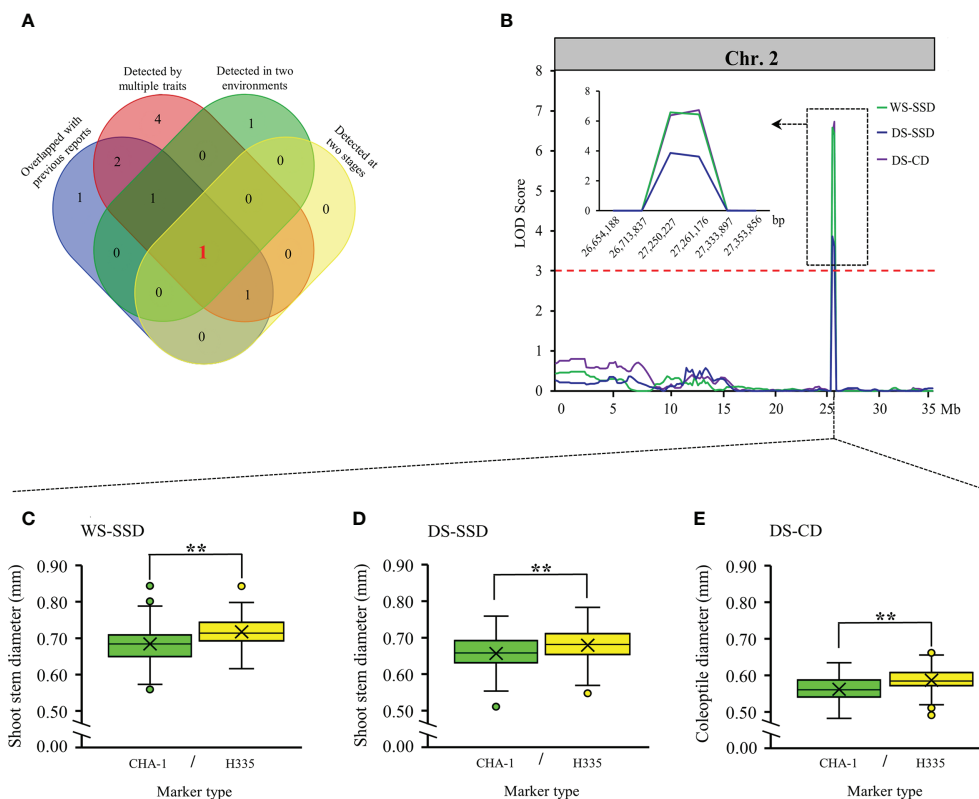


FIGURE 3

Summary of 20 loci associated with 11 traits related to anaerobic tolerance. **(A)** Phenotypic contribution rates of QTLs associated with 11 traits. **(B)** Number of increasing QTL alleles in various traits contributed by parents. **(C)** Heat map reveals pleiotropy of various QTLs. The different colors shown in the legend correspond to various levels of explanation of phenotypic variation. The blue star means detected in both seasons, the red star represents the simultaneous influence of multiple traits, the black star represents the trait that affects both shoots and roots for bud growth, and the green star indicates that both seed germination and bud growth are affected. **(D)** The interaction network of different traits and QTLs. The square represents locus, the circle represents trait; the dotted line represents the negative effect, the solid line represents the positive effect; the thickness of the line represents the LOD value, and the color of the line represents the PVE.



**FIGURE 4**  
Validation of reliable loci. **(A)** Venn diagrams showing unique and shared criteria for QTLs detected in our study. **(B)** locus 3 located on chromosome 2 identified by linkage analysis. The box shows a magnification of the QTL candidate interval region on chromosome 2. **(C-E)** Boxplots showing the distribution of phenotypic differences between the two alleles of locus 3. Differences between the genotypes were analyzed using Student's t-test, \*\* represents significance at the 0.01 level.

more phenotypes and represents conditions that are close to those of actual production.

## Different genetic mechanisms control anaerobic tolerance at germination stage and bud stage in the rice

In previous studies, we did not observe the emergence of genetic loci in mapping studies associated to anaerobic tolerance at bud stage. In our preliminary experiment, seeds at the pigeon breast stage or those whose shoot length was approximately 1 mm were treated with anaerobic treatment, just as the seeds without pre germination were treated directly. The final length of the rice coleoptiles under anaerobic conditions exceeded that of the rice coleoptiles under aerobic conditions, while the roots and primary leaves failed to grow. However, when rice seeds whose shoot length was approximately 3 mm were selected for anaerobic treatment, we observed the growth of roots and leaves. Of course, compared with that under aerobic conditions, the growth of buds and roots under anaerobic conditions was inhibited. In addition, among the 20 loci

we detected, only locus 3 and 4 were detected at germination and bud stages. Present findings revealed that the genetic mechanisms of anaerobic tolerance at germination and bud stage are different. With respect to anaerobic tolerance, locus 3 and 4 were identified at various stages, revealing that there may be an overlap between metabolic pathways of anaerobic tolerance at various stages of rice.

## Considerable evidence suggests that *OsTPP1* might involved in mediating the variations in anaerobic seedling establishment ability

Kretschmar et al. (2015) find T6P phosphatase gene, *OsTPP7*, fine mapping within *qAG-9-2* (Angaji et al., 2010), a key QTL for AG tolerance. *OsTPP7* is involved in metabolism of T6P, which is central to the energy sensor which determine catabolism or anabolism depending on the availability of local sucrose (Paul, 2008; Zhang et al., 2009). By representing low availability of sugar via enhanced T6P turnover, *OsTPP7* activity might increased the sink strength in the proliferating heterotrophic

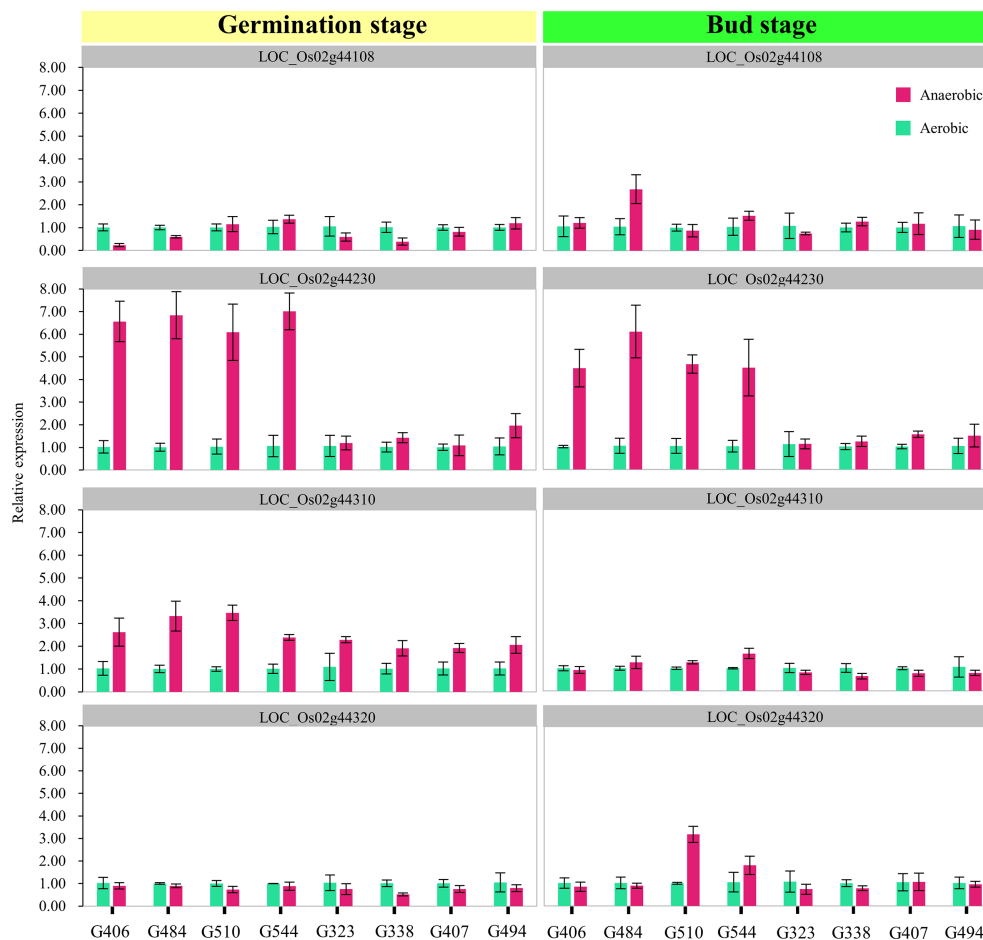


FIGURE 5

Expression analysis of candidate genes. The expression levels of four candidate genes in tissues (seeds + seedlings) of treated four-day-old seeds at the germination stage and bud stage respectively were measured using quantitative RT-PCR. The x-axis lists the eight genotypes whose phenotypes contrast (tolerant lines carrying H335 marker type alleles: G406, G484, G510, and G544; sensitive lines carrying CHA-1 marker type alleles: G323, G338, G407, and G494). The magenta and dark green boxes represent the control and submerged samples, respectively. The error bars correspond to the standard deviations (n = 3).

tissues, thus increasing starch mobilization to drive the kinetics of growth in germinating embryo and elongating coleoptile, which as a result enhances AG tolerance (Kretzschmar et al., 2015).

In the yeast and microbes, trehalose produced from glucose by the enzymes i.e., trehalose-6-phosphate synthase (TPS) and trehalose-6-phosphate phosphatase (TPP) works as metabolic regulator, sugar storage molecule and offers protection against abiotic stress (Wiemken, 1990; Strom and Kaasen, 1993). Thirteen *TREHALOSE-6-PHOSPHATE PHOSPHATASE* (TPP)-like genes are present in the rice (Ge et al., 2008), of which the products of *OsTPP1* and *OsTPP2* have reported to convert T6P to trehalose (Shima et al., 2007). In addition, *OsTPP1* over expression in the rice enhances tolerance to cold and salt stress (Ge et al., 2008). In particular, a recent study showed that *OsTPP1* regulates seed germination by crosstalk with abscisic acid in the rice (Wang et al., 2021). In our study, *OsTPP1* was derived from a genetic site that had a

relatively high contribution rate and reliability. Expression analysis demonstrated that expression of *OsTPP1* was significantly induced by the anaerobic environment during both the germination and bud stages. Based on this evidence, we speculate that *OsTPP1* may be one of a main factors influencing the phenotypic changes in our RIL population. This might be engaged in mediating the variations in anaerobic seedling establishment.

## Conclusion

In our study, using the GBS approach, we developed a RIL population along with the construction of a map of genetic linkage having an average of 0.95 cM genetic distance among adjacent markers. Genetic mapping of quantitative traits was performed for 12 traits related to anaerobic seedling establishment at germination

as well as bud stage during both the cropping seasons, a total of 20 loci were obtained. Among them, locus 3 was highly reliable and valuable for fine mapping. Within the interval, by combining gene annotation and expression analysis data, we found a promising candidate gene, *OsTPP1*. Present findings are useful for increasing our understanding of the genetic mechanism of anaerobic seedling establishment.

## Data availability statement

The data presented in the study are deposited in the Sequence Read Archive database ([www.ncbi.nlm.nih.gov/sra](http://www.ncbi.nlm.nih.gov/sra)) at NCBI (National Center for Biotechnology Information), accession number PRJNA857157. The names of the repository/repositories and accession number(s) can be found in the article/[Supplementary Material](#).

## Author contributions

HW, SF and JL designed the project, and JY performed all the experiments and wrote the manuscript. JW, JX, YX and GD assisted in conducting the experiments and analyzing the data. HW, SF and JY provided the direction for the study and the corrections of the manuscript. All authors contributed to the article and approved the submitted version.

## Funding

This research was funded by the grant from the Yunnan Fundamental Research Project (Grant No. 202201AU070059,

202201AT070034, 202201AT070150) and the scientific research fund project of Yunnan Provincial Department of Education (Grant No. 2022J0134). The funding agency had no input into experimental design, the conduct of the research or the analysis, interpretation of experimental results and in writing the manuscript.

## Conflict of interest

The authors declare that the research was conducted in the absence of any commercial or financial relationships that could be construed as a potential conflict of interest.

## Publisher's note

All claims expressed in this article are solely those of the authors and do not necessarily represent those of their affiliated organizations, or those of the publisher, the editors and the reviewers. Any product that may be evaluated in this article, or claim that may be made by its manufacturer, is not guaranteed or endorsed by the publisher.

## Supplementary material

The Supplementary Material for this article can be found online at: <https://www.frontiersin.org/articles/10.3389/fpls.2022.985080/full#supplementary-material>

## References

- Angaji, S. A. (2008). Mapping QTLs for submergence tolerance during germination in rice. *Afr. J. Biotechnol.* 7, 2551–2558.
- Angaji, S. A., Septiningsih, E. M., Mackill, D. J., and Ismail, A. M. (2010). QTLs associated with tolerance of flooding during germination in rice (*Oryza sativa* L.). *Euphytica* 172, 159–168. doi: 10.1007/s10681-009-0014-5
- Atwell, B. J., Waters, I., and Greenway, H. (1982). The effect of oxygen and turbulence on elongation of coleoptiles of submergence-tolerant and-intolerant rice cultivars. *J. Exp. Bot.* 33, 1030–1044. doi: 10.1093/jxb/33.5.1030
- Baltazar, M. D., Ignacio, J. C. I., Thomson, M. J., Ismail, A. M., Mendioro, M. S., and Septiningsih, E. M. (2014). QTL mapping for tolerance of anaerobic germination from IR64 and the *aus* landrace nanhi using SNP genotyping. *Euphytica* 197, 251–260. doi: 10.1007/s10681-014-1064-x
- Baltazar, M. D., Ignacio, J. C. I., Thomson, M. J., Ismail, A. M., Mendioro, M. S., and Septiningsih, E. M. (2019). QTL mapping for tolerance to anaerobic germination in rice from IR64 and the *aus* landrace kharsu 80A. *Breed. Sci.* 69, 227–233. doi: 10.1270/jsbbs.18159
- Broman, K. W., Wu, H., Sen, S., and Churchill, G. A. (2003). R/qtl: QTL mapping in experimental crosses. *Bioinformatics* 19, 889–890. doi: 10.1093/bioinformatics/btg112
- Chauhan, B. S., and Johnson, D. E. (2010). Relative importance of shoot and root competition in dry-seeded rice growing with junglerice (*Echinochloa colona*) and ludwigia (*Ludwigia hyssopifolia*). *Weed Sci.* 58, 295–299. doi: 10.1614/WS-D-09-00068.1
- Chen, S., Wang, J., Pan, Y., Ma, J., Zhang, J., Zhang, H., et al. (2012). Genetic analysis of seed germinability under submergence in rice. *Chin. Bull. Botany* 47, 28–35. doi: 10.3724/SP.J.1259.2012.00028
- Da, Y., VanRaden, P. M., and Schook, L. B. (2000). Detection and parameter estimation for quantitative trait loci using regression models and multiple markers. *Genet. Sel. Evol.* 32, 357–381. doi: 10.1186/1297-9686-32-4-357
- Gao, H., Zhang, C., He, H., Liu, T., Zhang, B., Lin, H., et al. (2020). Loci and alleles for submergence responses revealed by GWAS and transcriptional analysis in rice. *Mol. Breed.* 40, 1–16. doi: 10.1007/s11032-020-01160-6
- Ge, L., Chao, D., Shi, M., Zhu, M., Gao, J., and Lin, H. (2008). Overexpression of the trehalose-6-phosphate phosphatase gene *OsTPP1* confers stress tolerance in rice and results in the activation of stress responsive genes. *Planta* 228, 191–201. doi: 10.1007/s00425-008-0729-x
- Ghosal, S., Casal, C., Quilloy, F. A., Septiningsih, E. M., Mendioro, M. S., and Dixit, S. (2019). Deciphering genetics underlying stable anaerobic germination in rice: phenotyping, QTL identification, and interaction analysis. *Rice* 12, 1–15. doi: 10.1186/s12284-019-0305-y
- Guglielminetti, L., Perata, P., and Alpi, A. (1995). Effect of anoxia on carbohydrate metabolism in rice seedlings. *Plant Physiol.* 108, 735–741. doi: 10.1104/pp.108.2.735



- Hong, Y., Ho, T. D., Wu, C., Ho, S., Yeh, R., Lu, C., et al. (2012). Convergent starvation signals and hormone crosstalk in regulating nutrient mobilization upon germination in cereals. *Plant Cell*. 24, 2857–2873. doi: 10.1105/tpc.112.097741
- Hsu, S., and Tung, C. (2015). Genetic mapping of anaerobic germination-associated QTLs controlling coleoptile elongation in rice. *Rice* 8, 38. doi: 10.1186/s12284-015-0072-3
- Hsu, S., and Tung, C. (2017). RNA-Seq analysis of diverse rice genotypes to identify the genes controlling coleoptile growth during submerged germination. *Front. Plant Sci.* 8. doi: 10.3389/fpls.2017.00762
- Huang, X., Feng, Q., Qian, Q., Zhao, Q., Wang, L., Wang, A., et al. (2009). High-throughput genotyping by whole-genome resequencing. *Genome Res.* 19, 1068–1076. doi: 10.1101/gr.089516.108
- Hwang, Y. S., Thomas, B. R., and Rodriguez, R. L. (1999). Differential expression of rice  $\alpha$ -amylase genes during seedling development under anoxia. *Plant Mol. Biol.* 40, 911–920. doi: 10.1023/a:1006241811136
- Ismail, A. M., Ella, E. S., Vergara, G. V., and Mackill, D. J. (2009). Mechanisms associated with tolerance to flooding during germination and early seedling growth in rice (*Oryza sativa*). *Ann. Bot.* 103, 197–209. doi: 10.1093/aob/mcn211
- Jackson, M. B. (2008). Ethylene-promoted elongation: An adaptation to submergence stress. *Ann. Bot.* 101, 229–248. doi: 10.1093/aob/mcm237
- Jiang, L., Hou, M., Wang, C., and Wan, J. (2004). Quantitative trait loci and epistatic analysis of seed anoxia germinability in rice (*Oryza sativa*). *Rice Sci.* 11, 238–244.
- Jiang, L., Liu, S., Hou, M., Tang, J., Chen, L., Zhai, H., et al. (2006). Analysis of QTLs for seed low temperature germinability and anoxia germinability in rice (*Oryza sativa* L.). *Field Crop Res.* 98, 68–75. doi: 10.1016/j.fcr.2005.12.015
- Kim, S., and Reinke, R. (2018). Identification of QTLs for tolerance to hypoxia during germination in rice. *Euphytica* 214, 160. doi: 10.1007/s10681-018-2238-8
- Kong, W., Li, S., Zhang, C., Qiang, Y., and Li, Y. (2022). Combination of quantitative trait locus (QTL) mapping and transcriptome analysis reveals submerged germination QTLs and candidate genes controlling coleoptile length in rice. *Food Energy Secur.* 11, e354. doi: 10.1002/fes3.354
- Kretschmar, T., Pelayo, M. A. F., Trijatmiko, K. R., Gabunada, L. F. M., Alam, R., Jimenez, R., et al. (2015). A trehalose-6-phosphate phosphatase enhances anaerobic germination tolerance in rice. *Nat. Plants* 1, 15124. doi: 10.1038/nplants.2015.124
- Lasanthi-Kudahettige, R., Magneschi, L., Loreti, E., Gonzali, S., Licausi, F., Novi, G., et al. (2007). Transcript profiling of the anoxic rice coleoptile. *Plant Physiol.* 144, 218–231. doi: 10.1104/pp.106.093997
- Li, H., Handsaker, B., Wysoker, A., Fennell, T., Ruan, J., Homer, N., et al. (2009). The sequence Alignment/Map format and SAMtools. *Bioinformatics* 25, 2078–2079. doi: 10.1093/bioinformatics/btp352
- Liu, X., Zhang, H., Li, H., Li, N., Zhang, Y., Zhang, Q., et al. (2008). Fine-mapping quantitative trait loci for body weight and abdominal fat traits: Effects of marker density and sample size. *Poultry Sci.* 87, 1314–1319. doi: 10.3382/ps.2007-00512
- Loreti, E., van Veen, H., and Perata, P. (2016). Plant responses to flooding stress. *Curr. Opin. Plant Biol.* 33, 64–71. doi: 10.1016/j.pbi.2016.06.005
- Mahender, A., Anandan, A., and Pradhan, S. K. (2015). Early seedling vigour, an imperative trait for direct-seeded rice: an overview on physio-morphological parameters and molecular markers. *Planta* 241, 1027–1050. doi: 10.1007/s00425-015-2273-9
- Manangkil, O. E., Vu, H. T. T., Mori, N., Yoshida, S., and Nakamura, C. (2013). Mapping of quantitative trait loci controlling seedling vigor in rice (*Oryza sativa* L.) under submergence. *Euphytica* 192, 63–75. doi: 10.1007/s10681-012-0857-z
- Manigbas, N. L., Solis, R. O., Barroga, W. V., Noriel, A. J., Arocena, E. C., Padolina, T. F., et al. (2008). Development of screening methods for anaerobic germination and seedling vigor in direct wet-seeded rice culture. *Philipp. J. Crop Sci.* 33, 34–44.
- Meng, L., Li, H., Zhang, L., and Wang, J. (2015). QTL IciMapping: Integrated software for genetic linkage map construction and quantitative trait locus mapping in biparental populations. *Crop J.* 3, 269–283. doi: 10.1016/j.cj.2015.01.001
- Narsai, R., Howell, K. A., Carroll, A., Ivanova, A., Millar, A. H., and Whelan, J. (2009). Defining core metabolic and transcriptomic responses to oxygen availability in rice embryos and young seedlings. *Plant Physiol.* 151, 306–322. doi: 10.1104/pp.109.142026
- Paul, M. J. (2008). Trehalose 6-phosphate: a signal of sucrose status. *Biochem. J.* 412, e1–e2. doi: 10.1042/BJ20080598
- Rao, A. N., Johnson, D. E., Sivaprasad, B., Ladha, J. K., and Mortimer, A. M. (2007). Weed management in direct-seeded rice. *Adv. Agron.* 93, 153–255. doi: 10.1016/S0065-2113(06)93004-1
- Septingsih, E. M., Ignacio, J. C. I., Sendon, P. M. D., Sanchez, D. L., Ismail, A. M., and Mackill, D. J. (2013). QTL mapping and confirmation for tolerance of anaerobic conditions during germination derived from the rice landrace ma-zhan red. *Theor. Appl. Genet.* 126, 1357–1366. doi: 10.1007/s00122-013-2057-1
- Shibaya, T., Hori, K., Ogiso-Tanaka, E., Yamanouchi, U., Shu, K., Kitazawa, N., et al. (2016). *Hd18*, encoding histone acetylase related to arabidopsis FLOWERING LOCUS d, is involved in the control of flowering time in rice. *Plant Cell Physiol.* 57, 1828–1838. doi: 10.1093/pcp/pcw105
- Shima, S., Matsui, H., Tahara, S., and Imai, R. (2007). Biochemical characterization of rice trehalose-6-phosphate phosphatases supports distinctive functions of these plant enzymes. *FEBS J.* 274, 1192–1201. doi: 10.1111/j.1742-4658.2007.05658.x
- Smoot, M. E., Ono, K., Ruschinski, J., Wang, P., and Ideker, T. (2011). Cytoscape 2.8: new features for data integration and network visualization. *Bioinformatics* 27, 431–432. doi: 10.1093/bioinformatics/btq675
- Strom, A. R., and Kaasen, I. (1993). Trehalose metabolism in *Escherichia coli*: stress protection and stress regulation of gene expression. *Mol. Microbiol.* 8, 205–210. doi: 10.1111/j.1365-2958.1993.tb01564.x
- Su, L., Yang, J., Li, D., Peng, Z., Xia, A., Yang, M., et al. (2021). Dynamic genome-wide association analysis and identification of candidate genes involved in anaerobic germination tolerance in rice. *Rice* 14, 1. doi: 10.1186/s12284-020-00444-x
- Wang, Y. (2009). Screening of germplasm adaptable to direct seeding and discovery of favorable alleles for seed vigor and seedling anoxic tolerance in rice (*Oryza sativa* L.) (Nanjing Agricultural University).
- Wang, G., Li, X., Ye, N., Huang, M., Feng, L., Li, H., et al. (2021). *OsTPP1* regulates seed germination through the crosstalk with abscisic acid in rice. *New Phytol.* 230, 1925–1939. doi: 10.1111/nph.17300
- Wiemken, A. (1990). Trehalose in yeast, stress protectant rather than reserve carbohydrate. *Antonie Van Leeuwenhoek*. 58, 209–217. doi: 10.1007/BF00548935
- Xie, W., Feng, Q., Yu, H., Huang, X., Zhao, Q., Xing, Y., et al. (2010). Parent-independent genotyping for constructing an ultrahigh-density linkage map based on population sequencing. *Proc. Natl. Acad. Sci. U.S.A.* 107, 10578–10583. doi: 10.1073/pnas.1005931107
- Yamauchi, M., Aguilar, A. M., Vaughan, D. A., and Seshu, D. V. (1993). Rice (*Oryza sativa* L.) germplasm suitable for direct sowing under flooded soil surface. *Euphytica* 67, 177–184. doi: 10.1007/BF00040619
- Yamauchi, M., and Biswas, J. K. (1997). Rice cultivar difference in seedling establishment in flooded soil. *Plant Soil*. 189, 145–153. doi: 10.1023/A:1004250901931
- Yang, J., Sun, K., Li, D., Luo, L., Liu, Y., Huang, M., et al. (2019). Identification of stable QTLs and candidate genes involved in anaerobic germination tolerance in rice via high-density genetic mapping and RNA-seq. *BMC Genomics* 20, 355. doi: 10.1186/s12864-019-5741-y
- Yin, C. (2015). Development of different types of the indica  $\times$  japonica population and genetic mapping of important quantitative traits in rice (*Oryza sativa* L.) (Chinese Academy of Agricultural Sciences).
- Zhang, M., Lu, Q., Wu, W., Niu, X., Wang, C., Feng, Y., et al. (2017). Association mapping reveals novel genetic loci contributing to flooding tolerance during germination in indica rice. *Front. Plant Sci.* 8. doi: 10.3389/fpls.2017.00678
- Zhang, Y., Primavesi, L. F., Jhureea, D., Andralojc, P. J., Mitchell, R. A. C., Powers, S. J., et al. (2009). Inhibition of SNF1-related protein kinase1 activity and regulation of metabolic pathways by trehalose-6-phosphate. *Plant Physiol.* 149, 1860–1871. doi: 10.1104/pp.108.133934



## OPEN ACCESS

EDITED BY  
Milan Skalicky,  
Czech University of Life Sciences  
Prague, Czechia

REVIEWED BY  
Parvaiz Ahmad,  
Government Degree College,  
Pulwama, India  
Mohammad Shah Jahan,  
Sher-e-Bangla Agricultural  
University, Bangladesh

\*CORRESPONDENCE  
Futian Peng  
pft@sdaue.edu.cn  
Yuansong Xiao  
ysxiao@sdaue.edu.cn

SPECIALTY SECTION  
This article was submitted to  
Plant Abiotic Stress,  
a section of the journal  
Frontiers in Plant Science

RECEIVED 23 August 2022  
ACCEPTED 10 October 2022  
PUBLISHED 21 October 2022

CITATION  
Zhang B, Du H, Sun M, Wu X, Li Y,  
Wang Z, Xiao Y and Peng F (2022)  
Comparison of lauric acid and 12-  
hydroxylauric acid in the alleviation of  
drought stress in peach (*Prunus  
persica* (L.) Batsch).  
*Front. Plant Sci.* 13:1025569.  
doi: 10.3389/fpls.2022.1025569

COPYRIGHT  
© 2022 Zhang, Du, Sun, Wu, Li, Wang,  
Xiao and Peng. This is an open-access  
article distributed under the terms of  
the [Creative Commons Attribution  
License \(CC BY\)](#). The use, distribution  
or reproduction in other forums is  
permitted, provided the original author  
(s) and the copyright owner(s) are  
credited and that the original  
publication in this journal is cited, in  
accordance with accepted academic  
practice. No use, distribution or  
reproduction is permitted which does  
not comply with these terms.

# Comparison of lauric acid and 12-hydroxylauric acid in the alleviation of drought stress in peach (*Prunus persica* (L.) Batsch)

Binbin Zhang, Hao Du, Maoxiang Sun, Xuelian Wu, Yanyan Li, Zhe Wang, Yuansong Xiao\* and Futian Peng\*

College of Horticulture Science and Engineering, Shandong Agricultural University, Taian, China

Water shortage is a key factor that can restrict peach tree growth. Plants produce fatty acids and the fatty acid derivatives lauric acid (LA) and 12-hydroxylauric acid (LA-OH), which are involved in abiotic stress responses, but the underlying stress response mechanisms remain unclear. In this study, physiological examination revealed that in *Prunus persica* (L.) Batsch, pretreatment with 50 ppm LA-OH and LA reduced drought stress, efficiently maintained the leaf relative water content, and controlled the relative conductivity increase. Under drought stress, LA-OH and LA treatments prevented the degradation of photosynthetic pigments, increased the degree of leaf stomatal opening and enhanced the net photosynthetic rate. Compared with drought stress, LA-OH and LA treatment effectively increased the net photosynthetic rate by 204.55% and 115.91%, respectively, while increasing the Fv/Fm by 2.75% and 7.75%, respectively, but NPQ decreased by 7.67% and 37.54%, respectively. In addition, the level of reactive oxygen species increased under drought stress. The content of O<sub>2</sub><sup>-</sup> in LA-OH and LA treatment decreased by 12.91% and 11.24% compared to CK-D, respectively, and the content of H<sub>2</sub>O<sub>2</sub> decreased by 13.73% and 19.94%, respectively. At the same time, the content of malondialdehyde (MDA) decreased by 55.56% and 58.48%, respectively. We believe that the main reason is that LA-OH and LA treatment have improved the activity of superoxide dismutase (SOD), peroxidase (POD), and catalase (CAT). The application of exogenous LA increased the levels of soluble sugars, soluble proteins, proline and free amino acids under drought stress, and maintained the osmotic balance of cells. Compared with CK-D treatment, it increased by 24.11%, 16.89%, 29.3% and 15.04%, respectively. At the same time, the application of exogenous LA-OH also obtained similar results. In conclusion, exogenous LA-OH and LA can alleviate the damage to peach seedlings caused by drought stress by enhancing the photosynthetic and antioxidant capacities, increasing the activities of protective enzymes and regulating the contents of osmotic regulators, but the molecular mechanism is still in need of further exploration.

## KEYWORDS

*Prunus persica* (L.) Batsch, lauric acid, 12-hydroxylauric acid, drought stress, physiological indicators

## Highlights

- Exogenous LA-OH and LA enhanced the photosynthetic and fluorescent properties of drought-stressed leaves.
- LA-OH and LA treatment of *P. persica* could enhance osmoregulation and reduce oxidative stress.
- The equilibrium of reactive oxygen species might be better maintained under drought circumstances after LA-OH and LA pretreatment by increasing antioxidant enzyme activity.
- LA-OH and LA can improve the drought resistance of *P. persica*.

## Introduction

In recent years, with the exacerbation of global climate change and the destruction of the natural environment (Leng and Hall, 2019), drought stress has become common worldwide and is one of the most important factors affecting agricultural yields (Guo et al., 2014; Han et al., 2022). Drought stress directly affects every stage of plant growth and development, from seed emergence to final seed setting, resulting in a series of physiological and biochemical reactions and gene expression changes throughout the plant (Bocchini et al., 2018). The detrimental effects of drought stress on crops include plant growth inhibition, decreased photosynthetic activity, excessive formation of reactive oxygen species, disruption of oxidative metabolism balance, increased damage to membrane lipid peroxidation, and even plant mortality (Caser et al., 2019; Liang et al., 2019; Lozano-Montaña et al., 2021; Sun et al., 2022). Studies have indicated that drought is the most problematic factor exacerbating anthropogenic climate change (Del Buono, 2021). At present, strategies such as breeding and genetic modification are being used for drought (Chukwuneme et al., 2020; Maazou et al., 2016), including soil improvement and enhanced irrigation (Rauf et al., 2016). However, these methods are not very effective, because they not only consume a lot of time, but also have high labor and cost (Fahad et al., 2017; Ullah et al., 2017). Thus, finding efficient techniques to alleviate plant stress is critical.

Using bioregulators or organic acids to increase plant growth and improve drought tolerance has been demonstrated to be an effective and environmentally beneficial strategy (Li et al., 2017; Saidi et al., 2017; Xa lxo and Keshavkant, 2019). Fatty acids are bioactive compounds that are classified as short-chain (SCFA; <C8:0), medium-chain (MCFA; C8: 0–14: 0), or long-chain (LCFA; >C16: ω3–9) based on the length of their carbon atom chains (Beermann et al., 2003; Bocca et al., 2007). Lauric acid (LA), systematically designated dodecanoic acid, is a saturated fatty acid with similar properties to medium-chain fatty acids

(Sandhya et al., 2016). Although the role of LA in the water stress response remains to be elucidated, it is noteworthy that the presence of LA in *in vitro* culture medium has been found to promote resistance to drought stress during the pre-domestication stage by maintaining leaf water concentration, stomatal closure and nonphotochemical energy dissipation, all of which can change plant metabolic rates (Medeiros et al., 2015). Plants grown in this lauric acid medium exhibited increased photosynthesis during the recovery period. Studies have shown that in loquat, LA may have an effect similar to that of capric acid and abscisic acid (ABA) on improving stomatal sensitivity and drought resistance in leaves (Gugliuzza et al., 2020). Through the study of fatty acid oxidase in organisms, it has been found that fatty acid oxidation products seem to have important biological activities (Funk, 2001; Blée, 2002; Noverr et al., 2003). Plants, like certain other organisms, create hydroxy fatty acids primarily through enzymatic processes mediated by cytochrome P450-dependent fatty acid hydroxylases (Benveniste et al., 2005). Different fatty acid hydroxylase metabolites are involved in different aspects of plant development and responses to biotic and abiotic stresses (Kandel et al., 2006). Researchers have cloned the fatty acid-metabolizing enzyme CYP94C1 of the cytochrome P450 family from *Arabidopsis thaliana*. When recombinant yeast microsomes were incubated with lauric acid (C12:0) for 15 min, a major metabolite was formed, identified as 12-hydroxylauric acid (Kandel et al., 2007). Studies have shown that synthetic medium-chain-hydroxy fatty acid metabolites can act as systemic immune elicitors (Kutschera et al., 2019). Although 12-hydroxylauric acid can be employed as an immune activator in plants, few studies have been conducted on its role in plant responses to biotic stress.

Peach (*Prunus persica* (L.) Batsch) is a popular commercial fresh fruit worldwide. Peach development is heavily reliant on an appropriate amount of water (Eldem et al., 2012). Plants respond to drought stress by activating several response mechanisms that govern various physiological processes while also influencing the biochemical processes related to plant morphology (Bielsa et al., 2021). To prevent water loss, leaf pigment levels and photosynthetic activity are decreased and growth is managed through moderating stomatal closure and osmotic management (Belin et al., 2009). Stomatal conductance (Gs), leaf relative water content (RWC), relative electrolytic leakage (REL), plant antioxidant system, and a variety of other metrics have been used to investigate this physiological response (Verslues et al., 2006; Golldack et al., 2014; Lind et al., 2015). Drought stress can have a series of effects on cells, including an increase in the production of reactive oxygen species (ROS), destruction caused by membrane lipid peroxidation, inhibition of enzyme function, protein oxidation and changes in plant antioxidant systems (Li et al., 2011; Gao et al., 2020; Kaya et al., 2020). These characteristics provide strong theoretical support for plants' capacity to endure drought stress.

To better understand plant stress responses, we induced natural drought stress in 'Maotao' peach cultivar seedlings (*Prunus persica*

(L.) Batsch) in a greenhouse for this study. Over the course of the study, we investigated the effects of exogenous lauric acid (LA) and 12-hydroxylauric acid (LA-OH) on peach seedling responses to drought. Our findings indicate that exogenous LA and LA-OH can ameliorate the drought-associated oxidative damage and decrease in photosynthesis while also delaying drought-induced leaf senescence. These findings provide a strategy to boost agricultural production through enhanced drought tolerance.

## Materials and methods

### Experimental materials

This experiment was carried out at the Shandong Agricultural University experimental base, located in Tai'an city, Shandong Province, China (36°17'7459"N, 117°16'7712"E), in 2021. Uniform and plump peach seeds were selected and were soaked in a 400 ppm gibberellin solution for 24 hours before being placed in seedling trays. Once the peach seedlings reached approximately 5 cm in height, healthy seedlings of comparable size that were free of insect pests were selected for planting in pots. Each pot was a square shape (7 cm x 7 cm). The media in the pot was a 2:1 volume ratio blend of garden soil and vermiculite. Each pot of culture media weighed 200 g. The seedlings were maintained on a regular basis.

### Drought treatments

Peach seedlings that developed similarly were selected and split into three groups of 80 pots each. For three consecutive treatments, the seedlings were irrigated every five days with one of the following, depending on the group to which they were assigned: clean water, lauric acid (50 ppm, Sigma–Aldrich) or 12-hydroxylauric acid (50 ppm, Shanghai Macklin Biochemical Co., Ltd.). The reagent concentration was established by the results of earlier preparatory studies. We discovered that LA and LA-OH had no negative impact on the development of peach seedlings after the irrigation treatments. Then, each group of peach seedlings was split into two subgroups: one that received a regular watering treatment (CK, LA-OH, LA) and one that was exposed to natural drought conditions (CK-D, LA-OH-D, LA-D). There were 40 pots in each subgroup. Following a 14-day treatment period, leaves from all subgroups were washed carefully with tap water, frozen with liquid nitrogen, and then stored at -80°C until use.

### Calculation of the relative water content and relative electrolyte leakage of leaves

Three plants were chosen for each treatment, two leaves were removed from each plant and promptly placed in an aluminium

box of known weight, and the fresh weight (Wf) was determined. The leaves were submerged in distilled water for approximately 1 hour before being removed and weighed to determine the saturated fresh weight (WT) of the sample. The dry weight (Wd) was then obtained by drying the leaves to a constant weight. The relative water content (RWC) was determined using the following formula (Bielsa et al., 2021):  $(Wf - Wd) / (WT - Wd) \times 100\%$ .

The relative electrolyte leakage (REL) was measured with reference to Gao et al. (2020) but with slight modifications. Ten tiny discs were punched from ripe leaves and placed in a 20 mL centrifuge tube with 10 mL of deionized water. After 4 hours at room temperature, a Raymag DDS-307 conductivity meter was used to test the solution conductivity, designated S1. At the same time, the conductivity of the deionized water, designated S0, was measured. The centrifuge tube was then placed in a 100°C water bath for 20 min. After cooling, the mixture was shaken well, and the conductivity, designated S2, was measured. To represent the relative permeability of the plasma membrane, the relative electrolyte leakage was calculated using the following formula:  $REL (\%) = (S1 - S0) / (S2 - S0) \times 100\%$ .

### Determination of gas exchange and photosynthetic parameters

On the 14th day of the treatment period, photosynthesis was monitored from 10:00 to 11:30 am. We measured the following parameters with the CIRAS-3 portable photosynthetic system (PP Systems, Massachusetts, USA): net photosynthetic rate (Pn), transpiration rate (Tr), stomatal conductance (Gs), intercellular CO<sub>2</sub> concentration (Ci) and water use efficiency (WUE). The relative chlorophyll content (SPAD) was measured six times using a SPAD502 instrument, and the average value was calculated.

Samples (0.2 g) were taken from fresh, clean peach leaves and extraction was performed for 24 h in a 95% ethanol solution. We then used a Pharma-Spec UC-2450 ultraviolet spectrophotometer (Shimadzu, Kyoto, Japan) to measure the OD<sub>665</sub>, OD<sub>649</sub>, and OD<sub>470</sub> of the extract. To calculate leaf chlorophyll and carotenoid levels, we used the methods of Li et al., 2021.

We used the IMAGING-PAM Chlorophyll Fluorescence System (Heinz Walz, Effeltrich, Germany) to measure the following parameters: minimal fluorescence (F0), maximal fluorescence (Fm), maximum quantum efficiency (Fv/Fm), actual quantum efficiency (ΦPSII), photochemical quenching (qP), nonphotochemical quenching (NPQ), and electron transport rate (ETR). To determine Fv/Fm, the peach leaves were dark-adapted in a dark clip adaptor for 30 min.

### Stomatal aperture assay

Three leaves from the same part of each plant were collected 14 days later to assess the stomata morphology and degree of



opening. Colourless acrylic nail polish was applied evenly on the back of each collected peach leaf. After 5 min, tweezers were used to remove the nail polish after it had hardened. The piece treated with nail polish was then placed on a microscope slide and examined with a fluorescence microscope at 400× magnification (AXIO, Carl Zeiss, Germany). We chose three sites at random on each piece for imaging. To calculate and identify the degree of openness, stomatal aperture imprints were measured using ImageJ software (National Institutes of Health, Bethesda, Maryland, USA).

## Determination of osmotic regulatory substances

To calculate the total soluble sugar content (Li et al., 2021), 0.2 g of leaves was weighed, chopped and mixed. Then, 10 mL of distilled water was added and the leaf matter was placed in a boiling water bath for 30 min to create an extract, which was then filtered and diluted to a 25 mL volumetric flask. One millilitre of extract was mixed with 4 mL of 0.2% anthrone reagent, and the absorbance at 620 nm was measured.

The proline content in the leaves was then measured (Mehdizadeh et al., 2021). First, 5 mL of 3% sulfosalicylic acid was added to 0.5 g of leaf sample, and the sample was ground to prepare the homogenate, which was then boiled in a water bath for 10 min and cooled to room temperature. Then, 2 mL of supernatant was collected and added to 2 mL of glacial acetic acid and 3 mL of ninhydrin to generate a coloured liquid. The mixture was then heated in a boiling water bath for 40 min. In addition, 5 mL of toluene was added to the mixture for extraction, and the absorbance value of the toluene layer was measured using a spectrophotometer at 520 nm.

For enzyme extraction, 0.5 g fresh leaf sample were collected, and 0.1 mL of the extract was pipetted from the mixture and added to 5 mL of Coomassie Brilliant Blue G-250 reagent and mixed well. The mixture was allowed to rest for 2 min, and then the absorbance at 595 nm was recorded and the soluble protein concentration was assessed based on the standard curve (Xiao et al., 2020).

The method for measuring the total amount of free amino acids was based on Vardharajula et al., 2011, with slight modifications. Approximately 0.5 g of leaves was weighed, and 10% acetic acid was added to make a homogenate, which was then diluted to 100 mL. Then, 2 mL of sample extract was pipetted from the homogenate and mixed with 3 mL of ninhydrin reagent and 0.1% ascorbic acid aqueous solution. Next, the mixture was heated for 15 min in a boiling water bath and cooled to the colour of the solution, which was blue–violet. Then, 60% ethanol was added to 5 mL, and the absorbance was tested at 570 nm.

## Determination of leaf reactive oxygen species levels

We measured the hydrogen peroxide content in leaves using the methods of Xiao et al. (2020). Briefly, we placed cut-up leaf samples (0.1 g) in sterilized centrifuge tubes and then froze them with liquid nitrogen. After centrifugation at 60 rpm for 150 s, leaves were ground, frozen, and centrifuged again. The samples were then mixed with 1.5 mL of 0.1% trichloroacetic acid (TCA) and placed on ice. The samples were then centrifuged again at 12000 rpm for 15 min at 4°C. A 0.5 mL sample of supernatant was then collected and mixed with 0.5 mL of phosphate-buffered saline (PBS) and 1 mL of potassium iodide (KI). The resulting solution was shaken well and kept at 28 °C for 1 hour, after which we measured the absorbance at 390 nm.

We measured the  $O_2^-$  content in leaves using the methods of Han et al. (2022). Briefly, we chopped up 1 g sampled peach leaves and added 3 mL of phosphate buffer (pH = 7.8). The samples were then placed in an ice bath and were ground and then centrifuged at  $4000 \times g$  for 15 min. The supernatant was collected and mixed with 0.1 mL of 10 m mol/L hydroxylamine hydrochloride solution and incubated at 25°C for 20 min. We then added 1 mL of 17 m mol/L p-aminobenzene sulfonic acid and 1 mL of 7 m mol/L  $\alpha$ -naphthylamine solution and incubated the mixture at 25°C for 20 min. After that, we added an equal volume of chloroform to extract the pigment and centrifuged the mixture at 10000 r/min for 3 min. The pink extract was collected to measure the  $OD_{530}$ .

## Measurements of leaf lipid peroxidation

Malondialdehyde (MDA), a biomarker of lipid peroxidation caused by oxidative stress, was measured using the method described by Zhang et al. (2016), with some modifications. Briefly, we mixed 0.20 g leaf samples with 2 mL of 0.1% trichloroacetic acid (TCA) and ground the samples to prepare the homogenate. Samples were then centrifuged at 4000 r/min for 10 min. We collected 1 mL of supernatant and mixed it with 4 mL of 20% TCA (containing 0.5% thiobarbituric acid [TBA]), placed the mixture in a boiling water bath for 60 min for reaction to occur, and then cooled the mixture quickly on ice at 4 °C. The absorbance OD values at 600, 532 and 450 nm were measured after centrifugation at 4000 rpm for 10 min. MDA content was expressed as U/g·min.

## Determination of leaf SOD, POD and CAT activities

The mixed sample (0.5 g) was weighed and ground in liquid nitrogen, and 4 mL of phosphate buffer was added at a



concentration of 0.05 M pH 7.8 (0.3% EDTA with 0.1 mM, Triton-X100 and 4% polyvinylpyrrolidone) was ground fully into a centrifuge tube, with a 6 mL buffer flush applied twice at 4 °C and 12,000 r/min. After centrifugation for 20 min, the supernatant was collected and stored at 4°C until use.

Superoxide dismutase (SOD) activity was determined according to the method of Zhang et al. (2016), with some modifications. The reaction mixture consisted of 1  $\mu$ M nitro blue tetrazolium (NBT), 30  $\mu$ M EDTA, 60  $\mu$ M riboflavin, 14 mM methionine, 50 mM sodium phosphate buffer (pH 7.8), and 100  $\mu$ L of crude enzyme extract. After the samples were evenly mixed, they were incubated in a water bath at 37°C for 30 min, and then the absorbance was read at 560 nm.

Peroxidase (POD) activity was determined according to the methods of Liang et al. (2018), with some modifications. One millilitre of crude enzyme extract was mixed with 1.0 mL of guaiacol, 1.0 mL of H<sub>2</sub>O<sub>2</sub>, and 2 mL of 0.2 mM phosphate buffer (pH 5.0) and heated at 34°C for 3 min. To start the reaction, H<sub>2</sub>O<sub>2</sub> was added, and then the A470 value was measured as A1. The absorbance A2 was measured after 1 min and 30 s, and the POD activity was recorded in terms of activity per gram of fresh tissue.

Catalase (CAT) activity was determined according to the methods of Li et al. (2011), with slight modifications. Briefly, we added 0.2 mL of crude enzyme extract to 2.8 mL of 30 mM H<sub>2</sub>O<sub>2</sub> and measured the absorbance at 240 nm after 5 s. Then, we determined the initial absorption value A1 and the absorption value A2 after 1 min. Activity was expressed in CAT enzyme activity units, for which one unit equals a change of 0.01 in the A240 value per gram of tissue per minute per millilitre of reaction solution.

## Statistical analysis

SPSS 17.0 (IBM, New York, USA) statistical analysis software was used to perform one-way ANOVA and Duncan's multiple comparison test. Statistical significance, presented as lettered results in the tables below, was assumed at a level of 5% ( $P < 0.05$ ). Data on all tables are presented as the means  $\pm$  standard deviations (error bars).

## Results

### LA and LA-OH enhanced drought stress tolerance

Pretreatment with 50 ppm LA and LA-OH reduced the withering of peach leaves under drought stress (Figure 1). Under drought conditions, the RWC value of peach leaves decreased considerably. However, pretreatment with LA and LA-OH greatly slowed the reduction in water content (Figure 2A). During drought stress, the REL of untreated peach seedlings

increased dramatically, but the REL of plants pretreated with LA increased significantly (Figure 2B). These results indicate that under drought conditions, LA and LA-OH enhanced RWC while decreasing REL.

### Characteristics of photosynthetic parameters of leaves

CK treatment considerably decreased the net photosynthetic rate (Pn), stomatal conductance (Gs), transpiration rate (Tr), water use efficiency (WUE), and SPAD value under drought stress while dramatically increasing the intercellular CO<sub>2</sub> concentration (Ci) (Figure 3). Exogenous LA or LA-OH substantially slowed the decreases in Pn, Gs, Tr, WUE, and SPAD during drought stress ( $P < 0.05$ ). In comparison to the CK-D subgroup, the LA-D and LA-OH-D treatment subgroups exhibited increases in Pn, Gs, Tr, WUE, and SPAD of 204.55%, 54.82%, 134.14%, 33.13%, 28.09% and 115.91%, 18.76%, 104.87%, 4.47%, 19.03%, respectively. However, compared to the Ci values for the CK-D drought stress treatment subgroup, Ci in the LA and LA-OH drought stress treatment subgroups fell by 15.24% (LA-D) and 13.81% (LA-OH-D), demonstrating that exogenous LA and LA-OH can ameliorate drought stress by influencing the photosynthetic properties of peach leaves. The impact of LA was superior to that of LA-OH.

### The effect of exogenous LA and LA-OH on leaf stomatal characteristics

Under normal conditions, the stomatal opening of the drought-treated leaves was substantially less than that of the control leaves. Exogenous LA-OH and LA may enlarge the stomatal aperture of leaves (Figure 4A); compared to the CK-D treatment, the LA-OH-D and LA-D treatments considerably enhanced the average stomatal aperture, increasing it by 2.23 times and 2.41 times, respectively (Figure 4B).

### Effects of drought stress on leaf pigmentation

Drought stress reduced the concentrations of chlorophyll a, chlorophyll b, chlorophyll a+b, and carotenoids in the peach seedlings by 21.47%, 6.78%, 19.53%, and 29.30%, respectively. By contrast, the concentrations of chlorophyll a, chlorophyll b, chlorophyll a+b, and carotenoids in the LA-OH-D treatment subgroup increased by 8.01%, 2.00%, 5.36%, and 3.53%, respectively (Figure 5). In the LA-D treatment subgroup, the concentrations of chlorophyll b, chlorophyll a+b, and carotenoids increased by 12.85%, 19.19%, 13.92%, and 15.06%, respectively. Exogenous LA-OH and LA can stimulate the synthesis of

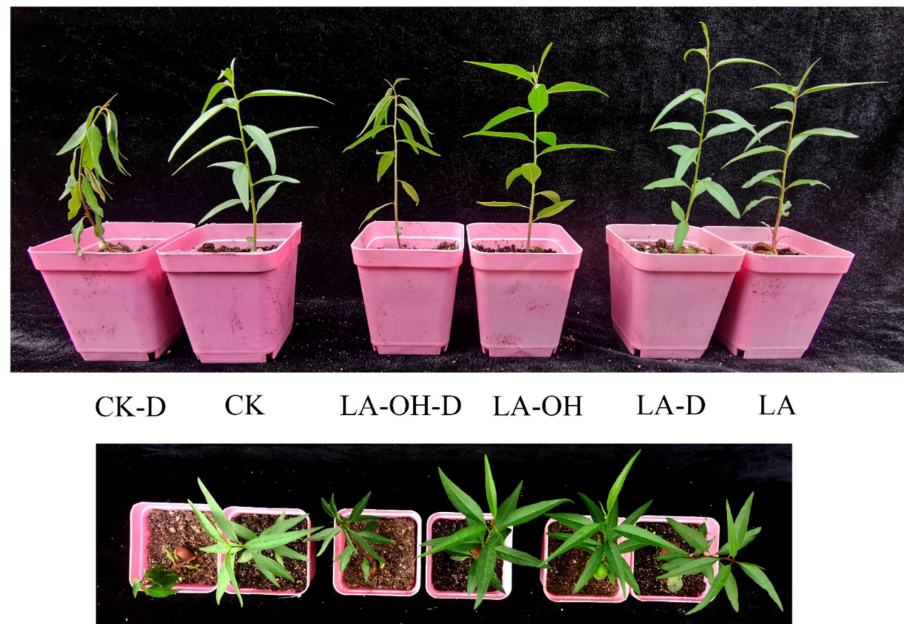


FIGURE 1

Drought tolerance of *P. persica* was increased by 12-Hydroxylauric acid and Lauric acid pretreatment. The detailed treatments of CK-D, CK, LA-OH-D, LA-OH, LA-D and LA are described in Materials and methods 2.2.

photosynthetic pigments in peach leaves under drought stress, with LA having a greater impact than LA-OH.

## The effects of LA and LA-OH on the osmotic control system of drought-stressed peach seedlings

Drought stress treatment dramatically enhanced the amounts of soluble sugar, proline, soluble protein, and free amino acids in

peach seedlings not treated with LA-OH or LA (Figure 6). The levels of soluble sugar, proline, soluble protein, free amino acids, and other organic osmotic regulators were much higher in drought-stressed plants treated with LA-OH and LA than in untreated drought-stressed plants. In contrast with the subgroups not treated with LA-OH or LA, the levels of soluble sugar, proline, soluble protein and free amino acids increased by 13.48%, 20.51%, 11.82% and 10.96%, respectively, in the LA-OH treatment subgroups. Under LA treatment, these levels increased by 24.11%, 29.30%, 16.89% and 15.04%, respectively.

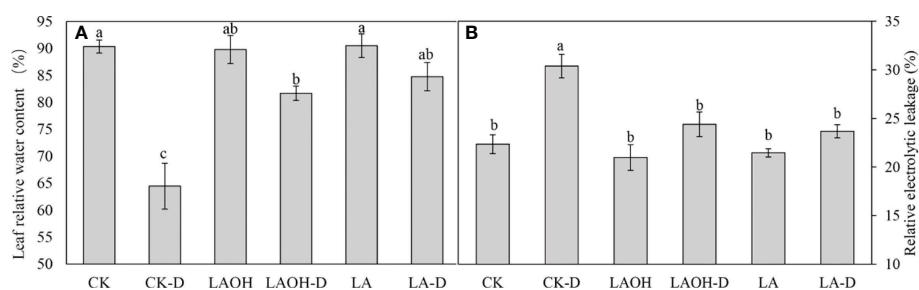
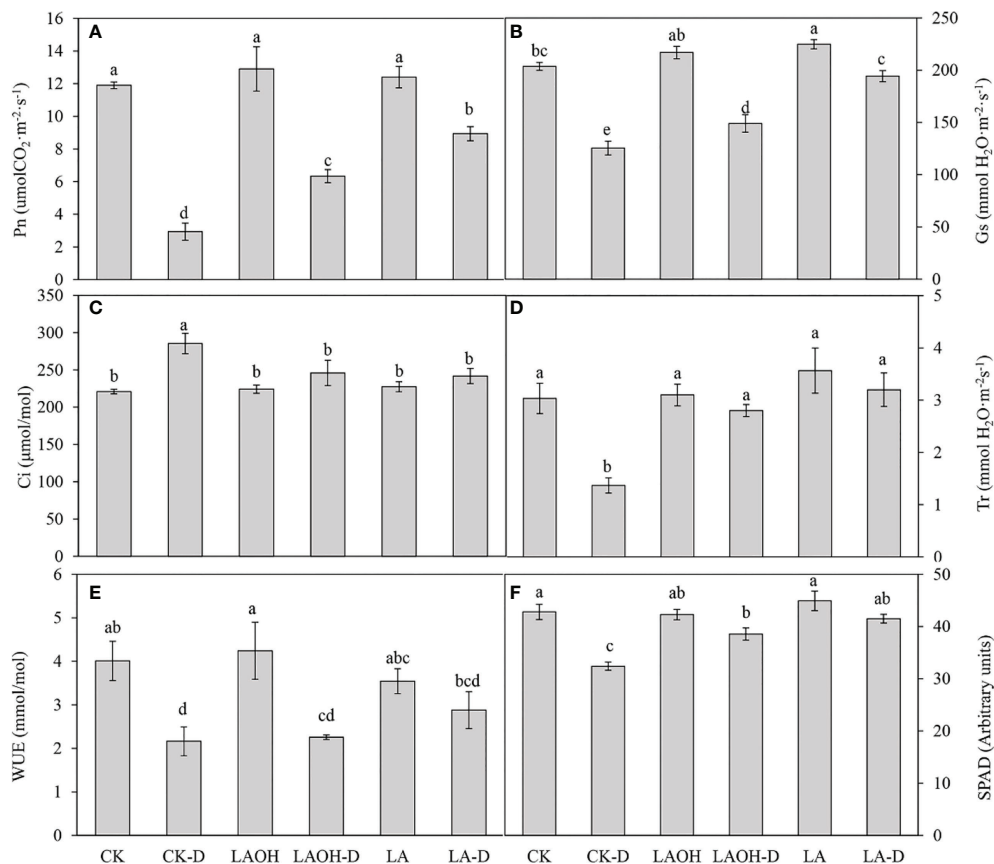


FIGURE 2

The effects of LA-OH and LA treatments on relative water content (A) and relative electrolyte leakage (B) in leaves under control and drought circumstances are shown in the graphs. The values represent the SD of the mean of three replicates. Duncan's test and ANOVA were used. Significant differences ( $P < 0.05$ ) are indicated by different letters.



**FIGURE 3**  
Effects of LA-OH and LA on the photosynthetic characteristics of *P. persica* under drought stress (A) Pn; (B) Gs; (C) Ci; (D) Tr; (E) WUE; (F) SPAD). Data are mean  $\pm$  SD ( $n = 3$ ). Duncan's test and ANOVA were used. Significant differences ( $P < 0.05$ ) are indicated by different letters.

## Changes in chlorophyll fluorescence in LA-OH and LA peach seedlings

In the absence of LA-OH or LA treatment, the initial fluorescence value ( $F_0$ ), maximum fluorescence value ( $F_m$ ), maximum quantum yield of PSII ( $F_v/F_m$ ), real photochemical efficiency of  $\Phi$ PSII ( $\Phi$ PSII), and photochemical quenching coefficient ( $qP$ ) of drought-treated peach tree seedlings were considerably reduced (Figure 7). LA-OH treatment in the LA-OH-D subgroup enhanced  $F_0$ ,  $F_m$ ,  $F_v/F_m$ ,  $\Phi$ PSII, and  $qP$  by 12.03%, 17.95%, 2.7%, 18.38%, and 5.07%, respectively, compared to the values for the CK-D subgroup. The impact of LA treatment was much greater than that of the LA-OH treatment, with LA treatment enhancing  $F_0$ ,  $F_m$ ,  $F_v/F_m$ ,  $\Phi$ PSII, and  $qP$  by 18.54%, 33.71%, 7.75%, 19.41%, and 11.39%, respectively. Under drought stress, the nonphotochemical quenching coefficient (NPQ) increased considerably in all treatment groups, with the CK-D treatment subgroup having the highest level, followed by the LA-OH-D treatment subgroup, with no significant difference between the two. Under drought

stress, the LA treatment resulted in the lowest NPQ level, which was substantially different from the levels in the CK-D and LA-OH-D subgroups. The corresponding colour photos of leaves show the state of the four parameters under various treatments (Figure 8A). LA-OH-D treatment and LA-D treatment effectively alleviated the damage caused by drought stress. The ETR-PAR light response curve (Figure 8B) revealed that the LA-OH-D and LA-D treatments greatly increased the  $ETR_{max}$  of peach tree seedlings by 38.84% and 51.45%, respectively.

## LA-OH and LA alleviated oxidative damage in peach seedlings under drought stress

We examined the levels of  $O_2^-$  and  $H_2O_2$  to investigate the influence of LA-OH and LA pretreatment on oxidative alterations. Under drought conditions,  $O_2^-$  and  $H_2O_2$  accumulated in peach leaves, and the levels of  $O_2^-$  and  $H_2O_2$  in peach leaves treated with LA-OH and LA were lower than

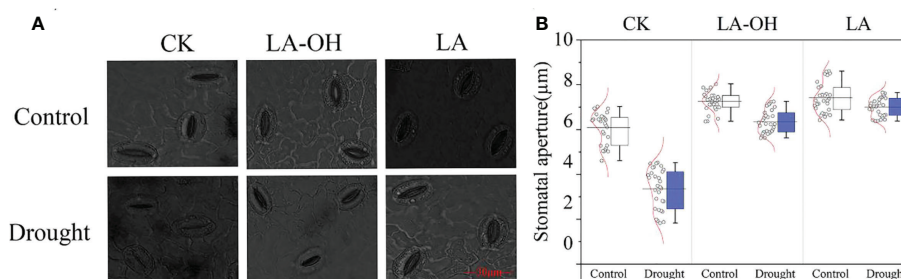


FIGURE 4

Effects of LA-OH and LA on the sizes of stomatal apertures of *P. persica* leaves under drought stress (A) light microscopeto visualize showed the characteristics of stomata; (B) Stomatal aperture area). Data are mean  $\pm$  SD (n = 3). Duncan's test and ANOVA were used. Significant differences (P < 0.05) are indicated by different letters.

those in leaves not treated with LA-OH or LA (Figure 9), suggesting that LA-OH and LA may mitigate ROS-induced oxidative damage. The SOD, POD, and CAT activity levels of peach leaves under drought stress increased considerably when compared to the activity levels of the control, but the SOD, POD, and CAT activity levels of peach leaves treated with LA-OH and LA were greater than those under drought stress without LA-OH or LA treatment, increasing by 5.37%, 16.74%, 3.36%, and 16.38%, 24.25%, 10.77%, respectively. Furthermore, the

antioxidant enzyme activity in the LA-D treatment subgroup was greater than that of the LA-OH-D treatment subgroup. Drought stress, on the other hand, considerably enhanced the MDA content in peach leaves when compared to the MDA content in the leaves of the control. The MDA content in peach leaves treated with LA-OH and LA was substantially lower than that in leaves under drought stress without LA-OH or LA treatment but was significantly higher than that of the control.

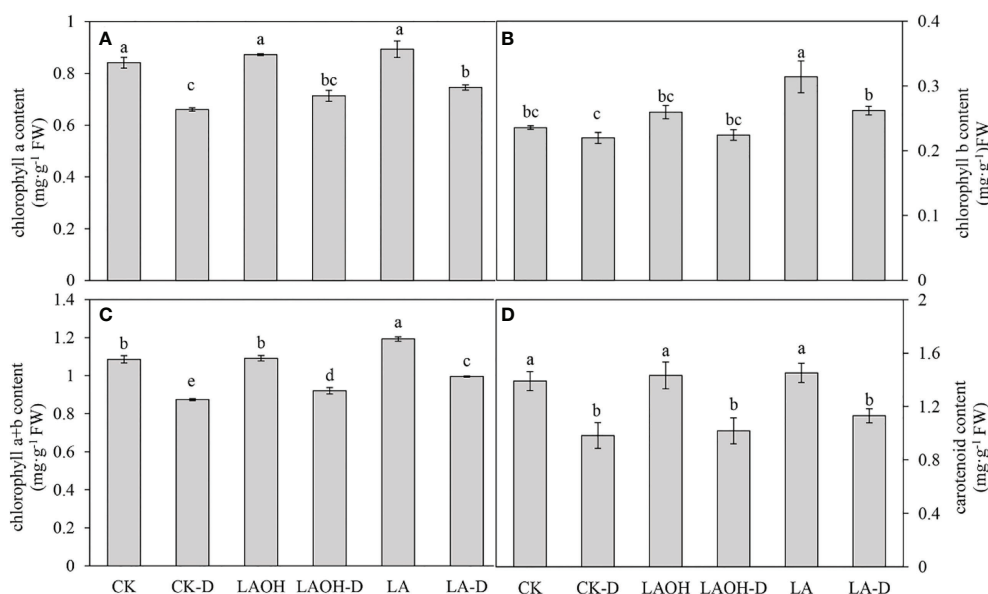


FIGURE 5

Effects of LA-OH and LA on photosynthetic pigment content in *P. persica* leaves under drought stress (A) chlorophyll a content; (B) chlorophyll b content; (C) chlorophyll a+b content; (D) carotenoid content). Data are mean  $\pm$  SD (n = 3). Duncan's test and ANOVA were used. Significant differences (P < 0.05) are indicated by different letters.

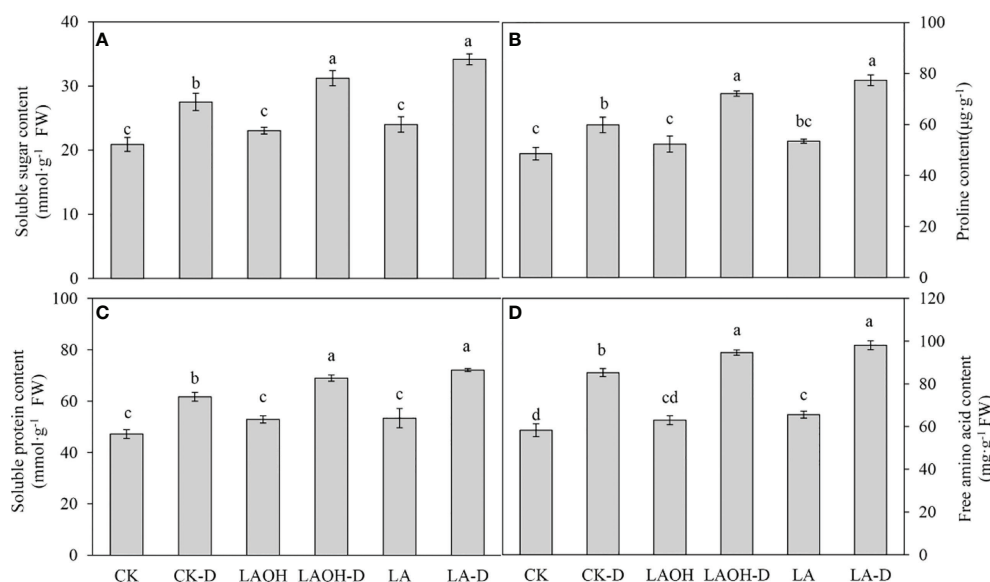


FIGURE 6

Effects of LA-OH and LA on osmoregulatory substances in *P. persica* under drought stress (A) soluble sugar content; (B) proline content; (C) soluble protein content; (D) free amino acid content. Data are mean  $\pm$  SD ( $n = 3$ ). Duncan's test and ANOVA were used. Significant differences ( $P < 0.05$ ) are indicated by different letters.

## Correlation analysis of LA-OH and LA with drought resistance

For the correlation study, the relative water content (RWC) of the peach leaves, as well as leaf pigment, osmotic regulatory system, stomatal aperture, and antioxidant system activity (i.e.,  $O_2^-$ ,  $H_2O_2$ , MDA, SOD, POD, CAT), were evaluated (Figure 10). The RWC of leaves was found to be positively correlated with stomatal aperture and leaf pigment content and was significantly correlated with stomatal aperture ( $r=0.85$ ), significantly positively correlated with chlorophyll a (Chl a) ( $r=0.80$ ), positively correlated with chlorophyll b (Chl b) ( $r=0.46$ ), significantly positively correlated with total chlorophyll (Chl t) ( $r=0.79$ ), and significantly positively correlated with carotenoid (Car) ( $r=0.65$ ). RWC was significantly negatively correlated with REL ( $r=-0.84$ ); negatively correlated with soluble sugar ( $r=-0.32$ ), proline ( $r=-0.22$ ), and soluble protein ( $r=-0.40$ ); and significantly negatively correlated with free amino acids ( $r=-0.48$ ). RWC was also significantly negatively correlated with  $O_2^-$  ( $r=-0.70$ ),  $H_2O_2$  ( $r=-0.69$ ) and MDA ( $r=-0.84$ ); negatively correlated with SOD ( $r=-0.16$ ) and POD ( $r=-0.45$ ); and significantly negatively correlated with CAT ( $r=-0.50$ ).

## Discussion

Fatty acids (FAs) are ubiquitous in nature and play an important role in many biological processes (Liu et al., 2008).

FAs are significant physiological molecules that play a role in cellular energy storage, membrane structure, and numerous signalling pathways (Corino et al., 2004; Shin et al., 2007). FAs are well recognized for their antibacterial and antifungal properties. (Agoramoorthy et al., 2007). Lauric acid (LA) is one of the most active medium-chain FAs (Dayrit, 2015), and its antimicrobial benefits in medicine (Carballeira, 2008; Liang et al., 2021) and plants have been described (Řiháková et al., 2001; Walters et al., 2003), although there have been few investigations on its role in boosting plant drought tolerance. LA not only promotes the *in vitro* growth of zygotic coconut (*Cocos nucifera* L.) embryos, but plants treated with LA in the predomestication stage can be used to improve crop drought resistance because of the role of LA in modulating the degree of stomatal opening and closing, maintaining the relative moisture content in leaves, and maintaining photosynthetic activity (Medeiros et al., 2015). Studies have shown that drought stress has a significant effect on loquat growth and metabolism and that among leaf metabolites, LA is involved in metabolism in loquat under drought conditions (Gugliuzza et al., 2020). According to research, the products of fatty acid oxidase in organisms appear to have vital biological actions (Funk, 2001; Blée, 2002). Moreover, it is now known, that they are engaged in a variety of biological activities. Different aspects of plant growth, as well as responses to biotic and abiotic stressors, entail oxidative products (Kandel et al., 2006; Nelson, 2006). In plants, 12-hydroxylauric acid (LA-OH) is mostly generated through a process mediated by cytochrome P450 fatty acid



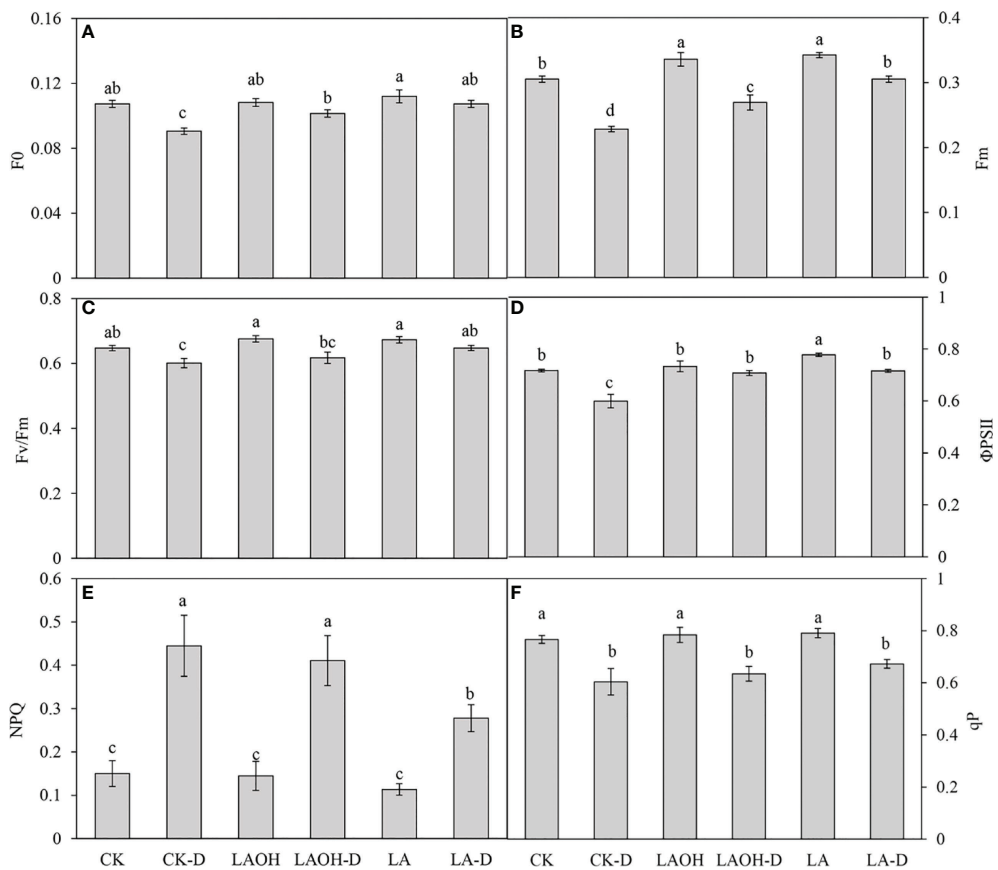


**FIGURE 7** Changes in chlorophyll fluorescence parameters of peach seedlings under drought conditions. (A) F<sub>0</sub>; (B) F<sub>m</sub>; (C) F<sub>v</sub>/F<sub>m</sub>; (D) ΦPSII; (E) NPQ; (F) qP. Duncan's test and ANOVA were used. Significant differences (P < 0.05) are indicated by different letters.

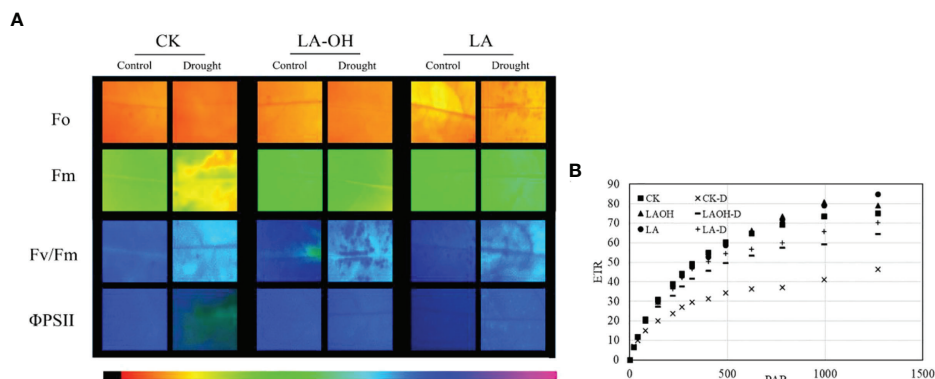


**FIGURE 8** Chlorophyll fluorescence parameters in leaves of the peach seedlings. (A) Chlorophyll fluorescence imaging of F<sub>0</sub>, F<sub>m</sub>, F<sub>v</sub>/F<sub>m</sub> and ΦPSII; The darker the color, the greater the F<sub>v</sub>/F<sub>m</sub>; (B) ETR-PAR.

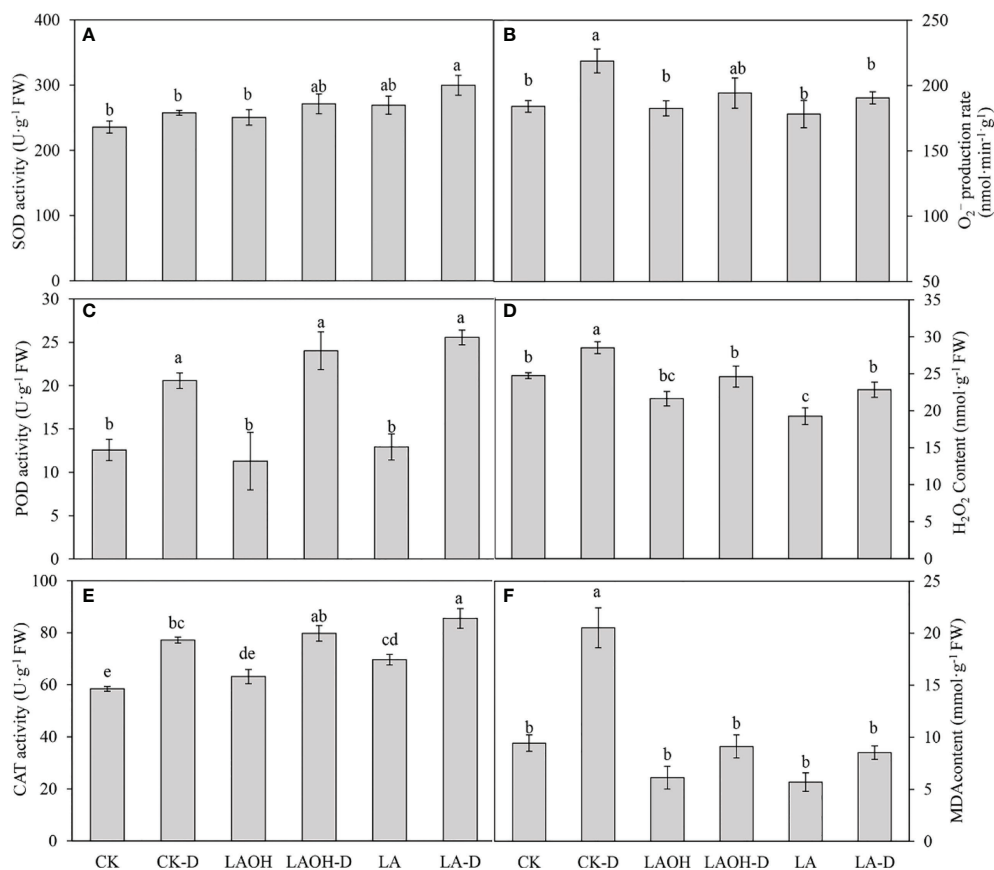


**FIGURE 9**  
Effects of LA and LA-OH on antioxidant enzyme activity and MDA content of *P. persica* leaves under drought stress (A) SOD; (B) O<sub>2</sub><sup>-</sup> production rate; (C) POD; (D) H<sub>2</sub>O<sub>2</sub> content; (E) CAT; (F) MDA content). Data are mean ± SD (n = 3). Duncan's test and ANOVA were used. Significant differences (P < 0.05) are indicated by different letters.

hydroxylases. Research indicates that the addition of hydroxylauric acid has a role in regulating plant development phenomena (Imaishi and Petkova-Andonova, 2007). It has been shown that LA and LA-OH activate the immune response in *Arabidopsis* by activating cytosolic calcium ([Ca<sup>2+</sup>]<sub>cyt</sub>) signalling (Kutschera et al., 2019). We first investigated the impacts of exogenous LA and LA-OH on plant photosynthetic performance under drought conditions, and we then investigated the mechanism of LA and LA-OH in photosynthesis by evaluating photosynthetic pigments, gas exchange parameters, and chlorophyll fluorescence parameters. We describe our findings by examining osmoregulation and antioxidant systems because the use of LA and LA-OH under abiotic stress has not been adequately studied.

The ability of plants to respond to drought stress is enhanced by maintaining the correct leaf water status (Han et al., 2022). Drought decreased the relative water content (RWC) of peach leaves, and after irrigating the seedlings with LA and LA-OH, RWC in subgroups receiving one of these two treatments was

considerably higher than RCW in the CK-D subgroup (Figure 2). Morphological observation of the seedling leaves revealed that the more severe the drought was, the more severe the water loss in the leaves, and the greater the degree of curling and folding of the leaves. Relative electrolytic leakage (REL) is a good predictor of membrane permeability and drought tolerance (Sun et al., 2018). Our findings revealed that the REL value of the CK-D treatment was greatly enhanced; however, the REL values of the LA-D and LA-OH-D treatment subgroups were not significantly different from those of the subgroups receiving LA or LA-OH treatments under drought conditions. The difference was not statistically significant, suggesting that LA and LA-OH treatment prevented cell damage under dry conditions.

Photosynthesis, the process through which plants obtain carbon and energy, is particularly susceptible to environmental stress (Muhammad et al., 2021). Research indicates that drought stress can disrupt pigment complexes, impede electron transport, damage chloroplast structure, and reduce photosynthetic rates (Liu et al.,

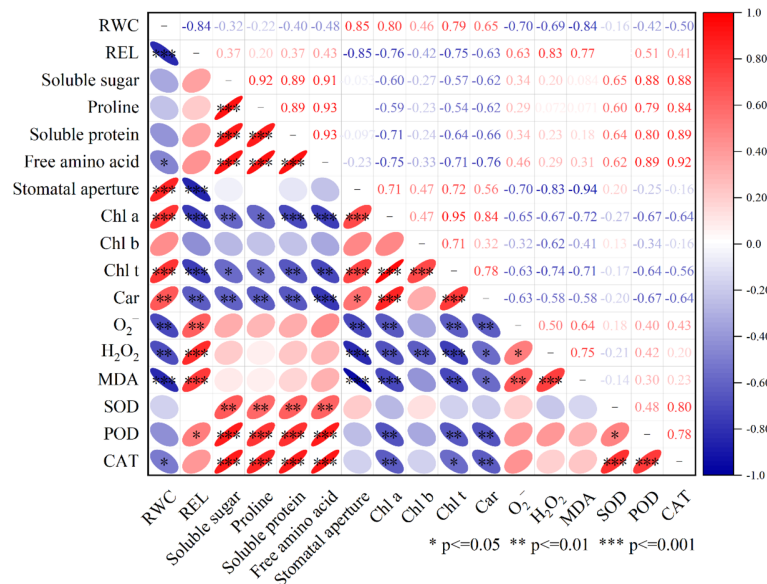


FIGURE 10

Pearson correlation analysis was done on RWC, REL, Soluble sugar, Proline, Soluble protein, Free amino acid, Stomatal aperture, Chl a, Chl b, Chl t, Car, O<sub>2</sub><sup>-</sup>, H<sub>2</sub>O<sub>2</sub>, MDA, SOD, POD, CAT after LA-OH and LA treatments under drought stress. \*\*\*—indicates 0.1% significant ( $p \leq 0.001$ ), \*\*—indicates 1% significant ( $p \leq 0.01$ ), and \*—indicates 5% significant ( $p \leq 0.05$ ).

2016; Li et al., 2018). Pn can be decreased under drought stress due to decreased chlorophyll content and stomatal conductance (Liang et al., 2018). In our study, drought reduced chlorophyll a, chlorophyll b, and carotenoid levels; however, the application of LA-OH and LA mitigated the deleterious effects of drought on chlorophyll content. Our findings agree with those of Moaveni (2011), who discovered that photosynthetic pigments are decreased in crops subjected to water stress. Drought stress reduces stomatal aperture, which results in a decrease in the Pn rate or in alterations to photosynthetic metabolism. Furthermore, drought decreases the CO<sub>2</sub> concentration and transpiration rate *via* stomata (Moaveni, 2011; Shahid et al., 2014). Our research revealed that LA-OH and LA treatments might stimulate stomatal opening in peach leaves while also significantly reducing stomatal aperture closure caused by drought. Our findings imply that LA-OH and LA increase plant drought tolerance through a variety of mechanisms, including by decreasing stomatal limitation, protecting chlorophyll from degradation, and improving photosynthetic capability.

Evaluation of chlorophyll fluorescence characteristics is an essential technique for determining plant water status during drought stress because these characteristics can rapidly, precisely, and safely indicate the effects of drought stress on plant photosynthesis (Maxwell and Johnson, 2000). F0 is a key metric for assessing plant stress damage, and Fm can indicate PS II electron transport capabilities following dark adaptation (Rao et al., 2021). Our investigation revealed that during drought stress, both F0 and Fm declined dramatically but that LA-OH and LA treatments could successfully delay the declining trend (Figure 8). Fv/Fm is an

excellent measure for determining the degree of damage to plant leaves, and Fv/Fm decreases with environmental stress (Pettigrew, 2004; Raja et al., 2020). Under drought stress, all three drought treatment subgroups (CK-D, LA-OD-D, and LA-D) exhibited a decline in Fv/Fm. Among the subgroups, the CK-D subgroup exhibited a markedly decreased Fv/Fm, while the LA-OH-D and LA-D subgroups exhibited the smallest decrease, showing that drought stress had a markedly impact on the seedlings in the CK treatment subgroup. The PS II response centre was damaged. As a result, its activity and light energy conversion efficiency were reduced. The seedlings in the LA-OH-D and LA-D subgroups, on the other hand, incurred less damage and showed marked tolerance to dry environments. During drought stress, the maximum quantum efficiency (Fv/Fm) of photosystem PS II, the actual quantum efficiency of PS II ( $\Phi$  PSII), and the photochemical quenching (qP) all declined, although the nonphotochemical quenching (NPQ) increased (Figures 7C, D). Gao et al. (2021) reported comparable results in apple. In our study, the reduction in these parameters was somewhat reversed after applying LA-OH and LA. The LA-OH and LA treatments not only reduced the drought-induced decreases in Fv/Fm and  $\Phi$  PSII but also promoted restoration of photosynthesis. Simultaneously, damage to a key component of the PS II response centre was minimized. The perceived electron transfer efficiency under real light intensity is represented by the photosynthetic electron transfer rate (ETR). Under normal conditions, this value reflects the electron capture efficiency of the PS II reaction centre. Plant ETR values are normally steady within a particular range, and their ETR decreases when they

are stressed (Rao et al., 2021). In this study, irrigation with LA-OH and LA under drought conditions significantly increased leaf  $ETR_{max}$ , indicating that improving leaf light energy use efficiency had a significant promoting effect, whereas the greatest decrease in leaf  $ETR_{max}$  was observed in the CK-D treatment subgroup, indicating that electron transport was severely hampered, in turn affecting photosynthetic capacity (Figure 9).

Plant resistance to abiotic stressors is heavily reliant on the accumulation of osmoprotectants (Jespersen et al., 2017). LA-OH and LA had substantial impacts on various osmolytes in our investigation. Plants under drought stress had higher levels of soluble sugar and soluble protein than those without LA-OH or LA treatment (Figure 6). The levels of proline and free amino acids in the plant are major regulators of cellular osmotic potential. The build-up of these biomolecules aids in cell membrane integrity and the prevention of osmotic and oxidative damage (Han et al., 2022). LA-OH and LA treatments have significantly boosted proline content in drought-stressed pecan seedlings in our past trial studies. Comparable results have been obtained in apple (Gao et al., 2021). In addition to its osmoregulatory role, proline accumulation under harsh conditions protects the photosynthetic system from damage (Khan et al., 2016).

It is critical for cells to maintain reactive oxygen species equilibrium and osmotic potential during drought (Wang et al., 2013). In our study, drought stress caused an excessive concentration of ROS in leaves, disrupting the plant cell membrane system and causing electrolyte leakage, which resulted in chlorophyll degradation. These modifications have been demonstrated to significantly limit photochemical processes, impair photosynthesis, and hasten leaf senescence (Gao et al., 2020). In the current investigation, the levels of  $O_2^-$ ,  $H_2O_2$ , and MDA in peach leaves increased dramatically under drought stress but decreased significantly following the application of LA-OH or LA (Figure 9). The antioxidant defence system in plants, which comprises enzymatic and nonenzymatic antioxidants, strictly controls the equilibrium of reactive oxygen species (Wang et al., 2013). According to studies, the external application of acetic acid can control reactive oxygen species homeostasis by increasing the activity of apple antioxidant enzymes, which guards the fruit against harm caused by reactive oxygen species during drought stress (Sun et al., 2022). Trehalose treatment has significantly increased the activity levels of SOD, CAT and POD enzymes in sunflower leaves under water stress, thus upregulating the oxidative defence system of plants, which has a considerable effect on promoting plant growth under drought stress conditions (Kosar et al., 2021). The LA-OH or LA treatment in our study greatly boosted the activity levels of SOD, POD, and CAT, according to our findings (Figure 9). Excess reactive oxygen species have been found to be eliminated by SOD, POD, and CAT enzymes in other studies. SOD can turn  $O_2^-$  into  $H_2O_2$ , and  $H_2O_2$  can subsequently be transformed back into  $H_2O$  through POD and CAT to reduce reactive oxygen species damage. Increasing the activity of enzymatic reactive oxygen species scavengers and the quantity of nonenzymatic reactive oxygen

species scavengers in grape has been shown to be beneficial (Wang and Li, 2006). We came to the same conclusion for peach seedlings.

The interplay of these indicators was investigated using Pearson's correlation analysis to assess how the use of LA-OH and LA increase plant tolerance under drought conditions. The correlation analysis in our study revealed that ROS and MDA were positively correlated with enzymatic antioxidants, while RWC was positively correlated with ROS, REL, reactive oxygen species, the osmotic regulation system, and the enzymatic antioxidant system (Figure 10). The results demonstrated that drought stress had a significant impact on the photosynthetic system, osmotic regulatory system, and reactive oxygen species enzymatic antioxidant system of peach seedlings and that LA-OH and LA could mitigate these effects to alleviate drought stress.

## Conclusion

In this study, both LA-OH and LA alleviated the growth of peach seedlings under drought stress. Drought stress can be alleviated *via* various mechanisms, including the following: (i) LA-OH and LA can effectively increase the chlorophyll content in peach leaves, increase the degree of leaf stomatal opening and enhance the net photosynthetic rate, thereby improving photosynthesis and reducing the damage caused by drought stress to the photosystem; (ii) LA-OH and LA can increase the contents of soluble sugar, soluble protein, proline, and free amino acids; alleviate osmotic stress; control the relative conductivity of leaves; and maintain the leaf water content; (iii) under drought stress, both LA-OH and LA may decrease the  $O_2^-$  and  $H_2O_2$  contents and lipid peroxidation level in tobacco plants, which is beneficial for the antioxidant system of peach seedlings. In general, both LA-OH and LA can help to decrease drought stress. The findings of this research shed light on the mechanism by which LA-OH and LA relieve drought stress in peach plants. Additional research is needed to better understand these pathways.

## Data availability statement

The raw data supporting the conclusions of this article will be made available by the authors, without undue reservation.

## Author contributions

BZ: substantial contributions to the conception or design of the work; or the acquisition, analysis, or interpretation of data for the work; HD: substantial contributions to the acquisition, analysis; MS: drafting the work or revising it critically for important intellectual content; XW and ZW: substantial

contributions to the interpretation of data for the work; YX: provide approval for publication of the content; FP: agree to be accountable for all aspects of the work in ensuring that questions related to the accuracy or integrity of any part of the work are appropriately investigated and resolved. All authors contributed to the article and approved the submitted version.

## Funding

This work was supported by the National Key Research and Development Program of China (2020YFD1000203), the National Modern Agro-industry Technology Research System Fund (Grant No. CARS-30-2-02).

## References

- Agoramoorthy, G., Chandrasekaran, M., Venkatesalu, V., and Hsu, M. (2007). Antibacterial and antifungal activities of fatty acid methyl esters of the blind-your-eye mangrove from India. *Braz. J. Microbiol.* 38, 739–742. doi: 10.1590/S1517-83822007000400028
- Beermann, C., Jelinek, J., Reinecker, T., Hauenschild, A., Boehm, G., and Klör, H. (2003). Short term effects of dietary medium-chain fatty acids and n-3 long-chain polyunsaturated fatty acids on the fat metabolism of healthy volunteers. *Lipids Health Disease*. 2, 1–10. doi: 10.1186/1476-511X-2-10
- Belin, C., Thomine, S., and Schroeder, J. I. (2009). “Water balance and the regulation of stomatal movements,” in A. Pareek, S. K. Sopory and H. J. Bohnert Govindjee eds. *Abiotic stress adaptation in plants*, (Dordrecht: Springer), 283–305. doi: 10.1007/978-90-481-3112-9\_14
- Benveniste, I., Bronner, R., Wang, Y., Compagnon, V., Michler, P., Schreiber, L., et al. (2005). CYP94A1, a plant cytochrome P450-catalyzing fatty acid  $\omega$ -hydroxylase, is selectively induced by chemical stress in vicia sativa seedlings. *Planta*. 221, 881–890. doi: 10.1007/s00425-005-1503-y
- Bielsa, B., Sanz, M.Á., and Rubio-Cabetas, M. J. (2021). ‘Garnem’ and myrobalan ‘P. 2175’: Two different drought responses and their implications in drought tolerance. *Horticulturae*. 7, 299. doi: 10.3390/horticulturae7090299
- Blée, E. (2002). Impact of phyto-oxylipins in plant defense. *Trends Plant sci.* 7, 315–322. doi: 10.1016/S1360-1385(02)02290-2
- Bocca, C., Bozzo, F., Gabriel, L., and Miglietta, A. (2007). Conjugated linoleic acid inhibits caco-2 cell growth via ERK-MAPK signaling pathway. *J. Nutr. Biochem.* 18, 332–340. doi: 10.1016/j.jnutbio.2006.07.001
- Bocchini, M., D’Amato, R., Ciancaleoni, S., Fontanella, M. C., Palmerini, C. A., Beone, G. M., et al. (2018). Soil selenium (Se) biofortification changes the physiological, biochemical and epigenetic responses to water stress in zea mays l. by inducing a higher drought tolerance. *Front. Plant sci.* 9, 389. doi: 10.3389/fpls.2018.00389
- Carballeira, N. (2008). New advances in fatty acids as antimalarial, antimycobacterial and antifungal agents. *Prog. Lipid Res.* 47, 50–61. doi: 10.1016/j.plipres.2007.10.002
- Caser, M., Chitarra, W., D’Angiolillo, F., Perrone, I., Demasi, S., Lovisolo, C., et al. (2019). Drought stress adaptation modulates plant secondary metabolite production in salvia dolomitica codd. *Ind. Crops products*. 129, 85–96. doi: 10.1016/j.indcrop.2018.11.068
- Chukwuneme, C. F., Babalola, O. O., Kutu, F. R., and Ojuederie, O. B. (2020). Characterization of actinomycetes isolates for plant growth promoting traits and their effects on drought tolerance in maize. *J. Plant Interactions*. 15, 93–105. doi: 10.1080/17429145.2020.1752833
- Corino, C., Filetti, F., Gambacorta, M., Manchisi, A., Magni, S., Pastorelli, G., et al. (2004). Influence of dietary conjugated linoleic acids (CLA) and age at slaughtering on meat quality and intramuscular collagen in rabbits. *Meat sci.* 66, 97–103. doi: 10.1016/S0309-1740(03)00024-X
- Dayrit, F. M. (2015). The properties of lauric acid and their significance in coconut oil. *J. Am. Oil Chemists’ Soc.* 92, 1–15. doi: 10.1007/s11746-014-2562-7
- Del Buono, D. (2021). Can biostimulants be used to mitigate the effect of anthropogenic climate change on agriculture? it is time to respond. *Sci. Total Environment*. 751, 141763. doi: 10.1016/j.scitotenv.2020.141763
- Eldem, V., Çelikkol Akçay, U., Ozhuner, E., Bakır, Y., Uranbey, S., and Unver, T. (2012). Genome-wide identification of miRNAs responsive to drought in peach (*Prunus persica*) by high-throughput deep sequencing. *PLoS One* 7, e50298. doi: 10.1371/journal.pone.0050298
- Fahad, S., Bajwa, A. A., Nazir, U., Anjum, S. A., Farooq, A., Zohaib, A., et al. (2017). Crop production under drought and heat stress: Plant responses and management options. *Front. Plant Sci.* 8:1147. doi: 10.3389/fpls.2017.01147
- Funk, C. D. (2001). Prostaglandins and leukotrienes: advances in eicosanoid biology. *science*. 294, 1871–1875. doi: 10.1126/science.294.5548.1871
- Gao, T., Shi, C., Li, Q., Wei, Z., Liu, L., and Feng, J. (2021). Drought tolerance monitoring of apple rootstock m. 9-T337 based on infrared and fluorescence imaging. *Photosynthetica*. 59, 458–467. doi: 10.32615/ps.2021.035
- Gao, T., Zhang, Z., Liu, X., Wu, Q., Chen, Q., Liu, Q., et al. (2020). Physiological and transcriptome analyses of the effects of exogenous dopamine on drought tolerance in apple. *Plant Physiol. Biochem.* 148, 260–272. doi: 10.1016/j.plaphy.2020.01.022
- Gollack, D., Li, C., Mohan, H., and Probst, N. (2014). Tolerance to drought and salt stress in plants: unraveling the signaling networks. *Front. Plant sci.* 5, 151. doi: 10.3389/fpls.2014.00151
- Gugliuzza, G., Talluto, G., Martinelli, F., Farina, V., and Lo Bianco, R. (2020). Water deficit affects the growth and leaf metabolite composition of young loquat plants. *Plants*. 9, 274. doi: 10.3390/plants9020274
- Guo, Y.-P., MI, F.-G., YAN, L.-J., REN, Y.-X., LV, S.-J., and FU, B.-Z. (2014). Physiological response to drought stresses and drought resistances evaluation of different Kentucky bluegrass varieties. *Acta Prataculturae Sin.* 23, 220. doi: 10.11686/cyxh2014042
- Han, D., Tu, S., Dai, Z., Huang, W., Jia, W., Xu, Z., et al. (2022). Comparison of selenite and selenate in alleviation of drought stress in nicotiana tabacum l. *Chemosphere*. 287, 132136. doi: 10.1016/j.chemosphere.2021.132136
- Imaishi, H., and Petkova-Andonova, M. (2007). Molecular cloning of CYP76B9, a cytochrome P450 from petunia hybrida, catalyzing the  $\omega$ -hydroxylation of capric acid and lauric acid. *Biosci. biotechnol. Biochem.* 71, 104–113. doi: 10.1271/bbb.60396
- Jespersen, D., Yu, J., and Huang, B. (2017). Metabolic effects of acibenzolar-s-methyl for improving heat or drought stress in creeping bentgrass. *Front. Plant sci.* 8, 1224. doi: 10.3389/fpls.2017.01224
- Kandel, S., Sauveplane, V., Compagnon, V., Franke, R., Millet, Y., Schreiber, L., et al. (2007). Characterization of a methyl jasmonate and wounding-responsive cytochrome P450 of arabidopsis thaliana catalyzing dicarboxylic fatty acid formation *in vitro*. *FEBS J.* 274, 5116–5127. doi: 10.1111/j.1742-4658.2007.06032.x
- Kandel, S., Sauveplane, V., Olry, A., Diss, L., Benveniste, I., and Pinot, F. (2006). Cytochrome P450-dependent fatty acid hydroxylases in plants. *Phytochem. Rev.* 5, 359–372. doi: 10.1007/s11101-006-9041-1

## Conflict of interest

The authors declare that the research was conducted in the absence of any commercial or financial relationships that could be construed as a potential conflict of interest.

## Publisher’s note

All claims expressed in this article are solely those of the authors and do not necessarily represent those of their affiliated organizations, or those of the publisher, the editors and the reviewers. Any product that may be evaluated in this article, or claim that may be made by its manufacturer, is not guaranteed or endorsed by the publisher.



- Kaya, C., Şenbayram, M., Akram, N. A., Ashraf, M., Alyemeni, M. N., and Ahmad, P. (2020). Sulfur-enriched leonardite and humic acid soil amendments enhance tolerance to drought and phosphorus deficiency stress in maize (*Zea mays* L.). *Sci. Rep.* 10, 1–13. doi: 10.1038/s41598-020-62669-6
- Khan, M., Khan, N. A., Masood, A., Per, T. S., and Asgher, M. (2016). Hydrogen peroxide alleviates nickel-inhibited photosynthetic responses through increase in use-efficiency of nitrogen and sulfur, and glutathione production in mustard. *Front. Plant Sci.* 7, 44. doi: 10.3389/fpls.2016.00044
- Kosar, F., Akram, N. A., Ashraf, M., Ahmad, A., Alyemeni, M. N., and Ahmad, P. (2021). Impact of exogenously applied trehalose on leaf biochemistry, achene yield and oil composition of sunflower under drought stress. *Physiol. Plantarum*. 172, 317–333. doi: 10.1111/ppl.13155
- Kutschera, A., Dawid, C., Gisch, N., Schmid, C., Raasch, L., Gerster, T., et al. (2019). Bacterial medium-chain 3-hydroxy fatty acid metabolites trigger immunity in arabidopsis plants. *Science*. 364, 178–181. doi: 10.1126/science.aau1279
- Leng, G., and Hall, J. (2019). Crop yield sensitivity of global major agricultural countries to droughts and the projected changes in the future. *Sci. Total Environment*. 654, 811–821. doi: 10.1016/j.scitotenv.2018.10.434
- Liang, C., Gao, W., Ge, T., Tan, X., Wang, J., Liu, H., et al. (2021). Lauric acid is a potent biological control agent that damages the cell membrane of phytophthora sojae. *Front. Microbiol.* 12:666761. doi: 10.3389/fmicb.2021.666761
- Liang, B., Ma, C., Zhang, Z., Wei, Z., Gao, T., Zhao, Q., et al. (2018). Long-term exogenous application of melatonin improves nutrient uptake fluxes in apple plants under moderate drought stress. *Environ. Exp. Botany*. 155, 650–661. doi: 10.1016/j.envexpbot.2018.08.016
- Liang, D., Ni, Z., Xia, H., Xie, Y., Lv, X., Wang, J., et al. (2019). Exogenous melatonin promotes biomass accumulation and photosynthesis of kiwifruit seedlings under drought stress. *Scientia Horticulturae*. 246, 34–43. doi: 10.1016/j.scienta.2018.10.058
- Li, Y., Lv, Y., Lian, M., Peng, F., and Xiao, Y. (2021). Effects of combined glycine and urea fertilizer application on the photosynthesis, sucrose metabolism, and fruit development of peach. *Scientia Horticulturae*. 289, 110504. doi: 10.1016/j.scienta.2021.110504
- Lind, C., Dreyer, I., López-Sanjurjo, E. J., von Meyer, K., Ishizaki, K., Kohchi, T., et al. (2015). Stomatal guard cells co-opted an ancient ABA-dependent desiccation survival system to regulate stomatal closure. *Curr. Biol.* 25, 928–935. doi: 10.1016/j.cub.2015.01.067
- Liu, E., Mei, X., Yan, C., Gong, D., and Zhang, Y. (2016). Effects of water stress on photosynthetic characteristics, dry matter translocation and WUE in two winter wheat genotypes. *Agric. Water Management*. 167, 75–85. doi: 10.1016/j.agwat.2015.12.026
- Liu, S., Ruan, W., Li, J., Xu, H., Wang, J., Gao, Y., et al. (2008). Biological control of phytopathogenic fungi by fatty acids. *Mycopathologia*. 166, 93–102. doi: 10.1007/s11046-008-9124-1
- Li, Z., Yu, J., Peng, Y., and Huang, B. (2017). Metabolic pathways regulated by abscisic acid, salicylic acid and  $\gamma$ -aminobutyric acid in association with improved drought tolerance in creeping bentgrass (*Agrostis stolonifera*). *Physiol. Plantarum*. 159, 42–58. doi: 10.1111/ppl.12483
- Li, Y., Zhao, H., Duan, B., Korpelainen, H., and Li, C. (2011). Effect of drought and ABA on growth, photosynthesis and antioxidant system of cotinus coggygia seedlings under two different light conditions. *Environ. Exp. Botany*. 71, 107–113. doi: 10.1016/j.envexpbot.2010.11.005
- Li, C., Zhao, Q., Gao, T., Wang, H., Zhang, Z., Liang, B., et al. (2018). The mitigation effects of exogenous melatonin on replant disease in apple. *J. pineal Res.* 65, e12523. doi: 10.1111/jpi.12523
- Lozano-Montaña, P. A., Sarmiento, F., Mejía-Sequera, L. M., Álvarez-Flórez, F., and Melgarejo, L. M. (2021). Physiological, biochemical and transcriptional responses of passiflora edulis sims f. edulis under progressive drought stress. *Scientia Horticulturae*. 275, 109655. doi: 10.1016/j.scienta.2020.109655
- Maazou, A.-R. S., Tu, J., Qiu, J., and Liu, Z. (2016). Breeding for drought tolerance in maize (*Zea mays* L.). *Am. J. Plant Sci.* 7, 1858. doi: 10.4236/ajps.2016.714172
- Maxwell, K., and Johnson, G. N. (2000). Chlorophyll fluorescence—a practical guide. *J. Exp. Botany*. 51, 659–668. doi: 10.1093/jexbot/51.345.659
- Medeiros, M. J., Oliveira, D. S., Oliveira, M. T., Willadino, L., Houllou, L., and Santos, M. G. (2015). Ecophysiological, anatomical and biochemical aspects of *in vitro* culture of zygotic syagrus coronata embryos and of young plants under drought stress. *Trees*. 29, 1219–1233. doi: 10.1007/s00468-015-1202-7
- Mehdizadeh, L., Farsaraei, S., and Moghaddam, M. (2021). Biochar application modified growth and physiological parameters of ocimum ciliatum L. and reduced human risk assessment under cadmium stress. *J. Hazardous Materials*. 409, 124954. doi: 10.1016/j.jhazmat.2020.124954
- Moaveni, P. (2011). Effect of water deficit stress on some physiological traits of wheat (*Triticum aestivum*). *Agric. Sci. Res. J.* 1, 64–68.
- Muhammad, I., Shalmani, A., Ali, M., Yang, Q.-H., Ahmad, H., and Li, F. B. (2021). Mechanisms regulating the dynamics of photosynthesis under abiotic stresses. *Front. Plant Sci.* 11, 2310. doi: 10.3389/fpls.2020.615942
- Nelson, D. R. (2006). Plant cytochrome P450s from moss to poplar. *Phytochem. Rev.* 5, 193–204. doi: 10.1007/s11101-006-9015-3
- Nover, M. C., Erb-Downward, J. R., and Huffnagle, G. B. (2003). Production of eicosanoids and other oxylipins by pathogenic eukaryotic microbes. *Clin. Microbiol. Rev.* 16, 517–533. doi: 10.1128/CMR.16.3.517-533.2003
- Pettigrew, W. (2004). Physiological consequences of moisture deficit stress in cotton. *Crop Sci.* 44, 1265–1272. doi: 10.2135/cropsci2004.1265
- Raja, V., Qadir, S. U., Alyemeni, M. N., and Ahmad, P. (2020). Impact of drought and heat stress individually and in combination on physio-biochemical parameters, antioxidant responses, and gene expression in solanum lycopersicum. *3 Biotech.* 10, 1–18. doi: 10.1007/s13205-020-02206-4
- Rao, L., Li, S., and Cui, X. (2021). Leaf morphology and chlorophyll fluorescence characteristics of mulberry seedlings under waterlogging stress. *Sci. Rep.* 11, 1–11. doi: 10.1038/s41598-021-92782-z
- Rauf, S., Al-Khayri, J. M., Zaharieva, M., Monneveux, P., and Khalil, F. (2016). “Breeding strategies to enhance drought tolerance in crops,” in J. M. Traits, S. Al-Khayri, M. Jain and D. V. Johnson eds. *Advances in plant breeding strategies: agronomic, abiotic and biotic stress traits*. (Cham: Springer), 397–pp 445. doi: 10.13140/2.1.2343.9682
- Řiháková, Z., Plocková, M., Filip, V., and Šmidrkal, J. (2001). Antifungal activity of lauric acid derivatives against aspergillus niger. *Eur. Food Res. Technol.* 213, 488–490. doi: 10.1007/s002170100416
- Saidi, I., Youssfi, N., and Borgi, M. A. (2017). Salicylic acid improves the antioxidant ability against arsenic-induced oxidative stress in sunflower (*Helianthus annuus*) seedling. *J. Plant Nutr.* 40:2326–2335. doi: 10.1080/01904167.2017.1310888
- Sandhya, S., Talukdar, J., and Bhaishya, D. (2016). Chemical and biological properties of lauric acid: A review. *Int. J. Adv. Res.* 4, 1123–1128. doi: 10.21474/IJAR01/952
- Shahid, M. A., Balal, R. M., Pervez, M. A., Garcia-Sanchez, F., Gimeno, V., Abbas, T., et al. (2014). Treatment with 24-epibrassinolide mitigates NaCl-induced toxicity by enhancing carbohydrate metabolism, osmolyte accumulation, and antioxidant activity in Pisum sativum. *Turk J. Bot.* 38, 511–525. doi: 10.3906/bot-1304-45
- Shin, S., Bajpai, V., Kim, H., and Kang, S. (2007). Antibacterial activity of eicosapentaenoic acid (EPA) against foodborne and food spoilage microorganisms. *LWT-Food Sci. Technol.* 40, 1515–1519. doi: 10.1016/j.lwt.2006.12.005
- Sun, X., Wang, P., Jia, X., Huo, L., Che, R., and Ma, F. (2018). Improvement of drought tolerance by overexpressing MdATG18a is mediated by modified antioxidant system and activated autophagy in transgenic apple. *Plant Biotechnol. J.* 16, 545–557. doi: 10.1111/pbi.12794
- Sun, T., Zhang, J., Zhang, Q., Li, X., Li, M., Yang, Y., et al. (2022). Exogenous application of acetic acid enhances drought tolerance by influencing the MAPK signaling pathway induced by ABA and JA in apple plants. *Tree Physiol* 42, 1827–1840. doi: 10.1093/treephys/tpac034
- Ullah, A., Sun, H., Yang, X., and Zhang, X. (2017). Drought coping strategies in cotton: increased crop per drop. *Plant Biotechnol. J.* 15, 271–284. doi: 10.1111/pbi.12688
- Vardharajula, S., Zulfikar Ali, S., Grover, M., Reddy, G., and Bandi, V. (2011). Drought-tolerant plant growth promoting bacillus spp.: effect on growth, osmolytes, and antioxidant status of maize under drought stress. *J. Plant Interactions*. 6, 1–14. doi: 10.1080/17429145.2010.535178
- Verslues, P. E., Agarwal, M., Katiyar-Agarwal, S., Zhu, J., and Zhu, J. K. (2006). Methods and concepts in quantifying resistance to drought, salt and freezing, abiotic stresses that affect plant water status. *Plant J.* 45, 523–539. doi: 10.1111/j.1365-313X.2005.02593.x
- Walters, D., Walker, R., and Walker, K. (2003). Lauric acid exhibits antifungal activity against plant pathogenic fungi. *J. Phytopathol.* 151, 228–230. doi: 10.1046/j.1439-0434.2003.00713.x
- Wang, L.-J., and Li, S.-H. (2006). Salicylic acid-induced heat or cold tolerance in relation to Ca<sup>2+</sup> homeostasis and antioxidant systems in young grape plants. *Plant Sci.* 170, 685–694. doi: 10.1016/j.plantsci.2005.09.005
- Wang, P., Sun, X., Li, C., Wei, Z., Liang, D., and Ma, F. (2013). Long-term exogenous application of melatonin delays drought-induced leaf senescence in apple. *J. pineal Res.* 54, 292–302. doi: 10.1111/jpi.12017
- Xa lxo, R., and Keshavkant, S. (2019). Melatonin, glutathione and thiourea attenuates lead and acid rain-induced deleterious responses by regulating gene expression of antioxidants in trigonella foenum graecum L. *Chemosphere*. 221, 1–10. doi: 10.1016/j.chemosphere.2019.01.029
- Xiao, Y., Wu, X., Sun, M., and Peng, F. (2020). Hydrogen sulfide alleviates waterlogging-induced damage in peach seedlings via enhancing antioxidative system and inhibiting ethylene synthesis. *Front. Plant Sci.* 11, 696. doi: 10.3389/fpls.2020.00696
- Zhang, X., Wang, X., Zhong, J., Zhou, Q., Wang, X., Cai, J., et al. (2016). Drought priming induces thermo-tolerance to post-anthesis high-temperature in offspring of winter wheat. *Environ. Exp. Botany*. 127, 26–36. doi: 10.1016/j.envexpbot.2016.03.004



## OPEN ACCESS

EDITED BY  
Milan Skalicky,  
Czech University of Life Sciences  
Prague, Czechia

REVIEWED BY  
Gholamreza Gohari,  
University of Maragheh, Iran  
Mahadi Hasan,  
Lanzhou University, China

\*CORRESPONDENCE  
Shokoofeh Hajihashemi  
hajihashemi@bkatu.ac.ir

SPECIALTY SECTION  
This article was submitted to  
Plant Abiotic Stress,  
a section of the journal  
Frontiers in Plant Science

RECEIVED 29 August 2022  
ACCEPTED 12 October 2022  
PUBLISHED 01 November 2022

CITATION  
Hajihashemi S, Jahantigh O and  
Alboghobeish S (2022) The redox  
status of salinity-stressed  
*Chenopodium quinoa* under  
salicylic acid and sodium  
nitroprusside treatments.  
*Front. Plant Sci.* 13:1030938.  
doi: 10.3389/fpls.2022.1030938

COPYRIGHT  
© 2022 Hajihashemi, Jahantigh and  
Alboghobeish. This is an open-access  
article distributed under the terms of  
the [Creative Commons Attribution  
License \(CC BY\)](#). The use, distribution  
or reproduction in other forums is  
permitted, provided the original  
author(s) and the copyright owner(s)  
are credited and that the original  
publication in this journal is cited, in  
accordance with accepted academic  
practice. No use, distribution or  
reproduction is permitted which does  
not comply with these terms.

# The redox status of salinity-stressed *Chenopodium quinoa* under salicylic acid and sodium nitroprusside treatments

Shokoofeh Hajihashemi\*, Omolbanin Jahantigh  
and Sahira Alboghobeish

Plant Biology Department, Faculty of Science, Behbahan Khatam Alanbia University of Technology,  
Khuzestan, Iran

Spreading the cultivation of crops with high nutritional values such as quinoa demands a wide area of research to overcome the adverse effects of environmental stress. This study aimed at investigating the role of salicylic acid (SA) and sodium nitroprusside (SNP) as a nitric oxide donor, priming at improving the antioxidant defense systems in boosting salinity tolerance in *Chenopodium quinoa*. These two treatments, SA (0.1 mM) and SNP (0.2 mM), individually or in combination, significantly improved the function of both enzymatic and non-enzymatic antioxidants. SA and SNP priming significantly reduced superoxide dismutase activity, which was accompanied by a significant decrease in hydrogen peroxide accumulation under salinity stress (100 mM NaCl). The SA and SNP treatment increased the activity of enzymatic antioxidants (e.g., catalase, ascorbate peroxidase, peroxidase, and glutathione reductase) and the accumulation of non-enzymatic antioxidants (e.g. ascorbate–glutathione pools,  $\alpha$ -tocopherol, phenols, flavonoids, anthocyanins, and carotenoids) to suppress the oxidative stress induced by salinity stress. Under SA and SNP treatment, the upregulation of antioxidant mechanisms induced a significant increase in chlorophyll fluorescence, chlorophylls, carotenoids, and proteins, as well as a significant reduction in the malondialdehyde content in salinity-stressed plants. In addition, the foliar application of SA or/and SNP led to a significant increase in the accumulation of osmoprotectant molecules of sugars and proline to overcome osmotic stress induced by salinity stress. In conclusion, SA and SNP priming can effectively combat salinity stress through improving the redox status of plants.

## KEYWORDS

antioxidants, membrane integrity, nitric oxide, osmoprotectants, photosynthetic pigments, quinoa

## Introduction

Quinoa (*Chenopodium quinoa* Willd.) is an annual dicotyledonous herbaceous crop in the Amaranthaceae family with agronomic and nutritional value. In about 7,000 years ago, it was domesticated in the Andean countries of South America, while it is reported to be widely cultured in more than 100 countries by 2021. The main edible part of quinoa is its gluten-free grains with high quantities of proteins, amino acids, minerals, and vitamins. Based on its nutritional value and health importance, it is considered to be a “superfood.” The United Nations General Assembly called 2013 as the “International Year of Quinoa” (Pathan and Siddiqui, 2022). Additionally, its salt, drought, and cold tolerance, in combination with the little requirement to fertilizers and water, has introduced quinoa as a preferable crop for cultivation all over the world (Pathan and Siddiqui, 2022).

An excessive level of salt in the soil or irrigation water limits plant growth and productivity (Mostofa et al., 2015). The plant's exposure to toxic levels of salt induces generation of excessive quantities of reactive oxygen species (ROS), such as superoxide anion ( $O_2^-$ ), hydroxyl radical (OH), and hydrogen peroxide ( $H_2O_2$ ), which can induce oxidation and malfunction in critical macro- and micromolecules in the plant cells. The induced oxidative stress because of the high accumulation of ROS can be mitigated through a complex series of ROS-scavenging or -detoxifying systems such as enzymatic and/or non-enzymatic antioxidants. Such antioxidant systems can improve the plant's potency to counteract ROS overaccumulation, so as to protect the cells against oxidative stress. The main antioxidants include ascorbate (AsA)–glutathione cycle enzymes and metabolites, peroxidase (POD), superoxide dismutase (SOD), catalase (CAT), phenolic compounds, and proline to overcome oxidative stress. Lipid peroxidation is one of the common injuries induced by the overaccumulation of ROS because of the degradation of lipids and proteins (Yadu et al., 2017).

Salinity stress is one of the most common environmental stress. Understanding the mechanisms involved in the defense response to stressors is very critical in finding new cues to produce stress tolerance plants. In particular, salicylic acid (SA), as a naturally occurring plant phenolic compound, is introduced as one of the natural plant hormones involved in the plant response to different abiotic stress, such as salinity (Rasheed et al., 2022), drought (Ahmad et al., 2021), and heavy metals (Kaya et al., 2020b). The exogenous application of SA could minimize the adverse effects of salinity stress on the physiological parameters of different plant species (Rasheed et al., 2022). SA is thought to protect the plants against environmental stress by balancing ROS accumulation and stabilizing macromolecules such as lipid membranes, proteins, and photosynthetic pigments (Kaya et al., 2020b).

Signaling molecules such as nitric oxide (NO) are found in all plants and implicated in various physiological, biochemical, and developmental processes, as well as responses to abiotic stress (Hajjhashemi et al., 2020b; Kolbert et al., 2021). NO serves

as a messenger of stress signals. As a result of its antioxidant capability, NO shows antistress effects and membrane and cell wall-stabilizing abilities. The exogenous application of NO has been proposed as an effective approach to enhance stress tolerance of crops, such as *Oryza sativa*, *C. quinoa*, *Glycine max*, and *Medicago truncatula* (Filippou et al., 2013; Mostofa et al., 2015; Hajjhashemi et al., 2020b; Jabeen et al., 2021).

Plants apply various strategies to improve tolerance to environmental stress, while some of them are time-consuming. Priming, acclaimed as preexposure of plant to elicitors, induces “stress memory” to enable quicker or more effective activation of diverse defense systems upon plant exposure to stressor (Aranega-Bou et al., 2014; Xiao et al., 2017). The pretreatment of plants with specific compounds or biological agents can maintain efficient action of defense mechanisms because of a higher content of stress-protective compounds under subsequently encountered stress. In this respect, priming practice can be done at various plant developmental stages or life cycle such as seed, seedling, or young plant (Wiszniewska, 2021). Small signaling compounds such as  $H_2O_2$  and NO and the phytohormone SA are the most frequently applied to induce priming effects in plants (Wiszniewska, 2021). Priming factors can either trigger the stressor itself or stimulate the defense mechanisms as a stress predictor (Wiszniewska, 2021).

However, the exogenously applied phytoprotectants such as plant hormones and signaling molecules were used to induce a significant protection in plant species subjected to stress throughout the last decades (Yadu et al., 2017); the protection mechanisms of phytoprotectants priming in alleviating the adverse effect of salinity stress needs to be studied more precisely, particularly in important crops. Because quinoa is an important crop, this study was conducted to investigate the effects of plant priming with SA and sodium nitroprusside (SNP), as an NO donor, and their combinations on maximizing plant stress tolerance. In this context, the enzymatic and non-enzymatic antioxidants, as well as photosynthetic pigments, membrane integrity and osmoprotectant molecules were studied in the present research.

## Materials and methods

### Plant cultivation and treatments

The planting experiment was conducted in Behbahan, Khuzestan, Iran, based on a pot culture using quinoa (*C. quinoa* Willd.) seeds obtained from Pakan Bazr Isfahan, Iran. Ten quinoa seeds were planted per each polyethylene pot containing equal amounts of soil and perlite. The pots were transferred to a room with a 16 h:8 h light/dark cycle and irrigated with tap water every 4 days. At the two leaves stages, four uniform plants were kept per pot to grow further, and extra plants were uprooted. Then, the pots were transferred to open-air conditions. As a completely randomized block in a split-plot design, the foliar treatment and NaCl irrigation were considered as the main plot and subplot, respectively. Each

treatment had four replications, that is, four pots per treatment. Each repetition included four plants per pot, so each treatment contained 16 quinoa plants. Before starting the salinity stress, priming was done on young plants with SA and SNP. Some prior characterization of multiple parameters was done to select a meaningful level of SA (0–0.2 mM), SNP (0–0.2 mM), and NaCl (0–200 mM). The results (not shown) revealed that 0.1 mM SA and 0.2 mM SNP were the most effective on reducing the adverse effects of salinity stress at 100 mM NaCl. In this respect, the 14-day-old plants were foliar sprayed with distilled water (control plants), SA (0.1 mM), SNP (0.2 mM), and a combination of SA and SNP every 5 days. The foliar application was done uniformly, with about 10-ml solution to the plants per pot, as a fine spray using an atomizer. The foliar application lasted for 1 month. One month after the first foliar treatment, the primed pots were divided into two groups of four pots each. The groups were irrigated with distilled water (control) or 100 mM of NaCl solution every 4 days. The plants were grown for further 1 month under salinity stress. At the end of NaCl irrigation regime, the chlorophyll (Chl) fluorescence was measured, and the plants were harvested for the purpose of doing further analysis. Figure 1 illustrates the scheme of the treated plants at the harvesting stage. Furthermore, the key physiological and biochemical parameters were studied in the collected plants.

### Analysis of hydrogen peroxide; malondialdehyde; total antioxidant power; and activity of superoxide dismutase, catalase, ascorbate peroxidase, polyphenol oxidase, peroxidase, and glutathione reductase enzymes

The  $H_2O_2$  content of fresh leaves was determined based on the Velikova et al. (2000) procedure. The malondialdehyde (MDA) content, as a lipid peroxidation indicator, was measured in the fresh leaves, using thiobarbituric acid, according to the Heath and Packer

(1968) method. The fresh leaves were used to quantify the total antioxidant power (FRAP) value, as already described by Szöllősi and Varga (2002). The activity of enzymes were appraised according to the standard protocols developed for SOD activity (Giannopolitis and Ries, 1977), CAT activity (Aebi, 1984), ascorbate peroxidase (APX) activity (Nakano and Asada, 1987), POD activity (Plewa et al., 1991), and glutathione reductase (GR) activity (Mannervik, 1999).

### Analysis of ascorbate and glutathione metabolites

The fresh leaves were extracted in cold metaphosphoric acid for the purpose of measuring both AsA and glutathione metabolites. The AsA and dehydroascorbate (DHA) contents were quantified according to the protocol of Kampfenkel et al. (1995). The oxidized glutathione (GSSG) and reduced glutathione (GSH) were measured using the procedure of Griffith (1980).

### Analysis of phenols, flavonoids, anthocyanins, and $\alpha$ -tocopherol

A protocol of using Folin's reagent was used for phenol assay based on the method of Singleton and Rossi (1965). The flavonoid content was measured in the fresh leaves based on the Zhishen et al. (1999) protocol. The anthocyanins of fresh leaves was colorimetrically measured as already described by Wagner (1979). The quantification of  $\alpha$ -tocopherol in the fresh leaves was done according to the Baker et al. (1980) method.

### Analysis of chlorophyll fluorescence and photosynthetic pigments

The Chl fluorescence was determined using a portable Chl fluorometer (Pocket PEA, Hansatech Instruments Ltd., King's

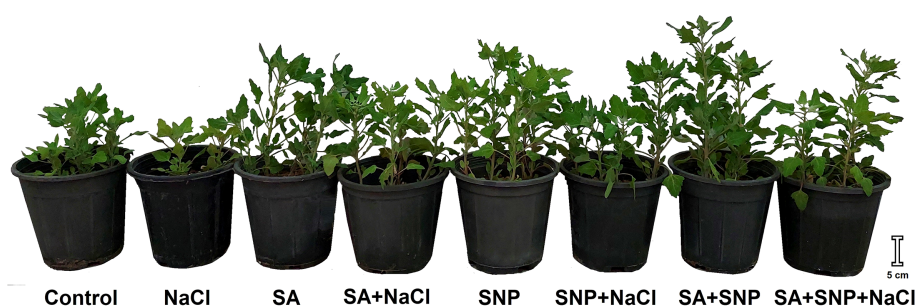


**FIGURE 1**  
Illustration of *Chenopodium quinoa* under different treatments of salicylic acid (SA) and sodium nitroprusside (SNP), and salinity stress at harvesting stage.



Lynn, Norfolk, England). The maximum quantum yield of photosystem II ( $F_v/F_m$ ) and efficiency of both photosystems I and II ( $PI_{abs}$ ) were examined on the surface of fully expanded apical leaves, which were previously adapted in dark for 30 min (Hajihashemi et al., 2018). The photosynthesis pigments of the fresh leaves were appraised by applying the procedure outlined by Wellburn (1994).

## Analysis of water soluble carbohydrates, proteins, proline, and free amino acids

The water soluble carbohydrates (WSC) content was determined according to the phenol-sulfuric acid protocol (Dubois et al., 1956). The total soluble protein content of fresh leaves was determined using the Bradford reagent (Bradford, 1976). The ninhydrin-based colorimetric assay of Bates et al. (1973) was followed to analyze the fresh leaves free proline content. The free amino acid content in the fresh leaves was measured by the procedure as previously optimized by Yemm et al. (1955). The applied methods in this study were described in detail in our earlier literatures (Hajihashemi and Ehsanpour, 2014; Hajihashemi et al., 2018; Hajihashemi et al., 2020b).

## Statistical analyses

The plant culture and treatment were repeated at three consecutive times, every time with four pots containing four plants as one replicate for each treatment. The values presented in figures are the means plus their respective standard error of three independent replicates. The data were subjected to 0.05% level of probability, employing the Tukey's test using the SPSS statistical (version 24) package. The superscripted letters presented above each column in the figures show the significant differences at  $p \leq 0.05$ .

## Results

Salinity stress led to oxidative stress as shown by a significant ( $p \leq 0.05$ ) increase in the  $H_2O_2$  and MDA contents, by 32% and 44%, respectively, with respect to the control plants (Figures 2A, B). The plant priming with both SA and SNP suppressed the accumulation of  $H_2O_2$  and MDA in both salt-stressed and non-stressed plants. The SNP treatment induced the largest average reduction in the  $H_2O_2$  and MDA contents in the non-stressed plants, by 49% and 35%, respectively, in comparison with the control plants. Under salinity stress, the average values of  $H_2O_2$  and MDA showed the highest reduction in response to SNP priming by 38% and 51%, respectively, less than their values in salinity stress without priming. Salinity stress decreased the total antioxidant activity, represented as FRAP, by 5% compared with

that in the control plants (Figure 2C). The individual foliar application of SA and SNP or their combination improved the FRAP value in both stressed and non-stressed plants. SA, SNP, and SA + SNP priming significantly ( $p \leq 0.05$ ) increased the FRAP value in the stressed plants by 10%, 15% and 14%, respectively, higher than that in the salt-stressed plants.

The antioxidant system includes enzymatic and non-enzymatic antioxidants. The upregulation of enzymatic and non-enzymatic antioxidants can lead to the reduction of ROS value below the threshold level and the suppression of oxidative stress induced by salinity stress. In this respect, the activity of SOD showed a significant ( $p \leq 0.05$ ) increase (55%), the activity of CAT and APX showed no significant changes, whereas the activity of POD and GR significantly ( $p \leq 0.05$ ) decreased (29% and 51%, respectively) in the salt-stressed plants, as compared with that in the control plants (Figures 2D–H). SA, SNP, and SA + SNP priming reversed the adverse effects of salinity stress on the activity of SOD, CAT, APX, POD, and GR. Under salinity stress, the activity of CAT, APX, POD, and GR in the SA-, SNP-, and SA + SNP-treated plants significantly ( $p \leq 0.05$ ) increased higher than their values in the stressed plants without treatment. Under salinity stress, the greatest increase in the activity of CAT (51%), APX (65%), POD (73%), and GR (60%) was achieved in the SNP-treated plants, with respect to the control plants. The foliar application of SA, SNP, and SA + SNP significantly ( $p \leq 0.05$ ) decreased the SOD activity in both stressed and non-stressed plants (Figure 2D). Under salinity stress, the SOD activity in the SA-, SNP-, and SA + SNP-treated plants decreased by 75%, less than its value in salinity stress alone.

To assess the SA and SNP function in tolerance to salinity stress, the redox status of AsA and GSH pools were measured in quinoa plants. Salinity stress significantly ( $p \leq 0.05$ ) decreased the AsA and GSH contents (50% and 41%, respectively) while significantly ( $p \leq 0.05$ ) increased the DHA and GSSG contents (53% and 57%, respectively), compared with the control plants (Figures 3A–D). SA, SNP, and SA + SNP priming reversed the adverse effects of salinity stress on the AsA and glutathione pools, which was followed by a significant ( $p \leq 0.05$ ) increase in the AsA and GSH values and a significant ( $p \leq 0.05$ ) reduction in the DHA and GSSG contents (Figures 3A–D). Under salinity stress, the greatest increase in the AsA and GSH contents was achieved in SNP priming, by 75% and 60%, respectively, with respect to their values in salinity stress alone. The values of DHA and GSSG in the stressed plants showed the highest reduction in the SA + SNP treatment by 43% and 56%, respectively, relative to salinity stress alone.

The evaluation of non-photosynthetic pigments revealed a significant ( $p \leq 0.05$ ) reduction in the phenol, flavonoid and anthocyanin contents in response to NaCl irrigation, by 13%, 36%, and 13%, respectively, as compared with the control plants (Figures 3E–G). SA, SNP, and SA + SNP priming significantly ( $p \leq 0.05$ ) increased the phenol, flavonoid, and anthocyanin contents in both stressed and non-stressed plants. Under stress



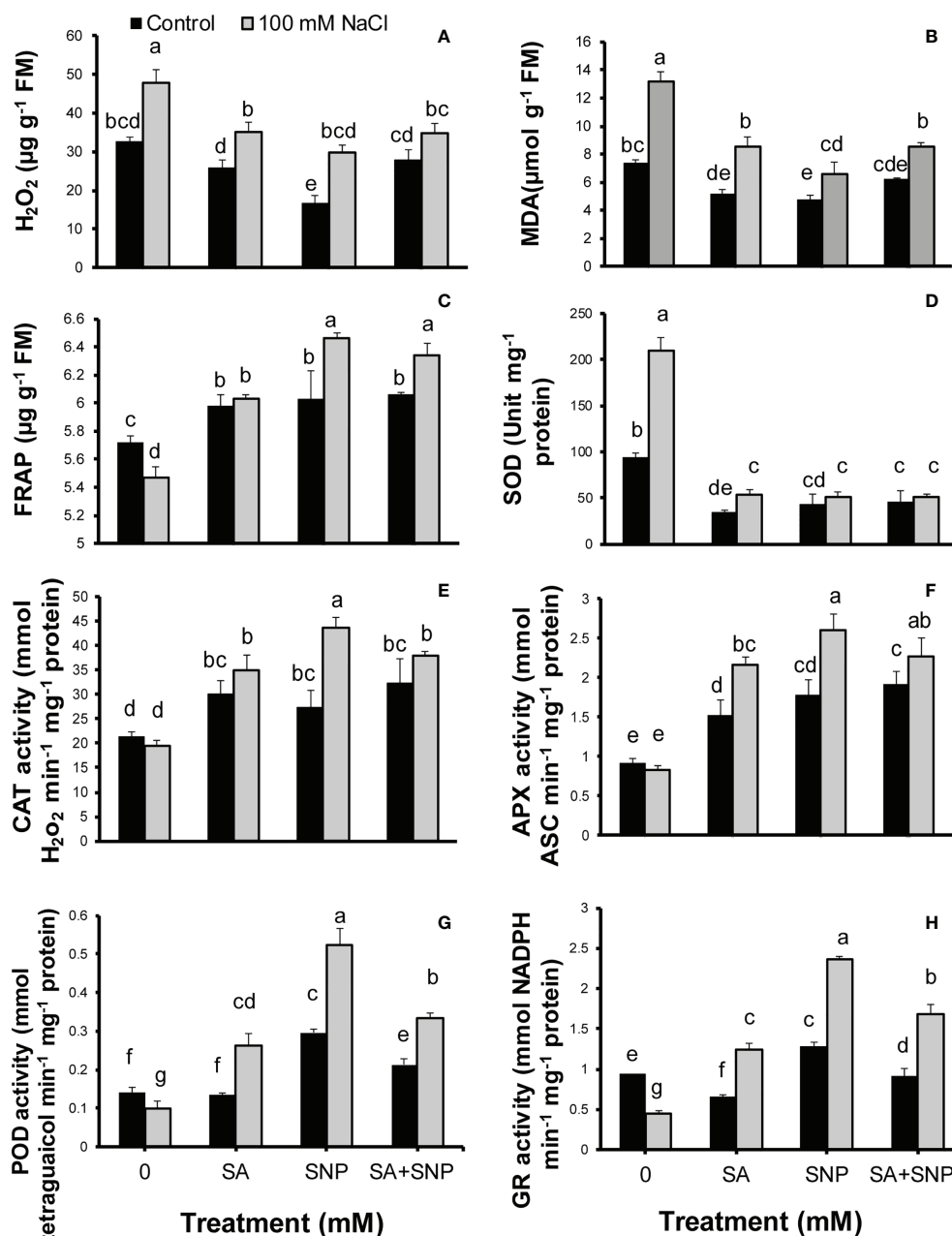


FIGURE 2

(A)  $H_2O_2$ , (B) malondialdehyde (MDA), (C) total antioxidant power (FRAP), (D) superoxide dismutase activity (SOD), (E) catalase activity (CAT), (F) ascorbate peroxidase activity (APX), (G) peroxidase activity (POD), and (H) glutathione reductase activity (GR) in *Chenopodium quinoa* under different treatments of salicylic acid (SA) and sodium nitroprusside (SNP), and salinity stress. Columns with different letters are significantly different at  $p < 0.05$ .

conditions, the greatest accumulation of phenols and flavonoids was achieved in the SNP treatment by 54% and 53%, respectively, greater than their contents in salinity stress alone. The greatest increase in the anthocyanins in the stressed plants was achieved in the SA + SNP treatment by 30% higher than that in salinity stress alone. The  $\alpha$ -tocopherol content, in a similar

trend to non-photosynthetic pigments, significantly ( $p \leq 0.05$ ) decreased in the stressed plants by 24% less than its value in the control plants (Figure 3H). The foliar application of SA, SNP, and SA + SNP reversed the adverse effect of salinity stress on  $\alpha$ -tocopherol, with the greatest increase observed in the SA treatment, by 49% higher than that in the control plants. The

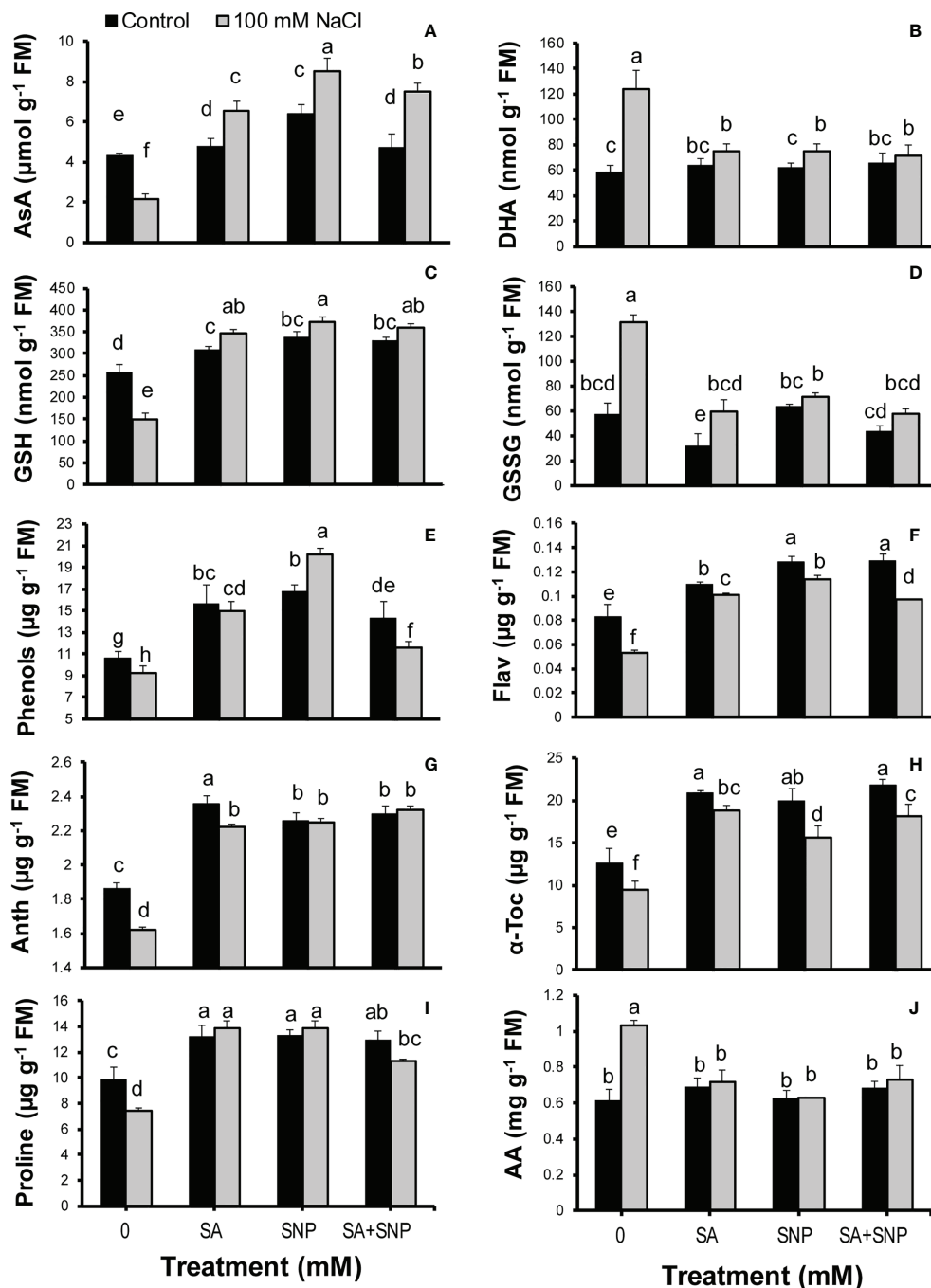


FIGURE 3

(A) Ascorbate (AsA), (B) dehydroascorbate (DHA), (C) reduced glutathione (GSH), (D) oxidized glutathione (GSSG), (E) phenols, (F) flavonoids (Flav), (G) anthocyanins (Anth), (H)  $\alpha$ -tocopherol ( $\alpha$ -Toc), (I) proline, and (J) total free amino acids (AA) in *Chenopodium quinoa* under different treatments of salicylic acid (SA) and sodium nitroprusside (SNP), and salinity stress. Columns with different letters are significantly different at  $p < 0.05$ .

proline content significantly ( $p \leq 0.05$ ) decreased (24%) in the salt-stressed plants, whereas the amount of total amino acids significantly ( $p \leq 0.05$ ) increased (40%) in response to salinity stress (Figures 3I, J). The foliar application of SA, SNP, and SA + SNP significantly ( $p \leq 0.05$ ) increased proline accumulation in

both stressed and non-stressed plants. Under stress conditions, individual SA and SNP primings were more effective than their combination in increasing the proline content, by 46% higher than that in salinity stress alone. In opposite to proline, the application of SA, SNP, and SA + SNP prevented the changes in

the accumulation of amino acids in both stressed and non-stressed plants.

Salinity stress suppressed photosynthesis-related traits such as  $F_v/F_m$ ,  $PI_{abs}$ , Chls a and b, and carotenoids in quinoa plants (Figures 4A–F). The  $F_v/F_m$  and  $PI_{abs}$  values in the salt-stressed plants were by 15% and 72%, respectively, less than their values in the control plants (Figures 4A, B). The SA, SNP, and SA + SNP treatments led to a significant ( $p \leq 0.05$ ) increase in the  $F_v/F_m$  and  $PI_{abs}$  values as compared with salinity stress alone. In parallel to Chl fluorescence parameters, the Chls a and b, total Chl, and carotenoid values significantly ( $p \leq 0.05$ ) decreased in the salt-stressed plants by 47%, 56%, 51%, and 34%, respectively,

relative to their values in the control plants (Figures 4C–F). The foliar application of SA, SNP, and SA + SNP, in the absence or presence of NaCl, promoted a significant ( $p \leq 0.05$ ) increase in the Chl and carotenoid values. The highest increase in Chls a and b, total Chl, and carotenoid contents was achieved in the SNP treatment by 34%, 31%, 33% and 42%, respectively, higher than them in the control plants.

Along with the observed reduction in the photosynthetic pigments in the salinity-stressed plants, the WSC content also showed a significant ( $p \leq 0.05$ ) reduction by 28% less than that in the control plants (Figure 4G). The SA, SNP, and SA + SNP treatments led to a significant ( $p \leq 0.05$ ) increase in the WSC

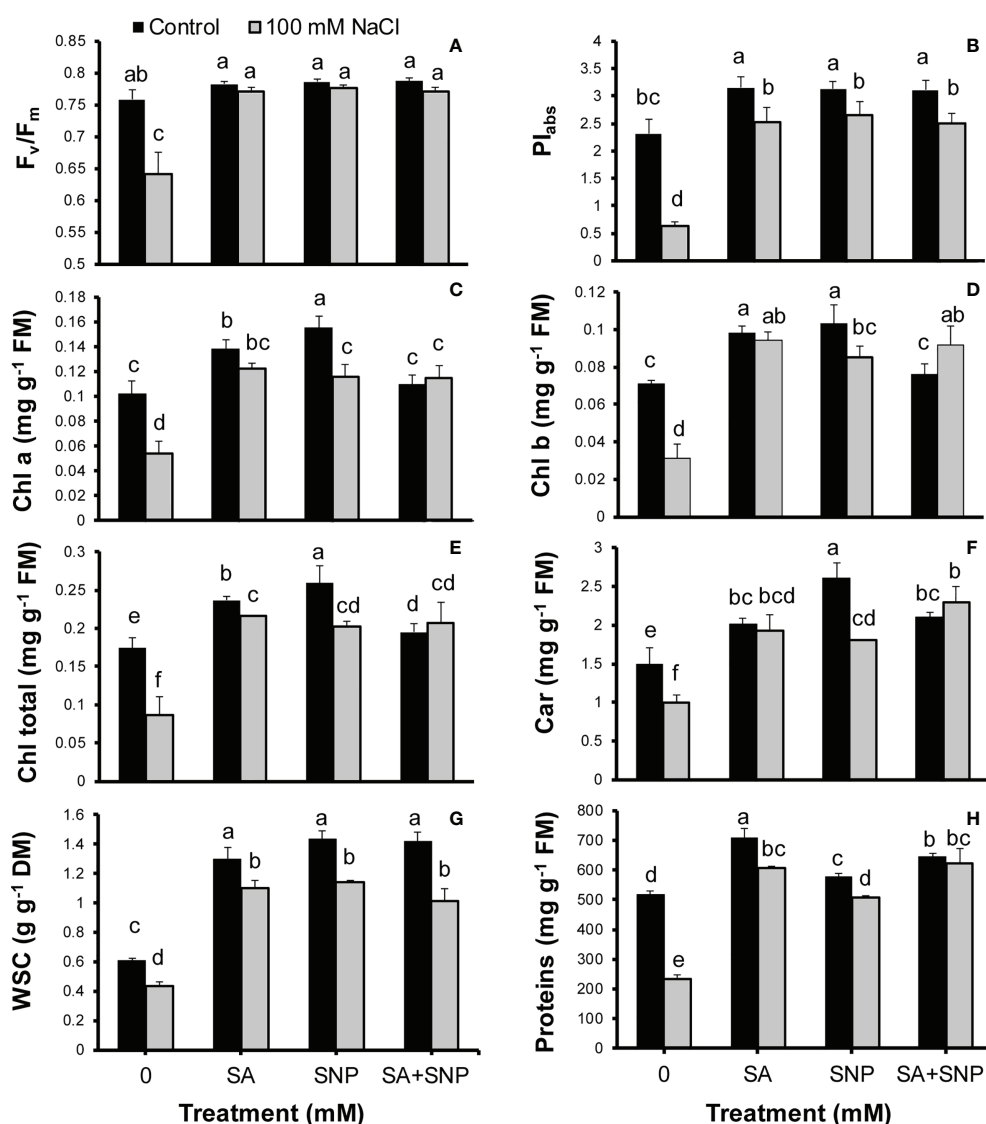


FIGURE 4

(A) Maximum quantum yield of photosystem II ( $F_v/F_m$ ), (B) efficiency of both photosystems I and II ( $PI_{abs}$ ), (C) chlorophyll a (Chl a), (D) Chl b, (E) total Chls, (F) carotenoids, (G) water soluble carbohydrate (WSC), and (H) proteins in *Chenopodium quinoa* under different treatments of salicylic acid (SA) and sodium nitroprusside (SNP), and salinity stress. Columns with different letters are significantly different at  $p < 0.05$ .

content in both stressed and non-stressed plants. The WSC content showed the greatest increase at the SNP application without or with NaCl irrigation by 58% and 47%, respectively, higher than that in the control plants (Figure 4G). Furthermore, the protein content significantly ( $p \leq 0.05$ ) reduced in response to salinity stress by 55% less than that in the control plants (Figure 4H). In parallel with the observed increase in the activity of antioxidant enzymes, the foliar application of SA, SNP, and SA + SNP significantly ( $p \leq 0.05$ ) increased the protein content in both stressed and non-stressed plants (Figure 4H). The greatest protein content was observed in the SA treatment by 27% higher than that in the control plants. SA, SNP, and SA + SNP priming in the stressed plants increased the protein content by 61%, 53% and 62%, respectively, relative to that in the stressed plants alone.

## Discussion

Soil salinization with sodium chloride ions induces malfunction in the physiological and biochemical mechanisms due to inducing either osmotic or oxidative stresses, leading to a reduction in the crops yield (Gupta et al., 2018; Gupta et al., 2021). Upon exposure to saline environment, plants employ antioxidants and osmoregulation mechanisms to tolerate salinity stress (Gupta et al., 2021). Two signaling molecules of NO and SA are introduced as robust tools to mitigate the adverse effects of salinity stress through engaging in an array of tasks against salinity-induced oxidative stress (Mostofa et al., 2015; Kaya et al., 2020a; Prakash et al., 2021). SA involves in stress tolerance due to scavenging free radical molecules such as NO and its related molecules, while NO triggers an increase in SA level with the potential of reducing NO-mediated oxidative stress (Prakash et al., 2021). However, the individual roles of NO and SA on enhancing antioxidant systems have been extensively studied (Mostofa et al., 2015; Kaya et al., 2020a; Hajihashemi, 2021; Prakash et al., 2021; Hajihashemi and Jahantigh, 2022); understanding their interactions and associated mechanisms in improving antioxidative systems can highlight future perspectives. This study was designed to evaluate how the antioxidant systems of salt-stressed quinoa plants respond to SA and SNP priming, and the consequence of physiological and biochemical processes was also evaluated to better understand the associated mechanisms toward stress tolerance.

The  $H_2O_2$  burst in response to environmental stress plays a critical role in triggering the defense mechanisms in plants to cope oxidative stress. Priming agents such as NO and SA used to stimulate plant antioxidant capacity and to counteract oxidative damages at the early stage of encountering stress (Aranega-Bou et al., 2014; Wiszniewska, 2021).

The results of this study showed that salinity stress induced a significant decrease in the FRAP value accompanied by the high accumulation of  $H_2O_2$ , which confirms the previous reports

based on the negative effects of salinity stress on the antioxidant systems (Mostofa et al., 2015; Hasanuzzaman et al., 2021). In opposite, SA, SNP, and SA + SNP priming promoted a significant increase in the FRAP value in the salinity-stressed quinoa plants, corresponding a significant decrease in  $H_2O_2$  accumulation. Under stress conditions, the function of SA + SNP treatment in improving the FRAP value was similar to individual SNP priming and significantly higher than the SA treatment, which declares no antagonistic effect of SA on NO at their applied concentrations in this study. As expected, an increase in the MDA level and a decline in the protein content concomitantly happened with the increase of ROS and reduction of FRAP value in the stressed quinoa plants, which corroborates previous reports (Mostofa et al., 2015; Prakash et al., 2021). The priming of plants with SA, SNP, and SA + SNP prevented the reduction in proteins and the increase in MDA because of salinity stress in a coordinated manner to previous reports (Mostofa et al., 2015; Kaya et al., 2020a; Prakash et al., 2021). Accordingly, the promotion of antioxidant power by SA, SNP, and SA + SNP, represented as an improvement in the FRAP value, was responsible for the observed reduction in ROS accumulation, and the common damages to the lipid and protein molecules in the salinity-stressed quinoa plants.

The promotion of enzymatic and non-enzymatic antioxidant mechanisms was achieved in response to SA, SNP, and SA + SNP priming in the stressed and non-stressed quinoa plants. As illustrated in Figure 5, SOD, CAT, APX, POD, and GR are the key ROS scavenging enzymes in plants (Hajihashemi and Ehsanpour, 2014; Hajihashemi, 2021; Kaya et al., 2020b). SA, SNP, and SA + SNP priming reduced  $H_2O_2$  accumulation in parallel with a significant decrease in the SOD activity under salinity stress, which approved the previous reports based on the key role of SA and SNP in reducing ROS accumulation (Mostofa et al., 2015; Yadu et al., 2017; Kaya et al., 2020b). In reverse to SOD, the foliar application of SA, SNP, and SA + SNP in the salinity-stressed plants led to a significant increase in the activity of CAT, APX, GR, and POD enzymes, which play a vital role in the  $H_2O_2$  detoxification (Figure 5) (Mostofa et al., 2015; Yadu et al., 2017). The findings of this study showed that the highest activity of antioxidant enzymes was achieved in the individual SNP treatment. Zottini et al. (2007) demonstrated the role of SA in inducing NO production in *Arabidopsis thaliana* by nitric oxide synthase-like enzymes. Kaya et al. (2020b) has shown that the application of cPTIO, an NO scavenger, upturned the upregulated activity of antioxidant enzymes induced by SA treatment. They have suggested that the accumulation of endogenous NO due to SA treatment involved in inducing antioxidant defense systems (Kaya et al., 2020b). The results of this study approved the previous reports based on the role of SA in modifying the activity of NO-regulated antioxidant enzymes such as SOD, CAT, APX, and GR (Mostofa et al., 2015). Based on the wide involvement of NO in the reduction of oxidative stress (Mostofa et al., 2015), it can be suggested that the salinity

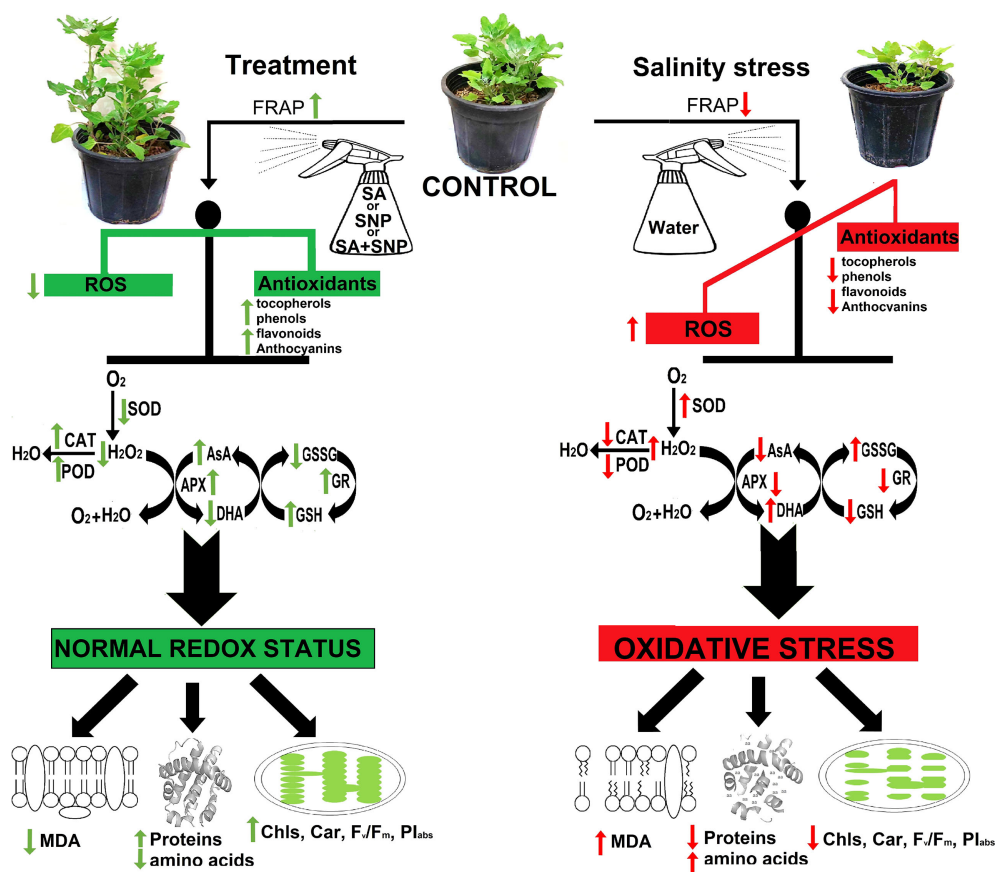


FIGURE 5

Summary of the most important events that occurred in *Chenopodium quinoa* under different treatments of salicylic acid (SA) and sodium nitroprusside (SNP), and salinity stress.

tolerance of quinoa in response to both SA and SNP treatment was due to the NO role in suppressing ROS accumulation.

AsA–glutathione cycle is one of the major antioxidant defense pathways in a plant cell with the main aim of detoxifying  $H_2O_2$  (Hasanuzzaman et al., 2019). In this cycle, APX decomposes  $H_2O_2$  to water with consuming AsA as an electron donor. Then, GR involves in the regeneration of AsA and GSH using NADPH, as the electron donor (Hasanuzzaman et al., 2019). In this study, salinity stress induced a substantial reduction in the AsA and GSH contents, interfering that salinity stress perturbed the whole antioxidant systems. As AsA has prominent responsibility in the redox function metabolism, recycling of AsA from DHA (using GSH) is a necessity to keep the redox balance and a higher total AsA pool (Hasanuzzaman et al., 2019). AsA functions as both a ROS scavenger and an electron donor in various reactions, which leads to be oxidized to DHA. DHA is very unstable and reduces back to AsA; otherwise, it will be lost within minutes. The recycling of AsA can provide its appropriate pool for suppressing oxidative stress in the stressed plant cells (Szarka

et al., 2012). In this study, SA and/or SNP priming in the salinity-stressed plants led to the overactivity of APX and GR, along with the changes in equilibrium between AsA and GSH. The achieved increase in the AsA/DHA and GSH/GSSG ratio in response to SA and/or SNP priming was followed with a significant reduction in the  $H_2O_2$  content in the salinity-stressed quinoa plants. In line with our findings, Kaya et al. (2020a) acclaimed the potential of combined application of SA plus NO to trigger the AsA–GSH cycle to improve salinity tolerance through suppressing oxidative stress. Despite the association of GR and GSH with AsA regeneration, the overexpression of GR has not led to an improvement in stress tolerance (Szarka et al., 2012). Accordingly, it can be suggested that the observed increase in GR and GSH in response to SA and/or SNP in the stressed plants can provide the reduction state of the AsA pool with coupling of the reactions of the AsA–GSH pathway. Quinoa priming with either SA or SNP is considered advantageous because of its effective response to salinity stress by neutralizing oxidative impairments as a result of enhanced antioxidant systems.



The non-enzymatic antioxidants system includes AsA, GSH,  $\alpha$ -tocopherol, flavonoids, phenols, carotenoids, and several osmoprotectants with roles in quenching the toxic by-products of ROS (Gupta and Huang, 2014; Hajihashemi et al., 2020a; Hasanuzzaman et al., 2021). Salinity stress in quinoa plants led to a significant reduction in the non-enzymatic antioxidant molecules such as  $\alpha$ -tocopherol, flavonoids, phenols, and carotenoids. AsA and GSH are introduced as the two major hydrophilic antioxidants in the plant cells (Szarka et al., 2012). Tocopherols are lipophilic free radical scavengers with the ability to donate the phenolic hydrogen to lipid free radicals.  $\alpha$ -Tocopherol is one of the most abundant antioxidants in leaves. AsA, as one of the most powerful  $H_2O_2$  scavengers, maintains the reduced state of  $\alpha$ -tocopherol (Szarka et al., 2012). The synergistic antioxidant effect of tocopherol, AsA, and GSH can be an interesting area of the present research. In parallel with AsA and GSH, the foliar application of SA and/or SNP increased  $\alpha$ -tocopherol accumulation in the stressed and non-stressed plants. It has already documented that a severe AsA deficiency in chloroplasts led to  $\alpha$ -tocopherol loss under stress conditions, which enhanced the importance of the AsA and GSH cycle in recycling reduced  $\alpha$ -tocopherol from the tocopheroxyl radical (Szarka et al., 2012; Hasanuzzaman et al., 2019). The reduction of oxidative stress induced by salinity stress in the SA- and/or SNP-treated quinoa plants, represented by the reduction of  $H_2O_2$  and membrane lipid peroxidation, increased the belief based on the several fold improvement of the antioxidants of tocopherol, AsA, and GSH in a coordinate manner. In addition, the observed increase in the photosynthetic and non-photosynthetic pigments of carotenoids, phenols, anthocyanins, and flavonoids with antioxidant property in the SA and/or SNP treatment in the salinity-stressed plants provided a strong evidence that the objective of avoiding oxidative damage can be achieved more efficiently by a joint effort of antioxidants.

Excess ROS generation and oxidative stress can lead to hampering photosynthesis, changing enzyme activities, disruption of membranes, and cell death (Hasanuzzaman et al., 2019). The chloroplast is one of the major sources of ROS in plant cells. It is well known that chloroplast, photosystems, Calvin cycle activity, and photosynthesis pathway are the maximum contributor of ROS and oxidative stress under abiotic stress (Hasanuzzaman et al., 2019). In the salinity-stressed plants, enhanced ROS accumulation can lead to damages in the photosynthetic system (Mostofa et al., 2015), which was obvious in this study by a significant reduction in the Chls a and b,  $F_v/F_m$ , and  $PI_{abs}$ . The limitation of  $CO_2$  fixation accompanies a reduction in the ATP and NADPH consumption, which results in a decline in the  $NADP^+$  content. The depletion of  $NADP^+$  as the main electron acceptor in photosystem I accelerates the transport of electrons to molecular oxygen resulting in  $H_2O_2$  accumulation. The elevated ROS content inhibits the damaged photosystem II repair and results in photoinhibition (Szarka et al., 2012). This may explain the

observed reduction in the  $F_v/F_m$  and  $PI_{abs}$  values in the salinity-stressed quinoa. Several research findings reported about the role of AsA and GSH in improving the Chls and carotenoids levels (Hasanuzzaman et al., 2019), which can explain the observed increase in the Chls,  $F_v/F_m$ , and  $PI_{abs}$  in response to SA and/or SNP application under salinity stress. Wang et al. (2010) have already reported that transgenic plants with a large AsA pool showed lower membrane damage and accumulated a higher level of Chl in the stressed plants.  $\alpha$ -Tocopherol accumulation in response to SA and/or SNP priming in the salinity-stressed quinoa plants can be another reason for enhanced ROS scavenging and to avoid oxidative damage to the plastids envelope (Szarka et al., 2012). Overall, the elegant evidence of the interplay between hydrophilic and lipophilic antioxidants has been documented in this study to better understand the early and effective role of the SA and/or NO priming in predicting oxidative stress and hampering oxidative damage to a photosynthetic system.

The overproduction of ROS in cells because of environmental stress is toxic and reactive, which can result in the oxidation of cellular components and damage Chls, proteins, lipids, and DNA (Wang et al., 2010; Hasanuzzaman et al., 2019). The enhanced MDA level in the salinity-stressed quinoa marked the high accumulation of  $H_2O_2$  and higher lipid peroxidation than in the control plants. A characteristic feature of MDA accumulation is damages to plant cellular compartment membrane including chloroplasts (Szarka et al., 2012). One response to salinity stress is generation of signaling molecules of SA and NO to combat ROS formation (Gupta et al., 2021). NO can directly react with lipid radicals to prevent lipid oxidation or activate enzymatic and non-enzymatic antioxidants including CAT, APX, GR, POD, and ASA–GSH pathway (Gupta et al., 2021). Besides, there is evidence that tocopherol mediated plant cell protection against lipid peroxidation. Tocopherols are lipophilic molecules with a hydrophobic prenyl tail associated with membrane lipids and a polar chromanol head exposed to membrane surface. Tocopherol synthesis is regulated in plant responses to environmental stress and stress-sensitive hormones such as SA (Noreen and Ashraf, 2010). The parallel enhanced  $\alpha$ -tocopherol and stabilized lipid membrane, represented as the reduction of MDA, demonstrated the potential of SA and NO in improving the antioxidant defense system to improve membrane integrity. In line with our results, Szarka et al. (2012) have proposed an interplay between hydrophilic (AsA) and lipophilic (tocopherol) antioxidants to prevent lipid peroxidation under stress conditions.

Under salinity stress conditions, the quinoa plant developed a significant increase in the total amino acids compared with the stress-free condition, and this imbalanced condition triggered reduced protein content. In salinity-tolerant plants, proteins and membrane lipids are protected from oxidative damage through enhanced antioxidant mechanism, which minimizes lipid and protein oxidation while preserving membrane integrity (Gupta et al., 2021). The utilization of SA and/or SNP managed to

alleviate the damage to cellular compounds such as proteins through activating the antioxidant systems to scavenge ROS, thereby restricting protein degradation and high amino acid accumulation. Regardless to total amino acids, salinity stress led to a significant reduction in the proline content in quinoa. One of the strategies used to mitigate against salinity stress is the accumulation of proline within the plant cells (Gupta et al., 2021). Under stress conditions, the foliar application of SA and/or SNP resulted in the high accumulation of proline in quinoa. The plant exposure to saline conditions induces a decline in the capacity of water absorbing from soil, resulting in osmotic stress. In order to overcome osmotic stress, the plant cells accumulate osmolytes, such as proline, sugars, organic acids, and polyamines, in favor of osmotic adjustment (Hajjhashemi, 2020; Hasanuzzaman et al., 2021; Gupta et al., 2021). In the salinity stress, SA and/or SNP priming increased the proline and sugar contents, suggesting that SA and NO could improve the water potential of cells by enhancing osmolytes, as has earlier been reported in maize and rice (Mostofa et al., 2015; Kaya et al., 2020b). The salinity stress-induced decline in the photosynthetic pigments and photosystems function triggered a significant reduction in the carbohydrate biosynthesis in quinoa, which was reversed by SA and/or SNP priming. As an osmoprotector, it is supposed that sugars can stabilize lipid membranes and proteins through substituting the water molecules in the hydrogen bond formation with phosphate groups of phospholipids and polar residues of polypeptides (Yadu et al., 2017). Overall, plant priming with the relevant molecules of SA and NO motivated various defense mechanisms to improve salinity tolerance in quinoa.

## Conclusion

The complex phenomenon of plant response to SA and NO priming involved dynamic changes in (A) the antioxidant systems including (a) high accumulation of non-enzymatic antioxidants (e.g., AsA, GSH, anthocyanins, flavonoids, phenols,  $\alpha$ -tocopherol, and carotenoids) and (b) regulation of enzymatic antioxidants activity (e.g., CAT, APX, POD, GR, and SOD) to combat formation of ROS; (B) osmolytes accumulation (e.g., proline and sugars) to overcome osmotic stress induced by salinity stress; and (C) protecting of cellular compounds against stress-induced

damages (e.g., Chls, lipid membrane, and proteins) to modulate the adverse effect of salinity stress in quinoa plants. In conclusion, the results of this study revealed the high potential of relevant molecules of SA and NO in reducing the adverse effect of salinity stress in plants through improving antioxidant defense systems and osmotic adjustment. However, the results revealed that none of SA and SNP at the applied concentrations in this study was superior to the other one. It should also be pointed that the combination of SA and SNP did not multiply their effect. Overall, the scheme of physiological mechanisms induced by the SA and NO priming of quinoa provided a promising strategy in crop production management under stress conditions.

## Data availability statement

The raw data supporting the conclusions of this article will be made available by the authors, without undue reservation.

## Author contributions

SH designed the experiment and wrote the manuscript. SH, OJ and SA conducted the experiment. SH and OJ analyzed the data. All authors contributed to the article and approved the submitted version.

## Conflict of interest

The authors declare that the research was conducted in the absence of any commercial or financial relationships that could be construed as a potential conflict of interest.

## Publisher's note

All claims expressed in this article are solely those of the authors and do not necessarily represent those of their affiliated organizations, or those of the publisher, the editors and the reviewers. Any product that may be evaluated in this article, or claim that may be made by its manufacturer, is not guaranteed or endorsed by the publisher.

## References

- Aebi, H. (1984). Catalase *in vitro*. *Methods enzymology* 105, 121–126. doi: 10.1016/S0076-6879(84)05016-3
- Ahmad, A., Aslam, Z., Naz, M., Hussain, S., Javed, T., Aslam, S., et al. (2021). Exogenous salicylic acid-induced drought stress tolerance in wheat (*Triticum aestivum* L.) grown under hydroponic culture. *PLoS One* 16, e0260556. doi: 10.1371/journal.pone.0260556
- Aranega-Bou, P., de la O Leyva, M., Finiti, I., García-Agustín, P., and González-Bosch, C. (2014). Priming of plant resistance by natural compounds. hexanoic acid as a model. *Front. Plant Sci.* 5, 488. doi: 10.3389/fpls.2014.00488
- Baker, H., Frank, O., and DeAngelis Feingold, B. S. (1980). Plasma tocopherol in man at various times after ingesting free or acetylated tocopherol. *Nutr. Rep. Int.* 21 (4), 531–536.

- Bates, L., Waldren, R., and Teare, I. (1973). Rapid determination of free proline for water-stress studies. *Plant Soil* 39, 205–207. doi: 10.1007/BF00018060
- Bradford, M. M. (1976). A rapid and sensitive method for the quantitation of microgram quantities of protein utilizing the principle of protein-dye binding. *Analytical Biochem.* 72, 248–254. doi: 10.1016/0003-2697(76)90527-3
- DuBois, M., Gilles, K. A., Hamilton, J. K., and Rebers Smith, P. T. F. (1956). Colorimetric method for determination of sugars and related substances. *Anal. Chem.* 28 (3), 350–356.
- Filippou, P., Antoniou, C., and Fotopoulos, V. (2013). The nitric oxide donor sodium nitroprusside regulates polyamine and proline metabolism in leaves of medicago truncatula plants. *Free Radical Biol. Med.* 56, 172–183. doi: 10.1016/j.freeradbiomed.2012.09.037
- Giannopolitis, C. N., and Ries, S. K. (1977). Superoxide dismutases: I. occurrence in higher plants. *Plant Physiol.* 59, 309–314. doi: 10.1104/pp.59.2.309
- Griffith, O. W. (1980). Determination of glutathione and glutathione disulfide using glutathione reductase and 2-vinylpyridine. *Analytical Biochem.* 106, 207–212. doi: 10.1016/0003-2697(80)90139-6
- Gupta, B., and Huang, B. (2014). Mechanism of salinity tolerance in plants: physiological, biochemical, and molecular characterization. *Int. J. Genomics* 2014, 1–18. doi: 10.1155/2014/701596
- Gupta, D. K., Palma, J. M., and Corpas, F. J. (2018). *Antioxidants and antioxidant enzymes in higher plants* (USA: Springer).
- Gupta, S., Schillaci, M., Walker, R., Smith, P., Watt, M., Roessner, U., et al. (2021). Alleviation of salinity stress in plants by endophytic plant-fungal symbiosis: Current knowledge, perspectives and future directions. *Plant Soil* 461, 219–244. doi: 10.1007/s11104-020-04618-w
- Hajjhashemi, S. (2020). Characterization of exogenous nitric oxide effect on crocus sativus response to different irrigation regimes. *J. Plant Growth Regul.* 40, 1510–1520. doi: 10.1007/s00344-020-10207-z
- Hajjhashemi, S., Brestic, M., Landi, M., and Skalicky, M. (2020a). Resistance of fritillaria imperialis to freezing stress through gene expression, osmotic adjustment and antioxidants. *Sci. Rep.* 10, 1–13. doi: 10.1038/s41598-020-63006-7
- Hajjhashemi, S., and Ehsanpour, A. A. (2014). Antioxidant response of stevia rebaudiana b. @ to polyethylene glycol and paclobutrazol treatments under in vitro culture. *Appl. Biochem. Biotechnol.* 172, 4038–4052. doi: 10.1007/s12010-014-0791-8
- Hajjhashemi, S., and Jahantigh, O. (2022). Nitric oxide effect on growth, physiological and biochemical processes, flowering, and postharvest performance of narcissus tazetta. *J. Plant Growth Regul.* 1–16. doi: 10.1007/s00344-022-10596-3
- Hajjhashemi, S., Noedoost, F., Geuns, J. M. C., Djalovic, I., and Siddique, K. H. M. (2018). Effect of cold stress on photosynthetic traits, carbohydrates, morphology, and anatomy in nine cultivars of stevia rebaudiana. *Front. Plant Sci.* 9. doi: 10.3389/fpls.2018.01430
- Hajjhashemi, S., Skalicky, M., Brestic, M., and Pavla, V. (2020b). Cross-talk between nitric oxide, hydrogen peroxide and calcium in salt-stressed chenopodium quinoa wild. At seed germination stage. *Plant Physiol. Biochem.* 154, 657–664. doi: 10.1016/j.plaphy.2020.07.022
- Hasanuzzaman, M., Bhuyan, M. B., Anee, T. I., Parvin, K., Nahar, K., Mahmud, J. A., et al. (2019). Regulation of ascorbate-glutathione pathway in mitigating oxidative damage in plants under abiotic stress. *Antioxidants* 8, 384. doi: 10.3390/antiox8090384
- Hasanuzzaman, M., Raihan, M. R. H., Masud, A. A. C., Rahman, K., Nowroz, F., Rahman, M., et al. (2021). Regulation of reactive oxygen species and antioxidant defense in plants under salinity. *Int. J. Mol. Sci.* 22, 9326. doi: 10.3390/ijms22179326
- Heath, R. L., and Packer, L. (1968). Photoperoxidation in isolated chloroplasts: I. kinetics and stoichiometry of fatty acid peroxidation. *Arch. Biochem. biophysics* 125, 189–198. doi: 10.1016/0003-9861(68)90654-1
- Jabeen, Z., Fayyaz, H. A., Irshad, F., Hussain, N., Hassan, M. N., and Li, J. (2021). Sodium nitroprusside application improves morphological and physiological attributes of soybean (Glycine max l.) under salinity stress. *PloS One* 16, e0248207. doi: 10.1371/journal.pone.0248207
- Kampfenk, K., Vanmontagu, M., and Inze, D. (1995). Extraction and determination of ascorbate and dehydroascorbate from plant tissue. *Analytical Biochem.* 225, 165–167. doi: 10.1006/abio.1995.1127
- Kaya, C., Ashraf, M., Alyemeni, M. N., and Ahmad, P. (2020a). The role of endogenous nitric oxide in salicylic acid-induced up-regulation of ascorbate-glutathione cycle involved in salinity tolerance of pepper (Capsicum annuum l.) plants. *Plant Physiol. Biochem.* 147, 10–20. doi: 10.1016/j.plaphy.2019.11.040
- Kaya, C., Ashraf, M., Alyemeni, M. N., Corpas, F. J., and Ahmad, P. (2020b). Salicylic acid-induced nitric oxide enhances arsenic toxicity tolerance in maize plants by upregulating the ascorbate-glutathione cycle and glyoxalase system. *J. Hazardous Materials* 399, 123020. doi: 10.1016/j.jhazmat.2020.123020
- Kolbert, Z., Szöllösi, R., Feigl, G., Kónya, Z., and Rónavári, A. (2021). Nitric oxide signalling in plant nanobiology: current status and perspectives. *J. Exp. Bot.* 72, 928–940. doi: 10.1093/jxb/eraa470
- Mannervik, B. (1999). Measurement of glutathione reductase activity. *Curr. Protoc. Toxicol.* 7.2, 1–7.2.4. doi: 10.1002/0471140856.tx0702s00
- Mostofa, M. G., Fujita, M., and Tran, L.-S. P. (2015). Nitric oxide mediates hydrogen peroxide- and salicylic acid-induced salt tolerance in rice (Oryza sativa l.) seedlings. *Plant Growth Regul.* 77, 265–277. doi: 10.1007/s10725-015-0061-y
- Nakano, Y., and Asada, K. (1987). Purification of ascorbate peroxidase in spinach chloroplasts; its inactivation in ascorbate-depleted medium and reactivation by monodehydroascorbate radical. *Plant Cell Physiol.* 28, 131–140. doi: 10.1093/oxfordjournals.pcp.a077268
- Noreen, S., and Ashraf, M. (2010). Modulation of salt (NaCl)-induced effects on oil composition and fatty acid profile of sunflower (Helianthus annuus l.) by exogenous application of salicylic acid. *J. Sci. Food Agric.* 90, 2608–2616. doi: 10.1002/jsfa.4129
- Pathan, S., and Siddiqui, R. A. (2022). Nutritional composition and bioactive components in quinoa (Chenopodium quinoa wild.) greens: A review. *Nutrients* 14, 558. doi: 10.3390/nul14030558
- Plewa, M. J., Smith, S. R., and Wagner, E. D. (1991). Diethyldithiocarbamate suppresses the plant activation of aromatic amines into mutagens by inhibiting tobacco cell peroxidase. *Mutat. research/fundamental Mol. Mech. mutagenesis* 247, 57–64. doi: 10.1016/0027-5107(91)90033-k
- Prakash, V., Singh, V., Tripathi, D., Sharma, S., and Corpas, F. J. (2021). Nitric oxide (NO) and salicylic acid (SA): A framework for their relationship in plant development under abiotic stress. *Plant Biol.* 23, 39–49. doi: 10.1111/plb.13246
- Rasheed, F., Anjum, N. A., Masood, A., Sofo, A., and Khan, N. A. (2020). The key roles of salicylic acid and sulfur in plant salinity stress tolerance. *J. Plant Growth Regul.* 41, 1–14. doi: 10.1007/s00344-020-10257-3
- Singleton, V., and Rossi, J. A. (1965). Colorimetry of total phenolics with phosphomolybdic-phosphotungstic acid reagents. *Am. J. Enology Viticulture* 16, 144–158.
- Szarka, A., Tomasskovic, B., and Bánhegyi, G. (2012). The ascorbate-glutathione- $\alpha$ -tocopherol triad in abiotic stress response. *Int. J. Mol. Sci.* 13, 4458–4483. doi: 10.3390/ijms13044458
- Szöllösi, R., and Varga, I. S. (2002). Total antioxidant power in some species of labiate (Adaptation of FRAP method). *Acta Biologica Szegediensis* 46, 125–127. Available at: <http://abs.bibl.u-szeged.hu/index.php/abs/article/view/2269>.
- Velikova, V., Yordanov, I., and Edreva, A. (2000). Oxidative stress and some antioxidant systems in acid rain-treated bean plants: protective role of exogenous polyamines. *Plant Sci.* 151, 59–66. doi: 10.1016/S0168-9452(99)00197-1
- Wagner, G. J. (1979). Content and vacuole/extravacuole distribution of neutral sugars, free amino acids, and anthocyanin in protoplasts. *Plant Physiol.* 64, 88–93. doi: 10.1104/pp.64.1.88
- Wang, Z., Xiao, Y., Chen, W., Tang, K., and Zhang, L. (2010). Increased vitamin c content accompanied by an enhanced recycling pathway confers oxidative stress tolerance in arabidopsis. *J. Integr. Plant Biol.* 52, 400–409. doi: 10.1111/j.1744-7909.2010.00921.x
- Wellburn, A. R. (1994). The spectral determination of chlorophylls a and b, as well as total carotenoids, using various solvents with spectrophotometers of different resolution. *J. Plant Physiol.* 144, 307–313. doi: 10.1016/S0176-1617(11)81192-2
- Wisniewska, A. (2021). Priming strategies for benefiting plant performance under toxic trace metal exposure. *Plants* 10, 623. doi: 10.3390/plants10040623
- Xiao, W., Liu, F.-L., and Jiang, D. (2017). Priming: A promising strategy for crop production in response to future climate. *J. Integr. Agric.* 16, 2709–2716. doi: 10.1016/S2095-3119(17)61786-6
- Yadu, S., Dewangan, T. L., Chandrakar, V., and Keshavkant, S. (2017). Imperative roles of salicylic acid and nitric oxide in improving salinity tolerance in pisin sativum l. *Physiol. Mol. Biol. Plants* 23, 43–58. doi: 10.1007/s12298-016-0394-7
- Yemm, E., Cocking, E., and Ricketts, R. (1955). The determination of amino acids with ninhydrin. *Analyst* 80, 209–214. doi: 10.1039/an9558000209
- Zhishen, J., Mengcheng, T., and Jianming, W. (1999). The determination of flavonoid contents in mulberry and their scavenging effects on superoxide radicals. *Food Chem.* 64, 555–559. doi: 10.1016/S0308-8146(98)00102-2
- Zottini, M., Costa, A., De Michele, R., Ruzzene, M., Carimi, F., and Lo Schiavo, F. (2007). Salicylic acid activates nitric oxide synthesis in arabidopsis. *J. Exp. Bot.* 58, 1397–1405. doi: 10.1093/jxb/erm001



## OPEN ACCESS

## EDITED BY

Hirofumi Saneoka,  
Hiroshima University, Japan

## REVIEWED BY

Juanjuan Yu,  
Henan Normal University, China  
Riyazuddin Riyazuddin,  
Hungarian Academy of Sciences  
(MTA), Hungary  
Sho Nishida,  
Saga University, Japan

## \*CORRESPONDENCE

Xuwu Sun  
sunxuwu@henu.edu.cn

<sup>†</sup>These authors have contributed  
equally to this work

## SPECIALTY SECTION

This article was submitted to  
Plant Abiotic Stress,  
a section of the journal  
Frontiers in Plant Science

RECEIVED 03 September 2022

ACCEPTED 31 October 2022

PUBLISHED 17 November 2022

## CITATION

Bawa G, Liu Z, Zhou Y, Fan S, Ma Q,  
Tissue DT and Sun X (2022) Cotton  
proteomics: Dissecting the stress  
response mechanisms in cotton.  
*Front. Plant Sci.* 13:1035801.  
doi: 10.3389/fpls.2022.1035801

## COPYRIGHT

© 2022 Bawa, Liu, Zhou, Fan, Ma, Tissue  
and Sun. This is an open-access article  
distributed under the terms of the  
[Creative Commons Attribution License](#)  
(CC BY). The use, distribution or  
reproduction in other forums is  
permitted, provided the original  
author(s) and the copyright owner(s)  
are credited and that the original  
publication in this journal is cited, in  
accordance with accepted academic  
practice. No use, distribution or  
reproduction is permitted which does  
not comply with these terms.

# Cotton proteomics: Dissecting the stress response mechanisms in cotton

George Bawa<sup>1†</sup>, Zhixin Liu<sup>1†</sup>, Yaping Zhou<sup>1†</sup>, Shuli Fan<sup>2</sup>,  
Qifeng Ma<sup>2</sup>, David T. Tissue<sup>3</sup> and Xuwu Sun<sup>1\*</sup>

<sup>1</sup>State Key Laboratory of Cotton Biology, Key Laboratory of Plant Stress Biology, School of Life Sciences, Henan University, Kaifeng, China, <sup>2</sup>State Key Laboratory of Cotton Biology, Institute of Cotton Research, Chinese Academy of Agricultural Sciences (ICR, CAAS), Anyang, China, <sup>3</sup>Hawkesbury Institute for the Environment, Western Sydney University, Richmond, NSW, Australia

The natural environment of plants comprises a complex set of biotic and abiotic stresses, and plant responses to these stresses are complex as well. Plant proteomics approaches have significantly revealed dynamic changes in plant proteome responses to stress and developmental processes. Thus, we reviewed the recent advances in cotton proteomics research under changing environmental conditions, considering the progress and challenging factors. Finally, we highlight how single-cell proteomics is revolutionizing plant research at the proteomics level. We envision that future cotton proteomics research at the single-cell level will provide a more complete understanding of cotton's response to stresses.

## KEYWORDS

adaptation, cotton, environmental stress, fiber development, proteomics

## Introduction

Cotton (*Gossypium* spp.) is an essential industrial crop cultivated throughout the world for the production of textile fiber and cottonseed oil (Li et al., 2007; Santhosh and Yohan, 2019; Zhao et al., 2022). However, stress conditions often affect cotton growth and development, thus decreasing cotton yield. Over the past decade, cotton yield and quality have been decreased by different abiotic stresses such as drought, shade, and temperature (Wang et al., 2014; Umbetev et al., 2015; Ullah et al., 2016; Guo et al., 2017; Li et al., 2020) and biotic stress such as fungal infections (Gao et al., 2013; Zhang T. et al., 2016; Zhang et al., 2017). As part of evolution, cotton plants have evolved several defense mechanisms that generate a rapid response to incoming stresses, enhancing tolerance to combat these unfavorable environmental factors (Wang et al., 2014; Guo et al., 2017; Kerry et al., 2018; Bawa et al., 2019; Zhou et al., 2019; Li et al., 2020; Bhat et al., 2022). Stress signals are recognized by plasma membrane or intracellular receptors, which



results in the activation of a signaling cascade related to post-translational modifications of the proteins, with signals transduced to transcription factors (TFs), thus activating transcriptional responses (Figure 1), suggesting that knowledge of cotton gene and protein identification, function, and expression pattern under stress conditions is essential for increasing cotton yield (Wang et al., 2012; Zhang et al., 2017; Nagamalla et al., 2021).

Recent knowledge has shown how transcriptome analysis has revealed the functions of a large number of stress-responsive genes in cotton (Han et al., 2019; Zhu H. et al., 2021). However, the up-regulated proteins and mRNA activities often do not correspond to each other as a result of post-translational activities (Pradet-Balade et al., 2001), which suggests that genome and transcriptome findings alone cannot be used to determine plant gene function and the regulatory mechanisms of plants under stress conditions. Meanwhile, other studies have shown that plant response to changing environmental conditions is directly linked with the upregulation of defense-related proteins (Kerry et al., 2018; Liu L. et al., 2019; Sinha et al., 2021), which means that proteomics could provide mechanistic insights into the function of differently expressed proteins during

cotton stress acclimation (Chen et al., 2020) and developmental processes (Zhu et al., 2018). The term “proteome” refers to the protein component of a given sample (organisms or plants), while “proteomics” refers to the quantification and identification of these proteins (Wilkins et al., 1996). Plant research uses proteomics approaches to understand plant growth dynamics and how plants respond to stress conditions to improve crop tolerance mechanisms, which increases crop yield and quality in our agricultural systems. In recent times, single-cell proteomics profiling has been used to study protein dynamics in plants. Single-cell proteomics allows the identification of many proteins expressed within thousands of individual cells at a given time (Clark et al., 2022). Single-cell-type proteomics treats biological samples as heterogeneous, which reveals the actual functions of cells in plant developmental processes (Dai and Chen, 2012; Potts et al., 2022). Recent breakthroughs in single-cell proteomics have enabled us to distinguish different cellular subpopulations through large-scale protein profiling (Clark et al., 2022). Hence, considering the constant regulation of cotton growth and development by different stress conditions, this review discusses the progress in cotton proteomics research. More importantly, we highlight how single-cell proteomics could

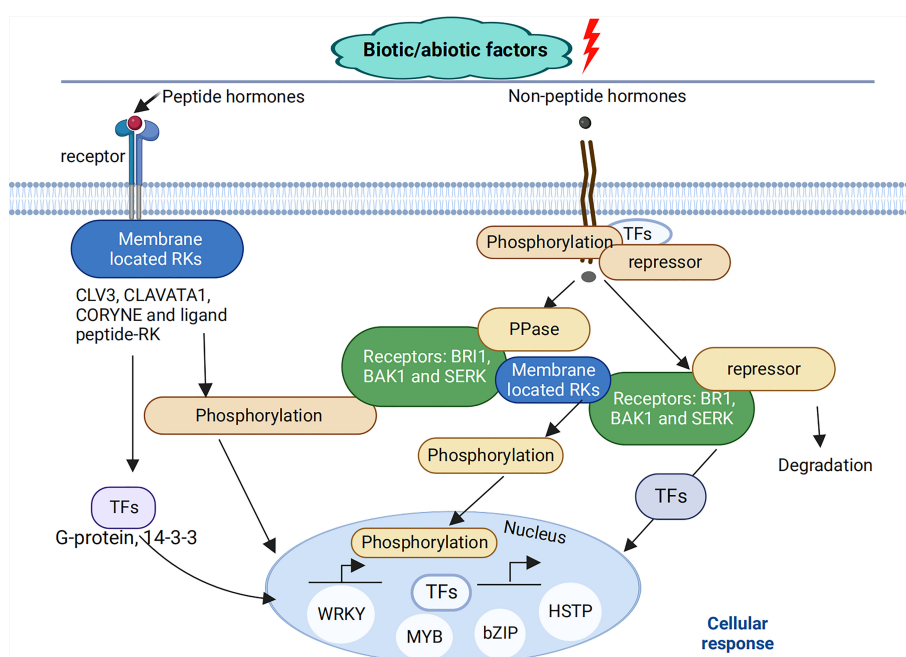


FIGURE 1

Plant cellular signaling cascades. Throughout their developmental period, plants are attacked by different biotic and abiotic stresses. These stress signals are recognized by membrane-located RPKs, which play an important role in plant signaling pathways either through peptide hormones such as CLAVATA3, CLAVATA1, CORYNE and other ligand peptides –RK interactions or non-peptide hormones, such as a membrane-bound receptor named brassinosteroid-insensitive 1 (BR1), which interacts with BCL2 antagonist/killer1 (BAK1), and somatic embryogenesis receptor-like kinase (SERK) shown to be involved in different signaling pathways under stress conditions. These transmembrane receptor-like kinases transmit signals through the plasma membrane, which activates a signaling cascade related to post-translational modifications of proteins, with signals activating the expression of transcription factors (TFs), such as myb-related protein (MYP), basic leucine zipper (bZIP), heat stress transcription factor (HSTP), WRKY, etc., as a form of response to these stresses.



revolutionize plant response to stress conditions in the coming years.

## Cotton proteomics approaches

Selecting a methodology for separating and identifying plant proteins is an important step to consider in plant proteomics analysis. A reliable analytical resolution in the separation and identification steps is required for a complete or successful extraction process. In response to stress, cotton plants activate defense genes to enhance tolerance through changes in defense protein expression levels (Wang et al., 2012; Tu et al., 2017). However, the regulation of gene expression in plants is controlled by several signal-sensing networks of phosphorylation and dephosphorylation activity (Abreu et al., 2013), which suggests that the application of proteomics at the cotton stress response level could assist in identifying key defense proteins involved in a particular stress condition. The cotton proteomic analysis comprises either gel-based method (protein separation using gel electrophoresis, quantification, spot digestion, and mass spectrometric analysis) or gel-free based method (protease breakdown of protein samples and liquid chromatographic separation and spectrometric analysis) (Champagne and Boutry, 2013). Despite the high labor and time-consuming nature of the two-dimensional gel electrophoreses (2-DE) approach, several developmental studies have used the technique for cotton protein quantification and separation (Coumans et al., 2009; Rabilloud and Lelong, 2011; Zhou et al., 2014; Li et al., 2015) (Table 1). The cotton gel-based technologies include 2-DE at the separation level and mass spectrometry (MS) at the identification level (Wang et al., 2011), which have been reviewed in cotton proteomic analysis (Zhou et al., 2014). In the 2-DE analysis, the protein spots are often stained with Coomassie brilliant blue and fluorescent dye (Chevalier et al., 2004). Using advanced

mass spectrometry, the 2-DE analysis enhances different proteins characterized in a single gel (Magdeldin et al., 2014). These advantages of the 2-DE make it more applicable in post-translational modifications (PTMs) of cotton protein analysis (Zhou et al., 2014). Again, the 2-DE analysis is considered essential because of its increased identification and quantification of proteins with different expressions under different conditions and comparative expression of protein complexes (O'Farrell, 1975; Heinemeyer et al., 2009; Rabilloud, 2012). As a result of its reliability, 2-DE has been used to effectively characterize cotton organelles and other tissues, including cotton leaf and root proteomics, successively (Coumans et al., 2009; Pang et al., 2010; Meng et al., 2011). To obtain higher protein spots in cotton, Yao et al. (2006) added polyvinylpyrrolidone (PVPP) into cotton grinding samples to remove unwanted compounds such as polyphenols and lipids. They also added 80% cold acetone in water to prevent protein pellets from lipid contamination. Further, cold acetone was used to clean the tissue powder while suspended in an extraction buffer to enhance extraction ability and supplemented with 2% SDS to promote the solubility of proteins, making this an efficient protocol for cotton protein extraction. However, cotton protein analysis with the 2-DE gel approach can sometimes be constrained by the sensitivity, linearity, and homogeneity of the staining processes and is in line with mass spectrometry. Protein identification using fluorescent dyes can sometimes be problematic since it combines sensitivity and compatibility with mass spectrometry techniques (Rabilloud and Lelong, 2011). Another constraint of the 2-DE gel analysis is its low-level identification of low abundant proteins (Rabilloud and Lelong, 2011). Again, the 2-DE approach can only separate up to about 30–50% of a tissue proteome and often cannot separate all the proteins in certain complex cotton tissues (Yao et al., 2006). The above-listed constraints of the 2-DE gel approach led to the development of gel-free proteomics technologies applied to cotton.

TABLE 1 Cotton proteomics studies according to stress type, tissue and method used.

| Stress type      | Organ/Tissue | Method                      | References             |
|------------------|--------------|-----------------------------|------------------------|
| Cadmium stress   | Leaves       | 2-DE                        | Daud et al. (2015)     |
| Drought          | Leaves       | 2-DE                        | Deeba et al. (2012)    |
| Drought          | Root         | Tandem Mass Tag-based (TMT) | Xiao et al. (2020)     |
| Drought          | Root         |                             | Zhang H. et al. (2016) |
| Nitrogen stress  | Fiber        | 2-DE                        | Wang et al. (2012)     |
| Low temperature  | Fiber        | 2-DE                        | Zheng et al. (2012)    |
| Fungal infection | Root         | 2-DE                        | Wang et al. (2011)     |
| Fungal infection | Root         | 2-DE                        | Coumans et al. (2009)  |
| Fungal infection | Root         | 2-DE                        | Zhao et al. (2012)     |
| Fungal infection | Root         | iTRAQ                       | Zhang et al. (2017)    |
| Salinity         | Root         | iTRAQ                       | Li et al. (2015)       |
| Low light        | Fiber        | 2-DE                        | Hu et al. (2017)       |

In addition to the 2-DE gel-based approach, various sophisticated gel-free proteomic techniques have also been exploited in cotton proteomic analysis, which suggests a growing level in the field of differential proteomics (Figure 2). The gel-free proteomic analysis has the ability to overcome certain challenges of the 2-DE gel approach, such as detection sensitivity, low-level detection of hydrophobic proteins, and high throughput worldwide proteome analysis of complex biological systems. The gel-free technique includes tag-based labeling, metabolic labeling, and label-free techniques. With tag labeling, various mass tags like ICAT, iTRAQ, TMT, and dimethyl labeling are introduced into the proteins, while the metabolic labeling techniques include SILAC and  $^{15}\text{N}$  labeling (Ritter et al., 2011). Various studies have shown that these gel-free approaches are more reproducible and reduce biases more effectively than the 2-DE gel method (Lee et al., 2010). A study conducted by Nouri and Komatsu (2010) investigated a proteomic analysis of soybean plasma membrane under osmotic stress with 4 and 8 protein spots shown as high and low abundance proteins, respectively, using the 2-DE gel technique, while 11 and 75 proteins were observed as high and low abundance proteins using nanoLC-MS. Using the same comparative method, Van Cutsem et al. (2011) extracted 680 and 850 proteins from *Nicotiana tabacum* trichomes via the 2-DE gel technique and gel-free method, respectively, which highlights the comparative advantage of the gel-free protein analysis over the gel-based method. However, despite the numerous advantages of the gel-free-based technique over the 2-DE gel approach, the gel-free technique has some challenges, limiting its application in cotton proteomics research in many laboratories. In the gel-free-based technique, peptides found in multiple proteins reduce the reliability of identified proteins, and the cost of this technology makes it more expensive for cotton proteomics analysis, thus limiting plant research progress.

Nevertheless, the 2-DE gel-based approach is commonly used alongside the mass-spectrometry technique for cotton proteomics analysis despite the substantial progress in other proteomics methods (Nouri and Komatsu, 2010; Van Cutsem et al., 2011), especially when dealing with several quantification comparison samples, and the lower cost of this technology makes its application easier and affordable for many cotton research laboratories (Table 1).

## Proteomics and stress adaptation in cotton

In their natural environments, biotic or abiotic stresses negatively regulate plant growth and development (Guo et al., 2019; Tang et al., 2019; Wu and Li, 2019; Li et al., 2020; Zhang et al., 2021; Liu et al., 2022B; Mostofa et al., 2022), which activates plant stress defense mechanisms (Sun et al., 2011; Shabala et al., 2014; Chen et al., 2017; Guo et al., 2019; Wu and Li, 2019; Li et al., 2020; Li et al., 2021; Lv et al., 2021; Zhang et al., 2021; Chieppa et al., 2022; Liu et al., 2022a; Solis et al., 2022; Wu et al., 2022) (Figure 1). Likewise, in the life of the most prestigious industrial crop, cotton growth and development is often regulated by different stress conditions that initiate several defense mechanisms at the physiological, cellular, and molecular levels, which include a change in plant height and leaf size, upregulation of antioxidant defense enzymes, and increase in the levels of defense-related genes and proteins (Nagamalla et al., 2021; Qamer et al., 2021). Since cotton's genomic sequence is already available, post-transcriptional investigations will positively impact cotton growth and development by understanding the regulatory mechanisms underlying how cotton plants respond to these stresses. Since its introduction into plant research, proteomics, an “omic” approach that

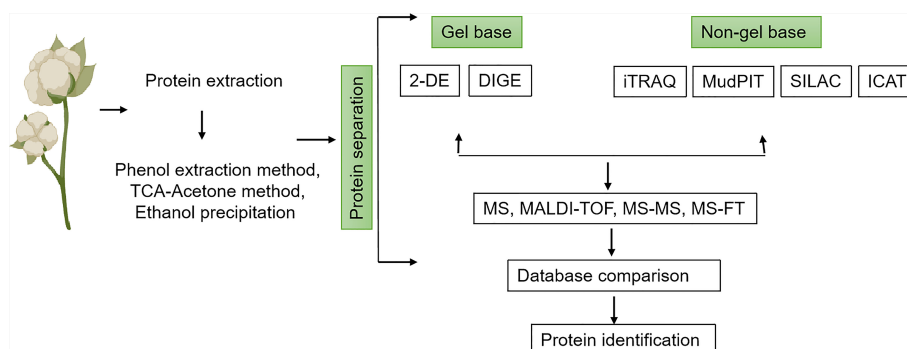


FIGURE 2

Schematic workflow of the different methods used in cotton proteomics analysis. Proteins are extracted from tissues of interest using any of the following methods: phenol extraction, TCA-Acetone, or ethanol precipitation. This is followed by protein separation either using a gel base (2-DE or DIGE) or a non-gel base (iTRAQ, MupPIT, SILAC, ICAT) method. Proteins can further be analyzed by MS, MALDI-TOF, MS-MS, or MS-TF. After analysis, data comparison is performed for final protein identification.

enhances the quantification and identification of differently expressed proteins, has enabled the identification of post-transcriptionally related proteins, which play a key role in plant response to stress. Biotic and abiotic stresses induce changes in protein expression in cotton, and using proteomics techniques provides information and understanding of the functions of the key proteins expressed under stress conditions (Gao et al., 2013; Liu L. et al., 2019). Thus, breeders can use the identification of these stress-responsive proteins to develop stress-tolerant cotton varieties. In addition to elucidating the functions of cotton proteins, proteomics also enhances our understanding of phenotypic variations during cotton stress adaptation processes. (Table 1) describes how cotton tissues or organs respond to stress conditions using various proteomics methods. In the case of abiotic stress, throughout cotton-growing areas globally, cotton growth and development have been affected by an increasing number of abiotic stresses, which negatively regulate cotton's physiological development (Wang et al., 2014; Snider et al., 2021). For instance, a study by Zheng et al. (2017) using iTRAQ-based quantitative proteomic analysis to analyze the mechanism involved in induced premature leaf senescence in two cotton genotypes under cold conditions showed 443 differential abundant proteins (DAPs) were identified from high-confidence proteins at four different stages between premature cotton and non-premature cotton genotypes, with 158 proteins being over-accumulated, 238 proteins down-regulated, and 47 proteins showing overlapped accumulation in all the different stages. The Gene Ontology enrichment analysis showed that cold-responsive and hormonal-related genes were more highly accumulated in the premature genotype than in the non-premature genotype. Significantly, 58 proteins were involved in abiotic stress,

hormonal signaling, and leaf greenness regulation, consisting of 26 cold-responsive proteins (Table 2). Together, this study demonstrated that changes in plant leaf development undergo several differential protein expressions, which require identification and functional classification using proteomics approaches. In addition, Nagamalla et al. (2021) investigated the molecular mechanisms underlying drought tolerance of two cotton genotypes, *Bacillus thuringiensis* cotton and hybrid cotton, using 2DE-DIGE proteomics analysis. It was observed in this study that 509 and 337 different proteins were expressed in *Bacillus thuringiensis* and the hybrid genotype, respectively, compared to their controls. Interestingly, the transcript analysis performed alongside the identified drought-related proteins confirmed a significant correlation in expression. *In silico* analysis of the differentially expressed proteins ATPase  $\beta$  subunit (ATPB), nucleobase-ascorbate transporter 9 (NAT9), early responsive to dehydration (ERD), late embryogenesis abundant (LEA) proteins, and embryo-defective 2001 (EMB2001) proteins were correlated with different drought-related genes such as late embryogenesis abundant (LEA), APETALA2/Ethylene Responsive Factor (AP2/ERF), WRKY, and neuronally altered carbohydrate (NAC). These different proteins played an important role in cotton drought response, especially in the *Bacillus thuringiensis* genotype. The significant drought response in the *Bacillus thuringiensis* genotype induced overexpression of photosynthetic proteins, which elevated lipid metabolism, induced cellular detoxification, decreased biosynthesis of unwanted proteins, improved stomatal functioning, and increased antioxidant activity such as catalase (CAT), superoxide dismutase (SOD), peroxidase (POD), and ascorbate peroxidase (APX) compared to the hybrid genotype, suggesting that proteomics technologies may provide a better

TABLE 2 List of proteins and related functions.

| Stress type      | Total proteins | Up-regulated proteins | Down-regulated proteins | Function   | References           |
|------------------|----------------|-----------------------|-------------------------|--|----------------------|
| Drought          | 110            |                       |                         | Cellular structure, antioxidants, and metabolism.  | Zhang et al. (2017)  |
| Low temperature  | 37             |                       |                         | Soluble sugar metabolism, cell wall loosening, cellular response, cellulose synthesis, cytoskeleton, and redox homeostasis.  | Zheng et al. (2012)  |
| Fungal infection | 68             | 51                    | 17                      | Stress defense, metabolism, and lipid biosynthesis.  | Wang et al. (2011)   |
| Fungal infection | 174            |                       |                         | ROS metabolism, induction of various histone-modifying, and DNA methylating.   | Zheng et al. (2017)  |
| Fungal infection | 188            |                       |                         | Stimulus-response, cellular and metabolic processes.   | Gao et al. (2013)    |
| Low light        | 49             |                       |                         | 39 proteins were involved in signal transduction, energy metabolism, cytoskeleton, nitrogen metabolism, and stress response. | Hu et al. (2017)     |
| Leaf senescence  | 195            | 91                    | 104                     | Nitrogen metabolism, photosynthetic, and diterpenoid biosynthesis.   | Liu L. et al. (2019) |
| Dwarfism         | 687            |                       |                         | Catalytic, binding, and transporter-related activity.  | Tu et al. (2017)     |

understanding of cotton's physiological response under drought stress, which could help in developing drought-tolerant and high-yielding cotton genotypes.

Similar to abiotic stress, biotic stress also regulates several physiological activities in cotton by introducing destructive pathogens at the growth stage. For example, [Zhang et al. \(2017\)](#) used an iTRAQ-based proteomic method to understand cotton pathogen interaction to further investigate pathogenic-related proteins involved in cotton's disease resistance or tolerance. In this study, a total of 174 differentially induced proteins were observed in cotton plants as a result of *R. solani* infection ([Table 2](#)). These differentially induced proteins played a significant role in reactive oxygen species (ROS) metabolism and induction of various histone-modifying and DNA-methylating proteins resulting from *R. solani* infection, suggesting that the redox homeostasis and epigenetic regulation were vital for cotton's resistance against *R. solani* infection. Further changes in phenylpropanoid biosynthesis-related protein expression in response to *R. solani* infection suggest a significant contribution of secondary metabolic activity in response to fungal infection in cotton. This study showed that the induction of different innate immunity-related proteins significantly contributes to cotton's resistance to pathogen attacks. Verticillium wilt causes huge annual losses in cotton yield ([Wang et al., 2016](#); [Dadd-Daigle et al., 2021](#)). [Wang et al. \(2011\)](#) demonstrated how different proteins are expressed in response to cotton and *Verticillium dahliae* (*V. dahliae*) interaction. This study conducted a comparative proteomic analysis between infected and non-infected cotton roots using 2-DE gel analysis. The findings showed that 51 up-regulated and 17 down-regulated proteins were involved in stress defense, metabolism, and lipid biosynthesis. Importantly, it was observed that ethylene defense signaling and biosynthesis were induced in cotton roots due to *V. dahliae* infection. It was also observed that the *Bet v 1* family proteins were possibly involved in cotton's defense against *V. dahliae* infection ([Table 2](#)). Gao and colleagues performed a comparative proteomics analysis to further understand the mechanisms of cotton's resistance to *V. dahliae* ([Gao et al., 2013](#)). The study uncovered 188 differentially expressed proteins by matrix-assisted laser desorption ionization time-of-flight/time-of-flight (MALDI-TOF/TOF) mass spectrometry analysis and classified them into 17 biological functional groups based on Gene Ontology annotation. Several of these proteins were related to stimulus-response, cellular, and metabolic processes. The study further highlighted several genes involved in secondary metabolism, reactive oxygen burst, and salicylic acid (SA) signaling in cotton's response to *V. dahliae* according to the analysis of GbSS12, a major regulator in the crosstalk between SA and jasmonic acid (JA) signaling pathways. In addition, three classes of genes involved in gossypol metabolism, brassinosteroids (BRs) signaling, and JA signaling were characterized using

virus-induced gene silencing (VIGs). Continuously, the study revealed that gossypol, BRs, and JA act as major players in contributing to cotton's resistance to *V. dahliae*, thus providing new insights into the molecular basis of cotton's defense against *V. dahliae*. Together, these studies highlight the major role of proteomics analysis in dissecting the stress response mechanisms in cotton.

## Proteomics: For improving cotton fiber quality

Proteomics techniques are applied to farm animals to enhance the nutraceutical activity of the milk proteome or to check the *in vivo* performance of livestock animals ([Bendixen et al., 2011](#); [Roncada et al., 2012](#); [D'Alessandro and Zolla, 2013](#)). In the last decade, there has been increasing use of proteomics approaches in crop plants such as cotton to promote quality fiber and increase yield through improved breeding programs ([Zhou et al., 2014](#); [Ahmad, 2016](#); [Liu et al., 2016](#)). Cotton fiber is a widely used raw material in the textile industry. However, stress conditions often negatively regulate cotton fiber development, which decreases cotton fiber quality and yield.

As depicted in [Table 2](#), several studies, including [Zheng et al. \(2012\)](#), used proteomics to show how low-temperature stress regulates protein expression during cotton fiber elongation using two cotton genotypes (low-temperature tolerant and low-temperature sensitive) planted at different sowing dates, which resulted in changes in environmental conditions. Proteomic investigations showed that a total of 37 proteins related to soluble sugar metabolism, cell wall loosening, cellular response, cellulose synthesis, cytoskeleton, and redox homeostasis were changed in response to the low-temperature stress according to the mass spectrometry identification, suggesting that the biosynthesis of these proteins was involved in the low-temperature tolerance of cotton fibers. This study's results also show how proteomics approaches have significantly improved cotton fiber development. Low light is one of the most important environmental conditions reducing cotton yield in many cotton-growing areas ([Pettigrew, 2001](#); [Wang et al., 2005](#); [Chen et al., 2014](#)), suggesting that the identification of proteins involved in cotton's response to low-light stress through proteomics has made a significant contribution to cotton fiber development. Using proteomic analysis, [Hu et al. \(2017\)](#) demonstrated how low-light conditions regulate cotton fiber elongation processes. The study showed that low-light stress decreased cotton fiber length. Proteomic analysis conducted at the four developmental stages (5, 10, and 15 days post-anthesis) indicated that 49 proteins were expressed under low light. Among these proteins, 39 were identified as well-known key low-light stress-responsive proteins significantly involved in signal transduction, energy metabolism, cytoskeleton structure, nitrogen (N) metabolism, and stress response. Moreover, the

reduced fiber length in this study was linked with the levels of signal-related protein (phospholipase D), cytoskeletal proteins, carbohydrate metabolism proteins, and stress-responsive proteins down-regulated under low-light stress. These changes in protein levels in response to low light suggest that a further determination of the functions of all the identified proteins will go a long way to promoting cotton fiber development under low light. Changes in plant nutrient levels regulate plant growth and development (Ahmed M. et al., 2020; Shrivastav et al., 2020). For instance, N, phosphorus (P), and potassium (K) are required in large quantities and are limited in many soils. The deficiencies of macronutrients and micronutrients decrease cotton yield (Ahmed N. et al., 2020). Recently, Iqbal et al. (2022) demonstrated that low P tolerance in cotton is regulated by root morphology and physiology. The study showed that low P decreased dry matter, photosynthesis, and carbon metabolism in cotton, which could directly affect the yield.

Among these nutrients that highly regulate cotton fiber development is N (Read et al., 2006; Saleem et al., 2010; Wang et al., 2012; Snider et al., 2021; Van Der Sluijs, 2022). Using proteomics analysis, Wang et al. (2012) demonstrated how low N stress regulates cotton fiber elongation. The study used different N application rates: 0 kg hm<sup>-2</sup> (N0), 240 kg hm<sup>-2</sup> (N1), and 480 kg hm<sup>-2</sup> (N2), equivalent to 0, 4.5, and 9.0 g per pot, respectively, where N0 represents N starvation, N1 normal N application, and N2 excess N application. The study showed that different nitrogen application rates regulate N biosynthesis in cotton fiber cells and fiber length, which revealed that cotton carbohydrate metabolism, antioxidants and hormonal, cell wall component synthesis, and amino acid metabolism-related proteins were significantly expressed during N stress (N0), with the carbohydrate metabolism proteins being the most expressed. Importantly, this study demonstrated that plants activate tolerance mechanisms such as expressing defense-related proteins for plant survival under stress conditions. Hence, the authors hypothesize that further functional analysis of the identified proteins could reveal the molecular mechanisms of cotton N tolerance for enhanced fiber quality. It can be concluded that understanding cotton fiber developmental changes under stress conditions using proteomics approaches will help decipher the molecular mechanisms governing stress tolerance in cotton, especially during fiber development.

## Proteomics: Toward physiological development of cotton

Proteomics technologies have been used to characterize proteome regulation throughout plant developmental processes. The plant growth process is constantly mediated by different stresses such as drought, temperature, and salinity (Afroz et al., 2011). Several studies have been conducted to understand how different proteins are expressed during plant

physiological development (Tu et al., 2017; Zhu S. et al., 2021). Likewise, changes in cotton's physiological activity during growth and development are regulated by changes in gene expression, which has a final consequence on protein levels and functions (Xu et al., 2013; Zhu S. et al., 2021). Proteomics techniques have been used to study proteome mediation during cotton developmental stages and different organ development. Various studies have been conducted to investigate the complete proteome profile of cotton during growth and development to understand the regulatory mechanisms underlying how proteomics approaches contribute to cotton stress tolerance mechanisms (Zhang Z. et al., 2016; Nagamalla et al., 2021). Here, we provide updates on how proteomics technologies contribute to certain physiological aspects of cotton's developmental process. Using proteomics analysis, Zhang H. et al. (2016) determined the effect of different cotton genotypes on drought stress using 2-DE and MALDI-TOF mass spectrometry to analyze the proteome of two cotton genotypes (drought-sensitive and drought-tolerant) exposed to drought stress. A total of 110 protein spots were detected and identified as related to cellular structure, antioxidants, and metabolism. Other proteins such as ascorbate peroxidase, UDP-D- glucose pyrophosphorylase and DNA (cytosine-5) methyltransferase were significantly up-regulated in the drought-tolerant than in the sensitive genotype. Again, among the two genotypes, proteins such as translation initiation factor 5A and fungal-related proteins were in high abundance in the drought-tolerant, while ribosomal protein S12, cysteine, and actin were highly decreased in the drought-sensitive genotype. This enhances our understanding of how different proteins are induced in the roots of different cotton genotypes under drought stress.

Leaf senescence occurs in plants as the plant ages but sometimes can be induced by environmental stresses such as drought, temperature, shade, and salt (Munné-Bosch and Alegre, 2004; Brouwer et al., 2012; Liu L. et al., 2019), which involves the breakdown of intracellular organelles and macromolecules (Lim et al., 2007). One important growth stage that causes changes in cotton protein dynamics is leaf senescence (Liu L. et al., 2019). Using the iTRAQ method, Liu L. et al. (2019) characterized the protein expression patterns during the senescence of cotton leaves under field conditions. As part of the developmental processes, it was observed that the photosynthetic rates and photosynthetic pigment activities of the field-grown cotton were sharply decreased during the senescence period, which suggests that, as cotton ages, certain metabolic activities, including proteins, are broken down, which speeds up leaf yellowing (Liu L. et al., 2019). A total of 195 different proteins were identified by mass spectrometry, with 91 proteins being up-regulated and 104 down-regulated. In addition to changes in the protein dynamics, genes related to cotton photosynthetic biosynthesis, N metabolism, and diterpenoid biosynthesis expression levels significantly changed during the senescence process, which provides an interesting



mechanism involved in proteome changes during cotton's physiological development (Liu L. et al., 2019). The stem is a critical part of cotton that is regulated by different stress conditions. Tu et al. (2017) conducted a study using the iTRAQ approach to investigate the key elements and signaling pathways involved in cotton dwarfism using proteomic analysis. Two different cotton lines, dwarf line LA-1 and high near-isogenic line LH-1, were used for the study. It was observed that a total of 4849 proteins were identified from the two cotton lines, and 697 showed differential accumulations. Most DAPs had catalytic, binding, and transporter-related activity and were involved in the metabolism and processing (protein) pathways. A total of 7 DAPs that were mainly related to phytohormone (2-gibberellin, 3-cytokinin) receptors, cytokinin oxidase, and cytokinin-N-glucosyltransferase were increased in LA-1, while GA 20-oxidase was decreased in LH-1. The authors hypothesized that the DELLA-independent GA signaling pathway induced the dwarfism in LA-1 and suggested that the cytokinin-related element 1-2, gibberellin-insensitive dwarf, 3- $\beta$ -dioxxygenase, and cytokinin oxidase could indicate dwarf cotton. The findings provide critical data for dwarf breeding in cotton and start a new race to determine the molecular regulatory mechanisms underlying dwarfism in cotton. We believe that proteomics can be used to unravel cotton's physiological response under stress conditions toward crop improvement.

## Single-cell proteomics: A powerful futuristic tool to revolutionize cotton proteomics research

Several biological processes involve the interaction of signal networks across a population of cells, organs, and whole tissues. Bulk-cell and tissue omics profiling technologies such as transcriptomics, proteomics, and metabolomics have been used to study cell type and gene expression in plant tissues. However, these bulk methods only generate the averages of cells, do not analyze a small number of cells, and cannot also provide heterogeneous cell information. Given that the heterogeneous cell information of individual cells can be obtained depending on the profiling method, single-cell expression profiling of plant tissues is the only holistic way of generating a deeper understanding of plant developmental processes or environmental adaptation (Dai and Chen, 2012; Clark et al., 2022). Proteomics of plant organs or tissues has uncovered several proteins in different plant cultivars during developmental changes or under varying environmental conditions (Baerenfaller et al., 2008; Hochholdinger et al., 2018; Liu Y. et al., 2019). However, several single-cell-type proteomics studies on cotton fiber, pollen grains, guard cells, and root hairs have proven to identify several important proteins ranging from defense, metabolism, signaling and transport, cytoskeleton, cell wall modification, lipid transfer, oxidation-reduction, among

others, more than their mother tissue or organs such as a leaf, flower, and root (Figure 3). This is because single-cell-type proteomics does not treat the sample as a homogeneous sample but rather as a heterogeneous sample, which reveals the cells' actual functions in biological processes. A number of single-cell-type proteomics studies involving pollen and fiber identified several proteins enriched in membrane trafficking, signal transduction, oxidation-reduction, N metabolism, cytoskeleton, cell wall modification, signaling, metabolism, stress defense, energy, protein synthesis and fate (Fernando, 2005; Dai et al., 2006; Petersen et al., 2006; Sheoran et al., 2007; Wu et al., 2008; Chen et al., 2009; Grobei et al., 2009; Pertl et al., 2009; Han et al., 2010; Hu et al., 2017; Zhou et al., 2019), while several organ/tissue studies involving flowers have demonstrated to be enriched in metabolism, stress and defense, photosynthesis, energy and protein synthesis and fate (Dafny-Yelin et al., 2005; Chua et al., 2010; Silveira and Carvalho, 2016) (Figure 3A). Also, different works of single-cell-type proteomics studies involving the guard cell have identified many proteins enriched in specialized metabolism, signaling, energy, transport, protein synthesis and fate, stress and defense, photosynthesis, lipid transfer, oxidation-reduction and cell-cell communication (Okamoto et al., 2004; Zhu et al., 2009; Lawrence et al., 2020; Balmant et al., 2021), while organ and tissue studies involving the leaf have demonstrated to be enriched in photosynthesis, cell organization, metabolism, stress and defense, and protein synthesis and fate (Wan and Liu, 2008; Khodadadi et al., 2017) (Figure 3B). In addition to those mentioned above, single-cell-type proteomics of root hair has identified several important proteins enriched in specialized metabolism, metabolism, synthesis and fate, energy, cell wall modification, signaling, stress and defense, and transport (Brechenmacher et al., 2008; Nestler et al., 2011; Brechenmacher et al., 2012), while organ/tissue studies involving roots have demonstrated to be enriched in transport mechanisms, energy, synthesis activity, signal transduction, transcription regulation, stress, and defense (Sun et al., 2017) (Figure 3C). Together, these studies enhanced our understanding of the role of particular proteins in cellular development, which highlighted insights into the molecular networks underlying the role of a particular type of plant cell and, to a large extent, revealed the significant difference between the proteomics of whole tissue or organ and single-cell-type proteomics.

## Conclusions and perspectives

Yield reduction in agricultural crops due to biotic and abiotic stress calls for understanding how plants respond to these stresses. In this post-genomic era, the integration of proteomics into the field of crop science will enrich genome annotation efforts and push forward the development of crop models for the elucidation of gene function influencing phenotypes for the success of field crops. Thus, studies involving cotton's response

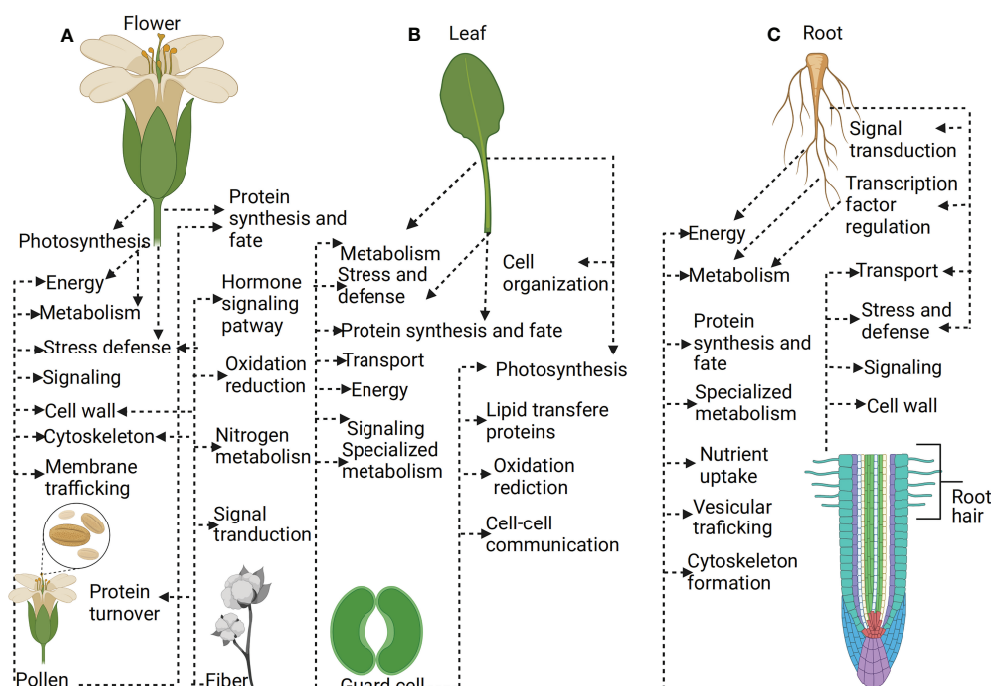


FIGURE 3

Plant single-cell type-proteomics. (A) Proteins expressed in flower versus protein expressed in the pollen (B) Proteins expressed in leaf versus protein expressed in the guard cell (C) Proteins expressed in root versus protein expressed in the root hair. Single-cell proteomics allows the identification of many proteins expressed within thousands of individual cells at a given time. Single-cell-type proteomics treats biological samples as heterogeneous, which reveals the actual function of cells in plant developmental processes or response to stress. The application of single cells proteomics has several advantages, such as providing specific information on cell function than the whole organ or tissue proteomics, which provide average information of cells.

to biotic and abiotic stresses at the proteome level have significantly contributed to our understanding of the molecular mechanisms underlying these responses. These studies have contributed to unraveling specific resistance and response traits displayed by plants under stress conditions. The proteins identified via proteomics analysis can further be investigated to finally assess their role in plant resistance processes, thus facilitating the efforts to develop stress-tolerant crops. Cotton proteomics enables the identification of key protein types responsible for a biological process under specific conditions in a particular tissue. Cotton proteomics also provides one of the best options for understanding the gene function and phenotypic changes during cotton fiber development and stress response, thus providing novel clues to guide further investigations and genetic improvement for high-quality cotton fiber. The past years have seen tremendous progress in studying low-abundance membrane proteins, leading to the development of different proteomics techniques. Meanwhile, further advances in proteomics technologies are required for higher precision. Considering the diverse and increasing number of recent single-cell proteomics studies reported (Clark et al., 2022; Potts et al., 2022), we believe that the application of high-throughput proteomics technology, such as single-cell proteomics, will

provide a better understanding of the mechanisms surrounding cotton stress tolerance.

## Author contributions

Conceptualization of the project: XS; writing of the first draft: GB and XS; literature revision: YZ, SF, QM, and DTT; supervision and validation: XS; all authors contributed to the article and approved the submitted version.

## Funding

This research was supported by the National Natural Science Foundation of China (31670233).

## Conflict of interest

The authors declare that the research was conducted in the absence of any commercial or financial relationships that could be construed as a potential conflict of interest.

## Publisher's note

All claims expressed in this article are solely those of the authors and do not necessarily represent those of their affiliated

## References

- Abreu, I. A., Farinha, A. P., Negrão, S., Gonçalves, N., Fonseca, C., Rodrigues, M., et al. (2013). Coping with abiotic stress: Proteome changes for crop improvement. *J. Proteomics* 93, 145–168. doi: 10.1016/j.jprot.2013.07.014
- Afroz, A., Ali, G. M., Mir, A., and Komatsu, S. (2011). Application of proteomics to investigate stress-induced proteins for improvement in crop protection. *Plant Cell Rep.* 30 (5), 745–763. doi: 10.1007/s00299-010-0982-x
- Ahmed, N., Ali, M. A., Danish, S., Chaudhry, U., Hussain, S., Hassan, W., et al. (2020). Role of macronutrients in cotton production. 81–104.
- Ahmed, M., Hasanuzzaman, M., Raza, M. A., Malik, A., and Ahmad, S. (2020). "Plant nutrients for crop growth, development and stress tolerance," In *Sustainable agriculture in the era of climate change*. Eds. R. Roychowdhury, S. Choudhury, M. Hasanuzzaman and S. Srivastava (Cham: Springer International Publishing) pp. 43–92.
- Baerenfaller, K., Grossmann, J., Grobei, M. A., Hull, R., Hirsch-Hoffmann, M., Yalovsky, S., et al. (2008). Genome-scale proteomics reveals arabidopsis thaliana gene models and proteome dynamics. *Science* 320 (5878), 938–941. doi: 10.1126/science.1157956
- Balmant, K., Lawrence, S., Duong, B., Zhu, F., Zhu, N., Nicklay, J., et al. (2021). Guard cell redox proteomics reveals a role of lipid transfer protein in plant defense. *J. Proteomics* 242, 104247. doi: 10.1016/j.jprot.2021.104247
- Bawa, G., Feng, L., Yan, L., Du, Y., Shang, J., Sun, X., et al. (2019). Pre-treatment of salicylic acid enhances resistance of soybean seedlings to fusarium solani. *Plant Mol. Biol.* 101 (3), 315–323. doi: 10.1007/s11103-019-00906-x
- Bendixen, E., Danielsen, M., Hollung, K., Gianazza, E., and Miller, I. (2011). Farm animal proteomics — a review. *J. Proteomics* 74 (3), 282–293. doi: 10.1016/j.jprot.2010.11.005
- Bhat, K. A., Mahajan, R., Pakhtoon, M. M., Urwat, U., Bashir, Z., Shah, A. A., et al. (2022). Low temperature stress tolerance: An insight into the omics approaches for legume crops. *Front. Plant Sci.* 13. doi: 10.3389/fpls.2022.888710
- Brechenmacher, L., Lee, J., Sachdev, S., Song, Z., Nguyen, T., Joshi, T., et al. (2008). Establishment of a protein reference map for soybean root hair cells. *Plant Physiol.* 149, 670–682. doi: 10.1104/pp.108.131649
- Brechenmacher, L., Nguyen, T., Hixson, K., Libault, M., Aldrich, J., Pasa-Tolic, L., et al. (2012). Identification of soybean proteins from a single cell type: The root hair. *Proteomics* 12 (22), 3365–3373. doi: 10.1002/pmic.201200160
- Brouwer, B., Ziolkowska, A., Bagard, M., Keech, O., and Gardestrom, P. (2012). The impact of light intensity on shade-induced leaf senescence. *Plant Cell Environ.* 35 (6), 1084–1098. doi: 10.1111/j.1365-3040.2011.02474.x
- Champagne, A., and Boutry, M. (2013). Proteomics of nonmodel plant species. *Proteomics* 13 (3–4), 663–673. doi: 10.1002/pmic.201200312
- Chen, Z.-H., Guang, C., Dai, F., Wang, Y., Hills, A., Ruan, Y.-L., et al. (2017). Molecular evolution of grass stomata. *Trends Plant Sci.* 22, 124–139. doi: 10.1016/j.tplants.2016.09.005
- Chen, J., Lv, F., Liu, J., Ma, Y., Wang, Y., Chen, B., et al. (2014). Effects of different planting dates and low light on cotton fibre length formation. *Acta Physiologiae Plantarum* 36 (10), 2581–2595. doi: 10.1007/s11738-014-1629-2
- Chen, C., Wang, C., Liu, Z., Cai, Z., Hua, Y., Mei, Y., et al. (2020). iTRAQ-based proteomic technique provides insights into salt stress responsive proteins in apocyni veneti folium (Apocynum venetum L.). *Environ. Exp. Bot.* 180, 104247. doi: 10.1016/j.envexpbot.2020.104247
- Chen, T., Wu, X., Chen, Y., Li, X., Huang, M., Zheng, M., et al. (2009). Combined proteomic and cytological analysis of Ca<sup>2+</sup>-calmodulin regulation in picea meyeri pollen tube growth. *Plant Physiol.* 149 (2), 1111–1126. doi: 10.1104/pp.108.127514
- Chevalier, F., Rofidal, V., Vanova, P., Bergoin, A., and Rossignol, M. (2004). Proteomic capacity of recent fluorescent dyes for protein staining. *Phytochemistry* 65 (11), 1499–1506. doi: 10.1016/j.phytochem.2004.04.019
- Chieppa, J., Power, S. A., Nielsen, U. N., and Tissue, D. T. (2022). Plant functional traits affect competitive vigor of pasture grasses during drought and following recovery. *Ecosphere* 13 (7), e4156. doi: 10.1002/ecs2.4156
- Chua, L., Shan, X., Wang, J., Peng, W., Zhang, G., and Xie, D. (2010). Proteomics study of COII-regulated proteins in arabidopsis flower. *J. Integr. Plant Biol.* 52, 4, 410–419. doi: 10.1111/j.1744-7909.2010.00938.x
- Clark, N. M., Elmore, J. M., and Walley, J. W. (2022). To the proteome and beyond: advances in single-cell omics profiling for plant systems. *Plant Physiol.* 188 (2), 726–737. doi: 10.1093/plphys/kiab429
- Coumans, J. V. F., Poljak, A., Raftery, M. J., Backhouse, D., and Peregrin-Gerk, L. (2009). Analysis of cotton (Gossypium hirsutum) root proteomes during a compatible interaction with the black root rot fungus thielaviopsis basicola. *Proteomics* 9 (2), 335–349. doi: 10.1002/pmic.200800251
- Dadd-Daigle, P., Kirkby, K., Chowdhury, P. R., Labbate, M., and Chapman, T. A. (2021). The verticillium wilt problem in Australian cotton. *Australas. Plant Pathol.* 50 (2), 129–135. doi: 10.1007/s13313-020-00756-y
- Dafny-Yelin, M., Guterman, I., Menda, N., Ovadis, M., Shalit, M., Pichersky, E., et al. (2005). Flower proteome: changes in protein spectrum during the advanced stages of rose petal development. *Planta* 222 (1), 37–46. doi: 10.1007/s00425-005-1512-x
- Dai, S., and Chen, S. (2012). Single-cell-type proteomics: toward a holistic understanding of plant function. *Mol. Cell. proteomics: MCP* 11 (12), 1622–1630. doi: 10.1074/mcp.R112.021550
- Dai, S., Li, L., Chen, T., Chong, K., Xue, Y., and Wang, T. (2006). Proteomic analyses of oryza sativa mature pollen reveal novel proteins associated with pollen germination and tube growth. *Proteomics* 6 (8), 2504–2529. doi: 10.1002/pmic.200401351
- D'Alessandro, A., and Zolla, L. (2013). Meat science: From proteomics to integrated omics towards system biology. *J. Proteomics* 78, 558–577. doi: 10.1016/j.jprot.2012.10.023
- Daud, M. K., Quiling, H., Lei, M., Ali, B., and Zhu, S. J. (2015). Ultrastructural, metabolic and proteomic changes in leaves of upland cotton in response to cadmium stress. *Chemosphere* 120, 309–320. doi: 10.1016/j.chemosphere.2014.07.060
- Deeba, F., Pandey, A. K., Ranjan, S., Mishra, A., Singh, R., Sharma, Y. K., et al. (2012). Physiological and proteomic responses of cotton (Gossypium herbaceum L.) to drought stress. *Plant Physiol. Biochem.* 53, 6–18. doi: 10.1016/j.plaphy.2012.01.002
- Fernando, D. D. (2005). Characterization of pollen tube development in pinus strobus (Eastern white pine) through proteomic analysis of differentially expressed proteins. *Proteomics* 5 (18), 4917–4926. doi: 10.1002/pmic.200500009
- Gao, W., Long, L., Zhu, L. F., Xu, L., Gao, W. H., Sun, L. Q., et al. (2013). Proteomic and virus-induced gene silencing (VIGS) analyses reveal that gossypol, brassinosteroids, and jasmonic acid contribute to the resistance of cotton to verticillium dahliae. *Mol. Cell. proteomics: MCP* 12 (12), 3690–3703. doi: 10.1074/mcp.M113.031013
- Grobei, M. A., Qeli, E., Brunner, E., Rehrauer, H., Zhang, R., Roschitzki, B., et al. (2009). Deterministic protein inference for shotgun proteomics data provides new insights into arabidopsis pollen development and function. *Genome Res.* 19 (10), 1786–1800. doi: 10.1101/gr.089060.108
- Guo, Y., Pang, C., Jia, X., Ma, Q., Dou, L., Zhao, F., et al. (2017). An NAM domain gene, GhNAC79, improves resistance to drought stress in upland cotton. *Front. Plant Sci.* 8, 1657. doi: 10.3389/fpls.2017.01657
- Guo, J., Zhou, Y., Li, J., Sun, Y., Shangguan, Y., Zhu, Z., et al. (2019). COE 1 and GUN1 regulate the adaptation of plants to high light stress. *Biochem. Biophys. Res. Commun.* 521, 184–189. doi: 10.1016/j.bbrc.2019.10.101
- Han, B., Chen, S., Dai, S., Yang, N., and Wang, T. (2010). Isobaric tags for relative and absolute quantification- based comparative proteomics reveals the features of plasma membrane-associated proteomes of pollen grains and pollen tubes from liliun davidii. *J. Integr. Plant Biol.* 52, 12, 1043–1058. doi: 10.1111/j.1744-7909.2010.00996.x
- Han, M., Lu, X., Yu, J., Chen, X., Wang, X., Malik, W. A., et al. (2019). Transcriptome analysis reveals cotton (Gossypium hirsutum) genes that are differentially expressed in cadmium stress tolerance. *Int. J. Mol. Sci.* 20 (6), 1479. doi: 10.3390/ijms20061479

- Heinemeyer, J., Scheibe, B., Schmitz, U. K., and Braun, H.-P. (2009). Blue native DIGE as a tool for comparative analyses of protein complexes. *J. Proteomics* 72 (3), 539–544. doi: 10.1016/j.jprot.2008.12.008
- Hochholdinger, F., Marcon, C., Baldauf, J. A., Yu, P., and Frey, F. P. (2018). Proteomics of maize root development. *Front Plant Sci.* 9, 143. doi: 10.3389/fpls.2018.00143
- Hu, W., Zheng, M., Wang, S., Meng, Y., Wang, Y., Chen, B., et al. (2017). Proteomic changes in response to low-light stress during cotton fiber elongation. *Acta Physiologiae Plantarum* 39 (9), 200. doi: 10.1007/s11738-017-2499-1
- Iqbal, A., Qiang, D., Xiangru, W., Huiping, G., Hengheng, Z., Xiling, Z., et al. (2022). Low phosphorus tolerance in cotton genotypes is regulated by root morphology and physiology. *J. Plant Growth Regul.* doi: 10.1007/s00344-022-10829-5
- Kerry, R. G., Mahapatra, G. P., Patra, S., Sahoo, S. L., Pradhan, C., Padhi, B. K., et al. (2018). Proteomic and genomic responses of plants to nutritional stress. *BioMetals* 31 (2), 161–187. doi: 10.1007/s10534-018-0083-9
- Khodadadi, E., Fakheri, B. A., Aharizad, S., Emamjomeh, A., Norouzi, M., and Komatsu, S. (2017). Leaf proteomics of drought-sensitive and -tolerant genotypes of fennel. *Biochim. Biophys. Acta (BBA) - Proteins Proteomics* 1865 (11, Part A), 1433–1444. doi: 10.1016/j.bbapap.2017.08.012
- Lawrence, S. R. 2nd, Gaitens, M., Guan, Q., Dufresne, C., and Chen, S. (2020). S-Nitroso-Proteome revealed in stomatal guard cell response to Flg22. *International journal of molecular sciences* 21, 5. doi: 10.3390/ijms21051688
- Lee, D.-G., Houston, N., Stevenson, S., Ladics, G., McClain, S., Privalle, L., et al. (2010). Mass spectrometry analysis of soybean seed proteins: Optimization of gel-free quantitative workflow. *Anal. Methods* 2, 1577–83. doi: 10.1039/C0AY00319K
- Li, H.-B., Qin, Y.-M., Pang, Y., Song, W.-Q., Mei, W.-Q., and Zhu, Y.-X. (2007). A cotton ascorbate peroxidase is involved in hydrogen peroxide homeostasis during fibre cell development 175, 3, 462–471. doi: 10.1111/j.1469-8137.2007.02120.x
- Li, T., Wu, R., Liu, Z., Wang, J., Guo, C., Zhou, Y., et al. (2021). GUN4 affects the circadian clock and seedlings adaptation to changing light conditions. *Int. J. Mol. Sci.* 23, 194. doi: 10.3390/ijms23010194
- Li, W., Fa, Z., Fang, W., Xie, D., Hou, J., Yang, X., et al. (2015). Identification of early salt stress responsive proteins in seedling roots of upland cotton (*Gossypium hirsutum* L.) employing iTRAQ-based proteomic technique. *Front. Plant Sci.* 6, 732. doi: 10.3389/fpls.2015.00732
- Li, Z., Wang, X., Cui, Y., Qiao, K., Zhu, L., Fan, S., et al. (2020). Comprehensive genome-wide analysis of thaumatin-like gene family in four cotton species and functional identification of GhTLP19 involved in regulating tolerance to verticillium dahlia and drought. *Front Plant Sci.* 11, 575015. doi: 10.3389/fpls.2020.575015
- Lim, P. O., Kim, H. J., and Nam, H. G. (2007). Leaf senescence. *Annu. Rev. Plant Biol.* 58, 1, 115–136. doi: 10.1146/annurev.arplant.57.032905.105316
- Liu, Z., Guo, C., Wu, R., Hu, Y., Zhou, Y., Wang, J., et al. (2022a). FLS2-RBOHD-PIF4 module regulates plant response to drought and salt stress. *Int. J. Mol. Sci.* 23 (3), 1080. doi: 10.3390/ijms23031080
- Liu, Z., Guo, C., Wu, R., Wang, J., Zhou, Y., Yu, X., et al. (2022b). Identification of the regulators of epidermis development under drought- and salt-stressed conditions by single-cell RNA-seq. *Int. J. Mol. Sci.* 23 (5), 2759. doi: 10.3390/ijms23052759
- Liu, L., Li, A., Chen, J., Wang, M., Zhang, Y., Sun, H., et al. (2019). iTRAQ-based quantitative proteomic analysis of cotton (*Gossypium hirsutum* L.) leaves reveals pathways associated throughout the aging process. *Acta Physiologiae Plantarum* 41, 144. doi: 10.1007/s11738-019-2921-y
- Liu, Y., Lu, S., Liu, K., Wang, S., Huang, L., and Guo, L. (2019). Proteomics: a powerful tool to study plant responses to biotic stress. *Plant Methods* 15 (1), 135. doi: 10.1186/s13007-019-0515-8
- Liu, D., Zhang, J., Liu, X., Wang, W., Liu, D., Teng, Z., et al. (2016). Fine mapping and RNA-seq unravels candidate genes for a major QTL controlling multiple fiber quality traits at the T1 region in upland cotton. *BMC Genomics* 17 (1), 295. doi: 10.1186/s12864-016-2605-6
- Lv, J., Baizhi, C., Ma, C., Qiao, K., Fan, S., and Ma, Q. (2021). Identification and characterization of the AINV genes in five *Gossypium* species with potential functions of GhAINVs under abiotic stress. *Physiologia plantarum* 173 (4), 2091–2102. doi: 10.1111/ppl.13559
- Magdeldin, S., Enany, S., Yoshida, Y., Xu, B., Zhang, Y., Zureena, Z., et al. (2014). Basics and recent advances of two dimensional- polyacrylamide gel electrophoresis. *Clin. Proteomics* 11 (1), 16. doi: 10.1186/1559-0275-11-16
- Meng, Y., Liu, F., Pang, C., Fan, S., Song, M., Wang, D., et al. (2011). Label-free quantitative proteomics analysis of cotton leaf response to nitric oxide. *J. Proteome Res.* 10 (12), 5416–5432. doi: 10.1021/pr200671d
- Mostofa, M., Abdelrahman, M., Rahman, M., Cuong, T., Nguyen, K., Watanabe, Y., et al. (2022). Karrikin receptor KAI2 coordinates salt tolerance mechanisms in *Arabidopsis thaliana*. *Plant Cell Physiol.* pccac121. doi: 10.1093/pcp/pccac121
- Munné-Bosch, S., and Alegre, L. (2004). Die and let live: leaf senescence contributes to plant survival under drought stress. *Funct. Plant biology: FPB* 31 (3), 203–216. doi: 10.1071/FP03236
- Nagamalla, S. S., Alaparathi, M. D., Mellacheruvu, S., Gundeti, R., Eerawandla, J. P. S., and Sagurthi, S. R. (2021). Morpho-physiological and proteomic response of bt-cotton and non-bt cotton to drought stress. *Front Plant Sci.* 12, 663576. doi: 10.3389/fpls.2021.663576
- Nestler, J., Schütz, W., and Hochholdinger, F. (2011). Conserved and unique features of the maize (*Zea mays* L.) root hair proteome. *J. Proteome Res.* 10 (5), 2525–2537. doi: 10.1021/pr200003k
- Nouri, M. Z., and Komatsu, S. (2010). Comparative analysis of soybean plasma membrane proteins under osmotic stress using gel-based and LC MS/MS-based proteomics approaches. *Proteomics* 10 (10), 1930–1945. doi: 10.1002/pmic.200900632
- O'Farrell, P. H. (1975). High resolution two-dimensional electrophoresis of proteins. *J. Biol. Chem.* 250 (10), 4007–4021. doi: 10.1016/S0021-9258(19)41496-8
- Okamoto, T., Higuchi, K., Shinkawa, T., Isobe, T., Lörz, H., Koshiba, T., et al. (2004). Identification of major proteins in maize egg cells. *Plant Cell Physiol.* 45 (10), 1406–1412. doi: 10.1093/pcp/pch161
- Pang, C. Y., Wang, H., Pang, Y., Xu, C., Jiao, Y., Qin, Y. M., et al. (2010). Comparative proteomics indicates that biosynthesis of pectic precursors is important for cotton fiber and arabidopsis root hair elongation. *Mol. Cell. proteomics: MCP* 9 (9), 2019–2033. doi: 10.1074/mcp.M110.000349
- Pertl, H., Schulze, W. X., and Obermeyer, G. (2009). The pollen organelle membrane proteome reveals highly spatial-temporal dynamics during germination and tube growth of lily pollen. *J. Proteome Res.* 8 (11), 5142–5152. doi: 10.1021/pr900503f
- Petersen, A., Dresselhaus, T., Grobe, K., and Becker, W.-M. (2006). Proteome analysis of maize pollen for allergy-relevant components. *Proteomics* 6 (23), 6317–6325. doi: 10.1002/pmic.200600173
- Pettigrew, W. T. (2001). Environmental effects on cotton fiber carbohydrate concentration and quality. *Crop Physiology Metabol.* 41 (4), 1108–1113. doi: 10.2135/cropsci2001.4141108x
- Potts, J., Li, H., Qin, Y., Wu, X., Hui, D., Nasr, K. A., et al. (2022). Using single cell type proteomics to identify Al-induced proteomes in outer layer cells and interior tissues in the apical meristem/cell division regions of tomato root-tips. *J. Proteomics* 255, 104486. doi: 10.1016/j.jprot.2022.104486
- Pradet-Balade, B., Boulmé, F., Beug, H., Müller, E. W., and Garcia-Sanz, J. A. (2001). Translation control: bridging the gap between genomics and proteomics? *Trends Biochem. Sci.* 26 (4), 225–229. doi: 10.1016/S0968-0004(00)01776-x
- Qamer, Z., Chaudhary, M. T., Du, X., Hinze, L., and Azhar, M. T. (2021). Review of oxidative stress and antioxidative defense mechanisms in *Gossypium hirsutum* L. @ in response to extreme abiotic conditions. *J. Cotton Res.* 4 (1), 9. doi: 10.1186/s42397-021-00086-4
- Rabilloud, T. (2012). The whereabouts of 2D gels in quantitative proteomics. *Methods Mol. Biol. (Clifton NJ)* 893, 25–35. doi: 10.1007/978-1-61779-885-6\_2
- Rabilloud, T., and Lelong, C. (2011). Two-dimensional gel electrophoresis in proteomics: A tutorial. *J. Proteomics* 74 (10), 1829–1841. doi: 10.1016/j.jprot.2011.05.040
- Read, J., Reddy, K., and Jenkins, J. (2006). Yield and fiber quality of upland cotton as influenced by nitrogen and potassium nutrition. *Eur. J. Agron.* 24, 282–290. doi: 10.1016/j.eja.2005.10.004
- Riter, L. S., Jensen, P. K., Ballam, J. M., Urbanczyk-Wochniak, E., Clough, T., Vitek, O., et al. (2011). Evaluation of label-free quantitative proteomics in a plant matrix: A case study of the night-to-day transition in corn leaf. *Anal. Methods* 3 (12), 2733–2739. doi: 10.1039/c1ay05473b
- Roncada, P., Piras, C., Soggiu, A., Turk, R., Urbani, A., and Bonizzi, L. (2012). Farm animal milk proteomics. *J. Proteomics* 75 (14), 4259–4274. doi: 10.1016/j.jprot.2012.05.028
- Saleem, M., Bilal, M., Awais, M., Shahid, M. Q., and Anjum, S. (2010). Effect of nitrogen on seed cotton yield and fiber qualities of cotton (*Gossypium hirsutum* L.) cultivars. *J. Anim. Plant Sci.* 20, 23–27.
- Santhosh, B., and Yohan, Y. (2019). Abiotic stress responses of cotton: A review. *Internat J. Chem. Studies* 7 (6), 795–798.
- Shabala, S., Bose, J., Shabala, L., Zeng, F., Wu, H., Zhu, M., et al. (2014). Abiotic stress tolerance and crop yield: a physiologist's perspective.
- Sheoran, I. S., Ross, A. R. S., Olson, D. J. H., and Sawhney, V. K. (2007). Proteomic analysis of tomato (*Lycopersicon esculentum*) pollen. *J. Exp. Bot.* 58 (13), 3525–3535. doi: 10.1093/jxb/erm199
- Shrivastav, P., Prasad, M., Singh, T. B., Yadav, A., Goyal, D., Ali, A., et al. (2020). “Role of nutrients in plant growth and development,” in *Contaminants in agriculture: Sources, impacts and management*. Eds. M. Naem, A. A. Ansari and S. S. Gill (Cham: Springer International Publishing), 43–59.
- Silveira, J. A. G., and Carvalho, F. E. L. (2016). Proteomics, photosynthesis and salt resistance in crops: An integrative view. *J. Proteomics* 143, 24–35. doi: 10.1016/j.jprot.2016.03.013



- Sinha, R., Bala, M., Ranjan, A., Lal, S. K., Sharma, T. R., Pattanayak, A., et al. (2021). "Proteomic approaches to understand plant response to abiotic stresses," in *Agricultural biotechnology: Latest research and trends*. Eds. D. Kumar Srivastava, A. Kumar Thakur and P. Kumar (Singapore: Springer Nature Singapore), 351–383.
- Snider, J., Harris, G., Roberts, P., Meeks, C., Chastain, D., Bange, M., et al. (2021). Cotton physiological and agronomic response to nitrogen application rate. *Field Crops Res.* 270, 108194. doi: 10.1016/j.fcr.2021.108194
- Solis, C. A., Yong, M. T., Zhou, M., Venkataraman, G., Shabala, L., Holford, P., et al. (2022). Evolutionary significance of NHX family and NHX1 in salinity stress adaptation in the genus *oryza*. *Int. J. Mol. Sci.* 23 (4), 2092. doi: 10.3390/ijms23042092
- Sun, X., Feng, P., Xu, X., Guo, H., Ma, J., Chi, W., et al. (2011). A chloroplast envelope-bound PHD transcription factor mediates chloroplast signals to the nucleus. *Nat. Commun.* 2 (1), 477. doi: 10.1038/ncomms1486
- Sun, X., Wang, Y., Xu, L., Li, C., Zhang, W., Luo, X., et al. (2017). Unraveling the root proteome changes and its relationship to molecular mechanism underlying salt stress response in radish (*Raphanus sativus* L.). *Front. Plant Sci.* 8, 1192. doi: 10.3389/fpls.2017.01192
- Tang, Z.-Q., Shang, J., Zhang, L., Du, J.-B., Yang, H., Zeng, S.-H., et al. (2019). Characterization of synergy between cucumber mosaic virus and alternaria alternata in nicotiana tabacum. *Physiol. Mol. Plant Pathol.* 108, 101404. doi: 10.1016/j.pmpp.2019.03.001
- Tu, X., Li, J., Wang, Q., and Liu, A. (2017). Quantitative proteomic analysis of upland cotton stem terminal buds reveals phytohormone-related pathways associated with dwarfism. *Biol. Plantarum* 61 (1), 106–114. doi: 10.1007/s10535-016-0644-0
- Ullah, K., Khan, N., Usman, Z., Ullah, R., Saleem, F. Y., Shah, S. A. I., et al. (2016). Impact of temperature on yield and related traits in cotton genotypes. *J. Integr. Agric.* 15 (3), 678–683. doi: 10.1016/S2095-3119(15)61088-7
- Umbetev, I., Bigaraev, O., and Baimakhanov, K. (2015). Effect of soil salinity on the yield of cotton in Kazakhstan. *Russian Agric. Sci.* 41 (4), 222–224. doi: 10.3103/S1068367415040205
- Van Cutsem, E., Simonart, G., Degand, H., Faber, A. M., Morsomme, P., and Boutry, M. (2011). Gel-based and gel-free proteomic analysis of nicotiana tabacum trichomes identifies proteins involved in secondary metabolism and in the (a)biotic stress response. *Proteomics* 11 (3), 440–454. doi: 10.1002/pmic.201000356
- Van Der Sluijs, M. H. J. (2022). Effect of nitrogen application level on cotton fibre quality. *J. Cotton Res.* 5 (1), 9. doi: 10.1186/s42397-022-00116-9
- Wang, X., Fan, S., Song, M., Pang, C., Wei, H., Yu, J., et al. (2014). Upland cotton gene GhFPF1 confers promotion of flowering time and shade-avoidance responses in arabidopsis thaliana. *PLoS One* 9 (3), e91869. doi: 10.1371/journal.pone.0091869
- Wang, Y., Liang, C., Wu, S., Zhang, X., Tang, J., Jian, G., et al. (2016). Significant improvement of cotton verticillium wilt resistance by manipulating the expression of gastrodia antifungal proteins. *Mol. Plant* 9 (10), 1436–1439. doi: 10.1016/j.molp.2016.06.013
- Wang, F. X., Ma, Y. P., Yang, C. L., Zhao, P. M., Yao, Y., Jian, G. L., et al. (2011). Proteomic analysis of the sea-island cotton roots infected by wilt pathogen verticillium dahliae. *Proteomics* 11 (22), 4296–4309. doi: 10.1002/pmic.201100062
- Wang, Q., Wang, Z., Song, X., Li, Y., Guo, Y., Wang, J., et al. (2005). [Effects of shading at blossoming and boll-forming stages on cotton fiber quality]. *Ying yong sheng tai xue bao = J. Appl. Ecol.* 16 (8), 1465–1468.
- Wang, Y., Zheng, M., Gao, X., and Zhou, Z. (2012). Protein differential expression in the elongating cotton (*Gossypium hirsutum* L.) fiber under nitrogen stress. *Sci. China Life Sci.* 55 (11), 984–992. doi: 10.1007/s11427-012-4390-z
- Wan, X. Y., and Liu, J. Y. (2008). Comparative proteomics analysis reveals an intimate protein network provoked by hydrogen peroxide stress in rice seedling leaves. *Mol. Cell. proteomics: MCP* 7 (8), 1469–1488. doi: 10.1074/mcp.M700488-MCP200
- Wilkins, M. R., Sanchez, J. C., Gooley, A. A., Appel, R. D., Humphrey-Smith, I., Hochstrasser, D. F., et al. (1996). Progress with proteome projects: why all proteins expressed by a genome should be identified and how to do it. *Biotechnol. Genet. Eng. Rev.* 13, 19–50. doi: 10.1080/02648725.1996.10647923
- Wu, X., Chen, T., Zheng, M., Chen, Y., Teng, N., Samaj, J., et al. (2008). Integrative proteomic and cytological analysis of the effects of extracellular Ca(2+) influx on pinus bungeana pollen tube development. *J. Proteome Res.* 7 (10), 4299–4312. doi: 10.1021/pr800241u
- Wu, H., and Li, Z. (2019). The importance of cl<sup>-</sup> exclusion and vacuolar cl<sup>-</sup> sequestration: Revisiting the role of cl<sup>-</sup> transport in plant salt tolerance. *Front. Plant Sci.* 10, 1418. doi: 10.3389/fpls.2019.01418
- Wu, R., Liu, Z., Wang, J., Guo, C., Zhou, Y., Bawa, G., et al. (2022). COE2 is required for the root foraging response to nitrogen limitation. *Int. J. Mol. Sci.* 23, 861. doi: 10.3390/ijms23020861
- Xiao, S., Liu, L., Zhang, Y., Sun, H., Zhang, K., Bai, Z., et al. (2020). Tandem mass tag-based (TMT) quantitative proteomics analysis reveals the response of fine roots to drought stress in cotton (*Gossypium hirsutum* L.). *BMC Plant Biol.* 20 (1), 328. doi: 10.1186/s12870-020-02531-z
- Xu, W.-L., Zhang, D.-J., Wu, Y.-F., Qin, L.-X., Huang, G.-Q., Li, J., et al. (2013). Cotton PRP5 gene encoding a proline-rich protein is involved in fiber development. *Plant Mol. Biol.* 82 (4), 353–365. doi: 10.1007/s11103-013-0066-8
- Yao, Y., Yang, Y.-W., and Liu, J.-Y. (2006). An efficient protein preparation for proteomic analysis of developing cotton fibers by 2-DE. *Electrophoresis* 27 (22), 4559–4569. doi: 10.1002/elps.200600111
- Zargar, SM, Gupta, N, Mir, RA, and Rai, V (2016). Shift from Gel Based to Gel Free Proteomics to Unlock Unknown Regulatory Page 9 of 19 Network in Plants: A Comprehensive Review. *J. Adv. Res. Biotech.* 1 (1), 19.
- Zhang, Z., Chao, M., Wang, S., Bu, J., Tang, J., Li, F., et al. (2016). Proteome quantification of cotton xylem sap suggests the mechanisms of potassium-deficiency-induced changes in plant resistance to environmental stresses. *Sci. Rep.* 6 (1), 21060.
- Zhang, M., Cheng, S. T., Wang, H. Y., Wu, J. H., Luo, Y. M., Wang, Q., et al. (2017). iTRAQ-based proteomic analysis of defence responses triggered by the necrotrophic pathogen rhizoctonia solani in cotton. *J. Proteomics* 152, 226–235. doi: 10.1016/j.jprot.2016.11.011
- Zhang, H., Ni, Z., Chen, Q., Guo, Z., Gao, W., Su, X., et al. (2016). Proteomic responses of drought-tolerant and drought-sensitive cotton varieties to drought stress. *Mol. Genet. Genomics* 291 (3), 1293–1303. doi: 10.1007/s00438-016-1188-x
- Zhang, X., Zhao, J., Wu, X., Hu, G., Fan, S., and Ma, Q. (2021). Evolutionary relationships and divergence of KNOTTED1-like family genes involved in salt tolerance and development in cotton (*Gossypium hirsutum* L.). *Front. Plant Sci.* 12. doi: 10.3389/fpls.2021.774161
- Zhang, T., Zhao, Y.-L., Zhao, J.-H., Wang, S., Jin, Y., Chen, Z.-Q., et al. (2016). Cotton plants export microRNAs to inhibit virulence gene expression in a fungal pathogen. *Nat. Plants* 2 (10), 16153. doi: 10.1038/nplants.2016.153
- Zhao, F., Fang, W., Xie, D., Zhao, Y., Tang, Z., Li, W., et al. (2012). Proteomic identification of differentially expressed proteins in gossypium thurberi inoculated with cotton verticillium dahliae. *Plant Sci.* 185–186, 176–184. doi: 10.1016/j.plantsci.2011.10.007
- Zhao, Z., Liu, Z., Zhou, Y., Wang, J., Zhang, Y., Yu, X., et al. (2022). Creation of cotton mutant library based on linear electron accelerator radiation mutation. *Biochem. Biophysics Rep.* 30, 101228. doi: 10.1016/j.bbrep.2022.101228
- Zheng, X., Fan, S., Wei, H., Tao, C., Ma, Q., Ma, Q., et al. (2017). iTRAQ-based quantitative proteomic analysis reveals cold responsive proteins involved in leaf senescence in upland cotton (*Gossypium hirsutum* L.). *Int. J. Mol. Sci.* 18 (9), 1984. doi: 10.3390/ijms18091984
- Zheng, M., Wang, Y., Liu, K., Shu, H., and Zhou, Z. (2012). Protein expression changes during cotton fiber elongation in response to low temperature stress. *J. Plant Physiol.* 169 (4), 399–409. doi: 10.1016/j.jplph.2011.09.014
- Zhou, X., Hu, W., Li, B., Yang, Y., Zhang, Y., Thow, K., et al. (2019). Proteomic profiling of cotton fiber developmental transition from cell elongation to secondary wall deposition. *Acta Biochim. Biophys. Sin.* 51 (11), 1168–1177. doi: 10.1093/abbs/gmz111
- Zhou, M., Sun, G., Sun, Z., Tang, Y., and Wu, Y. (2014). Cotton proteomics for deciphering the mechanism of environment stress response and fiber development. *J. Proteomics* 105, 74–84. doi: 10.1016/j.jprot.2014.03.017
- Zhu, H. G., Cheng, W. H., Tian, W. G., Li, Y. J., Liu, F., Xue, F., et al. (2018). iTRAQ-based comparative proteomic analysis provides insights into somatic embryogenesis in gossypium hirsutum L. *Plant Mol. Biol.* 96 (1–2), 89–102. doi: 10.1007/s11103-017-0681-x
- Zhu, M., Dai, S., McClung, S., Yan, X., and Chen, S. (2009). Functional differentiation of brassica napus guard cells and mesophyll cells revealed by comparative proteomics. *Mol. Cell. proteomics: MCP* 8 (4), 752–766. doi: 10.1074/mcp.M800343-MCP200
- Zhu, S., Li, Y., Zhang, X., Liu, F., Xue, F., Zhang, Y., et al. (2021). GhAlaRP, a cotton alanine rich protein gene, involves in fiber elongation process. *Crop J.* 9 (2), 313–324. doi: 10.1016/j.cj.2020.08.007
- Zhu, H., Song, J., Dhar, N., Shan, Y., Ma, X. Y., Wang, X. L., et al. (2021). Transcriptome analysis of a cotton cultivar provides insights into the differentially expressed genes underlying heightened resistance to the devastating verticillium wilt. *Cells* 10 (11), 2961. doi: 10.3390/cells10112961





## OPEN ACCESS

EDITED BY  
Kashmir Singh,  
Panjab University, India

REVIEWED BY  
Peifang Zhao,  
Yunnan Academy of Agricultural  
Sciences, China  
Shumayla,  
Panjab University, India

\*CORRESPONDENCE  
Zhaoliang Liu  
349159942@qq.com  
Zhen Wang  
wang798110510@163.com

<sup>†</sup>These authors have contributed  
equally to this work

SPECIALTY SECTION  
This article was submitted to  
Plant Abiotic Stress,  
a section of the journal  
Frontiers in Plant Science

RECEIVED 11 August 2022  
ACCEPTED 21 November 2022  
PUBLISHED 12 December 2022

CITATION  
Pang F, Niu J, Solanki MK, Nosheen S,  
Liu Z and Wang Z (2022) *PHD-finger*  
family genes in wheat (*Triticum*  
*aestivum* L.): Evolutionary  
conservatism, functional  
diversification, and active expression in  
abiotic stress.  
*Front. Plant Sci.* 13:1016831.  
doi: 10.3389/fpls.2022.1016831

COPYRIGHT  
© 2022 Pang, Niu, Solanki, Nosheen, Liu  
and Wang. This is an open-access  
article distributed under the terms of  
the [Creative Commons Attribution  
License \(CC BY\)](#). The use, distribution  
or reproduction in other forums is  
permitted, provided the original  
author(s) and the copyright owner(s)  
are credited and that the original  
publication in this journal is cited, in  
accordance with accepted academic  
practice. No use, distribution or  
reproduction is permitted which does  
not comply with these terms.

# *PHD-finger* family genes in wheat (*Triticum aestivum* L.): Evolutionary conservatism, functional diversification, and active expression in abiotic stress

Fei Pang<sup>1†</sup>, Junqi Niu<sup>1†</sup>, Manoj Kumar Solanki<sup>2</sup>,  
Shaista Nosheen<sup>3</sup>, Zhaoliang Liu<sup>1\*</sup> and Zhen Wang<sup>1\*</sup>

<sup>1</sup>College of Agriculture, Yulin Normal University, Yulin, China, <sup>2</sup>Plant Cytogenetics and Molecular Biology Group, Faculty of Natural Sciences, Institute of Biology, Biotechnology and Environmental Protection, University of Silesia in Katowice, Katowice, Poland, <sup>3</sup>School of Agricultural Engineering and Food Science, Shandong University of Technology, Zibo, China

Plant homeodomain (PHD) transcription factors (TFs) are a class of proteins with conserved Cys4-His-Cys3 domains that play important roles in plant growth and development and in response to abiotic stresses. Although characterization of *PHDs* has been performed in plants, little is known about their function in wheat (*Triticum aestivum* L.), especially under stress conditions. In the present study, 244 *TaPHDs* were identified in wheat using comparative genomics. We renamed them *TaPHD1-244* based on their chromosomal distribution, and almost all PHD proteins were predicted to be located in the nucleus. According to the unrooted neighbor-joining phylogenetic tree, gene structure, and motif analyses, *PHD* genes were divided into four clades. A total of 149 *TaPHD* genes were assigned to arise from duplication events. Furthermore, 230 gene pairs came from wheat itself, and 119, 186, 168, 7, 2, and 6 gene pairs came from six other species (*Hordeum vulgare*, *Zea mays*, *Oryza sativa*, *Arabidopsis thaliana*, *Brassica rapa*, and *Gossypium raimondii*, respectively). A total of 548 interacting protein branches were identified to be involved in the protein interaction network. Tissue-specific expression pattern analysis showed that *TaPHDs* were highly expressed in the stigma and ovary during flowering, suggesting that the *TaPHD* gene plays an active role in the reproductive growth of wheat. In addition, the qRT-PCR results further confirmed that these *TaPHD* genes are involved in the abiotic stress response of wheat. In conclusion, our study provides a theoretical basis for deciphering the molecular functions of *TaPHDs*, particularly in response to abiotic stress.

## KEYWORDS

*PHD-finger* genes, wheat, phylogenetic analysis, expression patterns, abiotic stress

## Introduction

Plants encounter various unfavorable growth conditions during their life cycle, such as pests and diseases, drought, and extreme temperatures. In response to adverse external environments, plants activate *in vivo* defense response mechanisms by inducing stress-responsive gene expression (Fujita et al., 2006; Zhu et al., 2019). Many plant-specific transcription factor (TF) family members are involved in plant-specific developmental processes and participate in and regulate the stress response of plants to the external environment, thereby improving their adaptation to adversity (Yamasaki et al., 2013). To date, some such transcription factors have been successively isolated from many species of plants, such as AP2/ERF (Mizoi et al., 2012), bHLH (Sun et al., 2018), MYB (Li et al., 2015), and WRKY (Rushton et al., 2010). Among these, the plant homeodomain (PHD)-finger transcription factor family is tissue-specific and plays an important role in plant growth, development, and transcriptional regulation by adversity. The PHD is a conserved zinc finger structural domain in biological evolution and is commonly distributed in eukaryotes ranging from yeast to plants and animals (Ogryzko et al., 1996; Gibbons et al., 1997; Kehle et al., 1998; Papoulas et al., 1998; Martin et al., 2006). A typical PHD domain consists of 50–80 amino acid residues with a characteristic Cys4-His-Cys3 sequence, which is arranged in a manner similar to RING (Cys3-His-Cys4) and LIM (Cys2-His-Cys5) (Aasland et al., 1995; Borden and Freemont, 1996). The most important function of the PHD domain is the specific recognition of various histone modifications and DNA sequences, thus acting in transcriptional regulation and participating in various biological processes in organisms (Li et al., 2006; Hu et al., 2011; Xi et al., 2011). For example, previous studies have shown that, in model plants, proteins containing PHD domains are involved in embryonic meristem germination, root development, photoperiod, vernalization, meiosis, and post-meiotic pollen development. PHD domains play an important role in plant growth and development (Mouriz et al., 2015).

PHD domains are a class of relatively small protein domains. Their relatively conserved cysteine and histidine can stabilize the normal spatial structure by binding zinc ions, so that the three-dimensional conformation of the entire domain is basically spherical (Kwan et al., 2003). In addition to the conserved Cys4-His-Cys3 residues, PHD proteins usually contain highly diverse sequences. These diverse sequences form genes with different biological functions within the *PHD-finger* family. For example, the PHD domain-containing protein MMD1 is involved in essential chromatin remodeling and transcriptional events during male meiosis (Yang et al., 2003). In *Arabidopsis*, the ALFIN1-like (AL) protein, which contains the PHD domain, plays a key role in seed germination (Molitor et al., 2014). Furthermore, the PHD-finger protein VIL1 is involved in the

photoperiod and vernalization pathways, as it regulates the expression of related floral repressors (Sung and Amasino, 2004). ATX1 and ATX2 have histone methyltransferase activities and regulate the development of roots, leaves, and floral organs, as well as the transcription of some stress genes (Saleh et al., 2008).

Since Schinder first discovered and identified PHD proteins in plants (Schindler et al., 1993), an increasing number of *PHDs* have been reported. To date, 59 *Oryza sativa* members (Sun et al., 2017), 108 *Gossypium hirsutum* members (Wu et al., 2021), 72 *Solanum tuberosum* members (Qin et al., 2019), 60 *Phyllostachys edulis* members (Gao et al., 2018), and 67 *Zea mays* members (Wang et al., 2015a) have been identified. It is known that PHD proteins not only participate in the regulation of plant growth and development but also play an important role in stress response, especially to abiotic stresses such as salt, high-temperature, low-temperature, and drought stress. In rice, overexpression of the *OsPHD1* gene can significantly improve resistance to low-temperature, high-salt, and drought stress (Liu et al., 2011). Overexpression of the PHD-finger transcription factor gene *OsMsr16* can enhance salt resistance in rice plants (Zhang et al., 2016). Wei et al. also found that *Arabidopsis thaliana* transgenic plants overexpressing soybean *GmPHD2* exhibited higher salt resistance, possibly because overexpression of *GmPHD2* enhanced the scavenging of oxidative substances (Wei et al., 2009). Furthermore, under abiotic stress, genes in the *PHD-finger* family in maize, cotton, and poplar show differential expression under salt, drought, and cold stress (Wang et al., 2015a; Wu et al., 2016; Wu et al., 2021). Thus, it can be seen that the *PHD* family genes play a crucial role in regulating plant resistance to stress.

Wheat is a major food crop worldwide and plays a crucial role in global food security. It is especially important to tap important resistance genes, breed new resistant wheat varieties, and improve the resistance of wheat itself (He et al., 2011). The *PHD-finger* gene family, which is essential for growth and development, has been identified and studied in many crops, but no systematic studies of the *PHD* gene family in wheat have been performed. In the present study, we identified *PHD-finger* family members in wheat for the first time and performed a comprehensive and systematic genome-wide analysis, including gene conserved motif analysis, phylogenetic relationships, Gene Ontology (GO) annotation analysis, covariance analysis, reciprocal relationship analysis, and subcellular localization. We also investigated the expression of PHD family proteins during growth and development, their specific expression in each organ, and their expression under multiple stresses of low temperature, high temperature, and drought. We lay the foundation for analyzing the functions of PHD proteins and regulating stress resistance and also provide theoretical references for the excavation of stress resistance genes and stress resistance breeding in wheat.

## Materials and methods

### Identification and classification analysis of *PHD* family genes in wheat

To identify *PHD* gene family members from wheat, whole genome data for *T. aestivum* (IWGSC RefSeq\_v1.1) were obtained from the Ensembl plant database (<http://plants.ensembl.org/info/website/ftp/index.html>), and the *PHD*-finger domain (PF00628) was downloaded from the PFAM database (<https://pfam.xfam.org/>). The *PHD* protein sequences from *A. thaliana* (70) and *O. sativa* (59) (Supplementary Table S1) (Sun et al., 2017) were used as query sequences to search against the wheat protein dataset using the BLASTP program, and the threshold was set as E-value < 1e-5. The NCBI-Batch CD-Search (Marchler-Bauer et al., 2017) (<https://www.ncbi.nlm.nih.gov/Structure/bwrpsb/bwrpsb.cgi>), PFAM database, and SMART database (<http://smart.embl.de/>) were used to further confirm the candidate *PHD*-finger genes of *T. aestivum*. There were other spliced transcripts in the candidate genes of these species, and we selected the first splice variant as a representative for subsequent analysis.

The protein sequences of *TaPHDs* were computed using the ExPASy server (Artimo et al., 2012) to obtain the theoretical isoelectric point (pI), molecular weight (MW), instability index (II), aliphatic index (AI), and grand average hydrophobicity (GRAVY). Plant-mPLoc (Chou and Shen, 2010) (<http://www.csbio.sjtu.edu.cn/cgi-bin/PlantmPLoc.cgi>) and BUSCA (Savojardo et al., 2018) (Bologna Unified Subcellular Component Annotator, <http://busca.biocomp.unibo.it>) were used to predict the subcellular localization of the *TaPHD* proteins.

### Phylogenetic analyses of *TaPHD* genes

The *PHD*-finger protein sequences of *T. aestivum*, *A. thaliana*, and *O. sativa* were used for phylogenetic analysis. Jalview 2.11 software (<http://www.jalview.org/>) with the MUSCLE method with default parameters was utilized to conduct multiple sequence alignment. Evolutionary analysis involved 342 amino acid sequences (all wheat *PHD* genes, and most rice and *Arabidopsis* *PHD* genes). These analyses were conducted in MEGA X (Kumar et al., 2018) using the neighbor-joining method (Saitou and Nei, 1987). The percentage of replicate trees in which the associated taxa clustered together in the bootstrap test (1000 replicates) is shown next to the branches. The evolutionary distances were computed using the Poisson correction method and were expressed as the number of amino acid substitutions per site. The iTOL website (<http://itol.embl.de/>) was used to visualize the phylogenetic tree.

### Gene duplication and Ka/Ks analysis of *TaPHD* genes

MCSanX software (Wang et al., 2012) was used to detect collinear regions between *TaPHD* genes as well as collinear blocks of *TaPHDs* with three monocotyledons (*H. vulgareto*, *Z. mays*, and *O. sativa*) and three dicotyledons (*A. thaliana*, *B. rapa*, and *G. raimondii*). Whole genome data for *H. vulgareto*, *Z. mays*, *O. sativa*, *A. thaliana*, *B. rapa*, and *G. raimondii* were obtained from the Ensembl plant database (<http://plants.ensembl.org/info/website/ftp/index.html>). All *TaPHD* genes were mapped to their respective loci in the wheat genome in a circular diagram using shinyCircos (Yu et al., 2018). Gene duplication events of *TaPHDs* and syntenic relationships between the aforementioned species were visualized using TBtools (v1.082) (Chen et al., 2020). The Ka/Ks values (non-synonymous substitution rate/synonymous substitution rate) were calculated after identification of duplicated genes, using the method of Nei and Gojobori as implemented in KaKs\_calculator (Zhang et al., 2006) based on the coding sequence alignments. Subsequently, the divergence time of collinear gene pairs was calculated using the duplication events formula  $T = Ks/(2\lambda \times 10^{-6})$  in millions of years (Mya), with  $\lambda = 6.5 \times 10^{-9}$  (Wang et al., 2015b).

### GO annotation and protein-protein interaction network analysis of *TaPHD* genes

GO annotation of *TaPHD* proteins was available from the KOBAS database (<http://kobas.cbi.pku.edu.cn/kobas3>) (Xie et al., 2011). The full-length amino acid sequences of *TaPHD* proteins were uploaded to the original program, followed by drawing and annotation. GO annotations were performed for three types of analyses: biological processes, molecular functions, and cellular composition. The GO annotation results were visualized using the online tool OmicStudio (<https://www.omicstudio.cn/tool>) (Ye et al., 2018). All the predicted *TaPHD* proteins were submitted to the STRING database (<https://string-db.org/cgi/input.pl>). The minimum required interaction score was set to a high confidence (0.700). The maximum number of interactors was no more than 10 on the first shell.

### Expression of *TaPHD* genes

Transcriptional data for *TaPHDs* were obtained from the wheat expression website (<http://www.wheat-expression.com/download>) (Borrill et al., 2016; Ramírez-González et al., 2018) and were used to explore the potential biological functions of

*TaPHD* genes in growth and development, abiotic and biotic stress, and other conditions. Systematic clustering analysis was performed based on the log2 of transcripts per million (TPM) values for the 244 *TaPHD* genes. R was used to display the expression patterns in a heat map, and OmicStudio (<https://www.omicstudio.cn/tool>) was used to display the histogram, volcano plot, and Venn diagram.

## Quantitative real-time PCR analyses (qRT-PCR) of *TaPHD* genes in response to environmental stresses

In this study, the seeds of the hexaploid common wheat variety “Zhengmai 7698” were surface-sterilized with 2% hydrogen peroxide, rinsed thoroughly with distilled water, and germinated with water saturation at 25°C for two days in Petri dishes on three layers of filter paper. The young seedlings were transformed and grown in 1/2 Hoagland’s culture solution under a 14 h light (25°C)/10 h dark (20°C) photoperiod. When the wheat grew to two leaves and one heart, the plants were subsequently treated with 16% polyethylene glycol 6000. For cold stress, wheat seedlings were exposed to 4°C for 12 h. For heat stress, wheat seedlings were exposed to 40°C for 12 h. New leaves of the three seedlings were collected as biological replicates, and each treatment had three replicates.

Total RNA was extracted using RNAiso Reagent (TaKaRa, Beijing, China) and Cdna was synthesized using the RT Master Mix Perfect RealTime kit (TaKaRa, Beijing, China). Quantitative real-time PCR was performed using the CFX Touch™ Real-Time PCR Detection System (Bio-Rad Laboratories, Hercules, CA, USA) and the SG Fast Qpcr Master Mix (Sangon Biotech, Shanghai, China). Relative expression levels were determined using the  $2^{-\Delta\Delta Ct}$  method (Livak and Schmittgen, 2001), and  $\beta$ -actin was used as the internal control to normalize the expression levels of *TaPHD* genes. Specific primers used for qRT-PCR are listed in [Supplementary Table S2](#).

## Determination of subcellular localization of TaPHD11, TaPHD19, and TaPHD133

Full-length open reading frames of *TaPHD11*, *TaPHD19*, and *TaPHD133* were obtained from “Zhengmai 7698” Cdna ([Supplementary Table S2](#)). The Coding sequence (CDS) of *TaPHD11*, *TaPHD19*, and *TaPHD133* were cloned into the pJIT16318 vector at the BamHI site using specific primers ([Supplementary Table S2](#)). The pJIT16318 vector contained a CaMV 35S promoter and C-terminal GFP. Transient expression assays were conducted as described by Cui et al. (2019). Approximately  $4 \times 10^4$  mesophyll protoplasts were isolated from 12-day-old wheat seedlings. The transfected protoplasts were incubated at 23°C for 12 h. The GFP fluorescence in the

transformed protoplasts was imaged using a confocal laser-scanning microscope (LSM 700; Zeiss).

## Results

### Identification and classification analysis of *PHD* genes in wheat

In this study, 244 *T. aestivum* genes were designated *PHD* genes with two query methods; HMM and BLASTP were used for identification, and three websites, NCBI-Batch CD-Search, PFAM database, and SMART database, were used for confirmation ([Supplementary Table S3](#)). These *PHD* genes were renamed *TaPHD1* to *TaPHD244*, based on the order of their chromosomal locations and physical positions.

To further determine the characteristics of *TaPHD* genes, the ExPASy Server online tool was used to analyze the protein characteristics ([Supplementary Table S3](#)). The shortest protein contained 216 amino acids (*TaPHD158*, *TaPHD175*) and the longest protein contained 2853 amino acids (*TaPHD204*); the molecular weight was between 24567.82 Da (*TaPHD158*) and 310347.53 Da (*TaPHD204*). The protein instability index showed that all *PHD* genes were unstable proteins. The isoelectric point of *TaPHD* genes varied markedly from 4.42 (*TaPHD36*) to 9.65 (*TaPHD78*), and the aliphatic index varied significantly from 48.13 (*TaPHD26/39/51*) to 97.51 (*TaPHD42*). The GRAVY of *TaPHD* proteins in wheat varied from 0.016 (*TaPHD160*) to -1.285 (*TaPHD23*), indicating that they were all hydrophilic proteins, except for *TaPHD160* ([Supplementary Table S3](#)). We used two methods (Plant-mPLOC and BUSCA) to predict the subcellular localization of the *TaPHD* proteins. The results showed that a few *TaPHDs* may be localized in the chloroplast, mitochondrion, or cytoplasm, and most members were predicted to be located in the nucleus ([Supplementary Table S3](#)).

### Multiple sequence alignment and phylogenetic analysis of *PHD* genes

Multiple sequence alignments of *PHD* domains were performed ([Figure 1](#)). Approximately 60 amino acids (aa) comprised a *PHD* domain containing basic Cys4-His-Cys3 sequence motifs in each *TaPHD*.

To evaluate the evolutionary relationships of *PHD* genes in *T. aestivum*, *O. sativa*, and *A. thaliana*, a neighbor-joining phylogenetic tree was constructed using full-length *PHD* proteins ([Figure 2](#) and [Supplementary Table S1](#)). Phylogenetic analysis showed that *PHD* family proteins can be divided into four clades (clades 1 to 4). *TaPHD* members were found in all clades. Clade 1 was the largest, with 95 *TaPHD* members, and clade 4 was the smallest, with only 38 members. The results



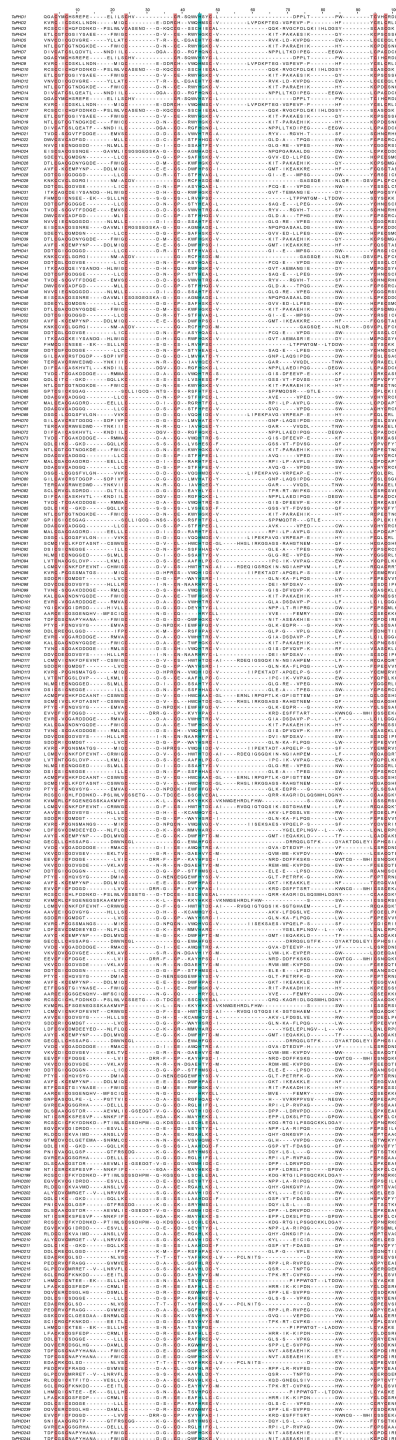
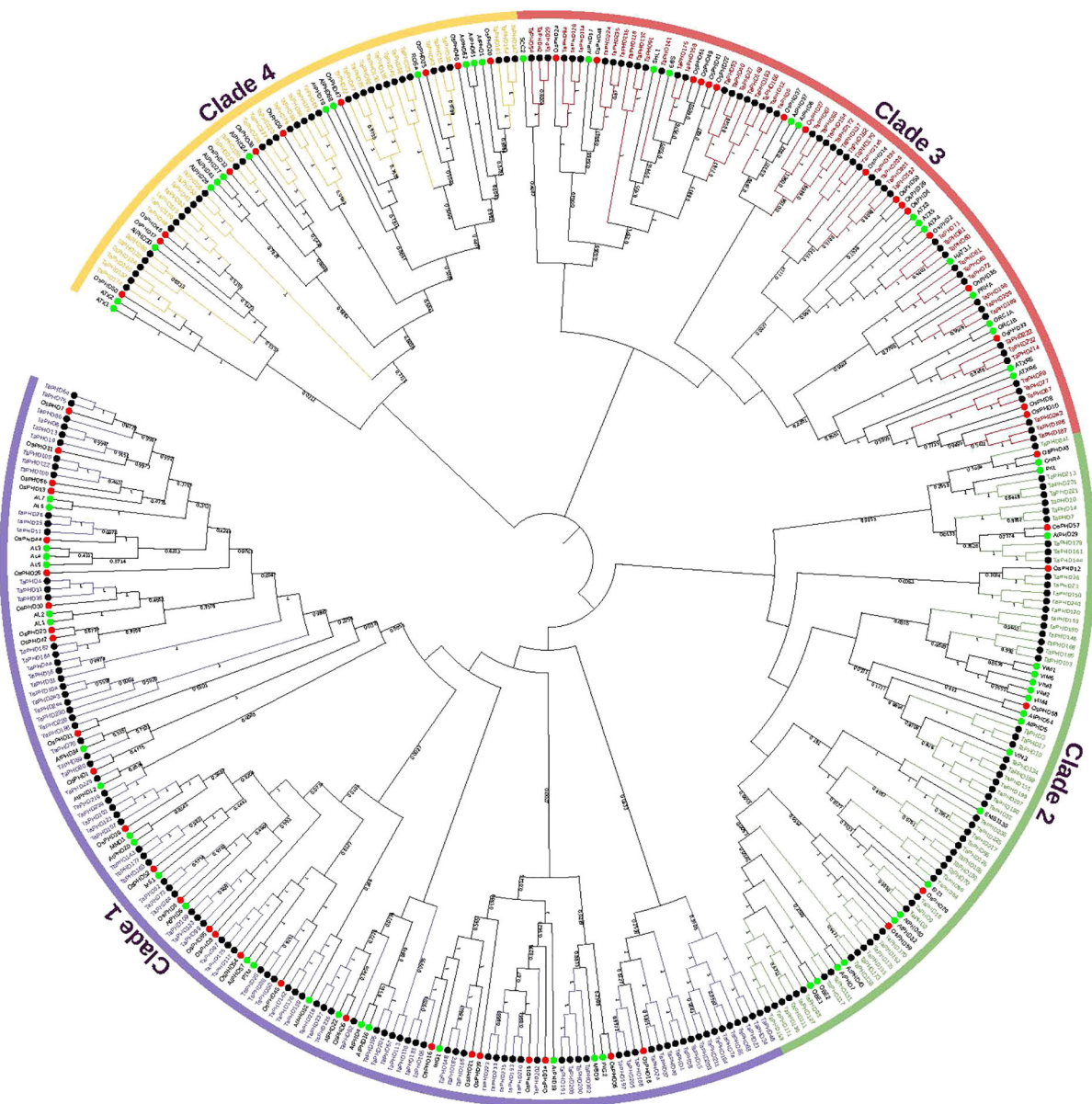


FIGURE 1

Protein sequence multiple alignment of the PHD-finger domains in TaPHD family proteins. The multiple alignment was conducted with the amino acid sequences within the predicted PHD domains by using Jalview software. The conserved amino acids (Cys4-His-Cys3) within the PHD-finger domains are shaded in red and blue.





**FIGURE 2**  
Phylogenetic tree of *PHD* genes in wheat, rice, and *Arabidopsis*. The tree was analyzed in MEGA X by using the neighbor-joining method. The PHDs from wheat, rice, and *Arabidopsis* are distinguished with black, red, and green dots. The PHD proteins were grouped into four distinct clades (clades 1–4), which are indicated by colored branches.

showed that there were many small branches under each clade, and almost every small branch had corresponding genes of rice and *Arabidopsis*. This indicates that the *TaPHD* gene is not an evolutionary characteristic of monocotyledonous and dicotyledonous plants, and that the *PHD* gene family was formed before the differentiation of these two types of plants.

Protein domains are often functional carriers. According to phylogenetic and domain analyses (NCBI-Batch CD-Search,

PFAM, and SMART database), 30 dominant types were identified in all wheat PHD proteins (Table 1). The results showed that among all wheat PHD proteins, 43 contained a typical PHD domain. The next most common, the jas-PHD and alfin-PHD domains, had 28 and 25 members, respectively; the PHD-Oberon\_cc domain and the PHD-RING domains had 11 members, and the remaining domain types had less than ten members. The results showed that wheat PHD proteins

TABLE 1 Types, names, and numbers of wheat *PHD*-finger genes.

| Domain type | Wheat triad                                  | Rice orthologs   | Arabidopsis thaliana orthologs | Gene number | Chr  | Genomes |
|-------------|--|------------------|--------------------------------|-------------|------|---------|
| PHD         | TaPHD1/TaPHD8/TaPHD15                        |                  |                                | 3           | 1    | ABD     |
|             | TaPHD5/TaPHD12                               |                  |                                | 2           | 1    | AB      |
|             | TaPHD21/TaPHD34/TaPHD46                      |                  |                                | 3           | 2    | ABD     |
|             | TaPHD62/TaPHD73/TaPHD84                      | OsPHD5           |                                | 3           | 3    | ABD     |
|             | TaPHD82                                      |                  |                                | 1           | 3    | D       |
|             | TaPHD94/TaPHD114/TaPHD128                    | OsPHD24          |                                | 3           | 4    | ABD     |
|             | TaPHD218/TaPHD226/TaPHD237                   | OsPHD24          |                                | 3           | 7    | ABD     |
|             | TaPHD98/TaPHD110/TaPHD124                    |                  |                                | 3           | 4    | ABD     |
|             | TaPHD99/TaPHD109/TaPHD123                    | OsPHD55          | AtPHD6                         | 3           | 4    | ABD     |
|             | TaPHD101/TaPHD107/TaPHD121                   | OsPHD19          | MS1,MMD1                       | 3           | 4    | ABD     |
|             | TaPHD143/TaPHD160/TaPHD177                   | OsPHD52          | MS1,MMD1                       | 3           | 5    | ABD     |
|             | TaPHD103                                     |                  |                                | 1           | 4    | A       |
|             | TaPHD137/TaPHD154/TaPHD172                   |                  |                                | 3           | 5    | ABD     |
|             | TaPHD146/TaPHD163/TaPHD180                   | OsPHD58          | AtPHD54                        | 3           | 5    | ABD     |
|             | TaPHD168/TaPHD185                            |                  |                                | 2           | 5    | BD      |
|             | TaPHD186                                     | OsPHD11          |                                | 1           | 5    | D       |
|             | TaPHD192/TaPHD201/TaPHD209                   | OsPHD14, OsPHD37 | AtPHD8,AtPHD37                 | 3           | 6    | ABD     |
| PHD-PHD     | TaPHD135/TaPHD152/TaPHD170                   | OsPHD59          | AtPHD32,AtPHD40                | 3           | 5    | ABD     |
|             | TaPHD144/TaPHD161/TaPHD178                   |                  | AtPHD29                        | 3           | 5    | ABD     |
|             | TaPHD216/TaPHD224/TaPHD235                   | OsPHD48          |                                | 3           | 7    | ABD     |
| Alifn-PHD   | TaPHD4/TaPHD11/TaPHD18                       | OsPHD30          | AL1,AL2                        | 3           | 1    | ABD     |
|             | TaPHD6/TaPHD13/TaPHD19                       | OsPHD31          | AL6,AL7                        | 3           | 1    | ABD     |
|             | TaPHD26/TaPHD39/TaPHD51                      | OsPHD44          | AL3,AL4,AL5                    | 3           | 2    | ABD     |
|             | TaPHD31/TaPHD44/TaPHD56                      |                  | AL1,AL2,AL3,AL4,AL5,AL6,AL7    | 3           | 2    | ABD     |
|             | TaPHD64/TaPHD75/TaPHD86                      | OsPHD7           | AL6,AL7                        | 3           | 3    | ABD     |
|             | TaPHD100/TaPHD108/TaPHD122                   | OsPHD56          | AL6,AL7                        | 3           | 4    | ABD     |
|             | TaPHD167/TaPHD184                            | OsPHD23, OsPHD42 | AL1,AL2                        | 2           | 5    | BD      |
|             | TaPHD104/TaPHD229/TaPHD230/TaPHD243/TaPHD244 |                  | AL1,AL2,AL3,AL4,AL5,AL6,AL7    | 5           | 4(7) | A(DD)UU |
| ARID-PHD    | TaPHD142/TaPHD159/TaPHD176                   |                  |                                | 3           | 5    | ABD     |
| RING-PHD    | TaPHD23/TaPHD36/TaPHD48                      | OsPHD46          | AtPHD30                        | 3           | 2    | ABD     |
|             | TaPHD93/TaPHD115/TaPHD129                    | OsPHD17          | AtPHD30                        | 3           | 4    | ABD     |
| ING-PHD     | TaPHD105/TaPHD119/TaPHD133                   | OsPHD16          | ING1                           | 3           | 4    | ABD     |
|             | TaPHD148/TaPHD165/TaPHD182                   | OsPHD21          | ING2                           | 3           | 5    | ABD     |

(Continued)

TABLE 1 Continued

| Domain type            | Wheat triad                         | Rice orthologs   | Arabidopsis thaliana orthologs  | Gene number | Chr  | Genomes |
|------------------------|-------------------------------------|------------------|---------------------------------|-------------|------|---------|
| BAH-PHD                | TaPHD27/TaPHD40/TaPHD53             | OsPHD41          | SHL1                            | 3           | 2    | ABD     |
|                        | TaPHD141/TaPHD158/TaPHD175          | OsPHD49, OsPHD51 | EBS                             | 3           | 5    | ABD     |
|                        | TaPHD149/TaPHD166/TaPHD183          | OsPHD22          | SHL1                            | 3           | 5    | ABD     |
| Jas-PHD                | TaPHD28/TaPHD41/TaPHD52             | OsPHD40          | AtPHD1,AtPHD61,AtPHD62          | 3           | 2    | ABD     |
|                        | TaPHD147/TaPHD164/TaPHD181          | OsPHD20          | AtPHD1,AtPHD61,AtPHD62          | 3           | 5    | ABD     |
|                        | TaPHD30/TaPHD43/TaPHD55             | OsPHD25          |                                 | 3           | 2    | ABD     |
|                        | TaPHD33/TaPHD45/TaPHD58             |                  | ROS4                            | 3           | 2    | ABD     |
|                        | TaPHD22/TaPHD35/TaPHD47             | OsPHD47          | AtPHD68,AtPHD70                 | 3           | 2    | ABD     |
|                        | TaPHD92/TaPHD116/TaPHD130           | OsPHD47          | AtPHD68,AtPHD70                 | 3           | 4    | ABD     |
|                        | TaPHD66/TaPHD76/TaPHD88             | OsPHD9           |                                 | 3           | 3    | ABD     |
|                        | TaPHD68/TaPHD78                     | OsPHD9           |                                 | 2           | 3    | AB      |
|                        | TaPHD106/TaPHD212                   | OsPHD32          | AtPHD24,AtPHD26,AtPHD27,AtPHD41 | 2           | 4(7) | A(A)    |
|                        | TaPHD220/TaPHD227/TaPHD238          | OsPHD38          | AtPHD24,AtPHD26,AtPHD27,AtPHD41 | 3           | 7    | ABD     |
| DDT-PHD                | TaPHD25/TaPHD38/TaPHD50             | OsPHD45          | DDP1,DDP2                       | 3           | 2    | ABD     |
|                        | TaPHD97/TaPHD112/TaPHD125           | OsPHD54          | DDP3                            | 3           | 4    | ABD     |
|                        | TaPHD138/TaPHD155/TaPHD173          | OsPHD54          | DDP3                            | 3           | 5    | ABD     |
| zf-HC5HC2H-PHD         | TaPHD59/TaPHD70/TaPHD80             | OsPHD1           |                                 | 3           | 3    | ABD     |
| PHD-Oberon_cc          | TaPHD91/TaPHD118/TaPHD132           |                  |                                 | 3           | 4    | ABD     |
|                        | TaPHD95/TaPHD111/TaPHD127           |                  | OBE1,OBE2                       | 3           | 4    | ABD     |
|                        | TaPHD136/TaPHD153/TaPHD171          |                  | OBE1,OBE2                       | 3           | 5    | ABD     |
|                        | TaPHD117/TaPHD131                   |                  |                                 | 2           | 4    | BD      |
| PHD-FN3                | TaPHD3/TaPHD10/TaPHD17              |                  | VIN3                            | 3           | 1    | ABD     |
|                        | TaPHD134/TaPHD151/TaPHD169          |                  | VIN3                            | 3           | 5    | ABD     |
|                        | TaPHD190/TaPHD199/TaPHD207          |                  | VIN3                            | 3           | 6    | ABD     |
| PHD-SANT               | TaPHD63/TaPHD74/TaPHD85             |                  |                                 | 3           | 3    | ABD     |
|                        | TaPHD194/TaPHD203/TaPHD211          |                  |                                 | 3           | 6    | ABD     |
| PHD-WHIM1              | TaPHD102/TaPHD191/TaPHD200/TaPHD208 |                  | MBD9                            | 4           | 6(4) | (A)ABD  |
| PHD-SET                | TaPHD67/TaPHD77/TaPHD89             | OsPHD8           | ATXR5,ATXR6                     | 3           | 3    | ABD     |
|                        | TaPHD187/TaPHD196/TaPHD242          | OsPHD10          | ATXR5,ATXR6                     | 3           | 6    | AB(U)   |
| PWWP-PHD-SET           | TaPHD60/TaPHD71/TaPHD81             | OsPHD2,OsPHD4    | ATX3,ATX4,ATX5                  | 3           | 3    | ABD     |
| PWWP-FYRN-FYRC-PHD-SET | TaPHD140/TaPHD157/TaPHD174          | OsPHD50          | ATX1,ATX2                       | 3           | 5    | ABD     |
| PHD-BAH                | TaPHD234                            |                  |                                 | 1           | 7    | D       |
| PHD-BAH-AAA            | TaPHD214/TaPHD222/TaPHD232          | OsPHD33          | ORC1A,ORC1B                     | 3           | 7    | ABD     |
| PHD-homeodomain        | TaPHD7/TaPHD14/TaPHD20              |                  | PRHA                            | 3           | 1    | ABD     |

(Continued)

TABLE 1 Continued

| Domain type                 | Wheat triad                | Rice orthologs   | Arabidopsis thaliana orthologs | Gene number | Chr  | Genomes |
|-----------------------------|----------------------------|------------------|--------------------------------|-------------|------|---------|
| PHD-PLN03142                | TaPHD61/TaPHD72/TaPHD83    | OsPHD35          | HAT3.1                         | 3           | 3    | ABD     |
|                             | TaPHD189/TaPHD198/TaPHD206 |                  |                                | 3           | 6    | ABD     |
|                             | TaPHD65/TaPHD87            |                  |                                | 2           | 3    | AD      |
|                             | TaPHD195/TaPHD204/TaPHD241 |                  |                                | 3           | 6    | ABD     |
| PHD-RING                    | TaPHD2/TaPHD9/TaPHD16      | OsPHD29          | SIZ1                           | 3           | 1    | ABD     |
|                             | TaPHD69/TaPHD79/TaPHD90    |                  | SIZ1                           | 3           | 3    | ABD     |
|                             | TaPHD96/TaPHD113/TaPHD126  |                  | SIZ1                           | 3           | 4    | ABD     |
|                             | TaPHD139/TaPHD156          |                  | SIZ1                           | 2           | 5    | AB      |
| PHD-JmjC-PLU1               | TaPHD219/TaPHD228/TaPHD239 |                  |                                | 3           | 7    | ABD     |
| AAA_34-PHD-Helicase_C_4     | TaPHD32/TaPHD57            | OsPHD27          | EMB1135                        | 2           | 2    | AD      |
|                             | TaPHD217/TaPHD225/TaPHD236 | OsPHD27          | EMB1135                        | 3           | 7    | ABD     |
| PHD-zf-HC5HC2H-zf-HC5HC2H   | TaPHD193/TaPHD202/TaPHD210 | OsPHD15, OsPHD34 | AtPHD18                        | 3           | 6    | ABD     |
|                             | TaPHD215/TaPHD223/TaPHD233 |                  |                                | 3           | 7    | ABD     |
| BRCT-BRCT-PHD               | TaPHD24/TaPHD37/TaPHD49    | OsPHD18          |                                | 3           | 2    | ABD     |
|                             | TaPHD188/TaPHD197/TaPHD205 | OsPHD18          |                                | 3           | 6    | ABD     |
| PHD-SWIB-GYF-Plus3          | TaPHD120/TaPHD150/TaPHD240 |                  |                                | 3           | 4(5) | (A)BU   |
| PHD-SWIB-Plus3-GYF          | TaPHD145/TaPHD162/TaPHD179 |                  |                                | 3           | 5    | ABD     |
| PHD-Chromo-Helicase_C-DUF   | TaPHD213/TaPHD221/TaPHD231 |                  | PKL                            | 3           | 7    | ABD     |
| PHD-Cohesin_HEAT-Nipped-B_C | TaPHD29/TaPHD42/TaPHD54    |                  | EMB2773                        | 3           | 2    | ABD     |

contained a canonical PHD domain or double PHD domains. Owing to their different domains, differentiation in function was achieved.

To better understand why *PHD-finger* genes are abundant in the wheat genome, we analyzed the homoeologous groups in

detail (Table 2). A total of 35.8% of wheat genes were present in homoeologous groups of three, also termed triads (A:B:D = 1:1:1) (Consortium et al., 2018). In contrast, 84.8% of the *PHD-finger* genes identified were present in triads (Table 2). Also, the percentage of *PHD-finger* genes with homoeolog-specific

TABLE 2 Groups of homoeologous *PHD-finger* genes in wheat.

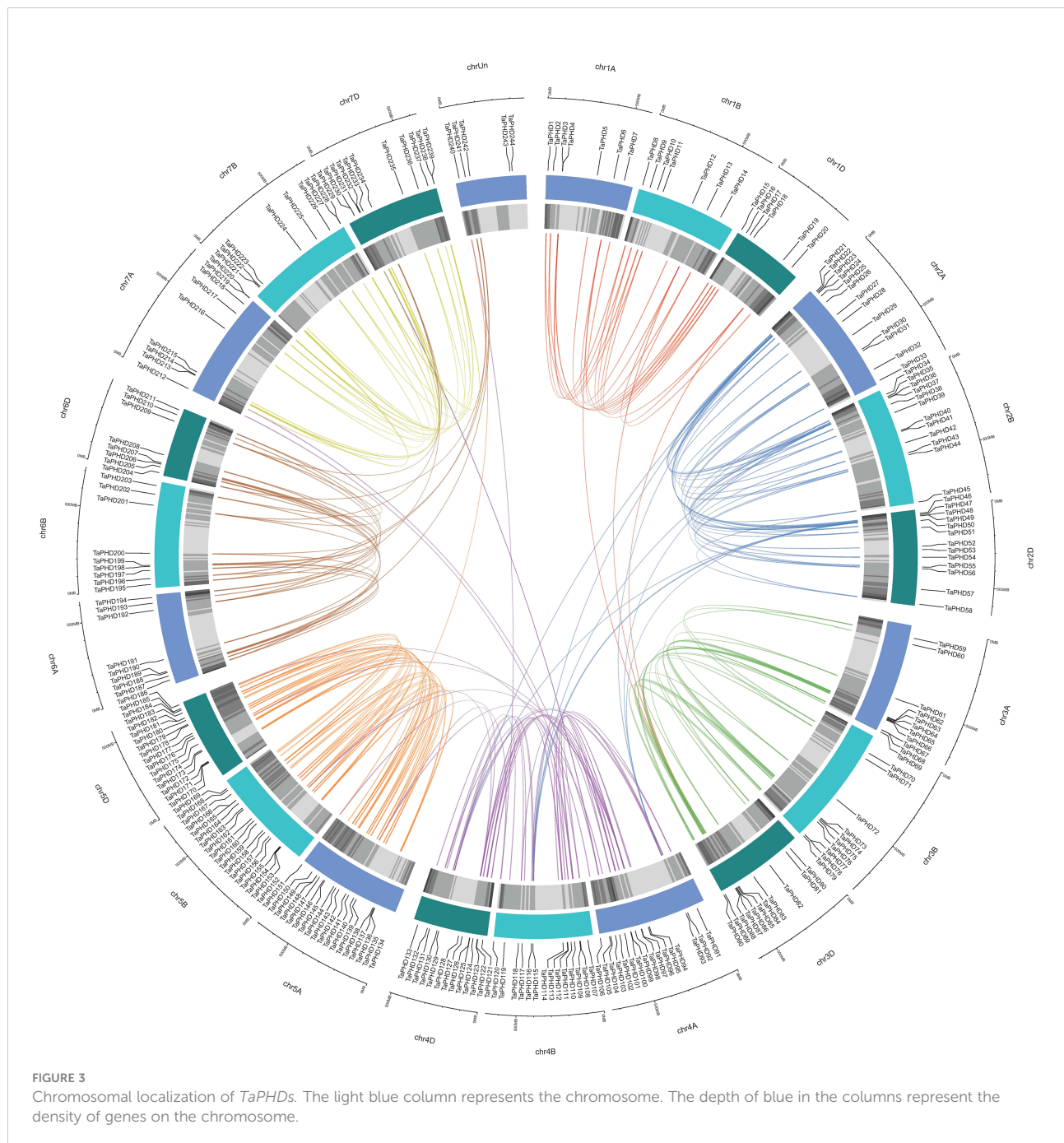
| Homoeologous group (A: B: D)         | All wheat genes <sup>1</sup> | Wheat <i>PHD-finger</i> genes (all) |                 |                         |
|--------------------------------------|------------------------------|-------------------------------------|-----------------|-------------------------|
|                                      |                              | Number of groups                    | Number of genes | % of genes <sup>2</sup> |
| 1: 1: 1                              | 35.8%                        | 69                                  | 207             | 84.8                    |
| n: 1: 1/1: n: 1/1: 1: n <sup>3</sup> | 5.7%                         | 1                                   | 4               | 1.6                     |
| 1: 1: 0/1: 0: 1/0: 1: 1              | 13.2%                        | 8                                   | 16              | 6.6                     |
| Other ratios <sup>4</sup>            | 8.0%                         | 3                                   | 11              | 4.5                     |
| Orphans/singletons                   | 37.1%                        | 4                                   | 4               | 1.6                     |
| Not categorized <sup>5</sup>         | -                            | -                                   | 2               | 0.8                     |
|                                      | 99.8%                        |                                     | 244             | 100.0                   |

<sup>1</sup>According to IWGSC (2018). <sup>2</sup>Percentage calculated with 244 genes. <sup>3</sup>For n > 1. <sup>4</sup>E.g., n:1:n or 0:1:n, n > 1. <sup>5</sup>See Table 1 and Table S3.

duplications was lower for *PHD-finger* genes than for all wheat genes (1.6% vs 5.7%; Table 2). Loss of one homoeolog, on the other hand, was less pronounced in *PHD-finger* genes (6.6% vs 13.2%; Table 2). Only four *PHD-finger* genes were orphans/singletons. Thus, the high homoeolog retention rate could partly explain the high number of wheat *PHD-finger* genes.

## Chromosomal location, gene duplication, and synteny analysis of *TaPHD* genes

Based on the reference GFF3 files, the physical positions of *PHD* genes on the corresponding chromosomes are shown in Figure 3. The identified *TaPHDs* could be mapped on every





chromosome and evenly across the three sub-genomes. The map shows that chromosomes 5B and 5D harbor the largest number of *TaPHD* genes (18), whereas chromosome 1D contains the least (6).

Gene duplication is an indispensable mechanism by which organisms create new genes with similar or different functions (Song et al., 2019). Therefore, we analyzed the duplication events that occurred in the *TaPHD* gene family. A total of 230 *PHD* gene pairs from wheat were identified as duplicated (Figure 4 and Supplementary Table S4). These similar *PHD* gene pairs had the same domain type and appeared in the same branch of the phylogenetic tree. Tandem and segment duplications are critical for the evolution of gene families to adapt to different environmental conditions. Interestingly, all the *TaPHD* gene pairs were associated with segmental duplication events. This suggests that this was the main route for expanding *PHD* genes

in wheat and the many homologous genes on different wheat chromosomes suggest the high conservation of the family. To further infer the evolutionary origin and homology of the wheat *PHD* family, we constructed a collinear chart comparing six species with wheat, including three monocotyledons (*H. vulgare*, *Z. mays*, and *O. sativa*) and three dicotyledons (*A. thaliana*, *B. rapa*, and *G. raimondii*) (Figure 5 and Supplementary Table S4). We identified pairwise homologues of the *TaPHD* genes and detected 119, 186, 168, 7, 2, and 6 pairs of homologous genes from *H. vulgare*, *Z. mays*, *O. sativa*, *A. thaliana*, *B. rapa*, and *G. raimondii*, respectively (Figure 5 and Supplementary Table S4). This implies that *TaPHD* genes share a strong evolutionary relationship with *ZmPHDs*, *HvPHDs*, and *OsPHDs*. Furthermore, these results indicated that the *PHD* gene family was differentiated between monocotyledonous and dicotyledonous plants. This also indicated that *TaPHD* genes

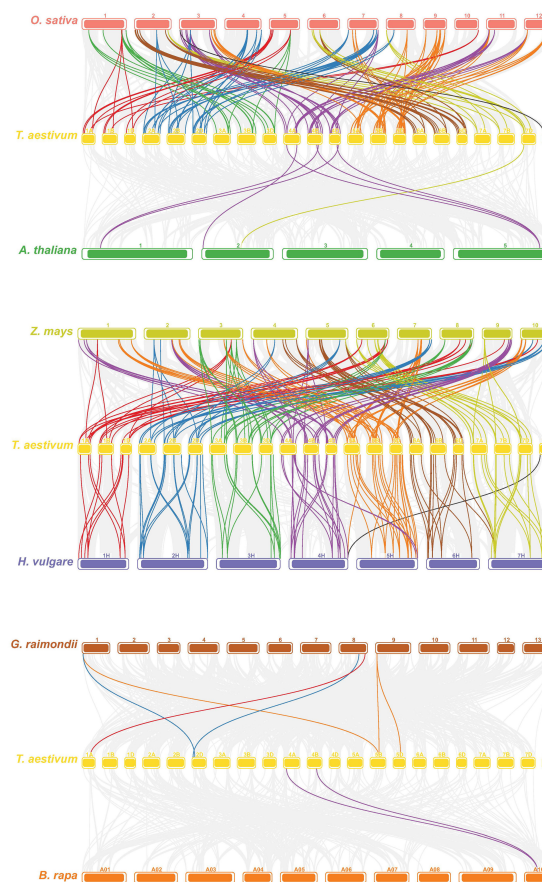


FIGURE 4

Synteny analysis of *PHD* genes in wheat. All *TaPHD* genes were mapped to their respective locus in the wheat genome in a circular diagram using shinyCircos (Yu et al., 2018). Subgenomes are indicated by different shades of blue (outer track), and chromosomal segments are indicated by shades of gray (inner track). Homoeologous *PHD* genes were inferred by phylogeny (for details see the Materials and Methods section) and linked with chromosome-specific colors.

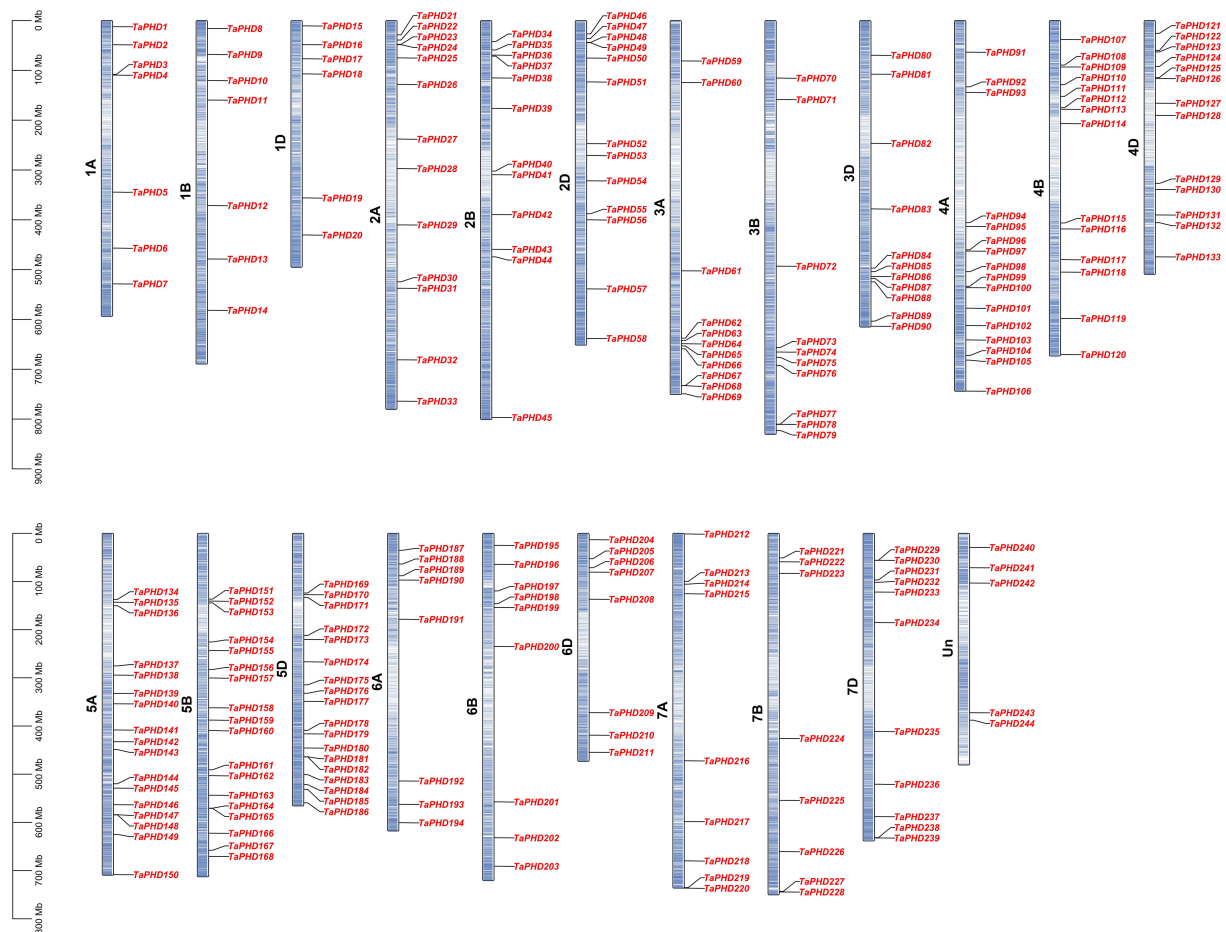


FIGURE 5

Synteny analysis of *PHD* genes between wheat and six representative plants (maize, barley, rice, *Arabidopsis*, cotton, and *Brassica rapa*). Each different species is replaced with a different color. The gray line in the background indicates a collinear block in the genome of wheat and other plants, while the line highlights the isomorphic *PHD* gene pair. Homoeologous *PHD* genes were inferred by phylogeny (for details see the Materials and Methods section) and linked with chromosome-specific colors.

had a strong evolutionary relationship with *ZmPHDs*, *HvPHDs*, and *OsPHDs*. The average differentiation time was: barley (12.78 Mya) < rice (22.09 Mya) < maize (60.87 Mya).

Ka/Ks, the non-synonymous substitution ratio, determines the selection pressure for duplicated genes. According to the results (Supplementary Table S4), only a very few *TaPHD* gene pairs had Ka/Ks ratios >1, suggesting that the evolution of *TaPHD* genes was accompanied by strong purifying selection. The Ka/Ks ratios between wheat and three monocotyledonous plants were calculated based on the collinear gene pairs. Except for very few genes, the values of the other collinear gene pairs were all below 1, which confirmed that the evolution of the wheat *PHD* gene family underwent strong purifying selection. However, the Ka/Ks ratios of the collinear gene pairs between wheat and the three dicots could not be calculated properly. This is because most synonymous mutation sites have synonymous mutations; that is, the degree of sequence divergence and

evolutionary distance is too large. Some *TaPHD* genes have formed at least five homologous gene pairs, such as *TaPHD9*, which may have played key roles in the evolution of the *PHD* gene family (Figure 5 and Supplementary Table S4).

## GO annotation analysis and protein-protein interaction network of *TaPHD* genes

We performed GO annotation analysis of the 244 *TaPHD* proteins, revealing that they may participate in a range of cellular components, molecular functions, and biological processes (Figure 6 and Supplementary Table S5). The 244 *TaPHD* proteins were assigned a total of 105 GO terms. In biological processes, the three most highly enriched categories were related to the regulation of DNA-templated transcription, heat

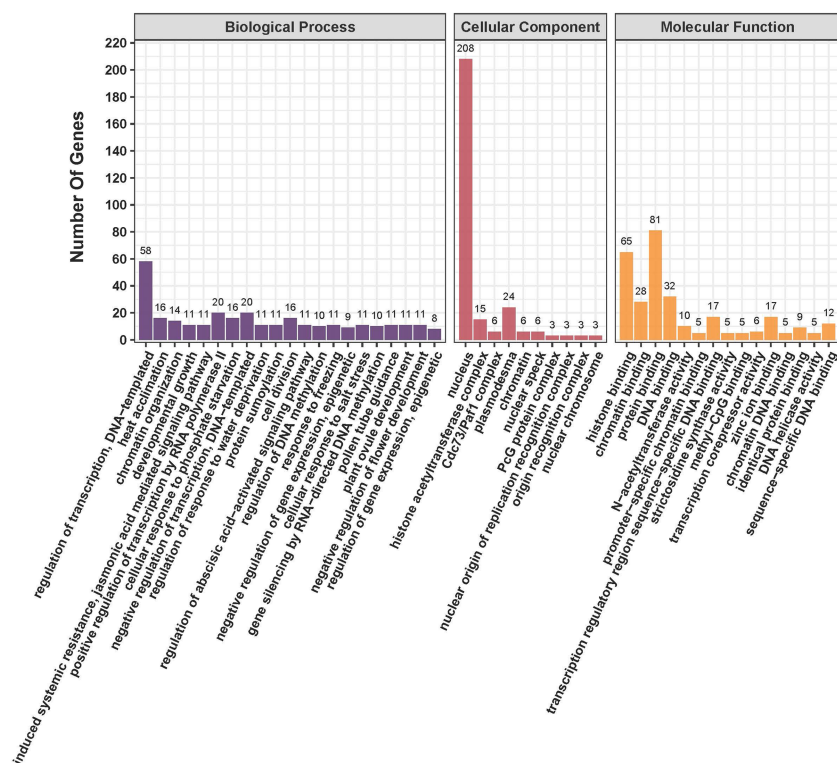


FIGURE 6

Functional annotation analysis of *TaPHD* genes. Gene Ontology (GO) classification based on *TaPHD* gene annotation. The GO terms are grouped into three main categories: purple for Biological Processes, red for Cellular Components, and yellow for Molecular Function.

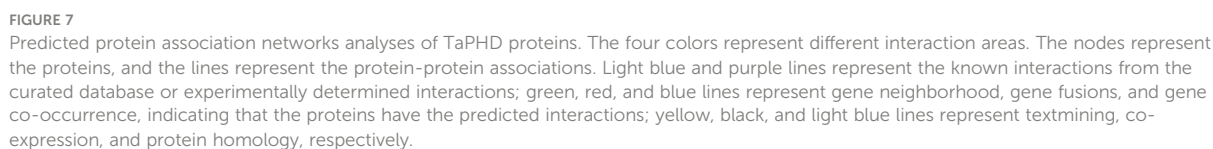
acclimation, and chromatin organization. Developmental growth and jasmonic acid-mediated systemic resistance were also particularly enriched. In the cellular component category, the most highly enriched categories were related to the nucleus, and 85% of the *TaPHDs* could participate in this process, whereas less than 10% of *TaPHDs* were involved in plasmodesma. Regarding molecular functions, the 65 most enriched *TaPHDs* were involved in histone binding, 28 *TaPHDs* were involved in chromatin binding, and 81 *TaPHDs* were related to protein binding.

To understand protein-protein interactions between *TaPHDs* and other proteins in wheat, we constructed a protein-protein interaction network (Figure 7 and Supplementary Table S6). A total of 89 *TaPHD* proteins and 548 interacting protein branches were identified. According to the strength of the interaction, we divided the 89 proteins into four interaction regions, which are represented by different colors, as shown in Figure 7. Some *TaPHDs*, such as *TaPHD15*, *TaPHD145*, and *TaPHD162*, could interact with up to 28 proteins, suggesting that these *TaPHD* proteins play a significant role in the regulation of protein networks. Notably, we found that these proteins had a PHD domain or a PHD-

SWIB-Plus3-GYF domain. Therefore, we believe that such domains are likely to play an important role in the PHD family.

## Expression analysis of *TaPHD* genes during growth and development

RNA-sequencing is a powerful tool for exploring certain gene transcription patterns using high-throughput sequencing methods (Wang et al., 2009). Systematic clustering analysis was performed based on the log2 of TPM values for 244 *TaPHD* genes (Figure 8A and Supplementary Table S7). The data showed that *TaPHD* gene expression showed great differences with the change in the growth period. In general, the expression of *TaPHDs* can be divided into three categories: the first group contains members that are widely expressed in many tissues under multiple developmental stage conditions; the second group contains those that are highly induced only at specific growth and development stages; and the last group includes members that do not appear to be expressed during growth and development. For example, *TaPHD100*, *TaPHD108*, and *TaPHD122* had high expression during most growth and



The lowest number of highly expressed genes (none) was found in the flag leaf blade at night in the flag leaf stage. Our results suggest that some *TaPHDs* may play important roles in many biological processes during wheat growth, especially during anthesis.

## Expression responses of *TaPHD* genes to abiotic/biotic stress

Frontiers in Plant Science



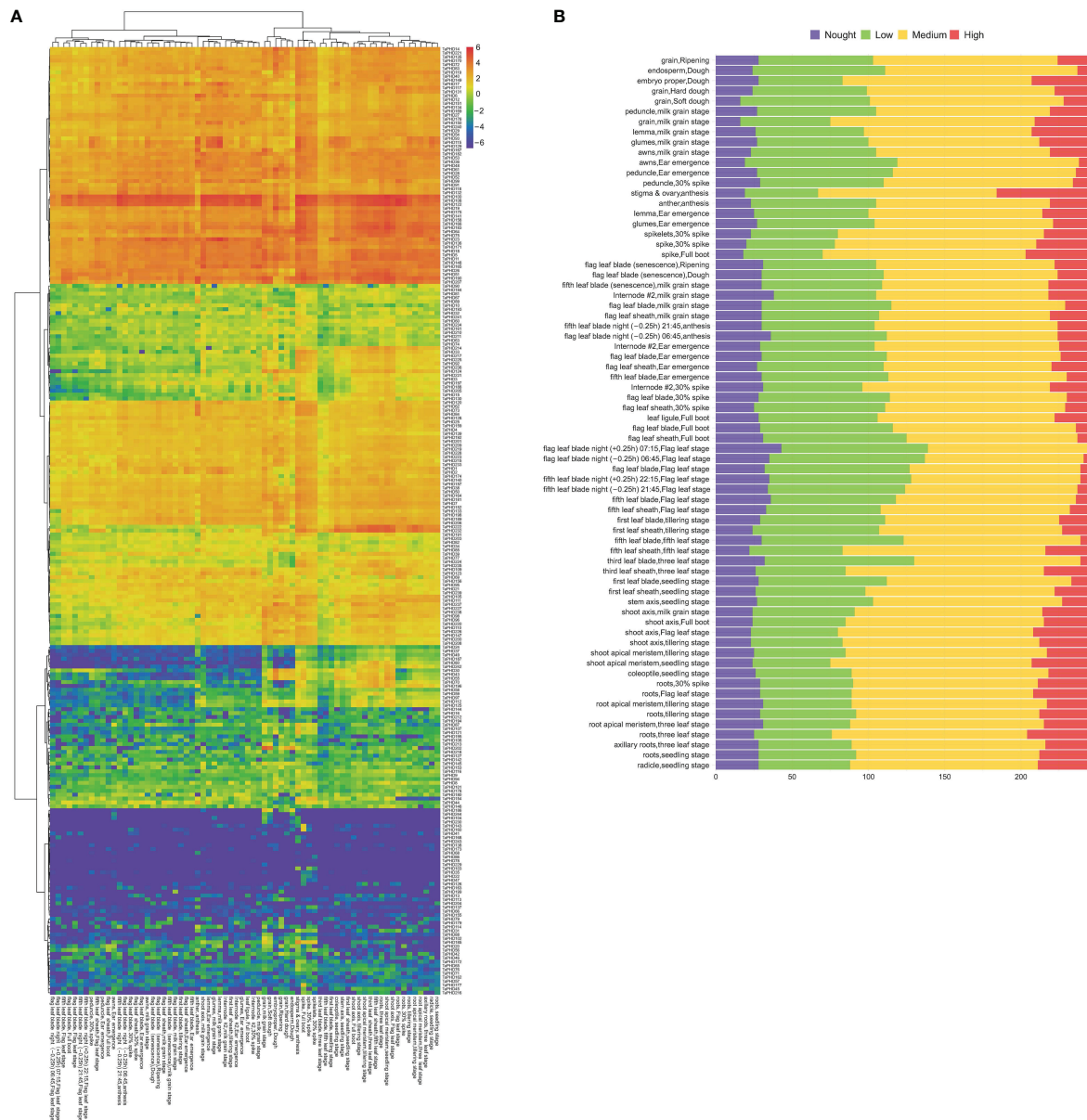


FIGURE 8

Transcriptome analyses of *TaPHDs* in different tissues. (A) Heat map of expression profiles for 244 *TaPHD* genes in different tissues. Red color indicates high expression levels; blue color indicates low expression levels. The gradual change of the color indicates different levels of gene log<sub>2</sub>-transformed expression. (B) Numbers of expressed genes in different tissues. High: TPM values >10, medium: 10 ≥ TPM values > 1, low: 1 ≥ TPM values > 0, none: TPM values = 0.

**S8.** During biological stress, we found that inoculation with *Fusarium*, powdery mildew, pathogen associated molecular patterns (PAMP), crown rot, *Septoria*, or stripe rust caused few changes in the expression of *TaPHD* genes. This suggests that *TaPHD* family members may not be associated with disease resistance.

Under abiotic stress, there are many *TaPHD* genes whose expression changes are more obvious under high-temperature,

drought, and cold conditions (Figures 9G–K and Supplementary Table S8). For example, after high-temperature treatment, the expression levels of many *TaPHD* genes (*TaPHD26*, *TaPHD75*, *TaPHD100*, *TaPHD115*, *TaPHD117*, and *TaPHD167*) were significantly altered compared to those in the experimental control group. In the drought starvation treatment, *TaPHD11*, *TaPHD19*, *TaPHD99*, *TaPHD141*, *TaPHD153*, and *TaPHD171* expression levels changed significantly. However, in the



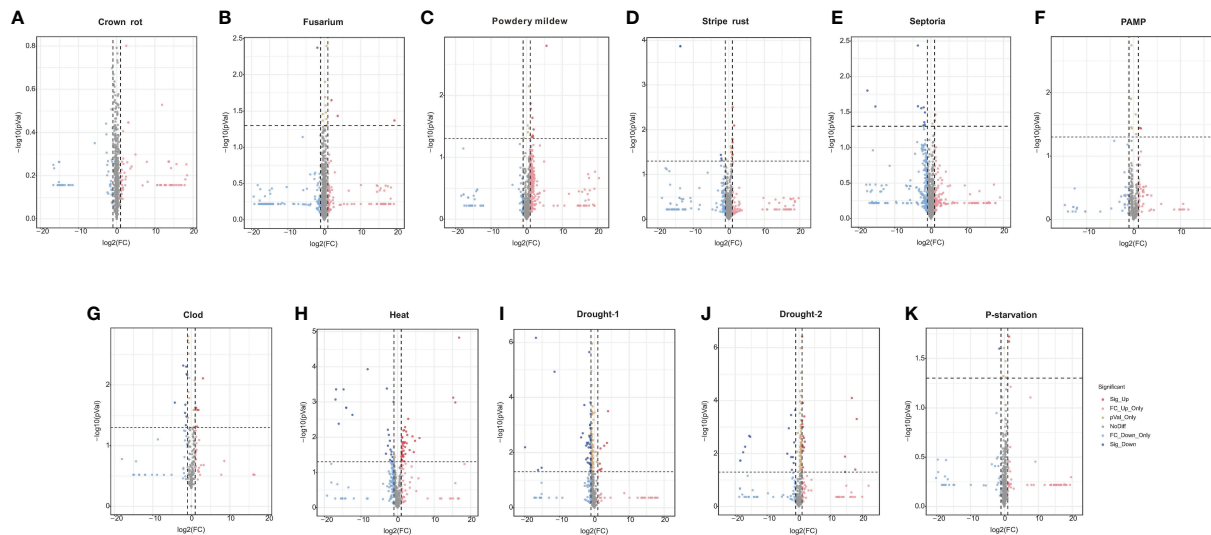


FIGURE 9

Expression of *TaPHDs* during different biological stress. Volcano map of expression profiles for 244 *TaPHD* genes under different biological/abiotic stresses, including (A) crown rot infection, (B) *Fusarium* infection, (C) powdery mildew infection, (D) stripe rust infection, (E) *Septoria tritici* infection and *Zymoseptoria tritici* infection, (F) PAMP (chitin and flg22 infection), (G) cold stress, (H) drought-1 (drought stress in Giza 168), (I) drought-2 (drought stress in Gemmiza 10), (J) heat stress, and (K) P-starvation. DEGs were defined as Fold Change > 1 and FDR < 0.05.

phosphorus starvation treatment, there were few changes in the expression of *TaPHD* genes. To further understand whether there is an intersection between the differential genes of the *PHD* family under drought, high-temperature, and low-temperature treatments, we drew a Venn diagram of DEGs in *TaPHD* genes during the four different transcriptomes (Figure 10, Supplementary Table S9). The data showed that *TaPHD215* and *TaPHD223* were significantly altered in every treatment. *TaPHD30*, *TaPHD96*, *TaPHD180*, *TaPHD174*, and *TaPHD239* gene expression varied greatly between the two drought and heat treatments. In addition, in cold and heat stress environments,

the expression levels of five genes (*TaPHD109*, *TaPHD118*, *TaPHD120*, *TaPHD167*, and *TaPHD178*) were significantly changed.

### qRT-PCR confirmed the response capability of *TaPHD* genes to abiotic stress conditions

To elucidate the possible regulatory mechanisms of *TaPHD* genes under cold, drought, and heat conditions, we performed

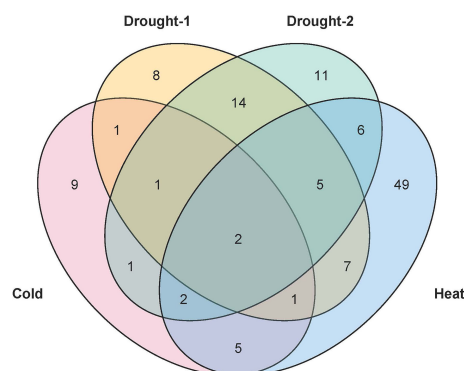


FIGURE 10

Venn diagram of DEGs in *TaPHD* genes during different abiotic stress. DEGs of *TaPHD* genes in different abiotic stress conditions, including cold stress, drought-1 (drought stress in Giza), drought-2 (drought stress in Gemmiza), and heat stress.

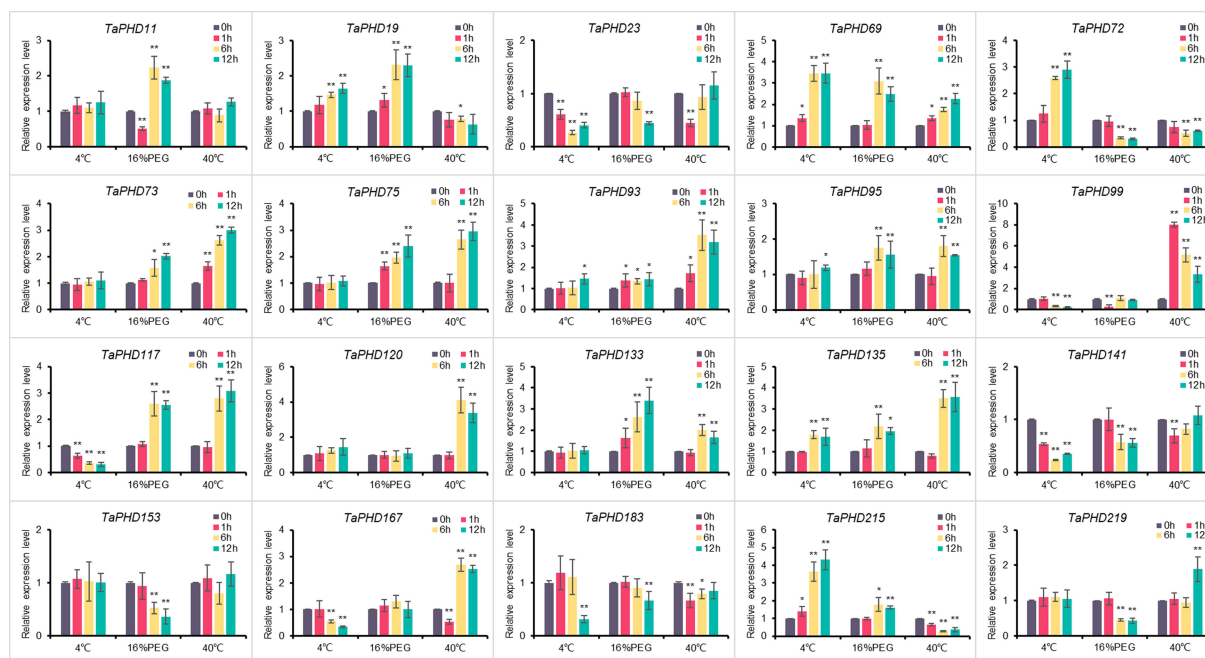


FIGURE 11

Relative expression levels of 20 genes under three different treatments. Expression of *TaPHD* genes in wheat were detected after 4°C, 16% PEG, and 40°C treatments for 0, 1, 6, and 12 h. Significant differences were determined by one-way ANOVA test: \*  $p < 0.05$ ; \*\*  $p < 0.01$ .

qRT-PCR analysis of 20 genes (Figure 11). The results showed that all 20 *TaPHDs* responded to different stress conditions and had different manifestations. Under low temperature stress induced by 4°C, the expression of five *TaPHDs* was significantly upregulated at different time points, and the expression of six *TaPHDs* was significantly downregulated at different time points compared with the control. In contrast, under 40°C-induced high-temperature stress, the expression of 12 *TaPHDs* was significantly upregulated at different time points compared with the control. The expression of five *TaPHDs* was inhibited at different time points. This indicated that compared with low temperature stress, high temperature stress could induce more changes in the expression of *TaPHDs* and could upregulate the expression more. In wheat under 16% PEG stress, the expression of ten *TaPHDs* was significantly upregulated at different time points. The expression of seven *TaPHDs* was inhibited at different time points. Among them, *TaPHD72* was most significantly inhibited, and it was downregulated four-fold at 6 and 12 h after treatment. The expression levels of *TaPHD69* and *TaPHD135* significantly increased after the three treatments. However, the expression levels of *TaPHD23* and *TaPHD141* significantly decreased after the three treatments. In addition, *TaPHD99* was strongly upregulated or downregulated by high temperature, low temperature, and PEG, and we speculated that this might be a key regulator of abiotic induction. In conclusion, we verified the effect of *PHD-finger* gene expression on the effect

of three abiotic stresses in wheat using qRT-PCR. These results indicate that *PHD-finger* genes play an important role in coping with abiotic stress in wheat.

## Subcellular localization of *TaPHD11*, *TaPHD19*, and *TaPHD133*

Previous studies have shown that most PHD finger proteins are localized in the nucleus, and only a few are localized in the membranes or other organelles (Gozani et al., 2003; Wu et al., 2016; Sun et al., 2017). For example, ZmPHD14 and ZmPHD19 are localized to the nucleus (Wang et al., 2015a). Also, GmPHD1 to GmPHD6 target the nucleus, and their nuclear localization requires the PHD domain (Wei et al., 2009). To better understand the functions of *TaPHDs*, we used Plant-mPloc and BUSCA to predict their subcellular localization. The results showed that more than 90% of the *TaPHD* proteins were localized in the nucleus (Table S1). In *Arabidopsis thaliana*, the *PHD* genes *AL5* and *AL6* play a very important role in improving the resistance of plants to abiotic stress. Therefore, we selected *TaPHD11* and *TaPHD19*, which are highly homologous to *AtALs*, for subcellular localization of wheat protoplasts. As shown in Figure 12, this suggests that, in wheat, the proteins *TaPHD11* and *TaPHD19* not only function in the nucleus but also in the membrane. In addition, research has shown that PHD

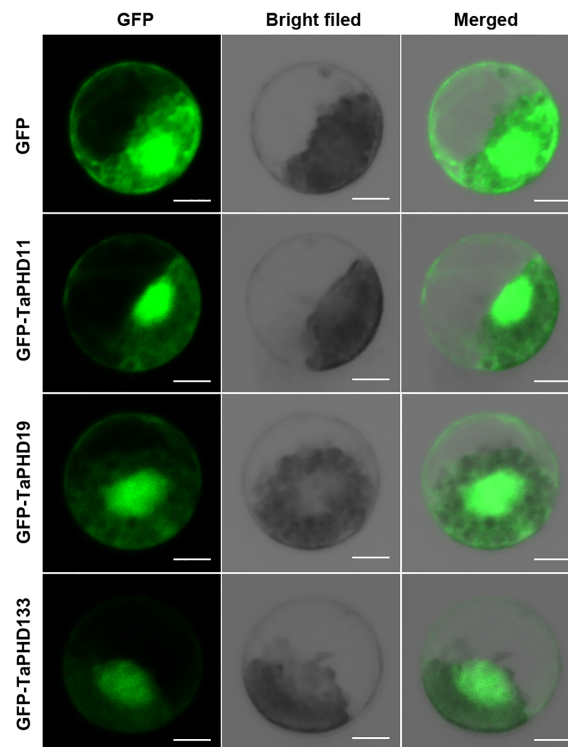


FIGURE 12

Subcellular location of *TaPHD11*, *TaPHD19*, and *TaPHD133*. Localization of *TaPHD* proteins under normal conditions. Images were observed under a confocal laser scanning microscope (LSM 700, Zeiss). Scale bars = 10  $\mu$ m.

finger ING2 is a phosphoinositide binding module and a nuclear PtdInsP receptor and suggests that PHD-phosphoinositide interactions directly regulate nuclear responses to DNA damage (Gozani et al., 2003). However, we studied the protein *TaPHD133*, which is highly homologous to ING1, and found that it is localized not only in the nucleus but also in the membrane. In summary, the subcellular localization of PHD proteins in wheat differs from that in other species.

## Discussion

As an important transcription factor in organisms, the *PHD* gene family not only plays a key role in regulating plant growth and development but also an important regulatory role when plants face biotic and abiotic stresses (Mouriz et al., 2015). In this study, we identified 244 *TaPHD* gene members in the wheat genome for the first time (Supplementary Table S3), which we divided into four large evolutionary branches. In terms of the number of genes, compared with the 59 and 67 *PHD* members in the diploid gramineous crops rice and maize, the *PHD* gene in wheat has a more exaggerated expansion and evolution. This is not only because the origin of wheat involves two polyploidy events, resulting in the existing allohexaploid bread wheat, but also

because segmental duplication contributes to the amplification of *TaPHD* genes. Gene duplication events are important for the rapid expansion and evolution of plant gene families (Cannon et al., 2004). Approximately 70%–80% of angiosperms experience duplication events (Blanc et al., 2003; Bowers et al., 2003), and in common wheat (*Triticum aestivum* L.), more than 85% of the sequences are duplicates (Walkowiak et al., 2020). Our research revealed the presence of several segmental duplication events during the evolution of *TaPHD* genes (Figures 4, 5). The proportion of *TaPHDs* with a 1:1:1 ratio of the three subgenomes A:B:D accounted for 84.8% of the total proportion (Table 2), which was much higher than the 35.8% observed for the whole wheat genome, indicating that the *PHD* gene family is highly conserved in the three subgenomes. When the *PHD* genes with different chaperone structural domains were subdivided (Table 1), the fold divergences were also different; for example, ING1, ING2, ROS1, EBS, and PKL were expanded 3-fold, while SHL1 was expanded 6-fold, and VIN3 and SIZ1 were expanded 9-fold and 11-fold, respectively. It is likely that the presence of many redundant genes has contributed to the stability of the genome of the hexaploid wheat species (Consortium et al., 2018). In terms of the covariance and evolutionary relationship of wheat *PHD* genes among species (Figure 5), the *PHD-finger* family diverged between monocotyledonous and dicotyledonous species, with the

average divergence time from the monocotyledonous species in the order of barley (12.78 Mya) < rice (22.09 Mya) < maize (60.87 Mya), indicating a more similar genetic structure to barley in terms of *PHD* genes.

Genes perform their functions through transcription and translation, and the expression patterns of genes reflect their function. *PHD* genes can regulate the growth and development of plants. Therefore, their expression in different plant tissues has also attracted much attention. Studies have shown that the expression patterns of the *PHD* gene family in different species are concentrated in different tissue types (Sun et al., 2017; Qin et al., 2019; Wu et al., 2021). Most of them have a high level of expression in reproductive organs, including rice (Sun et al., 2017) and potato (Qin et al., 2019). However, in cotton, *GhPHDs* genes have the highest expression levels in ovule and fiber tissues (Wu et al., 2021). This study showed that the *TaPHD* expression in various tissues of wheat showed great differences with the growth period. In particular, *TaPHD* expression was highest in the stigma and ovary at the flowering stage. A large number of *PHD* proteins regulate plant reproductive and developmental processes, which indicates that *TaPHDs* may play the same role in rice and potato. It also has a similar expression pattern in *Arabidopsis thaliana*, the model plant with the most in-depth research. Some genes have been identified as having key functions. For example, MMD1, MS1, VIM1, and SHL1 in *Arabidopsis* have been shown to play key roles in the reproductive growth stage (Yang et al., 2003; Woo et al., 2007; Fernández Gómez and Wilson, 2014). Moreover, *TaPHD100*, *TaPHD108*, and *TaPHD122*, which were highly orthologous to *AtAL6* and *AtAL7* are highly expressed during the whole growth period. In *Arabidopsis*, *AtAL6* and *AtAL7* are methylated by histones via the *PHD* domain, and the modification sites H3K4me3 and H3K4me2 bind to regulate the expression of target genes. Alfin-*PHD* domain proteins bind to di- or trimethylated histone H3 (H3K4me3/2) and affect plant growth and development in *Arabidopsis* (Winicov, 2000). It can be seen that these three genes may play an important role in the growth and development of wheat via methylated histones. Furthermore, we can also speculate the function of the *PHD* gene in wheat through the expression mode of a more highly homologous *PHD* gene. PWWP-*PHD*-SET domain proteins have histone methyltransferase activities and regulate the development of roots, leaves, and floral organs, as well as the transcription of some stress genes (Saleh et al., 2008). Therefore, *TaPHD100*, *TaPHD108*, and *TaPHD122*, which have high coincidence with the PWWP-*PHD*-SET domain, may play important roles in regulating the growth and development of wheat histone methylation (Lee et al., 2009). In addition, *TaPHD222* and *TaPHD232* are only highly expressed in shoots and roots; these two genes are highly orthologous to *ORC1A/B*. In contrast, in *Arabidopsis*, the *ORC1A/B* protein binds methyl groups through the *PHD* domain and functions as a transcriptional activator (De La Paz Sanchez and Gutierrez,

2009). Therefore, we infer that *TaPHD222* and *TaPHD232* are essential for root and shoot development. However, their function during development requires further verification.

The *PHD* family not only regulates plant growth and development but also responds to abiotic stresses. Existing research shows that the *PHD* genes *AL5* and *AL6* in *Arabidopsis* bind to the promoter regions of downstream target genes, thereby inhibiting various signaling pathways to improve the resistance of plants to abiotic stresses such as low temperature, drought, and high salt (Gozani et al., 2003; Wei et al., 2015). Notably, in this study, *TaPHD11* and *TaPHD19*, which are highly homologous to *ALs*, were upregulated only under induction by PEG treatment. Through qRT-PCR analysis, we also found that *TaPHD11* and *TaPHD19*, which are highly homologous to *AtALs*, were significantly upregulated only under drought treatment. This finding is different from the results of the previous study in *Arabidopsis*, indicating that *ALs* seem to have different responses to abiotic stress in monocotyledonous and dicotyledonous plants. Meanwhile, subcellular localization experiments also showed that *TaPHD11* and *TaPHD19* were localized in the nucleus and cell membrane, indicating that they function not only in the nucleus but also in the cell membrane of wheat. This suggests that there are differences in the responses of *PHD* genes to abiotic stresses among species.

This does not mean that the *PHD* gene expression pattern of monocotyledons and dicotyledons is completely different. *TaPHD69*, which is highly homologous to *AtSIZ1*, can be significantly upregulated under low-temperature, drought, and high-temperature conditions. *AtSIZ1* accumulates high levels of SUMOylated proteins through an ABA-independent pathway in response to abiotic stresses such as drought, low temperature, and heat shock (Catala et al., 2007). The accumulation of *TaPHD69* seems to be beneficial for plants to cope with abiotic stress, which is similar to the function of *AtSIZ1* in *Arabidopsis*. In rice, the cis-acting elements DRE/CRT in the *OsPHD13* and *OsPHD52* promoters are upregulated by as much as 15-fold under low-temperature stress. Overexpression of *OsPHD1* can significantly improve plant resistance to stress (drought, high salt, and low temperature) (Liu et al., 2011; Ahmar and Gruszka, 2022). In maize, the expression of subfamily IX *TaPHDs* responds to salt, drought, and ABA stress (Wang et al., 2015a). Among *TaPHDs*, 45 *TaPHDs* genes were significantly changed under two or three treatments, indicating that *TaPHDs* play an active role in plant responses to low-temperature, drought, or high-temperature stress. *TaPHD117* was significantly upregulated under high-temperature and drought treatments and significantly downregulated under low-temperature treatment and had distinct expression patterns in response to different treatments. Therefore, whether *TaPHDs* act as key genes in the roots to cope with abiotic stress requires further verification, but our results suggest that *TaPHDs* have potential functions in plant responses to abiotic stress.

## Data availability statement

The datasets presented in this study can be found in online repositories. The names of the repository/repositories and accession number(s) can be found in the article/[Supplementary Material](#).

## Author contributions

FP, ZL, and ZW designed the study. FP and MS conducted the experiments. JN and SN analyzed the data. FP, JN, ZL, and ZW wrote the manuscript. ZL and ZW revised and finalized the manuscript. All authors contributed to the article and approved the submitted version.

## Funding

The present study was supported by the Scientific Startup Foundation for Doctors of Yulin Normal University (CN) (Grant No. G2020ZK13).

## References

- Asland, R., Gibson, T. J., and Stewart, A. F. (1995). The PHD finger: implications for chromatin-mediated transcriptional regulation. *Trends Biochem. Sci.* 20, 56–59. doi: 10.1016/S0968-0004(00)88957-4
- Ahmar, S., and Gruszka, D. (2022). In-silico study of brassinosteroid signaling genes in rice provides insight into mechanisms which regulate their expression. *Front. Genet.* 13, 953458. doi: 10.3389/fgene.2022.953458
- Artimo, P., Jonnalagedda, M., Arnold, K., Baratin, D., Csardi, G., De Castro, E., et al. (2012). ExPASy: SIB bioinformatics resource portal. *Nucleic Acids Res.* 40, W597–W603. doi: 10.1093/nar/gks400
- Blanc, G., Hokamp, K., and Wolfe, K. H. (2003). A recent polyploidy superimposed on older large-scale duplications in the *Arabidopsis* genome. *Genome Res.* 13, 137–144. doi: 10.1101/gr.751803
- Borden, K. L., and Freemont, P. S. (1996). The RING finger domain: a recent example of a sequence-structure family. *Curr. Opin. Struct. Biol.* 6, 395–401. doi: 10.1016/S0959-440X(96)80060-1
- Borrill, P., Ramirez-Gonzalez, R., and Uauy, C. (2016). expVIP: a customizable RNA-seq data analysis and visualization platform. *Plant Physiol.* 170, 2172–2186. doi: 10.1104/pp.15.01667
- Bowers, J. E., Chapman, B. A., Rong, J., and Paterson, A. H. (2003). Unravelling angiosperm genome evolution by phylogenetic analysis of chromosomal duplication events. *Nature* 422, 433–438. doi: 10.1038/nature01521
- Cannon, S. B., Mitra, A., Baumgarten, A., Young, N. D., and May, G. (2004). The roles of segmental and tandem gene duplication in the evolution of large gene families in *Arabidopsis thaliana*. *BMC Plant Biol.* 4, 10. doi: 10.1186/1471-2229-4-10
- Catala, R., Ouyang, J., Abreu, I. A., Hu, Y., Seo, H., Zhang, X., et al. (2007). The *Arabidopsis* E3 SUMO ligase SIZ1 regulates plant growth and drought responses. *Plant Cell* 19, 2952–2966. doi: 10.1105/tpc.106.049981
- Chen, C., Chen, H., Zhang, Y., Thomas, H. R., Frank, M. H., He, Y., et al. (2020). TBtools: an integrative toolkit developed for interactive analyses of big biological data. *Mol. Plant* 13, 1194–1202. doi: 10.1016/j.molp.2020.06.009
- Chou, K.-C., and Shen, H.-B. (2010). Plant-mPLOC: a top-down strategy to augment the power for predicting plant protein subcellular localization. *PloS One* 5, e11335. doi: 10.1371/journal.pone.0011335
- Consortium, I. W. G. S., Appels, R., Eversole, K., Stein, N., Feuillet, C., Keller, B., et al. (2018). Shifting the limits in wheat research and breeding using a fully annotated reference genome. *Science* 361, eaar7191. doi: 10.1126/science.aar7191
- Cui, X.-Y., Gao, Y., Guo, J., Yu, T.-F., Zheng, W.-J., Liu, Y.-W., et al. (2019). BES/BZR transcription factor TaBZR2 positively regulates drought responses by activation of TaGST1. *Plant Physiol.* 180, 605–620. doi: 10.1104/pp.19.00100
- De La Paz Sanchez, M., and Gutierrez, C. (2009). *Arabidopsis* ORC1 is a PHD-containing H3K4me3 effector that regulates transcription. *Proc. Natl. Acad. Sci.* 106, 2065–2070. doi: 10.1073/pnas.0811093106
- Fernández Gómez, J., and Wilson, Z. A. (2014). A barley PHD finger transcription factor that confers male sterility by affecting tapetal development. *Plant Biotechnol. J.* 12, 765–777. doi: 10.1111/pbi.12181
- Fujita, M., Fujita, Y., Noutoshi, Y., Takahashi, F., Narusaka, Y., Yamaguchi-Shinozaki, K., et al. (2006). Crosstalk between abiotic and biotic stress responses: a current view from the points of convergence in the stress signaling networks. *Curr. Opin. Plant Biol.* 9, 436–442. doi: 10.1016/j.pbi.2006.05.014
- Gao, Y., Liu, H., Wang, Y., Li, F., and Xiang, Y. (2018). Genome-wide identification of PHD-finger genes and expression pattern analysis under various treatments in moso bamboo (*Phyllostachys edulis*). *Plant Physiol. Biochem.* 123, 378–391. doi: 10.1016/j.plaphy.2017.12.034
- Gibbons, R. J., Bachoo, S., Picketts, D. J., Aftimos, S., Asenbauer, B., Bergoffen, J., et al. (1997). Mutations in transcriptional regulator ATRX establish the functional significance of a PHD-like domain. *Nat. Genet.* 17, 146–148. doi: 10.1038/ng1097-146
- Gozani, O., Karuman, P., Jones, D. R., Ivanov, D., Cha, J., Lugovskoy, A. A., et al. (2003). The PHD finger of the chromatin-associated protein ING2 functions as a nuclear phosphoinositide receptor. *Cell* 114, 99–111. doi: 10.1016/S0092-8674(03)00480-X
- He, Z., Xia, X., Chen, X., and Zhuang, Q. (2011). Progress of wheat breeding in China and the future perspective. *Acta Agronom. Sin.* 37, 202–215. doi: 10.3724/SP.J.1006.2011.00202
- Hu, L., Li, Z., Wang, P., Lin, Y., and Xu, Y. (2011). Crystal structure of PHD domain of UHRF1 and insights into recognition of unmodified histone H3 arginine residue 2. *Cell Res.* 21, 1374–1378. doi: 10.1038/cr.2011.124

## Conflict of interest

The authors declare that the research was conducted in the absence of any commercial or financial relationships that could be construed as a potential conflict of interest.

## Publisher's note

All claims expressed in this article are solely those of the authors and do not necessarily represent those of their affiliated organizations, or those of the publisher, the editors and the reviewers. Any product that may be evaluated in this article, or claim that may be made by its manufacturer, is not guaranteed or endorsed by the publisher.

## Supplementary material

The Supplementary Material for this article can be found online at: <https://www.frontiersin.org/articles/10.3389/fpls.2022.1016831/full#supplementary-material>



- Kehle, J., Beuchle, D., Treuheit, S., Christen, B., Kennison, J. A., Bienz, M., et al. (1998). dMi-2, a hunchback-interacting protein that functions in *Polycomb* repression. *Science* 282, 1897–1900. doi: 10.1126/science.282.5395.1897
- Kumar, S., Stecher, G., Li, M., Knyaz, C., and Tamura, K. (2018). MEGA X: molecular evolutionary genetics analysis across computing platforms. *Mol. Biol. Evol.* 35, 1547–1549. doi: 10.1093/molbev/msy096
- Kwan, A. H., Gell, D. A., Verger, A., Crossley, M., Matthews, J. M., and Mackay, J. P. (2003). Engineering a protein scaffold from a PHD finger. *Structure* 11, 803–813. doi: 10.1016/S0969-2126(03)00122-9
- Lee, W. Y., Lee, D., Chung, W. I., and Kwon, C. S. (2009). Arabidopsis ING and Alfin1-like protein families localize to the nucleus and bind to H3K4me3/2 via plant homeodomain fingers. *Plant J.* 58, 511–524. doi: 10.1111/j.1365-3113X.2009.03795.x
- Li, H., Ilin, S., Wang, W., Duncan, E. M., Wysocka, J., Allis, C. D., et al. (2006). Molecular basis for site-specific read-out of histone H3K4me3 by the BPTF PHD finger of NURF. *Nature* 442, 91–95. doi: 10.1038/nature04802
- Li, C., Ng, C. K.-Y., and Fan, L.-M. (2015). MYB transcription factors, active players in abiotic stress signaling. *Environ. Exp. Bot.* 114, 80–91. doi: 10.1016/j.envexpbot.2014.06.014
- Liu, Y., Liu, C., Li, Z., Xia, M., Jiang, H., Cheng, B., et al. (2011). Overexpression of a plant homeodomain (PHD)-finger transcription factor, *OsPHD1*, can enhance stress tolerance in rice. *J. Agric. Biotechnol.* 19, 462–469. doi: 10.3969/j.issn.1674-7968.2011.03.009
- Livak, K. J., and Schmittgen, T. D. (2001). Analysis of relative gene expression data using real-time quantitative PCR and the  $2^{-\Delta\Delta CT}$  method. *Methods* 25, 402–408. doi: 10.1006/meth.2001.1262
- Marchler-Bauer, A., Bo, Y., Han, L., He, J., Lanczycki, C. J., Lu, S., et al. (2017). CDD/SPARCLE: functional classification of proteins via subfamily domain architectures. *Nucleic Acids Res.* 45, D200–D203. doi: 10.1093/nar/gkw1129
- Martin, D. G., Baetz, K., Shi, X., Walter, K. L., Macdonald, V. E., Wlodarski, M. J., et al. (2006). The Yng1p plant homeodomain finger is a methyl-histone binding module that recognizes lysine 4-methylated histone H3. *Mol. Cell. Biol.* 26, 7871–7879. doi: 10.1128/MCB.00573-06
- Mizoi, J., Shinozaki, K., and Yamaguchi-Shinozaki, K. (2012). AP2/ERF family transcription factors in plant abiotic stress responses. *Biochim. Biophys. Acta (BBA)-Gene Regul. Mech.* 1819, 86–96. doi: 10.1016/j.bbagr.2011.08.004
- Molitor, A. M., Bu, Z., Yu, Y., and Shen, W.-H. (2014). Arabidopsis AL PHD-PRC1 complexes promote seed germination through H3K4me3-to-H3K27me3 chromatin state switch in repression of seed developmental genes. *PLoS Genet.* 10, e1004091. doi: 10.1371/journal.pgen.1004091
- Mouriz, A., López-González, L., Jarillo, J. A., and Piñeiro, M. (2015). PHDs govern plant development. *Plant Signaling Behav.* 10, e993253. doi: 10.4161/15592324.2014.993253
- Ogryzko, V. V., Schiltz, R. L., Russanova, V., Howard, B. H., and Nakatani, Y. (1996). The transcriptional coactivators p300 and CBP are histone acetyltransferases. *Cell* 87, 953–959. doi: 10.1016/S0092-8674(00)82001-2
- Papoulas, O., Beek, S. J., Moseley, S. L., McCallum, C. M., Sarte, M., Shearn, A., et al. (1998). The drosophila trithorax group proteins BRM, ASH1 and ASH2 are subunits of distinct protein complexes. *Development* 125, 3955–3966. doi: 10.1242/dev.125.20.3955
- Qin, M., Luo, W., Zheng, Y., Guan, H., and Xie, X. (2019). Genome-wide identification and expression analysis of the PHD-finger gene family in *Solanum tuberosum*. *PLoS One* 14, e0226964. doi: 10.1371/journal.pone.0226964
- Ramírez-González, R., Borrill, P., Lang, D., Harrington, S., Brinton, J., Venturini, L., et al. (2018). The transcriptional landscape of polyploid wheat. *Science* 361, eaar6089. doi: 10.1126/science.aar6089
- Rushton, P. J., Somssich, I. E., Ringler, P., and Shen, Q. J. (2010). WRKY transcription factors. *Trends Plant Sci.* 15, 247–258. doi: 10.1016/j.tplants.2010.02.006
- Saitou, N., and Nei, M. (1987). The neighbor-joining method: a new method for reconstructing phylogenetic trees. *Mol. Biol. Evol.* 4, 406–425. doi: 10.1093/oxfordjournals.molbev.a040454
- Saleh, A., Alvarez-Venegas, R., Yilmaz, M., Le, O., Hou, G., Sadder, M., et al. (2008). The highly similar Arabidopsis homologs of trithorax ATX1 and ATX2 encode proteins with divergent biochemical functions. *Plant Cell* 20, 568–579. doi: 10.1105/tpc.107.056614
- Savojardo, C., Martelli, P. L., Fariselli, P., Profitti, G., and Casadio, R. (2018). BUSCA: an integrative web server to predict subcellular localization of proteins. *Nucleic Acids Res.* 46, W459–W466. doi: 10.1093/nar/gky320
- Schindler, U., Beckmann, H., and Cashmore, A. R. (1993). HAT3. 1, a novel Arabidopsis homeodomain protein containing a conserved cysteine-rich region. *Plant J.* 4, 137–150. doi: 10.1046/j.1365-3113X.1993.04010137.x
- Song, S., Hao, L., Zhao, P., Xu, Y., Zhong, N., Zhang, H., et al. (2019). Genome-wide identification, expression profiling and evolutionary analysis of auxin response factor gene family in potato (*Solanum tuberosum* group phureja). *Sci. Rep.* 9, 1755. doi: 10.1038/s41598-018-37923-7
- Sung, S., and Amasino, R. M. (2004). Vernalization in *Arabidopsis thaliana* is mediated by the PHD finger protein VIN3. *Nature* 427, 159–164. doi: 10.1038/nature02195
- Sun, M., Jia, B., Yang, J., Cui, N., Zhu, Y., and Sun, X. (2017). Genome-wide identification of the PHD-finger family genes and their responses to environmental stresses in *Oryza sativa* L. *Int. J. Mol. Sci.* 18, 2005. doi: 10.3390/ijms18092005
- Sun, X., Wang, Y., and Sui, N. (2018). Transcriptional regulation of bHLH during plant response to stress. *Biochem. Biophys. Res. Commun.* 503, 397–401. doi: 10.1016/j.bbrc.2018.07.123
- Walkowiak, S., Gao, L., Monat, C., Haberer, G., Kassa, M. T., Brinton, J., et al. (2020). Multiple wheat genomes reveal global variation in modern breeding. *Nature* 588, 277–283. doi: 10.1038/s41586-020-2961-x
- Wang, Z., Gerstein, M., and Snyder, M. (2009). RNA-Seq: a revolutionary tool for transcriptomics. *Nat. Rev. Genet.* 10, 57–63. doi: 10.1038/nrg2484
- Wang, Q., Liu, J., Wang, Y., Zhao, Y., Jiang, H., and Cheng, B. (2015a). Systematic analysis of the maize PHD-finger gene family reveals a subfamily involved in abiotic stress response. *Int. J. Mol. Sci.* 16, 23517–23544. doi: 10.3390/ijms161023517
- Wang, Y., Tang, H., Debarry, J. D., Tan, X., Li, J., Wang, X., et al. (2012). MCS-ScanX: a toolkit for detection and evolutionary analysis of gene synteny and collinearity. *Nucleic Acids Res.* 40, e49. doi: 10.1093/nar/gkr1293
- Wang, Y., Wang, Q., Zhao, Y., Han, G., and Zhu, S. (2015b). Systematic analysis of maize class III peroxidase gene family reveals a conserved subfamily involved in abiotic stress response. *Gene* 566, 95–108. doi: 10.1016/j.gene.2015.04.041
- Wei, W., Huang, J., Hao, Y.-J., Zou, H.-F., Wang, H.-W., Zhao, J.-Y., et al. (2009). Soybean GmPHD-type transcription regulators improve stress tolerance in transgenic Arabidopsis plants. *PLoS One* 4, e7209. doi: 10.1371/journal.pone.0007209
- Wei, W., Zhang, Y. Q., Tao, J. J., Chen, H. W., Li, Q. T., Zhang, W. K., et al. (2015). The alfin-like homeodomain finger protein AL5 suppresses multiple negative factors to confer abiotic stress tolerance in Arabidopsis. *Plant J.* 81, 871–883. doi: 10.1111/tpj.12773
- Winicov, I. (2000). Alfin1 transcription factor overexpression enhances plant root growth under normal and saline conditions and improves salt tolerance in alfalfa. *Plant J.* 210, 416–422. doi: 10.1007/PL00008150
- Woo, H. R., Pontes, O., Pikaard, C. S., and Richards, E. J. (2007). VIM1, a methylcytosine-binding protein required for centromeric heterochromatinization. *Genes Dev.* 21, 267–277. doi: 10.1101/gad.1512007
- Wu, S., Wu, M., Dong, Q., Jiang, H., Cai, R., and Xiang, Y. (2016). Genome-wide identification, classification and expression analysis of the PHD-finger protein family in *Populus trichocarpa*. *Gene* 575, 75–89. doi: 10.1016/j.gene.2015.08.042
- Wu, H., Zheng, L., Qian, G., Guo, M., Wang, Z., and Yang, Z. (2021). Response of phytohormone mediated plant homeodomain (PHD) family to abiotic stress in upland cotton (*Gossypium hirsutum* spp.). *BMC Plant Biol.* 21, 13. doi: 10.1186/s12870-020-02787-5
- Xie, C., Mao, X., Huang, J., Ding, Y., Wu, J., Dong, S., et al. (2011). KOBAS 2.0: a web server for annotation and identification of enriched pathways and diseases. *Nucleic Acids Res.* 39, W316–W322. doi: 10.1093/nar/gkr483
- Xi, Q., Wang, Z., Zaromytidou, A.-I., Zhang, X. H.-F., Chow-Tsang, L.-F., Liu, J. X., et al. (2011). A poised chromatin platform for TGF- $\beta$  access to master regulators. *Cell* 147, 1511–1524. doi: 10.1016/j.cell.2011.11.032
- Yamasaki, K., Kigawa, T., Seki, M., Shinozaki, K., and Yokoyama, S. (2013). DNA-Binding domains of plant-specific transcription factors: structure, function, and evolution. *Trends Plant Sci.* 18, 267–276. doi: 10.1016/j.tplants.2012.09.001
- Yang, X., Makaroff, C. A., and Ma, H. (2003). The Arabidopsis MALE MEIOCYTE DEATH1 gene encodes a PHD-finger protein that is required for male meiosis. *Plant Cell* 15, 1281–1295. doi: 10.1105/tpc.010447
- Ye, J., Zhang, Y., Cui, H., Liu, J., Wu, Y., Cheng, Y., et al. (2018). WEGO 2.0: a web tool for analyzing and plotting GO annotation 2018 update. *Nucleic Acids Res.* 46, W71–W75. doi: 10.1093/nar/gky400
- Yu, Y., Ouyang, Y., and Yao, W. (2018). shinyCircos: an R/Shiny application for interactive creation of circos plot. *Bioinformatics* 34, 1229–1231. doi: 10.1093/bioinformatics/btx763
- Zhang, X., Li, M., Zhang, B., Yin, X., Wang, M., and Xia, X. (2016). Possibility study on improving salt tolerance of rice by overexpressing PHD-finger transcription factor gene *OsMsr16*. *Genomics Appl. Biol.* 35, 1820–1827. doi: 10.13417/j.gab.035.001820
- Zhang, Z., Li, J., Zhao, X.-Q., Wang, J., Wong, G. K.-S., and Yu, J. (2006). KaKs-Calculator: calculating ka and ks through model selection and model averaging. *Genom. Proteomics Bioinf.* 4, 259–263. doi: 10.1016/S1672-0229(07)60007-2
- Zhu, Y.-X., Gong, H.-J., and Yin, J.-L. (2019). Role of silicon in mediating salt tolerance in plants: a review. *Plants* 8, 147. doi: 10.3390/plants8060147



## OPEN ACCESS

## EDITED BY

Arpna Kumari,  
The University of Tokyo, Japan

## REVIEWED BY

Faisal Zulfiqar,  
The Islamia University of Bahawalpur,  
Pakistan  
Sayed Mohammad Mohsin,  
Sher-e-Bangla Agricultural University,  
Bangladesh  
Musa Seymen,  
Selçuk University, Turkey

## \*CORRESPONDENCE

Huanxiu Li  
huanxiuli62@163.com  
Yi Tang  
tangyi@sicau.edu.cn

<sup>†</sup>These authors have contributed  
equally to this work and share  
first authorship

## SPECIALTY SECTION

This article was submitted to  
Plant Abiotic Stress,  
a section of the journal  
Frontiers in Plant Science

RECEIVED 20 October 2022

ACCEPTED 25 November 2022

PUBLISHED 15 December 2022

## CITATION

Liang L, Tang W, Lian H, Sun B,  
Huang Z, Sun G, Li X, Tu L, Li H  
and Tang Y (2022) Grafting promoted  
antioxidant capacity and carbon and  
nitrogen metabolism of bitter gourd  
seedlings under heat stress.  
*Front. Plant Sci.* 13:1074889.  
doi: 10.3389/fpls.2022.1074889

## COPYRIGHT

© 2022 Liang, Tang, Lian, Sun, Huang,  
Sun, Li, Tu, Li and Tang. This is an open-  
access article distributed under the  
terms of the [Creative Commons  
Attribution License \(CC BY\)](#). The use,  
distribution or reproduction in other  
forums is permitted, provided the  
original author(s) and the copyright  
owner(s) are credited and that the  
original publication in this journal is  
cited, in accordance with accepted  
academic practice. No use,  
distribution or reproduction is  
permitted which does not comply with  
these terms.

# Grafting promoted antioxidant capacity and carbon and nitrogen metabolism of bitter gourd seedlings under heat stress

Le Liang<sup>1†</sup>, Wen Tang<sup>1†</sup>, Huashan Lian<sup>2†</sup>, Bo Sun<sup>1</sup>, Zhi Huang<sup>1</sup>,  
Guochao Sun<sup>1</sup>, Xiaomei Li<sup>1,3</sup>, Lihua Tu<sup>4</sup>, Huanxiu Li<sup>5\*</sup>  
and Yi Tang<sup>5\*</sup>

<sup>1</sup>College of Horticulture, Sichuan Agricultural University, Chengdu, Sichuan, China, <sup>2</sup>Horticulture Research Institute, Chengdu Agricultural College, Chengdu, Sichuan, China, <sup>3</sup>Vegetable Germplasm Innovation and Variety Improvement Key Laboratory of Sichuan, Sichuan Academy of Agricultural Sciences, Chengdu, Sichuan, China, <sup>4</sup>College of Forestry, Sichuan Agricultural University, Chengdu, Sichuan, China, <sup>5</sup>Institute of Pomology and Olericulture, Sichuan Agricultural University, Chengdu, Sichuan, China

**Introduction:** Heat stress can limit vegetable growth, and this can lead to constraints on agricultural production. Grafting technologies, however, can be used to alleviate various plant stresses.

**Methods:** In this study, the differences in the heat stress impacts and recovery abilities of pumpkin and luffa rootstocks for bitter gourd were analyzed in terms of their antioxidant activity and carbon and nitrogen metabolism.

**Results:** Compared with the un-grafted and self-grafted bitter gourd, which suffered from heat stress at 40°C for 24 h, heterologously grafted bitter gourd showed higher heat stability of the cell membrane (relative conductivity and malondialdehyde content were reduced), reduced oxidative stress (antioxidant enzyme activity was increased and the reactive oxygen species content reduced), and increased enzyme activity (sucrose phosphate synthase, sucrose synthase, neutral invertase, and acid invertase) and sugar content (soluble sugar, sucrose, fructose, and glucose) in carbon metabolism. The enzyme activity (nitrate reductase, nitrite reductase, and glutamine synthetase) and product content (nitrate and nitrite) of nitrogen metabolism were also found to be increased, and this inhibited the accumulation of ammonium ions. After the seedlings were placed at 25°C for 24 h, the heterogeneous rootstocks could rapidly restore the growth of the bitter gourd seedlings by promoting the antioxidant and carbon and nitrogen metabolism systems. When luffa was used as rootstock, its performance on the indexes was better than that of pumpkin. The correlation between the various indicators was demonstrated using a principal component and correlation analysis.

**Discussion:** The luffa rootstock was found to be more conducive to reducing cell damage and energy loss in bitter melon seedlings caused by heat induction through the maintenance of intracellular redox homeostasis and the promotion of carbon and nitrogen metabolism.

#### KEYWORDS

carbohydrate, correlation analysis, luffa, nitrogen, pumpkin, PCA

## 1 Introduction

To ensure that there is an annual supply of various vegetables, autumn-delayed cultivation of protected plots has been introduced in different regions. This stubble arrangement of vegetable cultivation has been found to satisfy consumer needs. However, high temperatures in the autumn can lead to stunted growth and even death for some vegetables, which seriously affects their economic benefits. In the process of high temperature, plant cells will produce oxygen free radicals and their derivatives, namely reactive oxygen species (ROS), and make the balance between ROS generation and antioxidant defense system imbalance, thus triggering the excessive accumulation of ROS and inducing oxidative stress in plants (Hasanuzzaman et al., 2020a). It is worth noting that both enzymatic and non-enzymatic antioxidant defense systems can maintain the balance between detoxification and production of ROS. Among them, the endogenous defense mechanisms composed of different enzymes include: superoxide dismutase, SOD; catalase, CAT; peroxidase, POD; ascorbic acid peroxidase, APX; enzyme in the glutathione ascorbic acid cycle, AsA-GSH. Non-enzymatic antioxidants include ascorbic acid, AsA; glutathione, GSH; flavonoids, carotenoids, etc (Hasanuzzaman et al., 2020b). Under heat stress, the solubility of CO<sub>2</sub> and O<sub>2</sub> in plant leaf cells decreases, which consequently means that the amount of CO<sub>2</sub> fixed by ribulose-1,5-diphosphate carboxylation/oxygenase decreases, while the oxidation reaction in photorespiration and the CO<sub>2</sub> diffusion resistance increases, and these conditions are not conducive to leaf photosynthesis (Ara et al., 2013). Under 35 °C heat stress, the cell membranes in the leaves of cucumber (*Cucumis sativus* L.) seedlings were damaged due to the excessive accumulation of soluble protein, proline (Pro), malondialdehyde (MDA), and superoxide anion (O<sub>2</sub><sup>•−</sup>) (Ding et al., 2016). This resulted in reduced cell membrane fluidity and damaged the DNA, proteins, and lipids of the plant (Giordano et al., 2021). This also stimulates the activity of antioxidant enzymes and the expression of related genes such as glutathione reductase, SOD, POD, and CAT (Ding et al., 2016).

Carbon and nitrogen metabolism are two irreplaceable processes in plant growth and development but are affected by heat stress. Carbohydrates play a positive role in plant growth,

photosynthesis, carbon partitioning, lipid metabolism, osmotic homeostasis, protein synthesis, and gene expression under heat stress (Rosa et al., 2009; Sami et al., 2016), as they can help maintain the stability of the cell membrane (Lemoine, 2013). Heat stress can cause soluble sugars, fructose, and sucrose to accumulate in plant leaves (Yuan et al., 2014; Shan et al., 2016). Carbohydrates play a key role in osmoregulation and protect cell membranes from dehydration (Ruan et al., 2010), and increasing the carbohydrate content and the activity of sucrose-degrading enzymes can alleviate the physiological damage to leaves under heat stress (Loka et al., 2020). Moreover, leaf carbohydrate content is largely dependent on sucrose metabolism. Heat stress (40 °C) increased the sucrose content in melons (*Cucumis melo* L. cv. Hale's Best Jumbo), and this may be due to the upregulated expression of the sucrose transporter (Gil et al., 2012). Nitrogen metabolism in plants is closely related to photosynthesis and respiration, and plants can absorb inorganic nitrogen (NO<sub>3</sub><sup>−</sup> and NH<sub>4</sub><sup>+</sup>) from the soil. After NO<sub>3</sub><sup>−</sup> enters the cell, it is reduced to NO<sub>2</sub><sup>−</sup> by nitrate reductase (NR) and NO<sub>2</sub><sup>−</sup> is reduced to NH<sub>4</sub><sup>+</sup> by nitrite reductase (NiR). NH<sub>4</sub><sup>+</sup> is then assimilated into amino acids and other organic matter through the glutamine-glutamate cycle pathway (Liang et al., 2021), which requires energy for metabolism. However, various environmental stressors can lead to insufficient energy metabolism in plants, which further affects their absorption of inorganic nitrogen. When subjected to heat stress, the activities of NR, glutamine synthase (GS), glutamate synthase (GOGAT), and glutamate dehydrogenase (GDH) in the leaves of heat-tolerant plants were found to be higher, but the total amino acid level in the leaves did not change (Yuan et al., 2017).

There are numerous ways to alleviate the damage caused by heat stress in plants. Grafting is a type of vegetative asexual reproduction, and it utilizes plant totipotency to a plant branch or bud cambium and another plant stem or root cambium so that the two parts grow into a complete plant. The ability of plants to resist abiotic stress can be improved by grafting, mainly due to the resistance of the rootstock. Heat-resistant rootstocks have been shown to have strong growth and high ROS scavenging activity under heat stress conditions, and the glutathione and ascorbic acid contents in the seedlings were

also found to be high (Zhang et al., 2007). When luffa was used as a rootstock, CO<sub>2</sub> assimilation and the related enzyme activities of cucumber grafted seedlings were promoted (Li et al., 2014a). Under heat stress (40 °C), the leaves of the cucumber seedlings and self-grafted seedlings accumulated more ROS when luffa was used as the rootstock, the increase in hydrogen peroxide (H<sub>2</sub>O<sub>2</sub>) and O<sub>2</sub><sup>•−</sup> in the grafted seedlings was alleviated, and the activities of the antioxidant enzymes were increased, which improved the heat tolerance of the cucumber seedlings (Li et al., 2016). Li et al. have obtained similar results (Li et al., 2014b). However, the effects of grafting on carbon and nitrogen metabolism in melon vegetables have not been widely investigated.

Bitter gourd (*Momordica charantia* L.) is an annual climbing tender herb native to eastern India. It is widely planted worldwide, from tropical to temperate zones, and in particular, in the southern and northern areas of China. In the actual production process, bitter gourd seedlings will be exposed to excessive heat stress in the late autumn cultivation. Bitter gourd has been used as a rootstock with strong stress resistance in numerous studies. Using bitter gourd as a rootstock can improve the heat resistance (40 °C) of cucumber seedlings. Proteome analysis can increase the protein content involved in energy metabolism, defense responses, and protein and nucleic acid biosynthesis (Xu et al., 2018). Wei et al. (2019) found that cucumber plants grafted with bitter gourd could maintain the homeostasis of redox in cells after heat stress (40 °C). However, there are few reports on improving the heat resistance of bitter gourds using other resistant rootstocks. In this study, we analyzed the effects of different rootstocks on the heat tolerance of bitter gourd in terms of antioxidant activity and carbon and nitrogen metabolism levels and identified grafting mechanisms that could be utilized to improve stress resistance in bitter gourd.

## 2 Materials and methods

### 2.1 Materials

The experiment was conducted at the Chengdu Campus of the Sichuan Agricultural University from August to November 2021. The scion used was a bitter gourd (*Momordica charantia* L.), F-1437, hereafter referred to as M. Two types of rootstock were also utilized: pumpkin (*Cucurbita moschata* (Duch. ex Lam.) Duch. ex Poir.) hereafter referred to as C; and luffa (*Luffa cylindrica* L.), hereafter referred to as L. The stock and scion materials were obtained from the Chengdu Agricultural Vocational and Technical College.

### 2.2 Experimental design

The seeds of grafted rootstocks and scions were soaked in 45–55°C water for 30 minutes and were then soaked for 24 h after cooling. After the seeds expanded, they were put into a petri

dish containing wet filter paper to accelerate germination at 30 °C. When the white tip of the seeds reached 0.5 cm, they were sown. The stock was sown 2–3 days before the scion (perlite: vermiculite = 2:1). When the rootstock had one leaf and one heart and the first true leaf of the scion was unfolded, split grafting was performed. There were four grafting treatments: bitter gourd seedlings (M), self-grafted bitter gourd seedlings (MS), pumpkin as the rootstock and bitter gourd as the scion (MC), and luffa as the rootstock and bitter gourd as the scion (ML).

While grafting, a transparent plastic film was used to cover the grafts. After grafting, a black film was used to cover for shading. The cover must be placed for the whole day for shading, heat preservation, and moisture preservation over 1–3 days. Within 4–6 days after grafting, light was blocked from 10 a.m. to 3 p.m. every day, and the black film was removed for the rest of the time. The temperature in the small arch shed was controlled at 32 °C during the day and 20 °C at night, and the humidity was controlled at ~90%. After 7 days, the plants were placed under light all day, and the seedlings were gradually ventilated and cooled to keep the temperature at 25 °C during the day and 18 °C at night. After 10–15 days of grafting, the grafting clip was removed.

When the grafted seedlings had grown four leaves and one heart, seedlings were selected with uniform growth vigor and placed in an intelligent artificial incubator (Tianjin Taist Instrument Co., Ltd., RGX300EF) for pre-culture. There were 20 pots per treatment, 1 plant per pot, and 3 replicates per treatment. The pre-culture conditions were as follows: 25/18 °C, 12 h/12 h (day/night), light intensity 300 μmol·m<sup>−2</sup>·s<sup>−1</sup>, and relative humidity 80%. After 24 h of pre-culture, heat stress (H) was performed: 40 °C, 12/12 h (day/night), the light intensity was 300 μmol·m<sup>−2</sup>·s<sup>−1</sup>, and the relative humidity was set to 80%. After 24 h of heat treatment, all treated seedlings were placed in an incubator at 25 °C under a 12 h light/12 h dark cycle, the light intensity was 300 μmol·m<sup>−2</sup>·s<sup>−1</sup>, and the relative humidity was 80% for 24 h, to restore the growth of seedlings after heat stress (RH). The grafted seedlings were randomly arranged in an intelligent artificial incubator, and their positions were changed regularly to ensure consistent growth conditions and adequate moisture. Samples were collected and measured 24 h after heat stress (H) and 24 h after the recovery of growth (RH).

### 2.3 Determination of indices

#### 2.3.1 Relative conductivity and osmotic regulating substances

The relative conductivity of the leaves was measured using a conductance instrument (Shanghai INESA Scientific Instrument Co., Ltd, DDS-307). Soluble protein content was determined using the Coomassie brilliant blue G-250 method, MDA content



was determined using the thiobarbituric acid method, and Pro content was determined using the acid ninhydrin colorimetric method (Wang and Huang, 2015). The  $O_2^-$  content was determined using the p-aminobenzenesulfonic acid method (Ke et al., 2007) and the  $H_2O_2$  content was determined using potassium iodide spectrophotometry (Chakrabarty and Datta, 2008).

### 2.3.2 Antioxidant enzyme activity

In preparation for the antioxidant enzyme extract, leaves (0.5 g) were weighed and ground with 5 mL of 50 mmol·L<sup>-1</sup> phosphate buffer (pH 7.8) containing 0.2 mmol·L<sup>-1</sup> EDTA and 2% polyvinylpyrrolidone. The homogenate was centrifuged at 12000 × g for 20 min at 4 °C, and the supernatant was then used for the determination of antioxidant enzyme activity. SOD activity was measured using the nitroblue tetrazolium method, POD activity using the guaiacol method, and CAT activity using the ultraviolet (UV) absorption method (Wang and Huang, 2015).

### 2.3.3 Carbon metabolism and related enzyme activities

The total soluble sugar content was determined using the anthrone method (Wang and Huang, 2015), sucrose and fructose were determined using the Buysse and Merckx's method (1993), and glucose content was determined using a colorimetric method (Jones et al., 1977).

The enzyme solution was prepared according to the method of Holaday et al. (1992), and the activity of the sucrose phosphate synthase (SPS) was measured. To measure the activities of sucrose synthase (SS), neutral synthase (NI), and acid synthase (AI), enzyme solutions were prepared as previously described (Shahid et al., 2018).

### 2.3.4 Nitrogen metabolism and related enzyme activities

The free amino acid content was determined using the ninhydrin solution chromogenic method (Wang and Huang, 2015). The  $NO_3^-$  and  $NO_2^-$  contents were determined according to Cataldo et al. (2008). The  $NH_4^+$  content was determined according to the method described by Molins-Legua et al. (2006).

NR activity was measured using an *in vitro* method (Wang and Huang, 2015), NiR activity was measured according to the method described by Ramarao et al. (1983), and GS was measured according to the method of Lillo (1984).

## 2.4 Statistical analysis

All data were sorted using Excel 2010 software. Statistical analyses were conducted using SPSS 20.0 (IBM Corporation, Armonk, NY, USA). Data were analyzed using one-way analysis

of variance, followed by Duncan's new complex range method at a 5% level of significance ( $P < 0.05$ ). In order to study the relationship between various indicators, we conducted principal component analysis (PCA) and correlation analysis.

## 3 Results

### 3.1 Changes in the ROS and osmotic substance levels

After heat stress or recovery, the relative conductivity and MDA,  $O_2^-$ , and  $H_2O_2$  contents of the MC and ML decreased significantly when compared with the M and MS; at the same time, the protein and Pro contents increased significantly (Figure 1). In addition, when comparing ML with MC, regardless of heat stress or recovery, the relative conductivity and  $O_2^-$  content in the ML was lower than that of the MC (under heat stress, it decreased by 20.47% and 23.72% respectively, and decreased by 36.48% and 39.82% respectively after recovery), while the protein and MDA of the ML were not significantly different from those of the MC. After heat stress, the Pro content in the ML was significantly higher (17.36%) than that of the MC, but after recovery, there was no significant difference between the two. The results for the  $H_2O_2$  content levels were the opposite. When MS and M were compared, the contents of Pro,  $O_2^-$ , and  $H_2O_2$  did not differ significantly with the heat stress or after recovery, whereas the relative conductivity and MDA content of the MS were both significantly lower than those of the M. After the heat stress, the protein content of the MS was not significantly different from that of the M; however, after recovery, the protein content of the MS was significantly higher than that of the M.

### 3.2 Activity of antioxidant enzymes

When bitter melon seedlings were subjected to high-temperature stress or resumed growth at 25 °C, the activities of SOD, POD, and CAT in the MC and ML were significantly higher than those in the M and MS (Figure 2). At the same time, after heat stress or recovery, the CAT activity of the ML was significantly higher than that of the MC (increased by 25.18% and 32.14% respectively), whereas the SOD activity of the ML was not significantly different from that of the MC. In terms of POD activity, after the heat stress, there was no significant difference between the ML and MC; however, after recovery, the ML was significantly higher (26.73%) than that of the MC. After heat stress, the activity of the POD and CAT in the MS was not significantly different from that of the M, but the activity of the SOD was significantly increased (18.12%). After recovery, the activities of SOD and CAT in the MS were not significantly different from those in the M, but the activity of the POD was significantly increased.



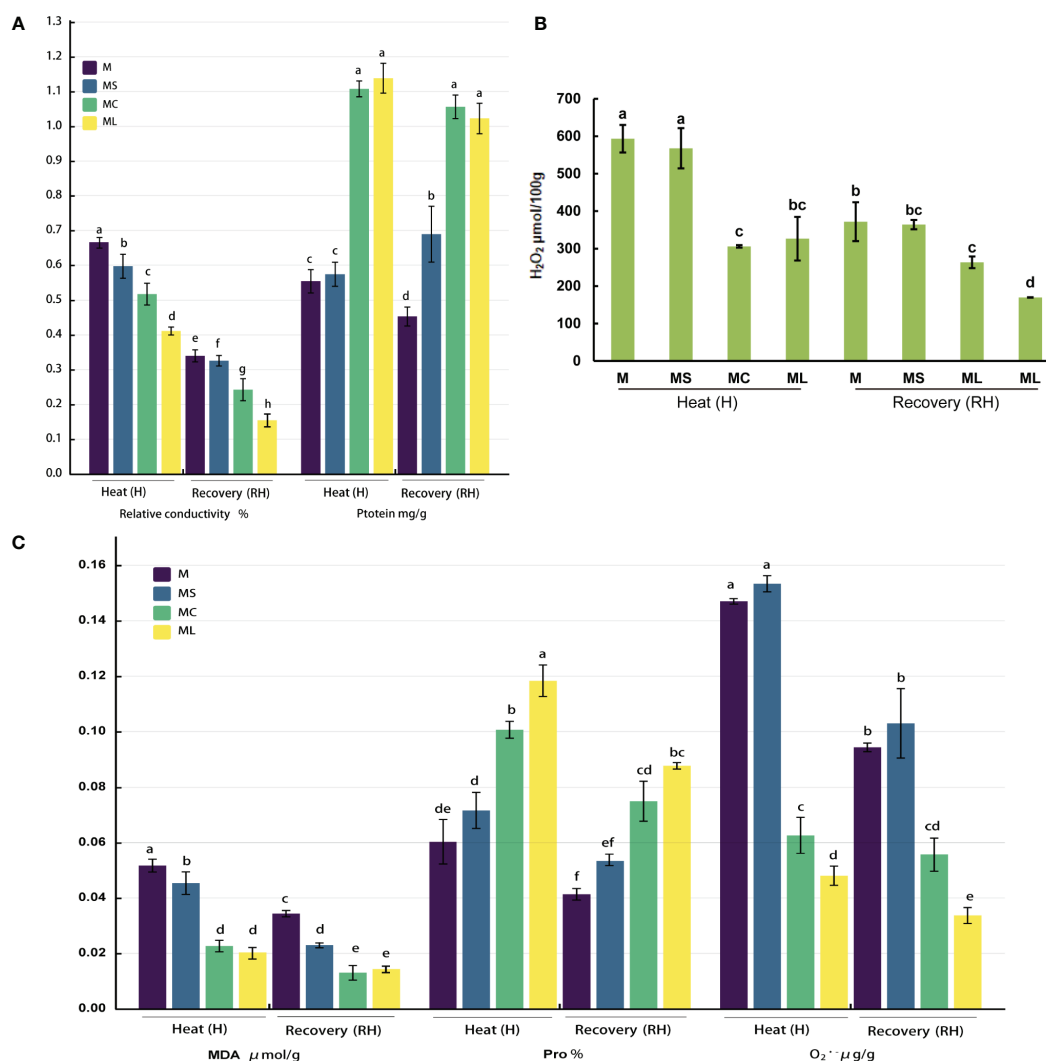


**FIGURE 1**  
Changes in the ROS and osmotic substance levels. **(A)** Relative conductivity and protein content. **(B)** H<sub>2</sub>O<sub>2</sub> content. **(C)** MDA, Pro and O<sub>2</sub><sup>-</sup> content. Values are the mean ( $\pm$  SE) of three replicates. Different letters indicate statistically significant differences between the treatment groups ( $P < 0.05$ ).

### 3.3 Carbon metabolite content

After heat stress or growth recovery, the soluble sugar, sucrose, fructose, and glucose contents in the ML and MC were significantly higher than those in the M and MS, and the soluble sugar and sucrose contents in the ML were significantly higher than those in the MC, the soluble sugar content increased by 57.74% and 14.27%, and the sucrose content increased by 52.01% and 42.94%, respectively (Figure 3). After heat stress, the fructose content of the ML was not significantly different from that of the MC; however, the fructose content of the ML was significantly higher (17.70%) than that of the MC after growth recovery. After heat stress, the glucose content in the ML and MC increased significantly (36.24%), but there was no

significant difference between ML and MC after growth recovery. After heat stress, the soluble sugar, fructose, and glucose contents of the MS were not significantly different to those of M, but the sucrose content of MS was significantly higher than that of M. After recovery at 25 °C, the soluble sugar, sucrose, and fructose contents in MS were significantly higher than those in M, but there was no significant difference in glucose.

### 3.4 Activity of carbon metabolism enzymes

The SPS, SS, and NI activities of MC and ML were significantly higher than those of M and MS after heat stress and recovery, and the

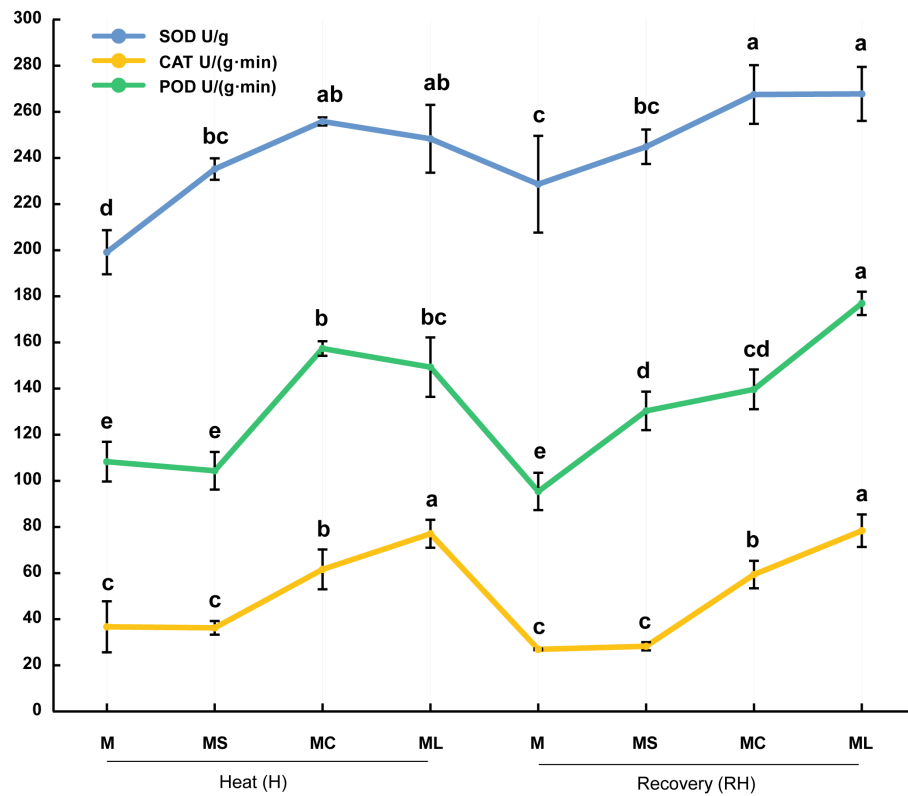


**FIGURE 2**  
Activity of antioxidant enzymes. Values are the mean ( $\pm$  SE) of three replicates. Different letters indicate statistically significant differences between the treatment groups ( $P < 0.05$ ).

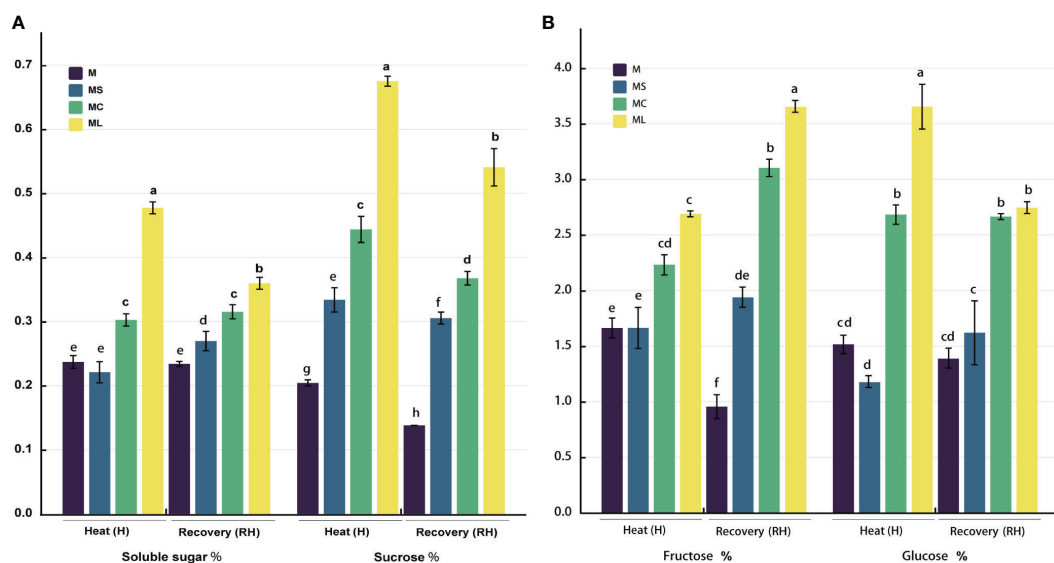


**FIGURE 3**  
Carbon metabolite content. (A) Soluble sugar and sucrose content. (B) Fructose and glucose content. Values are the mean ( $\pm$  SE) of three replicates. Different letters indicate statistically significant differences between the treatment groups ( $P < 0.05$ ).

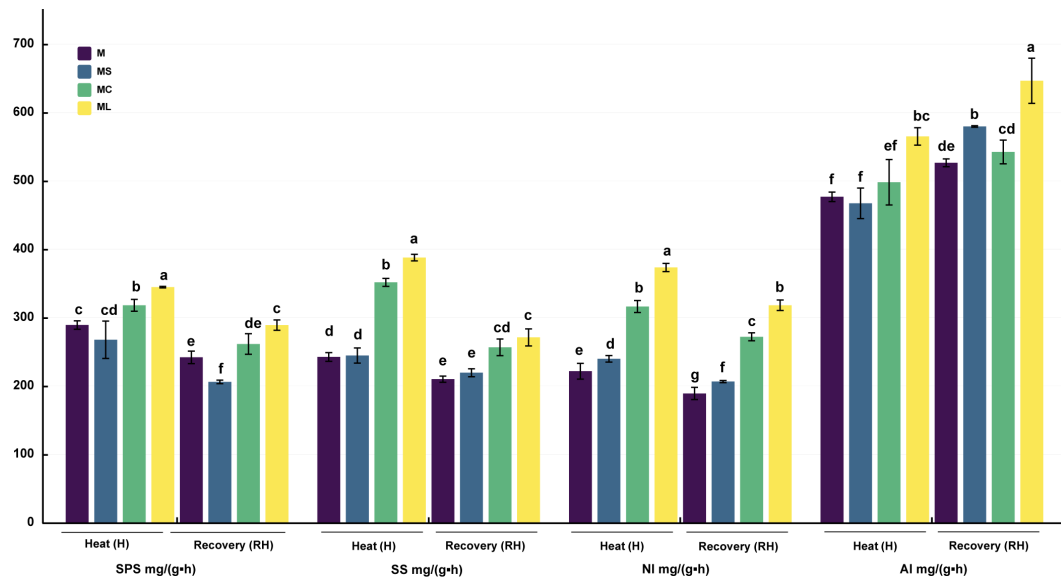


FIGURE 4

Activity of carbon metabolism enzymes. Values are the mean ( $\pm$  SE) of three replicates. Different letters indicate statistically significant differences between the treatment groups ( $P < 0.05$ ).

activities of ML were significantly higher than those of MC, except that the SS (RH) activities of ML and MC were not significantly different (Figure 4). Compared with MC, the SPS activity of ML significantly increased by 8.36% and 10.56% after heat stress and recovery, and the NI activity increased by 18.06% and 16.95% respectively, while the SS activity increased by 10.32% only after heat stress. After heat stress, the activities of SPS and SS in the MS were not significantly different from those in M; however, the

activities of NI were significantly increased. After the recovery of growth, the activities of the SPS, SS, and NI of MS were significantly reduced, with no significant difference, and were significantly increased when compared with that of M. For AI activity, after the heat stress or recovery, ML was significantly higher than that for other treatments. After heat stress, the AI activity of ML was significantly increased by 18.25%, 12.67% and 16.37% compared with M, MS and MC respectively, and 22.79%, 11.53% and 19.18% respectively after

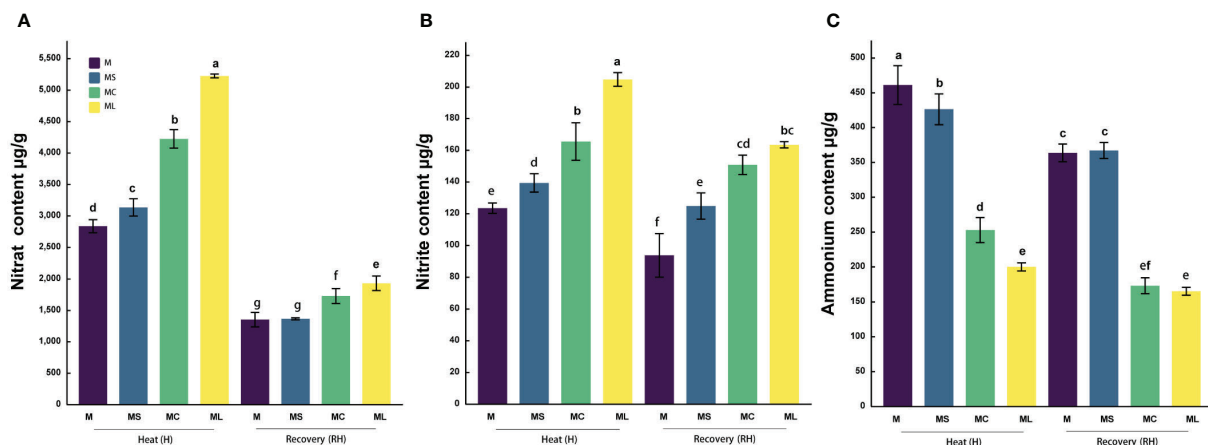


FIGURE 5

Nitrogen metabolite content. Values are the mean ( $\pm$  SE) of three replicates. Different letters indicate statistically significant differences between the treatment groups ( $P < 0.05$ ). (A) Nitrate content. (B) Nitrite content. (C) Ammonium content.

the recovery. After heat stress, there was no significant difference in the AI activity among the M, MS, and MC groups. After recovery, the AI activity of MS was significantly higher than that of M, and there was no significant change in MC.

### 3.5 Nitrogen metabolite content

After the heat stress and recovery, the  $\text{NO}_3^-$  and  $\text{NO}_2^-$  contents of the grafted seedlings in MC and ML were significantly higher than those of the MS and M, and the  $\text{NH}_4^+$  contents were significantly higher than those of MS and M (Figure 5). After heat stress, the  $\text{NO}_3^-$  and  $\text{NH}_4^+$  contents in the ML were significantly higher (23.6%) and lower (20.85%) than those in the MC, respectively, but there was no significant difference in  $\text{NO}_2^-$ . After recovery, the  $\text{NO}_3^-$  content in the ML was significantly higher (11.73%) than that in the MC, but the  $\text{NO}_2^-$  and  $\text{NH}_4^+$  contents were not significantly different from those in the MC. The  $\text{NO}_3^-$  and  $\text{NO}_2^-$  contents in the MS were significantly higher than those in the M after heat stress, 10.55% and 12.94% respectively, while the  $\text{NH}_4^+$  content was significantly reduced by 7.59%. After recovery, the  $\text{NO}_3^-$  and  $\text{NH}_4^+$  contents in the MS were not significantly different from those in the M, but the  $\text{NO}_2^-$  content increased significantly.

### 3.6 Activity of nitrogen metabolism enzymes

After heat stress and recovery, NR, NiR, and GS activities in the MC and ML of the grafted seedlings were significantly higher than those in the MS and M (Figure 6). Except after heat stress, there was no significant difference in NR activity between the MC, M, and MS. At the same time, after heat stress and recovery, the NR, NiR, and GS activities of ML were significantly higher than those of the MC. Compared with MC, the activities of NR, NiR and GS in ML increased by 35.67%, 29.09% and 25.96% respectively after heat stress, and increased by 33.20%, 13.37% and 11.56% respectively after recovery. After heat stress and recovery, there were no significant differences in the NR, NiR, and GS activities between the MS and M.

### 3.7 Principal component and correlation analysis

Two principal components were extracted from the principal component analysis, and the characteristic root values were  $> 1$  (Figure 7; Supplementary Table 1). The variance interpretation rates of the two principal components

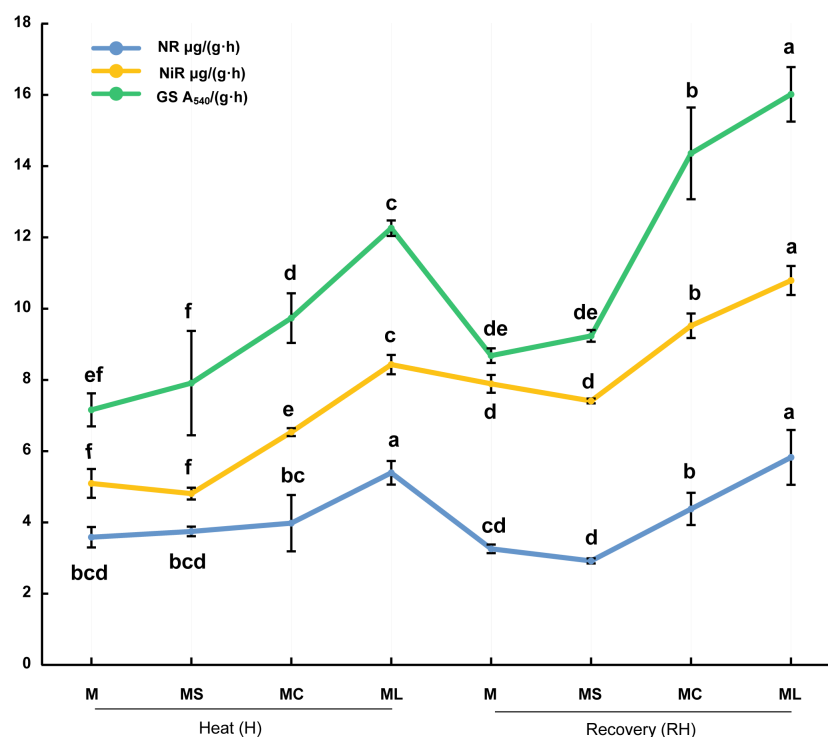


**FIGURE 6**  
Activity of nitrogen metabolism enzymes. Values are the mean ( $\pm$  SE) of three replicates. Different letters indicate statistically significant differences between the treatment groups ( $P < 0.05$ ).

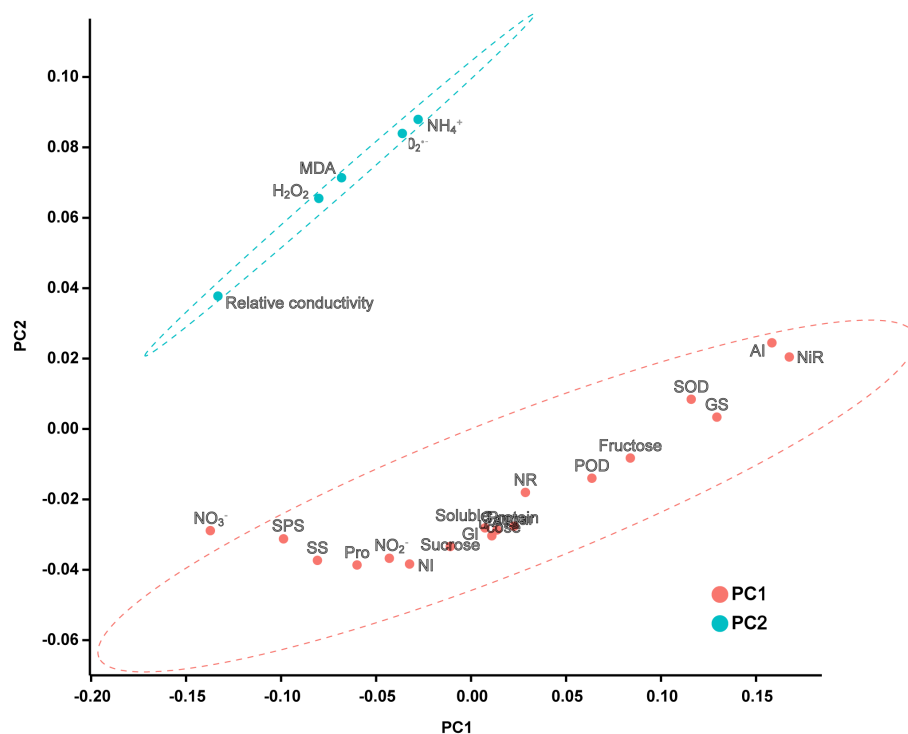


FIGURE 7

PCA score plot of each indicator. According to the principle that the eigenvalue is greater than 1, two principal components are extracted with a confidence interval of 95%.

were 65.791% (PC1) and 21.459% (PC2), and the cumulative variance interpretation rate was 87.250%. Relative conductivity, MDA,  $O_2^-$ ,  $H_2O_2$ , and  $NH_4^+$  were negatively correlated with PC1. The 23 indicators were divided into two groups: one group was composed of cell damage indicators and the other group was composed of antioxidants and carbon and nitrogen metabolism systems.

To further intuitively display the relationship between the various indicators, a correlation analysis of the data was conducted based on the heat map, as shown in Figure 8. The correlation coefficient values between relative conductivity and the 11 items of MDA,  $O_2^-$ ,  $H_2O_2$ , SOD, POD, fructose, AI,  $NO_3^-$ ,  $NH_4^+$ , NiR, and GS showed a significant difference ( $P < 0.05$ ,  $P < 0.01$ ). There was a significant positive correlation between relative conductivity and MDA,  $O_2^-$ ,  $H_2O_2$ , and  $NH_4^+$  (correlation coefficients were 0.826, 0.750, 0.859, and 0.721, respectively;  $P < 0.01$ ). There was a significant negative correlation between the relative conductivity and SOD ( $-0.685$ ,  $P < 0.01$ ), POD ( $-0.505$ ,  $P < 0.05$ ), fructose ( $-0.572$ ,  $P < 0.01$ ), AI ( $-0.840$ ,  $P < 0.01$ ),  $NO_3^-$  ( $0.483$ ,  $P < 0.05$ ), NiR ( $-0.933$ ,  $P < 0.01$ ), and GS ( $-0.802$ ,  $P < 0.01$ ). The correlation value between relative conductivity and the 11 items of protein, Pro, CAT, soluble sugar, sucrose, glucose, SPS, SS, NI,  $NO_2^-$ , and NR were not

significant ( $P > 0.05$ ), indicating that there was no correlation between relative conductivity and these 11 items.

## 4 Discussion

For optimal growth and development, vegetables often require an optimal temperature, and they can perceive slight changes in the ambient temperature, such as increases; these will greatly affect the physiological and metabolic processes of vegetables (Giordano et al., 2021). Photosynthesis is one of the processes most affected by temperature, and this can cause large disruptions to energy allocation and the final biomass production of vegetables. Previous studies have found that heat stress not only changes the structure of the thylakoid membrane and pigment protein complex (Rath et al., 2022), but also reduces leaf water potential (Weng et al., 2021). Exposure to stress temperatures leads to a decrease in  $CO_2$  assimilation, resulting in an increase in PSII electron transport, which in turn enables chloroplasts to accumulate large amounts of ROS (Zhou et al., 2007; Rath et al., 2022). Grafting is an ecologically sustainable agricultural practice that can improve stress resistance in vegetables. Moreover, studies have found that



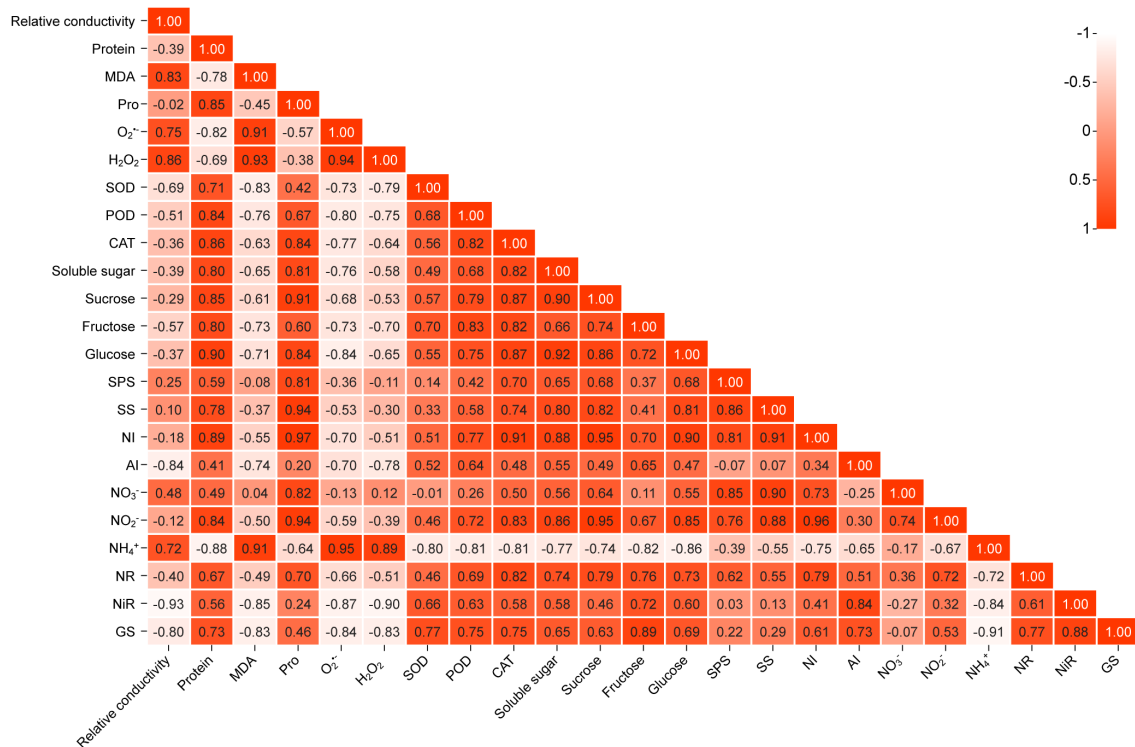


FIGURE 8

Correlation diagram of correlation of three indicators. Positive values indicate positive correlation, while negative values indicate negative correlation. The darker or lighter the color, the stronger the correlation between the indicators. All correlations in the figure reflect the absolute value of the Pearson correlation coefficient above the threshold ( $P < 0.05$ ,  $P < 0.01$ ).

the effects of grafting depend on the characteristics of the scion and rootstock as well as their interactions (Colla et al., 2010). In a grafting experiment using cucumber, the rootstock was found to significantly increase the activities of the antioxidant enzymes (CAT and POD), improve the accumulation of Pro, and reduce lipid peroxidation (MDA) content (Shehata, 2022). Moreover, by improving the carboxylation efficiency, transcription of defense-related genes, and scavenging activity of ROS, the oxidative stress of grafted watermelon seedlings was significantly reduced (Li et al., 2014a). In our study, after heat stress, the two different rootstocks increased the Pro and protein content, decreased relative conductivity and MDA content, and inhibited ROS ( $H_2O_2$  and  $O_2^{\cdot-}$ ) accumulation by promoting antioxidant enzyme (SOD, POD, and CAT) activities in the leaves of bitter melon seedlings, when compared with the self-rooted grafted seedlings. After recovery at 25 °C, the grafted seedlings of the pumpkin and luffa were still superior to the self-grafted and non-grafted seedlings for all indicators. At the same time, under heat stress or after recovery, the luffa had a more significant effect on alleviating oxidative damage in bitter melon seedlings. These results are similar to those reported by Shehata (2022) and Li et al. (2014b). Relative electrical conductivity and MDA represent cell integrity and membrane lipid peroxidation

in leaves, and their reduced values indicate that seedlings have higher stress resistance and that cell damage can be prevented. Previous studies have shown that increased Pro content can reduce photo inhibition to maintain electron conduction between the two photosystems (Ashraf and Foolad, 2007; Szabados and Saviouré, 2010; Padilla et al., 2021), which acts as a low molecular weight cellular antioxidant that removes free radicals and protects plants from oxidative damage (Anjum et al., 2012). During normal growth and development of plants, the production and removal of ROS in cells is balanced (Mittler, 2017), but the excessive accumulation of ROS not only destroys cellular components (carbohydrates, proteins, lipids, etc.), but also leads to cell death (Raja et al., 2017). Plants have enzymatic and non-enzymatic antioxidant defense systems; the enzymes in these systems mainly include SOD, POD, and CAT. SOD first converts  $O_2^{\cdot-}$  to  $H_2O_2$  in response to high-temperature stress, and the generated  $H_2O_2$  is further converted to  $H_2O$  by CAT or POD (Biczak, 2016). Cucumber seedlings using bitter melon (Tao et al., 2020), melon (Miao et al., 2019), or luffa (Li et al., 2016) as rootstocks all showed good antioxidant activity. Luffa is a type of gourd with strong heat tolerance, which is conducive to improving the oxidation resistance of scions. In plants, in addition to antioxidant enzymes, the role of

low molecular weight antioxidants can't be ignored. AsA has the potential to provide electrons as a coenzyme. It clears ROS by regulating the water state of cells (Hasanuzzaman et al., 2019). Tocopherol is mainly synthesized in the photosynthetic apparatus and protects the photosynthetic membrane by clearing ROS (Hasanuzzaman et al., 2014). Carotenoids are mainly responsible for pigment deposition and ROS quenching capacity. Flavonoids reduce plant cell damage by scavenging free radicals and protecting the cell membrane from membrane lipid peroxidation (Løvdal et al., 2010). Therefore, in the future research, more attention should be paid to the contribution of non-enzymatic antioxidants to abiotic stress resistance of plants.

In this study, heat stress increased the content of the total soluble sugar, sucrose, fructose, and glucose in grafted bitter gourd seedlings, especially in the two heterologous rootstocks. The accumulation of sugar in plant leaves depends on photosynthesis and the transport of carbohydrates, and the stress resistance of grafted plants can be achieved by significantly increasing the content of the total soluble sugar, reducing sugar, and sucrose (Turhan and Ergin, 2012). Grafted seedlings can degrade more starch, which is not only conducive to respiration and growth, but also to the maintenance of a high soluble sugar content (Sato et al., 2004), so that plants can accumulate more energy to resist stress. Interestingly, the contents of sucrose and fructose in the leaves of the self-grafted bitter gourd seedlings also increased correspondingly, which may be due to the transport of sugar and its accumulation at the grafting site or the formation of vascular bundles. This is similar to the results of Miao et al. (2019), in which it was suspected that the rapid accumulation of biomass in pumpkin/pumpkin compared to cucumber/cucumber and cucumber/pumpkin may be due to early vascular bundle reconnection. The bitter gourd seedlings grafted with luffa as rootstock had a higher sugar content to reduce the negative effects caused by heat stress. This may be because luffa roots have strong heat resistance (Zhang et al., 2007). The activities of AI, NI, SS, and SPS in plant leaves affect the contents of non-reducing sugars (sucrose) and reducing sugars (fructose and glucose). In this study, the contents of the non-reducing and reducing sugars were directly proportional to the related enzyme activities. In heterologous bitter gourd-grafted seedlings, the increase in leaf SPS activity promoted sucrose accumulation; SS and NI were conducive to the accumulation of glucose and fructose, while AI was inferior to the first three enzyme activities. This is similar to the results of Shahid et al. (2018), but in a study by Turhan and Ergin (2012), stress resistance was found to increase with the reduction of NI and SS activities in the bark tissue of 4-year-old sweet cherry-grafted trees. This phenomenon largely depends on where the samples are taken from and where the carbon is assimilated. The activities of SS increased, which could increase the sugar content in plant leaves, maintain the balance of cell sugar, and maintain the homeostasis and water potential of plant

cells. When growth resumed at 25 °C, the sugar content and related enzyme activities of the grafted bitter gourd seedlings were similar to those after heat stress. Therefore, pumpkin and luffa rootstocks are conducive to the rapid recovery of bitter gourd from heat stress.

Among the nitrogen metabolites,  $\text{NO}_3^-$  and  $\text{NO}_2^-$  contents in heterologously grafted bitter gourd seedlings after heat stress were significantly higher than those in non-grafted and self-grafted seedlings, whereas  $\text{NH}_4^+$  showed the opposite trend. Nitrogen metabolism includes nitrogen absorption, transport, amino acid metabolism, and assimilation (Kusano et al., 2011), all of which require energy. However, various environmental stresses lead to insufficient energy metabolism in plants, affecting the synthesis and metabolism of compounds, such as proteins, nucleotides, and chlorophyll (Dai et al., 2014). In watermelon (Yang et al., 2013) and tomato (Sánchez-Rodríguez et al., 2013), grafting promoted nitrogen metabolism in seedlings and improved  $\text{NO}_3^-$  assimilation efficiency and NR activity. In our results, under heat stress, grafting promoted nitrogen metabolism, and the  $\text{NH}_4^+$  accumulation of luffa rootstock was less than that of pumpkin rootstock. At the same time, compared with non-grafted and self-grafted seedlings, pumpkin and luffa rootstocks increased the activities of NR, NiR, and GS in the leaves of bitter gourd-grafted seedlings after heat stress, and the plants on luffa rootstocks showed better performance.  $\text{NH}_4^+$  can not only destroy the photosynthetic system of plants and cause them to experience toxicity but also lead to a reduction in nitrogen utilization efficiency (Skopelitis et al., 2006). The  $\text{NH}_4^+$  concentration in plants is not only dependent on NR and NiR catalysis but is also related to  $\text{NH}_4^+$  assimilation through the GS/GOGAT pathway. The increased activities of NR, NiR, and GS resulted in a simultaneous increase in  $\text{NH}_4^+$  formation and assimilation, effectively reducing  $\text{NH}_4^+$  accumulation. In addition, GSH, as a low molecular weight antioxidant and non-protein thiol, plays a key role in regulating intracellular defense by scavenging ROS during stress (Singh et al., 2016), and GSH maintains redox homeostasis as an integral part of the AsA-GSH cycle, so this may also indirectly inhibit the accumulation of  $\text{NH}_4^+$ , which needs to be proved by subsequent studies. The increase in enzyme activities related to nitrogen metabolism in heterologously grafted seedlings may be related to the promotion of photosynthesis and antioxidant defense systems of bitter gourd seedlings by grafting, as excessive accumulation of ROS may change the biosynthesis and activity of enzymes (Taïbi et al., 2016). The effects of nitrogen metabolites and enzyme activities under heat stress indicate that strong rootstocks can absorb more nitrogen and promote nitrogen assimilation in leaves. Grafting is also conducive to the recovery of seedlings by inhibiting the accumulation of  $\text{NH}_4^+$ . In future research, more attention should be paid to the molecular mechanism of grafting on carbon and nitrogen metabolism of bitter gourd and the improvement of stress resistance of bitter gourd by grafting.

## 5 Conclusions

We found that grafting bitter melon onto the roots of pumpkin and luffa can help to reduce heat-induced oxidative stress by increasing the scavenging activity of active oxygen, the carbon and nitrogen metabolite content, and the enzyme activity. The possible mechanism is that grafting is conducive to the metabolism of sucrose in bitter melon leaves, thus promoting the accumulation of non-reducing sugar and reducing sugar, maintaining the balance of cell sugar, the stable state of cells and water potential, and also providing the ability to absorb nitrogen in leaves to prevent cells from being poisoned by  $\text{NH}_4^+$ . The grafted seedlings of bitter melon were subjected to heat stress recovery at 25 °C. We found that pumpkin and luffa rootstocks could quickly restore the normal growth of seedlings. At 40 °C and 25 °C, the performance of the luffa rootstock was better than that of the pumpkin rootstock. Our research shows that the root system of the luffa has a large effect on the adaptability of the scions to heat stress, and this mechanism should be further explored to improve the stress resistance and productivity of plants.

## Data availability statement

The original contributions presented in the study are included in the article/Supplementary Materials. Further inquiries can be directed to the corresponding authors.

## Author contributions

LL, HL and YT conceived and designed the experiments. LT designed the experiment and provided grafting technology and guidance. LL, WT, HL and XL performed the experiments. LL,

WT and GS analyzed the data. LL and WT wrote the manuscript. LL, BS, ZH, HL and YT reviewed and revised the manuscript. All authors have read and approved the final version of the manuscript. All authors contributed to the article and approved the submitted version.

## Acknowledgments

We would like to thank Editage ([www.editage.cn](http://www.editage.cn)) for English language editing.

## Conflict of interest

The authors declare that the research was conducted in the absence of any commercial or financial relationships that could be construed as a potential conflict of interest.

## Publisher's note

All claims expressed in this article are solely those of the authors and do not necessarily represent those of their affiliated organizations, or those of the publisher, the editors and the reviewers. Any product that may be evaluated in this article, or claim that may be made by its manufacturer, is not guaranteed or endorsed by the publisher.

## Supplementary material

The Supplementary Material for this article can be found online at: <https://www.frontiersin.org/articles/10.3389/fpls.2022.1074889/full#supplementary-material>

## References

- Anjum, S. A., Farooq, M., Xie, X., Liu, X., and Ijaz, M. F. (2012). Antioxidant defense system and proline accumulation enables hot pepper to perform better under drought. *Sci. Hortic.* 140, 66–73. doi: 10.1016/j.scienta.2012.03.028
- Ara, N., Yang, J., Hu, Z., and Zhang, M. (2013). Determination of heat tolerance of interspecific (*Cucurbita maxima* × *Cucurbita moschata*) inbred line of squash 'Maxchata' and its parents through photosynthetic response. *Tarim. Bilim. Derg.* 19, 188–197. doi: 10.1501/Tarimbil\_0000001244
- Ashraf, M., and Foolad, M. R. (2007). Roles of glycine betaine and proline in improving plant abiotic stress resistance. *Environ. Exp. Bot.* 59 (2), 206–216. doi: 10.1016/j.envexpbot.2005.12.006
- Biczak, R. (2016). Quaternary ammonium salts with tetrafluoroborate anion: Phytotoxicity and oxidative stress in terrestrial plants. *J. Hazard. Mater.* 304, 173–185. doi: 10.1016/j.jhazmat.2015.10.055
- Bysses, J., and Merckx, R. (1993). An improved colorimetric method to quantify sugar content of plant tissue. *J. Exp. Bot.* 44 (10), 1627–1629. doi: 10.1093/jxb/44.10.1627
- Cataldo, D. A., Maroon, M., Schrader, L. E., and Youngs, V. L. (2008). Rapid colorimetric determination of nitrate in plant tissue by nitration of salicylic acid. *Commun. Soil. Sci. Plant* 6 (1), 71–80. doi: 10.1080/00103627509366547
- Chakrabarty, D., and Datta, S. K. (2008). Micropropagation of gerbera: lipid peroxidation and antioxidant enzyme activities during acclimatization process. *Acta Physiol. Plant* 30 (3), 325–331. doi: 10.1007/s11738-007-0125-3
- Colla, G., Rouphael, Y., Leonardi, C., and Bie, Z. (2010). Role of grafting in vegetable crops grown under saline conditions. *Sci. Hortic.* 127 (2), 147–155. doi: 10.1016/j.scienta.2010.08.004
- Dai, J., Duan, L., and Dong, H. (2014). Comparative effect of nitrogen forms on nitrogen uptake and cotton growth under salinity stress. *J. Plant Nutr.* 38 (10), 1530–1543. doi: 10.1080/01904167.2014.983126
- Ding, X., Jiang, Y., He, L., Zhou, Q., Yu, J., Hui, D., et al. (2016). Exogenous glutathione improves high root-zone temperature tolerance by modulating photosynthesis, antioxidant and osmolytes systems in cucumber seedlings. *Sci. Rep.* 6 (1), 35424. doi: 10.1038/srep35424

- Gil, L., Ben-Ari, J., Turgeon, R., and Wolf, S. (2012). Effect of CMV infection and high temperatures on the enzymes involved in raffinose family oligosaccharide biosynthesis in melon plants. *J. Plant Physiol.* 169 (10), 965–970. doi: 10.1016/j.jplph.2012.02.019
- Giordano, M., Petropoulos, S. A., and Roupheal, Y. (2021). Response and defence mechanisms of vegetable crops against drought, heat and salinity stress. *Agriculture* 11 (5), 463. doi: 10.3390/agriculture11050463
- Hasanuzzaman, M., Alam, M., Rahman, A., Hasanuzzaman, M., Nahar, K., and Fujita, M. (2014). Exogenous proline and glycine betaine mediated upregulation of antioxidant defense and glyoxalase systems provides better protection against salt-induced oxidative stress in two rice (*Oryza sativa* L.) varieties. *BioMed. Res. Int.* 2014, 757219. doi: 10.1155/2014/757219
- Hasanuzzaman, M., Bhuyan, M. H. M. B., Anee, T. I., Parvin, K., Nahar, K., Mahmud, J. A., et al. (2019). Regulation of ascorbate-glutathione pathway in mitigating oxidative damage in plants under abiotic stress. *Antioxidants* 8 (9), 384. doi: 10.3390/antiox8090384
- Hasanuzzaman, M., Bhuyan, M. H. M. B., Parvin, K., Bhuiyan, T. F., Anee, T. I., Nahar, K., et al. (2020b). Regulation of ROS metabolism in plants under environmental stress: A review of recent experimental evidence. *Int. J. Mol. Sci.* 21 (22), 8695. doi: 10.3390/ijms21228695
- Hasanuzzaman, M., Bhuyan, M. H. M. B., Zulfiqar, F., Raza, A., Mohsin, S. M., Mahmud, J. A., et al. (2020a). Reactive oxygen species and antioxidant defense in plants under abiotic stress: Revisiting the crucial role of a universal defense regulator. *Antioxidants* 9 (8), 681. doi: 10.3390/antiox9080681
- Holaday, A. S., Martindale, W., Aired, R., Brooks, A. L., and Leegood, R. C. (1992). Changes in activities of enzymes of carbon metabolism in leaves during exposure of plants to low temperature. *Plant Physiol.* 98 (3), 1105–1114. doi: 10.1104/pp.98.3.1105
- Jones, M. G. K., Outlaw, W. H., and Lowry, O. H. (1977). Enzymic assay of 10–7 to 10–14 moles of sucrose in plant tissues. *Plant Physiol.* 60 (3), 379–383. doi: 10.1104/pp.60.3.379
- Ke, D., Sun, G., and Wang, Z. (2007). Effects of superoxide radicals on ACC synthase activity in chilling-stressed etiolated mungbean seedlings. *Plant Growth Regul.* 51 (1), 83–91. doi: 10.1007/s10725-006-9150-2
- Kusano, M., Fukushima, A., Redestig, H., and Saito, K. (2011). Metabolomic approaches toward understanding nitrogen metabolism in plants. *J. Exp. Bot.* 62 (4), 1439–1453. doi: 10.1093/jxb/erq417
- Løvdaal, T., Olsen, K. M., Slimestad, R., Verheul, M., and Lillo, C. (2010). Synergetic effects of nitrogen depletion, temperature, and light on the content of phenolic compounds and gene expression in leaves of tomato. *Phytochemistry* 71 (5–6), 605–613. doi: 10.1016/j.phytochem.2009
- Lemoine, R. (2013). Source-to-sink transport of sugar and regulation by environmental factors. *Front. Plant Sci.* 4. doi: 10.3389/fpls.2013.00272
- Li, H., Ahammed, G. J., Zhou, G., Xia, X., Zhou, J., Shi, K., et al. (2016). Unraveling main limiting sites of photosynthesis under below- and above-ground heat stress in cucumber and the alleviatory role of luffa rootstock. *Front. Plant Sci.* 7. doi: 10.3389/fpls.2016.00746
- Liang, J., Chen, X., Guo, P., Ren, H., Xie, Z., Zhang, Z., et al. (2021). Grafting improves nitrogen-use efficiency by regulating the nitrogen uptake and metabolism under low-nitrate conditions in cucumber. *Sci. Hortic.* 289, 110454. doi: 10.1016/j.scienta.2021.110454
- Li, H., Liu, S. S., Yi, C. Y., Wang, F., Zhou, J., Xia, X. J., et al. (2014b). Hydrogen peroxide mediates abscisic acid-induced HSP70 accumulation and heat tolerance in grafted cucumber plants. *Plant Cell Environ.* 37, 2768–2780. doi: 10.1111/pce.12360
- Lillo, C. (1984). Diurnal variations of nitrite reductase, glutamine synthetase, glutamate synthase, alanine aminotransferase and aspartate aminotransferase in barley leaves. *Physiol. Plantarum* 61 (2), 214–218. doi: 10.1111/j.1399-3054.1984.tb05899.x
- Li, H., Wang, F., Chen, X. J., Shi, K., Xia, X. J., Considine, M. J., et al. (2014a). The sub/supraoptimal temperature-induced inhibition of photosynthesis and oxidative damage in cucumber leaves are alleviated by grafting onto figleaf gourd/luffa rootstocks. *Physiol. Plantarum* 152 (3), 571–584. doi: 10.1111/ppl.12200
- Loka, D. A., Derrick, M. O., Dimitrios, B., Christos, N., and Wei, H. (2020). Single and combined effects of heat and water stress and recovery on cotton (*Gossypium hirsutum* L.) leaf physiology and sucrose metabolism. *Plant Physiol. Bioch.* 146, 166–179. doi: 10.1016/j.plaphy.2020.01.015
- Miao, L., Li, S., Bai, L., Anwar, A., Li, Y., He, C., et al. (2019). Effect of grafting methods on physiological change of graft union formation in cucumber grafted onto bottle gourd rootstock. *Sci. Hortic.* 244, 249–256. doi: 10.1016/j.scienta.2018.09.061
- Mittler, R. (2017). ROS are good. *Trends Plant Sci.* 22 (1), 11–19. doi: 10.1016/j.tplants.2016.08.002
- Molins-Lagua, C., Meseguer-Lloret, S., Moliner-Martinez, Y., and Campins-Falco, P. (2006). A guide for selecting the most appropriate method for ammonium determination in water analysis. *Trend. Anal. Chem.* 25 (3), 282–290. doi: 10.1016/j.trac.2005.12.002
- Padilla, Y. G., Gisbert-Mullor, R., López-Serrano, L., López-Galarza, S., and Calatayud, A. (2021). Grafting enhances pepper water stress tolerance by improving photosynthesis and antioxidant defense systems. *Antioxidants* 10 (4), 576. doi: 10.3390/antiox10040576
- Raja, V., Majeed, U., Kang, H., Andrabi, K. I., and John, R. (2017). Abiotic stress: Interplay between ROS, hormones and MAPKs. *Environ. Exp. Bot.* 137, 142–157. doi: 10.1016/j.envexpbot.2017.02.010
- Ramarao, C. S., Patil, V. H., Dhak, B. D., and Kadrekar, S. B. (1983). A simple *in vivo* method for the determination of nitrite reductase activity in rice roots. *Z. Für. Pflanzenphysiol.* 109 (1), 81–85. doi: 10.1016/s0044-328x(83)80175-5
- Rath, J. R., Pandey, J., Yadav, R. M., Zamil, M. Y., Ramachandran, P., Mekala, N. R., et al. (2022). Temperature-induced reversible changes in photosynthesis efficiency and organization of thylakoid membranes from pea (*Pisum sativum*). *Plant Physiol. Bioch.* 185, 144–154. doi: 10.1016/j.plaphy.2022.05.036
- Rosa, M., Prado, C., Podazza, G., Interdonato, R., González, J. A., Hilal, M., et al. (2009). Soluble sugars—metabolism, sensing and abiotic stress: A complex network in the life of plants. *Plant Sign. Behav.* 4 (5), 388–393. doi: 10.4161/psb.4.5.8294
- Ruan, Y. L., Jin, Y., Yang, Y. J., Li, G. J., and Boyer, J. S. (2010). Sugar input, metabolism, and signaling mediated by invertase: Roles in development, yield potential, and response to drought and heat. *Mol. Plant* 3 (6), 942–955. doi: 10.1093/mp/ssq044
- Sami, F., Yusuf, M., Faizan, M., Faraz, A., and Hayat, S. (2016). Role of sugars under abiotic stress. *Plant Physiol. Bioch.* 109, 54–61. doi: 10.1016/j.plaphy.2016.09.005
- Sánchez-Rodríguez, E., Romero, L., and Ruiz, J. M. (2013). Role of grafting in resistance to water stress in tomato plants: Ammonia production and assimilation. *J. Plant Growth Regul.* 32 (4), 831–842. doi: 10.1007/s00344-013-9348-2
- Sato, F., Yoshioka, H., Fujiwara, T., Higashio, H., Urugami, A., and Tokuda, S. (2004). Physiological responses of cabbage plug seedlings to water stress during low-temperature storage in darkness. *Sci. Hortic.* 101 (4), 349–357. doi: 10.1016/j.scienta.2003.11.018
- Shahid, M. A., Balal, R. M., Khan, N., Zotarelli, L., Liu, G., Ghazanfar, M. U., et al. (2018). Ploidy level of citrus rootstocks affects the carbon and nitrogen metabolism in the leaves of chromium-stressed kinnow mandarin plants. *Environ. Exp. Bot.* 149, 70–80. doi: 10.1016/j.envexpbot.2018.02.010
- Shan, X., Zhou, H., Sang, T., Shu, S., Sun, J., and Guo, S. (2016). Effects of exogenous spermidine on carbon and nitrogen metabolism in tomato seedlings under high temperature. *J. Am. Soc. Hortic.* 141 (4), 381–388. doi: 10.12127/jashs.141.4.381
- Shehata, S. A. (2022). Grafting enhances drought tolerance by regulating stress-responsive gene expression and antioxidant enzyme activities in cucumbers. *BMC Plant Biol.* 22 (1), 408. doi: 10.1186/s12870-022-03791-7
- Singh, S., Tripathi, D. K., Chauhan, D. K., and Dubey, N. K. (2016). Glutathione and phytochelatin mediated redox homeostasis and stress signal transduction in plants. *Plant Metal Interaction*. 2016, 285–310. doi: 10.1016/b978-0-12-803158-2.00011-4
- Skopelitis, D. S., Paranychianakis, N. V., Paschalidis, K. A., Pliakonis, E. D., Delis, I. D., Yakoumakis, D. I., et al. (2006). Abiotic stress generates ROS that signal expression of anionic glutamate dehydrogenases to form glutamate for proline synthesis in tobacco and grapevine. *Plant Cell* 18 (10), 2767–2781. doi: 10.1105/tpc.105.038323
- Szabados, L., and Savouré, A. (2010). Proline: a multifunctional amino acid. *Trends Plant Sci.* 15 (2), 89–97. doi: 10.1016/j.tplants.2009.11.009
- Taibi, K., Taibi, F., Ait Abderrahim, L., Ennajah, A., Belkhdja, M., and Mulet, J. M. (2016). Effect of salt stress on growth, chlorophyll content, lipid peroxidation and antioxidant defense systems in phaseolus vulgaris L. *S. Afr. J. Bot.* 105, 306–312. doi: 10.1016/j.sajb.2016.03.011
- Tao, M. Q., Jahan, M. S., Hou, K., Shu, S., Wang, Y., Sun, J., et al. (2020). Bitter melon (*Momordica charantia* L.) rootstock improves the heat tolerance of cucumber by regulating photosynthetic and antioxidant defense pathways. *Plants* 9 (6), E692. doi: 10.3390/plants9060692
- Turhan, E., and Ergin, S. (2012). Soluble sugars and sucrose-metabolizing enzymes related to cold acclimation of sweet cherry cultivars grafted on different rootstocks. *Sci. World J.* 2012, 1–7. doi: 10.1100/2012/979682
- Wang, X., and Huang, J. (2015). *Principle and technology of plant physiology and biochemistry experiment (Third edition)* (Beijing: Higher Education Press).
- Wei, Y., Wang, Y., Wu, X. Y., Shu, S., Sun, J., and Guo, S. R. (2019). Redox and thylakoid membrane proteomic analysis reveals the momordica (*Momordica charantia* L.) rootstock-induced photoprotection of cucumber leaves under short-term heat stress. *Plant Physiol. Bioch.* 136, 98–108. doi: 10.1016/j.plaphy.2019.01.010
- Weng, J., Li, P., Rehman, A., Wang, L., Gao, X., and Niu, Q. (2021). Physiological response and evaluation of melon (*Cucumis melo* L.) germplasm resources under

high temperature and humidity stress at seedling stage. *Sci. Hortic.* 288, 10. doi: 10.1016/j.scienta.2021.110317

Xu, Y., Yuan, Y., Du, N., Wang, Y., Shu, S., Sun, J., et al. (2018). Proteomic analysis of heat stress resistance of cucumber leaves when grafted onto momordica rootstock. *Hortic. Res.* 5 (1), 53-71. doi: 10.1038/s41438-018-0060-z

Yang, Y., Lu, X., Yan, B., Li, B., Sun, J., Guo, S., et al. (2013). Bottle gourd rootstock-grafting affects nitrogen metabolism in NaCl-stressed watermelon leaves and enhances short-term salt tolerance. *J. Plant Physiol.* 170 (7), 653-661. doi: 10.1016/j.jplph.2012.12.013

Yuan, L., Tang, L., Zhu, S., Hou, J., Chen, G., Liu, F., et al. (2017). Influence of heat stress on leaf morphology and nitrogen-carbohydrate metabolisms in two wucai (*Brassica campestris* L.) genotypes. *Acta Soc Bot. Pol.* 86 (2), 3554-3570. doi: 10.5586/asbp.3554

Yuan, L., Zhu, S., Li, S., Shu, S., Sun, J., and Guo, S. (2014). 2,4-epibrassinolide regulates carbohydrate metabolism and increases polyamine content in cucumber exposed to  $\text{Ca}(\text{NO}_3)_2$  stress. *Acta Physiol. Plant* 36 (11), 2845-2852. doi: 10.1007/bf03030705

Zhou, Y., Huang, L., Zhang, Y., Shi, K., Yu, J., and Nogués, S. (2007). Chill-induced decrease in capacity of RuBP carboxylation and associated  $\text{H}_2\text{O}_2$  accumulation in cucumber leaves are alleviated by grafting onto figleaf gourd. *Annals. Bot.* 100 (4), 839-848. doi: 10.1093/aob/mcm181

Zhang, Y., Zhang, Y., Yu, J., and Zhou, Y. (2007). Adaptation of Cucurbit Species to Changes in Substrate Temperature: Root Growth, Antioxidants, and Peroxidation. *J. Plant Biol.* 50(5), 527-532.





## OPEN ACCESS

EDITED BY  
Milan Skalicky,  
Czech University of Life Sciences  
Prague, Czechia

REVIEWED BY  
Guanfu Fu,  
China National Rice Research Institute  
(CAAS), China  
Xuwu Sun,  
Henan University, China

\*CORRESPONDENCE  
Wenbang Tang  
✉ tangwenbang@163.com  
Guilian Zhang  
✉ zgl604@163.com

†These authors have contributed  
equally to this work

SPECIALTY SECTION  
This article was submitted to  
Plant Abiotic Stress,  
a section of the journal  
Frontiers in Plant Science

RECEIVED 08 November 2022  
ACCEPTED 05 December 2022  
PUBLISHED 20 December 2022

CITATION  
Zhang Y, Liu X, Su R, Xiao Y, Deng H,  
Lu X, Wang F, Chen G, Tang W and  
Zhang G (2022) 9-*cis*-  
epoxycarotenoid dioxygenase 1  
confers heat stress tolerance in rice  
seedling plants.  
*Front. Plant Sci.* 13:1092630.  
doi: 10.3389/fpls.2022.1092630

COPYRIGHT  
© 2022 Zhang, Liu, Su, Xiao, Deng, Lu,  
Wang, Chen, Tang and Zhang. This is an  
open-access article distributed under  
the terms of the [Creative Commons  
Attribution License \(CC BY\)](#). The use,  
distribution or reproduction in other  
forums is permitted, provided the  
original author(s) and the copyright  
owner(s) are credited and that the  
original publication in this journal is  
cited, in accordance with accepted  
academic practice. No use,  
distribution or reproduction is  
permitted which does not comply with  
these terms.

# 9-*cis*-epoxycarotenoid dioxygenase 1 confers heat stress tolerance in rice seedling plants

Yijin Zhang<sup>1,2†</sup>, Xiong Liu<sup>1,2†</sup>, Rui Su<sup>1,2</sup>, Yunhua Xiao<sup>1,2</sup>,  
Huabing Deng<sup>1,2</sup>, Xuedan Lu<sup>1,2</sup>, Feng Wang<sup>1,2</sup>, Guihua Chen<sup>1</sup>,  
Wenbang Tang<sup>1,2,3,4\*</sup> and Guilian Zhang<sup>1,2\*</sup>

<sup>1</sup>College of Agronomy, Hunan Agricultural University, Changsha, China, <sup>2</sup>Hunan Provincial Key Laboratory of Rice and Rapeseed Breeding for Disease Resistance, Changsha, China, <sup>3</sup>Hunan Hybrid Rice Research Center, Hunan Academy of Agricultural Sciences, Changsha, China, <sup>4</sup>State Key Laboratory of Hybrid Rice, Changsha, China

High temperature is one of the main constraints affecting plant growth and development. It has been reported that abscisic acid (ABA) synthesis gene 9-*cis*-epoxycarotenoid dioxygenase (*NCED*) positively regulates plant resistance to salt, cold, and drought stresses. However, little is known about the function of the *NCED* gene in heat tolerance of rice. Here, we found that *OsNCED1* was a heat stress inducible gene. Rice seedlings overexpressing *OsNCED1* showed enhanced heat tolerance with more abundant ABA content, whereas the knockout mutant *osnced1* accumulated less ABA and showed more sensitive to heat stress. Under heat stress, increased expression of *OsNCED1* could reduce membrane damage and reactive oxygen species (ROS) level of plants, and elevate the activity of antioxidant enzymes. Moreover, real time-quantitative PCR (RT-qPCR) analysis showed that overexpression of *OsNCED1* significantly activated the expression of genes involved in antioxidant enzymes, ABA signaling pathway, heat response, and defense. Together, our results indicate that *OsNCED1* positively regulates heat tolerance of rice seedling by raising endogenous ABA contents, which leads to the improved antioxidant capacity and activated expression of heat and ABA related genes.

## KEYWORDS

rice, seedling, heat stress, ABA, *OsNCED1*

## Introduction

Rice (*Oryza sativa* L.) is a major food crop cultivated in countries around the world, especially in Asia, and feeds more than 50% of the global population. Rising temperature due to global warming has a serious impact on rice production, and the damage may continue to rise in the future, particularly for Asian rice (Qin-Di et al., 2021). Growing

rice above its optimal growth temperature of 5°C results in a corresponding thermal response profile at the cellular and metabolic levels to maintain its own survival and growth (Barnabás et al., 2008). Heat stress is an essential environmental factor limiting rice growth and reproduction, causing different damage to different development stages of rice, and it will suffer from different degrees of heat stress from germination to seedling, anthesis, grain filling, and grain maturation stages (Qin-Di et al., 2021). It has been reported that rice yield decreases by 3.2% for every 1°C increasing in global temperature (Zhao et al., 2017). The difficulty of rice to maintain its normal ontogeny under high temperature conditions, including photosynthesis, respiration, enzyme activity, formation of organs of both sexes, nutrient uptake, and so on, which is the main reason why it affects rice yield (Barnabás et al., 2008).

Absciscic acid (ABA) is a sesquiterpenoid with 15 carbon atoms, which is synthesized indirectly by the carotenoid pathway in plants. The synthetic path of ABA is that zeaxanthin epoxidase (ZEP) catalyzes zeaxanthin (C<sub>40</sub>) to all-trans-violaxanthin, then the neoxanthin synthase (NSY) converts all-trans-violaxanthin to 9'-cis-neoxanthin, and finally the *cis* isomer is cracked by 9-cis-epoxycarotenoid dioxygenase (NCED) and product C<sub>15</sub> xanthotoxin, which is an important step of ABA biosynthesis (Chen et al., 2020). ABA plays a crucial role in regulating plant stress responses. Its biosynthesis is induced by several environmental stresses, such as drought, salt, and cold stress (Nambara and Marion-Poll, 2005). Studies have shown that the bloating germination of *Arabidopsis thaliana* seeds at elevated temperatures is associated with the induction of elevated ABA levels by the zeaxanthin epoxidase gene *ABA1* and the three 9-cis-epoxycarotenoid dioxygenase genes *NCED2*, *NCED5* and *NCED9* (Toh et al., 2008). Heat stress decreases auxin and gibberellin content, and increases endogenous ABA content in rice anthers (Tang et al., 2007). Exogenous ABA maintains carbon and energy balance of rice by increasing sucrose transport and accelerating sucrose metabolism, to prevent pollen abortion under heat stress, and improve seed setting rate (Rezaul et al., 2019). The bZIP transcription factor gene of the ABA signaling pathway, *ZmbZIP4*, can regulate ABA synthesis related genes to promote the synthesis of ABA to improve high temperature tolerance in maize (*Zea mays*) seedlings (Ma et al., 2018). The above findings indicate that ABA is involved in plant response to high-temperature stress, but the underlying mechanism of the effect of heat stress on endogenous ABA content in rice is still unclear.

9-cis-epoxycarotenoid dioxygenase (NCED) is a key rate limiting enzyme in ABA biosynthesis, and its activity affects endogenous ABA accumulation in plants (Kalladan et al., 2019). Overexpression of *NCED* promotes ABA synthesis in response to various abiotic stresses (Zhang et al., 2014; Huang et al., 2018), whereas knockdown of *NCED* reduces ABA accumulation, and

shows abiotic stress sensitive (Frey et al., 2012). The first *NCED* gene to be discovered was *viviparous 14* (*VP14*) in a maize mutant (Nambara and Marion-Poll, 2005), and *NCED* genes were subsequently isolated from other plant species, such as tomato (*Solanum lycopersicum*), *Arabidopsis*, and apple (Huang et al., 2018).

There are five members of the *NCED* family in rice, *OsNCED1*, *OsNCED2*, *OsNCED3*, *OsNCED4* and *OsNCED5* (Zhu et al., 2009). *OsNCED1* expression is elevated by salt and drought stress but repressed by water stress (Huang et al., 2018; Jiang et al., 2019). It has also been shown that the cis-acting element ABRE region exists in the *AhNCED1* promoter, and ABA treatment under water stress can increase promoter activity, promote *AhNCED1* gene and protein expression, and promote ABA synthesis to enhance water stress (Liang et al., 2009), and that the ectopic expression of *AhNCED1* will improve ABA accumulation to improve water stress tolerance in *Arabidopsis* plants (Wan and Li, 2006). In addition, *OsNCED1* could indirectly regulate the seed setting rate of rice under low temperature stress at flowering stage by regulating ABA metabolic pathway (Huang et al., 2018). Both *OsNCED2* and *OsNCED3* expression levels correlate with delayed seed germination (Zhu et al., 2009; Song et al., 2012). *OsNCED3* regulates seed dormancy, stomatal opening, plant growth and leaf senescence by altering ABA accumulation in rice (Huang et al., 2018). In addition, *OsNCED3*, *OsNCED4* and *OsNCED5* induce the expression and promote ABA production under water stress, which would affect plant growth and water stress (Teng et al., 2014; Zhang et al., 2015). We have reported that overexpression of *OsNCED1* improved high temperature stress tolerance at heading and anthesis stages of rice (Zhou et al., 2022). However, the roles of *OsNCED1* under heat stress in rice seedling stage remains unclear.

At present, little is known about the function of genes involved in the ABA synthesis pathway and signal regulation pathway in heat stress responses in rice. In this study, we constructed *OsNCED1* overexpressing and gene edited transgenic rice plants, and aimed to explore the biological function of *OsNCED1* under heat stress at the seedling stage of rice.

## Materials and methods

### Plant materials

The rice japonica variety Nipponbare (Nip), *OsNCED1* overexpression lines (Nip), 252 and *osnced1* mutants (252) were used in this study. 252 was an extreme heat tolerant individual of the recombinant inbred lines derived from a cross between the heat-tolerant rice line 996 and the sensitive line 4628. The overexpression vectors (pCAMBIA1300-*OsNCED1*) and gene editing vectors (pBWA(V)HU-ylcas9-

*osnced1*) were constructed, and respectively transformed into *Agrobacterium tumefaciens* EHA105, and then introduced into Nip and 252 plants. Positive transgenic lines were selected and further identified by PCR and real time-quantitative PCR. Overexpression lines (*OE-1* and *OE-2*) with higher transcript levels were used for further analysis, and *osnced1* mutants (*ko-1* and *ko-2*) were also obtained for further analysis by sequencing.

## High temperature treatment

Seeds of wild-type (Nip and 252), *OsNCED1* overexpression lines (*OE-1* and *OE-2*), and *osnced1* mutants (*ko-1* and *ko-2*) were soaked in water at 37°C for 2 d, and sown in a rice seedling box in light incubator, with the temperature was 25°C, the light intensity was 30000 lux, the light cycle was 12/12 h (light/dark), and the relative humidity was 70%, and germinated for 8 d. Subsequently, 8-day-old transgenic lines and wild-type (WT) were transferred to a light incubator at 45°C for 48 h, and moved to a light incubator with 25°C for recovery. Corresponding WT and transgenic lines were grown in a 25°C light incubator and were set as controls. After 7 days of recovery, the phenotypes of the treated and control plants were photographed and the survival rate of seedling was counted. Four biological replicates were performed for each treatment, and 30 seedlings were replicated for each treatment.

## Measurement of abscisic acid content

Eight-day-old transgenic lines and WT rice plants were transferred to a light incubator at 45°C for 48 h, while the corresponding WT and transgenic seedlings were placed in a light incubator with 25°C as controls. The corresponding WT and transgenic plants were sampled for the determination of ABA content before and 48 h after treatment, and the determination method was referred to the method as described previously (Huang et al., 2018). Briefly, 0.1 g of fresh plants was extracted with 1.5 ml of phytohormone extraction buffer and 2 ng of ABA-d6 internal standard was added, then sample was freeze-dried in nitrogen for 2 times. The ABA levels were quantified by liquid chromatography-tandem mass spectrometry (LC-MS/MS).

## Measurement of physiological indexes

Eight-day-old transgenic lines and WT rice seedlings were treated in a light incubator and exposed to heat stress (45°C) for 48 h, and those in a light incubator at 25°C served as controls. After 48 h of treatment, plants under high temperature stress and control conditions were used for the determination of relative electrolyte leakage rate, malondialdehyde (MDA) content, hydrogen peroxide (H<sub>2</sub>O<sub>2</sub>) content and superoxide

anion (O<sub>2</sub><sup>•−</sup>) content, superoxide dismutase (SOD) activity, peroxidase (POD) activity, and three biological replicates were performed. The electrolyte leakage rate conductivity of heat-treated and control plants was measured by the conductivity meter (DS-11A), the MDA content was measured by the thiobarbituric acid (TBA) colorimetric method, the SOD activity was measured by the riboflavin nitro blue tetrazolium (NBT) method, and the POD activity was measured by the guaiacol method. The electrolyte leakage rate, MDA content and antioxidant enzyme activities were determined by the method of Zhou et al. (2022), with a slight modification. Referring to the method of Sun et al. (2019), 3,3-diaminobenzidine (DAB) and nitro blue tetrazolium were used to detect the accumulation of H<sub>2</sub>O<sub>2</sub> and O<sub>2</sub><sup>•−</sup> in the leaves of plants. The content of H<sub>2</sub>O<sub>2</sub> and O<sub>2</sub><sup>•−</sup> of high temperature treated and control plants were determined using kits (BC3595, Solarbio).

## Quantitative real-time PCR analysis

The WT plants treated with high-temperature for 0 h, 2 h, 4 h, and 8 h, the transgenic and WT plants of high-temperature treated for 48 h and the control were collected, and the corresponding RNA was extracted after snap freezing with liquid nitrogen. RT-qPCR was used to determine the expression levels of *OsNCED1* along with the transcript levels of genes involved in antioxidant enzymes, ABA signaling pathway, heat response, and defense. Total RNA extraction was performed using RNA easy isolation reagent (R701-01, Vazyme) and was reverse transcribed for qPCR analysis using the HiScript<sup>®</sup> II Q RT SuperMIX for RT-qPCR (+gDNA wiper) kit (R223-01, Vazyme). Rice *OsActin1* was used as an internal reference gene, and primers for amplification were designed by Primer Premier 6.0. The relative changes in gene expression levels were quantitated based on three biological replicates via the 2<sup>−ΔΔCt</sup> method.

## Statistical analysis

All experiments were conducted in three biological replicates. Data are presented as mean ± SE, and statistical analysis was performed using DPS (version 7.05). Data were analyzed by one-way ANOVA and it was considered statistically significant at  $p < 0.05$ ,  $p < 0.01$ . Plotted using GraphPad Prism (version 8.01).

## Results

### Response of *OsNCED1* to heat stress at rice seedling stage

In our previous study, the quantitative proteomics technology of iTRAQ quantitative marker combined with LC-

MS/MS analysis was used to compare and analyze the difference of anther protein expression between heat tolerant rice line 996 and heat sensitive rice line 4628 under heat stress, and it was found that *OsNCED1* was significantly upregulated (Zhou et al., 2022). In order to further explore the response of *OsNCED1* to heat stress at rice seedling stage, RT-qPCR was used to detect the expression level of *OsNCED1* in seedling of Nip and 252, an extreme heat tolerant individual, at 45°C for 0 h, 2 h, 4 h, 8 h and 48 h. Upon heat stress, the expression of *OsNCED1* increased significantly in Nip and 252, peaked at 4 h and then decreased at 8 h of the heat stress (Figures 1A, B). These results indicated that *OsNCED1* responded to heat stress and its expression was strongly induced.

### Effects of heat stress on survival rate and endogenous ABA content of *OsNCED1* transgenic and WT seedlings

In order to study the role of *OsNCED1* in heat stress, two mutants, *ko-1* and *ko-2*, were constructed in the background of 252 (Figure 2A; Supplementary Figure 1). The *ko-1* and *ko-2* had two different mutation sites in the *OsNCED1* exons, which caused premature termination of *OsNCED1* protein. The overexpression lines *OE-1* and *OE-2* of *OsNCED1* were constructed in the background of Nip. And the expression levels of the overexpression lines *OE-1* and *OE-2* were 50.9 times and 30.9 times higher than that of Nip, respectively (Figure 2B). As shown in Figures 2C, D, upon heat stress, the survival rate of Nip was significantly lower than that of the two overexpression lines (*OE-1* and *OE-2*), while the survival rate of 252 was significantly higher than that of the two mutants (*ko-1*

and *ko-2*). Under the control conditions, there is no significant difference between transgenic plants and corresponding WT (Figure 2D). The results showed that *OsNCED1* positively regulated the heat stress of rice seedlings.

ABA is in a dynamic equilibrium in response to physiological changes and stimuli from the external environment in plants. NCED is a key rate limiting enzyme for ABA biosynthesis, and affects the accumulation of endogenous ABA (Kalladan et al., 2019). The ABA content under control and heat stress revealed that the ABA levels of the overexpression lines *OE-1* and *OE-2* under control conditions were 13.5 ng/g and 12.4 ng/g, respectively, and significantly higher than that of Nip (6.4 ng/g), whereas the ABA levels of the mutants *ko-1* and *ko-2* were 6.2 ng/g and 5.9 ng/g, respectively, and significantly lower than that of 252 (12.9 ng/g) (Figure 2E). The ABA contents of the transgenic and WT plants were significantly increased under heat stress, indicating that heat tolerance of rice might be improved by increasing the ABA content. Thus, *OsNCED1* might improve the tolerance to heat stress by affecting the accumulation of endogenous ABA in rice.

### Changes in membrane lipid peroxidation and antioxidant enzyme activities in *OsNCED1* transgenic and WT seedlings under heat stress

To reveal the underlying physiological mechanism which *OsNCED1* improves heat tolerance in rice, MDA content, relative electrolyte leakage rate, SOD activity and POD activity of *OsNCED1* transgenic and WT seedling were measured under heat stress. Malondialdehyde can reflect the rate and intensity of peroxidation of plant membrane lipids, and can also indirectly

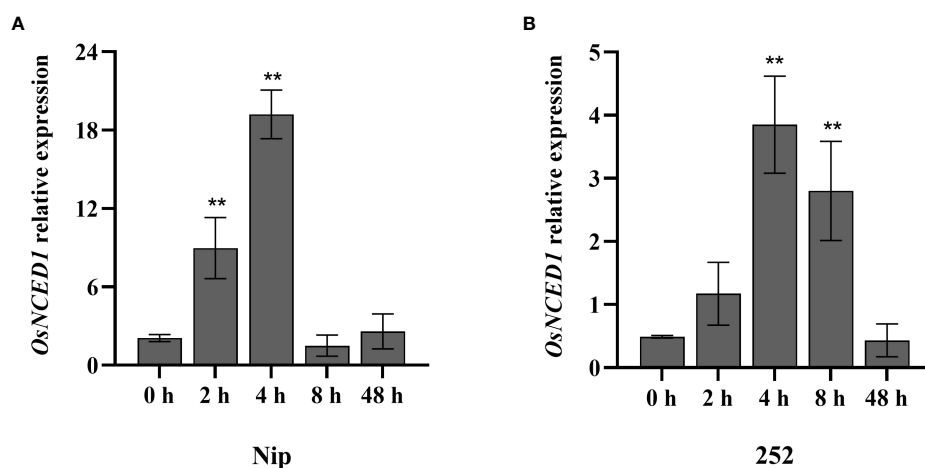


**FIGURE 1**  
Transcript level of *OsNCED1* in Nip and 252 under heat stress. (A) Transcript level of *OsNCED1* in Nip under heat stress. (B) Transcript level of *OsNCED1* in 252 under heat stress. Data are means  $\pm$  SD ( $n = 3$ ; \*\* $P < 0.01$ , Student's  $t$ -test).

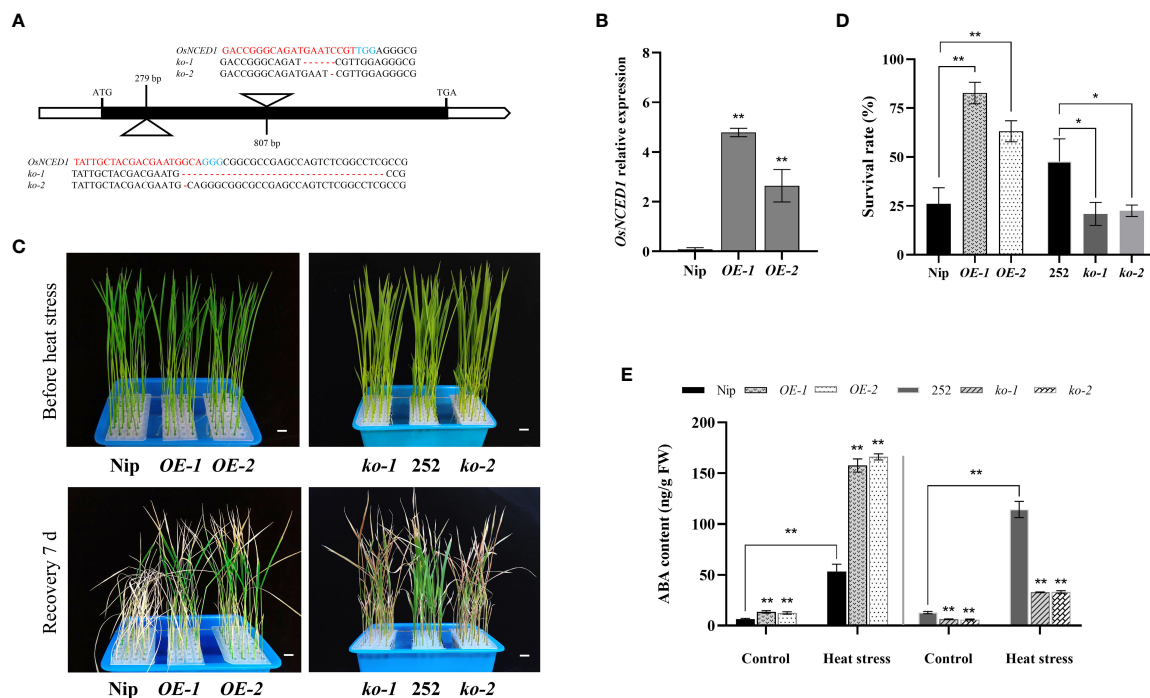


FIGURE 2

Phenotypic analyses of *OsNCED1* transgenic lines under heat stress. (A) The diagram of the two CRISPR/Cas9 target sites, and nucleotide mutation sequences of *ko-1* and *ko-2* lines. The base pairs in blue indicated protospacer adjacent motif (PAM), and the red represented small guide RNA (sgRNA) sequence. (B) Real-time quantitative PCR analysis of *OsNCED1* in *OsNCED1* overexpression lines *OE-1* and *OE-2*. Data are means  $\pm$  SD ( $n = 3$ ;  $^{**}P < 0.01$ , Student's *t*-test). (C) Phenotypes of two WT and *OsNCED1* transgenic rice seedlings before heat stress and 7 days after moderate temperature recovery. Bars = 1 cm. (D) Survival rates (%) of two WT and *OsNCED1* transgenic lines after heat stress for 48 h. Data are means  $\pm$  SD ( $n = 4$ ;  $^{*}P < 0.05$ ,  $^{**}P < 0.01$ , Student's *t*-test). (E) Endogenous ABA content in WT and *OsNCED1* transgenic lines under control and heat stress. Data are means  $\pm$  SD ( $n = 3$ ;  $^{*}P < 0.01$ , Student's *t*-test).

reflect the potential antioxidant capacity of plant cells (Rezaul et al., 2019). Relative electrolyte leakage rate conductivity is an important parameter to examine the membrane permeability of plant cells under abiotic stress (Huang et al., 2018). Under control conditions, there was no significant difference in MDA content and relative electrolyte leakage rate between transgenic and WT seedlings (Figures 3A, B). After 48 h of heat stress, the MDA content in both transgenic and WT seedlings increased significantly, but the increase of MDA content and relative electrolyte leakage rate of overexpression lines were significantly lower than that of Nip (Figures 3A, B), whereas the increase in the MDA content and relative electrolyte leakage rate of the mutants was significantly higher than that of 252, indicating that the increase in *OsNCED1* can reduce membrane damage in plants under heat stress.

Next, the activities of SOD and POD of transgenic and WT seedlings under heat stress were measured. As shown in Figures 3C, D, after 48 h of heat stress, the WT and transgenic lines showed higher activities of both antioxidative enzymes than that of the control, and the increases in antioxidative enzyme activities were significantly greater in the *OE-1* and *OE-2* lines than that of Nip, and the activities of antioxidant enzymes in *ko-*

*1* and *ko-2* lines were significantly lower than that of 252. These results suggested that *OsNCED1* could enhance seedling antioxidant enzyme activities under heat stress and attenuated membrane damage upon heat stress in rice seedling.

## Changes in reactive oxygen species levels in *OsNCED1* transgenic and WT seedlings under heat stress

To examine whether *OsNCED1* confers stress resistance to ROS, the accumulation of  $H_2O_2$  and  $O_2^-$  was examined under heat stress. The DAB and NBT staining result showed no obvious difference between the transgenic and WT seedling leaves under control conditions, whereas the leaves of the overexpression lines *OE-1* and *OE-2* seedlings under high-temperature stress stained lighter than that of Nip, whereas the leaves of the mutants *ko-1* and *ko-2* seedlings stained darker than that of 252 (Figures 4A, B).

Further the determination result of  $H_2O_2$  content and  $O_2^-$  content of *OsNCED1* transgenic and WT seedlings showed that Nip accumulated significantly more  $H_2O_2$  and  $O_2^-$  than that of



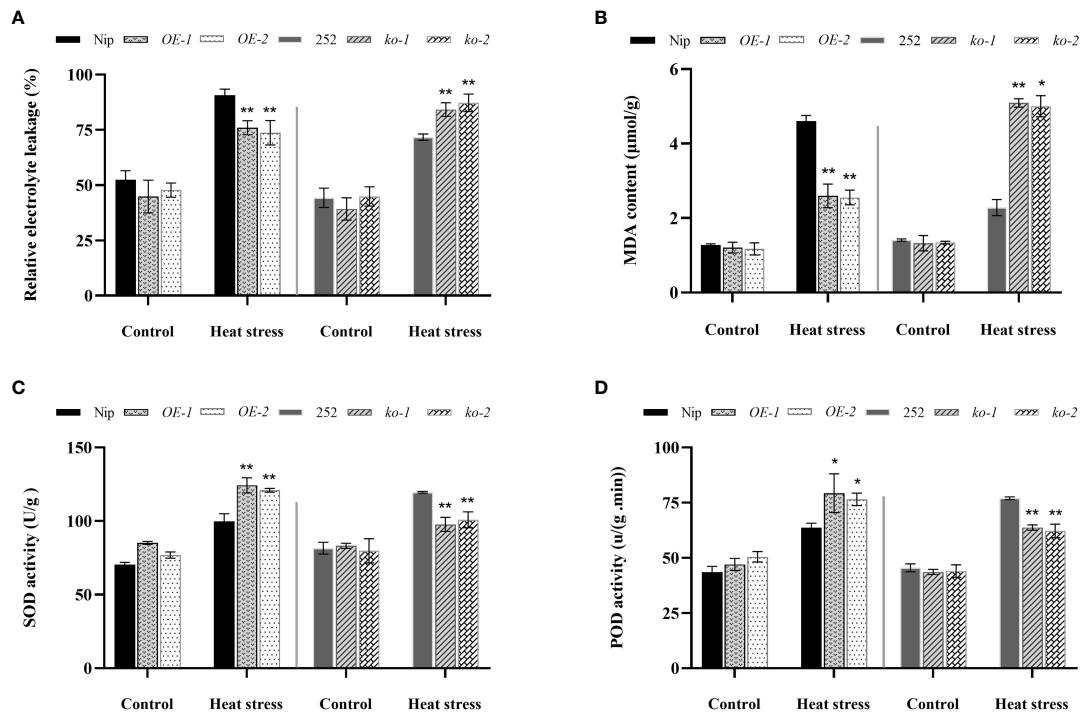


FIGURE 3

Changes in membrane lipid peroxidation and antioxidant enzyme activities in the transgenic lines and WT plants under heat stress. The electrolyte leakage rate (A) and MDA content (B) and SOD activity (C) and POD activity (D) in transgenic lines and WT after 48 h heat stress. Data are means  $\pm$  SD ( $n = 3$ ; \* $P < 0.05$ , \*\* $P < 0.01$ , Student's  $t$ -test).

overexpression lines *OE-1* and *OE-2*, and the  $H_2O_2$  content in Nip was 43% and 46% higher than that of overexpression lines *OE-1* and *OE-2*, respectively; the  $O_2^-$  content was 48% and 61% higher than that of overexpression lines *OE-1* and *OE-2*, respectively (Figures 4C, D). In addition, the accumulation of  $H_2O_2$  and  $O_2^-$  in 252 was significantly lower than that of the mutants, the  $H_2O_2$  content was 57% and 54% lower than that of the mutants *ko-1* and *ko-2*, respectively; the  $O_2^-$  content was 52% and 65% lower than that of the mutants *ko-1* and *ko-2*, respectively (Figures 4C, D). The results indicated that *OsNCED1* positively regulated plant antioxidant resistance under heat stress, and its overexpression could alleviate oxidative damage under heat stress.

## Transcriptional changes of antioxidant and defense related genes in *OsNCED1* transgenic and WT seedlings under heat stress

To elucidate the potential molecular mechanism of *OsNCED1* for heat tolerance, the transcript levels of several antioxidant and defense related genes in the transgenic and WT plants under control and heat stress conditions were detected by

RT-qPCR assays. These genes included three antioxidant genes (catalase encoding gene *OsCATB*, superoxide dismutase gene *Fe<sup>+</sup>SOD*, and ascorbate peroxidase *OsASP1*) (Feng et al., 2006; Ye et al., 2011; Li et al., 2015) and three defense genes (stress-responsive NAC transcription factor gene *osSNAC1*, AP2/EREBP transcription factor *OsDREB2A*, and late embryogenesis abundant enriched protein gene *OsLEA3*) (Hu et al., 2006; Xiao et al., 2007; Zhang et al., 2013), which had been shown to play critical roles in protecting rice against abiotic stress.

As shown in Figures 5A–C, there was no obvious difference in antioxidant genes between WT and transgenic lines seedlings under control conditions, but under heat stress, both WT and transgenic seedlings showed upregulated expression of antioxidant genes, especially *OsCATB*. Compared with Nip, the transcript levels of the three antioxidant related genes were significantly upregulated in the overexpression lines; the transcript levels of antioxidant related genes were significantly downregulated in the mutants compared to 252. Subsequently, the expression levels of three defense genes, *OsSNAC1*, *OsDREB2A* and *OsLEA3*, in the WT and *OsNCED1* transgenic lines under heat stress were examined. As shown in Figures 5D–F, the transcript levels of the three defense related genes were significantly higher in the overexpression lines than that of Nip

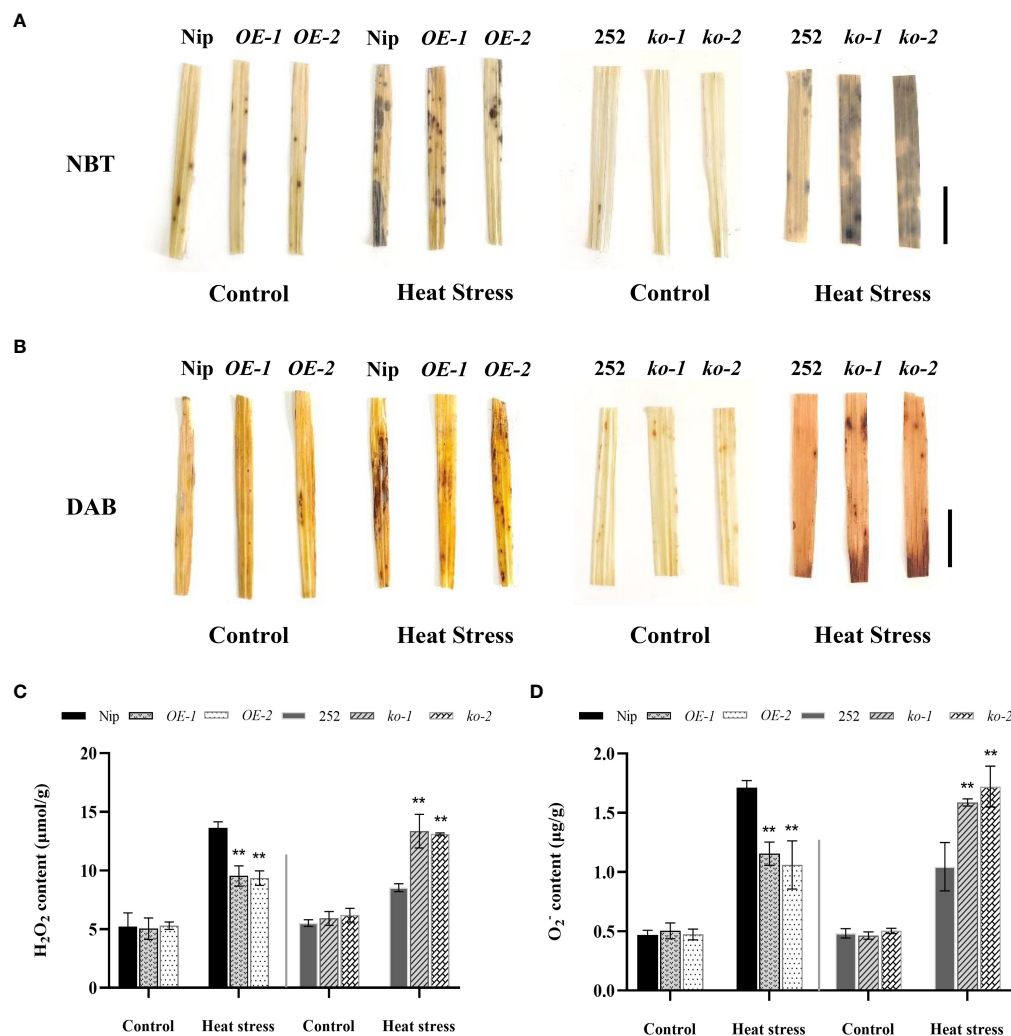


FIGURE 4

Accumulation of H<sub>2</sub>O<sub>2</sub> and O<sub>2</sub><sup>-</sup> in seedlings under heat stress. (A) O<sub>2</sub><sup>-</sup> production in leaf discs of WT and transgenic lines upon heat exposure. Bar = 1 cm. (B) H<sub>2</sub>O<sub>2</sub> accumulation in leaf discs of WT and transgenic lines upon heat exposure. Bar = 1 cm. (C) Quantitative measurement of total H<sub>2</sub>O<sub>2</sub> content in WT and transgenic lines upon heat exposure. (D) Quantitative measurement of total O<sub>2</sub><sup>-</sup> content in WT and transgenic lines upon heat exposure. Data are means ± SD (n = 3; \*\*P < 0.01, Student's t-test).

under heat stress, with *OsLEA3* upregulation being the most significant. The transcript levels of defense related genes in the two mutants were significantly lower than that of 252. These data suggested that *OsNCED1* induced the expression of antioxidant and defense related genes under heat stress.

### Transcriptional changes of genes related to heat and ABA responses in *OsNCED1* transgenic and WT seedlings under heat stress

The main function of HSPs was to regulate the folding and unfolding of proteins, as well as their subcellular localization and

degradation of unfolded and denatured proteins (Singh et al., 2016). SLG1 is able to interact with cytoplasmic tRNA 2-thiolated protein 1 (RCTU1) in rice to regulate tRNA thiolation levels and thus positively regulate rice heat tolerance (Xu et al., 2020). Therefore, the expression of HSPs genes and *SLG1* in *OsNCED1* transgenic and WT seedlings under heat stress was examined using RT-qPCR. As shown in Figures 6A–C, the transcript levels of *OsHSP70*, *OsHSP90* and *SLG1* of the overexpression lines were significantly higher than that of WT under 48 h heat stress, and the transcript levels of genes related to heat tolerance in the two mutants were significantly lower than that of 252. In contrast, there were no significant difference in the expression levels of these heat tolerance related genes between WT and transgenic lines under control conditions.

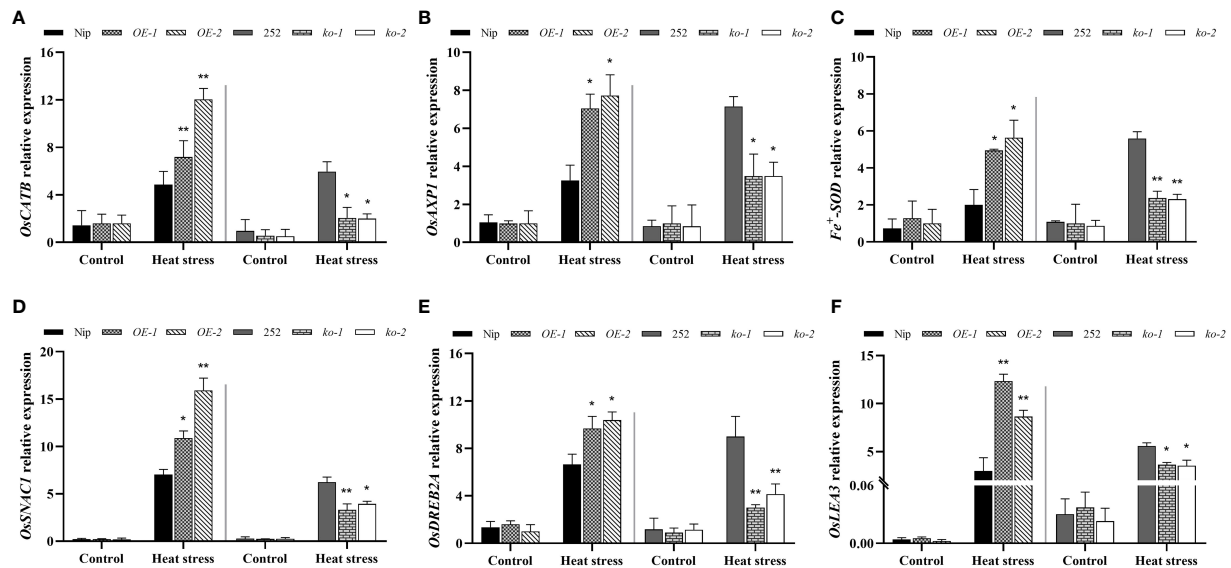


FIGURE 5

Transcriptional expression of antioxidant and defense related genes in seedlings of WT and transgenic lines under heat stress. Three antioxidant genes transcript levels of *OsCATB* (A), *OsAXP1* (B), and *Fe<sup>+</sup>SOD* (C). Seedlings of WT and transgenic lines were subjected to heat stress at 45°C for 48 h, and leaves were harvested for RNA extraction, cDNA synthesis and RT-qPCR analysis. For each RT-qPCR, rice reference gene *OsActin1* was used as a control to detect its transcript levels in different samples. Data are means  $\pm$  SD ( $n = 3$ ; \* $P < 0.05$ , \*\* $P < 0.01$ , Student's  $t$ -test). Three defense genes transcript levels of *OsSNAC1* (D), *OsDREB2A* (E), and *OsLEA3* (F). Data are means  $\pm$  SD ( $n = 3$ ; \* $P < 0.05$ , \*\* $P < 0.01$ , Student's  $t$ -test).

*OsNCED1* is involved in ABA biosynthesis, so the transcriptional change of ABA responsive genes between the transgenic lines and WT plants under heat stress was investigated. These ABA responsive genes included *OsbZIP46* (ABRE binding protein), *OsABI5* (ABRE binding factor), and *OsSAPK10* (stress-activated protein kinase), which have been shown to be involved in ABA responsive responses (Zou et al., 2008; Yang et al., 2011; Wang et al., 2020). As shown in Figures 6D–F, the transcript levels of the three ABA responsive genes in the overexpression lines showed greater upregulation under heat stress than that of Nip, and the mutants were upregulated less than 252. These results indicated that *OsNCED1* positively activated the expression of heat responsive genes and ABA responsive genes under heat stress.

## Discussion

Temperature is an important factor affecting rice growth and yield quality. With global warming, it is extremely important to understand how plants respond to high temperatures and breed high temperature tolerant rice varieties. Temperature of 10–15°C above ambient was generally considered as heat shock or heat stress in plants (Liu et al., 2018), whereas heat tolerance was the ability of plants to cope with heat stress, that was, the ability of plants to survive in an environment growing above the most

suitable temperature (Liu et al., 2016). The optimal growth temperature at the seedling stage of rice was 25–28°C, and heat stress at seedling stage (42–45°C) lead to increased water loss, leaf wilting and yellowing, impaired root growth, and severe or even seedling death (Liu et al., 2016; Liu et al., 2018). In this study, we showed that overexpression of *OsNCED1* increased the heat tolerance of rice seedlings, while *osnced1* seedlings exhibited reduced heat tolerance (Figure 2), indicating that *OsNCED1* positively regulates heat stress tolerance in rice seedling plants.

ABA is a hormone that is often involved in the stress response of plants. When subjected to abiotic stresses such as cold, drought and high temperature et al., plants will rapidly accumulate ABA to activate various stress responses. For example, ABA in grapes alleviated hyperthermic damage by increasing the accumulation of osmoregulation substances and endogenous hormone content (Lv et al., 2022). And *SlSnRK2.3* regulated ABA signaling pathway regulates stomatal movement under heat stress to improve the heat tolerance in tomato (Li et al., 2022). Moreover, brassinosteroids enhanced tolerance of canola seedlings to heat stress might be due to the induction of elevated endogenous ABA concentrations (Kurepin et al., 2008). It had also been shown in rice that the application of exogenous ABA alleviated pollen sterility under high-temperature stress and was responsible for improving heat tolerance in rice by promoting sucrose transport and metabolism in spikelets, antioxidant enzyme activity, maintaining carbon balance and

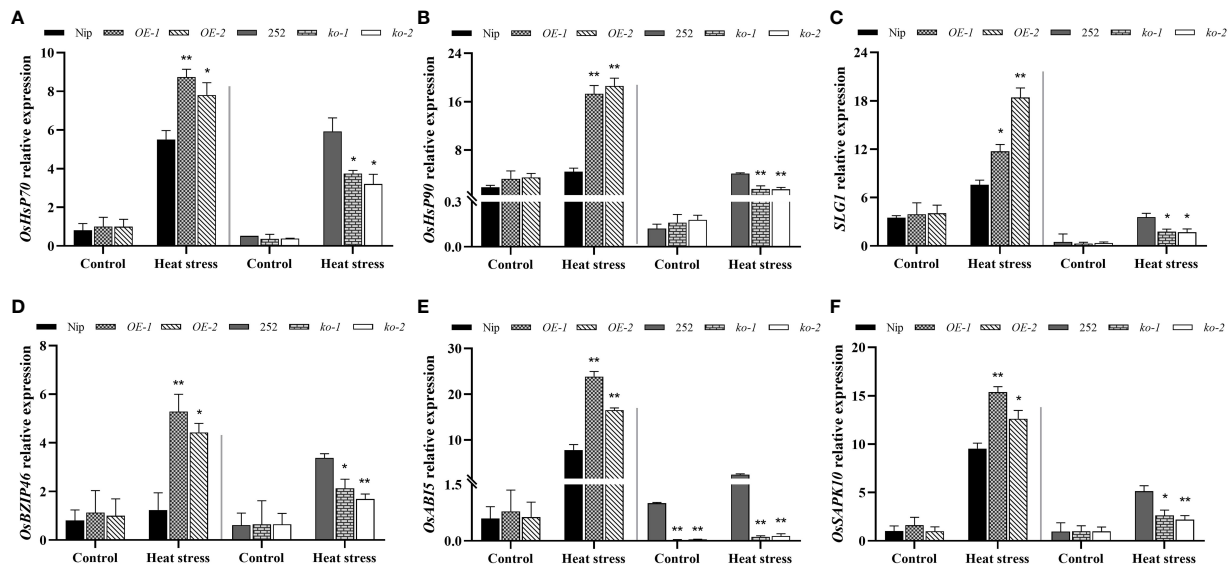


FIGURE 6

Transcriptional expression of heat tolerance and ABA related genes in WT and transgenic lines under heat stress. Three heat tolerance genes transcript levels of *OsHSP70* (A), *OsHSP90* (B), and *SLG1* (C). Seedlings of WT and transgenic lines were subjected to heat stress at 45°C for 48 h, and leaves were harvested for RNA extraction, cDNA synthesis and RT-qPCR analysis. For each RT-qPCR, rice reference gene *OsActin1* was used as a control to detect its transcript levels in different samples. Data are means  $\pm$  SD ( $n = 3$ ; \* $p < 0.05$ , \*\* $p < 0.01$ , Student's  $t$ -test). Three heat ABA related genes transcript levels of *OsbZIP46* (D), *OsABI5* (E), and *OsSAPK10* (F). Data are means  $\pm$  SD ( $n = 3$ ; \* $p < 0.05$ , \*\* $p < 0.01$ , Student's  $t$ -test).

energy balance (Rezaul et al., 2019). And high temperature stress promoted ABA accumulation to regulate seed germination (Liu et al., 2019). *NCED* genes contributed to higher ABA levels, and increased abiotic stress tolerance in plants (Bang et al., 2013). Our results suggested that *OsNCED1* enhanced rice seedling heat tolerance, possibly by regulating the endogenous ABA content. The reasons were as follows: firstly, the transcript levels of *OsNCED1* in both WT plants were rapidly induced under heat stress (Figure 1). Secondly, ABA content of transgenic plants and WT increased after heat stress; while ABA content of the overexpression lines were significantly higher than that of Nip, and ABA content in *osnced1* were lower than that in 252 (Figure 2). Thirdly, the transcript levels of ABA related genes were significantly upregulated in the overexpression lines under heat stress (Figures 5, 6). In support of this idea, previous reports had shown that ABA improved heat tolerance by inducing the accumulation of several HSPs, including HSP70 and HSP90 in plants (Li et al., 2014). There were also reports indicating that the expression of *OsLEA3* in rice seedlings was induced by ABA (Xiao et al., 2007). And *OsbZIP46* was involved in ABA signaling and abiotic stress response (Yang et al., 2011).

ROS were harmful substances reflecting oxidative metabolism. Both ROS production and scavenging affected protein, fat and nucleic acid damage and cell death (Raja et al., 2017). So, the dynamic balance of ROS was especially important for plant growth and development. Efficient enzymatic and

nonenzymatic antioxidant defense systems play an important role in scavenging ROS, reducing membrane lipid peroxidation, maintaining ROS dynamic balance and redox signals (Hasanuzzaman et al., 2018). SOD dismutates superoxide to hydrogen peroxide, while peroxidases (PODs) further decompose hydrogen peroxide to water and molecular oxygen (Wang et al., 2016). MDA accumulation and the electrolyte leakage rate well reflected the degree of cell damage. In this study, the activities of SOD and POD were increased in both the transgenic and WT seedling under heat stress, and among them, the *OsNCED1* overexpression lines showed higher SOD activity and POD activity, lower MDA content, electrolyte leakage rate and  $O_2^-$  content than Nip, thereby decreased cell membrane damage and oxidative stress, whereas the knockout lines happened to do the opposite, resulting in its poor survival (Figures 3, 4). Consistent with the antioxidant enzyme activities, we detected that the *OsNCED1* overexpression lines showed a significant upregulation in the transcript levels of the antioxidant related genes *OsCATB*, *Fe<sup>+</sup>SOD* and *OsAXP1* under heat stress, and the *osnced1* mutants, although somewhat upregulated, it was not upregulated as much as 252 (Figure 5). Therefore, *OsNCED1* overexpression lines might be to maintain the structure and function of cells under heat stress by regulating their own enzyme system activity and content of osmotic protective substances to scavenge toxic substances such as free radicals. Consistent with this paper, it was reported that

copper/zinc superoxide dismutase 1 (*CSD1*) and *CSD2* in *Arabidopsis* altered the redox status and scavenged ROS of cells to regulate heat tolerance (Guan et al., 2013). Similarly, there was also evidence that transgenic potatoes overexpressing *CuZnSOD* and *APX* had higher tolerance to high temperature and oxidative stress (Kim et al., 2010). On the contrary, the loss of *AXP1* and *CAT2* reduced the tolerance of *Arabidopsis* to high temperature stress (Vanderauwera et al., 2011). Reports had suggested that ABA in plants actively participated in antioxidant defense mechanisms through various MAPK cascades, such as ABA transiently activates MPK6 to regulate the expression of catalase 1 (*CAT1*), and maintaining ROS homeostasis (Raja et al., 2017).

Acting as a second messenger of ROS generating signals,  $H_2O_2$  has a dual role in regulating plant physiological processes, since low concentrations of  $H_2O_2$  initiate various signals in cells, whereas high concentrations of  $H_2O_2$  cause oxidative damage (Quan et al., 2008; Gill and Tuteja, 2010). ABA as a stress signal plays an important role in abiotic stresses, but there are different claims about the interaction between  $H_2O_2$  and ABA under abiotic stress. Our study showed that high-temperature treatment elevated endogenous ABA in the overexpression plants (Figure 2E), accompanied by reduced  $H_2O_2$  content (Figures 4B, C), reduced oxidative damage, to improve heat tolerance at the seedling stage of rice. Consistent with our results, *OsASR6* interacted with *OsNCED1* to enhance endogenous ABA content and reduce  $H_2O_2$  accumulation to improve rice salt tolerance (Zhang et al., 2022). In addition, the ABA accumulation in the *OsIAA18* overexpressing rice seedlings was significantly higher than that in WT under both salt and drought stress, and the genes of ABA synthesis and signaling pathways were also evidently upregulated, along with obviously lower level of  $H_2O_2$  and improved salt and drought (Wang et al., 2021). However, it has been shown that, under drought conditions, ABA induces ROS production and increases  $H_2O_2$  content in *Arabidopsis* guard cells, which activates calcium ion channels to promote stomatal closure and reduces water loss (Pei et al., 2000). It has also been shown that exogenous ABA induces  $H_2O_2$  production via *OsDMI3* in rice zhonghua11 (Shi et al., 2012). We speculated that *OsNCED1* in this study might reduce membrane damage and ROS levels in plants under heat stress by regulating ABA content. However, the exact role of *OsNCED1* in ROS homeostasis under heat stress requires further investigation. Our study provides a valuable resource for the potential exploitation of *OsNCED1* in the genetic improvement of heat tolerance in rice. Future studies on *OsNCED1* will include determining how other genes, together with *OsNCED1*, are involved in other physiological functions not observed in *osnced1* mutants. In addition, other novel regulatory functions of *OsNCED1* can be investigated by identifying its interacting proteins.

## Data availability statement

The original contributions presented in the study are included in the article/Supplementary Material. Further inquiries can be directed to the corresponding authors.

## Author contributions

YZ and XiL: investigation, writing-original draft. WT and GZ: conceptualization, supervision. RS and XuL: formal analysis. FW, HD, YX, GC and GZ: writing-review and editing. All author contributed to the article and approved the submitted version.

## Funding

This research was funded by the National Natural Science Foundation of China (31871599 and 31901528), the Natural Science Foundation of Hunan province (2021JJ30350), the Double first-class construction project of Hunan Agricultural University (SYL2019007), and the Hunan postgraduate scientific research innovation project (CX20200672). The APC was funded by the National Natural Science Foundation of China.

## Conflict of interest

The authors declare that the research was conducted in the absence of any commercial or financial relationships that could be construed as a potential conflict of interest.

## Publisher's note

All claims expressed in this article are solely those of the authors and do not necessarily represent those of their affiliated organizations, or those of the publisher, the editors and the reviewers. Any product that may be evaluated in this article, or claim that may be made by its manufacturer, is not guaranteed or endorsed by the publisher.

## Supplementary material

The Supplementary Material for this article can be found online at: <https://www.frontiersin.org/articles/10.3389/fpls.2022.1092630/full#supplementary-material>



## References

- Bang, S. W., Park, S. H., Jeong, J. S., Kim, Y. S., Jung, H., Ha, S. H., et al. (2013). Characterization of the stress-inducible OsNCED3 promoter in different transgenic rice organs and over three homozygous generations. *Planta* 237, 211–224. doi: 10.1007/s00425-012-1764-1
- Barnabás, B., Jäger, K., and Fehér, A. (2008). The effect of drought and heat stress on reproductive processes in cereals. *Plant Cell Environ.* 31, 11–38. doi: 10.1111/j.1365-3040.2007.01727.x
- Chen, K., Li, G. J., Bressan, R. A., Song, C. P., Zhu, J. K., and Zhao, Y. (2020). Abscisic acid dynamics, signaling, and functions in plants. *J. Integr. Plant Biol.* 62, 25–54. doi: 10.1111/jipb.12899
- Feng, W., Hongbin, W., Bing, L., and Jinfa, W. (2006). Cloning and characterization of a novel splicing isoform of the iron-superoxide dismutase gene in rice (*Oryza sativa* L.). *Plant Cell Rep.* 24, 734–742. doi: 10.1007/s00299-005-0030-4
- Frey, A., Effroy, D., Lefebvre, V., Seo, M., Perreau, F., Berger, A., et al. (2012). Epoxycarotenoid cleavage by NCED5 fine-tunes ABA accumulation and affects seed dormancy and drought tolerance with other NCED family members. *Plant J.* 70, 501–512. doi: 10.1111/j.1365-313X.2011.04887.x
- Gill, S. S., and Tuteja, N. (2010). Reactive oxygen species and antioxidant machinery in abiotic stress tolerance in crop plants. *Plant Physiol. Biochem.* 48, 909–930. doi: 10.1016/j.plaphy.2010.08.016
- Guan, Q., Lu, X., Zeng, H., Zhang, Y., and Zhu, J. (2013). Heat stress induction of *miR398* triggers a regulatory loop that is critical for thermotolerance in *Arabidopsis*. *Plant J.* 74, 840–851. doi: 10.1111/tpj.12169
- Hasanuzzaman, M., Oku, H., Nahar, K., Bhuyan, M. H. M. B., Mahmud, J. A., Baluska, F., et al. (2018). Nitric oxide-induced salt stress tolerance in plants: ROS metabolism, signaling, and molecular interactions. *Plant Biotechnol. Rep.* 12, 77–92. doi: 10.1007/s11816-018-0480-0
- Huang, Y., Guo, Y., Liu, Y., Zhang, F., Wang, Z., Wang, H., et al. (2018). 9-*cis*-epoxycarotenoid dioxygenase 3 regulates plant growth and enhances multi-abiotic stress tolerance in rice. *Front. Plant Sci.* 9. doi: 10.3389/fpls.2018.00162
- Hu, H., Dai, M., Yao, J., Xiao, B., Li, X., Zhang, Q., et al. (2006). Overexpressing a NAM, ATAF, and CUC (NAC) transcription factor enhances drought resistance and salt tolerance in rice. *Proc. Natl. Acad. Sci. U. S. A.* 103, 12987–12992. doi: 10.1073/pnas.0604882103
- Jiang, D., Zhou, L., Chen, W., Ye, N., Xia, J., and Zhuang, C. (2019). Overexpression of a microRNA-targeted NAC transcription factor improves drought and salt tolerance in rice via ABA-mediated pathways. *Rice* 12, 76. doi: 10.1186/s12284-019-0334-6
- Kalladan, R., Lasky, J. R., Sharma, S., Kumar, M. N., Juenger, T. E., Des Marais, D. L., et al. (2019). Natural variation in 9-*cis*-epoxycarotenoid dioxygenase 3 and ABA accumulation. *Plant Physiol.* 179, 1620–1631. doi: 10.1104/pp.18.01185
- Kim, M. D., Kim, Y. H., Kwon, S. Y., Yun, D. J., Kwak, S. S., and Lee, H. S. (2010). Enhanced tolerance to methyl viologen-induced oxidative stress and high temperature in transgenic potato plants overexpressing the *CuZnSOD*, *APX* and *NDPK2* genes. *Physiol. Plant* 140, 153–162. doi: 10.1111/j.1399-3054.2010.01392.x
- Kurepin, L. V., Qaderi, M. M., Back, T. G., Reid, D. M., and Pharis, R. P. (2008). A rapid effect of applied brassinolide on abscisic acid concentrations in *Brassica napus* leaf tissue subjected to short-term heat stress. *Plant Growth Regul.* 55, 165–167. doi: 10.1007/s10725-008-9276-5
- Liang, J., Yang, L., Chen, X., Li, L., Guo, D., Li, H., et al. (2009). Cloning and characterization of the promoter of the 9-*cis*-epoxycarotenoid dioxygenase gene in *Arachis hypogaea* L. *Biosci. Biotechnol. Biochem.* 73, 2103–2106. doi: 10.1271/bbb.90133
- Li, Y., Gao, Z., Lu, J., Wei, X., Qi, M., Yin, Z., et al. (2022). SiSNRK2.3 interacts with SiSUI1 to modulate high temperature tolerance via abscisic acid (ABA) controlling stomatal movement in tomato. *Plant Sci.* 321, 111305. doi: 10.1016/j.plantsci.2022.111305
- Li, H., Liu, S. S., Yi, C. Y., Wang, F., Zhou, J., Xia, X. J., et al. (2014). Hydrogen peroxide mediates abscisic acid-induced HSP70 accumulation and heat tolerance in grafted cucumber plants. *Plant Cell Environ.* 37, 2768–2780. doi: 10.1111/pce.12360
- Li, Z., Su, D., Lei, B., Wang, F., Geng, W., Pan, G., et al. (2015). Transcriptional profile of genes involved in ascorbate glutathione cycle in senescing leaves for an early senescence leaf (*esl*) rice mutant. *J. Plant Physiol.* 176, 1–15. doi: 10.1016/j.jplph.2014.09.020
- Liu, J., Hasanuzzaman, M., Wen, H., Zhang, J., Peng, T., Sun, H., et al. (2019). High temperature and drought stress cause abscisic acid and reactive oxygen species accumulation and suppress seed germination growth in rice. *Protoplasma* 256, 1217–1227. doi: 10.1007/s00709-019-01354-6
- Liu, J., Sun, X., Xu, F., Zhang, Y., Zhang, Q., Miao, R., et al. (2018). Suppression of *OsMDHAR4* enhances heat tolerance by mediating H<sub>2</sub>O<sub>2</sub>-induced stomatal closure in rice plants. *Rice* 11, 38. doi: 10.1186/s12284-018-0230-5
- Liu, J., Zhang, C., Wei, C., Liu, X., Wang, M., Yu, F., et al. (2016). The RING finger ubiquitin E3 ligase OsHTAS enhances heat tolerance by promoting H<sub>2</sub>O<sub>2</sub>-induced stomatal closure in rice. *Plant Physiol.* 170, 429–443. doi: 10.1104/pp.15.00879
- Lv, J., Dong, T., Zhang, Y., Ku, Y., Zheng, T., Jia, H., et al. (2022). Metabolomic profiling of brassinolide and abscisic acid in response to high-temperature stress. *Plant Cell Rep.* 41, 935–946. doi: 10.21203/rs.3.rs-1060645/v1
- Ma, H., Liu, C., Li, Z., Ran, Q., Xie, G., Wang, B., et al. (2018). ZmbZIP4 contributes to stress resistance in maize by regulating ABA synthesis and root development. *J. Plant Physiol.* 178, 753–770. doi: 10.1104/pp.18.00436
- Nambara, E., and Marion-Poll, A. (2005). Abscisic acid biosynthesis and catabolism. *Annu. Rev. Plant Biol.* 56, 165–185. doi: 10.1146/annurev.arplant.56.032604.144046
- Pei, Z. M., Murata, Y., Benning, G., Thomine, S., Klüsener, B., Allen, G. J., et al. (2000). Calcium channels activated by hydrogen peroxide mediate abscisic acid signalling in guard cells. *Nature* 406, 731–734. doi: 10.1038/35021067
- Qin-Di, D., Gui-Hua, J., Xiu-Neng, W., Zun-Guang, M., Qing-Yong, P., Shiyun, C., et al. (2021). High temperature-mediated disturbance of carbohydrate metabolism and gene expression regulation in rice: a review. *Plant Signal. Behav.* 16, 1862564. doi: 10.1080/15592324.2020.1862564
- Quan, L. J., Zhang, B., Shi, W. W., and Li, H. Y. (2008). Hydrogen peroxide in plants: a versatile molecule of the reactive oxygen species network. *J. Integr. Plant Biol.* 50, 2–18. doi: 10.1111/j.1744-7909.2007.00599.x
- Raja, V., Majeed, U., Kang, H., Andrabi, K. I., and John, R. (2017). Abiotic stress: Interplay between ROS, hormones and MAPKs. *Environ. Exp. Bot.* 137, 142–157. doi: 10.1016/j.envexpbot.2017.02.010
- Rezaul, I. M., Baohua, F., Tingting, C., Weimeng, F., Caixia, Z., Longxing, T., et al. (2019). Abscisic acid prevents pollen abortion under high-temperature stress by mediating sugar metabolism in rice spikelets. *Physiol. Plant* 165, 644–663. doi: 10.1111/ppl.12759
- Shi, B., Ni, L., Zhang, A., Cao, J., Zhang, H., Qin, T., et al. (2012). OsDMI3 is a novel component of abscisic acid signaling in the induction of antioxidant defense in leaves of rice. *Mol. Plant* 5, 1359–1374. doi: 10.1093/mp/sss068
- Singh, R. K., Jaishankar, J., Muthamilarasan, M., Shweta, S., Dangi, A., and Prasad, M. (2016). Genome-wide analysis of heat shock proteins in *C4* model, foxtail millet identifies potential candidates for crop improvement under abiotic stress. *Sci. Rep.* 6, 32641. doi: 10.1038/srep32641
- Song, S., Dai, X., and Zhang, W. H. (2012). A rice f-box gene, *OsFbx352*, is involved in glucose-delayed seed germination in rice. *J. Exp. Bot.* 63, 5559–5568. doi: 10.1093/jxb/ers206
- Sun, K., Wang, H., and Xia, Z. (2019). The maize bHLH transcription factor bHLH105 confers manganese tolerance in transgenic tobacco. *Plant Sci.* 280, 97–109. doi: 10.1016/j.plantsci.2018.11.006
- Tang, R.-S., Zheng, J.-C., Jin, Z.-Q., Zhang, D.-D., Huang, Y.-H., and Chen, L.-G. (2007). Possible correlation between high temperature-induced floret sterility and endogenous levels of IAA, GAs and ABA in rice (*Oryza sativa* L.). *Plant Growth Regul.* 54, 37–43. doi: 10.1007/s10725-007-9225-8
- Teng, K., Li, J., Liu, L., Han, Y., Du, Y., Zhang, J., et al. (2014). Exogenous ABA induces drought tolerance in upland rice: the role of chloroplast and ABA biosynthesis-related gene expression on photosystem II during PEG stress. *Acta Physiol. Plant* 36, 2219–2227. doi: 10.1007/s11738-014-1599-4
- Toh, S., Imamura, A., Watanabe, A., Nakabayashi, K., Okamoto, M., Jikumaru, Y., et al. (2008). High temperature-induced abscisic acid biosynthesis and its role in the inhibition of gibberellin action in *Arabidopsis* seeds. *Plant Physiol.* 146, 1368–1385. doi: 10.1104/pp.107.113738
- Vanderauwera, S., Suzuki, N., Miller, G., van de Cotte, B., Morsa, S., Ravanat, J. L., et al. (2011). Extranuclear protection of chromosomal DNA from oxidative stress. *Proc. Natl. Acad. Sci. U. S. A.* 108, 1711–1716. doi: 10.1073/pnas.1018359108
- Wang, Y., Hou, Y., Qiu, J., Wang, H., Wang, S., Tang, L., et al. (2020). Abscisic acid promotes jasmonic acid biosynthesis via a 'SAPK10-bZIP72-AOC' pathway to synergistically inhibit seed germination in rice (*Oryza sativa*). *New Phytol.* 228, 1336–1353. doi: 10.1111/nph.16774
- Wang, F., Liu, J., Zhou, L., Pan, G., Li, Z., Zaidi, S. H., et al. (2016). Senescence-specific change in ROS scavenging enzyme activities and regulation of various SOD isozymes to ROS levels in psf mutant rice leaves. *Plant Physiol. Biochem.* 109, 248–261. doi: 10.1016/j.plaphy.2016.10.005
- Wang, F., Niu, H., Xin, D., Long, Y., Wang, G., Liu, Z., et al. (2021). *OsIAA18*, an Aux/IAA transcription factor gene, is involved in salt and drought tolerance in rice. *Front. Plant Sci.* 12. doi: 10.3389/fpls.2021.738660
- Wan, X. R., and Li, L. (2006). Regulation of ABA level and water-stress tolerance of *Arabidopsis* by ectopic expression of a peanut 9-*cis*-epoxycarotenoid dioxygenase gene. *Biochem. Biophys. Res. Commun.* 347, 1030–1038. doi: 10.1016/j.bbrc.2006.07.026

- Xiao, B., Huang, Y., Tang, N., and Xiong, L. (2007). Over-expression of a *LEA* gene in rice improves drought resistance under the field conditions. *Theor. Appl. Genet.* 115, 35–46. doi: 10.1007/s00122-007-0538-9
- Xu, Y., Zhang, L., Ou, S., Wang, R., Wang, Y., Chu, C., et al. (2020). Natural variations of *SLG1* confer high-temperature tolerance in *indica* rice. *Nat. Commun.* 11, 5441. doi: 10.1038/s41467-020-19320-9
- Yang, X., Yang, Y. N., Xue, L. J., Zou, M. J., Liu, J. Y., Chen, F., et al. (2011). Rice ABI5-Like1 regulates abscisic acid and auxin responses by affecting the expression of ABRE-containing genes. *Plant Physiol.* 156, 1397–1409. doi: 10.1104/pp.111.173427
- Ye, N., Zhu, G., Liu, Y., Li, Y., and Zhang, J. (2011). ABA controls H<sub>2</sub>O<sub>2</sub> accumulation through the induction of *OsCATB* in rice leaves under water stress. *Plant Cell Physiol.* 52, 689–698. doi: 10.1093/pcp/pcr028
- Zhang, Q., Liu, Y., Jiang, Y., Li, A., Cheng, B., and Wu, J. (2022). *OsASR6* enhances salt stress tolerance in rice. *Int. J. Mol. Sci.* 23, 9340. doi: 10.3390/ijms23169340
- Zhang, X. X., Tang, Y. J., Ma, Q. B., Yang, C. Y., Mu, Y. H., Suo, H. C., et al. (2013). *OsDREB2A*, a rice transcription factor, significantly affects salt tolerance in transgenic soybean. *PLoS One* 8, e83011. doi: 10.1371/journal.pone.0083011
- Zhang, W., Yang, H., You, S., Xu, Y., Ran, K., and Fan, S. (2014). Cloning, characterization and functional analysis of the role *MhNCED3*, a gene encoding 9-*cis*-epoxycarotenoid dioxygenase in *Malus hupehensis* rehd., plays in plant tolerance to osmotic and Cd<sup>2+</sup> stresses. *Plant Soil* 381, 143–160. doi: 10.1007/s11104-014-2120-y
- Zhang, D. P., Zhou, Y., Yin, J. F., Yan, X. J., Lin, S., Xu, W. F., et al. (2015). Rice G-protein subunits *qPE9-1* and *RGB1* play distinct roles in abscisic acid responses and drought adaptation. *J. Exp. Bot.* 66, 6371–6384. doi: 10.1093/jxb/erv350
- Zhao, C., Liu, B., Piao, S., Wang, X., Lobell, D. B., Huang, Y., et al. (2017). Temperature increase reduces global yields of major crops in four independent estimates. *Proc. Natl. Acad. Sci. U. S. A.* 114, 9326–9331. doi: 10.1073/pnas.1701762114
- Zhou, H., Wang, Y., Zhang, Y., Xiao, Y., Liu, X., Deng, H., et al. (2022). Comparative analysis of heat-tolerant and heat-susceptible rice highlights the role of *OsNCED1* gene in heat stress tolerance. *Plants* 11, 1062. doi: 10.3390/plants11081062
- Zhu, G., Ye, N., and Zhang, J. (2009). Glucose-induced delay of seed germination in rice is mediated by the suppression of ABA catabolism rather than an enhancement of ABA biosynthesis. *Plant Cell Physiol.* 50, 644–651. doi: 10.1093/pcp/pcp022
- Zou, M., Guan, Y., Ren, H., Zhang, F., and Chen, F. (2008). A bZIP transcription factor, *OsABI5*, is involved in rice fertility and stress tolerance. *Plant Mol. Biol.* 66, 675–683. doi: 10.1007/s11103-008-9298-4



## OPEN ACCESS

EDITED BY  
Hirofumi Saneoka,  
Hiroshima University, Japan

REVIEWED BY  
Amit Kumar Mishra,  
Mizoram University, India  
Reiaz Ul Rehman,  
University of Kashmir, India

\*CORRESPONDENCE  
Supriya Tiwari  
✉ supriyabhu@gmail.com

SPECIALTY SECTION  
This article was submitted to  
Plant Abiotic Stress,  
a section of the journal  
Frontiers in Plant Science

RECEIVED 16 December 2022  
ACCEPTED 07 February 2023  
PUBLISHED 22 February 2023

CITATION  
Sahoo A, Madheshiya P, Mishra AK and  
Tiwari S (2023) Combating ozone stress  
through N fertilization: A case study of  
Indian bean (*Dolichos lablab* L.).  
*Front. Plant Sci.* 14:1125529.  
doi: 10.3389/fpls.2023.1125529

COPYRIGHT  
© 2023 Sahoo, Madheshiya, Mishra and  
Tiwari. This is an open-access article  
distributed under the terms of the [Creative  
Commons Attribution License \(CC BY\)](#). The  
use, distribution or reproduction in other  
forums is permitted, provided the original  
author(s) and the copyright owner(s) are  
credited and that the original publication in  
this journal is cited, in accordance with  
accepted academic practice. No use,  
distribution or reproduction is permitted  
which does not comply with these terms.

# Combating ozone stress through N fertilization: A case study of Indian bean (*Dolichos lablab* L.)

Ansuman Sahoo, Parvati Madheshiya, Ashish Kumar Mishra  
and Supriya Tiwari\*

Laboratory of Ecotoxicology, Centre of Advanced Study in Botany, Institute of Science, Banaras  
Hindu University, Varanasi, India

The present study investigates the efficiency of nitrogen (N) amendments in the management of ozone (O<sub>3</sub>) stress in two varieties (Kashi Sheetal and Kashi Harittima) of Indian bean (*Dolichos lablab* L.). Two O<sub>3</sub> concentrations, ambient (44.9 ppb) and elevated (74.64 ppb) were used, and each O<sub>3</sub> concentration has 3 nitrogen (N) dose treatments viz recommended (N1), 1.5 times recommended (N2), 2 times recommended (N3) and no nitrogen, which served as control (C). The experiment concluded Kashi Sheetal as O<sub>3</sub> tolerant, as compared to Kashi Harittima. N amendments were effective in the partial amelioration of O<sub>3</sub> stress, with N2 being the most effective nitrogen dose, at both ambient and elevated O<sub>3</sub> concentrations. Kashi Sheetal has been determined to be O<sub>3</sub> tolerant due to greater endogenous levels of H<sub>2</sub>O<sub>2</sub> accumulation and enzymatic antioxidant contents with O<sub>3</sub> exposure. The O<sub>3</sub>-sensitive variety, Kashi Harittima, responded more positively to N treatments, at both O<sub>3</sub> concentrations. The positive effect of N amendments is attributed to the stimulated antioxidative enzyme activity, rather than the biophysical processes like stomatal conductance. Strengthened defense upon N amendments was attributed to the enhanced activities of APX and GR in Kashi Sheetal, while in Kashi Harittima, the two enzymes (APX and GR) were coupled by SOD and CAT as well, during the reproductive phase. Yield (weight of seeds plant<sup>-1</sup>) increments upon N (N2) amendments were higher in Kashi Harittima (O<sub>3</sub> sensitive), as compared to Kashi Sheetal (O<sub>3</sub> tolerant) at both ambient and elevated O<sub>3</sub> concentration, due to higher antioxidant enzymatic response and greater rate of photosynthesis in the former.

## KEYWORDS

nitrogen amendments, ozone, antioxidants, stomatal conductance, dolichos

## 1 Introduction

Over the past few decades, speedy industrial growth and unrestrained urbanization in developing nations have greatly increased the concentration of primary and secondary pollutants in the atmosphere (Dhevagi et al., 2021). The concentration of phytotoxic secondary pollutant tropospheric ozone (O<sub>3</sub>) depends on the levels of certain primary air

pollutants such as nitrogen oxides ( $\text{NO}_x$ ), and volatile organic compounds (VOCs). In recent years, tropospheric ozone has shown a severe impact on plants because of its high oxidative potential (Duque et al., 2021). Background  $\text{O}_3$  concentration in the troposphere has increased by 36% since pre-industrial times (Mukherjee and Hazra, 2022). Nearly one-quarter of the world is currently at risk of high  $\text{O}_3$  and it is predicted that the levels could rise to 20% by 2050 (Meehl et al., 2018). Because of chemical interactions between  $\text{O}_3$  precursors, industrial pollutants, and sunlight, surface ozone levels are increasing at a rate of 0.5 to 2.5 percent each year (Wang et al., 2022). Because it has a negative impact on people's health, plants, and the ecosystem worldwide, the rising concentration of ground-level  $\text{O}_3$  has become a global issue (Mills et al., 2013). Even if strict adherence to the air quality regulations of 2000 is maintained, the  $\text{O}_3$ -induced damage is projected to worsen, according to future emission scenario legislation taking emissions for the year 2030 (CLE-2030) (Van Dingenen et al., 2009). A number of modeling studies have depicted high tropospheric ozone concentration in the future thus making the study of the impact of elevated ozone on plants even more important.

The stomata are the primary entry point for ozone into plant leaves (Stella et al., 2013). Ozone quickly reacts with intracellular components and forms reactive oxygen species (ROS) such as hydrogen peroxide ( $\text{H}_2\text{O}_2$ ), superoxide radicals ( $\text{O}_2^-$ ), and hydroxyl radicals ( $\text{OH}^\bullet$ ) inside the leaf (Zhang et al., 2017). These ROS enhance the antioxidant defense response downstream, which mitigates the fatal consequences of accumulating ROS. Contradictorily, when ROS generation surpasses the antioxidant efficiency, plants show ozone vulnerability in the form of foliar injury symptoms, alteration in metabolic processes, yield loss, and other ozone-related effects (Singh et al., 2014; Singh et al., 2018; Hayes et al., 2020). Excessive ROS levels within the cells brought on by  $\text{O}_3$  damage the membranes (lipid peroxidation), oxidize proteins, degrade RNA and DNA, enhance the production of secondary metabolites, degrade chlorophyll, and ultimately result in apoptosis (Choudhury et al., 2017). However, a vast variety of antioxidants and ROS-scavenging enzymes such as catalase (CAT), superoxide dismutase (SOD), glutathione reductase (GR), and ascorbate peroxidase (APX), produced by cells upon  $\text{O}_3$  exposure to attenuate the impacts of ROS in the cells (Picchi et al., 2017). In order to maintain steady development in plants and to aid in the damage repair caused by various stressors, nutrient supplements have frequently been utilized (Sahoo and Tiwari, 2021). Nitrogen (N) is the fourth most common element in living things and is theoretically an important component that supports plant development (Sahoo and Tiwari, 2021). Nitrogen amendment not only maintains greater protein levels it can also be used for repair processes and facilitates the remobilization of nutrients to reproductive parts, sustaining better production (Zeng et al., 2017). Nitrogen applications tend to improve the photosynthetic potential of the plant which can be commonly coupled with stomatal conductance (Zhang et al., 2018). The addition of nitrogen may partly counteract the detrimental effects of  $\text{O}_3$  on a few plants' morphological characteristics (Yendrek et al., 2013). Plants can either strengthen their antioxidant defense against an

$\text{O}_3$ -induced ROS surge, fix more carbon to use for  $\text{O}_3$ -induced injury, or direct more biomass into reproductive organs to sustain greater yields in response to N amendments (Podda et al., 2019).

A significant portion of India's protein needs is fulfilled by pulses, one of the country's essential crops, which are grown on an area of 28.3 million hectares and produced approximately 25.7 million metric tonnes in the fiscal year 2020–21 (Statista, 2021). In Asia, where the mean ambient ozone concentration ranged between 35 and 75 ppb during the growing season of the crop, legumes had a substantial production loss of 10 to 66 percent (Emberson et al., 2009). *Dolichos lablab* L. is a versatile crop, several plant components may be consumed as food, animal feed, and green manure (Davari et al., 2018; Rana et al., 2021). It is a low-cost source of protein and micronutrients when compared to other legumes, highlighting the importance of its study in view of food security and nutrition in near future (Letting et al., 2021). These micronutrients, which play a significant role in the diets of resource-limited households in rural areas, include phosphorus, fiber, niacin, and thiamine (Letting et al., 2021). The most recent study shows how efficient lablab bean extracts are at preventing the spread of viral illnesses like influenza and SARS-CoV-2, which has been called a global pandemic (Liu et al., 2020). To the best of our knowledge, the sensitivity of *Dolichos lablab* L. varieties towards tropospheric ozone has not been defined. The present work is the first effort to characterize the sensitivity of two varieties of *Dolichos lablab* L. towards  $\text{O}_3$  stress. In addition, it also exemplifies the efficiency of nitrogen amendments in the management of  $\text{O}_3$  stress and the mechanistic approach adopted therein. Through our work, we hypothesize that the ameliorative effect of N amendments in  $\text{O}_3$ -stressed plants is mostly credited to the antioxidant response rather than the biophysical parameters like stomatal conductance.

## 2 Materials and methods

### 2.1 Experimental area

The area of study was the Botanical Garden at Banaras Hindu University, Varanasi. It is a sub-urban site located in the Indian subcontinent at  $25^{\circ}14'$  N latitude,  $82^{\circ}03'$  E longitude, and 76.19 m above sea level. The crop was grown during the winter season from November 2021 to March 2022. A subtropical humid climate prevails in the area, with distinctive summer, rainy, and winter seasons. The soil is sandy loam in texture (sand 45%, silt 28%, clay 27%) having an organic carbon content of 0.67%, pH 7.4, nitrogen content of 0.12%, and phosphorus content of 0.065%.

### 2.2 Plant material

Two varieties of Indian bean (*Dolichos lablab* L.) namely, Kashi Sheetal and Kashi Harittima were used for the experiment. The seeds of the above varieties were procured from the Indian Institute of Vegetable Research, Varanasi (IIVR-IARI). Kashi Sheetal is a semi-pole type variant with low-temperature tolerance. It is very rich in protein and can give a yield of about 18–20 tonnes/hectare.

The color of flowers of this variety is violet and the pods were green with a dark red lining at their edges. Kashi Harittima is reasonably resistant to Dolicho's yellow mosaic virus and also exhibits tolerance against aphids and pod borers. It is a high-yielding variety with parchment-free green-colored pods and white flowers.

## 2.3 Experimental design

The study was carried out by installing custom-built open-top chambers (OTCs) in the experimental area under ambient field circumstances. The diameter of the OTCs was 1.5m and the height was 1.8m. OTCs were set up in the botanical garden and were categorized as ambient O<sub>3</sub> OTCs and elevated O<sub>3</sub> OTCs (ambient + 30 ppb) on the basis of O<sub>3</sub> concentrations maintained in them. The experimental setup is explained in Figure 1. Each level of O<sub>3</sub> treatment was further supplemented with 3 doses of nitrogen amendments viz recommended (AN1 and EN1), 1.5 times recommended (AN2 and EN2) and 2 times recommended (AN3 and EN3). For each O<sub>3</sub> treatment, control was also maintained (AC and EC), wherein no N treatment was given (Figure 2). Each treatment was replicated thrice. The nitrogen fertilizer was applied to the soil and the treatment was given in two phases i.e., one in the vegetative phase and the other in the reproductive phase. In OTCs, seeds were hand sown in accordance with standard agricultural procedures. Ozone was produced by the ozone generator (A1G, Faraday, India) and then transported through a connecting tube to the OTCs designated for elevated O<sub>3</sub>. For ozone formation, the generator utilized high-frequency corona discharge technology. The release of ozone into the growth chamber was set at multiple points at the base of the OTCs. The experimental setup and design are displayed in Figure 1.

## 2.4 Ozone monitoring

Continuous O<sub>3</sub> monitoring was done throughout the experiment. The concentrations of elevated ozone were standardized once the OTCs were mounted in the field. Ozone generators were calibrated to create the necessary levels of elevated

ozone (ambient + 30 ppb). Using an automated real-time O<sub>3</sub> monitoring instrument (Model APOA 370, HORIBA Ltd., Japan), eight-hour O<sub>3</sub> monitoring (9:00-17:00 h) was carried out during the growth period.

## 2.5 Histochemical localization of H<sub>2</sub>O<sub>2</sub>

By using a histochemical analysis, the test plants' flag leaves in the reproductive phase were studied *in-situ* localization of accumulated hydrogen peroxide (H<sub>2</sub>O<sub>2</sub>). For each cultivar, three randomly chosen leaf samples from different treatments were taken. The procedure given by Thordal-Christensen et al. (1997) was followed for studying the *in-situ* localization of H<sub>2</sub>O<sub>2</sub> in leaves using 3, 3'-Diaminobenzidine (DAB).

## 2.6 Physiological parameters

Photosynthetic rate (A), stomatal conductance (g<sub>s</sub>), and internal CO<sub>2</sub> concentration (C<sub>i</sub>) were analyzed by using a portable photosynthetic instrument (CIRAS-3, PP SYSTEMS). All these parameters were measured for both ambient and elevated conditions. Three randomly chosen plants per plot had their fourth fully grown leaf from the top examined for physiological parameters. At 40 DAG and 60 DAG, measurements were made between 9:00 and 10:30 hours on cloud-free days. The instrument was calibrated utilizing a known source of CO<sub>2</sub> set at 510 ppm and the photosynthetic active radiation (PAR) set at 1200 mmol m<sup>-2</sup> s<sup>-1</sup>.

## 2.7 Enzymatic antioxidants and lipid peroxidation

For the enzymatic assay, 0.2 gm of fresh weight of leaf was taken and homogenized using liquid nitrogen. 5 ml of extracting buffer was used to homogenize the leaf tissues in order to extract antioxidant enzymes. The buffer was prepared using 1 M phosphate buffer of pH 7.0 of polyvinylpyrrolidone (PVP), phenyl methane sulfonyl fluoride (PMSF), Ethylenediaminetetraacetic acid

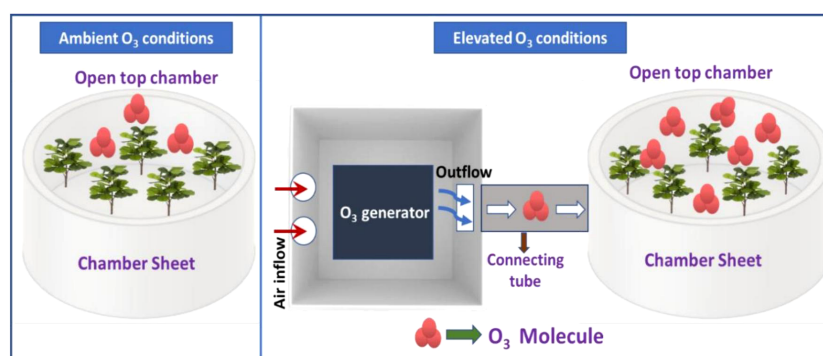


FIGURE 1  
Diagrammatic representation of experimental setup.



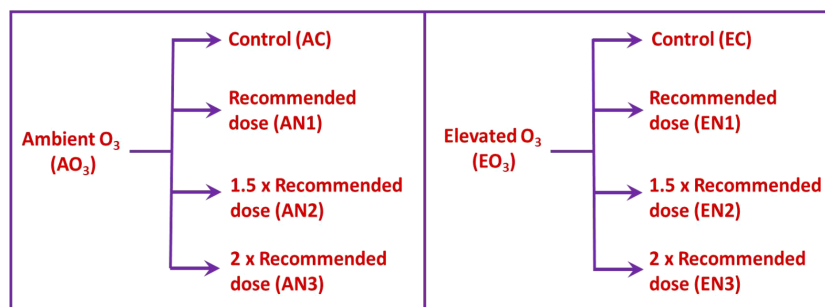


FIGURE 2

The different patterns of nitrogen amendments under ambient and elevated O<sub>3</sub> conditions.

(EDTA), and Triton-X-100 at 4°C. Antioxidant enzymes like superoxide dismutase (SOD), ascorbate peroxidase (APX), catalase (CAT), and glutathione reductase (GR) were estimated by the protocols (Fridovich, 1975; Nakano and Asada, 1981; Aebi, 1984; Anderson, 1996). The method developed by Heath and Packer (Heath and Packer, 1968) was used to estimate the malondialdehyde (MDA) content which represents lipid peroxidation. Leaf tissues (0.5 g) were extracted in 5% TCA, and 4 mL of 20% TCA containing 0.5% TBA was added. Following centrifugation, the sample mixture's absorbance was measured at 532 and 600 nm.

## 2.8 Yield

In order to determine yield, five plants per OTC were harvested in the first week of March and quantified for yield attributes. The number of seeds plant<sup>-1</sup>, the weight of seeds plant<sup>-1</sup>, and the test weight per 1000 seeds were estimated for each treatment.

## 2.9 Statistical analysis

All the statistical tests were executed using SPSS software (SPSS Inc. version 25.0, IBM Corp, New York). The three-way ANOVA was performed to examine the significance of the age of sampling, nitrogen treatment, and varieties of beans. Using the Shapiro-Wilk test, the normality of each dataset was examined, and the

distribution was determined to be normal in all instances since the P values were all over the threshold of significance (0.05). For both cultivars, the data was examined *via* principal component analysis (PCA). The correlation matrix and regression technique were used to perform the PCA.

## 3 Results

### 3.1 O<sub>3</sub> monitoring

During the growth period of the crop, the mean concentration of ambient O<sub>3</sub> and elevated O<sub>3</sub> was found to be 44.9 ppb and 74.64 ppb, respectively. The ambient O<sub>3</sub> concentration ranged from 29 ppb to 66 ppb and the elevated O<sub>3</sub> concentration ranged between 58 ppb to 97 ppb (Figure 3).

### 3.2 Histochemical localization

Histochemical detection of H<sub>2</sub>O<sub>2</sub> in the leaves of both varieties of *Dolichos lablab* L. indicated the presence of H<sub>2</sub>O<sub>2</sub> (Figure 4). The interaction of H<sub>2</sub>O<sub>2</sub> with DAB under elevated O<sub>3</sub> (EO<sub>3</sub>) as compared to ambient O<sub>3</sub> (AO<sub>3</sub>) produced a stronger reddish-brown stain in the leaf tissues of plants of both varieties. As compared with Kashi Harittima, leaves of Kashi Sheetal contained higher concentrations of H<sub>2</sub>O<sub>2</sub>. Furthermore, as nitrogen amendment amounts are increased, the H<sub>2</sub>O<sub>2</sub> content of both varieties of Indian bean decreased significantly.

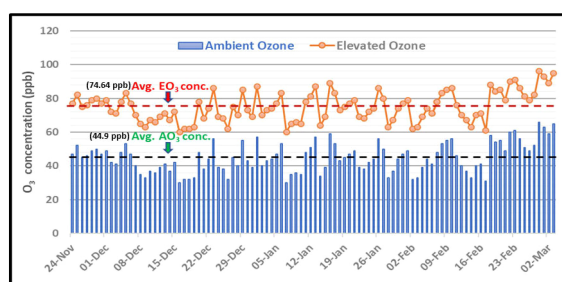


FIGURE 3

Mean 8h O<sub>3</sub> concentrations during the growth period of Hyacinth beans.

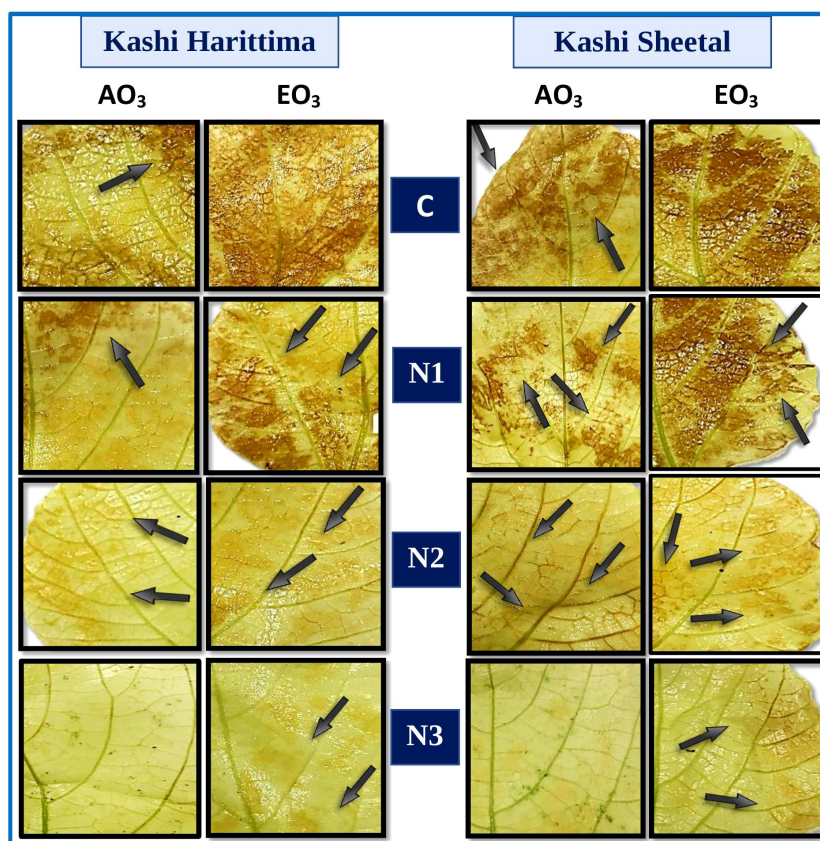


FIGURE 4

Histochemical localization of hydrogen peroxide ( $\text{H}_2\text{O}_2$ ) stained with DAB (brown color) in two varieties of *Dolichos lablab* L. exposed to  $\text{AO}_3$  and  $\text{EO}_3$  under different nitrogen fertilization levels.

### 3.3 Lipid peroxidation and antioxidative enzymatic activity

Plants grown in elevated  $\text{O}_3$  conditions showed significantly higher levels of lipid peroxidation (LPO) in their leaves than plants grown in ambient  $\text{O}_3$  conditions in both varieties of *Dolichos lablab* L. (Figures 5, 6). All three types of nitrogen treatments (N1, N2, and N3) showed significantly decreased lipid peroxidation as compared to control in both Kashi Sheetal and Kashi Harittima. For both varieties, the degree of lipid peroxidation was higher during the reproductive period than during the vegetative phase (Figures 5, 6). In both the vegetative and reproductive stages, Kashi Harittima plants had increased lipid peroxidation than Kashi Sheetal plants. The differences in the level of lipid peroxidation between treatments N2 and N3 were non-significant for both phases of growth. The results of the four-way ANOVA show that LPO varied significantly due to two individual factors such as age and treatment. Significant variations in LPO were also observed due to interactions of age with variety, ozone, and treatment factors (Table 1).

Antioxidative enzyme tests revealed that plants grown under  $\text{EO}_3$  conditions had much higher levels of enzymatic activity than in  $\text{AO}_3$ . In both growth phases, Kashi Sheetal plants had greater APX activity than Kashi Harittima plants (Figures 5, 6). At all ages and in

both varieties of Indian bean, there was no significant difference in the activity of the APX enzyme between the N2 and N3 treatments as compared to the control. N1 and N2 treatments showed significantly higher activities of APX in comparison to control in both  $\text{EO}_3$  and  $\text{AO}_3$  conditions. APX activity was significantly higher in the reproductive phase in both the varieties at  $\text{EO}_3$  and  $\text{AO}_3$  conditions. Results of four-way ANOVA revealed that APX varied significantly due to all individual factors and their interactions except age\*ozone\*variety and age\*ozone\*treatment (Table 1). Similar results were also revealed for activities of other antioxidative enzymes like CAT, GR, and SOD where the activity of these enzymes increased in reproductive stages of growth (Figures 5, 6). N1, N2, and N3 treatments showed significantly higher values of enzymatic activity as compared to the control but there was no significant difference between N2 and N3 treatments. The activity of CAT, GR, and SOD enzymes also increased significantly in the  $\text{EO}_3$  conditions as compared to  $\text{AO}_3$  conditions at all ages and this accounts for both varieties of *Dolichos lablab* L. (Figures 5, 6). GR and SOD showed significant variations for all four individual factors and some of their interactions such as age\*variety and age\*treatment. CAT showed significant variations for all individual factors and their interactions except age and its interaction with ozone and variety (Table 1).

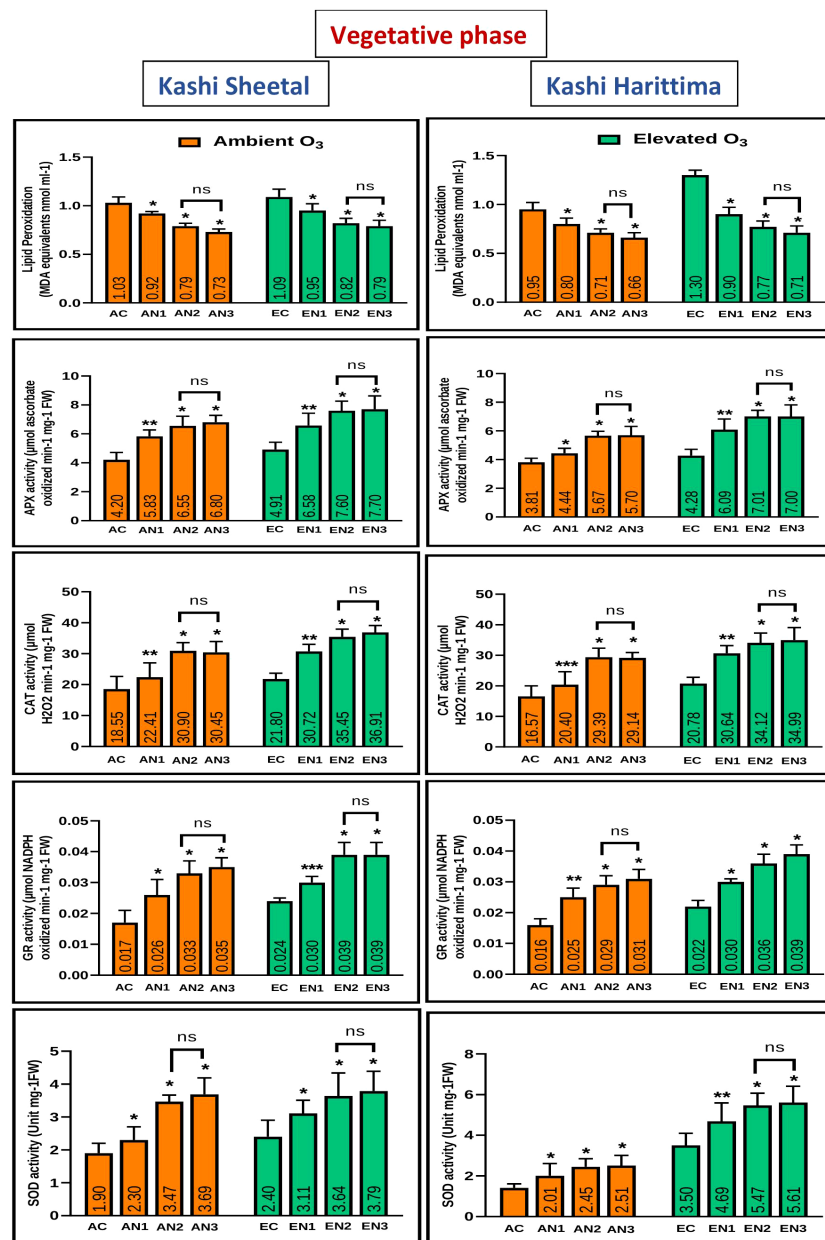


FIGURE 5

Variations in antioxidative enzymes in both varieties of *Dolichos lablab* L grown under AO<sub>3</sub> and EO<sub>3</sub> in the vegetative phase. Values are mean ± SE. Level of significance between AO<sub>3</sub> and EO<sub>3</sub> treated plants based on t-test; ns; not significant; \*, P ≤ 0.05; \*\*, P ≤ 0.01; \*\*\*, P ≤ 0.001.

### 3.4 Photosynthetic rate, stomatal gas conductance, and internal CO<sub>2</sub> concentration

Significantly higher rates of photosynthesis were observed in Kashi Sheetal plants at both ages and in all types of N treatment as compared to Kashi Harittima plants. The plants of both varieties grown in EO<sub>3</sub> conditions showed a considerable reduction in the rate of photosynthesis in comparison to plants grown in AO<sub>3</sub> conditions. In the vegetative phase, the Kashi Sheetal showed an 11.2, 25.5, and 26.5% increase at AO<sub>3</sub> and 8, 24.1, and 27.4% increase at EO<sub>3</sub> for N1, N2, and N3 treatments, respectively (Table 2). There was a 12.3, 26.9, and 28% increase at AO<sub>3</sub> and a

13, 28, and 30% increase at EO<sub>3</sub> for N1, N2, and N3 treatments, respectively of the Kashi Harittima variety in the vegetative phase (Table 2). Similarly in the reproductive phase, the Kashi Sheetal showed a 14.7, 30.3, and 28.4% increase at AO<sub>3</sub> and 14.8, 27.8, and 26.5% increase at EO<sub>3</sub> for N1, N2, and N3 treatments, respectively (Table 3). There was an 11.5, 24.2, and 26.3% increase at AO<sub>3</sub> and a 10.2, 22.7, and 25% increase at EO<sub>3</sub> for N1, N2, and N3 treatments, respectively of the Kashi Harittima variety in the reproductive phase (Table 3). After analyzing the degree of percent changes between the N treatments and control in both varieties, the N2 treatment was the most effective treatment in increasing the rate of photosynthesis. According to the four-way ANOVA results, the rate of photosynthesis varied significantly for all individual factors, and

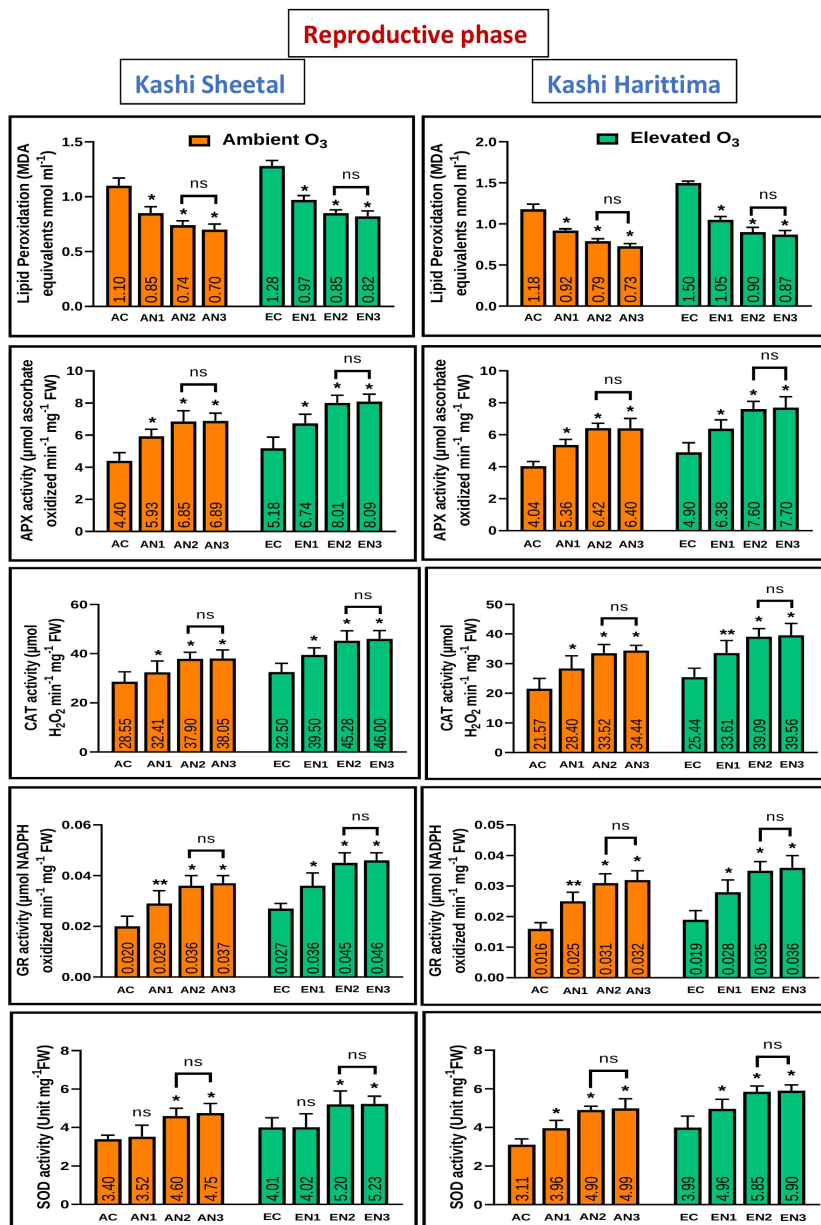


FIGURE 6

Variations in antioxidative enzymes in both varieties of *Dolichos lablab* L grown under AO<sub>3</sub> and EO<sub>3</sub> in the reproductive phase. Values are mean  $\pm$  SE. Level of significance between AO<sub>3</sub> and EO<sub>3</sub> treated plants based on t-test; ns; not significant; \*,  $P \leq 0.05$ ; \*\*,  $P \leq 0.01$ ; \*\*\*,  $P \leq 0.001$ .

some of their interactions such as age\*variety, variety\*treatment, and age\*variety\*treatment (Table 1). Similar results were also observed for stomatal gas conductance and internal CO<sub>2</sub> concentration in both the varieties of *Dolichos lablab* under AO<sub>3</sub> and EO<sub>3</sub> conditions. For both parameters, the Kashi Sheetal variety showed better results in all types of N treatments as compared to Kashi Harittima. The values of stomatal gas conductance and internal CO<sub>2</sub> concentration were significantly reduced in EO<sub>3</sub> conditions in comparison to AO<sub>3</sub> for both varieties at all ages. Stomatal gas conductance and internal CO<sub>2</sub> concentration varied significantly for all four individual factors and the interactions of age with ozone, variety, and treatment (Table 1).

### 3.5 Yield

There was a significant reduction in the weight of seeds plant<sup>-1</sup> for both varieties under EO<sub>3</sub> conditions as compared to AO<sub>3</sub> conditions. For the Kashi Sheetal variety, there was a 20.7, 34.5, and 35.4% increase at AO<sub>3</sub> and 26.8, 35.8, and 36.8% increase at EO<sub>3</sub> for N1, N2, and N3 treatments, respectively in comparison to control (Table 4). There was a 22.4, 42.6, and 43.8% increase at AO<sub>3</sub> and a 28.7, 40.4, and 41.2% increase at EO<sub>3</sub> for N1, N2, and N3 treatments, respectively of the Kashi Harittima variety as compared to control (Table 4). There was a significant reduction in the test weight of 1000 seeds for both varieties under EO<sub>3</sub> conditions as

TABLE 1 F-ratio and level of significance of selected biochemical and physiological characteristics of *Dolichos lablab* L.

|                                   | LPO | APX | GR  | CAT | SOD | A   | g <sub>s</sub> | Ci  |
|-----------------------------------|-----|-----|-----|-----|-----|-----|----------------|-----|
| AGE                               | **  | *** | **  | ns  | ns  | *** | ***            | *** |
| OZONE                             | ns  | *** | *** | *** | *** | *** | ***            | *** |
| VARIETY                           | ns  | *** | *** | *** | *** | *** | ***            | *** |
| TREATMENT                         | *** | *** | *** | *** | *** | *** | ***            | *** |
| AGE * OZONE                       | *** | *** | ns  | ns  | *** | ns  | **             | *   |
| AGE * VARIETY                     | *** | *** | *   | ns  | *   | *   | ***            | *   |
| AGE * TREATMENT                   | *   | *** | *   | *** | **  | ns  | ***            | *** |
| OZONE * VARIETY                   | ns  | *** | *   | **  | *** | ns  | ns             | ns  |
| OZONE * TREATMENT                 | ns  | **  | **  | *** | **  | ns  | **             | *** |
| VARIETY * TREATMENT               | ns  | *** | **  | *** | ns  | *** | ns             | ns  |
| AGE * OZONE * VARIETY             | *   | ns  | ns  | *   | *   | ns  | ns             | *** |
| AGE * OZONE * TREATMENT           | ns  | ns  | **  | *** | ns  | ns  | ns             | ns  |
| AGE * VARIETY * TREATMENT         | **  | *   | ns  | *   | ns  | *** | *              | ns  |
| OZONE * VARIETY * TREATMENT       | ns  | *** | ns  | *   | ns  | ns  | ns             | **  |
| AGE * OZONE * VARIETY * TREATMENT | ns  | *   | ns  | ns  | ns  | ns  | ns             | ns  |

\*,  $P < 0.05$ ; \*\*,  $P < 0.01$ ; \*\*\*,  $P < 0.001$ ; ns; not significant.

compared to AO<sub>3</sub> conditions except for the control of both varieties. For the Kashi Sheetal variety, there was a 9.7, 16.1, and 17.3% increase at AO<sub>3</sub> and 8.01, 12.4, and 12.9% increase at EO<sub>3</sub> for N1, N2, and N3 treatments, respectively in comparison to control. There was a 14.4, 20.2, and 20.6% increase at AO<sub>3</sub> and an 18.8, 28.4, and 28.9% increase at EO<sub>3</sub> for N1, N2, and N3 treatments, respectively of the Kashi Harittima variety as compared to control (Table 4). The percent change of all treatments was higher for the Kashi Harittima variety in comparison to the Sheetal variety. Only the N2 and N3 treatments of the Harittima variety were significant for the number of seeds plant<sup>-1</sup> as compared to the control. All the other values of Sheetal and Harittima varieties for the number of seeds plant<sup>-1</sup> were found to be insignificant.

## 4 Discussion

Sicard et al. (2017) predicted a rise in O<sub>3</sub> concentration under all climate change scenarios and identified South Asia as one of the primary O<sub>3</sub> hotspot regions. Intense irradiance, elevated temperature, and low moisture are the ideal circumstances for O<sub>3</sub> generation in the Indo-Gangetic plains, where high episodes of O<sub>3</sub> are common occurrences (Sarkar and Agrawal, 2010). In monitoring studies conducted at the current experimental site between 2002 - 2012, the concentration of O<sub>3</sub> was clearly on the rise (Tiwari and Agrawal, 2018). The results of the present experiment evidently revealed the presence of high ozone episodes during the reproductive phase of both varieties of *Dolichos lablab* L. The increased O<sub>3</sub> levels during the reproductive phase can be reasoned by the high temperature in the months of January, February, and March as compared to November and

December months. High O<sub>3</sub> concentrations have also been recorded in earlier experiments conducted at the current experimental location during the same time period (Singh et al., 2018; Yadav et al., 2019).

Out of the two varieties of *Dolichos lablab* L. exposed to ambient and elevated O<sub>3</sub> concentrations, Kashi Sheetal had higher endogenously generated H<sub>2</sub>O<sub>2</sub> in its control leaves as compared to Kashi Harittima, as evident through the histochemical assay of H<sub>2</sub>O<sub>2</sub> localization (Figure 4). Related findings have reported that cultivars with higher levels of endogenous H<sub>2</sub>O<sub>2</sub> are more tolerant than cultivars with lower levels of H<sub>2</sub>O<sub>2</sub> (Caregnato et al., 2013; Yadav et al., 2019; Gupta and Tiwari, 2020). Caregnato et al. (2013) reported significantly higher H<sub>2</sub>O<sub>2</sub> localization in the leaves of two varieties of *Phaseolus vulgaris* L. grown in EO<sub>3</sub> conditions in comparison to AO<sub>3</sub> conditions. The high H<sub>2</sub>O<sub>2</sub> localization in the leaves is because of the excessive ROS generated due to severe oxidative stress which happens due to elevated O<sub>3</sub> fumigation. With an increased dose of nitrogen treatments, there was a significant degree of reduction in the amount of H<sub>2</sub>O<sub>2</sub> localization in the leaves of both varieties (Figure 4). It was reported that H<sub>2</sub>O<sub>2</sub> was produced in the leaves of *Cymopsis tetragonoloba* L. Taub. (Cluster bean) was significantly decreased with increasing nitrogen amendment doses (Gupta and Tiwari, 2020). It is suggested that the surplus nitrogen available to the plant gets allocated to improve the antioxidative potential of the plants which results in improved scavenging of the H<sub>2</sub>O<sub>2</sub> (Podda et al., 2019). It is noted that N2 treatment was found to be sufficient in the management of O<sub>3</sub> stress under both O<sub>3</sub> exposure conditions.

Malondialdehyde is an intermediate product that is exclusively produced during the process of membrane lipid peroxidation, so measuring the MDA content gives an approximation of the degree



TABLE 2 Effect of N treatment (C, control; N1, recommended N dose; N2, 1.5-times recommended N dose and N3, 2-times recommended N dose) on physiological parameters of *Dolichos lablab* L. under AO<sub>3</sub> at vegetative stage and reproductive stage.

| a) N treatment     | Rate of photosynthesis<br>(A; $\mu\text{molCO}_2 \text{ m}^{-2} \text{ s}^{-1}$ ) | Stomatal gas conductance<br>(g <sub>s</sub> ; $\text{mmolCO}_2 \text{ m}^{-2} \text{ s}^{-1}$ ) | Internal CO <sub>2</sub><br>(C <sub>i</sub> ; $\mu\text{mol mol}^{-1}$ ) |
|--------------------|---|---|--|
| Vegetative Phase   |   |   |  |
| C                  | 9.8 <sup>c</sup> ± 0.42   | 132.9 <sup>c</sup> ± 3.71   | 310.4 <sup>c</sup> ± 4.5   |
| N1                 | 10.7 <sup>b</sup> ± 0.55  | 139.6 <sup>b</sup> ± 2.48   | 323.0 <sup>b</sup> ± 2.6   |
| N2                 | 12.3 <sup>a</sup> ± 0.82  | 155.4 <sup>a</sup> ± 3.03   | 340.9 <sup>a</sup> ± 3.1   |
| N3                 | 12.4 <sup>a</sup> ± 0.23  | 154.2 <sup>a</sup> ± 3.11   | 343.5 <sup>a</sup> ± 2.9   |
| Reproductive Phase |   |   |  |
| C                  | 10.2 <sup>c</sup> ± 0.35  | 136.9 <sup>c</sup> ± 3.69   | 318.1 <sup>c</sup> ± 3.2   |
| N1                 | 11.7 <sup>b</sup> ± 0.42  | 147.3 <sup>b</sup> ± 4.5  | 329.4 <sup>b</sup> ± 2.9   |
| N2                 | 13.3 <sup>a</sup> ± 0.7   | 160.7 <sup>a</sup> ± 2.99   | 349.6 <sup>a</sup> ± 3.5   |
| N3                 | 13.1 <sup>a</sup> ± 0.93  | 159.3 <sup>a</sup> ± 4.02   | 350.5 <sup>a</sup> ± 4.0   |
| b) N treatment     | Rate of photosynthesis<br>(A; $\mu\text{molCO}_2 \text{ m}^{-2} \text{ s}^{-1}$ ) | Stomatal gas conductance<br>(g <sub>s</sub> ; $\text{mmolCO}_2 \text{ m}^{-2} \text{ s}^{-1}$ ) | Internal CO <sub>2</sub><br>(C <sub>i</sub> ; $\mu\text{mol mol}^{-1}$ ) |
| Vegetative Phase   |   |   |  |
| C                  | 8.9 <sup>c</sup> ± 0.31   | 126.3 <sup>c</sup> ± 2.98   | 303.4 <sup>c</sup> ± 3.6   |
| N1                 | 10.0 <sup>b</sup> ± 0.64  | 133.5 <sup>b</sup> ± 3.42   | 315.7 <sup>b</sup> ± 2.7   |
| N2                 | 11.3 <sup>a</sup> ± 0.7   | 145.7 <sup>a</sup> ± 3.9  | 331.6 <sup>a</sup> ± 3.0   |
| N3                 | 11.4 <sup>a</sup> ± 0.85  | 146.8 <sup>a</sup> ± 2.66   | 331.0 <sup>a</sup> ± 2.2   |
| Reproductive Phase |   |   |  |
| C                  | 9.5 <sup>c</sup> ± 0.7  | 133.4 <sup>c</sup> ± 2.6  | 310.4 <sup>c</sup> ± 2.5   |
| N1                 | 10.6 <sup>b</sup> ± 0.58  | 140.7 <sup>b</sup> ± 4.45   | 310.4 <sup>c</sup> ± 2.5   |
| N2                 | 11.8 <sup>a</sup> ± 0.67  | 148.3 <sup>a</sup> ± 2.5  | 335.9 <sup>a</sup> ± 3.5   |
| N3                 | 12.0 <sup>a</sup> ± 0.55  | 149.1 <sup>a</sup> ± 3.36   | 336.1 <sup>a</sup> ± 2.8   |

Values are mean ± SE. a) Kashi Sheetal, b) Kashi Harittima.

of lipid peroxidation. Biochemical analysis of lipid peroxidation showed higher MDA content in the EO<sub>3</sub> conditions in both varieties of *Dolichos lablab* L. as compared to AO<sub>3</sub> at both developmental stages (Figures 5, 6). The findings suggest that greater O<sub>3</sub> influx under EO<sub>3</sub> conditions resulted in significant membrane damage in both kinds of Indian beans at both development phases. A 90.2% increase in MDA contents in *Vigna mungo* L. varieties was reported on exposure to EO<sub>3</sub> conditions as compared to AO<sub>3</sub> conditions (Dhevagi et al., 2021). Since lipid peroxidation is an important marker of O<sub>3</sub> stress tolerance (Iglesias et al., 2006), Kashi Sheetal which showed a lesser degree of membrane lipid peroxidation under EO<sub>3</sub> conditions as compared to Kashi Harittima, was considered to be more tolerant of the two experimental varieties. The level of MDA content in the leaves of both varieties of *Dolichos lablab* L. was significantly reduced upon nitrogen treatments at both the O<sub>3</sub> concentrations. Similar findings were also reported by Pandey et al. (2018) in which MDA content in the leaves of *Triticum aestivum* L. was significantly decreased with increased nitrogen amendments. Podda et al. (2019) also found that nitrogen treatment had a beneficial impact on O<sub>3</sub>-exposed plants, seeing a

substantial decrease in MDA and improved membrane stability after nitrogen treatment at both AO<sub>3</sub> and EO<sub>3</sub> conditions. It was observed that Kashi Sheetal produced a lesser amount of MDA in comparison to the Kashi Harittima, at all the nitrogen treatments during both developmental stages, indicating Kashi Harittima to be less efficient in scavenging the O<sub>3</sub>-induced ROS leading to higher membrane disintegration than the Kashi Sheetal upon nitrogen treatments under both O<sub>3</sub> exposure conditions. This observation points towards the higher sensitivity of the Kashi Harittima towards ozone stress. Furthermore, there was a negligible difference in the response between the N2 and N3 treatments for both varieties upon both O<sub>3</sub> exposure conditions, which specifies the sufficiency of N2 treatment in alleviating O<sub>3</sub> stress in the Indian bean. Pearson's correlation coefficient test has shown a significant negative correlation of MDA contents with the enzymatic activities, suggesting a reduction in membrane lipid peroxidation of O<sub>3</sub>-stressed plants upon N amendments (Figure 7).

The presence of an efficient antioxidant defense mechanism allows the higher plants to perceive and decipher ROS signals into necessary cellular responses (Yadav et al., 2019). In the current

**TABLE 3** Effect of N treatment (C, control; N1, recommended N dose; N2, 1.5-times recommended N dose and N3, 2-times recommended N dose) on physiological parameters of *Dolichos lablab* L. under EO<sub>3</sub> at vegetative stage and reproductive stage. Values are mean  $\pm$  SE. a) Kashi Sheetal, b) Kashi Harittima.

| a) N treatment     | Rate of photosynthesis<br>(A; $\mu\text{molCO}_2 \text{ m}^{-2} \text{ s}^{-1}$ ) | Stomatal gas conductance<br>(g <sub>s</sub> ; $\text{mmolCO}_2 \text{ m}^{-2} \text{ s}^{-1}$ ) | Internal CO <sub>2</sub><br>(Ci; $\mu\text{mol mol}^{-1}$ ) |
|--------------------|---|---|---|
| Vegetative Phase   |   |   |   |
| C                  | 9.1 <sup>c</sup> $\pm$ 0.28   | 124.5 <sup>b</sup> $\pm$ 2.66   | 299.0 <sup>c</sup> $\pm$ 4.8                                |
| N1                 | 9.9 <sup>b</sup> $\pm$ 0.45   | 129.7 <sup>b</sup> $\pm$ 3.78   | 308.2 <sup>b</sup> $\pm$ 6.9                                |
| N2                 | 11.3 <sup>a</sup> $\pm$ 0.62  | 144.1 <sup>a</sup> $\pm$ 4.4  | 320.7 <sup>a</sup> $\pm$ 5.1                                |
| N3                 | 11.6 <sup>a</sup> $\pm$ 0.3   | 145.7 <sup>a</sup> $\pm$ 3.15   | 322.4 <sup>a</sup> $\pm$ 4.7                                |
| Reproductive Phase |   |   |   |
| C                  | 9.4 <sup>c</sup> $\pm$ 0.52   | 127.4 <sup>c</sup> $\pm$ 4.2  | 306.2 <sup>c</sup> $\pm$ 4.0                                |
| N1                 | 10.8 <sup>b</sup> $\pm$ 0.67  | 130.0 <sup>b</sup> $\pm$ 3.91   | 314.7 <sup>b</sup> $\pm$ 5.3                                |
| N2                 | 12.0 <sup>a</sup> $\pm$ 0.45  | 148.6 <sup>a</sup> $\pm$ 2.58   | 325.0 <sup>a</sup> $\pm$ 3.8                                |
| N3                 | 11.9 <sup>a</sup> $\pm$ 0.3   | 149.1 <sup>a</sup> $\pm$ 4.56   | 327.1 <sup>a</sup> $\pm$ 6.1                                |
| b) N treatment     | Rate of photosynthesis<br>(A; $\mu\text{molCO}_2 \text{ m}^{-2} \text{ s}^{-1}$ ) | Stomatal gas conductance<br>(g <sub>s</sub> ; $\text{mmolCO}_2 \text{ m}^{-2} \text{ s}^{-1}$ ) | Internal CO <sub>2</sub><br>(Ci; $\mu\text{mol mol}^{-1}$ ) |
| Vegetative Phase   |   |   |   |
| C                  | 8.2 <sup>c</sup> $\pm$ 0.42   | 117.5 <sup>c</sup> $\pm$ 3.41   | 292.5 <sup>c</sup> $\pm$ 3.6                                |
| N1                 | 9.3 <sup>b</sup> $\pm$ 0.57   | 123.3 <sup>b</sup> $\pm$ 2.9  | 301.6 <sup>b</sup> $\pm$ 4.8                                |
| N2                 | 10.5 <sup>a</sup> $\pm$ 0.39  | 135.0 <sup>a</sup> $\pm$ 4.57   | 314.2 <sup>a</sup> $\pm$ 5.2                                |
| N3                 | 10.7 <sup>a</sup> $\pm$ 0.66  | 136.2 <sup>a</sup> $\pm$ 3.95   | 316.1 <sup>a</sup> $\pm$ 6.8                                |
| Reproductive Phase |   |   |   |
| C                  | 8.8 <sup>c</sup> $\pm$ 0.44   | 124.7 <sup>c</sup> $\pm$ 4.2  | 303.5 <sup>c</sup> $\pm$ 5.5                                |
| N1                 | 9.7 <sup>b</sup> $\pm$ 0.8  | 133.1 <sup>b</sup> $\pm$ 3.52   | 310.6 <sup>b</sup> $\pm$ 6.4                                |
| N2                 | 10.8 <sup>a</sup> $\pm$ 0.35  | 148.4 <sup>a</sup> $\pm$ 4.67   | 321.4 <sup>a</sup> $\pm$ 2.9                                |
| N3                 | 11.0 <sup>a</sup> $\pm$ 0.61  | 150.0 <sup>a</sup> $\pm$ 3.69   | 321.9 <sup>a</sup> $\pm$ 4.7                                |

experiment, it was observed that the endogenous level of antioxidants was higher in Kashi Sheetal as compared to Kashi Harittima, at ambient O<sub>3</sub> exposure, suggesting high tolerance of O<sub>3</sub> stress in Kashi Sheetal. All the antioxidative enzymes showed higher activity under EO<sub>3</sub> conditions as compared to AO<sub>3</sub> conditions and this applies to both varieties at all developmental stages. Similar findings have also been reported by Pandey et al. (2018) in which the activities of antioxidative enzymes increased under EO<sub>3</sub> conditions in two cultivars of *Triticum aestivum* L. It has been proved that the sustenance and regeneration of the antioxidative enzymatic pool indicate a strengthened defense response capable of O<sub>3</sub> detoxification (Caregnato et al., 2013). In the present study, N amendments enhanced the antioxidant activities in both varieties, thereby proving its potential in the management of O<sub>3</sub> injury. It was observed that the antioxidative system of O<sub>3</sub> sensitive variety Kashi Harittima responded more positively at elevated O<sub>3</sub>, compared to ambient O<sub>3</sub>. At elevated O<sub>3</sub>, Kashi Harittima was capable of sustaining higher increments in the enzyme activities at both developmental stages, which evidently proves that N amendments were more favorable in encountering O<sub>3</sub> stress in this variety, as

compared to Kashi Sheetal. As per the PCA analysis, it was observed that Kashi Harittima, as the sensitive variety, demonstrated a stronger association of enzymatic anti-oxidants in component 1 as compared with the Kashi Sheetal (Figure 8). In the ascorbate-glutathione pathway, APX is the essential enzyme known for scavenging H<sub>2</sub>O<sub>2</sub> by using ascorbic acid as an electron donor, whereas GR catalyzes glutathione reduction with ascorbate regeneration in plants (Ashraf, 2009). In the present experiment, N amendments intensified the role of APX and GR in inducing the plant's defense system in both varieties. The higher APX and GR activity can be owed to the greater H<sub>2</sub>O<sub>2</sub> level in EO<sub>3</sub> conditions than in AO<sub>3</sub>, thereby ensuring the scavenging of the H<sub>2</sub>O<sub>2</sub> in order to curtail O<sub>3</sub> stress. Under stressful circumstances, Almeselmani et al. (2006) also observed an increment in APX and GR activity in the tolerant wheat cultivars HD77 and HD2817. The lower levels of H<sub>2</sub>O<sub>2</sub> in Kashi Harittima, upon N amendments at elevated O<sub>3</sub> treatment, can be explained by higher increments in CAT activity. Upon N amendments, whereas, Kashi Harittima was able to uphold the activities of SOD and CAT, in elevated O<sub>3</sub>-treated plants, Kashi Sheetal showed lesser increments in the response of these two

TABLE 4 Variations in the number of seeds plant<sup>-1</sup>, wt. of seeds plant<sup>-1</sup>, and test wt. per 1000 seeds of both varieties of *Dolichos lablab* L. grown under AO<sub>3</sub> and EO<sub>3</sub>.

|                 | Number of seeds plant <sup>-1</sup> |                          | Weight of seeds plant <sup>-1</sup> (g) |                 | Test wt. per 1000 seeds (g) |                            |
|-----------------|-------------------------------------|--------------------------|---|-----------------|-----------------------------|----------------------------|
|                 | AO <sub>3</sub>                     | EO <sub>3</sub>          | AO <sub>3</sub>                         | EO <sub>3</sub> | AO <sub>3</sub>             | EO <sub>3</sub>            |
| Kashi Sheetal   |                                     |                          |   |                 |                             |                            |
| C               | 70.8 ± 5.3                          | 64.1 <sup>ns</sup> ± 3.2 | 134.5 ± 11.2                            | 121.7* ± 13.8   | 405.9 ± 15.9                | 378.2 <sup>ns</sup> ± 10.4 |
| N1              | 81.2 ± 4.5                          | 77.2 <sup>ns</sup> ± 2.8 | 162.4 ± 13.5                            | 154.4* ± 11.6   | 445.3 ± 14.6                | 408.5* ± 11.2              |
| N2              | 96.0 ± 3.9                          | 89.6 <sup>ns</sup> ± 4.3 | 181.0 ± 12.9                            | 165.3* ± 10.7   | 471.6 ± 20.8                | 425.1** ± 15.0             |
| N3              | 98.8 ± 6.2                          | 90.0 <sup>ns</sup> ± 5.7 | 182.2 ± 13.4                            | 166.5** ± 9.2   | 476.3 ± 19.5                | 427.0*** ± 16.7            |
| Kashi Harittima |                                     |                          |   |                 |                             |                            |
| C               | 67.2 ± 5.1                          | 56.8 <sup>ns</sup> ± 3.3 | 120.9 ± 10.6                            | 112.3* ± 14.8   | 375.2 ± 14.5                | 311.8 <sup>ns</sup> ± 12.6 |
| N1              | 78.4 ± 3.5                          | 70.0 <sup>ns</sup> ± 4.4 | 148.1 ± 12.1                            | 144.6* ± 17.1   | 429.3 ± 13.6                | 370.6* ± 11.9              |
| N2              | 92.4 ± 4.1                          | 79.6*** ± 6.7            | 172.5 ± 13.3                            | 157.7** ± 16.3  | 451.0 ± 17.7                | 400.5** ± 14.4             |
| N3              | 93.2 ± 4.0                          | 79.2*** ± 4.1            | 173.9 ± 12.7                            | 158.6*** ± 10.4 | 452.5 ± 15.9                | 402.1** ± 15.3             |

Values are mean ± SE (ns; not significant; \*, P ≤ 0.05; \*\*, P ≤ 0.01; \*\*\*, P ≤ 0.001).

enzymes, during the reproductive stage. It is to be noted that with a gradual increase in the dose of nitrogen treatments, there was a significant surge in the activities of the antioxidative enzymes in both varieties of *Dolichos lablab* L. at all growth stages. But the degree of increment of the activities of enzymes was insignificant between N2 and N3 treatments, suggesting the adequacy of N2 treatment in the management of O<sub>3</sub> stress.

O<sub>3</sub> exposure is known to adversely affect the physiological parameters of plants, rate of photosynthesis, and stomatal conductance being directly affected (Singh et al., 2014; Tetteh et al., 2016; Dhevagi et al., 2021). This reduced photosynthetic rate caused by elevated ozone may be related to the degradation of the chloroplast structure, which prevents the production of chlorophyll under these conditions (Biswas and Jiang, 2011). In the present study, N supplementation resulted in the improvement of these two parameters in both the varieties of *Dolichos lablab*, at both O<sub>3</sub> exposure conditions, further justifying the potential role of N amendments in depreciating O<sub>3</sub> stress. This is further proved by significant correlation coefficient values of different physiological parameters of O<sub>3</sub>-exposed plants upon N amendments (Tables 2, 3). Increased g<sub>s</sub> upon N amendments have been reported in wheat (Wall et al., 2000), larch (Mao et al., 2014), cluster bean (Gupta and

Tiwari, 2020), etc. A decrease in g<sub>s</sub> along with an increased A upon N amendments and O<sub>3</sub> exposure in poplar has been reported by Zhang et al. (2018). A comparison of the physiological response of both varieties revealed that upon N supplementation, Kashi Harittima showed higher increments in A and g<sub>s</sub>, in comparison to Kashi Sheetal at all ages under both AO<sub>3</sub> and EO<sub>3</sub> conditions. Since the O<sub>3</sub>-induced depreciation of cellular performance largely depends upon O<sub>3</sub> flux, which is directly controlled by stomatal movement (Yadav et al., 2019), increased stomatal conductance in O<sub>3</sub>-exposed plants of Indian bean in the present study, does not account for the reported improvement in the plant's performance upon N amendments. It has been reported that the application of a higher N dose leads to an increased influx of O<sub>3</sub>, which may lead to the depletion of the antioxidant pool (Harmens et al., 2017; Marzuoli et al., 2018). Non-significant variations in g<sub>s</sub> due to O<sub>3</sub> x variety and O<sub>3</sub> x treatment interactions (Table 1) further prove that g<sub>s</sub> does not play any substantial role in the ameliorative effect of N amendments in the experimental plants. These observations lead to the conclusion that the upturn in the rate of photosynthesis upon N amendments in O<sub>3</sub>-exposed plants can be attributed to the enhanced activities of the enzymatic antioxidant pool, thus proving our hypothesis. Increased enzymatic antioxidants upon N

|     | A      | Gs     | Ci     | T      | LPO    | APX    | CAT    | GR     | SOD    |
|-----|--------|--------|--------|--------|--------|--------|--------|--------|--------|
| A   | 1      | 0.981  | 0.97   | 0.966  | -0.814 | 0.9    | 0.892  | 0.93   | 0.932  |
| Gs  | 0.981  | 1      | 0.975  | 0.961  | -0.821 | 0.876  | 0.852  | 0.931  | 0.916  |
| Ci  | 0.97   | 0.975  | 1      | 0.974  | -0.774 | 0.947  | 0.907  | 0.967  | 0.97   |
| T   | 0.966  | 0.961  | 0.974  | 1      | -0.856 | 0.93   | 0.931  | 0.937  | 0.935  |
| LPO | -0.814 | -0.821 | -0.774 | -0.856 | 1      | -0.699 | -0.714 | -0.799 | -0.744 |
| APX | 0.9    | 0.876  | 0.947  | 0.93   | -0.699 | 1      | 0.957  | 0.934  | 0.971  |
| CAT | 0.892  | 0.852  | 0.907  | 0.931  | -0.714 | 0.957  | 1      | 0.878  | 0.927  |
| GR  | 0.93   | 0.931  | 0.967  | 0.937  | -0.799 | 0.934  | 0.878  | 1      | 0.972  |
| SOD | 0.932  | 0.916  | 0.97   | 0.935  | -0.744 | 0.971  | 0.927  | 0.972  | 1      |

FIGURE 7

Pearson's correlation coefficient for physiological and biochemical parameters of two varieties of Hyacinth bean at EO<sub>3</sub>.

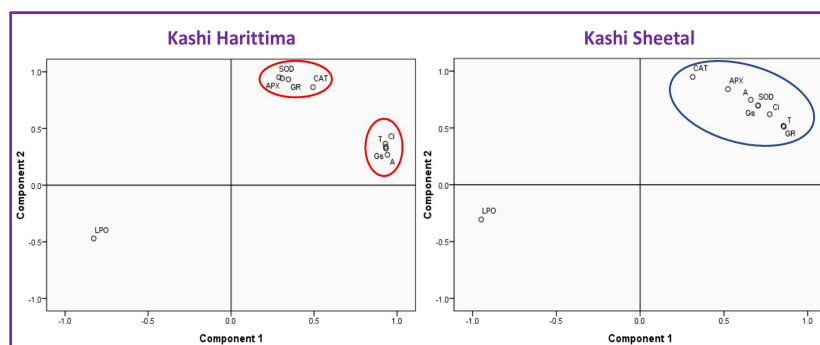


FIGURE 8

Principle Component Analysis (PCA) showed the association of considered parameters on two different components; i.e., component 1 and component 2. The parameters studied are APX, GR, SOD, CAT, LPO,  $\text{Cl}$ ,  $g_s$ , and (A) Association of studied parameters in Kashi Harittima, (B) association of studied parameters in Kashi Sheetal.

implementation, ensure the scavenging of  $\text{O}_3$ -induced oxidative entities, thus rendering protection to photosynthetic machinery in the chloroplasts.

The analysis of yield parameters showed a significant reduction in the  $\text{EO}_3$  conditions in comparison to  $\text{AO}_3$  conditions which accounts for both varieties of *Dolichos lablab* L. at all ages of growth (Table 4). An earlier study found that the yield of selected varieties of wheat (HUW 234 and 468, HD 3086 and 3118) and black gram (CO6 and VBN 1-8) were markedly reduced under  $\text{EO}_3$  as compared to  $\text{AO}_3$  (Yadav et al., 2019; Dhevagi et al., 2021). Both varieties of the Indian bean exhibited a significant increase in the weight of grains  $\text{plant}^{-1}$  upon all doses of N amendments (N1, N2, and N3). However, the difference in the magnitude of the increase in yield of N2 and N3 was inconsequential for both varieties indicating the sufficiency of N2 treatment in ameliorating oxidative conditions. Interestingly, the  $\text{O}_3$ -sensitive Kashi Harittima variety showed a higher percent increment in the number/weight of seeds  $\text{plant}^{-1}$  upon N amendments as compared to Kashi Sheetal (Table 4). Higher enhancement in the antioxidative enzyme activity and greater increments in the rate of photosynthesis explain the higher yield improvements in Kashi Harittima. A previous experiment also reported similar findings in which an  $\text{O}_3$ -sensitive wheat cultivar showed a higher percent increment in response to N amendments as compared to an  $\text{O}_3$ -tolerant wheat cultivar under both  $\text{AO}_3$  and  $\text{EO}_3$  conditions (Pandey et al., 2018). The above results prove our first hypothesis that nitrogen treatments assist in strengthening the antioxidative enzyme pool for defense against oxidative stress conditions. In the present study, the analysis of  $\text{H}_2\text{O}_2$  localization, antioxidative enzymes, physiological traits, and yield revealed that the Kashi Sheetal variety outperformed the Kashi Harittima variety in every aspect proving the second hypothesis that the differential response of the varieties to varied  $\text{O}_3$  conditions helps in determining their sensitivity to  $\text{O}_3$  stress. The more positive response of the  $\text{O}_3$ -sensitive varieties upon N exposure provides a promising feature and can be used for promoting the farming of  $\text{O}_3$ -sensitive varieties, thereby boosting agricultural production.

## 5 Conclusion

This experiment justifies the use of N amendments as an effective measure for the management of  $\text{O}_3$  injury. The higher endogenous levels of  $\text{H}_2\text{O}_2$  accumulation and enzymatic antioxidant contents upon  $\text{O}_3$  exposure have established Kashi Sheetal to be  $\text{O}_3$  tolerant. The interaction between N amendments and  $\text{O}_3$  exposure had a more positive effect on  $\text{O}_3$ -sensitive Kashi Harittima, as compared to Kashi Sheetal. Since the increased stomatal conductance upon N fertilization does not restrict the entry of  $\text{O}_3$  in plants, the higher photosynthetic rate, and subsequently yield were maintained by a stimulated enzymatic antioxidative response in plants at both  $\text{O}_3$  exposure conditions. The enzymatic response showed significant variations due to ozone and treatment and ozone and variety interactions, whereas the variations of stomatal conductance were insignificant, proving our theory. A more positive response of Kashi Harittima to N supplementation at both  $\text{O}_3$  exposure conditions can be associated with the sustenance of its higher enzymatic response at the reproductive stage as well, which was more prominent at the  $\text{EO}_3$  condition. The current study proved that N2 treatment (1.5 times recommended dose) was sufficient to partially ameliorate  $\text{O}_3$  stress and that larger nitrogen doses may not be more successful in doing so because they did not confer any further perks on the plant's growth and development. However, more experiments are required to establish a dose-response relationship between N fertilization and  $\text{O}_3$  exposure doses.

## Data availability statement

The original contributions presented in the study are included in the article/supplementary material. Further inquiries can be directed to the corresponding author.

## Author contributions

Conceptualization, writing-original draft, AS. Data curation, PM. Software, AM. Conceptualization, supervision, ST. All authors contributed to the article and approved the submitted version.

## Funding

Council of Scientific and Industrial Research, India 09/013 (0785)/2018-EMR-I

## Acknowledgments

The authors would like to acknowledge the Head of the Department of Botany, Banaras Hindu University for providing the necessary facilities. The authors would like to thank the Council

of Scientific and Industrial Research (CSIR)-HRDG, New Delhi, for providing fellowships.

## Conflict of interest

The authors declare that the research was conducted in the absence of any commercial or financial relationships that could be construed as a potential conflict of interest.

## Publisher's note

All claims expressed in this article are solely those of the authors and do not necessarily represent those of their affiliated organizations, or those of the publisher, the editors and the reviewers. Any product that may be evaluated in this article, or claim that may be made by its manufacturer, is not guaranteed or endorsed by the publisher.

## References

- Aebi, H. (1984). Catalase *in vitro*. *Methods enzymology* 105, 121–126. doi: 10.1016/S0076-6879(84)05016-3
- Almeselmani, M., Deshmukh, P. S., Sairam, R. K., Kushwaha, S. R., and Singh, T. P. (2006). Protective role of antioxidant enzymes under high-temperature stress. *Plant Sci. J.* 171, 382–388. doi: 10.1016/j.plantsci.2006.04.009
- Anderson, M. E. (1996). Glutathione. *Free radicals: Pract. approach*, 213–226.
- Ashraf, M. (2009). Biotechnological approach of improving plant salt tolerance using antioxidants as markers. *Biotechnol. Adv.* 27, 84–93. doi: 10.1016/j.biotechadv.2008.09.003
- Biswas, D. K., and Jiang, G. M. (2011). Differential drought-induced modulation of ozone tolerance in winter wheat species. *J. Exp. Bot.* 62, 4153–4162. doi: 10.1093/jxb/err104
- Caregnato, F. F., Bortolin, R. C., Junior, A. M. D., and Moreira, J. C. F. (2013). Exposure to elevated ozone levels differentially affects the antioxidant capacity and the redox homeostasis of two subtropical *Phaseolus vulgaris* L. varieties. *Chemosphere* 93, 320–330. doi: 10.1016/j.chemosphere.2013.04.084
- Choudhury, F. K., Rivero, R. M., Blumwald, E., and Mittler, R. (2017). Reactive oxygen species, abiotic stress and stress combination. *Plant J.* 90, 856–867. doi: 10.1111/tj.13299
- Davari, S. A., Gokhale, N. B., Palsande, V. N., and Kasture, M. C. (2018). Wal (*Lablab purpureus* L.): An unexploited potential food legumes. *Int. J. Chem. Stud.* 6, 946–949.
- Dhevagi, P., Ramya, A., Priyatharshini, S., and Poornima, R. (2021). Effect of elevated tropospheric ozone on vigna mungo L. varieties. *Ozone: Sci. Engineering* 44, 1–21.
- Duque, L., Poelman, E. H., and Steffan-Dewenter, I. (2021). Effects of ozone stress on flowering phenology, plant-pollinator interactions and plant reproductive success. *Environ. pollut.* 272, 115953. doi: 10.1016/j.envpol.2020.115953
- Emberson, L. D., Bükler, P., Ashmore, M. R., Mills, G., Jackson, L. S., Agrawal, M., et al. (2009). A comparison of north American and Asian exposure-response data for ozone effects on crop yields. *Atmospheric Environ.* 43, 1945–1953. doi: 10.1016/j.atmosenv.2009.01.005
- Fridovich, I. (1975). Superoxide dismutases. *Annu. Rev. Biochem.* 44, 147–159. doi: 10.1146/annurev.bi.44.070175.001051
- Gupta, G. S., and Tiwari, S. (2020). Role of antioxidant pool in management of ozone stress through soil nitrogen amendments in two cultivars of a tropical legume. *Funct. Plant Biol.* 48, 371–385. doi: 10.1071/FP20159
- Harmens, H., Hayes, F., Sharps, K., Mills, G., and Calatayud, V. (2017). Leaf traits and photosynthetic responses of betula pendula saplings to a range of ground-level ozone concentrations at a range of nitrogen loads. *J. Plant Physiol.* 211, 42–52. doi: 10.1016/j.jplph.2017.01.002
- Hayes, F., Sharps, K., Harmens, H., Roberts, I., and Mills, G. (2020). Tropospheric ozone pollution reduces the yield of African crops. *J. Agron. Crop Sci.* 206, 214–228. doi: 10.1111/jac.12376
- Heath, R. L., and Packer, L. (1968). Photoperoxidation in isolated chloroplasts: I. kinetics and stoichiometry of fatty acid peroxidation. *Arch. Biochem. biophysics* 125, 189–198. doi: 10.1016/0003-9861(68)90654-1
- Iglesias, D. J., Calatayud, Á., Barreno, E., Primo-Millo, E., and Talon, M. (2006). Responses of citrus plants to ozone: leaf biochemistry, antioxidant mechanisms, and lipid peroxidation. *Plant Physiol. Biochem.* 44, 125–131. doi: 10.1016/j.plaphy.2006.03.007
- Letting, F. K., Venkataramana, P. B., and Ndakidemi, P. A. (2021). Breeding potential of lablab [*Lablab purpureus* (L.) sweet]: a review on characterization and bruchid studies towards improved production and utilization in Africa. *Genet. Resour. Crop Evol.* 68, 3081–3101. doi: 10.1007/s10722-021-01271-9
- Liu, Y. M., Shahed-Al-Mahmud, M., Chen, X., Chen, T. H., Liao, K. S., Lo, J. M., et al. (2020). Carbohydrate-binding protein from the edible lablab beans effectively blocks the infections of influenza viruses and SARS-CoV-2. *Cell Rep.* 32, 108016. doi: 10.1016/j.celrep.2020.108016
- Mao, Q., Watanabe, M., Makoto, K., Kita, K., and Koike, T. (2014). High nitrogen deposition may enhance growth of a new hybrid larch F1 growing at two phosphorus levels. *Landscape Ecol. Eng.* 10, 1–8. doi: 10.1007/s11355-012-0207-2
- Marzuoli, R., Monga, R., Finco, A., Chiesa, M., and Gerosa, G. (2018). Increased nitrogen wet deposition triggers negative effects of ozone on the biomass production of *Carpinus betulus* L. young trees. *Environ. Exp. Bot.* 152, 128–136. doi: 10.1016/j.envexpbot.2017.10.017
- Meehl, G. A., Tebaldi, C., Tilmes, S., Lamarque, J. F., Bates, S., Pendergrass, A., et al. (2018). Future heat waves and surface ozone. *Environ. Res. Lett.* 13 (6), 064004. doi: 10.1088/1748-9326/aabdc
- Mills, G., Wagg, S., and Harmens, H. (2013). Ozone pollution: impacts on ecosystem services and biodiversity. *Centre Ecol. Hydrology*.
- Mukherjee, A., and Hazra, S. (2022). "Impact of elevated CO<sub>2</sub> and O<sub>3</sub> on field crops and adaptive strategies through agro-technology," in *Response of field crops to abiotic stress* (CRC Press), 177–190.
- Nakano, Y., and Asada, K. (1981). Hydrogen peroxide is scavenged by ascorbate-specific peroxidase in spinach chloroplasts. *Plant Cell Physiol.* 22, 867–880.
- Pandey, A. K., Ghosh, A., Agrawal, M., and Agrawal, S. B. (2018). Effect of elevated ozone and varying levels of soil nitrogen in two wheat (*Triticum aestivum* L.) cultivars: Growth, gas exchange, antioxidant status, grain yield and quality. *Ecotoxicology Environ. Saf.* 158, 59–68. doi: 10.1016/j.ecoenv.2018.04.014
- Picchi, V., Monga, R., Marzuoli, R., Gerosa, G., and Faoro, F. (2017). The ozone-like syndrome in durum wheat (*Triticum durum* L.): Mechanisms underlying the different symptomatic responses of two sensitive cultivars. *Plant Physiol. Biochem.* 112, 261–269. doi: 10.1016/j.plaphy.2017.01.011
- Podda, A., Pisuttu, C., Hoshika, Y., Pellegrini, E., Carrari, E., Lorenzini, G., et al. (2019). Can nutrient fertilization mitigate the effects of ozone exposure on an ozone-sensitive poplar clone? *Sci. Total Environ.* 657, 340–350. doi: 10.1016/j.scitotenv.2018.11.459



- Rana, R., Sayem, A. S. M., Sabuz, A. A., Rahman, M., and Hos-Sain, A. (2021). Effect of lablab bean (*Lablab purpureus* L.) seed flour on the physicochemical and sensory properties of biscuits. *Int. J. Food Sci. Agric.* 5, 52–57. doi: 10.26855/ijfsa.2021.03.008
- Sahoo, A., and Tiwari, S. (2021). Role of soil nitrogen amendments in management of ozone stress in plants: a study of the mechanistic approach. *J. Emerging Technol. Innovative Res.* 8, 739–755.
- Sarkar, A., and Agrawal, S. B. (2010). Elevated ozone and two modern wheat cultivars: an assessment of dose dependent sensitivity with respect to growth, reproductive and yield parameters. *Environ. Exp. Bot.* 69, 328–337. doi: 10.1016/j.envexpbot.2010.04.016
- Sicard, P., Anav, A., De Marco, A., and Paoletti, E. (2017). Projected global ground-level ozone impacts on vegetation under different emission and climate scenarios. *Atmospheric Chem. Phys.* 17, 12177–12196. doi: 10.5194/acp-17-12177-2017
- Singh, A. A., Agrawal, S. B., Shahi, J. P., and Agrawal, M. (2014). Assessment of growth and yield losses in two *Zea mays* L. cultivars (quality protein maize and non-quality protein maize) under projected levels of ozone. *Environ. Sci. Pollut. Res.* 21, 2628–2641. doi: 10.1007/s11356-013-2188-6
- Singh, A. A., Fatima, A., Mishra, A. K., Chaudhary, N., Mukherjee, A., Agrawal, M., et al. (2018). Assessment of ozone toxicity among 14 Indian wheat cultivars under field conditions: growth and productivity. *Environ. Monit. Assess.* 190, 1–14. doi: 10.1007/s10661-018-6563-0
- Statista (2021). Global No.1 business data platform.
- Stella, P., Personne, E., Lamaud, E., Loubet, B., Trebs, I., and Cellier, P. (2013). Assessment of the total, stomatal, cuticular, and soil 2-year ozone budgets of an agricultural field with winter wheat and maize crops. *J. Geophys. Res. Biogeosci.* 118, 1120–1132. doi: 10.1002/jgrg.20094
- Tetteh, R., Yamaguchi, M., and Izuta, T. (2016). Effect of ambient levels of ozone on photosynthetic components and radical scavenging system in leaves of African cowpea varieties. *Afr. Crop Sci. J.* 24, 127–142. doi: 10.4314/acsj.v24i2.2
- Thordal-Christensen, H., Zhang, Z., Wei, Y., and Collinge, D. B. (1997). Subcellular localization of H<sub>2</sub>O<sub>2</sub> in plants. H<sub>2</sub>O<sub>2</sub> accumulation in papillae and hypersensitive response during the barley–powdery mildew interaction. *Plant J.* 11, 1187–1194. doi: 10.1046/j.1365-313X.1997.11061187.x
- Tiwari, S., and Agrawal, M. (2018). *Tropospheric ozone and its impacts on crop plants* Vol. 1007 (Springer International Publishing), 978–973.
- Van Dingenen, R., Dentener, F. J., Raes, F., Krol, M. C., Emberson, L., and Cofala, J. (2009). The global impact of ozone on agricultural crop yields under current and future air quality legislation. *Atmos. Environ.* 43, 604–618. doi: 10.1016/j.atmosenv.2008.10.033
- Wall, G. W., Adam, N. R., Brooks, T. J., Kimball, B. A., Pinter, P. J., LaMorte, R. L., et al. (2000). Acclimation response of spring wheat in a free-air CO<sub>2</sub> enrichment (FACE) atmosphere with variable soil nitrogen regimes. 2. net assimilation and stomatal conductance of leaves. *Photosynthesis Res.* 66, 79–95. doi: 10.1023/A:1010646225929
- Wang, C., Lin, J., Niu, Y., Wang, W., Wen, J., Lv, L., et al. (2022). Impact of ozone exposure on heart rate variability and stress hormones: A randomized-crossover study. *J. Hazardous Materials* 421, 126750. doi: 10.1016/j.jhazmat.2021.126750
- Yadav, D. S., Rai, R., Mishra, A. K., Chaudhary, N., Mukherjee, A., Agrawal, S. B., et al. (2019). ROS production and its detoxification in early and late sown cultivars of wheat under future O<sub>3</sub> concentration. *Sci. Total Environ.* 659, 200–210. doi: 10.1016/j.scitotenv.2018.12.352
- Yendrek, C. R., Leisner, C. P., and Ainsworth, E. A. (2013). Chronic ozone exacerbates the reduction in photosynthesis and acceleration of senescence caused by limited N availability in *Nicotiana sylvestris*. *Global Change Biol.* 19, 3155–3166. doi: 10.1111/gcb.12237
- Zeng, J., Sheng, H., Liu, Y., Wang, Y., Wang, Y., Kang, H., et al. (2017). High nitrogen supply induces physiological responsiveness to long photoperiod in barley. *Front. Plant Sci.* 8, 569. doi: 10.3389/fpls.2017.00569
- Zhang, L., Hoshika, Y., Carrari, E., Cotrozzi, L., Pellegrini, E., and Paoletti, E. (2018). Effects of nitrogen and phosphorus imbalance on photosynthetic traits of poplar Oxford clone under ozone pollution. *J. Plant Res.* 131, 915–924. doi: 10.1007/s10265-018-1071-4
- Zhang, L., Xiao, S., Chen, Y. J., Xu, H., Li, Y. G., Zhang, Y. W., et al. (2017). Ozone sensitivity of four pakchoi cultivars with different leaf colors: physiological and biochemical mechanisms. *Photosynthetica* 55, 478–490. doi: 10.1007/s11099-016-0661-4



## OPEN ACCESS

## EDITED BY

Milan Skalicky,  
Czech University of Life Sciences Prague,  
Czechia

## REVIEWED BY

Reiaz Ul Rehman,  
University of Kashmir, India  
Tahmina Islam,  
University of Dhaka, Bangladesh  
Jun Liu,  
Institute of Crop Sciences, Chinese  
Academy of Agricultural Sciences, China

## \*CORRESPONDENCE

Ying Zhao

✉ Tianshi198937@126.com

Jianguo Zhang

✉ zhangjianguo72@163.com

Yuhu Zuo

✉ zuoyhu@163.com

†These authors have contributed equally to  
this work

## SPECIALTY SECTION

This article was submitted to  
Plant Abiotic Stress,  
a section of the journal  
Frontiers in Plant Science

RECEIVED 05 December 2022

ACCEPTED 23 February 2023

PUBLISHED 09 March 2023

## CITATION

Li X, Cai Q, Yu T, Li S, Li S, Li Y, Sun Y,  
Ren H, Zhang J, Zhao Y, Zhang J and  
Zuo Y (2023) *ZmG6PDH1* in glucose-6-  
phosphate dehydrogenase family enhances  
cold stress tolerance in maize.  
*Front. Plant Sci.* 14:1116237.  
doi: 10.3389/fpls.2023.1116237

## COPYRIGHT

© 2023 Li, Cai, Yu, Li, Li, Li, Sun, Ren, Zhang,  
Zhao, Zhang and Zuo. This is an open-  
access article distributed under the terms of  
the [Creative Commons Attribution License](#)  
(CC BY). The use, distribution or  
reproduction in other forums is permitted,  
provided the original author(s) and the  
copyright owner(s) are credited and that  
the original publication in this journal is  
cited, in accordance with accepted  
academic practice. No use, distribution or  
reproduction is permitted which does not  
comply with these terms.

# *ZmG6PDH1* in glucose-6-phosphate dehydrogenase family enhances cold stress tolerance in maize

Xin Li<sup>1,2†</sup>, Quan Cai<sup>2†</sup>, Tao Yu<sup>2†</sup>, Shujun Li<sup>2</sup>, Sinan Li<sup>2</sup>, Yunlong Li<sup>2</sup>,  
Yan Sun<sup>2</sup>, Honglei Ren<sup>2</sup>, Jiajia Zhang<sup>3</sup>, Ying Zhao<sup>3\*</sup>,  
Jianguo Zhang<sup>2\*</sup> and Yuhu Zuo<sup>1\*</sup>

<sup>1</sup>National Coarse Cereals Engineering Research Center, Heilongjiang Provincial Key Laboratory of Crop-Pest Interaction Biology and Ecological Control, Heilongjiang Bayi Agricultural University, Daqing, Heilongjiang, China, <sup>2</sup>Key Lab of Maize Genetics and Breeding, Heilongjiang Academy of Agricultural Sciences, Harbin, Heilongjiang, China, <sup>3</sup>College of Agriculture, Northeast Agricultural University, Harbin, Heilongjiang, China

Glucose-6-phosphate dehydrogenase (G6PDH) is a key enzyme in the pentose phosphate pathway responsible for the generation of nicotinamide adenine dinucleotide phosphate (NADPH), thereby playing a central role in facilitating cellular responses to stress and maintaining redox homeostasis. This study aimed to characterize five *G6PDH* gene family members in maize. The classification of these *ZmG6PDHs* into plastidic and cytosolic isoforms was enabled by phylogenetic and transit peptide predictive analyses and confirmed by subcellular localization imaging analyses using maize mesophyll protoplasts. These *ZmG6PDH* genes exhibited distinctive expression patterns across tissues and developmental stages. Exposure to stressors, including cold, osmotic stress, salinity, and alkaline conditions, also significantly affected the expression and activity of the *ZmG6PDHs*, with particularly high expression of a cytosolic isoform (*ZmG6PDH1*) in response to cold stress and closely correlated with G6PDH enzymatic activity, suggesting that it may play a central role in shaping responses to cold conditions. CRISPR/Cas9-mediated knockout of *ZmG6PDH1* on the B73 background led to enhanced cold stress sensitivity. Significant changes in the redox status of the NADPH, ascorbic acid (ASA), and glutathione (GSH) pools were observed after exposure of the *zmG6pdh1* mutants to cold stress, with this disrupted redox balance contributing to increased production of reactive oxygen species and resultant cellular damage and death. Overall, these results highlight the importance of cytosolic *ZmG6PDH1* in supporting maize resistance to cold stress, at least in part by producing NADPH that can be used by the ASA-GSH cycle to mitigate cold-induced oxidative damage.

## KEYWORDS

*ZmG6PDH1*, enzyme activity, expression, cold stress, CRISPR/Cas9, maize (*Zea mays* L.)

## Introduction

Glucose-6-phosphate dehydrogenase (G6PDH, EC 1.1.1.49) is a ubiquitously expressed enzyme responsible for catalyzing the rate-limiting first step of the pentose phosphate pathway (PPP) in which b-D-glucose-6-phosphate (G6P) is oxidized to 6-phosphogluconolactone and oxidized nicotinamide adenine dinucleotide phosphate (NADP<sup>+</sup>) is reduced to yield NADPH (Chen et al., 2022). NADPH, produced through PPP-mediated oxidation, functions as a reducing agent essential for redox homeostasis and lipid biosynthesis (Esposito, 2016). In parallel, the non-oxidative arm of the PPP is responsible for generating a range of metabolic intermediates, including ribose-5-phosphate, which is required for nucleotide biosynthesis, and erythrose 4-phosphate, which serves as a precursor molecule for aromatic amino acids and coenzymes (Corpas et al., 2021).

G6PDH gene family members have been characterized in many plant species, including soybean (Zhao et al., 2020), strawberry (Zhang et al., 2020), wheat (Tian et al., 2021), tomato (Landi et al., 2016), barley (Zhao et al., 2015), and *Arabidopsis* (Yang et al., 2019; Linnenbrügger et al., 2022), where they function as critical regulators of growth and development. The different G6PDH isoforms are classified according to their subcellular localizations, with each regulated by distinct mechanisms and playing different roles in plant metabolic activity (Feng et al., 2020; Landi et al., 2021). Plastid G6PDH isoforms include P1-G6PDH, which is similar to algal forms of this enzyme and is only expressed in green tissues, and P2-G6PDH, primarily expressed in roots and heterotrophic tissue types (Cardi et al., 2013; Preiser et al., 2019). Cytosolic G6PDH isoforms are estimated to account for 60–80% of total G6PDH activity measured within plant cells (Scharte et al., 2009; Zhang et al., 2020). In *Arabidopsis*, the cytosolic G6PDH knockdown can suppress seed oil accumulation, highlighting a pivotal role for Cy-G6PDH as a regulator of lipid biosynthesis in developing seeds (Ruan et al., 2022).

G6PD activity levels are positively correlated with a range of biotic and abiotic stressors, including fungal pathogen infection, ABA exposure, cell death responses, cold stress, drought, salt stress, nutrient starvation, and aluminum toxicity (Feng et al., 2020; Zhao et al., 2020; He et al., 2021; Huang et al., 2022). Scharte et al. demonstrated that G6PDH activity levels were elevated in the resistant *Nicotiana tabacum* Samsun NN cultivar in response to *Phytophthora nicotianae* infection, whereas the same was not true in the susceptible Xanthi cultivar (Scharte et al., 2009). G6PDH enzymatic responses to heavy metal stress in *Phaseolus vulgaris* L. and wheat are reportedly regulated by aluminum or zinc (Van Assche et al., 1988). RNAi studies have confirmed that the G6PDH isoenzyme shapes drought tolerance and flowering in tobacco plants (Begcy et al., 2012). The *A. thaliana* Cy-G6PDH isoform engages in specific regulatory functions resulting from Thr467 phosphorylation mediated by glycogen synthase kinase 3 (ASKa), with this activity possibly associated with a sugar-sensing signal in response to salt stress (Yang et al., 2019). G6PDH transcript levels in *Triticum aestivum* L. exposed to 0.15 M NaCl stress also reportedly rise with time, peaking after 12 h (Nemoto and

Sasakuma, 2000). Zhang et al. determined that G6PDH is also a key enzyme in *Oryza sativa* cells in suspension when exposed to salt stress, maintaining redox homeostasis by regulating G6PDH and NADPH oxidase activity (Zhang et al., 2013). Cold stress represents a severe physiological constraint for plants, negatively affecting both growth rates and development. Several researchers reported the tolerance of G6PDH to cold stress (Yang et al., 2014; Zhang et al., 2014; Landi et al., 2021). *PsG6PDH* overexpression in transgenic tobacco plants increased the induction of cold stress response-related genes, suggesting a role for this enzyme in the coordination of plant responses to low temperature stress (Lin et al., 2005). A remarkable increase of the expression levels of cytosolic and plastidic G6PDH has been found in strawberry (*Fragaria ananassa*) exposed to cold stress (Zhang et al., 2020). Cytosolic- and peroxisome-located G6PDHs showed a central role in acclimation to cold stress at various growth stages of barley (*Hordeum vulgare*) and *Arabidopsis thaliana* (Tian et al., 2021). While G6PDH activity is thus known to be central to the induction of plant responses to abiotic stressors, the specific relationships between its enzymatic reactions and stress tolerance are not fully understood.

The roles of G6PDH isoforms as coordinators of stress response-related activities have been documented in many plants, but little is known about their function in maize (*Zea mays* L.). Maize is the most widely produced crop in the world and is a significant component of animal feed and raw material used in industrial applications (Sheoran et al., 2021). Five maize G6PDH (*ZmG6PDH*) gene family members were characterized in this study. Transit peptide analyses were initially used to predict the localization of these *ZmG6PDH*s within cells, further confirmed by transient expression of GFP-tagged *ZmG6PDH*s in maize protoplasts. The transcriptional profiles of *ZmG6PDH* were further analyzed using high-throughput sequencing and qPCR in multiple organs and response to various abiotic stressors. The results showed that the transcription of one cytosolic isoform (*ZmG6PDH1*) was sensitive to cold stress and was correlated with G6PDH enzyme activity levels. Knockout of *ZmG6PDH1* reduced the tolerance of transgenic maize seedlings to cold stress, with corresponding reductions in the NADPH/NADP<sup>+</sup>, GSH/GSSG (reduced/oxidized glutathione), and ASA/DHA (ascorbic acid/dehydroascorbate) ratios, together with higher levels of reactive oxygen species (ROS) production. These findings suggest that these *ZmG6PDH*s may be important regulators of plant growth and stress response activity, with cytosolic *ZmG6PDH1* being the primary isoform responsible for regulating cellular redox pools and mitigating oxidative stress.

## Materials and methods

### Maize G6PDH gene family identification

Maize G6PDH isoforms were identified using known *A. thaliana* G6PDH sequences as queries to perform a BLASTP search against the maize genome (<http://www.maizesequence.org>).

Protein sequences for candidate ZmG6PDHs exhibiting >90% sequence identity and an E-value of  $<10^{-10}$  were downloaded. Phytozome v13 (<https://phytozome-next.jgi.doe.gov/>) was then used to acquire details regarding the genetic characteristics of these *ZmG6PDH* family genes, including chromosome location, coding sequence length, and protein length. The ExPASy server (<http://expasy.org/>) was used to determine the molecular mass and isoelectric points of these proteins, and predictions of transit peptides and subcellular localization were conducted using TargetP 2.0 (<http://www.cbs.dtu.dk/services/TargetP/>) and CELLO 2.5 (<http://cello.life.nctu.edu.tw/>) (Yu et al., 2004).

## Evolutionary, synteny, and gene structural analyses

Full-length G6PDH protein sequences from *Z. mays* (ZmG6PDH1-5), *Solanum lycopersicum* (SlG6PDH1-4), *Setaria italica* (SiG6PDH1-5), *Triticum aestivum* (TaG6PDH1-5), *Solanum tuberosum* (StG6PDH1-4), *Brassica oleracea* (BoG6PDH1-5), *Phaseolus vulgaris* (PvG6PDH1-5), *Sorghum bicolor* (SbG6PDH1-4), and *A. thaliana* (AtG6PDH1-6) were utilized to construct a neighbor-joining phylogenetic tree by MEGA 5.0 software with the bootstrap values performed on 1000 replicates (Tamura et al., 2011). These amino acid sequences were aligned with ClustalW with standard settings (gap opening penalty: 10 and gap extension penalty: 0.2) (Larkin et al., 2007). The GSDS database (<http://gsds.cbi.pku.edu.cn/index.php>) confirmed G6PDH gene structural characteristics by aligning coding regions and associated genomic regions. The NCBI and maize genetics and genomics databases were used to obtain *A. thaliana* and *Z. mays* genomic and coding sequences for G6PDHs. Syntenic blocks among the G6PDHs encoded by *Z. mays*, *P. vulgaris*, *A. thaliana*, *S. lycopersicum*, *S. italica*, *T. aestivum*, *S. tuberosum*, *B. oleracea*, and *S. bicolor* were then established based on the plant genome duplication database (PGDD, <http://chibba.agtec.uga.edu/duplication/>) (Lee et al., 2012). Gene IDs and other details regarding G6PDHs utilized for these analyses are compiled in Supplementary Table S1.

## ZmG6PDH promoter analyses

Key *cis*-acting elements in the promoter regions of candidate *ZmG6PDHs* were identified using the maize genetics and genomics database to obtain the region 2.0 kb upstream of the ATG start codon for each of these genes. The PlantCARE database (<http://bioinformatics.psb.ugent.be/webtools/plantcare/html/>) was then used to predict *cis*-acting elements within these regions, presented using IBS 2.0 (Liu et al., 2015).

## Subcellular localization analyses

The complete coding regions corresponding to the five identified *ZmG6PDHs* from the inbred B73 maize variety were amplified by

RT-PCR using high-fidelity KOD-Plus-DNA polymerase and gene-specific primers (Supplementary Table S2). The amplified genes were inserted into the pBI121 vector, containing a GFP tag and a CaMV35S promoter. The resultant *pBI121-ZmG6PDHs::GFP* fusion proteins were transiently transformed into the maize mesophyll protoplasts isolated from leaves of 14-day-old seedlings using polyethylene glycol (PEG)-mediated protoplast transformation technique (Yoo et al., 2007). The localization of these proteins was then visualized using confocal laser-scanning microscopy (LSM 710, Carl Zeiss, Jena, Germany) with respective excitation/emission wavelengths of 488 nm/507–535 nm and 610 nm/650–750 nm for GFP and chlorophyll autofluorescence.

## ZmG6PDH expression analyses

Patterns of *ZmG6PDH* gene expression across tissues, including leaves, stems, roots, ears, mature seeds, brace roots, and tassels, were analyzed using high-throughput sequencing data in the Phytozome database. The data were compiled into heatmaps subjected to hierarchical clustering performed with TBtools (Chen et al., 2020), and the values were normalized and subjected to log2 transformation. *ZmG6PDH* expression across different stages of seed development was characterized by extracting total RNA from maize seeds 5, 10, 15, 20, 25, and 30 days after flowering (DAF), with *ZmG6PDH* expression profiles at 5DAF used as a baseline for subsequent expression level changes. *ZmG6PDH* transcriptional profiles in response to different forms of abiotic stress were evaluated by subjecting maize seedlings at the three-leaf stage to salt stress (150 mM NaCl), alkali stress (100 mM NaHCO<sub>3</sub>), osmotic stress (20% w/v PEG [MW: 6000 g/M]), and cold stress (incubation at 4°C). At 0, 3, 6, 12, and 24 h following the initiation of these treatments, total RNA was extracted from the leaves of the seedlings. Levels of *ZmG6PDH* expression in maize leaves under non-stressed conditions served as a baseline for these analyses, while *ZmGAPDH* and *ZmACTIN* were used for normalization (Kong et al., 2013; Zhang et al., 2014). All qPCR assays were performed using three technical and three biological replicates, with relative *ZmG6PDH* expression levels determined through the  $2^{-\Delta\Delta C_t}$  method.

## CRISPR/Cas vector construction and maize transformation

A CRISPR/Cas9 approach was used to generate mutations in the *ZmG6PDH1* coding regions. Two guide RNAs targeting sites in the *ZmG6PDH1* gene were designed with the CRISPR-P 2.0 web tool (Liu et al., 2017) based on the B73 reference genome (Table S3), with these guide RNAs then being introduced into the pBUE411 vector (Xing et al., 2014). The resultant pBUE411 binary vector was introduced into *Agrobacterium tumefaciens* strain EHA105. *Agrobacterium*-mediated transformation was conducted with 10–15 DAP immature zygotic embryos (Char et al., 2017). The genome editing results were evaluated by PCR amplification and Sanger sequencing of target regions, and the expression of *ZmG6PDH1* in



gene-edited mutants was assessed by qPCR and enzyme activity analyses.

Dry weight values for both mutant and wild-type (WT) plants were assessed on day 5 following treatment at 4°C, with plant height and root length also being recorded. Samples of leaves were collected on day 3 of treatment to analyze biochemical and physiological parameters therein. Experiments were repeated at least three times with 10 to 20 plants, and all images depict representative results. Total chlorophyll, chlorophyll a, and chlorophyll b levels in the top secondary fully expanded leaves were analyzed as reported previously (Wellburn, 1994) using 80% (v/v) acetone. Photochemical efficiency ( $F_v/F_m$ ) was analyzed with a pulse-modulated fluorometer (FMS2, Hansatech, UK), and leaf photosynthetic characteristics ( $P_n$ , net photosynthetic rate) were evaluated with a portable open photosynthesis system (Li-6400; Li-Cor, Inc., NE, USA).

## Biochemical and physiological analyses

G6PDH activity was measured using a modified version of a previously reported protocol (Wakao and Benning, 2005). The total reaction volume of the assay was 1 mL containing 3.3 mM  $MgCl_2$ , 50 mM Hepes-Tris (pH 7.8), 0.5 mM  $NADPNa_2$ , 0.5 mM D-glucose-6-phosphate disodium salt, and an appropriate amount of enzyme extracts. The absorbance of the supernatant was read at 340 nm using an ultraviolet spectrophotometer (U3900, Hitachi High-Technologies, Japan). The redox status of the NADPH, ASA, and GSH pools was examined by evaluating the levels of the oxidized ( $NADP^+$ , DHA, GSSG) and reduced (NADPH, ASA, GSH) forms of these intermediates by spectrophotometry, as previously described (Nagalakshmi and Prasad, 2001; Queval and Noctor, 2007).

Superoxide ( $O_2^-$ ) and hydrogen peroxide ( $H_2O_2$ ) levels were also analyzed by spectrophotometry as previously described (Fryer et al., 2002). Thiobarbituric acid-reactive substances (TBARS) and electrolyte leakage (EL) levels were used to assess membrane leakage, as detailed previously (Hodges et al., 1999; Zhao et al., 2019). Leaf tissues (0.5 g) were ground in ice extracted with 10 mL 0.1% (w/v) trichloroacetic acid (TCA), and then the homogenate was centrifuged at 10 000 g for 10 min at 4°C. Supernatants were then collected for analyses of TBARS contents. The total reaction volume of the TBARS assay was 2 mL containing 0.5 mL of the supernatant and 1.5 mL 0.5% (w/v) thiobarbital acid in 15% TCA. The absorbance of supernatant was read at 532 nm.

ROS scavenging abilities were examined by homogenizing 0.5 g of maize in 0.2 mL extraction buffer (1% PVP, 1.5 mM EDTA, 0.5 mM ASC,  $K_2HPO_4$ - $KH_2PO_4$ , pH 7.0), with homogenates then being centrifuged at 12 000 g for 20 min at 4°C (Nakano and Asada, 1981; Takashi et al., 1997). The supernatants were then analyzed for the activity levels of monodehydro-ascorbate reductase (MDAR), glutathione reductase (GR), glutathione peroxidase (GPX), dehydroascorbate reductase (DHAR), and ascorbate peroxidase (APX) according to the instructions provided with commercial kits (Solarbio, China).

## Statistical analysis

A minimum of three biological replicates were used per experiment. Results are given as means  $\pm$  SD and were compared with Student's t-tests using SPSS 22.0.  $P < 0.05$  was the significance threshold.

## Results

### Maize G6PDH gene family identification and categorization

Initial analyses of the *Z. mays* genome led to the tentative identification of five genes encoding G6PDH isoforms named *ZmG6PDH1-5* (Table 1). The full-length coding sequences for these genes were between 1527 and 2748 bp, encoding proteins ranging from 508-915 amino acids in length. Isoelectric points and molecular weights for the candidate *ZmG6PDHs* encoded by these genes ranged from 6.26-9.22 and 57.63-103.03 kDa, respectively (Table 1). TargetP 1.1 and CELLO 2.5 were then utilized to detect putative N-terminal transit peptide (TP) sequences, predicting that *ZmG6PDH1* and *ZmG6PDH5* were localized in the cytosol while the three other isoforms were expected to localize to the plastid compartment (Table 1).

The evolutionary history and classification of these *ZmG6PDHs* were explored by aligning their full-length protein sequences with those of homologous G6PDH enzymes encoded by *S. bicolor* (StG6PDH1-4), *S. italica* (SiG6PDH1-5), *S. lycopersicum* (SlG6PDH1-4), *A. thaliana* (AtG6PDH1-6), *T. aestivum* (TaG6PDH1-5), *S. tuberosum* (StG6PDH1-4), *P. vulgaris* (PvG6PDH1-5), and *B. oleracea* (BoG6PDH1-5) to construct a phylogenetic tree (Figure 1A). In this analysis, these plant G6PDHs were broadly classified into Clade I (cytosolic isoforms) and Clade II (plastidic isoforms). The cytosolic (Cy) G6PDH isoforms, including *ZmG6PDH1* and 5, as well as two *Arabidopsis* Cy-G6PDHs (AtG6PDH5, 6) (Wakao et al., 2008). Members of Clade II were further subdivided into class a (including *ZmG6PDH4* and AtG6PDH1), class b (*ZmG6PDH2* and AtG6PDH2, 3), and class c (*ZmG6PDH3* and the inactive-G6PDH isoform AtG6PDH4). These *ZmG6PDHs* were closely related to homologs from monocot sorghum plants within individual clusters, consistent with the evolutionary history of these plant lineages and associated G6PDH isoforms.

Structural analyses of the proteins encoded by these five *ZmG6PDHs* revealed the presence of a bi-domain structure akin to that reported for *A. thaliana* G6PDHs, including both an N-terminal  $NADP^+$ -binding domain (PF00479) and a C-terminal G6PD domain (PF02781) (Figure 1B). Highly conserved substrate-binding (RIDHYLGKE) and  $NADP^+$ -binding (NEFVIRLQP) motifs were evident in all five *ZmG6PDHs* (Figure S1). Based on the above results, these *ZmG6PDHs* were classified into three plastidic G6PDH isoforms (*ZmG6PDH2*, 3, and 4) and two cytosolic G6PDH isoforms (*ZmG6PDH1* and 5). These



TABLE 1 Basic information of the five maize *G6PDH* genes (*ZmG6PDHs*).

| Gene Name       | Gene ID             | Previous Identifiers | Gene location              | ORF length (bp) | Protein length | Isoelectric point | Molecular weight (kDa) | Subcellular localization |
|-----------------|---------------------|----------------------|----------------------------|-----------------|----------------|-------------------|------------------------|--------------------------|
| <i>ZmG6PDH1</i> | Zm00001d003252_T003 | GRMZM2G130230_T01    | Zm2<br>37085168-37093582   | 1527            | 508            | 6.31              | 57.63                  | Cytoplasm                |
| <i>ZmG6PDH2</i> | Zm00001d025015_T002 | GRMZM2G177077_T01    | Zm10<br>99381158-99387758  | 1959            | 652            | 7.91              | 72.81                  | Chloroplast              |
| <i>ZmG6PDH3</i> | Zm00001d047587_T005 | GRMZM2G426964_T01    | Zm9<br>134182737-134185295 | 2748            | 915            | 6.26              | 103.03                 | Chloroplast              |
| <i>ZmG6PDH4</i> | Zm00001d029502_T001 | GRMZM2G179521_T01    | Zm1<br>72102454-72121802   | 1929            | 642            | 9.22              | 71.97                  | Chloroplast              |
| <i>ZmG6PDH5</i> | Zm00001d017119_T003 | GRMZM2G031107_T02    | Zm5<br>181440754-181446379 | 1557            | 518            | 6.66              | 58.62                  | Cytoplasm                |

findings highlight the relationships between the specific functions of these G6PDH isoforms and their underlying evolution.

***ZmG6PDH* syntenic relationships and gene structure analyses**

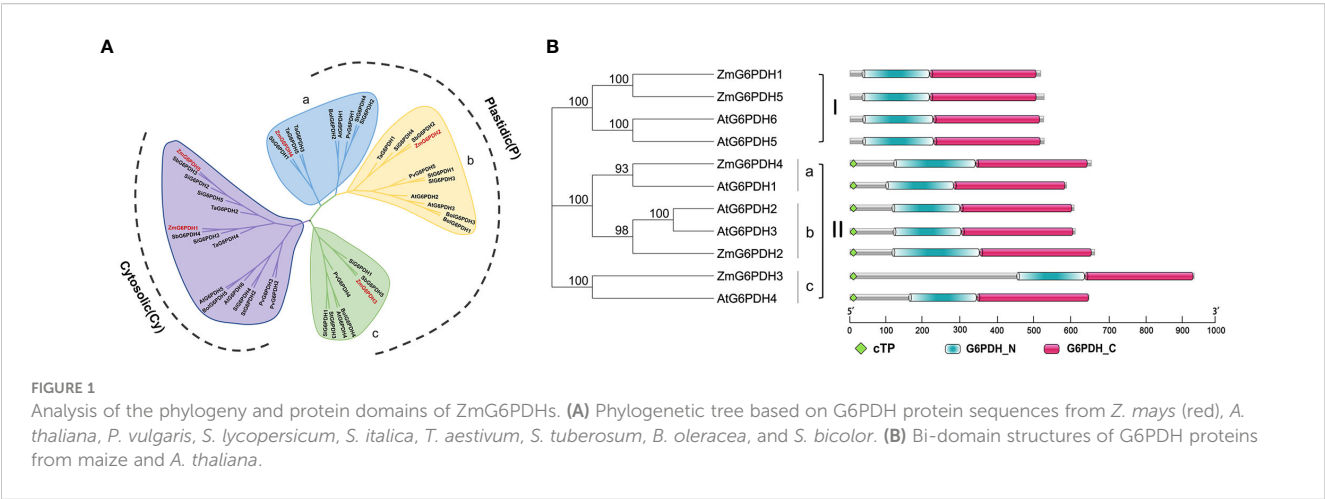
Over the past three million years, the maize genome has expanded to 2.3 gigabases due to two rounds of genomic duplication mediated by long-terminal-repeat retrotransposon proliferation. Synteny analyses of *G6PDHs* from *Z. mays*, *A. thaliana*, *P. vulgaris*, *S. lycopersicum*, *S. italica*, *T. aestivum*, *S. tuberosum*, *B. oleracea*, and *S. bicolor* were conducted to explore the possible functional roles of these *ZmG6PDHs*. The five *ZmG6PDHs* were scattered across five of the ten maize chromosomes (Figure 2A), with one gene per chromosome. *ZmG6PDH1* and *ZmG6PDH5* were identified as a pair of syntenic genes on chromosomes 2 and 5, respectively, consistent with the fact that only two *Arabidopsis* *G6PDH* genes are syntenic

(Figure 2A; Table S4). Notably, no paralogous or orthologous *GPDH* gene pairs were detected in the other plant species included in this study.

The structural diversity of the *ZmG6PDHs* was further explored by comparing the exon/intron sizes and localizations with those of *AtG6PDHs*, showing that the exon-intron structures of *G6PDHs* in the same clusters were largely similar, particularly regarding the number of exons (Figure 2B). For example, *G6PDH* genes in cluster I contained 15 exons, while those in cluster II contained 8-12 exons of nearly identical lengths. These data highlight the conservation of *ZmG6PDH* genes regarding gene sequences and exon-intron organization within phylogenetic groups.

**Identification of regulatory elements in *ZmG6PDH* promoter regions**

Putative *cis*-acting elements that may play a role in the transcriptional regulation of *ZmG6PDHs* were identified by



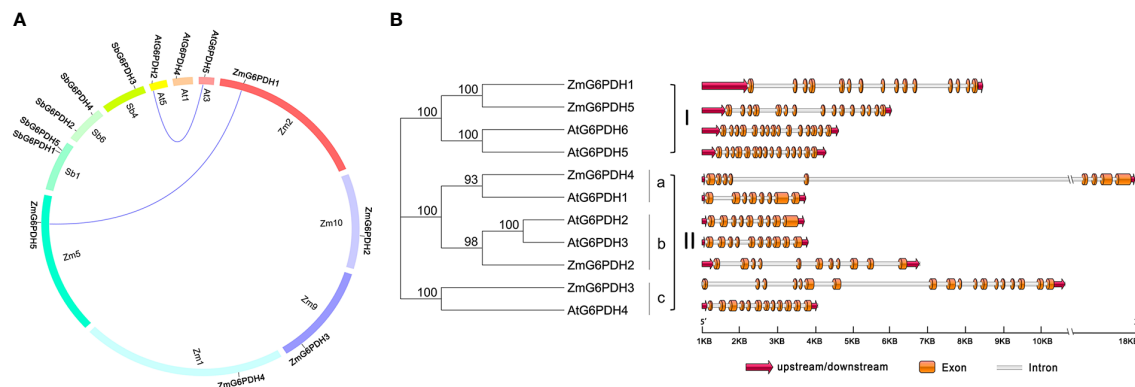


FIGURE 2

Syntenic and exon-intron structural analyses of genes in the *ZmG6PDH* family. (A) *ZmG6PDH* genes were subjected to syntenic analyses together with corresponding genes from *A. thaliana* and *S. bicolor*. Chromosomes are represented by circles, with the collinear regions of the *G6PDH* genes denoted by colored curved regions. (B) *AtG6PDH* and *ZmG6PDHs* gene family exon-intron organization. Blue arrows denote untranslated region (UTR) sequences. Colored boxes and gray lines represent exons and introns, respectively.

analyzing the region 2.0 kb upstream of the translation start site (ATG) for each of these genes. The majority of these *ZmG6PDHs* contained several stress-responsive *cis*-acting elements, including the anoxic-inducible ARE element, which was present in all genes other than *ZmG6PDH3* (Figure 3). The drought response-related MBS element was present in the *ZmG6PDH4* and *ZmG6PDH5* promoter regions, while the stress and defense response-related TC-rich repeat element was observed in the *ZmG6PDH1*, *ZmG6PDH2*, and *ZmG6PDH4* promoters, and the cold-responsive LTR element was observed in the *ZmG6PDH1*, *ZmG6PDH2*, *ZmG6PDH4*, and *ZmG6PDH5* promoters (Figure 3). All these *ZmG6PDH* promoters contained at least one hormone-responsive *cis*-acting element, such as the ABA-responsive element (ABRE) and gibberellin-responsive element (GARE).

## Assessment of *ZmG6PDH* subcellular localization

The localization of all five *ZmG6PDHs* was next verified by cloning their coding sequences; these sequences have been submitted to GenBank under the following accession numbers: *ZmG6PDH1* (ON962526), *ZmG6PDH2* (ON962527), *ZmG6PDH3* (ON962528), *ZmG6PDH4* (ON962529) and *ZmG6PDH5* (ON962530). These cloned coding region sequences were introduced in-frame with an N-terminal sequence encoding GFP. A positive control vector and GFP-tagged *ZmG6PDH* proteins were transiently transfected into maize mesophyll protoplasts. While free GFP was distributed evenly throughout all cell regions other than the vacuoles and chloroplasts (Figure 4), *ZmG6PDH2*, 3, and 4

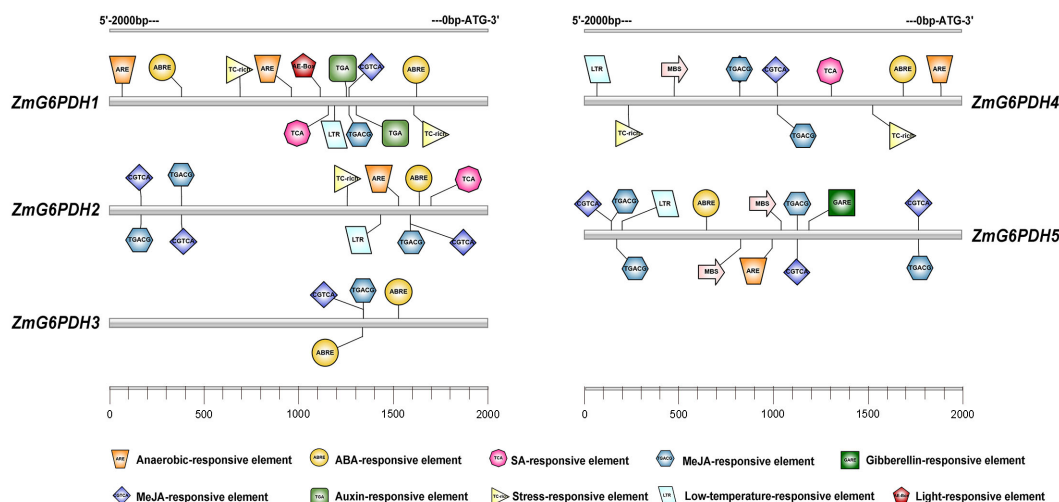
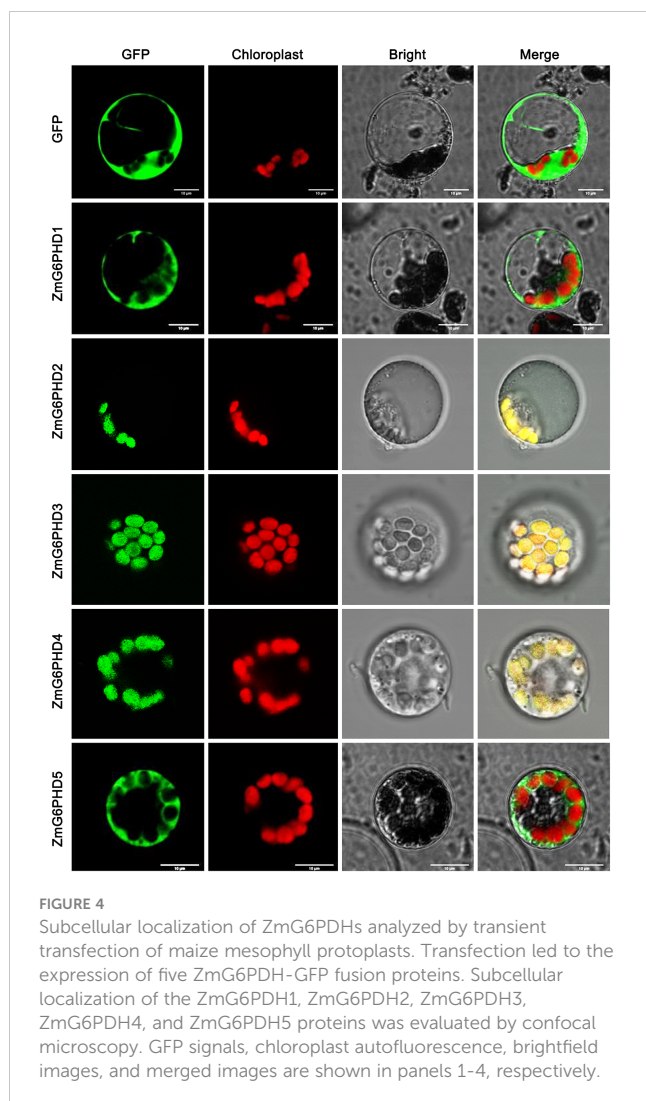


FIGURE 3

Predicted *cis*-acting elements within the 2.0-kb promoter region upstream of the start codons of *ZmG6PDHs*. Differently colored boxes show relative *cis*-acting element positions for each *ZmG6PDH*.



specifically localized to the chloroplast compartment, and ZmG6PDH1 and ZmG6PDH5 were only detected in the cytosol (Figure 4). These findings were consistent with the predictive analyses described above.

## Analyses of ZmG6PDHs expression across different tissues and stages of development

Next, ZmG6PDH expression levels were systematically evaluated in multiple tissues and seeds on days 5, 10, 15, 20, 25, and 30 after flowering *via* qPCR. The ZmG6PDHs showed tissue-specific expression patterns (Figure 5A). ZmG6PDH1, 3, and 5 were primarily detected in leaf blade samples, whereas ZmG6PDH2 and ZmG6PDH4 were primarily detected in tassel samples. Most ZmG6PDHs were expressed at low levels in stem, ear, silk, and brace root samples. These results suggest that ZmGPDHs may play a range of roles in the growth and development of maize plants. When these expression levels were assessed in seeds throughout development, all ZmG6PDHs were found to be expressed at relatively high levels during the early-middle stage of

development from 10-20 DAF (Figure 5B), whereas they were expressed at low levels during later stages of maturation and development at 25-30 DAF except for ZmG6PDH1 (Figure 5B). Maximal ZmG6PDH1 expression in developing seeds was evident at 25 DAF.

## Analyses of ZmG6PDH expression and activity levels under abiotic stress conditions

Members of the G6PDH gene family play vital roles in stress adaptation in various model plants (Yang et al., 2019; Linnenbrügger et al., 2022). ZmG6PDH transcriptional profiles were examined in response to low temperature (4°C), alkali (150 mM NaHCO<sub>3</sub>), salt (200 mM NaCl), and drought (20% PEG) stress treatment conditions to explore the potential roles of these genes in maize abiotic stress responses. Alkali treatment resulted in the upregulation of most of these ZmG6PDHs (Figure 6A), with cytosolic ZmG6PDHs exhibiting particularly high transcription levels at 6 h post-stimulation. ZmG6PDH2, 3, and 5 upregulation were also observed during the middle stages of salt stress, and at 12 h post-treatment, the ZmG6PDH2 levels were significantly higher than those of other analyzed genes. All ZmG6PDHs other than ZmG6PDH3 were upregulated at 6 h under osmotic stress conditions, with maximum upregulation at 12 h post-treatment. Cold stress significantly increased ZmG6PDH expression; ZmG6PDH1 was the most cold-inducible gene, reaching maximum expression levels after incubation at 4°C for 6 h (Figure 6A).

Measurement of enzyme activity showed that the activities of the G6PDHs in maize plants rose in response to salt, alkali, drought, and osmotic stressors (Figure 6B). Roughly 10-15-fold increases in G6PDH activity levels were detected in response to these treatments relative to control conditions, with even more pronounced upregulation being observed in response to cold stress such that enzymatic activity rapidly increased within 6 h of incubation at 4°C (Figure 6B). Throughout alkali stress treatment, G6PDH activity levels initially rose to a peak at 12 h and then decreased. Under osmotic stress conditions, G6PDH activities peaked at 6 h and then rose again from 12-24 h. Correlation analyses indicated that G6PDH activity under abiotic stress conditions was consistent with the transcripts of ZmG6PDH1, suggesting that it encodes the primary G6PDH isoform involved in cold stress responses (Figure 6C).

## Analyses of the effects of ZmG6PDH1 knockout on abiotic stress responses

To fully understand how ZmG6PDH1 regulates cold stress responses in plants, a CRISPR/Cas9 approach was next used to knock out this gene. Two gRNAs specific for ZmG6PDH1 (gRNA1 and gRNA2) were cloned into the binary vector p0195 (Figures 7A, B) under the control of the maize U6 promoter. The resultant constructs were then introduced into *Agrobacterium tumefaciens*, and maize embryos from the inbred B73 line were transformed *via* *Agrobacterium*-mediated transformation. In total, 20 T0 plants were collected harboring mutations at the target site, as

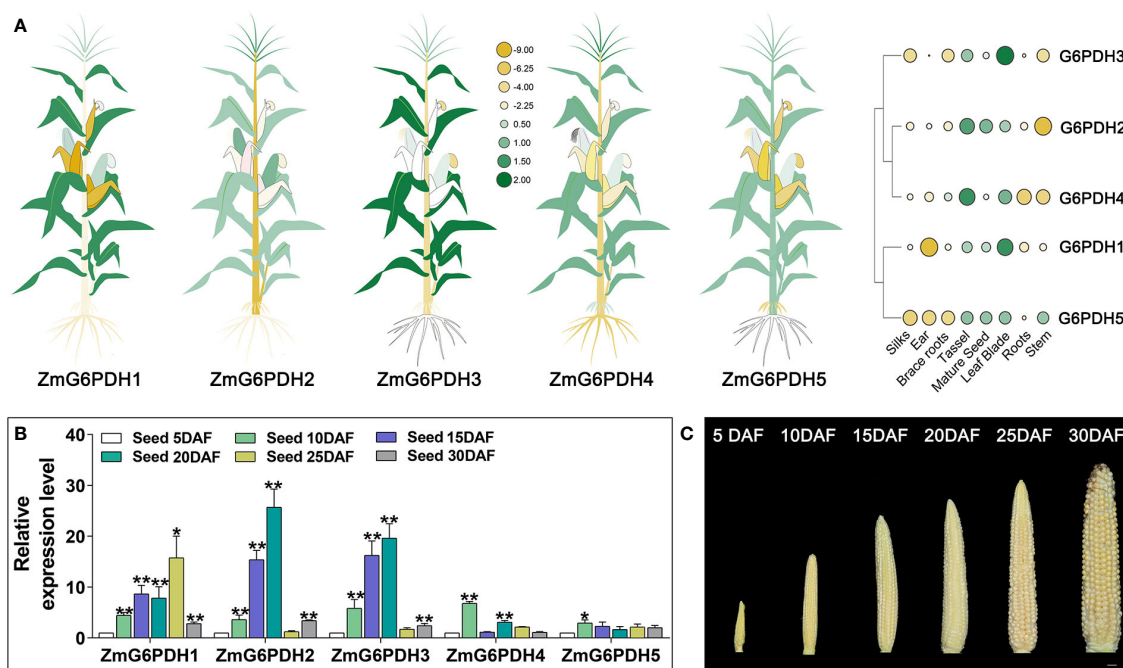


FIGURE 5

Transcripts of *ZmG6PDHs* in various tissues. **(A)** *ZmG6PDH* transcript levels were investigated in different tissues using the Phytozome database. Heatmap construction was performed using TBtools based on log2 expression levels. In the heatmaps, green and yellow indicate high and low transcription levels, respectively. Larger circles indicate higher levels of transcription. **(B)** Transcriptional profiles and **(C)** physiological phenotypes corresponding to *ZmG6PDHs* at 5, 10, 15, 20, 25, and 30 days after flowering (DAF). The expression of *ZmG6PDHs* in developing seeds at 5 DAF was used as an internal reference. Three biological replicate samples were analyzed per tissue. \**P* < 0.05, \*\* *P* < 0.01; Student's *t*-test.

confirmed through PCR and Sanger sequencing (Figure S1). Gene editing occurs at both target sites, making deletions more common than insertions (Figure 7C). Large 33 bp deletions were observed between the target sites of sgRNA1 and sgRNA2 (Figure 7C). Single nucleotide insertions were the most common type observed at these target sites, each target site, with 40% of insertions being 'G' (50%), 'T' (25%), or 'A' (25%) residues. In total, 8 (40%) of the 20 T0 plants were found to be successfully generated mutants, and 75% and 63% of the mutant T0 plants exhibited homozygous mutations at the respective sgRNA1 and sgRNA2 target sites.

Amino acid sequences for these mutant strains were analyzed, revealing differences in the sequences due to insertions and deletions of varying lengths that contributed to frameshifts and premature translational termination such that the gene was not appropriately expressed (Figure 7D). Varying levels of mutation were thus observed in these target genes in the resultant transgenic plants. Measurement of the expression and enzyme activity of *ZmG6PDH1* in the CRISPR-edited maize lines (*c1-c10*) (Figure S1) showed that *ZmG6PDH1* levels were 3–10-fold lower than in WT plants (Figure S1). Consistently, G6PDH activity in these edited lines was 2–4-fold below that in WT controls (Figure S1). These results thus confirmed successful *ZmG6PDH1* knockout in the transgenic plants.

T3 plants generated from the progeny of two editing events (*c1* and *c2*) were used for downstream use. These mutants harbored either a homozygous 1-bp insertion (gRNA1) or a 14-bp deletion (gRNA2), respectively, and these mutations were stably inherited through the T0, T1, and T2 generations as indicated through targeted sequencing

analyses. No apparent differences in seeds of visible growth phenotypes (such as plant height, ear height, kernels per ear, or kernels per ear row) were evident when comparing WT and mutant lines under normal growth conditions (Figure 7E; Table S5). In contrast, upon exposure of 3-week-old soil-grown seedlings to cold stress (4°C) for 4 days, the *ZmG6PDH1*-knockout plants were more sensitive to cold stress than were WT plants, as indicated by decreased height and root elongation, together with lower root and leaf dry weight (Figures 7F, H). Significant reductions in G6PDH enzyme activity levels were observed in the *c1* and *c2* lines, whereas they were increased in WT plants under normal and stress conditions (Figure 7G), indicating a potential link between *ZmG6PDH1* and G6PDH activity. In addition, mutant plants exhibited lower average total chlorophyll, chlorophyll a, chlorophyll b, and carotenoid levels as compared to WT plants under cold stress conditions (Figure 7I), together with a significant drop in the chlorophyll fluorescence parameter ( $F_v/F_m$ ) and net photosynthetic rate (Figure 7I). Together, these results supported a positive role for cytosolic *ZmG6PDH1* as a regulator of maize cold tolerance.

## The impact of *ZmG6PDH1* knockout on cell redox pairs under cold stress conditions

G6PDHs have previously been shown to help maintain proper carbon flow and NADPH generation within the PPP (Chen et al., 2022).





FIGURE 6

Expression and activity of *ZmG6PDHs* in response to abiotic stressors. (A) *ZmG6PDH* expression profiles and (B) enzymatic activity levels were measured in maize leaves exposed to 120 mM NaCl, 100 mM NaHCO<sub>3</sub>, 20% PEG, or 4°C conditions for 0, 1, 3, 6, or 12 h \**P* < 0.05, \*\* *P* < 0.01 vs. control; Student's *t*-test. (C) Correlation coefficients between *ZmG6PDH* expression and G6PDH enzyme activity. Correlations between pairs of traits are shown as individual ellipse charts; colors and slopes indicate the magnitude of correlations. Ellipses corresponding to negative and positive correlations are shown in red and blue, respectively.

NADPH redox status was initially analyzed to confirm the ability of cytosolic *ZmGPDH1* to modulate the redox state within cells under cold stress conditions. Under normal conditions, the NADPH levels and NADPH/NADP<sup>+</sup> ratios in the *c1* and *c2* lines were reduced relative to WT plants (Figure 8A). Increases in the NADPH/NADP<sup>+</sup> ratios were evident in all mutant lines exposed to cold-stress conditions, and these *zmG6pdh1* mutants exhibited NADH levels persistently lower than those of WT plants, thereby reducing the overall NADH/NADP<sup>+</sup> ratio despite a pronounced stress-induced increase in NADH levels, suggesting that the cytosolic G6PDH encoded by *ZmG6PDH1* regulates NADPH/NADP<sup>+</sup> homeostasis (Figure 8A).

To more fully explore whether *ZmG6PDH1* gene knockout had any effect on other redox pairs, the redox status of the GSH and ASA pools was also analyzed. No changes in reduced/oxidized GSH and ASA levels were evident under normal growth conditions when comparing WT and mutant plants (Figures 8B, C). However, after cold-stress exposure, GSH and ASA levels increased significantly in the WT plants than in the *zmG6pdh1* mutants. These differences

coincided with a reduction in the ASA/DHA and GSH/GSSG ratios in *zmG6pdh1* mutants compared with WT plants. Together, these findings indicated that *ZmG6PDH1*-knockout plants could not provide the reducing equivalent NADPH needed for the biosynthesis of ASA and GSH, highlighting a key role for the cytosolic G6PDH encoded by *ZmG6PDH1* as a regulator of the biosynthesis of ASA and GSH under cold-stress conditions.

## The impact of *ZmG6PDH1* knockout on ROS accumulation and antioxidant enzyme levels under low-temperature stress conditions

The redox state of plants is closely tied to ROS production and processing under stress conditions (Foyer and Noctor, 2005). The reduced NADP(H), ASA, and GSH pools seen in the *zmG6pdh1*



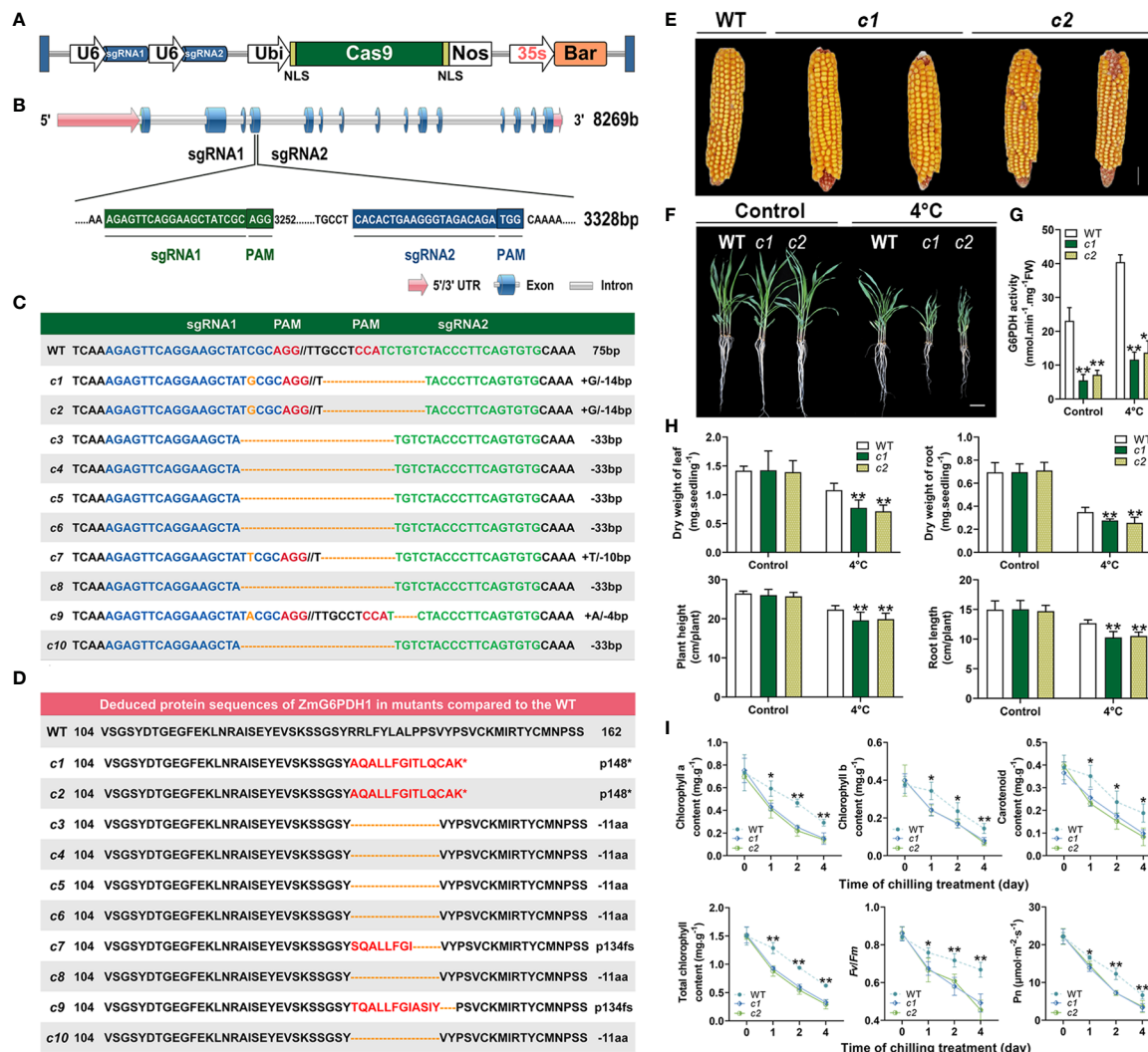


FIGURE 7

Phenotypic characteristics of *ZmG6PDH1* mutant plants exposed to cold stress. (A) Schematic overview of the T-DNA structure of the CRISPR/Cas9 constructs. (B) *ZmG6PDH1* gene structure and target sites. (C) Gene-edited allele sequences in individual *zmg6pdh1* mutants compared with the WT B73 reference sequence shown above. Red letters denote the PAM, and blue and green indicate target sequences. Deletions and insertions are shown as dashes and orange letters, respectively. Sequence changes relative to the B73 reference genome are annotated on the right. (D) Deduced *ZmG6PDH1* protein sequences in independent *zmg6pdh1* single mutants compared with the B73 reference sequence. An asterisk represents stop codons. (E) Mature seed performance comparisons in WT and gene-edited *ZmG6PDH1* mutants. (F) The phenotypic characteristics of *zmg6pdh1* mutant plants grown in pots and exposed to cold stress. (G) G6PDH enzymatic activity levels and (H) dry weight, plant height, and root length were compared in WT and *zmg6pdh1* mutant plants cultivated under control or 4°C treatment conditions. (I) Chlorophyll a, chlorophyll b, carotenoid, total chlorophyll, Fv/Fm, and Pn levels in the leaves of WT and *zmg6pdh1* mutant plants following exposure to 4°C conditions for 4 days. Data are means  $\pm$  SEs ( $n \geq 5$ ). \* $P < 0.05$ , \*\* $P < 0.01$  vs. WT; Student's *t*-test.

mutants thus highlighted a need to assess levels of ROS, including those of hydrogen peroxide ( $H_2O_2$ ) and superoxide radicals ( $O_2^-$ ), demonstrating that ROS levels were similar in WT and mutant plants under normal conditions. Under cold-stress conditions, however, the levels of ROS in the mutant lines were roughly double those in WT plants (Figures 9A, B). TBARS and electrolyte leakage levels related to oxidative damage to the cell membrane were also significantly increased in c1 and c2 relative to WT plants exposed to cold stress (Figures 9C, D). These data indicate that *ZmG6PDH1* deficiencies contribute to stress-driven ROS accumulation and associated lipid peroxidation. These higher

levels of ROS generation can induce the activation of systems responsible for ROS scavenging. Accordingly, levels of activity for antioxidant enzymes, including MDAR, APX, GR, DHAR, and GPX, were assessed. As expected, the activities of these enzymes were more significant in response to cold stress, with lower antioxidant enzyme activity levels seen in the *zmg6pdh1* mutants compared with the WT plants (Figures 9E-I). Overall, these findings indicated that the *zmg6pdh1* mutants showed significantly impaired antioxidant and redox systems, consistent with an important role for *ZmG6PDH1* as a modulator of redox homeostasis and ROS scavenging under cold stress conditions.

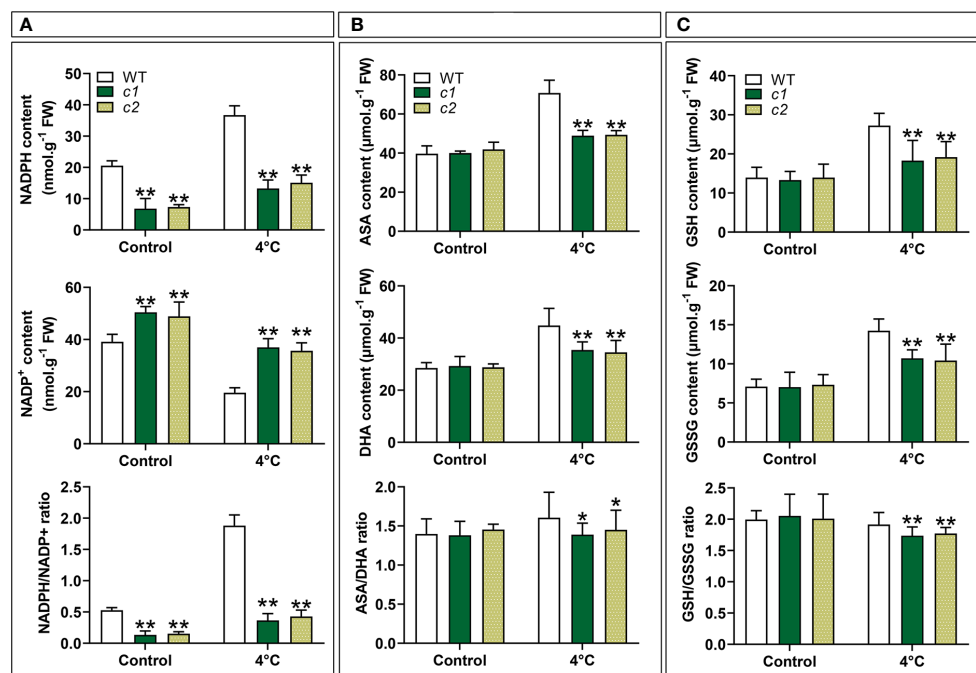


FIGURE 8

The impact of low-temperature exposure on the redox state of the NADPH, ASA, and GSH pools in WT and *zmg6pdh1* mutant leaves under control and 4°C treatment conditions. (A) NADH content, NAD<sup>+</sup> content, and the NADH/NAD<sup>+</sup> ratio. (B) ASA content, DHA content, and the ASA/DHA ratio. (C) GSH content, GSSG content, and the GSH/GSSG ratios. Data are means  $\pm$  SD (n=3). \*P < 0.05, \*\* P < 0.01 vs. WT; Student's t-test.

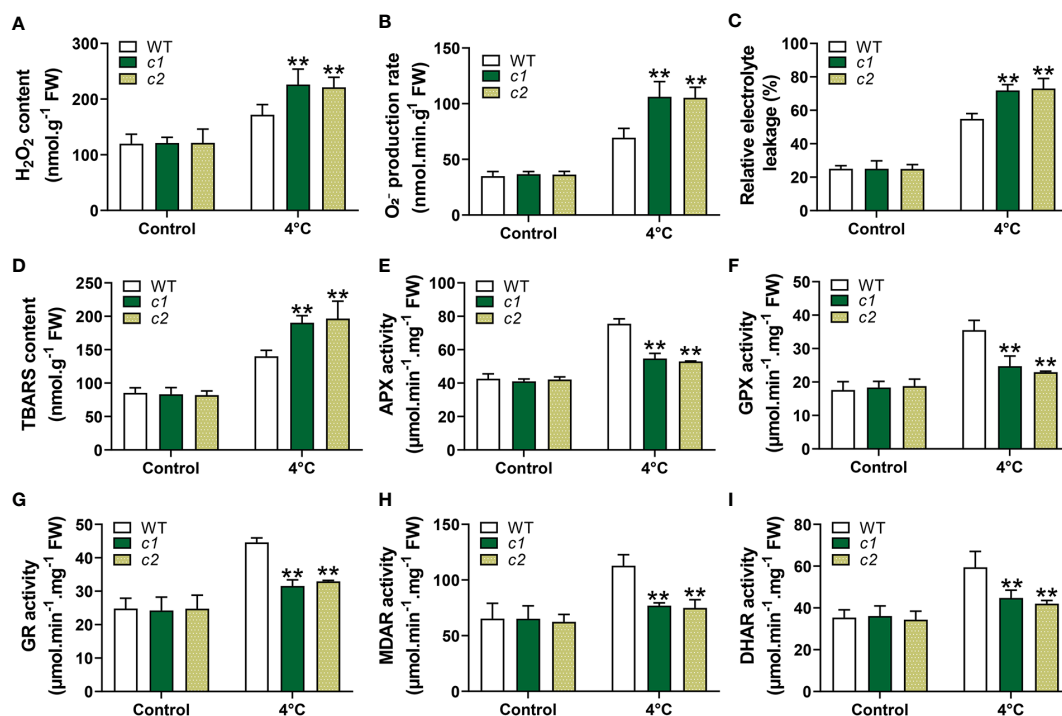


FIGURE 9

ROS levels and associated antioxidant response activities in WT and *zmg6pdh1* mutant leaves under control or 4°C treatment conditions. (A) O<sub>2</sub><sup>-</sup>, (B) H<sub>2</sub>O<sub>2</sub>, (C) relative electrolyte leakage, and (D) TBARS levels were analyzed in WT and *zmg6pdh1* mutants exposed to 4°C conditions. Levels of (E) APX, (F) GPX, (G) GR, (H) MDAR, and (I) DHAR activities were measured to assess antioxidant activity. FW, fresh weight. Data are means  $\pm$  SD (n=3). \*P < 0.05, \*\* P < 0.01 vs. WT; Student's t-test.

## Discussion

Maize (*Zea mays* L.) is a major global cereal crop widely used to prepare animal feed, industrial materials, and biofuel (Sheoran et al., 2021). G6PDHs have been identified as important regulators of many plant species' growth and abiotic stress responses (Wakao and Benning, 2005; Landi et al., 2021; Tian et al., 2021). While G6PDHs have been cloned successfully from a range of plants, including soybean (Zhao et al., 2020), tobacco (Yang et al., 2022), tomato (Landi et al., 2016), barley (Cardi et al., 2013), wheat (Nemoto and Sasakuma, 2000), and *Arabidopsis* (Wakao and Benning, 2005), little is known regarding this gene family in maize. Five maize G6PDH family members were identified (*ZmG6PDH1-5*; Table 1). Much as has been reported for other G6PDHs (Landi et al., 2021), the identified *ZmG6PDHs* contained key conserved protein domains (PF00479, PF02781) (Figure 1B). All five of these proteins expressed the conserved NEFVIRLQP motif (Figure S1), as has been reported for NADP<sup>+</sup>-dependent G6PDH isoforms with analogous NADP<sup>+</sup>-binding fragments corresponding to NEFVIRLQP (Yang et al., 2014; Zhang et al., 2020). The presence of signal peptides determines the localization of G6PDHs within plant cells, and transient expression of GFP-tagged versions of these *ZmG6PDHs* in maize mesophyll protoplasts was performed to evaluate their subcellular localization (Figure 4), demonstrating that *ZmG6PDH2*, 3, and 4 fusion proteins localized to the chloroplast compartment whereas *ZmG6PDH1* and 5 localized to the cytosol (Figure 4). These findings were consistent with prior *in silico* predictions and the phylogenetic clades to which these *ZmG6PDHs* were assigned. Prior studies hypothesized that *AtG6PDHs* would localize to the plastid or cytosolic compartments based on their targeting signals and transmembrane domains, but there was a lack of experimental evidence to support these predictions (Wakao and Benning, 2005; Landi et al., 2021).

G6PDH family enzymes reportedly play essential roles in the biosynthesis of lipids during plant seed development (Yang et al., 2019). Here, *ZmG6PDH* expression was observed in all analyzed tissues, with these levels being particularly high in leaves, tassels, and developing seeds (Figure 5). This is consistent with earlier results on *Arabidopsis* and soybean, with high levels of the *AtG6PDHcy* isoform detected in developing siliques (Yang et al., 2019) and high expression of soybean G6PDHs observed during seed development (Zhao et al., 2020). These tissue-specific expression patterns suggest key physiological roles for these *ZmG6PDHs* as regulators of maize development (Figure 5). Further physiological analyses were thus conducted to examine the *ZmG6PDH*-mediated regulation of abiotic stress adaptation. More NADPH is required to maintain a normal redox state in plants under abiotic stress (Yang et al., 2014). As indicated by our results, this may increase G6PDH. The *ZmG6PDHs* were significantly upregulated in response to salt, alkali, osmotic, and drought stress (Figures 6A, B), in line with the *AtG6PDH* (Wakao and Benning, 2005), *HbG6PDH* (Long et al., 2016), *PsG6PDH* (Lin et al., 2005) and *ScG6PDH* (Begcy et al., 2012; Yang et al., 2014) activity and expression patterns reported previously. Notably, a cytosolic isoform (*ZmG6PDH1*) responds vigorously to cold stress (Figure 6C), suggesting it is an important regulator of these cold stress responses. Similar results have been observed in poplar (*Populus suaveolens*) and sugarcane (*Saccharum officinarum*): a cytosolic G6PDH from *Populus*

*suaveolens* was identified as an important mediator of enhanced cold resistance in tobacco plants (Lin et al., 2005); and a cytosolic *ScG6PDH* in sugarcane also played a positive role in response to cold stress (Yang et al., 2014), while the associated functional verification is required.

Two homozygous *ZmG6PDH1* mutants generated using a CRISPR/Cas9 approach were isolated to confirm these results further. Morphologically, these *ZmG6PDH1* knockout mutants appeared comparable to WT plants (Figure 7). However, both mutant strains showed increased sensitivity to cold stress seen in the reductions in fresh weight, height, and root length after cold exposure (Figure 7). Cytosolic *ZmG6PDH1* deficiency may thus influence the ability of plants to adapt to cold conditions and may be capable of exacerbating growth suppression under cold temperatures. Cytosolic G6PDHs have been shown to supply NADPH and thus modulate cells' redox status (Valderrama et al., 2006). Consistently, the *zmG6pdh1* mutants in this study showed increased NADP<sup>+</sup> levels and reduced NADPH formation compared with WT plants (Figures 8A), with a corresponding drop in the cellular NADPH/NADP<sup>+</sup> ratio (Figures 8A), indicating that the impaired metabolic activity in these plants had profoundly compromised NADPH generation. Evident decreases in ASA/DHA and GSH/GSSG levels were also evident in both *zmG6pdh1* mutants as compared to WT plants (Figure 8B), indicating that the loss of *ZmG6PDH1* affected the redox status of the ASA pool beyond the immediate increase in this NADPH/NADP<sup>+</sup> ratio. Overall, these findings highlighted the critical role that *ZmG6PDH1* plays as a modulator of the cellular redox homeostasis of the GSH, ASA, and NADP(H) pools under cold stress conditions, in line with prior evidence (Wang et al., 2016).

*ZmG6PDH1* deficiency also resulted in increases in ROS, including chloroplastic ROS (Figures 9A, B), seen by the significantly reduced chlorophyll content in *zmG6pdh1* mutant plants exposed to cold stress (Figures 7I). Membrane damage in *zmG6pdh1* mutant plants was more severe, shown by the greater TBARS content and electrolyte leakage under stress conditions (Figures 9C, D), emphasizing that knockout of *ZmG6PDH1* led to significant ROS accumulation and associated increases in lipid peroxidation. ASA and GSH are non-enzymatic antioxidant members of the ASA-GSH cycle responsible for their regeneration, enabling them to eliminate excess ROS within cells (Noctor and Foyer, 1998). *ZmG6PDH1* may thus regulate the ASA-GSH cycle to influence ROS metabolism.

Enzymatic antioxidants in the ASA-GSH cycle play a key role in maintaining redox balance within cells and include APX, GR, GPX, MDAR, and DHAR (Noctor and Foyer, 1998; Foyer and Noctor, 2005). GR maintains a robust GSH pool within cells that is required to ensure active protein functionality, as it can prevent non-specific mixed disulfide bond formation and the consequent aggregation or inactivation of proteins (Couto et al., 2016). APX can utilize ASA as an electron donor for H<sub>2</sub>O<sub>2</sub> scavenging, oxidizing it to yield MDHA (Gill and Tuteja, 2010). GPX is the key enzyme responsible for repairing lipid peroxidation and an essential enzymatic mediator of antioxidant protection against membrane damage (Foyer and Noctor, 2005). Reduced GSH and DHA act as substrates of DHAR, a key enzyme for reduced ASA. MDAR utilizes NADPH as an electron donor to catalyze the processing of monodehydroascorbate (MDHA) into DHA and ASA (Singh

et al., 2015). Here, cold treatment was found to strongly induce APX, GR, GPX, MDAR, and DHAR activity in WT plants (Figures 9E-I), resulting in higher levels of GSH and ASA accumulation and decreases in ROS levels, whereas the same was not observed in *zmg6pdh1* mutants. Significant decreases in GSH, ASA, and NADPH levels, together with reductions in the activities of these key enzymes in the *zmg6pdh1* mutant plants, highlight the key role that *ZmG6PDH1* plays as a modulator of the ASA-GSH redox cycle, providing the NADPH necessary for the biosynthesis of GSH and ASA. Redox signaling plays an essential role in inter-organizational communication and nuclear gene expression regulation (Wolin et al., 2007; Kopczewski and Kuźniak, 2013). The low levels of NADPH in *zmg6pdh1* mutants were related to the impairment of the oxidative pentose phosphate pathway. Changes in the metabolic redox state ( $\text{NADP}^+/\text{NADPH}$  ratio) can represent a sensor for environmental fluctuation and serve as signals that coordinate the nuclear gene expression with the physiological response to cold stress. Together, these data demonstrate the important role of *ZmG6PDH1* as a regulator of cold tolerance through its ability to influence the cellular redox state and ROS-scavenging system, thus helping to balance ROS generation and to alleviate associated cellular toxicity.

## Conclusion

In conclusion, five *G6PDH* genes encoded by *Z. mays* were systematically identified and characterized. Phylogenetic and subcellular localization analyses enabled the classification of these *ZmG6PDHs* into cytosolic and plastidic isoforms. The expression of these different *ZmG6PDH* family members varied in response to particular abiotic stressors underscoring the distinct regulatory roles played likely by these enzymes. Cytosolic *ZmG6PDH1* expression was responsive to cold stress exposure and highly correlated with *G6PDH* activity levels, indicating that it is likely to play a key role in cold stress responses. Following this gene's CRISPR/Cas9-mediated knockout, *zmg6pdh1* mutant seedlings exhibited increased cold stress sensitivity compared with WT seedlings. Further research indicated that this gene encodes an active *G6PDH* enzyme form that maintains ASA and GSH redox homeostasis to mitigate oxidative damage induced by cold exposure.

## Data availability statement

The datasets presented in this study can be found in online repositories. The names of the repository/repositories and accession number(s) can be found in the article/supplementary material.

## References

Begcy, K., Mariano, E. D., Gentile, A., Lembke, C. G., Zingaretti, and Marli, S. J. P. O. (2012). A novel stress-induced sugarcane gene confers tolerance to drought, salt and oxidative stress in transgenic tobacco plants. *PLoS One* 7(9), e44697. doi: 10.1371/journal.pone.0044697

## Author contributions

XL, QC, and TY designed and conceived the experiments. XL performed the experiments. XL, ShL, SiL, YL, YS, HR, and JJZ analyzed the data and interpreted the results. XL prepared the manuscript. YZ, JGZ, and YHZ conceived the experiments and revised the manuscript. All authors agreed to be accountable for all aspects of the work, ensuring that questions related to the accuracy or integrity of any part of the work are appropriately investigated and resolved, and approved the final version to be published. All authors contributed to the article and approved the submitted version.

## Funding

This study was financially supported by the National Key R&D Program of China (2021YFD1201001-3, 2021YFD1201000), Heilongjiang Provincial Department of Finance Research Expenses (CZKYF2021-2-B024), National Key Laboratory (JD22A010), Young Scientists of Heilongjiang Province (2021QKPY005), National Maize Industry System (CARS-02-07), Reconstruction and Innovative Utilization of Crop Germplasm Bank in Cold Region (zy22001).

## Conflict of interest

The authors declare that the research was conducted in the absence of any commercial or financial relationships that could be construed as a potential conflict of interest.

## Publisher's note

All claims expressed in this article are solely those of the authors and do not necessarily represent those of their affiliated organizations, or those of the publisher, the editors and the reviewers. Any product that may be evaluated in this article, or claim that may be made by its manufacturer, is not guaranteed or endorsed by the publisher.

## Supplementary material

The Supplementary Material for this article can be found online at: <https://www.frontiersin.org/articles/10.3389/fpls.2023.1116237/full#supplementary-material>

Cardi, M., Chibani, K., Castiglia, D., Cafasso, D., Pizzo, E., Rouhier, N., et al. (2013). Overexpression, purification and enzymatic characterization of a recombinant plastidial glucose-6-phosphate dehydrogenase from barley (*Hordeum vulgare* cv. nure) roots. *Plant Physiol. Biochem.* 73, 266–273. doi: 10.1016/j.plaphy.2013.10.008



- Char, S. N., Neelakandan, A. K., Nahampun, H., Frame, B., Main, M., Spalding, M. H., et al. (2017). An agrobacterium-delivered CRISPR/Cas9 system for high-frequency targeted mutagenesis in maize. *Plant Biotechnol. J.* 15, 257–268. doi: 10.1111/pbi.12611
- Chen, C., Chen, H., Zhang, Y., Thomas, H. R., Frank, M. H., He, Y., et al. (2020). TBtools: An integrative toolkit developed for interactive analyses of big biological data. *Mol. Plant* 13, 1194–1202. doi: 10.1016/j.molp.2020.06.009
- Chen, P. H., Tjong, W. Y., Yang, H. C., Liu, H. Y., Stern, A., and Chiu, D. T. (2022). Glucose-6-Phosphate dehydrogenase, redox homeostasis and embryogenesis. *Int. J. Mol. Sci.* 23(4), 2017. doi: 10.3390/ijms23042017
- Corpas, F. J., González-Gordo, S., and Palma, J. M. (2021). Nitric oxide and hydrogen sulfide modulate the NADPH-generating enzymatic system in higher plants. *J. Exp. Bot.* 72, 830–847. doi: 10.1093/jxb/eraa440
- Couto, N., Wood, J., and Barber, J. (2016). The role of glutathione reductase and related enzymes on cellular redox homeostasis network. *Free Radic. Biol. Med.* 95, 27–42. doi: 10.1016/j.freeradbiomed.2016.02.028
- Esposito, S. (2016). Nitrogen assimilation, abiotic stress and glucose 6-phosphate dehydrogenase: The full circle of reductants. *Plants (Basel)*. 5 (2), 24. doi: 10.3390/plants5020024
- Feng, R., Wang, X., He, L., Wang, S., Li, J., Jin, J., et al. (2020). Identification, characterization, and stress responsiveness of glucose-6-phosphate dehydrogenase genes in highland barley. *Plants (Basel)*. 9 (12), 1800. doi: 10.3390/plants9121800
- Foyer, C. H., and Noctor, G. (2005). Redox homeostasis and antioxidant signaling: A metabolic interface between stress perception and physiological responses. *Plant Cell* 17, 1866–1875. doi: 10.1105/tpc.105.033589
- Fryer, M. J., Oxborough, K., Mullineaux, P. M., and Baker, N. R. (2002). Imaging of photo-oxidative stress responses in leaves. *J. Exp. Bot.* 53 (372), 1249–1254.
- Gill, S. S., and Tuteja, N. (2010). Reactive oxygen species and antioxidant machinery in abiotic stress tolerance in crop plants. *Plant Physiol. Biochem.* 48, 909–930. doi: 10.1016/j.plaphy.2010.08.016
- He, Q., Li, P., Zhang, W., and Bi, Y. (2021). Cytoplasmic glucose-6-phosphate dehydrogenase plays an important role in the silicon-enhanced alkaline tolerance in highland barley. *Funct. Plant Biol.* 48, 119–130. doi: 10.1071/FP20084
- Hodges, D. M., Delong, J. M., Forney, C. F., and Prange, R. K. (1999). Improving the thiobarbituric acid-reactive-substances assay for estimating lipid peroxidation in plant tissues containing anthocyanin and other interfering compounds. *Planta* 207, 604–611. doi: 10.1007/s004250050524
- Huang, J., Han, R., Ji, F., Yu, Y., Wang, R., Hai, Z., et al. (2022). Glucose-6-phosphate dehydrogenase and abscisic acid mediate programmed cell death induced by aluminum toxicity in soybean root tips. *J. Hazard. Mater.* 425, 127964. doi: 10.1016/j.jhazmat.2021.127964
- Kong, X., Lv, W., Jiang, S., Zhang, D., Cai, G., Pan, J., et al. (2013). Genome-wide identification and expression analysis of calcium-dependent protein kinase in maize. *BMC Genomics* 14, 433. doi: 10.1186/1471-2164-14-433
- Kopczewski, T., and Kuźniak, E. (2013). Redox signals as a language of interorganellar communication in plant cells. *Open Life Sci.* 8, 1153–1163. doi: 10.2478/s11535-013-0243-4
- Landi, S., Capasso, G., and Esposito, S. (2021). Different G6PDH isoforms show specific roles in acclimation to cold stress at various growth stages of barley (*Hordeum vulgare*) and arabidopsis thaliana. *Plant Physiol. Biochem.* 169, 190–202. doi: 10.1016/j.plaphy.2021.11.017
- Landi, S., Nurcato, R., De Lillo, A., Lentini, M., Grillo, S., and Esposito, S. (2016). Glucose-6-phosphate dehydrogenase plays a central role in the response of tomato (*Solanum lycopersicum*) plants to short and long-term drought. *Plant Physiol. Biochem.* 105, 79–89. doi: 10.1016/j.plaphy.2016.04.013
- Larkin, M. A., Blackshields, G., Brown, N. P., Chenna, R., McGettigan, P. A., McWilliam, H., et al. (2007). Clustal W and Clustal X version 2.0. *Bioinformatics*. 23 (21), 2947–8. doi: 10.1093/bioinformatics/btm404
- Lee, T.-H., Tang, H., Wang, X., and Paterson, A. H. (2012). PGDD: A database of gene and genome duplication in plants. *Nucleic Acids Res.* 41, D1152–D1158. doi: 10.1093/nar/gks1104
- Lin, S. Z., Zhang, Z. Y., Liu, W. F., Lin, Y. Z., Zhang, Q., and Zhu, B. Q. (2005). Role of glucose-6-phosphate dehydrogenase in freezing-induced freezing resistance of populus suaveolens. *Zhi. Wu. Sheng. Li. Yu. Fen. Zi. Sheng. Wu. Xue. Xue. Bao.* 31, 34–40.
- Linnenbrügger, L., Doering, L., Lansing, H., Fischer, K., Eirich, J., Finkemeier, I., et al. (2022). Alternative splicing of arabidopsis G6PD5 recruits NADPH-producing OPPP reactions to the endoplasmic reticulum. *Front. Plant Sci.* 13, 909624. doi: 10.3389/fpls.2022.909624
- Liu, H., Ding, Y., Zhou, Y., Jin, W., Xie, K., and Chen, L. L. (2017). CRISPR-p 2.0: An improved CRISPR-Cas9 tool for genome editing in plants. *Mol. Plant* 10, 530–532. doi: 10.1016/j.molp.2017.01.003
- Liu, W., Xie, Y., Ma, J., Luo, X., Nie, P., Zuo, Z., et al. (2015). IBS: An illustrator for the presentation and visualization of biological sequences. *Bioinformatics* 31, 3359–3361. doi: 10.1093/bioinformatics/btv362
- Long, X., He, B., Fang, Y., and Tang, C. (2016). Identification and characterization of the glucose-6-Phosphate dehydrogenase gene family in the para rubber tree, *hevea brasiliensis*. *Front. Plant Sci.* 7, 215. doi: 10.3389/fpls.2016.00215
- Nagalakshmi, N., and Prasad, M. N. (2001). Responses of glutathione cycle enzymes and glutathione metabolism to copper stress in *scenedesmus bijugatus*. *Plant Sci.* 160, 291–299. doi: 10.1016/S0168-9452(00)00392-7
- Nakano, Y., and Kozi, A. (1981). Hydrogen peroxide is scavenged by ascorbate-specific peroxidase in spinach chloroplasts. *Plant Cell Physiol.* 22 (5), 867–880. doi: 10.1093/oxfordjournals.pcp.a076232
- Nemoto, Y., and Sasakuma, T. (2000). Specific expression of glucose-6-phosphate dehydrogenase (G6PDH) gene by salt stress in wheat (*Triticum aestivum* L.). *Plant Sci.* 158, 53–60. doi: 10.1016/S0168-9452(00)00305-8
- Noctor, G., and Foyer, C. H. (1998). ASCORBATE AND GLUTATHIONE: Keeping active oxygen under control. *Annu. Rev. Plant Physiol. Plant Mol. Biol.* 49, 249–279. doi: 10.1146/annurev.arplant.49.1.249
- Preiser, A. L., Fisher, N., Banerjee, A., and Sharkey, T. D. (2019). Plastidic glucose-6-phosphate dehydrogenases are regulated to maintain activity in the light. *Biochem. J.* 476, 1539–1551. doi: 10.1042/BCJ20190234
- Queval, G., and Noctor, G. (2007). A plate reader method for the measurement of NAD, NADP, glutathione, and ascorbate in tissue extracts: Application to redox profiling during arabidopsis rosette development. *Anal. Biochem.* 363, 58–69. doi: 10.1016/j.ab.2007.01.005
- Ruan, M., He, W., Sun, H., Cui, C., Wang, X., Li, R., et al. (2022). Cytosolic glucose-6-phosphate dehydrogenases play a pivotal role in arabidopsis seed development. *Plant Physiol. Biochem.* 186, 207–219. doi: 10.1016/j.plaphy.2022.07.017
- Scharte, J., Schön, H., Tjaden, Z., Weis, E., and Von Schaewen, A. (2009). Isoenzyme replacement of glucose-6-phosphate dehydrogenase in the cytosol improves stress tolerance in plants. *Proc. Natl. Acad. Sci. U.S.A.* 106, 8061–8066. doi: 10.1073/pnas.0812902106
- Sheoran, S., Kumar, S., Kumar, P., Meena, R. S., and Rakshit, S. (2021). Nitrogen fixation in maize: breeding opportunities. *Theor. Appl. Genet.* 134, 1263–1280. doi: 10.1007/s00122-021-03791-5
- Singh, V. P., Singh, S., Kumar, J., and Prasad, S. M. (2015). Investigating the roles of ascorbate-glutathione cycle and thiol metabolism in arsenate tolerance in ridged luffa seedlings. *Protoplasma* 252, 1217–1229. doi: 10.1007/s00709-014-0753-6
- Takashi, U., Yasushi, M., Satoshi, S., Kyoichi, K., Kozi, A., and Hideo, T. (1997). Induction of enzymes involved in the ascorbate-dependent antioxidative system, namely, ascorbate peroxidase, monodehydroascorbate reductase and dehydroascorbate reductase, after exposure to air of rice (*Oryza sativa*) seedlings germinated under water. *Plant and Cell Physiol.* 38 (5), 541–549. doi: 10.1093/oxfordjournals.pcp.a029203
- Tamura, K., Peterson, D., Peterson, N., Stecher, G., Nei, M., and Kumar, S. J. M. B. (2011). MEGA5: Molecular evolutionary genetics analysis using maximum likelihood, evolutionary distance, and maximum parsimony methods. *Mol. Biol. Evol.* 28 (10), 2731–2739. doi: 10.1093/molbev/msr121
- Tian, Y., Peng, K., Bao, Y., Zhang, D., Meng, J., Wang, D., et al. (2021). Glucose-6-phosphate dehydrogenase and 6-phosphogluconate dehydrogenase genes of winter wheat enhance the cold tolerance of transgenic arabidopsis. *Plant Physiol. Biochem.* 161, 86–97. doi: 10.1016/j.plaphy.2021.02.005
- Valderrama, R., Corpas, F. J., Carreras, A., Gómez-Rodríguez, M. V., Chaki, M., Pedrajas, J. R., et al. (2006). The dehydrogenase-mediated recycling of NADPH is a key antioxidant system against salt-induced oxidative stress in olive plants. *Plant. Cell Environ.* 29, 1449–1459. doi: 10.1111/j.1365-3040.2006.01530.x
- Van Assche, F., Cardinaels, C., and Clijsters, H. (1988). Induction of enzyme capacity in plants as a result of heavy metal toxicity: dose-response relations in *phaseolus vulgaris* L., treated with zinc and cadmium. *Environ. pollut.* 52, 103–115. doi: 10.1016/0269-7491(88)90084-X
- Wakao, S., Andre, C., and Benning, C. (2008). Functional analyses of cytosolic glucose-6-phosphate dehydrogenases and their contribution to seed oil accumulation in arabidopsis. *Plant Physiol.* 146, 277–288. doi: 10.1104/pp.107.108423
- Wakao, S., and Benning, C. (2005). Genome-wide analysis of glucose-6-phosphate dehydrogenases in arabidopsis. *Plant J.* 41, 243–256. doi: 10.1111/j.1365-313X.2004.02293.x
- Wang, H., Yang, L., Li, Y., Hou, J., Huang, J., and Liang, W. (2016). Involvement of ABA- and H<sub>2</sub>O<sub>2</sub>-dependent cytosolic glucose-6-phosphate dehydrogenase in maintaining redox homeostasis in soybean roots under drought stress. *Plant Physiol. Biochem.* 107, 126–136. doi: 10.1016/j.plaphy.2016.05.040
- Wellburn, A. R. (1994). The spectral determination of chlorophylls a and b, as well as total carotenoids, using various solvents with spectrophotometers of different resolution. *J. Plant Physiol.* 144, 307–313. doi: 10.1016/S0176-1617(11)81192-2
- Wolin, M. S., Ahmad, M., Gao, Q., and Gupta, S. A. (2007). Cytosolic NAD(P)H regulation of redox signaling and vascular oxygen sensing. *Antioxid. Redox Signaling* 9, 671–678. doi: 10.1089/ars.2007.1559
- Xing, H. L., Dong, L., Wang, Z. P., Zhang, H. Y., Han, C. Y., Liu, B., et al. (2014). A CRISPR/Cas9 toolkit for multiplex genome editing in plants. *BMC Plant Biol.* 14, 327. doi: 10.1186/s12870-014-0327-y
- Yang, Y., Fu, Z., Su, Y., Zhang, X., Li, G., Guo, J., et al. (2014). A cytosolic glucose-6-phosphate dehydrogenase gene, ScG6PDH, plays a positive role in response to various abiotic stresses in sugarcane. *Sci. Rep.* 4, 7090. doi: 10.1038/srep07090
- Yang, D., Peng, Q., Cheng, Y., and Xi, D. (2022). Glucose-6-phosphate dehydrogenase promotes the infection of chilli vein mottle virus through affecting



ROS signaling in *nicotiana benthamiana*. *Planta* 256, 96. doi: 10.1007/s00425-022-04010-1

Yang, L., Wang, X., Chang, N., Nan, W., Wang, S., Ruan, M., et al. (2019). Cytosolic glucose-6-phosphate dehydrogenase is involved in seed germination and root growth under salinity in *arabidopsis*. *Front. Plant Sci.* 10, 182. doi: 10.3389/fpls.2019.00182

Yoo, S.-D., Cho, Y.-H., and Sheen, J. (2007). *Arabidopsis* mesophyll protoplasts: A versatile cell system for transient gene expression analysis. *Nat. Protoc.* 2, 1565. doi: 10.1038/nprot.2007.199

Yu, C. S., Lin, C. J., and Hwang, J. K. (2004). Predicting subcellular localization of proteins for gram-negative bacteria by support vector machines based on n-peptide compositions. *Protein Sci.* 13, 1402–1406. doi: 10.1110/ps.03479604

Zhang, L., Liu, J., Wang, X., and Bi, Y. (2013). Glucose-6-phosphate dehydrogenase acts as a regulator of cell redox balance in rice suspension cells under salt stress. *Plant Growth Regul.* 69, 139–148. doi: 10.1007/s10725-012-9757-4

Zhang, Y., Luo, M., Cheng, L., Lin, Y., Chen, Q., Sun, B., et al. (2020). Identification of the cytosolic glucose-6-phosphate dehydrogenase gene from

strawberry involved in cold stress response. *Int. J. Mol. Sci.* 21 (19), 7322. doi: 10.3390/ijms21197322

Zhang, Z., Zhang, J., Chen, Y., Li, R., Wang, H., Ding, L., et al. (2014). Isolation, structural analysis, and expression characteristics of the maize (*Zea mays* L.) hexokinase gene family. *Mol. Biol. Rep.* 41, 6157–6166. doi: 10.1007/s11033-014-3495-9

Zhao, Y., Cui, Y., Huang, S., Yu, J., Wang, X., Xin, D., et al. (2020). Genome-wide analysis of the glucose-6-phosphate dehydrogenase family in soybean and functional identification of GmG6PDH2 involvement in salt stress. *Front. Plant Sci.* 11, 214. doi: 10.3389/fpls.2020.00214

Zhao, Y., Liu, M., He, L., Li, X., Wang, F., Yan, B., et al. (2019). A cytosolic NAD<sup>+</sup>-dependent GPDH from maize (*ZmGPDH1*) is involved in conferring salt and osmotic stress tolerance. *BMC Plant Biol.* 19 (1), 16. doi: 10.1186/s12870-018-1597-6

Zhao, C., Wang, X., Wang, X., Wu, K., Li, P., Chang, N., et al. (2015). Glucose-6-phosphate dehydrogenase and alternative oxidase are involved in the cross tolerance of highland barley to salt stress and UV-b radiation. *J. Plant Physiol.* 181, 83–95. doi: 10.1016/j.jplph.2015.03.016



## OPEN ACCESS

## EDITED BY

Arpna Kumari,  
The University of Tokyo, Japan

## REVIEWED BY

Anuj Kumar,  
University of Arkansas, United States  
Guanfu Fu,  
China National Rice Research Institute  
(CAAS), China  
Bo Shen,  
Hangzhou Normal University, China  
Tao Wu,  
College of Plant Science,  
Jilin University, China

## \*CORRESPONDENCE

Kaifeng Jiang  
✉ jiangkf67@126.com  
Jiakui Zheng  
✉ zhen6102@126.com

<sup>†</sup>These authors have contributed equally to this work

## SPECIALTY SECTION

This article was submitted to  
Plant Abiotic Stress,  
a section of the journal  
Frontiers in Plant Science

RECEIVED 27 September 2022

ACCEPTED 17 February 2023

PUBLISHED 09 March 2023

## CITATION

Li G, Zhang T, Yang L, Qin J, Yang Q,  
Cao Y, Luo J, Li X, Gao L, Chen Q, He X,  
Huang Y, Liu C, He L, Zheng J and Jiang K  
(2023) Sterile line Dexiang074A enhances  
drought tolerance in hybrid rice.  
*Front. Plant Sci.* 14:1054571.  
doi: 10.3389/fpls.2023.1054571

## COPYRIGHT

© 2023 Li, Zhang, Yang, Qin, Yang, Cao, Luo,  
Li, Gao, Chen, He, Huang, Liu, He, Zheng  
and Jiang. This is an open-access article  
distributed under the terms of the [Creative  
Commons Attribution License \(CC BY\)](#). The  
use, distribution or reproduction in other  
forums is permitted, provided the original  
author(s) and the copyright owner(s) are  
credited and that the original publication in  
this journal is cited, in accordance with  
accepted academic practice. No use,  
distribution or reproduction is permitted  
which does not comply with these terms.

# Sterile line Dexiang074A enhances drought tolerance in hybrid rice

Gengmi Li<sup>1,2†</sup>, Tao Zhang<sup>1†</sup>, Li Yang<sup>1†</sup>, Jian Qin<sup>1</sup>, Qianhua Yang<sup>1</sup>,  
Yingjiang Cao<sup>1</sup>, Jing Luo<sup>1</sup>, Xiangzhao Li<sup>1</sup>, Lei Gao<sup>1</sup>,  
Qian Chen<sup>1,2</sup>, Xingping He<sup>1</sup>, Yong Huang<sup>1</sup>, Chuantao Liu<sup>1</sup>,  
Ling He<sup>1</sup>, Jiakui Zheng<sup>1\*</sup> and Kaifeng Jiang<sup>1\*</sup>

<sup>1</sup>Key Laboratory of Southwest Rice Biology and Genetic Breeding, Ministry of Agriculture/Luzhou Branch of National Rice Improvement Center, Rice and Sorghum Research Institute, Sichuan Academy of Agricultural Sciences, Deyang, China, <sup>2</sup>Biology and Molecular Biology Research Center, Rice and Sorghum Research Institute, Sichuan Academy of Agricultural Sciences, Deyang, China

Heterosis has been widely used in rice breeding, especially in improving rice yield. But it has rarely been studied in rice abiotic stress, including the drought tolerance, which is becoming one of the most important threaten in decreasing rice yield. Therefore, it is essential to studying the mechanism underlying heterosis in improving drought tolerance of rice breeding. In this study, Dexiang074B (074B) and Dexiang074A (074A) served as maintainer lines and sterile lines. Mianhui146 (R146), Chenghui727 (R727), LuhuiH103 (RH103), Dehui8258 (R8258), Huazhen (HZ), Dehui938 (R938), Dehui4923 (R4923), and R1391 served as restorer lines. The progeny were Dexiangyou (D146), Deyou4727 (D4727), Dexiang 4103 (D4103), Deyou8258 (D8258), Deyou Huazhen (DH), Deyou 4938 (D4938), Deyou 4923 (D4923), and Deyou 1391 (D1391). The restorer line and hybrid offspring were subjected to drought stress at the flowering stage. The results showed that Fv/Fm values were abnormal and oxidoreductase activity and MDA content were increased. However, the performance of hybrid progeny was significantly better than their respective restorer lines. Although the yield of hybrid progeny and restorer lines decreased simultaneously, the yield in hybrid offspring is significantly lower than the respective restorer line. Total soluble sugar content was consistent with the yield result, so we found that 074A can enhance drought tolerance in hybrid rice.

## KEYWORDS

rice, drought stress, heterosis, hybrid rice, total soluble sugar content

## Introduction

Rice is an important agricultural crop worldwide, and irrigated rice accounts for 70% of total rice production (Tiwari et al., 2020). It feeds more than half of the world's population. As the human population surges, rice production will need to double by 2030 to meet global demand. Crop plants face a variety of abiotic stresses (You and Chan, 2015). Drought stress is one of the abiotic stresses that can inhibit crop growth and reduce crop yield in the field (Moore et al., 2009; Clark et al., 2013; Robles et al., 2018; Fu et al., 2019;

Wang et al., 2019). To cope with climate change and environmental degradation, drought-tolerant rice varieties can be cultivated to reduce the risk of crop yield decline (Harris-Shultz et al., 2019). Because they are non-mobile organisms, it is important to coordinate genetic networks in rice to adapt to various biotic and abiotic stresses (Manhes et al., 2021; Song et al., 2023). For example, *STH1* encodes a negative regulator of salt tolerance in rice. Studies on *STH1* gene reveal a new mechanism for the synergistic regulation of salt tolerance and heading date in rice (Xiang et al., 2022). In *Arabidopsis*, sumoylation of NF-YC10 promotes the assembly of NF-YC complexes to enhance plant tolerance to high temperature stress (Huang et al., 2022). Among all abiotic stresses, drought stress is the most lethal because it can occur at any point in the rice plant life cycle, though it is especially damaging during another development (Guo et al., 2016). The phenomena of white anthers and sterile pollen grains finally caused yield loss in rice under water-deficit environments (Serraj et al., 2009). Drought stress may affect another compartment formation and microspore release by interfering with normal homeostasis of sugars, hormones, and reactive oxygen species (ROS) (Yu et al., 2019). Under drought stress conditions, many genes related to plant another development, including defective pollen wall (*DPW*) and tapetum degeneration deferred (*TDR*), are differentially expressed (Jin et al., 2013; Ma et al., 2017). However, the regulatory network that mediates the interaction between drought tolerance and fertility is complex and remains an obstacle to addressing their contradictions. Improving drought tolerance in rice without negatively affecting fertility remains a major challenge for rice breeders.

Under abiotic stress conditions, plants often sacrifice their fertility for survival. Therefore, fertility and stress resistance often oppose each other. In rice, drought tolerance may reduce seed fertility. In abiotic environments, the effects of drought on rice growth can be partly attributed to the accumulation of ROS (Halliwell, 2006). In this context, ROS generally refers to hydrogen peroxide ( $H_2O_2$ ) and superoxide ( $O_2^-$ ), which can cause lipid peroxidation, protein degradation, nucleotide damage, and cell death (Anjum et al., 2011; Xu et al., 2016). In order to prevent oxidative damage, superoxide dismutase (SOD), catalase (CAT), peroxidase (POD), and ascorbic acid peroxidase (APX) scavenge active oxygen to reduce the impact of drought on cell oxidative damage and protect plant cells from active oxygen damage (Gill and Tuteja, 2010). Quantification of these enzymes is considered a general indicator of drought tolerance (Farooq et al., 2009; He et al., 2018). Malondialdehyde (MDA) is one of the products of cell membrane lipid peroxidation, and it can also aggravate cell membrane damage. The production of MDA can reflect the degree of membrane lipid peroxidation and indirectly reflect the antioxidant capacity of plant tissues (Sheoran et al., 2015). After drought stress, *Arabidopsis* and rice plants transformed with *sbWRKY30* genes and became tolerant to drought stress by changing the configurations of their root systems. Their proline content and their activities of SOD, POD, and CAT were higher than those of wild-type plants, and their MDA content was lower than that of wild-type plants. Gene *sbWRKY30* has a positive regulatory role in drought stress (Yang et al., 2020).

It is estimated that 50% of global rice production is affected by drought (Ren et al., 2019). The main nutrient in the rice grain is starch, with a content ranging from 81.23% to 92.73% (Omar et al., 2016). Starch is an ( $\alpha$ -1,4)polyglucose-linked polymer. X-ray diffraction experiments showed that approximately 70% of the starch particles in rice were amorphous (mainly amylose), and the remaining 30% were amylopectin (Sajilata et al., 2006). Drought forcing during grain filling promoted plant senescence and redeployment of the carbon pool from vegetative tissues to grains (Yang et al., 2002), increased the grain filling rate, and shortened the grain filling period (Yang et al., 2001a). Sucrose is the main form of disaccharide transport in plants involved in photosynthate transport. In general, sucrose is transported by phloem to various organs (Eom et al., 2012; Ruan, 2012; De Schepper et al., 2013). Sucrose is not only the basis of physiological metabolism but also a signal molecule that plants use to coordinate physiological activities. It is the basic carbon skeleton monomer and energy source for seed formation and development, and it plays an important role in plant growth and seed development (Ruan et al., 2010; Ruan, 2012). It was previously reported that the transcription levels of *AtSWEET11*, *AtSWEET12*, and *AtSUC2* genes in *Arabidopsis* leaves were upregulated under drought stress conditions, resulting in enhanced response to sucrose export (Durand et al., 2016). Drought stress decreased photosynthetic carbon assimilation and seriously affected grain quality (Liu et al., 2017; Raed and Raju, 2018). In the study of soybean seed yield and drought, drought stress reduced the leaf photosynthesis rate, shoot biomass, and seed weight by 63.93%, 33.53%, and 41.65%, respectively. Drought stress increased the soluble sugar content, sucrose phosphatase content, and sucrose synthase and acid convertase activities; upregulated the expression of *GmSPS1*, *GmSuSy2*, and *GMA-INV*; and decreased the starch content by 15.13%. During seed development, drought stress increased the activities of sucrose synthesis and degradation enzymes, the expression levels of metabolism-related genes, and the expression levels of sucrose transporter genes during early seed development.

074B is a hybrid rice maintainer line with high combining ability as a parent, and 074A is the contra sterile line. 074B is used as a rice backbone parent line in Sichuan Province (Li et al., 2021). The hybrid offspring of 074A have efficient nitrogen utilization, high grain quality, and drought resistance. D4103 and D4727, two of its offspring, were recognized as super rice by the Ministry of Agriculture, China. Thus, 074A won the first prize in the Sichuan Province Science and Technology Progress Award. The effects of 17 cultivated rice varieties (074B, R146, D146, R727, D4727, RH103, D4103, R8258, D8258, HZ, DH, R938, D4938, R4923, D4923, R1391, and D1391) in southwest China on water stress tolerance in rice have been studied. In the present study, we used these 17 cultivars in a pot drought treatment experiment to make an assessment of the maintainer line 074B and to better promote the usage. These experiments were generally carried out during the later stage of rice growth (the main ear was exposed; i.e., the drought treatment was started 3–5 days before the beginning of the ear period) to allow the study of the mechanism underlying adaptation to water stress in 17 rice cultivars planted in southwest China. The

research included the effects of water stress on the phenotype and yield of cultivated rice in southwest China, Fv/Fm, MDA, antioxidant enzyme activity, dry matter accumulation, and the percentage of dry matter in the panicle relative to the whole plant.

## Materials and methods

### Plant materials and growth conditions

The experiment was carried out at Fuyang Experimental Base at the China National Rice Research Institute from June to September 2020 and 2021, and the results showed the same trend in both years. The data collected in 2021 were used in this paper for analysis. Potting soil was used in the experiment. Each plastic bucket was 40 cm high and 30 cm in diameter, with 2 cm holes on the bottom. Rubber plugs in the bottom of the bucket were used for drainage and plugging during drought treatment. The organic matter content in the potting soil was 36.1 g/kg, total nitrogen 2.70 g/kg, total phosphorus 0.62 g/kg, total potassium 20.4 g/kg, alkali-hydrolyzed nitrogen 239 mg/kg, ammonium nitrogen 9.8 mg/kg, available phosphorus 24.1 mg/kg, and available potassium 62 mg/kg. The pH was 6.5, and each pot was loaded with 10 kg of dry soil. We used 074B as a maintainer line, 074A as a sterile line, and R146, R727, RH103, R8258, HZ, R938, R4923, and R1391 as restorer lines. The progenies were D146, D4727, D4103, D8258, HZ, D4938, D4923, and D1391 (Table 1). Rice was soaked at 37°C for 2 days and seed germination for 1 day and then sown 1 day later. After 30 days of seedling growth, the seedlings were transplanted into plastic buckets with six seedlings per pot and 20 pots per variety, including 10 pots for control treatment and 10 pots for drought stress treatment. All the pots were placed under a plastic rain shelter randomly. We kept the rice plants under normal watering conditions until the emergence of the first panicle. Then, the potted plants were divided into two groups. The control groups continued to have a shallow water layer. The rubber plugs of the 10 pots for drought stress groups were pulled out, and the water was drained out till the water potential at a soil depth of 20 cm dropped to −50 kPa. We

then started the timer, waited another 48 h, and then started rehydration until the plants were mature and harvested.

### Measurement of seed setting rate and dry matter weight

When the rice plants fully matured, the remaining three pots were harvested to determine the rice seed setting rate and yield per pot. The rice plants in each pot were separated into three parts for assessing dry weight: leaves, shoots and sheaths, and panicles. The total dry matter weight was calculated as the total weight of all three groups of parts, and the weight of panicles was calculated as panicle weight/the total dry matter weight.

### Fv/Fm measurement

Before rehydration, chlorophyll fluorescence was measured with a portable chlorophyll fluorescence spectrometer (PAM-2500 chlorophyll fluorescence system; Heinz Walz, Effeltrich, Germany) for the maximum chlorophyll fluorescence measurement. Rice flag leaves were wrapped in aluminum foil to simulate a dark environment, and the maximum fluorescence electron efficiency was measured after 30 min of dark treatment (Yu et al., 2020).

### Malondialdehyde measurement

Before rehydration, approximately 0.2 g of frozen leaves was homogenized in 2 ml of 5% trichloroacetic acid, and then 2 ml of 0.6% (m/v) thiobarbituric acid was added. The reaction mixture was placed in a boiling water bath for 30 min and then placed in cold water for rapid cooling. When the container reached room temperature, the absorbance of the mixture was measured at 450, 532, and 600 nm. The MDA content was calculated using the following formula:  $C = 6.45 \times (A_{532} - A_{600}) - 0.56 \times A_{450}$  (Dionisio-Sese and Tobita, 1998).

TABLE 1 Genetic relationships between sterile, maintainer, restorer lines, and offspring.

| Parents of three-line hybrid rice |                    |                    | Varieties (hybrid offspring) |
|-----------------------------------|--------------------|--------------------|------------------------------|
| Male sterile line                 | Maintainer line    | Restorer lines     |                              |
| Dexiang074A (074A)                | Dexiang074B (074B) | Mianhui146 (R146)  | Dexiangyou (D146)            |
|                                   |                    | Chenghui727 (R727) | Deyou4727 (D4727)            |
|                                   |                    | Luhui103 (RH103)   | Dexiang4103 (D4103)          |
|                                   |                    | Dehui8258 (R8258)  | Deyou8258 (D8258)            |
|                                   |                    | Huazhen (HZ)       | Deyou Huazhen (DH)           |
|                                   |                    | Dehui938 (R938)    | Deyou 4938 (D4938)           |
|                                   |                    | Dehui4923 (R4923)  | Deyou 4923 (D4923)           |
|                                   |                    | R1391              | Deyou 1391 (D1391)           |

## Measurement of antioxidant enzyme activities

Before rehydration, approximately 0.5 g of frozen spikelets was ground into a fine powder with the help of liquid nitrogen and then homogenized in 50 mM of sodium phosphate buffer (pH 7.0). The homogenate was centrifuged at 13,000 g for 15 min at 4°C, and the supernatant was stored in a refrigerator at −20°C for further use. The POD activity was measured following the method described by Chance and Maehly (1964), in which guaiacol was converted to tetraguaiacol and then monitored at 470 nm. CAT activity was measured according to a previously described method by Bergmeyer with some modifications (Bergmeyer et al., 1974). The CAT reaction mixture contained 25 mM of sodium phosphate buffer (pH 7.0) and 40 mM of H<sub>2</sub>O<sub>2</sub> and was initiated by adding enzyme supernatant, and the change in the reaction solution in absorbance at 240 nm was recorded every 30 s for 2 min. One unit of CAT activity was defined as the amount capable of causing a change in absorbance of 0.01 unit/min.

## Measurement of total soluble sugar content

At the end of drought treatment, the panicles were sampled for assessment of total soluble sugar. Total soluble sugar content was determined using the anthrone-sulfate colorimetric method with some modifications (Dubois et al., 1956). A total of 0.5 g of panicle was mixed with 10 ml of ddH<sub>2</sub>O and boiled three times for a total of 30 min. After filtration, the extract was treated with anthrone, soaked in boiling water for 10 min, and cooled to room temperature, and the absorbance was measured at 620 nm with a spectrophotometer.

## Statistical analyses

SPSS 17.0 (SPSS, Chicago, IL, USA) was used for data analysis. A t-test was conducted to compare the differences between restorer lines and drought-stress plants. Variance (ANOVA) was conducted to compare the difference with a least significant difference (LSD) test at  $p = 0.05$ .

## Results

### Phenotype and yield statistics of progeny and restorer lines

In order to study the drought tolerance of the hybrid progeny of maintainer line 074B, we used 074B as a maintainer line, 074A as a sterile line, and R146, R727, RH103, R8258, HZ, R938, R4923, and R1391 as restorer lines. The progeny were D146, D4727, D4103, D8258, DH, D4938, D4923, and D1391. As shown in Figure 1, the seed setting rate decreased for both the control and hybrid offspring groups, but that of the control group decreased more seriously than that of the hybrid offspring group, indicating that drought caused more serious damage to the restorer line. The yield of maintainer line 074B decreased by 17.8% after drought treatment, while that of R146 and D146 decreased by 39.1% and 37.4%, respectively. The yield of R727 and its progeny D4727 decreased by 62.3% and 38.3%, respectively, while that of RH103 and D4103 decreased by 46% and 26%, respectively. HZ and its offspring DH decreased by 43.5% and 8.3%, respectively. The yield of R938 and progeny D4938 decreased by 74.6% and 55.7%, respectively; the yield of R4923 and D4923 decreased by 41.1% and 28.8%, respectively. The production of R1391 and offspring D1391 decreased by 58.7% and 24.6%, respectively. Compared with that of the control group, the yield of the offspring decreased less than that of the restorer groups. However, the yield of R8258 and its offspring D8258 decreased by 40.9% and 39.9%, respectively; the decrease in the yield of progeny was consistent with that of the restorer line D8258 (Figure 2). The data of the number of grains per panicle, number of panicles per basin, seed setting rate, 1,000-grain weight, and relative seed setting rate of 074B hybrid progeny can also fully explain how the 074B hybrid progeny has drought tolerance (Supplementary Table 1). The seed setting rate of R1391 decreased by 51.4%, which was twice as much as that of D1391 (25.2%). The number of grains per panicle (R727) and hybrid offspring (D4727) decreased by 25.6% and 0.3%, respectively. The 1,000-grain weight of R1391 and its progeny D1391 decreased by 2.4% and 0.07%, respectively. As shown, drought reduced the rice yield, but drought treatment conserved part of the rice yield of 074B hybrids to different degrees.

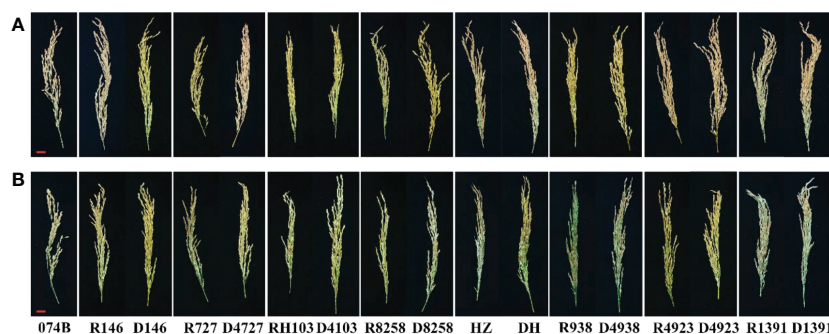
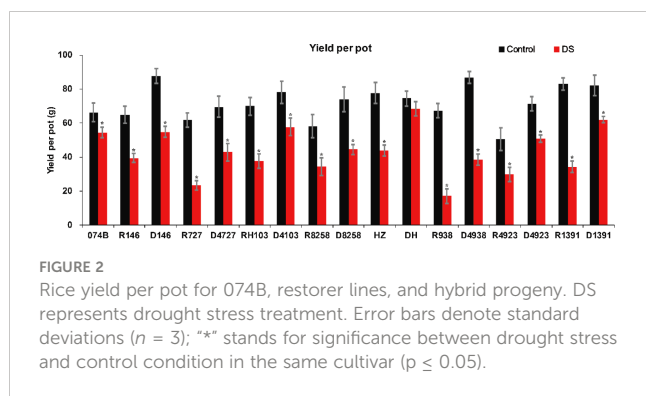


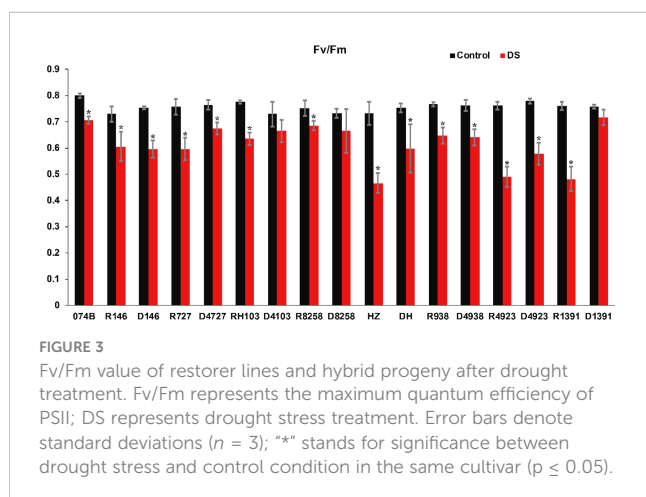
FIGURE 1  
Rice panicles of progeny and restorer lines. (A) Panicles under control conditions. (B) Panicles under drought treatment conditions. Bar = 2 cm.





## Effects of drought on Fv/Fm and MDA content of progeny and restorer lines

In order to distinguish the drought resistance of hybrids and restorer lines, we measured Fv/Fm and MDA content. The higher the value, the lower the stress status of the plant, and the better its health status. The lower the value, the worse the health status of those under strong stress conditions. The results shown in Figure 3 indicated that the Fv/Fm values of the male parent and hybrid offspring in the restorer line ranged from 0.7 to 0.8, indicating that the restorer line grew normally. After drought treatment, the Fv/Fm value of the maintainer line 074B decreased by 11.7%. The Fv/Fm values of the treatment group were lower than those of the restorer line; the Fv/Fm values of R727 and progeny D4727 decreased by 21.5% and 11.7%, respectively. The Fv/Fm values of RH103 and progeny D4103 decreased by 18% and 8.9%, respectively. The Fv/Fm values of HZ and its descendant DH decreased by 36.6% and 20.6%, respectively. The Fv/Fm values of R4923 and D4923 decreased by 35.8% and 26%, respectively. The Fv/Fm values of R1391 and D1391 decreased by 36.8% and 5.4%, respectively. Two sets of data showed no difference in Fv/Fm values between restorer lines and crosses. The Fv/Fm values of R8258 and D8258 decreased by 8.7% and 9.3%, respectively, and those of R938 and its descendant D4938 decreased by 15.7% and 15.7%, respectively. The Fv/Fm values of R146 and progeny D146 decreased by 17.3% and 21%, respectively. This was the only group of hybrid progeny whose Fv/Fm values showed that the restorer line was better at

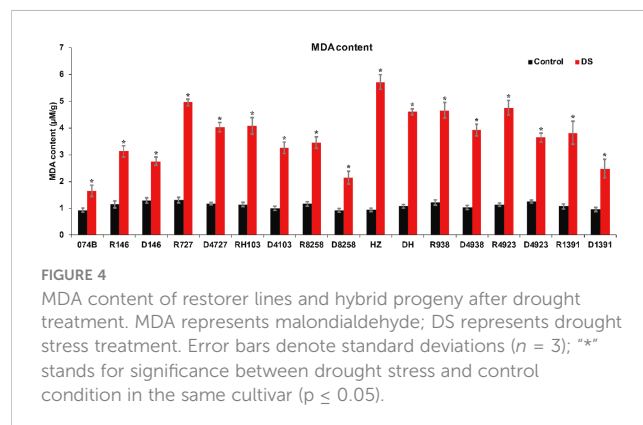


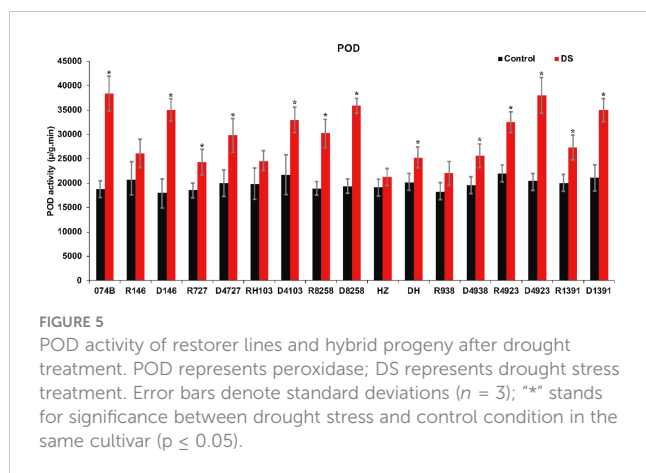
tolerating drought than its hybrid progeny. These results indicated that the parents and hybrid progeny were indeed affected by drought stress.

MDA is the product of the disintegration of membrane lipid peroxidation, and it is an important parameter of the potential antioxidant capacity of plants. It can indirectly reflect the degree of tissue peroxidation damage. MDA content is a commonly used index in the study of resistance physiology. It can reflect the degree of stress damage for plants. To assess the drought resistance of 074B hybrid progeny, MDA content was measured in the spikes of restorer lines and hybrid progeny. The results showed that the MDA content of both restorer lines and hybrid progeny increased significantly after drought treatment. MDA content increased by 78.3% after drought treatment in 074B. After drought treatment, the MDA content of HZ and DH increased by 500.6% and 330.2%. R727 and progeny D4727 increased by 276.8% and 242.4%, respectively. The MDA content in RH103 and progeny D4103 increased by 256.9% and 225.6%, while the MDA content in R4923 and D4923 increased by 320.8% and 188.9%, respectively. Finally, for R1391 and offspring D1391, the content of MDA increased by 255.4% and 156.2% (Figure 4). Only one group showed no significant difference in MDA content—R938 and hybrid offspring D4938—which saw an increase of 281.3% and 277%, respectively. The significant increase in MDA content indicated that the parents and hybrid progeny were indeed affected by drought stress.

## Effects of drought on antioxidant enzyme activities in plants

Plants contain a large number of peroxidases. These serve as markers of peroxisome, an oxidoreductase. Their activity changes constantly during plant growth and development, and POD activity can reflect the degree of stress damage to plants. In this study, POD activity was measured in the spikes of maintainer lines and hybrid progeny. The results shown in Figure 5 indicated that POD activity in both parents and hybrids increased significantly after drought treatment. POD activity increased by 105% in 074B after drought treatment. After drought treatment, POD activity in R146 and



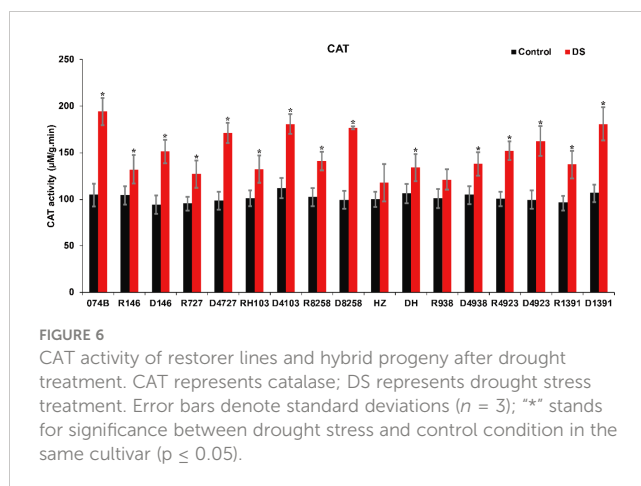


progeny D146 increased by 26.4% and 94.2%, respectively, and for R727 and progeny D4727, POD activity increased by 31.4% and 48.7%, respectively. In RH103 and progeny D4103, POD activity increased by 23.7% and 52.2%, respectively. Therefore, the POD activity of the hybrid progeny was significantly higher than that of the restorer lines after drought stress, indicating that the parents and hybrid progeny were indeed affected by drought stress and that the hybrid progeny could better cope with the effects of drought stress.

As a marker enzyme of peroxisomes, CAT is an oxidoreductase, and it can decompose  $H_2O_2$  to produce molecular oxygen and water and remove hydrogen peroxide from plants to prevent it from poisoning the cells. CAT activity can reflect the degree of stress damage to plants. In this study, CAT activity was measured in the spikes of restorer lines and hybrid progeny. The results showed that the CAT activity of both parents and crosses increased significantly after drought treatment. CAT activity increased by 84.8% after drought treatment in 074B. After drought treatment, the CAT activity of R146 and progeny D146 increased by 26.3% and 60.9%, respectively. For R727 and progeny D4727, the value increased by 33.1% and 73.7%, respectively, while CAT activity increased by 30.8% and 61.0% in RH103 and D4103, respectively. The CAT activity in other restorer lines and their offspring also increased (Figure 6). This indicated that catalase activity was improved in restorer lines and their offspring. The CAT activity of hybrid progeny was significantly greater than that of the restorer line, indicating that plants of hybrid progeny were indeed more resistant to drought stress than the restorer line.

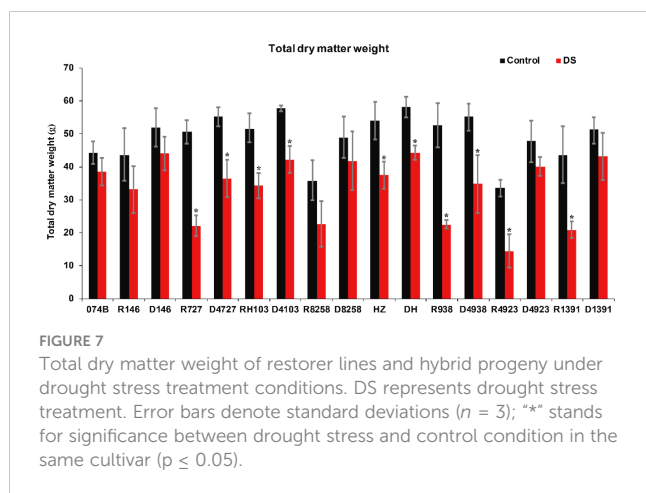
## Effect of drought on plant dry matter weight

Drought stress seriously affected the rate of accumulation of dry matter. During the flowering period, drought stress shortened the grain filling time, reduced the average and maximum rates of grain filling, and advanced the time at which the rate of grain filling peaked. It also affected the total amount of dry matter in plants. In this study, the degree of drought damage to plants was studied by measuring the amount of dry matter and the percentage of dry matter in the panicle



relative to the whole plants in restorer lines and hybrid progeny. The results showed that the dry matter of restorer lines and hybrid progeny decreased significantly after drought treatment (Figure 7). After drought treatment, the amount of 074B dry matter decreased by 12.8%. The amount of dry matter in R146 and progeny D146 decreased by 23.9% and 15.1%, respectively. The dry matter of R727 and progeny D4727 decreased by 56.3% and 34.2%, respectively, as well as decreased by 33.5% and 27.0% for RH103 and progeny D4103, respectively. Similarly, the dry matter also showed a downward trend in the following comparisons: R8258 (36.8%) and progeny D8258 (14.2%), HZ (30.7%) and its progeny DH (24.0%), R938 (57.4%) and progeny D4938 (37.1%), and R4923 (57.1%) and progeny D4923 (16.4%). The amount of dry matter showed a downward trend after the plants were subjected to drought stress, and the amount of dry matter in hybrid progeny was significantly lower than in the restorer line, indicating that the hybrid progeny were indeed more tolerant to drought stress than the restorer line.

Drought stress not only affected the rate of dry matter accumulation but also affected the rate of grain filling due to drought stress, which shortened the flowering period and affected the rate of grain filling. The amount of dry matter in the panicle was also affected. In this study, the percentage of dry matter in the panicle relative to the whole plant also confirmed that the plants were under drought stress. This study measured the percentage of dry matter in the panicle relative to the whole plant in restorer lines and hybrid progeny. The percentage of dry matter in the panicle relative to the whole plant in both restorer lines and hybrid progeny was significantly lower after drought treatment. The percentage of dry matter in the panicle relative to the whole plant decreased by 12.4% after 074B drought treatment. After drought treatment, the percentage of dry matter in the panicle relative to the whole plant between the restorer lines and progeny, R146 and D146, decreased by 29.5% and 16.0%, respectively. In R727 and progeny D4727, it decreased by 32.4% and 17.2%, respectively. In RH103 and progeny D4103, it decreased by 25.1% and 15.7%, respectively. In R8258 and its progeny D8258, it decreased by 23.5% and 15.5%, respectively. HZ and its progeny DH decreased by 22.3% and 8.3%, respectively. In R938 and progeny D4938, it decreased by 42.5% and 28.0%, respectively. In R4923 and progeny D4923, it decreased by 25.0%



and 18.8%, respectively. In R1391 and progeny D1391, it decreased by 39.8% and 22.0%, respectively (Figure 8). The percentage of dry matter in the panicle relative to the whole plant showed a downward trend after drought stress, and the restorer line had significantly less dry matter than the hybrid progeny, indicating that the hybrid progeny were indeed more tolerant to drought stress than the restorer line.

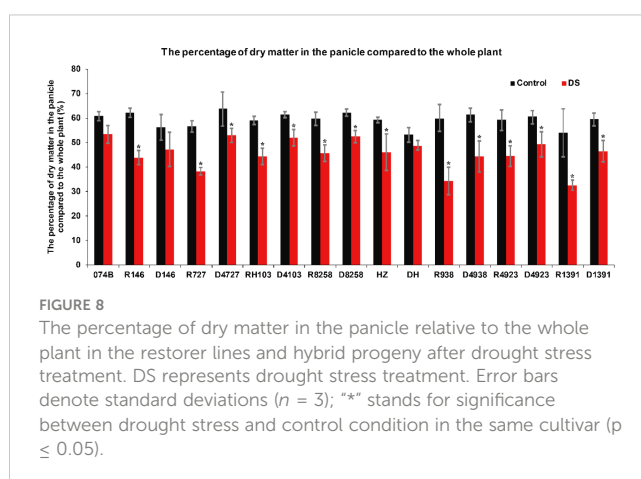
## Effects of drought on total soluble sugar content in plants

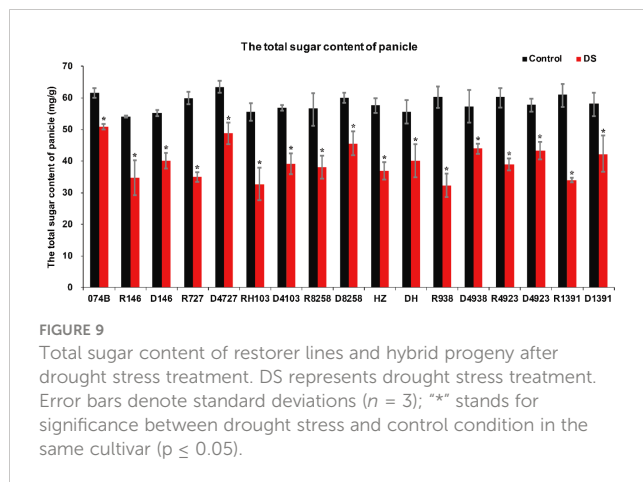
Drought stress decreased photosynthetic carbon assimilation and affected grain quality. In previous studies on soybean seeds and drought, drought stress reduced the rate of photosynthesis in the leaves; reduced shoot biomass and seed weight; increased soluble sugar content in the leaves, sucrose phosphate synthase, sucrose synthase, and acid convertase activities; and reduced starch content. The levels of starch, fructose, and glucose in seeds were decreased by drought stress during the later stages of grain filling. In this study, the index of the total sugar content of plants can also confirm that plants are under drought stress. In this study, the total sugar content of restorer lines and hybrid progeny was determined. The results showed that the total sugar content of restorer lines and hybrid progeny was significantly lower after drought treatment. The total sugar content of 074B decreased by 17.3% after drought treatment. After drought treatment, compared with the restorer line, the total sugar content in R146 and progeny D146 decreased by 35.5% and 25.0%, respectively, and in R727 and progeny D4727, the content decreased by 41.5% and 23.1%, respectively. The total sugar content decreased by 41.2% and 31.2% in RH103 and progeny D4103, respectively, while 46.4% and 23.2% total sugar content decreased in R8258 and progeny D8258, respectively. The total sugar content in other restorer lines and their progeny decreased in our results (Figure 9). The total sugar content showed a downward trend after the plants were subjected to drought stress, and the total sugar content of each restorer line was lower than that of its hybrid progeny, indicating that the hybrid progeny plants indeed had greater tolerance to drought stress than the restorer line.

## Discussion

Rice drought tolerance often has readily visible morphological, physiological, and biochemical characteristics as well as different genetic regulatory mechanisms (Yue et al., 2006). Although a large number of drought tolerance genes have been cloned in rice, marker-assisted selection breeding for drought tolerance has progressed slowly. Some factors have kept the progress slow: first, a considerable number of drought-tolerant genes have only been verified at the seedling stage and not at the reproductive stage. Second, these genes have little effect, so the drought tolerance of plants has not been significantly improved. Third, some genes have negative effects on plant growth, yield, or quality (Xia et al., 2019). Our present study showed that hybrids from Dexiang074A (074A) could significantly enhance yield, quality, and drought tolerance (Figure 1; Li et al., 2021).

It has been reported that many physiological indexes were used to evaluate the rice tolerance to drought stress such as Fv/Fm, MDA, and ROS (Wang et al., 2021). MDA is the product of membrane lipid peroxidation induced by ROS accumulation, often accumulated under stress conditions, which is consistent with our present study (Figure 4). There is a feedback mechanism of the ROS accumulation existing, which leads to an increase of antioxidant enzymes including POD and CAT (Mittler et al., 2022). In our present study, we found that the POD and CAT activities were increased under drought stress, while those of the hybrid offspring were higher than those of the restorer lines (Figures 5, 6). Except for the ROS system, carbohydrate transportation and distribution are often affected by water conditions (Jing et al., 2022). Moderate drought stress can effectively promote the transport of non-structural carbohydrates stored in stems and sheaths to panicles (Yang et al., 2001b). Under normal conditions, the contribution of stem and sheath assimilates to yield is approximately 20%, and it can increase to 50% under drought-stress conditions. This phenomenon is closely related to stomata (Chaves et al., 2002). Because stomatal conductance and CO<sub>2</sub> absorption are reduced under drought conditions, the generation of crop photosynthetic products is limited. Assimilates stored in stems and sheaths before grain filling become the main source of grain filling (Plaut et al., 2004). The total soluble carbohydrate decreased with an increase in





moisture deficit stress level (Shatpathy et al., 2019). In our present study, we found that the total sugar content was decreased by drought stress, and the total sugar content of hybrid offspring was generally higher than that of restorer lines (Figure 9). Also, the percentage of dry matter in the panicle relative to the whole plant showed the same trend, decreased by drought stress and less in hybrid than in the respective restorer lines (Figure 8). Therefore, we concluded that the 074A used as a sterile line could improve the hybrid tolerance than the respective restorer lines.

Heterosis, including dominance, super dominance, and epistasis effects, refers to the phenomenon that progeny of diverse varieties of a species or crosses between species exhibit greater biomass, speed of development, and fertility than both parents (Liu et al., 2020). In breeding, researchers select higher relative water content, ear length, grain number per ear, biomass, leaf drying, and drought recovery rate to improve rice drought tolerance and yield and obtain new varieties with high yield and drought tolerance (Jabran et al., 2017). Parents with high drought tolerance screened by identification of drought response indices were used to develop drought-tolerant varieties (Ouk et al., 2006). Lafitte et al. (2006) initiated large-scale backcross breeding involving more than 160 parent varieties from 25 countries to improve drought tolerance. After drought treatment, several lines with significant changes in drought response were selected, and drought-tolerant lines were crossed with one to three recurrent parents to evaluate  $BC_2F_2$  under drought conditions. Although drought stress results in a very low seed setting rate of backcross parents, many drought-tolerant backcross progeny lines produce seeds under drought stress, so they can provide drought-tolerant seed resources for rice-growing areas. Under drought stress during the reproductive period, directly selected seeds yielded 25% to 34% more than random lines. When assessed at similar levels of drought stress, it was noted that parent selection was particularly important in drought-tolerant breeding (Kamarudin et al., 2018). In addition, Verulkar et al. (2010) found that when severe drought stress occurred during the breeding period, selection leans toward greater gains under similar stress levels (yield reduction of 65% or greater under stress) than selection under non-stress conditions with no yield reduction under non-stress conditions (Verulkar et al., 2010). Recent studies indicated the grain yield of major quantitative trait loci (QTLs) with large effects

(32%–33% variation) under drought conditions (Vikram et al., 2016; Fontes et al., 2021). In the present study, 074A was used as the female parent, eight hybrids were used as the research materials, and the results indicated that the hybrids' yield was better than that of the restorer line parents' (Figure 2). It has been reported that the  $F_1$  hybrid rice combination from a cross between 103S and IR17525 enhanced grain yield under drought stress (Cuong et al., 2014). This is consistent with our present study, which showed that the hybrid combination, with obvious heterosis in drought stress, generally performed better than the parents in dry matter, enzyme activity, yield, and other characteristics. In addition, the heterosis value of dry matter accumulation under drought stress is slightly decreased when compared with normal conditions. For dry matter accumulation, the heterosis value increased much more in the hybrids under drought pressure than under normal conditions. After the drought recovery, the dry matter accumulation of all hybrid offspring remained unchanged, indicating the potential of using 074A to produce drought-tolerant hybrids. The utilization of rice heterosis was generally carried out around the yield in China (Ouyang et al., 2022). Hybrid offspring of female parent 074A showed not only heterosis of yield but also enhanced drought tolerance. However, no similar studies on rice male parents have been reported. Therefore, the collection and creation of drought-resistant germplasm resources of rice female parents may be an effective way for drought-resistant breeding of high-yield hybrid rice.

## Conclusion

Dexiang074B (074B) and Dexiang074A (074A) here served as maintainer lines and sterile lines. Mianhui146 (R146), Chenghui727 (R727), LuhuiH103 (RH103), Dehui8258 (R8258), Huazhen (HZ), Dehui938 (R938), Dehui4923 (R4923), and R1391 served as restorer lines. The progeny were Dexiangyou (D146), Deyou4727 (D4727), Dexiang4103 (D4103), Deyou8258 (D8258), Deyou Huazhen (DH), Deyou 4938 (D4938), Deyou 4923 (D4923), and Deyou 1391 (D1391). 074B, restorer lines, and offspring were used for drought stress treatment; the results of the study found that compared with the restorer lines, the offspring of 074A sterile lines in all in the determination of drought index have excellent performance. The decline in the yield was less pronounced for the offspring of 074A than for the restorer line. These hybrids are generally drought tolerant. Currently, the most concerning issue is the yield of crops under various stress conditions. The yield traits D4727 and DHZ showed the best performance, indicating that these two varieties have the least impact on yield under low-water conditions. This method can provide ideas for breeding for different stress conditions such as drought and low and high temperatures. The results of other drought tolerance indexes also showed that 074A progeny exhibited considerable drought tolerance. However, the yield traits of the 074A offspring showed excellent performance alongside drought resistance, indicating that this breeding method can allow the plant to cope with severe environmental changes, indicating that 074A may contain drought resistance genes and other novel genes with drought functions.



## Data availability statement

The original contributions presented in the study are included in the article/Supplementary Material. Further inquiries can be directed to the corresponding authors.

## Author contributions

Data curation: JQ, YC, and QY. Funding acquisition: GL, JZ, KJ, and TZ. Investigation: JL, XL, QC, XH, YH, CL, and LH. Writing the original draft: GL, TZ, and LY. Writing—review and editing: KJ, JZ, and GL. All authors contributed to the article and approved the submitted version.

## Funding

This work was funded by the National Natural Science Foundation of China (Grant 31901520), the Sichuan Key Project of Rice Breeding (2021YFYZ0016), the Key Science and Technology Project of Sichuan Province (2022ZDZX0012-02), the 1 + 9 Open Competition Project of Sichuan Academy of Agricultural Sciences (1 + 9KJGG002, 1 + 9KJGG001), Independent Innovation of Sichuan Province (2022CCZX066), Sichuan Youth Innovation Research Team of Science and Technology (Grant

2020JDTD0031), and Key Projects of Rice and Sorghum Research Institute (2020SZDYF008, 2020SZDYF001, and 2020SZDYF003).

## Conflict of interest

The authors declare that the research was conducted in the absence of any commercial or financial relationships that could be construed as a potential conflict of interest.

## Publisher's note

All claims expressed in this article are solely those of the authors and do not necessarily represent those of their affiliated organizations, or those of the publisher, the editors and the reviewers. Any product that may be evaluated in this article, or claim that may be made by its manufacturer, is not guaranteed or endorsed by the publisher.

## Supplementary material

The Supplementary Material for this article can be found online at: <https://www.frontiersin.org/articles/10.3389/fpls.2023.1054571/full#supplementary-material>

## References

- Anjum, S., Xie, X. Y., Wang, L. C., Saleem, M., Man, C., and Lei, W. (2011). Morphological, physiological and biochemical responses of plants to drought stress. *Afr. J. Agric. Res.* 6, 2026–2032. doi: 10.5897/AJAR10.027
- Bergmeyer, H. V., Gowehn, K., and Grassel, M. (1974). *Methods of enzymatic analysis* (Inc New York: Academic press).
- Chance, B., and Maehly, A. C. (1964). Assay of catalases and peroxidases. *Preparation and assay of enzymes. Meth. Enzymol.* 2, 764–775. doi: 10.1016/S0076-6879(55)02300-8
- Chaves, M. M., Pereira, J. S., Maroco, J., Rodrigues, M. L., Ricardo, C. P., Osório, M. L., et al. (2002). How plants cope with water stress in the field. photosynthesis and growth. *Annal Bot.* 89 Spec No (7), 907–916. doi: 10.1093/aob/mcf105
- Clark, C., Lin, Y., Bierwagen, B., Eaton, L., Langholtz, M., Morefield, P., et al. (2013). Growing a sustainable biofuels industry: Economics, environmental considerations, and the role of the conservation reserve program. *Environ. Res. Lett.* 8, 221–229. doi: 10.1088/1748-9326/8/2/025016
- Cuong, P. V., Hang, D. T. T., Hanh, T. T., Araki, T., Yoshimura, A., and Mochizuki, T. (2014). Photosynthesis and panicle growth responses to drought stress in F<sub>1</sub> hybrid rice (*Oryza sativa* L.) from a cross between thermo-sensitive genic male sterile (TGMS) line 103S and upland rice IR17525. *J. Fac. Agric. Kyushu Univ.* 59 (2), 273–277. doi: 10.5109/1467627
- De Schepper, V., De Swaef, T., Bauweraerts, I., and Steppe, K. (2013). Phloem transport: A review of mechanisms and controls. *J. Exp. Bot.* 64 (16), 4839–4850. doi: 10.1093/jxb/ert302
- Dionisio-Sese, M., and Tobita, S. (1998). Antioxidant responses of rice seedlings to salinity stress. *Plant Sci.* 135, 1–9. doi: 10.1016/S0168-9452(98)00025-9
- Dubois, M., Gilles, H. A., Hamilton, J. K., Rebers, P. A., and Smith, F. (1956). Colorimetric method for determination of sugars and related substances. *Analytical Chem.* 28, 22–25. doi: 10.1021/ac60111a017
- Durand, M., Porcheron, B., Hennion, N., Maurousset, L., Lemoine, R., and Pourtau, N. (2016). Water deficit enhances c export to the roots in arabidopsis thaliana plants with contribution of sucrose transporters in both shoot and roots. *Plant Physiol.* 170 (3), 1460–1479. doi: 10.1104/pp.15.01926
- Eom, J. S., Choi, S. B., Ward, J. M., and Jeon, J. S. (2012). The mechanism of phloem loading in rice (*Oryza sativa*). *Mol. Cells* 33 (5), 431–438. doi: 10.1007/s10059-012-0071-9
- Farooq, M., Wahid, A., Kobayashi, N., Fujita, D., and Basra, S. M. A. (2009). Plant drought stress: Effects, mechanisms and management. *Agron. Sustain. Dev.* 29 (1), 185–212. doi: 10.1051/agro:2008021
- Fontes, F., Gorst, A., and Palmer, C. (2021). Threshold effects of extreme weather events on cereal yields in India. *Climatic Change* 165, 26. doi: 10.1007/s10584-021-03051-x
- Fu, H., Chen, Y., Yang, X., Di, J., Xu, M., and Zhang, B. (2019). Water resource potential for large-scale sweet sorghum production as bioenergy feedstock in northern China. *Sci. Total Environ.* 653, 758–764. doi: 10.1016/j.scitotenv.2018.10.402
- Gill, S. S., and Tuteja, N. (2010). Reactive oxygen species and antioxidant machinery in abiotic stress tolerance in crop plants. *Plant Physiol. Biochem.* 48 (12), 909–930. doi: 10.1016/j.plaphy.2010.08.016
- Guo, C., Yao, L., You, C., Wang, S., Cui, J., Ge, X., et al. (2016). MID1 plays an important role in response to drought stress during reproductive development. *Plant J.* 88 (2), 280–293. doi: 10.1111/tpj.13250
- Halliwell, B. (2006). Reactive species and antioxidants. redox biology is a fundamental theme of aerobic life. *Plant Physiol.* 141 (2), 312–322. doi: 10.1104/pp.106.077073
- Harris-Shultz, K. R., Hayes, C. M., and Knoll, J. E. (2019). Mapping QTLs and identification of genes associated with drought resistance in sorghum. *Methods Mol. Biol.* 1931, 11–40. doi: 10.1007/978-1-4939-9039-9\_2
- He, F., Wang, H. L., Li, H. G., Su, Y., Li, S., Yang, Y., et al. (2018). PeCHYR1, a ubiquitin E3 ligase from populus euphratica, enhances drought tolerance via ABA-induced stomatal closure by ROS production in populus. *Plant Biotechnol. J.* 16 (8), 1514–1528. doi: 10.1111/pbi.12893
- Huang, J. W., Huang, J. J., Feng, Q. Y., Shi, Y. Q., Wang, F. G., Zheng, K. Y., et al. (2022). SUMOylation facilitates the assembly of a nuclear factor-γ complex to enhance thermotolerance in *Arabidopsis*. *J. Integr. Plant Biol.* doi: 10.1111/jipb.13396
- Jabran, K., Ullah, E., Akbar, N., Yasin, M., Zaman, U., Nasim, W., et al. (2017). Growth and physiology of basmati rice under conventional and water-saving production systems. *Arch. Agron. Soil Sci.* 63, 1465–1476. doi: 10.1080/03650340.2017.1285014
- Jin, Y., Yang, H., Wei, Z., Ma, H., and Ge, X. (2013). Rice male development under drought stress: phenotypic changes and stage-dependent transcriptomic reprogramming. *Mol. Plant* 6 (5), 1630–1645. doi: 10.1093/mp/sst067



- Jing, X. Q., Li, W. Q., Zhou, M. R., Shi, P. T., Zhang, R., Shalmani, A., et al. (2022). Rice carbohydrate-binding Malectin-Like protein, OsCBM1, contributes to drought-stress tolerance by participating in NADPH oxidase-mediated ROS production. *Rice* 15, 3. doi: 10.1186/s12284-022-00551-x
- Kamarudin, Z. S., Yusop, M. R., Mohamed, M. T. M., Ismail, M. R., and Harun, A. R. (2018). Growth performance and antioxidant enzyme activities of advanced mutant rice genotypes under drought stress condition. *Agronomy* 8 (12), 279. doi: 10.3390/agronomy8120279
- Lafitte, H. R., Li, Z. K., Vijayakumar, C. H. M., Gao, Y. M., Shi, Y., Xu, J. L., et al. (2006). Improvement of rice drought tolerance through backcross breeding: Evaluation of donors and selection in drought nurseries. *Field Crops Res.* 97, 77–86. doi: 10.1016/j.fcr.2005.08.017
- Li, G., Yang, Q., Li, D., Zhang, T., Yang, L., Qin, J., et al. (2021). Genome-wide SNP discovery and QTL mapping for economic traits in a recombinant inbred line of *Oryza sativa*. *Food Energy Secur.* 10, 313–328. doi: 10.1002/fes3.274
- Liu, J., Li, M. J., Zhang, Q., Wei, X., and Huang, X. H. (2020). Exploring the molecular basis of heterosis for plant breeding. *J. Integr. Plant Biol.* 62 (3), 287–298. doi: 10.1111/jipb.12804
- Liu, J. G., Wang, Y., Song, D. X., Wang, D. X., Cui, L. J., Sun, E. Y., et al. (2017). Effects on sunflower dry matter accumulation and yield of drought stress at flowering stages. *Liaoning Agric. Sci.* 3, 1–8. doi: 10.3969/j.issn.1002-1728.03.001
- Ma, J., Li, R., Wang, H., Li, D., Wang, X., Zhang, Y., et al. (2017). Transcriptomics analyses reveal wheat responses to drought stress during reproductive stages under field conditions. *Front. Plant Sci.* 8. doi: 10.3389/fpls.2017.00592
- Manhes, A., Ortiz-Moreno, F. A., He, P., and Shan, L. (2021). Plant plasma membrane-resident receptors: Surveillance for infections and coordination for growth and development. *J. Integr. Plant Biol.* 63, 79–101. doi: 10.1111/jipb.13051
- Mittler, R., Zandalinas, S. I., Fichman, Y., and Breusegem, F. V. (2022). Reactive oxygen species signaling in plant stress responses. *Nat. Rev. Mol. Cell Biol.* 23, 663–679. doi: 10.1038/s41580-022-00499-2
- Moore, J. P., Le, N. T., Brandt, W. F., Driouch, A., and Farrant, J. M. (2009). Towards a systems-based understanding of plant desiccation tolerance. *Trends Plant Sci.* 14 (2), 110–117. doi: 10.1016/j.tplants.2008.11.007
- Omar, K., Salih, B., Abdulla, N., Hussin, B., and Rassul, S. (2016). Evaluation of starch and sugar content of different rice samples and study their physical properties. *Indian J. Natural Sci.* 6, 11084–11093.
- Ouk, M., Basnayake, J., Tsubo, M., Fukai, S., Fischer, K. S., Cooper, M., et al. (2006). Use of drought response index for identification of drought tolerant genotypes in rainfed lowland rice. *Field Crops Res.* 99, 54–58. doi: 10.1016/j.fcr.2006.03.003
- Ouyang, Y. D., Li, X., and Zhang, Q. F. (2022). Understanding the genetic and molecular constitutions of heterosis for developing hybrid rice. *J. Genet. Genomics* 49, 385–393. doi: 10.1016/j.jgg.2022.02.022
- Plaut, Z., Butow, B. J., Blumenthal, C., and Wrigley, C. (2004). Transport of dry matter into developing wheat kernels and its contribution to grain yield under post-anthesis water deficit and elevated temperature. *Field Crops Res.* 86, 185–198. doi: 10.1016/j.fcr.2003.08.005
- Raed, E., and Raju, S. (2018). Canola responses to drought, heat, and combined stress: shared and specific effects on carbon assimilation, seed yield, and oil composition. *Front. Plant Sci.* 9. doi: 10.3389/fpls.2018.01224
- Ren, Y., Wang, X., Zhang, J. S., Nie, S. H., Wu, G. M., Geng, H. W., et al. (2019). Screening and identification of drought resistance of central Asian barley varieties at germination stage. *Xinjiang Agric. Sci.* 56. doi: 10.6048/j.issn.1001-4330.2019.05.0
- Robles, P., Navarro-Cartagena, S., Ferrández-Ayela, A., Núñez-Delegido, E., and Quesada, V. (2018). The characterization of *arabidopsis mterf6* mutants reveals a new role for mTERF6 in tolerance to abiotic stress. *Int. J. Mol. Sci.* 19 (8). doi: 10.3390/ijms19082388
- Ruan, Y. L. (2012). Signaling role of sucrose metabolism in development. *Mol. Plant* 5 (4), 763–765. doi: 10.1093/mp/sss046
- Ruan, Y. L., Jin, Y., Yang, Y. J., Li, G. J., and Boyer, J. S. (2010). Sugar input, metabolism, and signaling mediated by invertase: Roles in development, yield potential, and response to drought and heat. *Mol. Plant* 3 (6), 942–955. doi: 10.1093/mp/ssp044
- Sajilata, M. G., Singhal, R. S., and Kulkarni, P. R. (2006). Resistant starch-a review. *Compr. Rev. Food Sci. Food Saf.* 5 (1), 1–17. doi: 10.1111/j.1541-4337.2006.tb00076.x
- Serraj, R., Kumar, A., McNally, K., Slamet-Loedin, I., Bruskiewich, R., Mauleon, R., et al. (2009). Chapter 2 improvement of drought resistance in rice. *Adv. Agron.* 103, 41–99. doi: 10.1016/S0065-2113(09)03002-8
- Shatpathy, P., Dwivedi, S. K., and Dash, A. (2019). Assessment of physiological traits for adaptation to flowering stage water deficit in rainfed lowland rice (*Oryza sativa* L.). *Int. J. Curr. Microbiol. Appl. Sci.* 8, 245–255. doi: 10.20546/ijcmas.2019.810.025
- Sheoran, S., Thakur, V., Narwal, S., Turan, R., Mamrutha, H. M., Singh, V., et al. (2015). Differential activity and expression profile of antioxidant enzymes and physiological changes in wheat (*Triticum aestivum* L.) under drought. *Appl. Biochem. Biotechnol.* 177 (6), 1282–1298. doi: 10.1007/s12010-015-1813-x
- Song, J., Sun, P. P., Kong, W. N., Xie, Z. Z., Li, C. L., and Liu, J. H. (2023). SnRK2.4-mediated phosphorylation of ABF2 regulates ARGININE DECARBOXYLASE expression and putrescine accumulation under drought stress. *New Phytol.* doi: 10.1111/nph.18526
- Tiwari, P., Indoliya, Y., Singh, P., Singh, P., Singh, P., Srivastava, S., et al. (2020). Auxin-salicylic acid cross-talk ameliorates OsMYB-R1 mediated defense towards heavy metal, drought and fungal stress. *J. Hazard. Mater.* 399, 122811. doi: 10.1016/j.jhazmat.2020.122811
- Verulkar, S. B., Mandal, N. P., Dwivedi, J. L., Singh, B. N., Sinha, P. K., Mahato, R. N., et al. (2010). Breeding resilient and productive genotypes adapted to drought-prone rainfed ecosystem of India. *Field Crops Res.* 117, 197–208. doi: 10.1016/j.fcr.2010.03.005
- Vikram, P., Kadam, S., Singh, B. P., Lee, Y. J., Pal, J. K., Singh, S., et al. (2016). Genetic diversity analysis reveals importance of green revolution gene (*Sd1* locus) for drought tolerance in rice. *Agric. Res.* 5, 1–12. doi: 10.1007/s40003-015-0199-x
- Wang, J. Y., Li, C. M., Li, L., Reynolds, M., Mao, X. G., and Jing, R. L. (2021). Exploitation of drought tolerance-related genes for crop improvement. *Int. J. Mol. Sci.* 22, 9108. doi: 10.3390/ijms221910265
- Wang, X., Liu, H., Yu, F., Hu, B., Jia, Y., Sha, H., et al. (2019). Differential activity of the antioxidant defence system and alterations in the accumulation of osmolyte and reactive oxygen species under drought stress and recovery in rice (*Oryza sativa* L.) tillering. *Sci. Rep.* 9 (1), 8543. doi: 10.1038/s41598-019-44958-x
- Xia, H., Luo, Z., Xiong, J., Ma, X. S., Lou, Q. J., Wei, H. B., et al. (2019). Bi-directional selection in upland rice leads to its adaptive differentiation from lowland rice in drought resistance and productivity. *Mol. Plant* 12, 170–184. doi: 10.1016/j.molp.2018.12.011
- Xiang, Y. H., Yu, J. J., Liao, B., Shan, J. X., Ye, W. W., Dong, N. Q., et al. (2022). An  $\alpha/\beta$  hydrolase family member negatively regulates salt tolerance but promotes flowering through three distinct functions in rice. *Mol. Plant* 15. doi: 10.1016/j.molp.2022.10.017
- Xu, Y., Burgess, P., Zhang, X., and Huang, B. (2016). Enhancing cytokinin synthesis by overexpressing *ipt* alleviated drought inhibition of root growth through activating ROS-scavenging systems in *Agrostis stolonifera*. *J. Exp. Bot.* 67 (6), 1979–1992. doi: 10.1093/jxb/erw019
- Yang, Z., Chi, X., Guo, F., Jin, X., Luo, H., Hawar, A., et al. (2020). SbWRKY30 enhances the drought tolerance of plants and regulates a drought stress-responsive gene, SbRD19, in sorghum. *J. Plant Physiol.* 246–247, 153142. doi: 10.1016/j.jplph.2020.153142
- Yang, J., Zhang, J., Liu, L., Wang, Z., and Zhu, Q. (2002). Carbon remobilization and grain filling in Japonica/Indica hybrid rice subjected to postanthesis water deficits. *Agron. J.* 94, 102–109. doi: 10.2134/agronj2002.0102
- Yang, J., Zhang, J., Wang, Z., and Zhu, Q. (2001a). Activities of starch hydrolytic enzymes and sucrose-phosphate synthase in the stems of rice subjected to water stress during grain filling. *J. Exp. Bot.* 52 (364), 2169–2179. doi: 10.1093/jxb/52.364.2169
- Yang, J. C., Zhang, J. H., Wang, Z. Q., Zhu, Q. S., and Wang, W. (2001b). Remobilization of carbon reserves in response to water deficit during grain filling of rice. *Field Crops Res.* 71 (1), 47–55. doi: 10.1016/S0378-4290(01)00147-2
- You, J., and Chan, Z. (2015). ROS regulation during abiotic stress responses in crop plants. *Front. Plant Sci.* 6. doi: 10.3389/fpls.2015.01092
- Yu, P. H., Jiang, N., Fu, W. M., Zheng, G. J., Li, G. Y., Feng, B. H., et al. (2020). ATP hydrolysis determines cold tolerance by regulating available energy for glutathione synthesis in rice seedling plants. *Rice* 13 (1), 23. doi: 10.1186/s12284-020-00383-7
- Yu, J., Jiang, M., and Guo, C. (2019). Crop pollen development under drought: From the phenotype to the mechanism. *Int. J. Mol. Sci.* 20 (7). doi: 10.3390/ijms20071550
- Yue, B., Xue, W., Xiong, L., Yu, X., Luo, L., Cui, K., et al. (2006). Genetic basis of drought resistance at reproductive stage in rice: Separation of drought tolerance from drought avoidance. *Genetics* 172 (2), 1213–1228. doi: 10.1534/genetics.105.045062



## OPEN ACCESS

## EDITED BY

Arpna Kumari,  
The University of Tokyo, Japan

## REVIEWED BY

Hayssam M. Ali,  
King Saud University, Saudi Arabia  
Manzer H. Siddiqui,  
King Saud University, Saudi Arabia

## \*CORRESPONDENCE

Khalid Rehman Hakeem  
✉ kur.hakeem@gmail.com  
Reiaz Ul Rehman  
✉ reiazbiores@gmail.com

<sup>†</sup>These authors have contributed  
equally to this work and share  
first authorship

## SPECIALTY SECTION

This article was submitted to  
Plant Abiotic Stress,  
a section of the journal  
Frontiers in Plant Science

RECEIVED 26 September 2022

ACCEPTED 31 January 2023

PUBLISHED 10 March 2023

## CITATION

Mushtaq NU, Alghamdi KM, Saleem S,  
Tahir I, Bahieldin A, Henrissat B,  
Alghamdi MK, Rehman RU and Hakeem KR  
(2023) Exogenous zinc mitigates salinity  
stress by stimulating proline metabolism in  
proso millet (*Panicum miliaceum* L.).  
*Front. Plant Sci.* 14:1053869.  
doi: 10.3389/fpls.2023.1053869

## COPYRIGHT

© 2023 Mushtaq, Alghamdi, Saleem, Tahir,  
Bahieldin, Henrissat, Alghamdi, Rehman and  
Hakeem. This is an open-access article  
distributed under the terms of the [Creative  
Commons Attribution License \(CC BY\)](#). The  
use, distribution or reproduction in other  
forums is permitted, provided the original  
author(s) and the copyright owner(s) are  
credited and that the original publication in  
this journal is cited, in accordance with  
accepted academic practice. No use,  
distribution or reproduction is permitted  
which does not comply with these terms.

# Exogenous zinc mitigates salinity stress by stimulating proline metabolism in proso millet (*Panicum miliaceum* L.)

Naveed Ul Mushtaq<sup>1†</sup>, Khalid M. Alghamdi<sup>2†</sup>, Seerat Saleem<sup>1</sup>,  
Inayatullah Tahir<sup>3</sup>, Ahmad Bahieldin<sup>2</sup>, Bernard Henrissat<sup>4</sup>,  
Mohammed Khalid Alghamdi<sup>2</sup>, Reiaz Ul Rehman<sup>1\*</sup>  
and Khalid Rehman Hakeem<sup>2,5,6\*</sup>

<sup>1</sup>Department of Bioresources, School of Biological Sciences, University of Kashmir, Srinagar, India,

<sup>2</sup>Department of Biological Sciences, Faculty of Science, King Abdulaziz University,

Jeddah, Saudi Arabia, <sup>3</sup>Department of Botany, School of Biological Sciences, University of Kashmir,

Srinagar, India, <sup>4</sup>UMR7257 CNRS - Aix-Marseille University, Marseille, France, <sup>5</sup>Princess Dr. Najla Bint

Saud Al-Saud Center for Excellence Research in Biotechnology, King Abdulaziz University,

Jeddah, Saudi Arabia, <sup>6</sup>Department of Public Health, Daffodil International University, Dhaka, Bangladesh

Salinity is one of the most concerning ecological restrictions influencing plant growth, which poses a devastating threat to global agriculture. Surplus quantities of ROS generated under stress conditions have negative effects on plants' growth and survival by damaging cellular components, including nucleic acids, lipids, proteins and carbohydrates. However, low levels of ROS are also necessary because of their role as signalling molecules in various development-related pathways. Plants possess sophisticated antioxidant systems for scavenging as well as regulating ROS levels to protect cells from damage. Proline is one such crucial non-enzymatic osmolyte of antioxidant machinery that functions in the reduction of stress. There has been extensive research on improving the tolerance, effectiveness, and protection of plants against stress, and to date, various substances have been used to mitigate the adverse effects of salt. In the present study Zinc (Zn) was applied to elucidate its effect on proline metabolism and stress-responsive mechanisms in proso millet. The results of our study indicate the negative impact on growth and development with increasing treatments of NaCl. However, the low doses of exogenous Zn proved beneficial in mitigating the effects of NaCl by improving morphological and biochemical features. In salt-treated plants, the low doses of Zn (1 mg/L, 2 mg/L) rescued the negative impact of salt (150mM) as evidenced by increase in shoot length (SL) by 7.26% and 25.5%, root length (RL) by 21.84% and 39.07% and membrane stability index (MSI) by 132.57% and 151.58% respectively. The proline content improved at all concentrations with maximum increase of 66.65% at 2 mg/L Zn. Similarly, the low doses of Zn also rescued the salt induced stress at 200mM NaCl. The enzymes related to proline biosynthesis were also improved at lower doses of Zn. In salt treated plants

(150mM), Zn (1 mg/L, 2 mg/L) increased the activity of P5CS by 19.344% and 21%. The P5CR and OAT activities were also improved with maximum increase of 21.66% and 21.84% at 2 mg/L Zn respectively. Similarly, the low doses of Zn also increased the activities of P5CS, P5CR and OAT at 200mM NaCl. Whereas P5CDH enzyme activity showed a decrease of 82.5% at 2mg/L Zn+150mM NaCl and 56.7% at 2mg/L Zn+200 mM NaCl. These results strongly imply the modulatory role of Zn in maintaining of proline pool during NaCl stress.

#### KEYWORDS

P5CS, zinc, proline, salt stress, millets

## Introduction

Plants are impacted by both biotic and abiotic stress conditions which inhibit the uptake of water and nutrients, compromise membrane permeability and hamper development (Arif et al., 2020). These alterations also affect the metabolism of hormones, and the exchange of gasses and result in the production of ROS at a faster rate. The salinity stress reduces primary photochemistry of photosystem and reduced photosynthetic pigments, exhibited enhanced chlorophyll degradation and leakage of electrolytes (Siddiqui et al., 2019; Akhter et al., 2021). Continuous exposure to such conditions finally causes plant senescence and death (EL Sabagh et al., 2021). Salt stress in plants is one of the most significant ecological restrictions influencing plant growth and development which poses a devastating threat to global agriculture (Mushtaq et al., 2021). Worldwide, the rate of salinity is high which affects approximately 20% of the world's land and it has been steadily increasing for a few decades (Khan et al., 2022). The overuse of fertilizers and outdated irrigation practices are primarily to blame for excessive salt levels in agricultural lands (Ladeiro, 2012). An excessive amount of salt causes hyperosmotic and hyperionic conditions, accumulation of Na<sup>+</sup> and Cl<sup>-</sup> ions and the generation of ROS (Rahman et al., 2016). The increased ROS quantities impact the plants negatively by damaging cellular components, including nucleic acids, lipids, proteins, and carbohydrates (Das and Roychoudhury, 2014; Saleem et al., 2021). However, moderate levels of ROS are necessary as they function as a signalling molecule (Mittler, 2017; Marcec and Tanaka, 2021). On the other hand, plants have a sophisticated antioxidant system that scavenges and regulates the levels of ROS to protect cells from damage (Kapoor et al., 2019). Proline is one such crucial non-enzymatic osmolyte that plays a function in stress reduction (Alamri et al., 2019; Iqbal et al., 2021). Besides its role in plant improvement, proline is also involved in flowering, pollen, embryos, and leaf growth. As a response to stress, proline is typically boosted in the cytosol to regulate the osmotic environment (Meena et al., 2019). Apart from its function as an osmolyte, it also works as a metal chelator and antioxidant molecule during stressful situations (Hayat et al., 2012). Proline accumulation enhances heavy metal tolerance, and improved resistance to drought or salinity stress in plants and algae (Hmida-Sayari et al., 2005; Zhao

et al., 2022). There has been extensive research on improving the tolerance, effectiveness, and protection of plants against stress, and to date, various substances have been used to mitigate the adverse effects of salt. Microelements are thought to help plants cope with salt stress (Abideen et al., 2022) and throughout their life cycle, plants require these elements to survive in contrasting environmental conditions. Deficiencies of these elements can significantly affect a plant's growth, development, and survival. In the context of requirement, certain elements may not be required by all the plants, but are advantageous to particular plant species, and are therefore called beneficial elements. Beneficial elements consist of zinc (Zn), cobalt (Co), selenium (Se) and silicon (Si) (Kaur et al., 2016). Research indicates that these elements are beneficial to plant growth and development in both optimal and stressful environments. In order to enable plants to cope with stress adversities and survive, beneficial elements regulate essential acclimation responses through molecular, physiological, and biochemical mechanisms (Kumari et al., 2022). They increase abiotic stress tolerance in plants by an intricate crosstalk with other plant growth regulators such as phytohormones, ROS and other signalling molecules (Tiwari et al., 2017; Khan et al., 2021). However, their beneficiary and essentiality is debatable, with little evidence indicating necessity. In the era of climate change, a restored understanding of beneficial elements may also be beneficial to improving stress tolerance, plant health, plant nutritional value and crop productivity. As a result, the principles behind the impacts of beneficial components in plants need to be explored, and the field provides a chance to gain more insights that might aid in achieving sustainable agricultural yield and plant adaptation to abiotic stress conditions. Micronutrients such as boron (B), chloride (Cl), copper (Cu), iron (Fe), manganese (Mn), molybdenum (Mo), nickel (Ni), and zinc (Zn) are required in much lesser amounts by the plant (Thapa et al., 2021). It is difficult to specify the precise numbers of micronutrients since certain elements are still not clearly classified as essential or beneficial. 17 of the 92 natural elements found in plants are considered essential nutrients. Among these 17 elements, 8 are micronutrients which include iron (Fe), zinc (Zn), copper (Cu), manganese (Mn), molybdenum (Mo), chlorine (Cl), boron (B), and nickel (Ni) (Mondal and Bose, 2019). Micronutrients are involved in almost all metabolic and cellular activities, including primary and secondary metabolism, energy metabolism, cell defense, gene

regulation, hormone sensing, signal transduction, and reproduction. Micro nutrients also play vital roles in plant growth, development and food grain production, enhancing tolerance to abiotic stress, maintaining water potential, provide protection against environmental extremities and pathogen (Tripathi et al., 2015; Chrysargyris et al., 2022).

Zinc is one of the cardinal micronutrients which mitigates stress in plants (Dimkpa et al., 2019; Venugopalan et al., 2022). Studies reported that the use of Zn has improved plant growth, pigment content, carbohydrates, proteins, antioxidants, and the plant defence system (Noreen et al., 2021; Shah et al., 2022; Wei et al., 2022). It aids in membrane stability, hormone production, starch and sucrose turnover, RNA and DNA structure stabilization, gene expression, auxin formation, photosynthesis, and protection against drought, cold, salt, and pathogens (Umair Hassan et al., 2020; Hassanein et al., 2021; Rai-Kalal and Jajoo, 2021). Zinc deficiency in rice was reported to mediate the induction of CAZymes (Carbohydrate-Active enZymes) involved in starch synthesis/transport *via* up-regulation of genes encoding these CAZymes (Suzuki et al., 2012). These enzymes mainly belong to CAZy classes glycoside hydrolase (GH) and glycosyltransferases (GT) (Diricks et al., 2015; Stam et al., 2006) (<http://www.cazy.org>). Interestingly, the ability of rice plants to withstand the low level of Zn in their cells is prompted by the accumulation of starch mediated by certain CAZymes of the Kyoto Encyclopedia of Genes and Genomes (KEGG) pathway “Sucrose and Starch Metabolism” (map00500). These CAZymes include 4-alpha-glucanotransferase (EC 2.4.1.25) and 1,4-alpha-glucan branching enzyme (EC 2.4.1.18) that act on the transfer of  $\alpha$ -1,4-glucosidic bond, respectively, from maltose to amylose, and eventually to starch (<https://www.brenda-enzymes.org/>) (Lombard et al., 2014).

The normal concentration of Zn in most plants is between 25 to 150 ppm, however, this small amount of Zn plays a key role in more than 300 enzymes, such as alkaline phosphatase, carbonic anhydrase, alcohol dehydrogenase, and Cu-Zn superoxide dismutase (Malik et al., 2011; Solanki, 2021). It also has a structural role in the stabilization of proteins such as Zn cluster, Zn finger and RING finger domains/motifs. In crop plants, zinc is transported directly from the soil either in  $Zn^{2+}$  form and get accumulated in the roots of plants before being translocated to the shoots and leaves *via* xylem (Vatansever et al., 2017). In plants, Zn homeostasis is maintained by ZIP (Zn, iron-permease family/ZRT, IRT proteins) family uptake transporters in a coordinated regulation mechanism. Other proteins involved in the translocation of Zn are the heavy metal ATPase (HMA) family and the metal tolerant proteins (MTP) family (Olsen and Palmgren, 2014). ZIP family participates in the Zn influx into cell cytosol, while HMA mediates Zn efflux into the apoplast. Zn sequestration into the vacuoles and endoplasmic reticulum are facilitated by the MTP family (Gupta et al., 2016).

We hypothesized that a stressor (NaCl) and a mitigant (Zn) would have an impact on the proline biosynthesis which would reflect as a response on plant fitness. Thus to understand this process

we aimed to visualize the merit of using Zn as a mitigant against salt stress (NaCl) and to understand the role of Zn in regulating proline pathway under salt stress in proso millet. Thus we studied proline metabolism, proline accumulation and enzyme activities related to proline biosynthesis. We also elucidated plant growth parameters after the application of zinc (zinc sulfate).

## Material and methods

### Plant growth and treatments

The seeds of proso millet (*Panicum miliaceum* L.) were collected and identified at the Centre for Biodiversity and Taxonomy, University of Kashmir. The seeds were sterilized using 70% (v/v) ethanol for 1 minute and washed with sterile distilled water. Surface sterilization of seeds was performed using 10% sodium hypochlorite solution for 10 min followed by rinsing with sterilized distilled water. The seeds were sown in pots, 20 cm in diameter and containing autoclaved sand. Each pot of specific diameter contained 900grams of sand and 1gram of seeds (approx. 500 seeds). A controlled environment with a  $26 \pm 1^\circ\text{C}$  temperature and a 16-h photoperiod was maintained (Khalid et al., 2008; Desoky et al., 2019). Three sets of plants were grown with three replicates each and the treatments viz., 0, 150 and 200 mM of NaCl were given to the pots as per (Shah et al., 2020) and the Zinc (Zn) treatments 1 to 5 mg/L were provided in the form of zinc sulfate ( $ZnSO_4$ ). The Hoagland's nutrient medium (pH 6.5) containing all macro and micro nutrients was used as a nutrient source for the growth of plants. Till 14<sup>th</sup> day of sowing, plants were nourished with Hoagland's nutrient medium and afterwards both salt and Zinc were applied with nutrient solution. For maintaining concentrations of treatments throughout the stress period, treatments were repeated every third day till harvesting. The experiment was performed in a complete randomized design and each treatment was replicated three times (Supplementary Table 1). The plants were harvested after 22 days of sowing for morphological (Shoot length, root length, total length, leaf height and area), physiological and biochemical analysis.

### Determination of plant growth parameters and tolerance index

Following the experiment, 10 plants were taken at random from each treatment and gently cleansed four times with deionized water to remove adherent sand from the root surfaces. Following this, the morphological parameters were examined (Singh et al., 2008; Kausar et al., 2012; Dikobe et al., 2021). To evaluate the capacity of plants to thrive under high saline environments, the tolerance index (TI) was calculated by the equation given by Wilkin (Wilkins, 1957):

$$\text{Tolerance Index (TI \%)} = \text{MLT} / \text{MLC} \times 100$$

MLT = Mean length (root, shoot) of the longest root/shoot in treated plants, MLC = Mean length (root, shoot) of longest root/shoot in control.

### Fresh weight/dry weight/relative water content

The biomass accumulation (BA) of 10 plants was determined by drying in an incubator at  $70^\circ\text{C}$  for 48 hours. To calculate relative water content (RWC), the fresh weight (FW) of leaves was taken. Following this, the dry weights (DW) of leaves were taken by drying



in an oven at 70°C for 48 h (Afzal and Mansoor, 2012). RWC was analyzed using the formula:

$$RWC (\%) = FW - DW / FW \times 100$$

## The membrane stability index and electrolyte leakage

The membrane stability index (MSI) and Electrolyte leakage (EL) was determined by the method of Singh (Singh et al., 2008). Leaves were sterilized 3 times with distilled water before being chopped into small pieces and put in vials containing 10 mL of double distilled water. For the initial electrical conductivity of the solution (EC1), the vials were placed in a water bath at 40°C for 30 minutes. To obtain the final electrical conductivity (EC2), the vials were subjected to boiling temperature in a water bath for 10 minutes and then allowed to cool before taking EC2 readings. The EL and MSI were measured by using the following formulae;

$$EL (\%) = (EC1/EC2) \times 100$$

$$MSI (\%) = [1 - (EC1/EC2)] \times 100$$

## Photosynthetic pigments and chlorophyll stability index

0.2g of leaf sample was homogenized in 10ml of 80% acetone under dark conditions. Total chlorophyll, chlorophyll a and chlorophyll b were measured following the standard methods (Lichtenthaler, 1987; Hou et al., 2018);. For calculating anthocyanin, the pre-frozen leaf samples (0.1g) were homogenized in 10 ml of acidified methanol (methanol, double distilled water and concentrated HCl in the ratio of 80:20:1) in dark conditions (Benazzouk et al., 2020). Carotenoids, total phenolics and total flavonoid content were calculated as per Golkar and Taghizadeh and Benazzouk et al. (Golkar and Taghizadeh, 2018; Benazzouk et al., 2020). The stability of chlorophyll was measured by the chlorophyll stability index (CSI) as per Sairam et al. (Sairam et al., 1997) by the following formula;

$$CSI = (Total\ Chl.\ under\ stress / Total\ Chl.\ under\ control) \times 100$$

## 2, 2-Diphenyl-1-Picrylhydrazyl activity

The DPPH-radical scavenging activity was calculated using the method given by Sethi et al. (Sethi et al., 2020). To measure the radical scavenging activity of the methanolic extract, 0.1 ml of extract was allowed to inhibit 3.9 ml of DPPH. UV-VIS spectrophotometer was used to measure the absorbance of the reaction mixture at 517 nm and the percentage of DPPH radical scavenging activity was calculated by the following equation:

The percentage inhibition (IP) of absorbance was determined using the following equation:

$$IP (\%) = [A_{control} - A_{sample} / A_{control}] \times 100$$

Where,  $A_{control}$  is the absorbance of the control reaction and  $A_{sample}$  is the absorbance in the presence of a methanolic sample.

## Ferric reducing antioxidant power

The antioxidant capacity of the samples was determined spectrophotometrically using the method of Rajurkar and Hande with some modifications (Rajurkar and Hande, 2011). At low pH the electron donating antioxidants reduction of  $Fe^{3+}$  TPTZ complex (colourless complex) to  $Fe^{2+}$ -tripyrildyltriazine (blue coloured complex) takes place which was read at 593 nm after 4 minutes. The sample (10  $\mu$ l) was added to a 300  $\mu$ l FRAP reaction mixture containing 300 mM acetate buffer, 10 ml TPTZ in 40 mM HCl and 20 mM  $FeCl_3$  in the proportion of 10:1:1 at 37°C. Ferrous ammonium sulphate was used as a standard for calculating FRAP activity.

## Proline content estimation

The ninhydrin method was used to assess the proline content of the leaves as per Zhu et al. (Zhu et al., 2020) with some modifications. Leaves (0.5 g) collected were extracted in 3 percent (w/v) sulfosalicylic acid. The leaves were weighed and finely grounded using liquid nitrogen. The mixture was kept as such for a few minutes and was centrifuged at 12,000 g for 10 min. The supernatant obtained after centrifuge was used to estimate proline content. The supernatant was combined with 2 ml of acid ninhydrin and 2 ml of glacial acetic acid and placed in a 100°C water bath for 1 hour. The reaction was stopped by immersing the test tubes in an ice bath. Further 4 ml toluene was added to the mixture and the absorbance at 520 nm was measured with a spectrophotometer. The content of proline was measured using a proline standard curve made with different concentrations.

## Enzyme extraction and assays

To find out the activity of proline metabolism enzymes, the leaf samples was homogenized in an extraction buffer containing 100 mM Tris-HCl, 1 mM EDTA, 10 mM  $MgCl_2$ , 10 mM  $\beta$ -mercaptoethanol, 2 mM PMSF, 4 mM DTT, and 2% PVPP (pH 7.5). The homogenate was centrifuged at 4°C at 10,000 g for 20 min. The supernatant was stored at -80°C for enzyme assays. Pyrroline-5-carboxylate synthase (P5CS),  $\Delta$ -pyrroline-5-carboxylate reductase (P5CR),  $\delta$ -ornithine amino transferase (OAT),  $\Delta$ -pyrroline-5-carboxylate dehydrogenase (P5CDH) and proline dehydrogenase (ProDH) assays were performed following standard protocols with some modifications (Parida et al., 2008; Spoljarevic et al., 2011; Da Rocha et al., 2012; Koenigshofer and Loeppert, 2019; Zhu et al., 2020)

## Pyrroline-5-carboxylate synthase activity

This study determined the P5CS activity based on the utilization of NADPH during the reaction catalyzed by the enzyme. At 25°C, the



P5CS activity was performed in a final volume of 2 mL of 100mM Tris-HCl buffer (pH 7.5) containing 25mM MgCl<sub>2</sub>, 75mM Na-glutamate, 10mM ATP, 0.4mM NADPH, and the enzyme extract. Using UV-Vis spectrometer, NADPH consumption was monitored as a decrease in absorption at 340 nm as a function of time.

### Δ-pyrroline-5-carboxylate reductase activity

P5CR activity was determined by measuring the proline-dependent reduction of NAD<sup>+</sup> (the reverse reaction). At 25°C, the reaction was performed in a final volume of 2 mL of 200mM sodium glycinate buffer (pH 10.3), 20mM proline, 15mM NAD<sup>+</sup> (pH 5-7), and the enzyme extract. To measure the formation of NADH, absorbance at 340 nm was monitored by using UV-Vis spectrometer.

### Ornithine amino transferase activity

To determine the activity of δ-OAT, pyrroline 5-carboxylate (P5C) was measured for 30 minutes using the ninhydrin method. In a final volume of 1 mL, the reaction mixture contained 100 mM Tris-HCl (pH 8.0), 20 mM α-ketoglutarate, 50 mM L-ornithine, and the enzyme extract. The mixture was incubated for 30 min at 37°C. Using 0.2 mL of 2% (w/v) ninhydrin and 3 N perchloric acids the reaction was stopped. After incubating at 100°C for 5 min and centrifugation at 12,000g for 10 min, the precipitation was dissolved in 1.5 mL of ethanol. Now, the mixture was incubated at 100°C for 5 minutes. Following this, 10 minutes of centrifugation at 12,000g was carried out and the precipitate obtained was dissolved in 1.5 mL of ethanol. The clear supernatant was read at 510nm using UV-VIS spectrophotometer. One unit of δ-OAT activity was represented as the micromoles of P5C formed per mg of protein per hour.

### Δ-pyrroline-5-carboxylate dehydrogenase activity

A mixture of 50 mM Tris-HCl buffer (pH 7.0), 0.1 mM NAD<sup>+</sup>, and 0.3 mM P5C was used in the P5CDH reaction. An enzymatic extract of 0.2 mL was added to a final volume of 2.0 mL to start the reaction. An enzyme extract-free blank was prepared from the reaction mixture. A linear decrease in absorbance at 340 nm was observed after mixing for 5 minutes, and enzyme activity was measured after 2 minutes at 30°C. The molar extinction coefficient of NAD(P)H was used to quantify P5CDH activity and expressed as nmol NADH formed mg<sup>-1</sup> protein min<sup>-1</sup>.

### Proline dehydrogenase activity

ProDH enzyme extract was incubated at 28°C in a reaction buffer containing 100 mM Na<sub>2</sub>CO<sub>3</sub>-NaHCO<sub>3</sub> (pH 10.3), 20 mM L-proline, and 10 mM NAD<sup>+</sup> to determine its activity, and then ProDH dependent NAD<sup>+</sup> reduction was measured at 340 nm. The quantity of enzyme catalyzing the synthesis of 1 μmol of NADH per minute is defined as one unit of ProDH activity.

### Protein estimation

The protein content of the plants was determined according to Bradford (Bradford, 1976), using Bovine serum albumin (BSA) as a standard.

### Statistical analysis

All experiments were conducted in triplicates (n = 3), except for FM, BA, and RWC where 10 replicates were used. Using GraphPad Prism 8, two-way ANOVA was carried out and the results in the graphs were given as arithmetic mean ± standard error (SE). Tukey's post-hoc test was employed for identifying statistical differences at the 0.05 probability level.

## Results

### Growth and tolerance index of salt-stressed and Zn treated plants

Morphological parameters were measured after 22 days of sowing, and it was observed that the shoot length (SL) decreased significantly under salt stress in a dose-dependent manner. As can be seen from Figure 1A maximum decrease in SL was reported at 200mM NaCl (28.84%), while as a decrease of 7.43% in SL was observed at 150mM NaCl in comparison to control. However, the exogenous application of Zn was not only seen to alleviate the negative effects of salt on SL, but also increase the SL under normal conditions. In comparison to control the low doses of Zn (1 mg/L and 2mg/L) were seen to be more efficient in terms of salt stress alleviation by showing an increase in SL by 10.44% and 32.38% respectively. However, the higher doses of Zn (3, 4, 5 mg/L) were seen to be toxic as evidenced by a decrease in SL by 1.59%, 1.76%, and 18.4%, respectively. In salt-treated plants, the low doses of Zn rescued the negative impact as the SL increased by 7.26% and 25.5% in treatments 150 mM NaCl +1 mg/L Zn and 150 mM NaCl +2 mg/L Zn treated plants respectively in comparison to plants treated only with 150 mM NaCl. Similarly, the treatments 200 mM NaCl, + 1 mg/L Zn, 2mg/L were also reported to be effective in rescuing salt damage on SL (Figure 1A).

The root length (RL) also decreased at 200mM NaCl (28.66%), while as a decrease of 22.47% in RL was observed at 150mM NaCl in comparison to control (no salt/Zn treatment). However, the exogenous application of Zn alleviated the negative effects of salt on RL. We report an 8.79%, 32.24% and 24.1% increase in RL at 1 mg/L, 2mg/L and 3mg/L Zn respectively in comparison to control plants. The higher doses of Zn (4, 5 mg/L) were seen to be toxic as there was a decrease in RL at these concentrations by 6.1% and 1.6% respectively in comparison to control. In salt-treated plants, Zn rescued the negative impact of salt on RL, and we observed an increase of 21.84%, 39.07%, 10.5% and 5.88% in 150 mM NaCl+1 mg/L, 150 mM NaCl+2mg/L, 150 mM NaCl+3 mg/L and 150 mM NaCl+4 mg/L treated plants respectively in comparison to plants treated only with 150 mM NaCl. However, RL decreased by 5.4% in plants treated with 150 mM NaCl +4 mg/L treated plants as compared to 150 mM NaCl.

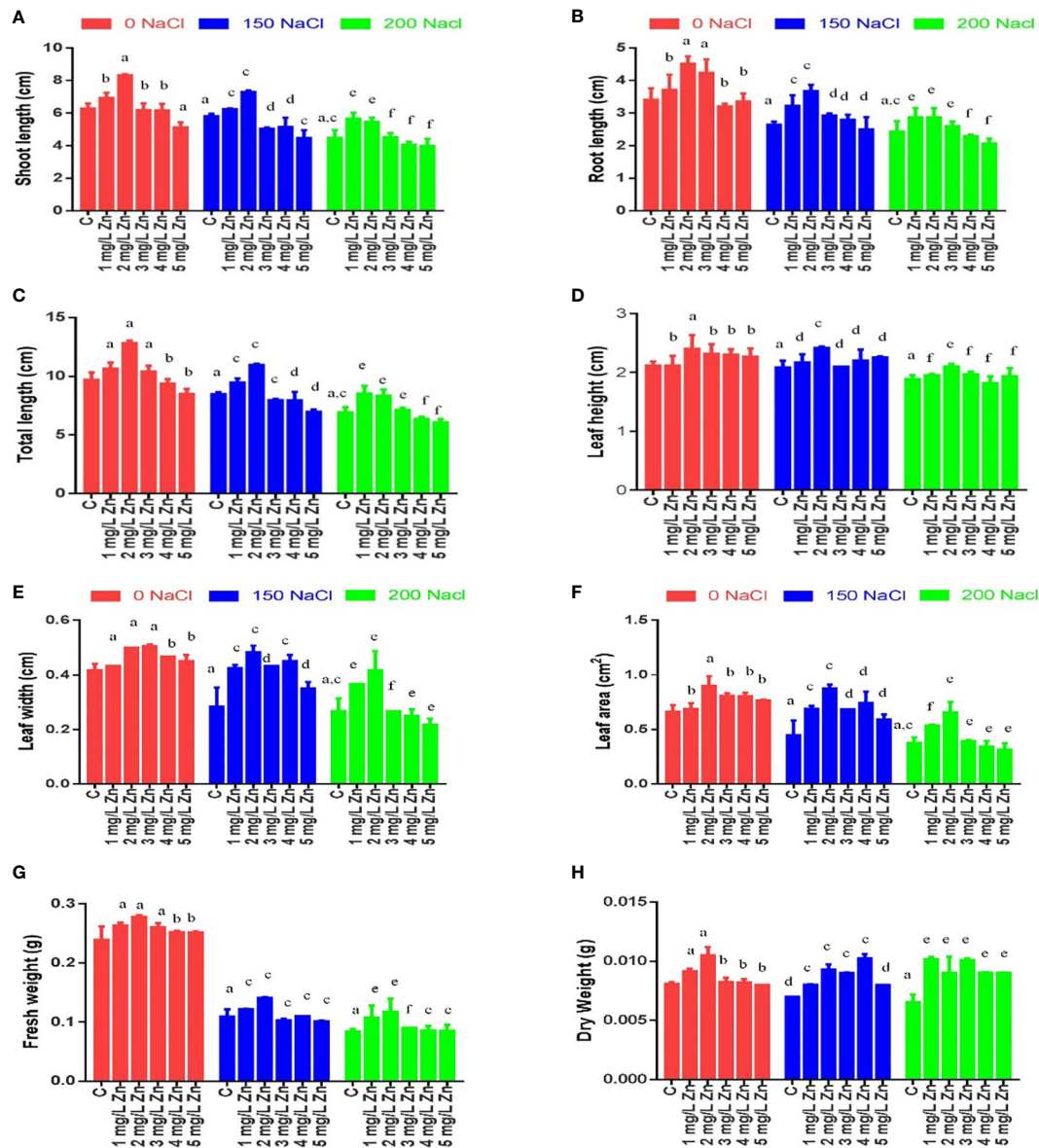


**FIGURE 1**  
Effects of NaCl and Zn on morphological parameters: (A) Shoot length (B) Root length (C) Total length (D) Leaf height (E) Leaf width (F) Leaf area (G) Fresh weight and (H) dry weight. The different letters on bars represent the significant differences (a, significant; b, non-significant compared to control; c, significant; d, non-significant compared to 150 mM NaCl and e, significant; f, non-significant compared to 200 mM NaCl at  $p \leq 0.05$ ).

Similarly, at 200 mM NaCl, a low dose (1 mg/L, 2 mg/L, and 3 mg/L) of Zn was found to be effective in rescuing salt damage. An increasing in RL by 17.8%, 17.8% and 6.84% at 1 mg/L, 2 mg/L, and 3 mg/L was observed however application of 4 mg/L and 5 mg/L Zn decreased RL when compared to plants treated with 200 mM salt (Figure 1B).

The total length (TL) in proso millet under salt stress decreased by 12.72% at 150 mM NaCl and by 28.78% at 200 mM NaCl. We report a 9.86%, 32.33% and 7.45% increase in TL at 1 mg/L, 2 mg/L and 3 mg/L Zn respectively in comparison to control plants. The higher doses of Zn (4, 5 mg/L) were seen to be toxic as there was a decrease in TL at these concentrations by 3.32% and 12.5% respectively in comparison to control. In salt-treated plants, Zn mitigated the negative impact of salt on TL, and we observed an increase of 11.82% and 29.7% in 150 mM NaCl+1 mg/L, 150 mM NaCl+ 2 mg/L treated plants respectively in comparison to plants treated only with 150 mM NaCl. However,

TL decreased by 5.9%, 6% and 17.6% in plants treated with 150 mM NaCl+3 mg/L, 150 mM NaCl+4 mg/L and 150 mM NaCl +5 mg/L respectively as compared to 150 mM NaCl. Similarly, at 200 mM NaCl, low doses (1 mg/L, 2 mg/L, and 3 mg/L) of Zn were found to be effective in rescuing salt damage. An increase in TL by 23.5%, 20.6% and 3.22% at 200 mM NaCl+1 mg/L, 200 mM NaCl+2 mg/L, and 200 mM NaCl +3 mg/L was observed however application of 200 mM NaCl+4 mg/L and 200 mM NaCl+5 mg/L Zn decreased TL when compared to plants treated with 200 mM NaCl (Figure 1C).

The leaf height (LH) in proso millet under salt stress decreased by 1.57% at 150 mM NaCl and by 11.02% at 200 mM NaCl. However, the application of 1 mg/L Zn does not affect LH. We found 13.39%, 9.45%, 8.66% and 7.09% increase in LH at 2 mg/L, 3 mg/L, 4 mg/L and 5 mg/L Zn respectively in comparison to control plants. In salt-treated plants, Zn mitigated the negative impact of salt on LH, and we

observed an increase of 4%, 16%, 0.8%, 5.6% and 8% in 150 mM NaCl +1 mg/L, 150 mM NaCl+2mg/L, 150 mM NaCl+3mg/L, 150 mM NaCl+4mg/L and 150 mM NaCl+5mg/L treated plants respectively in comparison to plants treated only with 150 mM NaCl. Similarly, at 200 mM NaCl, (1 mg/L, 2mg/L, and 3mg/L) of Zn were found to be effective in rescuing salt damage. An increasing in LH by 3.54%, 11.5% and 4.42% at 1 mg/L, 2mg/L, and 3mg/L when compared to plants treated with 200 mM NaCl (Figure 1D).

The leaf width (LW) in proso millet under salt stress decreased by 32% at 150mM NaCl and by 36% at 200mM NaCl. However, after the application Zn we found 4%, 20%, 12% and 12% and 8% increase in LW at 1mg/L, 2mg/L, 3mg/L, 4 mg/L and 5 mg/L Zn respectively in comparison to control plants. In salt-treated plants, Zn mitigated the negative impact of salt on LW, and we observed an increase of 50%, 70.5%, 52.9%, 58.8% and 23.58% in 150 mM NaCl+1 mg/L, 150 mM NaCl+2mg/L, 150 mM NaCl+3mg/L, 150 mM NaCl +4mg/L and 150 mM NaCl+ 5mg/L treated plants respectively in comparison to plants treated only with 150 mM NaCl. Similarly, at 200 mM NaCl, low levels of Zn (1 mg/L and 2mg/L) were found to be effective in rescuing salt damage. An increasing in LW by 37.5% and 56.25% was found at 1 mg/L and 2mg/L, whereas at 3mg/L no change in LW was observed when compared to plants treated with 200 mM NaCl. However, higher concentrations (4 mg/L and 5mg/L) of Zn showed a toxic effect and decreased LW (Figure 1E).

The leaf area (LA) in proso millet under salt stress decreased by 32.66% at 150mM NaCl and by 43.3% at 200mM NaCl. However, after the application of Zn we found 4%, 35.9%, 22% and 21% and 15.35% increase in LA at 1mg/L, 2mg/L, 3mg/L, 4 mg/L and 5 mg/L Zn respectively in comparison to control plants. In salt-treated plants, Zn mitigated the negative impact of salt on LA, and we observed an

increase of 54.76%, 96.44.5%, 53.08%, 66.91% and 32.52% in 150 mM NaCl+1 mg/L, 150 mM NaCl+2mg/L, 150 mM NaCl+3mg/L, 150 mM NaCl+4mg/L and 150 mM NaCl+5mg/L treated plants respectively in comparison to plants treated only with 150 mM NaCl. Similarly, at 200 mM NaCl, low levels of Zn (1 mg/L, 2mg/L and 3mg/L) were found to be effective in rescuing salt damage. An increase in LA by 42.8%, 74.47% and 4.77% was found at 200 mM NaCl+1 mg/L, 200 mM NaCl + 2mg/L and 200 mM NaCl +3mg/L when compared to plants treated with 200 mM NaCl. However, higher concentrations (4 mg/L and 5mg/L) of Zn showed a toxic effect by decreasing LA (Figure 1F).

Tolerance index (TI) improved in the plants treated with Zn in comparison to NaCl treatments only. The TI in shoots decreased by 4.91% at 150 mM NaCl and 19.12% at 200 mM NaCl concerning control. However, after the application of Zn we found 8.19% and 37.7% increase in TI at 1mg/L and 2mg/L, respectively in comparison to control plants. It was also seen that higher doses of Zn proved toxic as they decreased TI. In salt-treated plants, Zn mitigated the negative impact of NaCl, and we observed an increase of 8.04% and 24.7% in 150 mM NaCl +1 mg/L and 150 mM NaCl + 2mg/L respectively in comparison to plants treated only with 150 mM NaCl. The higher doses (150 mM NaCl+3mg/L, 150 mM NaCl+4mg/L and 150 mM NaCl+5mg/L) proved toxic as they decreased TI by 12%, 0.5% and 14.9% respectively in comparison to plants treated only with 150 mM NaCl. Similarly, at 200 mM NaCl, low levels of Zn (1 mg/L and 2mg/L) were found to be effective in rescuing salt damage. An increase in TI by 22.9% and 5.4% were found at 200 mM NaCl+1 mg/L and 200 mM NaCl+2mg/L when compared to plants treated with 200mM salt. However, higher concentrations of Zn showed toxic effect by decreasing TI (Table 1).

TABLE 1 Effect of Zn and collective effect of salt and Zn on root tolerance index (root TI %), shoot tolerance index (shoot TI %) and RWC of proso millet (PM).

| Parameter    | Treatments                |                            |                             |                             |                            |                           |                           |                            |                            |
|--------------|---------------------------|----------------------------|-----------------------------|-----------------------------|----------------------------|---------------------------|---------------------------|----------------------------|----------------------------|
|              | C                         | 1mg/L Zn                   | 2mg/L Zn                    | 3mg/L Zn                    | 4mg/L Zn                   | 5mg/L Zn                  | 150mM NaCl                | 150mM NaCl +1mg/L Zn       | 150mM NaCl +2mg/L Zn       |
| TI % (Root)  | 99.5 ± 0.7                | 103.9 ± 1.34 <sup>a</sup>  | 129.7 ± 0.98 <sup>a</sup>   | 135.63 ± 0.90 <sup>a</sup>  | 97.02 ± 0.041 <sup>a</sup> | 95.53 ± 0.8 <sup>a</sup>  | 74.05 ± 0.64 <sup>a</sup> | 104.94 ± 1.33 <sup>c</sup> | 111.87 ± 1.23 <sup>c</sup> |
| TI % (Shoot) | 100 ± 0                   | 107.59 ± 0.84 <sup>a</sup> | 136.85 ± 1.2 <sup>a</sup>   | 94.54 ± 0.76 <sup>a</sup>   | 99.5 ± 0.70 <sup>a</sup>   | 89.53 ± 0.7 <sup>a</sup>  | 94.54 ± 0.76 <sup>a</sup> | 101.86 ± 1.22 <sup>c</sup> | 118.03 ± 0.76 <sup>c</sup> |
| RWC (%)      | 96.4 ± 0.008              | 96.47 ± 0.097 <sup>a</sup> | 96.56364 ± 0.2 <sup>a</sup> | 96.63 ± 0.32 <sup>a</sup>   | 96.6 ± 0.28 <sup>a</sup>   | 96.6 ± 0.27 <sup>a</sup>  | 93 ± 0 <sup>a</sup>       | 93.16 ± 0.23 <sup>d</sup>  | 93.33 ± 0.46 <sup>c</sup>  |
| Parameter    | Treatments                |                            |                             |                             |                            |                           |                           |                            |                            |
|              | 150mM NaCl+3mg/L Zn       | 150mM NaCl +4mg/L Zn       | 150mM NaCl +5mg/L Zn        | 200mM NaCl                  | 200 mM NaCl +1mg/L Zn      | 200 mM NaCl+2mg/L Zn      | 200 mM NaCl+3 mg/L Zn     | 200 mM NaCl +4mg/L Zn      | 200 mM NaCl +5mg/L Zn      |
| TI % (Root)  | 83.90 ± 0.57 <sup>c</sup> | 86.13 ± 0.19 <sup>c</sup>  | 65.83 ± 1.17 <sup>c</sup>   | 62.37 ± 0.52 <sup>a,c</sup> | 93.55 ± 0.79 <sup>c</sup>  | 75.24 ± 0.34 <sup>c</sup> | 78.11 ± 0.44 <sup>c</sup> | 67.83 ± 1.15 <sup>c</sup>  | 55.44 ± 0.62 <sup>c</sup>  |
| TI % (Shoot) | 83.05 ± 0.78 <sup>c</sup> | 94.01 ± 0.73 <sup>c</sup>  | 80.43 ± 0.61 <sup>c</sup>   | 80.43 ± 0.61 <sup>a,c</sup> | 98.72 ± 1.02 <sup>c</sup>  | 85.12 ± 0.17 <sup>c</sup> | 74.97 ± 1.38 <sup>c</sup> | 69.19 ± 0.28 <sup>c</sup>  | 72.33 ± 0.47 <sup>c</sup>  |
| RWC (%)      | 92.04 ± 1.35 <sup>c</sup> | 91.95 ± 1.47 <sup>c</sup>  | 94.4 ± 3 <sup>c</sup>       | 91.3 ± 0.003 <sup>a</sup>   | 91.55 ± 0.35 <sup>f</sup>  | 91.890.83 <sup>c</sup>    | 90.11 ± 1.6 <sup>c</sup>  | 90.02 ± 1.8 <sup>c</sup>   | 89.88 ± 2.00 <sup>c</sup>  |

Values represent the % change with respect to control. The different letters on bars represent the significance.

The TI in roots also decreased by 25.49% at 150mM NaCl and 37.25% at 200mM NaCl with respect to control. However, after the application of Zn we found 4.9%, 30.3% and 36.27% increase in TI of root at 1mg/L, 2mg/L and 3mg/L Zn, respectively in comparison to control plants. However higher doses of Zn proved toxic as they decreased TI. In salt-treated plants, Zn mitigated the negative impact of NaCl, and we observed an increase of 42.1%, 51.3%, 13.15% and 15.78% in 150 mM NaCl+1 mg/L, 150 mM NaCl+2mg/L, 150 mM NaCl+3mg/L and 150 mM NaCl+4mg/L respectively in comparison to plants treated only with 150 mM NaCl. The higher doses (150 mM NaCl+5mg/L) proved toxic as they decreased TI by 10.52% respectively in comparison to plants treated only with 150 mM NaCl. An increasing in TI by 50%, 20.31%, 25% and 9.37 were found at 200 mM NaCl+1 mg/L, 200 mM NaCl+2mg/L, 200 mM NaCl +3mg/L and 200 mM NaCl+4mg/L when compared to plants treated with 200 mM NaCl. However, higher concentrations of Zn showed a toxic effect by decreasing TI (Table 1).

The fresh weight (FW) of proso millet decreased by 55.15% at 150mM NaCl and 65% at 200 mM NaCl with respect to control. However, after the application of Zn we found a 16.5%, 23.3% and 14.34% increase in FW at 1mg/L, 2mg/L and 3mg/L Zn, respectively in comparison to control plants. However higher doses of Zn (4mg/L and 5mg/L Zn) increased it by 12.1% each. In NaCl treated plants, Zn mitigated the negative impact of NaCl, and we observed an increase of 20% and 42% in 150 mM NaCl+1 mg/L and 2mg/L+150 mM NaCl treated plants respectively in comparison to plants treated only with 150 mM NaCl. An increasing in FW by 51.5%, 65.2% and 12.04% were found at 1 mg/L+200 mM NaCl, 2mg/L+200 mM NaCl and 3mg/L+200 mM NaCl treated plants in comparison to 200 mM NaCl. However higher doses prove toxic (Figure 1G).

A similar trend was observed in the case of dry weight (DW) of proso millet, as DW decreased by 12.5% at 150 mM NaCl and 12.5% at 200 mM NaCl with respect to control. However, after the application of Zn, we found a 12.5% increase in DW at 1mg/L and 2mg/L Zn, respectively in comparison to control plants. It was seen that higher doses of Zn did not affect DW. In salt-treated plants, Zn mitigated the negative impact of NaCl, and we observed that all doses applied, increased DW with a maximum increase of 42.85% in 4mg/L +150 mM NaCl treated plants in comparison to plants treated only with 150 mM NaCl. All the doses of Zn increased DW and maximum increasing of 42.8% was found in 1mg/L+200 mM NaCl to 3mg/L +200 mM NaCl treated plants in comparison to 200mM salt (Figure 1H).

RWC decreased noticeably as NaCl treatments increased. In proso millet, the decrease in RWC was 3.52–5.3% at 150–200 mM with respect to control. However, after the application Zn we found that all the doses increased RWC with a maximum increase of 0.48% at 3mg/L Zn with respect to control plants. In NaCl-treated plants, Zn mitigated the negative impact of salt, and we observed that increased RWC of 0.35% and 0.711% at 1mg/L+150 mM NaCl and 2mg/L+150 mM NaCl treated plants in comparison to plants treated only with 150 mM NaCl. Higher doses (3mg/L+150 mM NaCl, 4mg/L+150 mM NaCl, and 5mg/L+150 mM NaCl) showed toxic effect as they reduced RWC in comparison to plants treated only with 150 mM NaCl. An increase in RWC by 0.55% and 1.29% at 1 mg/L+200 mM NaCl and 2mg/L+200 mM NaCl was observed in comparison to plants treated with 200mM salt (Table 1).

## Effect on membrane stability index and electrolyte leakage

The MSI is an important feature that measures the influence of stress on cell membrane electrolyte conductivity. In general, a higher MSI indicates greater tolerance to salt stress. Figure 2D shows that with the increase in salt stress, MSI reduces considerably. The decrease in MSI from 61.5% to 65.04% at 150–200 mM NaCl was observed with respect to control. However, after the application Zn we found that MSI increased. The MSI after the application Zn were increased by 1.38% and 0.34% at 1mg/L and 2mg/L, Zn respectively in comparison to control plants. The higher doses of Zn (3mg/L, 4 mg/L and 5 mg/L) were toxic as they decreased MSI by 17.99%, 24.4% and 26.9% with respect to control plants. In salt treated plants, Zn mitigated the negative impact of salt as it increased MSI by 132.57%, 151.58%, 129.56%, 95.47% and 51.6% in 1 mg/L+150 mM NaCl, 2mg/L+150 mM NaCl, 3mg/L+150 mM NaCl, 4mg/L+150 mM NaCl and 5mg/L+150 mM NaCl treated plants respectively in comparison to plants treated only with 150 mM NaCl. Similarly, an increase in MSI by all the doses of Zn was found when compared to plants treated with 200mM salt. The maximum increase of 141.98% in MSI was at 2 mg/L +200NaCl.

EL is dependent on MSI and is inversely proportional to it, so an increase in salt stress increased the EL. The increase in EL from 271.94% to 287.29% at 150–200 mM NaCl was observed with respect to control. However, after the application Zn we found that EL decreased. The EL after the application of Zn were decreased by 6.1% and 1.51% at 1mg/L and 2mg/L, Zn respectively in comparison to control plants. The higher doses of Zn (3mg/L, 4 mg/L and 5 mg/L) were toxic as they increased EL by 79.4%, 107.84% and 118.97% with respect to control plants. In salt-treated plants, Zn mitigated the negative impact of salt as it decreased EL by 60.6%, 69.16%, 59.12%, 43.56% and 23.54% in 1 mg/L+150 mM NaCl, 2mg/L+150 mM NaCl, 3mg/L+150 mM NaCl, 4mg/L+150 mM NaCl and 5mg/L+150 mM NaCl treated plants respectively in comparison to plants treated only with 150 mM NaCl. Similarly, a decrease in EL by all the doses of Zn was found when compared to plants treated with 200mM salt. The maximum decrease of 56.6% in EL was at 2 mg/L +200 NaCl (Figure 2C).

## Biochemical effects of salinity and zinc on total chlorophyll, chlorophyll a and chlorophyll b

The total chlorophyll content (TCC), chlorophyll a (Chl a) and chlorophyll b (Chl b) concentrations were affected by Zn, NaCl and Zn with NaCl treatments (Figure 3). The levels of total chlorophyll, chlorophyll a, chlorophyll b in the proso millet leaves were significantly reduced with the rising salinity levels. The TCC decreased at 200 mM NaCl (27.56%), while, a decrease of 26.6% was observed at 150 mM NaCl in comparison to control (no salt/Zn treatment). However, the exogenous application of Zn alleviated the negative effects of salt. We report a 1.9%, 13.7% and 20.0% increase in TCC at 1 mg/L, 2mg/L and 4mg/L Zn respectively in comparison to control plants. The higher doses of Zn (5 mg/L) were seen to be toxic as there was a decrease in TCC by 20.06% in comparison to the



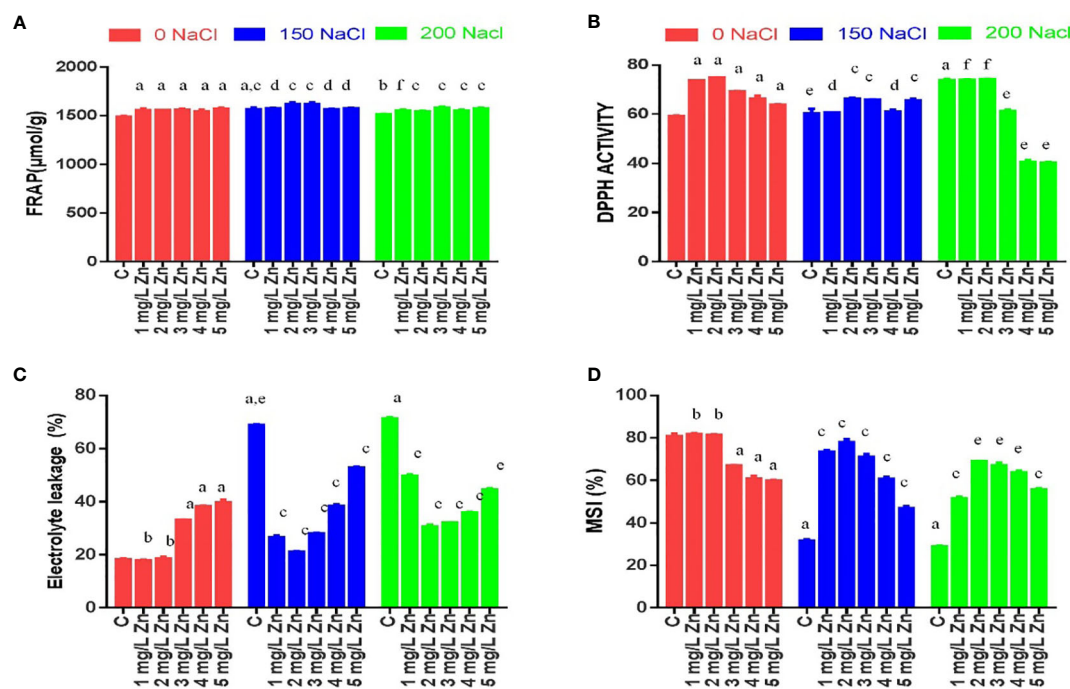


FIGURE 2

Effects of NaCl and Zn on membrane stability and antioxidant potential: (A) FRAP (B) DPPH (C) Electrolyte leakage (D) Membrane stability index. The different letters on bars represent the significant differences (a, significant; b, non-significant compared to control; c, significant; d, non-significant compared to 150 mM NaCl and e, significant; f, non-significant compared to 200 mM at  $p \leq 0.05$ ).

control. In NaCl-treated plants, Zn mitigated the negative impact of NaCl on TCC, and we observed an increase of TCC at all Zn concentrations with maximum increases of 91.93% at 4 mg/L+150 mM NaCl treated plants in comparison to plants treated only with 150 mM NaCl. Similarly, all the doses of Zn increased TCC at 200 mM NaCl and the maximum increase of 37.2% at 4 mg/L was observed in comparison to plants treated with 200 mM NaCl. The Chl a decreased at 150mM NaCl (10.4%) and 200mM NaCl (12.55%) and in comparison to control (no salt/Zn treatment). However, the exogenous application of Zn alleviated the negative effects of salt. We report a 13% and 99% increase in Chl a at 1 mg/L and 2 mg/L Zn respectively in comparison to control plants. The higher doses of Zn decreased Chl a in comparison to the control. In NaCl-treated plants, Zn mitigated the negative impact of NaCl on Chl a, and we observed an increase of Chl a at 1 mg/L, 2mg/L Zn, 3 mg/L and 5mg/L Zn concentrations with maximum increases of 114.85% at 150 mM NaCl +2 mg/L treated plants in comparison to plants treated only with 150 mM NaCl. Similarly, all the doses of Zn increased Chl a at 200mM level and the maximum increase of 35.5% at 2 mg/L was observed in comparison to plants treated with 200 mM NaCl. The Chl b decreased at 150mM NaCl (35.36%) and 200mM NaCl (34.9%) in comparison to control (no salt/Zn treatment). We report a 40.5% increase in Chl b at 4mg/L Zn respectively in comparison to control plants. In salt-treated plants, Zn mitigated the negative impact of salt on Chl b, and we observed an increase of Chl b at all the concentrations with maximum increases of 163.86% at 4 mg/L+150 mM NaCl treated plants in comparison to plants treated only with 150 mM NaCl. Similarly, all the doses of Zn increased Chl b at 200 mM level and the

maximum increase of 44.42% at 4 mg/L was observed in comparison to plants treated with 200 mM NaCl (Figure 3C).

## Effects of salinity and zinc on carotenoids, anthocyanin, total phenolic content, flavonoids and chlorophyll stability index

Like chlorophyll, carotenoid concentration was also reduced following salt treatments, with a drop of 9.5–21.19%. at 150–200 mM NaCl with reference to control. The supplementation of 3 mg/L and 4 mg/L Zn increased carotenoids by 60.75% and 1.33% respectively with reference to control. Furthermore, when Zn was administered with NaCl treatments, carotenoid concentration improved with a maximum increase of 136.10% at 4 mg/L Zn with reference to 150 mM NaCl and an increase of 72.50% at 4 mg/L Zn with reference to 200 mM NaCl treated plants (Figure 3H).

Anthocyanin content was also reduced following salt treatments, with a drop of 44.06–42.88% at 150–200 mM NaCl respectively with reference to control. However, the supplementation of Zn alone decreased anthocyanin content with reference to control. Moreover, when Zn was administered with NaCl treatments, anthocyanin concentration improved by 36.17% only at 4 mg/L Zn with reference to 150 mM NaCl and an increase of 52.06% at 5 mg/L Zn with reference to 200 mM NaCl treated plants (Figure 3G).

Total phenolic content (TPC) was also reduced following NaCl treatments, with a drop of 10.14–14.49% at 150–200 mM NaCl respectively with reference to control. However, the supplementation



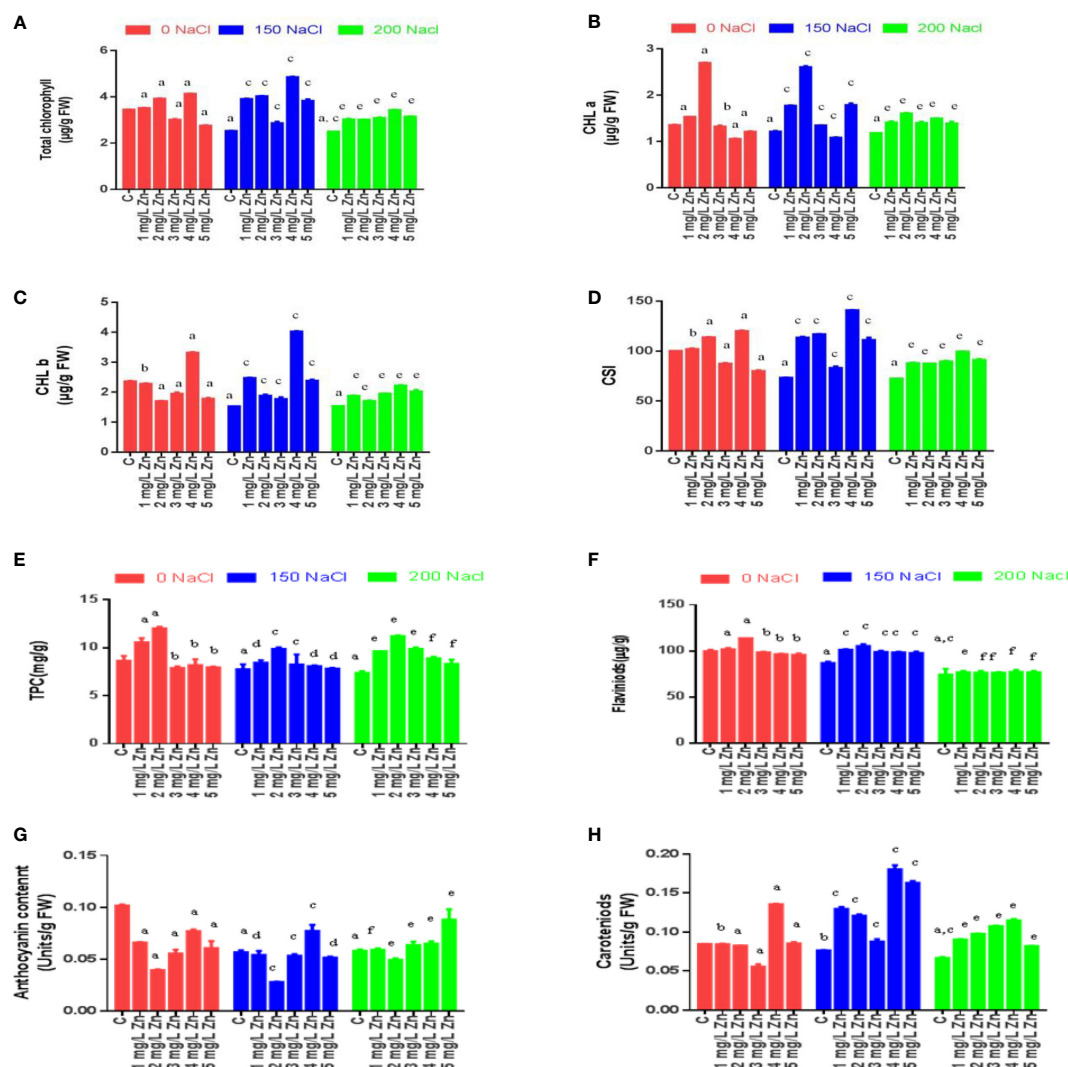


FIGURE 3

Effects of NaCl and Zn on photosynthetic pigments, chlorophyll stability index and total phenolic contents: (A) Total chlorophyll (B) Chlorophyll a (C) Chlorophyll b (D) Chlorophyll stability index (E) Total phenolic content (F) Flavonoids (G) Anthocyanin (H) Carotenoids. The different letters on bars represent the significant differences (a, significant; b, non-significant compared to control; c, significant; d = non-significant compared to 150 mM NaCl and e, significant; f, non-significant compared to 200 mM at  $p \leq 0.05$ ).

of Zn increased TPC content by 22.46% and 39.13% at 1 mg/L and 2 mg/L Zn with reference to control. However higher doses of Zn proved toxic and reduced TPC with reference to control. When Zn was administered with salt treatments, TPC improved at all concentrations and the maximum increase of 27.4% at 2 mg/L Zn with reference to 150 mM NaCl and of 51.6% at 2 mg/L Zn with reference to 200 mM NaCl treated plants (Figure 3E).

Flavonoid content (FC) also reduced following salt treatments, with a drop of 13.6–25.5% at 150–200 mM NaCl respectively with reference to control. However, the supplementation of Zn increased FC content by 2% and 14% at 1 mg/L and 2 mg/L Zn with reference to control. However higher doses of Zn proved toxic and reduced FC with reference to control. When Zn was administered with salt treatments, FC improved at all concentrations and the maximum increase of 21.26% at 2 mg/L Zn with reference to 150 mM NaCl and

4.02% at 4 mg/L Zn with reference to 200 mM NaCl treated plants (Figure 3F).

The chlorophyll stability index (CSI) is a cardinal aspect that determines the photosynthetic ability of a plant. Figure 3D that with the increase in salt CSI reduces considerably. The decrease in CSI from 26.6% to 27.56% at 150–200 mM NaCl was observed with respect to control. However, after the application Zn we found that CSI increased. The CSI after the application of Zn were increased by 2% and 13.7% at 1mg/L and 2mg/L Zn respectively in comparison to control plants. The higher doses of Zn (3mg/L, 4 mg/L and 5 mg/L) were toxic as they decreased CSI. In salt treated plants, Zn mitigated the negative impact of salt as it increased CSI by 54.6%, 59.24%, 13.22%, 92% and 11.06% in 1 mg/L+150 mM NaCl, 2mg/L+150 mM NaCl, 3mg/L+150 mM NaCl, 4mg/L+150 mM NaCl and 5mg/L+150 mM NaCl treated plants respectively in comparison to plants treated

only with 150 mM NaCl. Similarly, an increase in CSI by all the doses of Zn was found when compared to plants treated with 200 mM NaCl. The maximum increase of 37.2% in CSI was at 4 mg/L +200 NaCl.

## DPPH and FRAP activities in response to salinity and zinc

In response to salinity, the DPPH antioxidant capacity of leaf extracts, increased by 2.05% at 150mM NaCl and by 24.76% at 200 mM NaCl with reference to control plants. All the doses of Zn increased DPPH activity and the maximum increase of 26.5% was observed at 2 mg/L Zn with reference to control plants. However, when Zn was administered with salt treatments, it increased DPPH activity and a maximum increase of 9.65% at 2 mg/L Zn with reference to 150 mM NaCl. An increasing in DPPH activity by 0.62% was found at 2 mg/L+200 mM NaCl treated plants in comparison to 200 mM NaCl. However higher doses prove toxic (Figure 2B).

Similar results were observed for FRAP antioxidant capacity. FRAP activity increased by 5.4% at 150 mM NaCl and by 2.54% at 200 mM NaCl with reference to control plants. All the doses of Zn increased FRAP activity and the maximum increase of 6.12% was observed at 5 mg/L Zn with reference to control plants. However, when Zn was administered with salt treatments, it increased FRAP activity and a maximum increase of 3.43% at 2mg/L and 3mg/L Zn with reference to 150 mM NaCl. All the concentrations of Zn increased FRAP activity and the maximum increase of 4.21% was found at 3mg/L+200 mM NaCl treated plants in comparison to 200 mM NaCl (Figure 2A).

## Effects of salinity and zinc on proline and enzymes of proline pathway

The proline content (PC) in proso millet under salt stress increased by 71.65% at 150 mM NaCl and 141.73% at 200 mM NaCl. However, the supplementation of Zn further increased PC content by 1.18% and 5.54% at 1 mg/L and 2 mg/L Zn with reference to control. However higher doses of Zn proved toxic and reduced PC with reference to control. When Zn was administered with salt treatments, PC improved at all concentrations and the maximum increase of 66.65% at 2 mg/L Zn with reference to 150 mM NaCl and 27.5% at 2 mg/L Zn with reference to 200 mM NaCl treated plants (Figure 4A).

P5CS activity in proso millet under salt stress increased by 30% at 150 mM NaCl and increased by 66.6% at 200 mM NaCl. The application of Zn (1 mg/L and 2 mg/L) had a positive impact on the activity of P5CS as it increased by 4.66% and 26.96%, whereas the application of higher doses of Zn (3 mg/L, 4 mg/L and 5 mg/L) decreased it in comparison to control. In salt treated plants, a lower concentration of Zn further increased the activity of P5CS by 19.344% and 21% at 150 mM NaCl+1 mg/L and 2mg/L+150 mM NaCl treated plants respectively in comparison to plants treated only with 150 mM NaCl. However higher doses of Zn (3 mg/L, 4 mg/L and 5 mg/L) decreased it in comparison to 150 mM NaCl. An increase in P5CS activity by 0.64% and 3% were found at 1 mg/L+200 mM NaCl and

2mg/L+200 mM NaCl treated plants respectively in comparison to 200 mM NaCl. However higher doses prove toxic in comparison to 200 mM NaCl (Figure 4B).

Similar results were observed for P5CR activity. P5CR activity in under salt stress increased by 29.5% at 150 mM NaCl and 91.3% at 200 mM NaCl. However, the supplementation of Zn increased P5CR activity by 2.01%, 5.86 and 2.42% at 1 mg/L, 2 mg/L and 3 mg/L Zn respectively with reference to control. It was seen that higher doses of Zn proved toxic and reduced P5CR activity with reference to control. When Zn was administered with salt treatments, P5CR activity improved at lower concentrations (1 mg/L and 2 mg/L) and the maximum increase of 21.66% at 2 mg/L Zn with reference to 150 mM NaCl and 4% at 2 mg/L Zn with reference to 200 mM NaCl treated plants was observed. However higher doses of Zn proved toxic and reduced P5CR activity (Figure 4C).

The activity of OAT also increased under salt stress by 27.85% at 150mM NaCl and 32% at 200 mM NaCl. However, all the doses of Zn increased OAT activity and the maximum increase of 13.65% was observed at 1 mg/L Zn with reference to control. When Zn was administered with salt treatments, OAT activity improved at lower concentrations (1 mg/L and 2 mg/L) and the maximum increase of 21.84% at 2 mg/L Zn with reference to 150 mM NaCl and 11.73% at 1 mg/L Zn with reference to 200 mM NaCl treated plants was observed. However higher doses of Zn reduced OAT activity (Figure 4D).

The activity of PDH activity decreased under salt stress by 33.5% at 150 mM NaCl and 58.48% at 200 mM NaCl. However, all the doses of Zn decreased PDH activity and the maximum decrease of 70.38% was observed at 1 mg/L Zn with reference to control. When Zn was administered with salt treatments, PDH activity further decreased at all concentrations and the maximum decrease of 67.09% at 2 mg/L Zn with reference to 150 mM NaCl and 62.51% at 5 mg/L Zn with reference to 200 mM NaCl treated plants was observed. The activity of P5CDH activity decreased under salt stress by 52.65% at 150mM NaCl and 60.68% at 200mM NaCl. However, all the doses of Zn decreased P5CDH activity and the maximum decrease of 61% was observed at 2 mg/L Zn with reference to control. When Zn was applied with salt, it decreased the activity of P5CDH by 57.5% and 82.5% at 1 mg/L and 2 mg/L Zn respectively in comparison to 150 mM NaCl. The decrease in P5CDH activity by 33.7% and 56.7% at 1 mg/L and 2mg/L was observed, however application of 3 mg/L, 4 mg/L and 5 mg/L Zn increased P5CDH when compared to plants treated with 200 mM NaCl (Figures 4E, F).

## Discussion

Salt stress has negative consequences on plant growth and plants respond to this by accumulating wide range of metabolic products, principally, amino acids accumulate in plants, which are fundamental to plant developmental processes. There is an optimistic relationship between proline amassing and stress in plants which points towards its role in stress mitigation by osmotic adjustments. The present study aimed to study the role of Zn in stimulating proline metabolism and stress-responsive elements. To assess plant salt tolerance in proso millet, the morphological features were studied. The results of our study indicate that NaCl (150mM, 200mM NaCl) has a negative impact on growth and development in proso millet and the maximum damage

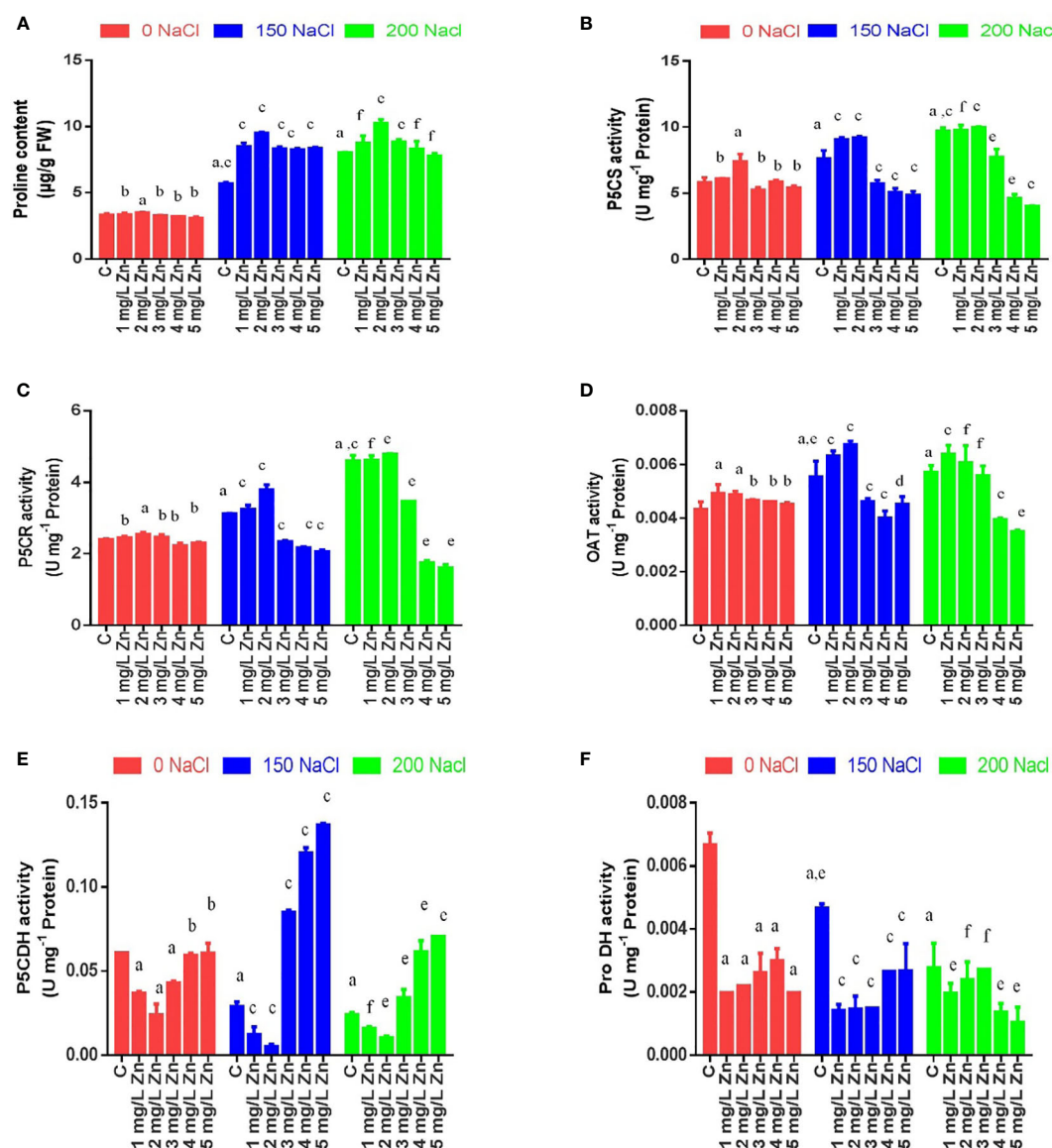


FIGURE 4

Effects of NaCl and Zn on total proline content and enzymes activities related to proline biosynthetic pathway: (A) Proline content (B) P5CS activity (C) P5CR activity (D) OAT activity (E) P5CDH activity (F) ProDH activity. The different letters on bars represent the significant differences (a, significant; b, non-significant compared to control; c, significant; d, non-significant compared to 150 mM NaCl and e, significant; f, non-significant compared to 200 mM at  $p \leq 0.05$ ).

was observed at higher salt levels. The results were in agreement with previous studies which indicated that salinity decreases growth, SL, RL, DW, FW, LW, and LA as observed in millets viz., *Pennisetum glaucum* L., *Eleusine coracana* L., *Setaria italica* L. and *Paspalum scrobiculatum* L. (Khushdil et al., 2019; Kothai and Roselin Roobavathi, 2020; Mukami et al., 2020; Rathinapriya et al., 2020; Mahmoud and Abdelhameed, 2021) and other plants *Lactuca sativa* L. *Tetragonia tetragonoides*, *Portulaca oleracea* L., *Oenanthe javanica* and *Tetragonia decumbens* (Hnilickova et al., 2019; Kumar et al., 2021; Sogoni et al., 2021). In the present study exogenous Zn was applied for mitigation of NaCl stress in *Panicum miliaceum* L. and it was observed that low doses of Zn have a beneficial effect on overall plant performances (morphological and biochemical features) which is in concurrence with earlier reports

wherein application of Zn mitigated salt stress in *Oryza sativa* L., *Vigna radiata* L., *Pistacia vera* L. *Ocimum basilicum* L. and *Pisum sativum* L. (Said-Al Ahl and Mahmoud, 2010; Tavallali et al., 2010; Nadeem et al., 2020; Al-Zahrani et al., 2021; Elshoky et al., 2021). Furthermore, there was a dose-dependent decrease in RWC and MSI due to salt stress and the addition of low doses of Zn significantly improved these parameters in stressed plants. In previous studies, Zn also improved RWC and MSI when applied to stress plants like *Solanum melongena* L., *Zea mays* L., *Oryza sativa* L. and *Abelmoschus esculentus* (Tufail et al., 2018; Nadeem et al., 2020; Ali et al., 2021; Raza et al., 2021; Semida et al., 2021b). An increase in growth and pigments by foliar application of Zn may be attributed to the crucial role of zinc on the biological and metabolism activity of

plants. Besides, salinity stress can also negatively affect the plants by reducing the amount of photosynthetic pigments (flavonoids, total phenolics, chlorophyll, carotenoid, and anthocyanin) which has been previously observed in many plants including citrus, rice, cucumber, melon, wheat (Dionisio-Sese and Tobita, 2000; López Climent et al., 2008) (Pour et al., 2017; Hawrylak et al., 2019) (Sairam and Srivastava, 2002). The decrease in pigments contents under salt stress may be due to membrane deterioration, changes in size and number of chloroplasts, damage and injury to grana and thylakoids. The decrease of these pigments may be caused by their deterioration due to the ROS generated during salt stress (Subramanyam et al., 2019). In our study, the applications of Zn improved the photosynthetic pigments which is in accordance with several studies on wheat, tomato, rice and maize (Mathpal et al., 2015; Liu et al., 2016; Faizan et al., 2021; Rai-Kalal and Jajoo, 2021). Furthermore, it is also evidenced in other studies that the foliar application of zinc proved positive by decreasing the injurious effect of salinity on pigments in okra plants, wheat, mungbean and rice (Tufail et al., 2018; Abou-Zeid et al., 2021; Al-Zahrani et al., 2021; Zafar et al., 2021). Similarly, Our findings revealed that applications of Zn improved the flavonoid, anthocyanin, total phenolic content. Similar results were reported in many plants like *Brassica juncea*, *Hordeum vulgare* and *Capsicum annuum* in which zinc improved these parameters. These pigments are essential for photosynthesis and protection of cells and the enhanced flavonoids content is directly related to better photosynthetic efficiency, superoxide radical scavenging and works as chelators in salt-stressed plants (Ahmad et al., 2017; García-López et al., 2018; Ali et al., 2022). The CSI is cardinal aspect that determines the photosynthetic ability of a plant and a higher CSI indicates greater tolerance to salt stress. In our study CSI decreased at 150–200 mM NaCl, as observed previously under various stresses in rice, mulberry and wheat (Mohan et al., 2000; Kumar et al., 2003; Babu et al., 2007; Abou-Zeid and Ismail, 2018). The application of Zn improved the CSI in accordance with previous studies on *Senna occidentalis*, *Solanum melongena* L. and *Triticum aestivum* L. (Farghali, 1997; Abou-Zeid and Ismail, 2018; Semida et al., 2021a). In response to salinity, the DPPH antioxidant capacity of leaf extracts, increased at 150mM NaCl and 200 mM NaCl with reference to control plants. Lower doses of Zn was found to further increased DPPH activity when given along with salt. Similar results were observed for FRAP antioxidant capacity as its activity also increased at 150mM NaCl and 200 mM NaCl with reference to control plants. Similarly, in many plants it was observed that salt increased both DPPH and FRAP activity in many plants like *Carthamus tinctorius* L., *Gossypium hirsutum* L., *Salsola baryosma*, *Trianthema triquetra*, *Zygophyllum simplex*, *Oryza sativa* L., *Nicotiana tubaccum* L., *Crocus sativus* L. and *Triticum aestivum* L. (Xie et al., 2008; Daiponmak et al., 2010; Sharma and Ramawat, 2014; Golkar and Taghizadeh, 2018) (Mazaheri-Tirani and Dayani, 2020; Rahaiee et al., 2020; Thakur et al., 2021). For osmoprotection, plants accumulate compatible solutes such as proline under salinity stress. Proline promotes osmotic regulation by balancing cellular structures, removing free radicals and protecting cellular redox potential. In reaction to stress, proline boosting usually take places in cytosol as it adds to the osmotic adjustment. A higher accumulation of proline in plants improves their drought and salinity resistance (Surekha et al., 2014). The reducing equivalent NADPH causes

reduction of glutamate to P5C, which is converted to proline. In this process NADP<sup>+</sup> is generated, which is employed as an electron acceptor, inhibiting singlet oxygen and ROS formation under stress circumstances. Furthermore, NADP<sup>+</sup> generated by proline biosynthesis may restore depleted NADP<sup>+</sup> pools caused by Calvin cycle suppression under stress (Szabados and Savouré, 2010). In our study, PC increased under salt stress at both 150mM and 200mM NaCl. The Zn supplementation at low concentrations further increased PC content with reference to control. When Zn was administered along with salt treatments, PC improved at all concentrations which is verified by similar results obtained in *Mangifera indica* L., *Triticale* and *Triticum aestivum* L. (Arough et al., 2016; Elsheery et al., 2020; Faizan et al., 2021). Increased proline results in neutralization of the detrimental effect of stress (Hossain et al., 2010; Sofy et al., 2020) which may be due to increased activity of proline biosynthetic genes (P5CS, P5CR and OAT) and decreased activity of catabolic enzymes (ProDH and P5CDH). The P5CS enzyme, one of two main enzymes involved in proline biosynthesis from glutamate precursors, has been shown to play an important role in proline accumulation. P5CS activity in proso millet under salt stress increased at 150mM and 200mM NaCl. These findings corroborate with observations in cactus pear, carrot, rape seed, sugarcane and mustard (Han and Hwang, 2003; Silva-Ortega et al., 2008; Guerzoni et al., 2014; Kubala et al., 2015; Chandra et al., 2018). The application of low doses of Zn (1 mg/L and 2 mg/L) had a positive impact on the activity of P5CS as it increased further in comparison to control which is in accordance with various studies (Qiao et al., 2015; Luo et al., 2019; Sadati et al., 2022). Similarly, P5CR activity increased under salt stress at 150mM and 200mM NaCl as reported earlier in green gram, lentil, rice and wheat under salt stress (Misra and Gupta, 2005; Nounjan et al., 2012; Tavakoli et al., 2016). However the supplementation of Zn at lower doses further increased the P5CR activity, but the higher doses of Zn proved toxic and reduced P5CR activity. Besides, when Zn was administered with salt treatments, P5CR activity improved at lower concentrations (1 mg/L and 2 mg/L) which are in agreement with studies on exogenous application of different mitigants (Misra and Gupta, 2005; Farhadi and Ghassemi-Golezani, 2020; Zhang et al., 2020). The activity of OAT also increased under salt stress at 150mM and 200mM NaCl, besides all the doses of Zn increased OAT activity as reported previously (Da Rocha et al., 2012; Gao et al., 2019). When Zn was administered with salt treatments, OAT activity improved at lower concentrations (1 mg/L and 2 mg/L) as observed in *Arabidopsis thaliana* plantlets which showed enhanced proline content, P5CS mRNA and OAT (Roosens et al., 1998). Over expression of *Arabidopsis*  $\delta$ OAT gene in tobacco and rice had amplified proline content and increased stress tolerance (Roosens et al., 2002). The role of P5CDH and ProDH in catalyzing the degradation of proline is well known and in our study as expected the activities of PDH and P5CDH decreased under salt stress at 150mM and 200mM NaCl. However, Zn also helped to decreased ProDH and P5CDH activities and with combined treatment of NaCl and Zn the enzyme activities decreased further. The decreased activities leads to reduced catabolism of proline and hence accumulation of proline under stressful conditions which is in accordance with studies on chinese cabbage, rice, sweet potato and cucumber (Lopez-Carrion et al., 2008; Liu et al., 2014; Benitez et al., 2016; Naliwajski and Skłodowska, 2021).



## Conclusions

Salt stress significantly limited growth resulting in lowering of shoot length, root length, leaf area, leaf width, lead to imbalances in photosynthetic parameters, chlorophyll, membrane stability and impacted biochemical parameters related to proline biosynthesis in proso millet. Based on current research, it is evident that Zn in lower doses is very effective which provided remedial effect to salt-stressed proso millet by improving osmotic substances, antioxidant activities, photosynthetic pigments and salt stress-responsive elements. Moreover, Zn also protected proso millet through the amelioration of proline biosynthesis. The activities of enzymes governing the synthesis of proline were increased whereas the activities of the enzyme responsible for the breakdown of proline were decreased. The results proved low doses of zinc were beneficial in alleviating salt stress in proso millet and an approach like this might boost the growth and yield of plants grown under saline conditions. However, there are still many questions to be answered regarding zinc's ability to alleviate the adverse effects of salt stress in plants. Thus deeper studies are required to answer the mechanistic role of Zn in plants and to understand the system/s governing salt stress tolerance by proline and its enzymes.

## Data availability statement

The original contributions presented in the study are included in the article/[Supplementary material](#). Further inquiries can be directed to the corresponding authors.

## Author contributions

Conceptualization: NM, KA, SS, IT, AB, RR and KH. Data curation: NM, SS, RR and KH. Formal analysis: NM, KA, SS, IT, AB, RR and KH. Funding acquisition: NM, SS, AB, RR and KH.

## References

- Abideen, Z., Waqif, H., Munir, N., El-Keblawy, A., Hasnain, M., Radicetti, E., et al. (2022). Algal-mediated nanoparticles, phycochar, and biofertilizers for mitigating abiotic stresses in plants: A review. *Agronomy* 12 (8), 1788. doi: 10.3390/agronomy12081788
- Abou-Zeid, H., and Ismail, G. (2018). The role of priming with biosynthesized silver nanoparticles in the response of *triticum aestivum* L to salt stress. *Egyptian J. Bot.* 58 (1), 73–85. doi: 10.21608/ejbo.2017.1873.1128
- Abou-Zeid, H. M., Ismail, G. S. M., and Abdel-Latif, S. A. (2021). Influence of seed priming with ZnO nanoparticles on the salt-induced damages in wheat (*Triticum aestivum* L.) plants. *J. Plant Nutr.* 44 (5), 629–643. doi: 10.1080/01904167.2020.1849288
- Afzal, M., and Mansoor, S. (2012). Effect of mobile phone radiations on morphological and biochemical parameters of mung bean (*Vigna radiata*) and wheat (*Triticum aestivum*) seedlings. *Asian J. Agric. Sci.* 4 (2), 149–152.
- Ahmad, P., Ahanger, M. A., Alyemeni, M. N., Wijaya, L., Egamberdieva, D., Bhardwaj, R., et al. (2017). Zinc application mitigates the adverse effects of NaCl stress on mustard [*Brassica juncea* (L.) czern & coss] through modulating compatible organic solutes, antioxidant enzymes, and flavonoid content. *J. Plant Interact.* 12 (1), 429–437. doi: 10.1080/17429145.2017.1385867
- Akhter, M. S., Noreen, S., Mahmood, S., Ashraf, M., Alsahli, A. A., and Ahmad, P. (2021). Influence of salinity stress on PSII in barley (*Hordeum vulgare* L.) genotypes, probed by chlorophyll-a fluorescence. *J. King Saud University-Sci.* 33 (1), 101239. doi: 10.1016/j.jksus.2020.101239
- Methodology: NM, KA, SS, IT, AB, RR and KH. Software: AB, RR and KH. Validation: NM, KA, RR and KH. Visualization: RR and KH. Writing – original draft: NM, KA, SS, IT, AB, RR and KH. Writing – review & editing: KA, AB, RR, BH and KH. All authors contributed to the article and approved the submitted version.
- Alamri, S. A., Siddiqui, M. H., Al-Khaishany, M. Y., Khan, M. N., Ali, H. M., and Alakeel, K. A. (2019). Nitric oxide-mediated cross-talk of proline and heat shock proteins induce thermotolerance in *Vicia faba* L. *Environ. Exp. Bot.* 161, 290–302. doi: 10.1016/j.envexpbot.2018.06.012
- Ali, M., Niaz, Y., Abbasi, G. H., Ahmad, S., Malik, Z., Kamran, M., et al. (2021). Exogenous zinc induced NaCl tolerance in okra (*Abelmoschus esculentus*) by ameliorating osmotic stress and oxidative metabolism. *Commun. Soil Sci. Plant Anal.* 52 (7), 743–755. doi: 10.1080/00103624.2020.1869761
- Ali, B., Saleem, M. H., Ali, S., Shahid, M., Sagir, M., Tahir, M. B., et al. (2022). Mitigation of salinity stress in barley genotypes with variable salt tolerance by application of zinc oxide nanoparticles. *Front. Plant Sci.* 13, 973782. doi: 10.3389/fpls.2022.973782
- Al-Zahrani, H. S., Alharby, H. F., Hakeem, K. R., and Rehman, R. U. (2021). Exogenous application of zinc to mitigate the salt stress in *vigna radiata* (L.) wilczek–evaluation of physiological and biochemical processes. *Plants* 10 (5)1005. doi: 10.3390/plants10051005
- Arif, Y., Singh, P., Siddiqui, H., Bajguz, A., and Hayat, S. (2020). Salinity induced physiological and biochemical changes in plants: An omic approach towards salt stress tolerance. *Plant Physiol. Biochem.* 156, 64–77. doi: 10.1016/j.plaphy.2020.08.042
- Arough, Y. K., SHARIFI, R. S., Sedghi, M., and Barmaki, M.J.N.B.H.A.C.-N. (2016). Effect of zinc and bio fertilizers on antioxidant enzymes activity, chlorophyll content, soluble sugars and proline in triticale under salinity condition. *sNotulae Botan. Horti Agrobotan. Cluj-Napoca* 44 (1), 116–124. doi: 10.15835/nbha44110224

## Acknowledgments

This research work was funded by Institutional Fund Projects under grant no (IFPRC-219-130-2020). Therefore, authors gratefully acknowledge technical and financial support from the Ministry of Education and King Abdulaziz University, Jeddah, Saudi Arabia.

## Conflict of interest

The authors declare that the research was conducted in the absence of any commercial or financial relationships that could be construed as a potential conflict of interest.

## Publisher's note

All claims expressed in this article are solely those of the authors and do not necessarily represent those of their affiliated organizations, or those of the publisher, the editors and the reviewers. Any product that may be evaluated in this article, or claim that may be made by its manufacturer, is not guaranteed or endorsed by the publisher.

## Supplementary material

The Supplementary Material for this article can be found online at: <https://www.frontiersin.org/articles/10.3389/fpls.2023.1053869/full#supplementary-material>



- Babu, S., Sheeba, A., Yogameenakshi, P., Anbumalaramathi, J., and Rangasamy, P. (2007). Effect of salt stress in the selection of salt tolerant hybrids in rice (*Oryza sativa* L.) under *in vitro* and *in vivo* condition. *Asian J. Plant Sci.* 6 (1), 137–142. doi: 10.3923/ajps.2007.137.142
- Benazzouk, S., Dobrev, P. I., Djazouli, Z.-E., Motyka, V., and Lutts, S. (2020). Positive impact of vermicompost leachate on salt stress resistance in tomato (*Solanum lycopersicum* L.) at the seedling stage: A phytohormonal approach. *Plant Soil* 446 (1), 145–162. doi: 10.1007/s11104-019-04361-x
- Benitez, L. C., Vighi, I. L., Auler, P. A., do Amaral, M. N., Moraes, G. P., dos Santos Rodrigues, G., et al. (2016). Correlation of proline content and gene expression involved in the metabolism of this amino acid under abiotic stress. *Acta Physiol. Plantarum* 38 (11), 1–12. doi: 10.1007/s11738-016-2291-7
- Bradford, M. M. (1976). A rapid and sensitive method for the quantitation of microgram quantities of protein utilizing the principle of protein-dye binding. *Anal. Biochem.* 72 (1-2), 248–254. doi: 10.1016/0003-2697(76)90527-3
- Chandra, D., Srivastava, R., Glick, B. R., and Sharma, A. K. (2018). Drought-tolerant pseudomonas spp. improve the growth performance of finger millet (*Eleusine coracana* (L.) gaertn.) under non-stressed and drought-stressed conditions. *Pedosphere* 28 (2), 227–240. doi: 10.1016/S1002-0160(18)60013-X
- Chrysargyris, A., Höfte, M., Tzortzakakis, N., Petropoulos, S. A., and Di Gioia, F. (2022). Micronutrients: The borderline between their beneficial role and toxicity in plants. *Front. Plant Sci.* 13. doi: 10.3389/fpls.2022.88974-621-7
- Daiponmak, W., Theerakulpisut, P., Thanonkao, P., Vanavichit, A., and Prathepha, P. (2010). Changes of anthocyanin cyanidin-3-glucoside content and antioxidant activity in Thai rice varieties under salinity stress. *Sci. Asia* 36, 286–291. doi: 10.2306/scienceasia1513-1874.2010.36.286
- Da Rocha, I. M. A., Vitorello, V. A., Silva, J. S., Ferreira-Silva, S. L., Viégas, R. A., Silva, E. N., et al. (2012). Exogenous ornithine is an effective precursor and the  $\delta$ -ornithine amino transferase pathway contributes to proline accumulation under high n recycling in salt-stressed cashew leaves. *J. Plant Physiol.* 169 (1), 41–49. doi: 10.1016/j.jplph.2011.08.001
- Das, K., and Roychoudhury, A. (2014). Reactive oxygen species (ROS) and response of antioxidants as ROS-scavengers during environmental stress in plants. *Front. Environ. Sci.* 2, 53. doi: 10.3389/fenvs.2014.00053
- Desoky, E., Ibrahim, S. A., and Merwad, A. (2019). Mitigation of salinity stress effects on growth, physio-chemical parameters and yield of snapbean (*Phaseolus vulgaris* L.) by exogenous application of glycine betaine. *Int. Lett. Natural Sci.* 76, 60–70. doi: 10.18052/www.scipress.com/ILNS.76.60
- Dikobe, T. B., Mashile, B., Sinthumule, R. R., and Ruzvidzo, O. (2021). Distinct morpho-physiological responses of maize to salinity stress. *Am. J. Plant Sci.* 12 (6), 946–959. doi: 10.4236/ajps.2021.126064
- Dimkpa, C. O., Singh, U., Bindraban, P. S., Elmer, W. H., Gardea-Torresdey, J. L., and White, J. C. (2019). Zinc oxide nanoparticles alleviate drought-induced alterations in sorghum performance, nutrient acquisition, and grain fortification. *Sci. Tot. Environ.* 688, 926–934. doi: 10.1016/j.scitotenv.2019.06.392
- Dionisio-Sese, M. L., and Tobita, S. (2000). Effects of salinity on sodium content and photosynthetic responses of rice seedlings differing in salt tolerance. *J. Plant Physiol.* 157 (1), 54–58. doi: 10.1016/S0176-1617(00)80135-2
- Diricks, M., De Bruyn, F., Van Daele, P., Walmagh, M., and Desmet, T. (2015). Identification of sucrose synthase in nonphotosynthetic bacteria and characterization of the recombinant enzymes. *Appl Microbiol Biotechnol.* 99, 8465–8474.
- Elsheery, N. I., Helaly, M. N., El-Hoseiny, H. M., and Alam-Eldein, S. M. (2020). Zinc oxide and silicone nanoparticles to improve the resistance mechanism and annual productivity of salt-stressed mango trees. *Agronomy* 10 (4), 558. doi: 10.3390/agronomy10040558
- Elschoky, H. A., Yotsova, E., Farghali, M. A., Farroh, K. Y., El-Sayed, K., Elzorkany, H. E., et al. (2021). Impact of foliar spray of zinc oxide nanoparticles on the photosynthesis of pism sativum L. under salt stress. *Plant Physiol. Biochem.* 167, 607–618. doi: 10.1016/j.plaphy.2021.08.039
- Faizan, M., Bhat, J. A., Chen, C., Alyemeni, M. N., Wijaya, L., Ahmad, P., et al. (2021). Zinc oxide nanoparticles (ZnO-NPs) induce salt tolerance by improving the antioxidant system and photosynthetic machinery in tomato. *Plant Physiol. Biochem.* 161, 122–130. doi: 10.1016/j.plaphy.2021.02.002
- Farghali, K. (1997). Diurnal variations of chlorophyll and dry matter contents of senna occidentalis in response to zinc and soil moisture. *Biol. plantarum* 40 (3), 419–424. doi: 10.1023/A:1001126316498
- Farhadi, N., and Ghassemi-Golezani, K. (2020). Physiological changes of mentha pulegium in response to exogenous salicylic acid under salinity. *Scientia Hort.* 267, 109325. doi: 10.1016/j.scienta.2020.109325
- Gao, W., Feng, Z., Bai, Q., He, J., and Wang, Y. (2019). Melatonin-mediated regulation of growth and antioxidant capacity in salt-tolerant naked oat under salt stress. *Int. J. Mol. Sci.* 20 (5), 1176. doi: 10.3390/ijms20051176
- García-López, J. I., Zavala-García, F., Olivares-Sáenz, E., Lira-Saldivar, R. H., Diaz Barriga-Castro, E., Ruiz-Torres, N. A., et al. (2018). Zinc oxide nanoparticles boosts phenolic compounds and antioxidant activity of *Capsicum annuum* L. during germination. *Agronomy* 8 (10), 215. doi: 10.3390/agronomy8100215
- Golkar, P., and Taghizadeh, M. (2018). *In vitro* evaluation of phenolic and osmolite compounds, ionic content, and antioxidant activity in safflower (*Carthamus tinctorius* L.) under salinity stress. *Plant Cell Tissue Organ Culture (PCTOC)* 134 (3), 357–368. doi: 10.1007/s11240-018-1427-4
- Guerzoni, J. T. S., Belintani, N. G., Moreira, R. M. P., Hoshino, A. A., Domingues, D. S., and Vieira, L. G. E. (2014). Stress-induced  $\Delta$ 1-pyrroline-5-carboxylate synthetase (P5CS) gene confers tolerance to salt stress in transgenic sugarcane. *Acta Physiol. Plantarum* 36 (9), 2309–2319. doi: 10.1007/s11738-014-1579-8
- Gupta, N., Ram, H., and Kumar, B. (2016). Mechanism of zinc absorption in plants: Uptake, transport, translocation and accumulation. *Rev. Environ. Sci. Bio/Technol.* 15 (1), 89–109. doi: 10.1007/s11157-016-9390-1
- Han, K.-H., and Hwang, C.-H. (2003). Salt tolerance enhanced by transformation of a P5CS gene in carrot. *J. Plant Biotechnol.* 5 (3), 157–161.
- Hassanein, Y. Z., Abdel-Rahman, S., Soliman, W. S., and Salaheldin, S. (2021). Growth, yield, and quality of roselle (*Hibiscus sabdariffa* L.) plants as affected by nano zinc and bio-stimulant treatments. *Horticult. Environ. Biotechnol.* 62 (6), 879–890. doi: 10.1007/s13580-021-00371-w
- Hawrylak, B., Rubinowska, K., Molas, J., Woch, W., Matraszek-Gawron, R., and Szczurowska, A. (2019). Selenium-induced improvements in the ornamental value and salt stress resistance of plectranthus scutellarioides (L.) r. br. *Horticulturae* 31 (1), 213–221. doi: 10.2478/hort-2019-0016
- Hayat, S., Hayat, Q., Alyemeni, M. N., Wani, A. S., Pichtel, J., Ahmad, A., et al. (2012). Role of proline under changing environments: A review. *Plant Signaling Behav.* 7 (11), 1456–1466. doi: 10.4161/psb.21949
- Hmida-Sayari, A., Gargouri-Bouzd, R., Bidani, A., Jaoua, L., Savouré, A., and Jaoua, S. (2005). Overexpression of  $\Delta$ 1-pyrroline-5-carboxylate synthetase increases proline production and confers salt tolerance in transgenic potato plants. *Plant Sci.* 169 (4), 746–752. doi: 10.1016/j.plantsci.2005.05.025
- Hnilickova, H., Hnilická, F., Orsák, M., and Hejnák, V. (2019). Effect of salt stress on growth, electrolyte leakage,  $na^+$  and  $k^+$  content in selected plant species. *Plant Soil Environ.* 65 (2), 90–96. doi: 10.17221/620/2018-PSE
- Hossain, M. A., Hasanuzzaman, M., and Fujita, M. (2010). Up-regulation of antioxidant and glyoxalase systems by exogenous glycinebetaine and proline in mung bean confer tolerance to cadmium stress. *Physiol. Mol. Biol. Plants* 16 (3), 259–272. doi: 10.1007/s12298-010-0028-4
- Hou, K., Bao, D., and Shan, C. (2018). Cerium improves the vase life of liliun longiflorum cut flowers through ascorbate-glutathione cycle and osmoregulation in the petals. *Scientia Hort.* 227, 142–145. doi: 10.1016/j.scienta.2017.09.040
- Iqbal, Z., Sarkhosh, A., Balal, R. M., Gómez, C., Zubair, M., Ilyas, N., et al. (2021). Silicon alleviate hypoxia stress by improving enzymatic and non-enzymatic antioxidants and regulating nutrient uptake in muscadine grape (*Muscadinia rotundifolia* michx.). *Front. Plant Sci.* 11, 618873. doi: 10.3389/fpls.2020.618873
- Kapoor, D., Singh, S., Kumar, V., Romero, R., Prasad, R., and Singh, J. (2019). Antioxidant enzymes regulation in plants in reference to reactive oxygen species (ROS) and reactive nitrogen species (RNS). *Plant Gene* 19, 100182. doi: 10.1016/j.plgene.2019.100182
- Kaur, S., Kaur, N., Siddique, K. H., and Nayyar, H. (2016). Beneficial elements for agricultural crops and their functional relevance in defence against stresses. *Arch. Agron. Soil Sci.* 62 (7), 905–920. doi: 10.1080/03650340.2015.1101070
- Kausar, A., Ashraf, M. Y., Ali, I., Niaz, M., and Abbass, Q. (2012). Evaluation of sorghum varieties/lines for salt tolerance using physiological indices as screening tool. *Pakistan Joournal Bot.* 44 (1), 47–52.
- Khalid, H., Muhammad, A., and Muhammad, Y. A. (2008). Relationship between growth and ion relation in pearl millet (*Pennisetum glaucum* (L.) r. br.) at different growth stages under salt stress. *Afr. J. Plant Sci.* 2 (3), 023–027.
- Khan, M. I. R., Ashfaq, F., Chhillar, H., Irfan, M., and Khan, N. A. (2021). The intricacy of silicon, plant growth regulators and other signaling molecules for abiotic stress tolerance: An entrancing crosstalk between stress alleviators. *Plant Physiol. Biochem.* 162, 36–47. doi: 10.1016/j.plaphy.2021.02.024
- Khan, A., Khan, A. A., Khan, M. J., Ijaz, M., and Hassan, S. S. (2022). Combined effect of organic amendments and seed placement techniques on sorghum yield under salt-stressed conditions. *J. Soil Sci. Plant Nutr.* 22, 4752–4767. doi: 10.1007/s42729-022-00957-y
- Khushdil, F., Jan, F. G., Jan, G., Hamayun, M., Iqbal, A., Hussain, A., et al. (2019). Salt stress alleviation in pennisetum glaucum through secondary metabolites modulation by *aspergillus terreus*. *Plant Physiol. Biochem.* 144, 127–134. doi: 10.1016/j.plaphy.2019.09.038
- Koenigshofer, H., and Loeppert, H.-G. (2019). The up-regulation of proline synthesis in the meristematic tissues of wheat seedlings upon short-term exposure to osmotic stress. *J. Plant Physiol.* 237, 21–29. doi: 10.1016/j.jplph.2019.03.010
- Kothai, N., and Roselin Roobavathi, M. (2020). Evaluation of salinity stress effects on seed germination and seedling growth and estimation of protein contents in kodo millet (*Paspalum scrobiculatum* L.). *J. Stress Physiol. Biochem.* 16 (4), 70–81.
- Kubala, S., Wojtyła, L., Quinet, M., Lechowska, K., Lutts, S., and Garnczarska, M. (2015). Enhanced expression of the proline synthesis gene P5CSA in relation to seed osmopriming improvement of brassica napus germination under salinity stress. *J. Plant Physiol.* 183, 1–12. doi: 10.1016/j.jplph.2015.04.009
- Kumar, S., Li, G., Yang, J., Huang, X., Ji, Q., Liu, Z., et al. (2021). Effect of salt stress on growth, physiological parameters, and ionic concentration of water dropwort (*Oenanthe javanica*) cultivars. *Front. Plant Sci.* 12, 660409. doi: 10.3389/fpls.2021.660409
- Kumar, S. G., Reddy, A. M., and Sudhakar, C. (2003). NaCl Effects on proline metabolism in two high yielding genotypes of mulberry (*Morus alba* L.) with contrasting salt tolerance. *Plant Sci.* 165 (6), 1245–1251. doi: 10.1016/S0168-9452(03)00332-7

- Kumari, V. V., Banerjee, P., Verma, V. C., Sukumaran, S., Chandran, M. A. S., Gopinath, K. A., et al. (2022). Plant nutrition: An effective way to alleviate abiotic stress in agricultural crops. *Int. J. Mol. Sci.* 23 (15), 8519. doi: 10.3390/ijms23158519
- Ladeiro, B. (2012). Saline agriculture in the 21st century: Using salt contaminated resources to cope food requirements. *J. Bot.* 2012, 1–7. doi: 10.1155/2012/310705
- Lichtenthaler, H. K. (1987). “Chlorophylls and carotenoids: Pigments of photosynthetic biomembranes,” in *Methods in enzymology*, vol. 148. (Academic Press), 350–382.
- Liu, H., Gan, W., Rengel, Z., and Zhao, P. (2016). Effects of zinc fertilizer rate and application method on photosynthetic characteristics and grain yield of summer maize. *J. Soil Sci. Plant Nutr.* 16 (2), 550–562. doi: 10.4067/S0718-95162016005000045
- Liu, D., He, S., Zhai, H., Wang, L., Zhao, Y., Wang, B., et al. (2014). Overexpression of IbP5CR enhances salt tolerance in transgenic sweetpotato. *Plant Cell Tissue Organ Culture (PCTOC)* 117 (1), 1–16. doi: 10.1007/s12400-013-0415-y
- Lombard, V., Golaconda Ramulu, H., Drula, E., Coutinho, P. M., and Henrissat, B. (2014). The carbohydrate-active enzymes database (CAZy) in 2013. *Nucleic Acids Res* 42 (D1), D490–D495.
- Lopez-Carrion, A., Castellano, R., Rosales, M., Ruiz, J., and Romero, L. (2008). Role of nitric oxide under saline stress: Implications on proline metabolism. *Biol. Plantarum* 52 (3), 587–591. doi: 10.1007/s10535-008-0117-1
- López Climent, M. F., Arbona, V., Pérez-Clemente, R. M., and Gómez-Cadenas, A. (2008). Relationship between salt tolerance and photosynthetic machinery performance in citrus. *Environ. Exp. Bot.* 62 (2), 176–184. doi: 10.1016/j.envexpbot.2007.08.002
- Luo, H., Du, B., He, L., He, J., Hu, L., Pan, S., et al. (2019). Exogenous application of zinc (Zn) at the heading stage regulates 2-acetyl-1-pyrroline (2-AP) biosynthesis in different fragrant rice genotypes. *Sci. Rep.* 9 (1), 1–10. doi: 10.1038/s41598-019-56159-7
- Mahmoud, N. E., and Abdelhameed, R. M. (2021). Superiority of modified graphene oxide for enhancing the growth, yield, and antioxidant potential of pearl millet (*Pennisetum glaucum* L.) under salt stress. *Plant Stress* 2, 100025. doi: 10.1016/j.stress.2021.100025
- Malik, N., Chamon, A., Mondol, M., Elahi, S., and Faiz, S. (2011). Effects of different levels of zinc on growth and yield of red amaranth (*Amaranthus* sp.) and rice (*Oryza sativa*, variety-BR49). *J. Bangladesh Assoc. Young Res.* 1 (1), 79–91. doi: 10.3329/jbayr.v1i1.6836
- Marcec, M. J., and Tanaka, K. (2021). Crosstalk between calcium and ROS signaling during flg22-triggered immune response in arabidopsis leaves. *Plants* 11 (1), 14. doi: 10.3390/plants11010014
- Mathpal, B., Srivastava, P. C., Shankhdhar, D., and Shankhdhar, S. C. (2015). Improving key enzyme activities and quality of rice under various methods of zinc application. *Physiol. Mol. Biol. Plants* 21 (4), 567–572. doi: 10.1007/s12298-015-0321-3
- Mazaheri-Tirani, M., and Dayani, S. (2020). *In vitro* effect of zinc oxide nanoparticles on nicotiana tabacum callus compared to ZnO micro particles and zinc sulfate (ZnSO<sub>4</sub>). *Plant Cell Tissue Organ Culture (PCTOC)* 140 (2), 279–289. doi: 10.1007/s11240-019-01725-0
- Meena, M., Divyanshu, K., Kumar, S., Swapnil, P., Zehra, A., Shukla, V., et al. (2019). Regulation of l-proline biosynthesis, signal transduction, transport, accumulation and its vital role in plants during variable environmental conditions. *Heliyon* 5 (12), e02952. doi: 10.1016/j.heliyon.2019.e02952
- Misra, N., and Gupta, A. K. (2005). Effect of salt stress on proline metabolism in two high yielding genotypes of green gram. *Plant Sci.* 169 (2), 331–339. doi: 10.1016/j.plantsci.2005.02.013
- Mittler, R. (2017). ROS are good. *Trends Plant Sci.* 22 (1), 11–19. doi: 10.1016/j.tplants.2016.08.002
- Mohan, M., Narayanan, S. L., and Ibrahim, S. (2000). Chlorophyll stability index (CSI): Its impact on salt tolerance in rice. *Int. Rice Res. Notes* 25 (2), 38–39.
- Mondal, S., and Bose, B. (2019). Impact of micronutrient seed priming on germination, growth, development, nutritional status and yield aspects of plants. *J. Plant Nutr.* 42 (19), 2577–2599. doi: 10.1080/01904167.2019.1655032
- Mukami, A., Ng'etich, A., Syombua, E., Oduor, R., and Mbinda, W. (2020). Varietal differences in physiological and biochemical responses to salinity stress in six finger millet plants. *Physiol. Mol. Biol. Plants* 26 (8), 1569–1582. doi: 10.1007/s12298-020-00853-8
- Mushtaq, N. U., Saleem, S., Rasool, A., Shah, W. H., Hakeem, K. R., and Rehman, R. U. (2021). Salt stress threshold in millets: Perspective on cultivation on marginal lands for biomass. *Phyton* 90 (1), 51. doi: 10.32604/phyton.2020.012163
- Nadeem, F., Azhar, M., Anwar-ul-Haq, M., Sabir, M., Samreen, T., Tufail, A., et al. (2020). Comparative response of two rice (*Oryza sativa* L.) cultivars to applied zinc and manganese for mitigation of salt stress. *J. Soil Sci. Plant Nutr.* 20 (4), 2059–2072. doi: 10.1007/s42729-020-00275-1
- Naliwajski, M., and Skłodowska, M. (2021). The relationship between the antioxidant system and proline metabolism in the leaves of cucumber plants acclimated to salt stress. *Cells* 10 (3), 609. doi: 10.3390/cells10030609
- Noreen, S., Sultan, M., Akhter, M. S., Shah, K. H., Ummara, U., Manzoor, H., et al. (2021). Foliar fertigation of ascorbic acid and zinc improves growth, antioxidant enzyme activity and harvest index in barley (*Hordeum vulgare* L.) grown under salt stress. *Plant Physiol. Biochem.* 158, 244–254. doi: 10.1016/j.plaphy.2020.11.007
- Nounjan, N., Nghia, P. T., and Theerakulpisut, P. (2012). Exogenous proline and trehalose promote recovery of rice seedlings from salt-stress and differentially modulate antioxidant enzymes and expression of related genes. *J. Plant Physiol.* 169 (6), 596–604. doi: 10.1016/j.jplph.2012.01.004
- Olsen, L. I., and Palmgren, M. G. (2014). Many rivers to cross: The journey of zinc from soil to seed. *Front. Plant Sci.* 5, 30. doi: 10.3389/fpls.2014.00030
- Parida, A. K., Dagaonkar, V. S., Phalak, M. S., and Aurangabadkar, L. P. (2008). Differential responses of the enzymes involved in proline biosynthesis and degradation in drought tolerant and sensitive cotton genotypes during drought stress and recovery. *Acta Physiol. Plantarum* 30 (5), 619–627. doi: 10.1007/s11738-008-0157-3
- Pour, A., Ahmadi, J., Mehrabi, A. A., Etminan, A., Moghaddam, M., and Siddique, K. H. (2017). Physiological responses to drought stress in wild relatives of wheat: Implications for wheat improvement. *Acta Physiol. Plantarum* 39 (4), 1–16. doi: 10.1007/s11738-017-2403-z
- Qiao, X., Wang, P., Shi, G., and Yang, H. (2015). Zinc conferred cadmium tolerance in lemma minor I. via modulating polyamines and proline metabolism. *Plant Growth Regul.* 77 (1), 1–9. doi: 10.1007/s10725-015-0027-0
- Rahaiee, S., Ranjbar, M., Azizi, H., Govahi, M., and Zare, M. (2020). Green synthesis, characterization, and biological activities of saffron leaf extract-mediated zinc oxide nanoparticles: A sustainable approach to reuse an agricultural waste. *Appl. Organomet. Chem.* 34 (8), e5705. doi: 10.1002/aoc.5705
- Rahman, A., Nahar, K., Hasanuzzaman, M., and Fujita, M. (2016). Calcium supplementation improves Na<sup>+</sup>/K<sup>+</sup> ratio, antioxidant defense and glyoxalase systems in salt-stressed rice seedlings. *Front. Plant Sci.* 7, 609. doi: 10.3389/fpls.2016.00609
- Rai-Kalal, P., and Jajoo, A. (2021). Priming with zinc oxide nanoparticles improve germination and photosynthetic performance in wheat. *Plant Physiol. Biochem.* 160, 341–351. doi: 10.1016/j.plaphy.2021.01.032
- Rajurkar, N. S., and Hande, S. (2011). Estimation of phytochemical content and antioxidant activity of some selected traditional Indian medicinal plants. *Indian J. Pharm. Sci.* 73 (2), 146. doi: 10.4103/0250-474X.91574
- Rathinapriya, P., Pandian, S., Rakkammal, K., Balasangeetha, M., Alexpandi, R., Satish, L., et al. (2020). The protective effects of polyamines on salinity stress tolerance in foxtail millet (*Setaria italica* L.), an important C4 model crop. *Physiol. Mol. Biol. Plants* 26 (9), 1815–1829. doi: 10.1007/s12298-020-00869-0
- Raza, H. M. A., Bashir, M. A., Rehman, A., Jan, M., Raza, Q.-U.-A., and Berlyn, G. P. (2021). Potassium and zinc co-fertilization provide new insights to improve maize (*Zea mays* L.) physiology and productivity. *Pakistan J. Bot.* 53 (6), 2059–2065. doi: 10.30848/PJB2021-6(28)
- Roosens, N. H., Bitar, F. A., Loenders, K., Angenon, G., and Jacobs, M. (2002). Overexpression of ornithine-δ-aminotransferase increases proline biosynthesis and confers osmotolerance in transgenic plants. *Mol. Breed.* 9 (2), 73–80. doi: 10.1023/A:1026791932238
- Roosens, N. H., Thu, T. T., Iskandar, H. M., and Jacobs, M. (1998). Isolation of the ornithine-δ-aminotransferase cDNA and effect of salt stress on its expression in arabidopsis thaliana. *Plant Physiol.* 117 (1), 263–271. doi: 10.1104/pp.117.1.263
- Sabagh, E. L., Islam, M. S., Skalicky, M., Ali Raza, M., Singh, K., Anwar Hossain, M., et al. (2021). Salinity stress in wheat (*Triticum aestivum* L.) in the changing climate: Adaptation and management strategies. *Front. Agron.* 3, 661932. doi: 10.3389/fagro.2021.661932
- Sadati, S. Y. R., Godehkahriz, S. J., Ebadi, A., and Sedghi, M. (2022). Zinc oxide nanoparticles enhance drought tolerance in wheat via physio-biochemical changes and stress genes expression. *Iranian J. Biotechnol.* 20 (1), e3027. doi: 10.30498/ijb.2021.280711.3027
- Said-Al Ahl, H., and Mahmoud, A. A. (2010). Effect of zinc and/or iron foliar application on growth and essential oil of sweet basil (*Ocimum basilicum* L.) under salt stress. *Ocean J. Appl. Sci.* 3 (1), 97–111.
- Sairam, R., Deshmukh, P., and Shukla, D. (1997). Tolerance of drought and temperature stress in relation to increased antioxidant enzyme activity in wheat. *J. Agron. Crop Sci.* 178 (3), 171–178. doi: 10.1111/j.1439-037X.1997.tb00486.x
- Sairam, R., and Srivastava, G. (2002). Changes in antioxidant activity in sub-cellular fractions of tolerant and susceptible wheat genotypes in response to long term salt stress. *Plant Sci.* 162 (6), 897–904. doi: 10.1016/S0168-9452(02)00037-7
- Saleem, S., Mushtaq, N. U., Shah, W. H., Rasool, A., Hakeem, K. R., and Rehman, R. U. (2021). Morpho-physiological, biochemical and molecular adaptation of millets to abiotic stresses: A review. *Phyton* 90 (5), 1363. doi: 10.32604/phyton.2021.014826
- Semida, W. M., Abdelkhalik, A., Mohamed, G. F., Abd El-Mageed, T. A., Abd El-Mageed, S. A., Rady, M. M., et al. (2021a). Foliar application of zinc oxide nanoparticles promotes drought stress tolerance in eggplant (*Solanum melongena* L.). *Plants* 10 (2), 421.
- Semida, W. M., Abdelkhalik, A., Mohamed, G. F., Abd El-Mageed, T. A., Abd El-Mageed, S. A., Rady, M. M., et al. (2021b). Foliar application of zinc oxide nanoparticles promotes drought stress tolerance in eggplant (*Solanum melongena* L.). *Plants* 10 (2), 421. doi: 10.3390/plants10020421
- Sethi, S., Joshi, A., Arora, B., Bhowmik, A., Sharma, R., and Kumar, P. (2020). Significance of FRAP, DPPH, and CUPRAC assays for antioxidant activity determination in apple fruit extracts. *Eur. Food Res. Technol.* 246 (3), 591–598. doi: 10.1007/s00217-020-03432-z
- Shah, A. A., Ahmed, S., Malik, A., Naheed, K., Hussain, S., Yasin, N. A., et al. (2022). Potassium silicate and zinc oxide nanoparticles modulate antioxidant system, membranous h<sup>+</sup>-ATPase and nitric oxide content in faba bean (*Vicia faba*) seedlings exposed to arsenic toxicity. *Funct. Plant Biol.* 50 (2), 146–159. doi: 10.1071/FP21301
- Shah, W. H., Rasool, A., Tahir, I., and Rehman, R. U. (2020). Exogenously applied selenium (Se) mitigates the impact of salt stress in *Setaria italica* L. and *Panicum miliaceum* L. *Nucleus* 63, 327–339. doi: 10.1007/s12327-020-00326-z

- Sharma, V., and Ramawat, K. G. (2014). Salt stress enhanced antioxidant response in callus of three halophytes (*Salsola baryosma*, *trianthema triquetra*, *zygophyllum simplex*) of thar desert. *Biol. plantarum* 69 (2), 178–185. doi: 10.2478/s11756-013-0298-8
- Siddiqui, M. H., Alamri, S., Al-Khaishany, M. Y., Khan, M. N., Al-Amri, A., Ali, H. M., et al. (2019). Exogenous melatonin counteracts NaCl-induced damage by regulating the antioxidant system, proline and carbohydrates metabolism in tomato seedlings. *Int. J. Mol. Sci.* 20 (2), 353. doi: 10.3390/ijms20020353
- Silva-Ortega, C. O., Ochoa-Alfaro, A. E., Reyes-Agüero, J. A., Aguado-Santacruz, G. A., and Jiménez-Bremont, J. F. (2008). Salt stress increases the expression of p5cs gene and induces proline accumulation in cactus pear. *Plant Physiol. Biochem.* 46 (1), 82–92. doi: 10.1016/j.plaphy.2007.10.011
- Singh, A., Kumar, J., and Kumar, P. (2008). Effects of plant growth regulators and sucrose on post harvest physiology, membrane stability and vase life of cut spikes of gladiolus. *Plant Growth Regul.* 55 (3), 221–229. doi: 10.1007/s10725-008-9278-3
- Sofy, M. R., Seleiman, M. F., Alhammad, B. A., Alharbi, B. M., and Mohamed, H. I. (2020). Minimizing adverse effects of pb on maize plants by combined treatment with jasmonic, salicylic acids and proline. *Agronomy* 10 (5), 699. doi: 10.3390/agronomy10050699
- Sogoni, A., Jimoh, M. O., Kambizi, L., and Laubscher, C. P. (2021). The impact of salt stress on plant growth, mineral composition, and antioxidant activity in tetragonia decumbens mill.: An underutilized edible halophyte in south Africa. *Horticulturae* 7 (6), 140. doi: 10.3390/horticulturae7060140
- Solanki, M. (2021). The zn as a vital micronutrient in plants. *J. Microbiol. Biotechnol. Food Sci.* 11 (3), e4026–e4026. doi: 10.15414/jmbfs.4026
- Spoljarevic, M., Agić, D., Lisjak, M., Gumze, A., Wilson, I. D., Hancock, J. T., et al. (2011). The relationship of proline content and metabolism on the productivity of maize plants. *Plant Signaling Behav.* 6 (2), 251–257. doi: 10.4161/psb.6.2.14336
- Stam, M. R., Danchin, E. G., Rancurel, C., Coutinho, P. M., and Henrissat, B. (2006). Dividing the large glycoside hydrolase family 13 into subfamilies: Towards improved functional annotations of  $\alpha$ -amylase-related proteins. *Protein Eng Des Sel.* 19 (12), 555–562.
- Subramanyam, K., Du Laing, G., and Van Damme, E. J. (2019). Sodium selenate treatment using a combination of seed priming and foliar spray alleviates salinity stress in rice. *Front. Plant Sci.* 10, 116. doi: 10.3389/fpls.2019.00116
- Surekha, C., Kumari, K. N., Aruna, L., Suneetha, G., Arundhati, A., and Kavi Kishor, P. (2014). Expression of the vigna aconitifolia P5CSF129A gene in transgenic pigeonpea enhances proline accumulation and salt tolerance. *Plant Cell Tissue Organ Culture (PCTOC)* 116 (1), 27–36. doi: 10.1007/s11240-013-0378-z
- Suzuki, M., Bashir, K., Inoue, H., Takahashi, M., Nakanishi, H., and Nishizawa, N. K. (2012). Accumulation of starch in Zn-deficient rice. *Rice* 5, 1–8.
- Szabados, L., and Savouré, A. (2010). Proline: A multifunctional amino acid. *Trends Plant Sci.* 15 (2), 89–97. doi: 10.1016/j.tplants.2009.11.009
- Tavakoli, M., Poustini, K., and Alizadeh, H. (2016). Proline accumulation and related genes in wheat leaves under salinity stress. *J. Agric. Sci. Technol.* 18 (3), 707–716.
- Tavallali, V., Rahemi, M., Eshghi, S., Kholdebarin, B., and Ramezani, A. (2010). Zinc alleviates salt stress and increases antioxidant enzyme activity in the leaves of pistachio (*Pistacia vera* L'Badami') seedlings. *Turkish J. Agric. Forest.* 34 (4), 349–359. doi: 10.3906/tar-0905-10
- Thakur, S., Asthir, B., Kaur, G., Kalia, A., and Sharma, A. (2021). Zinc oxide and titanium dioxide nanoparticles influence heat stress tolerance mediated by antioxidant defense system in wheat. *Cereal Res. Commun.* 50, 385–396. doi: 10.1007/s42976-021-00190-w
- Thapa, S., Bhandari, A., Ghimire, R., Xue, Q., Kidwaro, F., Ghatrehsamani, S., et al. (2021). Managing micronutrients for improving soil fertility, health, and soybean yield. *Sustainability* 13 (21), 11766. doi: 10.3390/su132111766
- Tiwari, S., Lata, C., Singh Chauhan, P., Prasad, V., and Prasad, M. (2017). A functional genomic perspective on drought signalling and its crosstalk with phytohormone-mediated signalling pathways in plants. *Curr. Genomics* 18 (6), 469–482. doi: 10.2174/1389202918666170605083319
- Tripathi, D. K., Singh, S., Singh, S., Mishra, S., Chauhan, D., and Dubey, N. (2015). Micronutrients and their diverse role in agricultural crops: Advances and future prospective. *Acta Physiol. Plantarum* 37 (7), 1–14. doi: 10.1007/s11738-015-1870-3
- Tufail, A., Li, H., Naeem, A., and Li, T. (2018). Leaf cell membrane stability-based mechanisms of zinc nutrition in mitigating salinity stress in rice. *Plant Biol.* 20 (2), 338–345. doi: 10.1111/plb.12665
- Umar Hassan, M., Aamer, M., Umer Chattha, M., Haiying, T., Shahzad, B., Barbanti, L., et al. (2020). The critical role of zinc in plants facing the drought stress. *Agriculture* 10 (9), 396. doi: 10.3390/agriculture10090396
- Vatansever, R., Ozyigit, I. I., and Filiz, E. (2017). Essential and beneficial trace elements in plants, and their transport in roots: A review. *Appl. Biochem. Biotechnol.* 181 (1), 464–482. doi: 10.1007/s12010-016-2224-3
- Venugopalan, V. K., Nath, R., Sengupta, K., Pal, A. K., Banerjee, S., Banerjee, P., et al. (2022). Foliar spray of micronutrients alleviates heat and moisture stress in lentil (*Lens culinaris medik*) grown under rainfed field conditions. *Front. Plant Sci.* 13. doi: 10.3389/fpls.2022.847743
- Wei, C., Jiao, Q., Agathokleous, E., Liu, H., Li, G., Zhang, J., et al. (2022). Hormetic effects of zinc on growth and antioxidant defense system of wheat plants. *Sci. Tot. Environ.* 807, 150992. doi: 10.1016/j.scitotenv.2021.150992
- Wilkins, D. (1957). A technique for the measurement of lead tolerance in plants. *Nature* 180 (4575), 37–38. doi: 10.1038/180037b0
- Xie, Z., Duan, L., Tian, X., Wang, B., Eneji, A. E., and Li, Z. (2008). Coronatine alleviates salinity stress in cotton by improving the antioxidative defense system and radical-scavenging activity. *J. Plant Physiol.* 165 (4), 375–384. doi: 10.1016/j.jplph.2007.06.001
- Zafar, S., Hasnain, Z., Aslam, N., Mumtaz, S., Jaafar, H. Z., Wahab, P. E. M., et al. (2021). Impact of zn nanoparticles synthesized via green and chemical approach on okra (*Abelmoschus esculentus* L.) growth under salt stress. *Sustainability* 13 (7), 3694. doi: 10.3390/su13073694
- Zhang, X., Zhang, H., Zhang, H., and Tang, M. (2020). Exogenous melatonin application enhances rhizophagus irregularis symbiosis and induces the antioxidant response of medicago truncatula under lead stress. *Front. Microbiol.* 11, 516. doi: 10.3389/fmicb.2020.00516
- Zhao, Y., He, Y., Wang, X., Qu, C., and Miao, J. (2022). Proline metabolism regulation in spartina alterniflora and SaP5CS2 gene positively regulates salt stress tolerance in transgenic arabidopsis thaliana. *J. Plant Interact.* 17 (1), 632–642. doi: 10.1080/17429145.2022.2080291
- Zhu, Y., Jiang, X., Zhang, J., He, Y., Zhu, X., Zhou, X., et al. (2020). Silicon confers cucumber resistance to salinity stress through regulation of proline and cytokinins. *Plant Physiol. Biochem.* 156, 209–220. doi: 10.1016/j.plaphy.2020.09.014





## OPEN ACCESS

## EDITED BY

Milan Skalicky,  
Czech University of Life Sciences Prague,  
Czechia

## REVIEWED BY

Pushan Bag,  
University of Oxford, United Kingdom  
Ravi Raghavbhai Sonani,  
University of Virginia, United States

## \*CORRESPONDENCE

Ajay Kumar  
✉ [ajaykumar\\_bhu@yahoo.com](mailto:ajaykumar_bhu@yahoo.com)  
Rajan Kumar Gupta  
✉ [rajang.bot@bhu.ac.in](mailto:rajang.bot@bhu.ac.in)

RECEIVED 18 January 2023

ACCEPTED 24 May 2023

PUBLISHED 23 June 2023

## CITATION

Yadav P, Singh RP, Alodaini HA,  
Hatamleh AA, Santoyo G, Kumar A and  
Gupta RK (2023) Impact of dehydration on  
the physicochemical properties of *Nostoc  
caldicola* BOT1 and its untargeted  
metabolic profiling through UHPLC-HRMS.  
*Front. Plant Sci.* 14:1147390.  
doi: 10.3389/fpls.2023.1147390

## COPYRIGHT

© 2023 Yadav, Singh, Alodaini, Hatamleh,  
Santoyo, Kumar and Gupta. This is an open-  
access article distributed under the terms of  
the [Creative Commons Attribution License  
\(CC BY\)](https://creativecommons.org/licenses/by/4.0/). The use, distribution or  
reproduction in other forums is permitted,  
provided the original author(s) and the  
copyright owner(s) are credited and that  
the original publication in this journal is  
cited, in accordance with accepted  
academic practice. No use, distribution or  
reproduction is permitted which does not  
comply with these terms.

# Impact of dehydration on the physiochemical properties of *Nostoc caldicola* BOT1 and its untargeted metabolic profiling through UHPLC-HRMS

Priya Yadav<sup>1</sup>, Rahul Prasad Singh<sup>1</sup>, Hissah Abdulrahman Alodaini<sup>2</sup>,  
Ashraf Atef Hatamleh<sup>2</sup>, Gustavo Santoyo<sup>3</sup>, Ajay Kumar<sup>1\*</sup>  
and Rajan Kumar Gupta<sup>1\*</sup>

<sup>1</sup>Laboratory of Algal Research, Centre of Advanced Study in Botany, Institute of Science, Banaras Hindu University, Varanasi, India, <sup>2</sup>Department of Botany and Microbiology, College of Science, King Saud University, Riyadh, Saudi Arabia, <sup>3</sup>Instituto de Investigaciones Químico-Biológicas, Universidad Michoacana de San Nicolás de Hidalgo, Morelia, Mexico

The global population growth has led to a higher demand for food production, necessitating improvements in agricultural productivity. However, abiotic and biotic stresses pose significant challenges, reducing crop yields and impacting economic and social welfare. Drought, in particular, severely constrains agriculture, resulting in unproductive soil, reduced farmland, and jeopardized food security. Recently, the role of cyanobacteria from soil biocrusts in rehabilitating degraded land has gained attention due to their ability to enhance soil fertility and prevent erosion. The present study focused on *Nostoc caldicola* BOT1, an aquatic, diazotrophic cyanobacterial strain collected from an agricultural field at Banaras Hindu University, Varanasi, India. The aim was to investigate the effects of different dehydration treatments, specifically air drying (AD) and desiccator drying (DD) at various time intervals, on the physicochemical properties of *N. caldicola* BOT1. The impact of dehydration was assessed by analyzing the photosynthetic efficiency, pigments, biomolecules (carbohydrates, lipids, proteins, osmoprotectants), stress biomarkers, and non-enzymatic antioxidants. Furthermore, an analysis of the metabolic profiles of 96-hour DD and control mats was conducted using UHPLC-HRMS. Notably, there was a significant decrease in amino acid levels, while phenolic content, fatty acids, and lipids increased. These changes in metabolic activity during dehydration highlighted the presence of metabolite pools that contribute to the physiological and biochemical adjustments of *N. caldicola* BOT1, mitigating the impact of dehydration to some extent. Overall, present study demonstrated the accumulation of biochemical and non-enzymatic antioxidants in dehydrated mats, which could be utilized to stabilize unfavorable environmental conditions. Additionally, the strain *N. caldicola* BOT1 holds promise as a biofertilizer for semi-arid regions.

## KEYWORDS

*Nostoc caldicola*, dehydration, chlorophyll fluorescence, osmoprotectants, metabolomics, UHPLC-HRMS

## Introduction

The rising concentrations of CO<sub>2</sub> in the atmosphere are causing significant changes in meteorological patterns and reductions in precipitation in the majority of the globe. In these alarming scenarios, cyanobacteria seem to be an efficient and potential candidate for the protection of soil erosion and detention (Wigley and Jones, 1985; Belnap et al., 2016; Ebi and Loladze, 2019; WMO, 2021). Exopolysaccharide (EPS) produced by cyanobacteria aids in nutrient management and water retention in the medium, producing favorable circumstances for microbe survival in nutrient-limited and dry environments (Colica et al., 2014; Chamizo et al., 2019).

In previous studies, various authors have reported on drought-tolerant cyanobacteria and their use as biofertilizers for non-water-logging crops (Abd-Alla et al., 1994; Kuraganti et al., 2020). In addition, the bio-priming of seeds like *Acacia hilliana*, *Senna notabilis*, *Grevillea wickhamii*, *Eucalyptus gamophylla*, and *Oryza sativa* with *Microcoleus* sp., *Anabaena oryzae*, *Nostoc punctiformae*, and *Nostoc* sp. resulted in improved the germination and growth of seeds under drought conditions (Chua et al., 2020; Yadav et al., 2022a).

In biocrust, some cyanobacteria have been reported as dominant and pioneer organisms, which promote the succession of pioneer species via secreting EPS and increase soil fertility (Lan et al., 2013; Park et al., 2017; Mugnai et al., 2018). Some of the cyanobacterial species like *Calothrix parietina*, *Scytonema crispum*, *Scytonema hyalinum*, *Nostoc* sp., *N. calcicola*, and *N. commune* commonly form biocrusts on dry lands, resulting in survivability in extreme desiccation and heat environments (Dojani et al., 2014; Büdel et al., 2016; Becerra-Absalón et al., 2019; Roncero-Ramos et al., 2019).

Several cyanobacteria have the ability to grow and thrive even in extremely dry environments, and these cyanobacterial species play a crucial role in the maintenance of moisture content, solubilization and mobilization of phosphorus and nitrogen fixation, etc. (Deinlein et al., 2014; Garlapati et al., 2019; Gr et al., 2021). Therefore, these cyanobacterial strains can be used for draught stress management. However, relatively little evidence has been reported on the cyanobacterial-mediated improvement of plant growth under harsh environmental conditions, like drought, low and high temperatures,

ultraviolet radiation, freezing, and hot springs (Castenholz, 1992; Zakhia et al., 2008; Tashyreva and Elster, 2016; Yadav et al., 2022b). *N. calcicola* is an alkaliphilic halotolerant, filamentous nitrogen-fixing cyanobacterium, generally grown in the range of 0.5 to 2 M concentrations of salt (Singh V, et al., 2015). In previous studies, cyanobacterial species like *N. calcicola*, *Nostoc commune*, and *Microcoleus* sp. have been effectively used in the restoration of sodic lands and saline areas because they are remarkably tolerant to salt stress (Thapar et al., 2008). Studies have reported that *Anabaena variabilis* and *N. calcicola* can withstand NaCl concentration in the range of 0.1 to 0.8 M and effectively sequester heavy metals such as Cd (II), Cu(II), and Co(II) (Usmonkulova et al., 2022). *A. variabilis* and *N. calcicola* have also been found to reduce the chlorogenic compound hexachlorocyclohexane (Kadirova et al., 2012a). *N. calcicola* not only acts as a biofertilizer but also as a biostimulator of the development and growth of higher plants by synthesizing the growth hormones auxin and gibberellins (Kadirova and Shakirov, 2012b; Yadav et al., 2022a).

In previous studies, various authors have reported the growth of cyanobacteria strains on granite, sandstone, limestone, and marble (Singh V, et al., 2015). However, under extreme conditions, they form biofilms composed of EPSs containing polysaccharides, glycoproteins, lipopolysaccharides, glycolipids, and other extracellular enzymes (Yang et al., 2009). The EPS produced by these cyanobacterial strains helps in its protection and crust formation.

Recent developments in “omics” technologies have made it possible to compare the amounts of chemical compounds in desiccation-tolerant versus desiccation-sensitive organisms by quantitatively monitoring their abundance in a high-throughput way. The Ultra-high-performance liquid chromatography high-resolution mass spectrometry (UHPLC-HRMS) method can identify metabolites in low concentrations and has a higher capacity to limit false discovery rates (Khan et al., 2019).

In this present study, we evaluated the effect of desiccation on various biochemical properties like pigments, proteins, carbohydrates, and lipids of *N. calcicola* BOT1. We also evaluated osmoprotectants, stress biomarkers, and non-enzymatic antioxidant tests to understand the survival mechanism of the strain under dehydration stress. Furthermore, we performed UHPLC-HRMS to detect metabolites from the control and 96 h DD mats to understand how these metabolites relate to the organism's survivability in drought conditions.

## Material and methods

### Isolation and purification of the cyanobacterial strain

The filamentous test organisms were collected from the rice field located at the B.H.U. Varanasi, India campus. Then, the samples were serially diluted and cultured in the basal growth medium (BG-11N<sup>-</sup>) nitrogen-free broth medium for 15 days before being spread on the agar plates (Rippka et al., 1979).

The cyanobacterial colonies grown on the agar plate were picked aseptically and transferred to 100 ml BG-11N<sup>-</sup> containing medium in 250 ml flasks. Then, further isolated colonies were

**Abbreviations:** AD, Air drying; DD, desiccator drying; RWC, relative water content; EPS, exopolysaccharide; DDW, double distilled water; SEM, scanning electron microscopy; PAM, pulse amplitude modulation; ChlF, chlorophyll fluorescence; Fm, maximum fluorescence intensity; (Fo), minimum fluorescence intensity; Fv/Fm, maximum photochemical quantum yield of the PSII; ETRmax, maximum electron transport rate; Y(II), effective photochemical quantum yield; Y(NO), quantum yield of non-regulated energy dissipation; Y (NPQ), quantum yield of regulated energy dissipation; NPQ, non-photochemical fluorescence quenching; qP, puddle model-based coefficient of photochemical fluorescence quenching; qL, lake model-based coefficient of photochemical fluorescence quenching; ROS, reactive oxygen species; PC, phycocyanin; PE, phycoerythrin; APC, allophycocyanin; TPBP, total phycobiliproteins; TBA, 2-thiobarbituric acid; TCA, trichloroacetic acid; MDA, malondialdehyde; TPC, total phenolic content; TFC, total flavonoid content; GAE, gallic acid equivalent; FDA, fluorescein diacetate; PI, propidium iodide; UHPLC-HRMS, ultra-high-performance liquid chromatography-high resolution mass spectrometry.



transferred to a new BG-11N<sup>−</sup> plate and incubated at 25 ± 2°C, under the 55 μmol photons m<sup>−2</sup>s<sup>−1</sup> illumination provided by a cool fluorescent tube light.

## Culture conditions

The mother cultures were grown in a conical flask with 200 ml of BG-11N<sup>−</sup> (pH 7.4) medium for 25 days at 25 ± 2°C under 55 μmol photons m<sup>−2</sup>s<sup>−1</sup> light intensity with a 14:10 h day-night photoperiod. The growth media containing cyanobacteria were manually shaken 3–5 times a day for proper growth and suspension formation. Then, 10% mother cultures of isolates (at exponential phase) were aseptically transferred into a 2 L conical flask containing 1300 ml of BG-11 N<sup>−</sup> medium and grown under the above-described culture conditions.

## Identification of isolate by light and scanning electron microscopy

The isolates were first observed under light microscopy by preparing temporary slides. The shape, size, and color of the thallus, the width and length of the trichome, the presence and position of heterocysts, branching in filaments, hormogonia, and akinetes were considered during taxonomic characterization (Desikachary, 1959; Komárek, 2013). The detailed morphology of the isolates was visualized using SEM. Cyanobacterial filaments were placed at the center of the cover slip, dried, and chemically fixed with 2.5% (v/v) glutaraldehyde. After complete drying, they were washed with double-distilled water (DDW) then further dehydrated with increasing ethanol concentrations (30%, 50%, 90%, and 100%) and again air dried. An Sc 7620 sputter coater was used to coat the dried cyanobacterial samples with gold-palladium at a thickness of 30 Å for 5 min. Further, these coated samples were used for their morphological identification under SEM (EVO18 Research ZEISS- Germany) (Sadiq et al., 2011).

## Molecular characterization of cyanobacteria isolates

For molecular characterization genomic DNA of the cyanobacteria isolate was extracted using the traditional xanthogenate technique (Tillett and Neilan, 2000). For the partial amplification of the 16S rRNA gene, a forward primer (359F, 5'-GGG GAA TYT TCC GCA ATG GG-3') and a reverse primer (781R, 5'-GAC TAC TGG GGT ATC TAA TCC CAT T-3') were used (Nübel et al., 1997). The 16S rRNA amplification was performed using 25 μl aliquots containing 30–50 μg DNA template, 200 μM dinucleotide triphosphates, 0.4 μM of forward and reverse primers, 1 U/μl Taq Polymerase and 1.5 μM MgCl<sub>2</sub>, (BioRad, DNA Engine, Peltier Thermal Cycler). The reaction mixture was incubated in a Thermal cycler for DNA amplification (Singh P, et al., 2015). The amplified products were sequenced by Sanger's method and the obtained sequence was compared with the NCBI database using BLAST tool. MEGA 11

software was used for making maximum likelihood tree for phylogenetic analysis (Guindon and Gascuel, 2003).

## Experimental setup for study

The culture of an early exponential growth phase was harvested throughout centrifugation at 3158 g for 10 min, and the obtained cell pellets were used to make an artificial mat on Petri dishes (90 mm in diameter). We employed two practical dehydration methods for dehydration treatment: the cyanobacterial mat was exposed to laminar airflow for air drying (AD) in the first, and the cyanobacterial mat was placed in a desiccation chamber using calcium chloride fused for desiccation drying (DD) in the second. At various dehydration treatments, including 0, 6, 12, 24, 48, and 96 hours, an *N. calicicola* BOT1 mat was harvested from each dehydrated plate and used for physicochemical analysis. Each of the experiments was carried out in three biological replicates.

## Relative water content

Relative water content was calculated using the following equation:

$$(\% \text{ of water}) = (\text{FW} - \text{DW})/\text{FW} \times 100 \%$$

Here, FW denotes the fresh weight of cyanobacteria samples and DW denotes the dry weight determined after chemical drying and air drying in the laminar flow.

## Evaluation of chlorophyll fluorescence (ChlF)

Through the study of ChlF parameters using the pulse-amplitude modulation (PAM-2500, Walz, Germany), the impact of dehydration stress on photosystem II (PSII) and the redox potential of the photosynthetic electron transport chain was evaluated *in-vivo* (Ogawa et al., 2017). As a non-destructive indicator of photosynthetic activity, ChlF was used, and a variety of photosynthetic metrics were used to gauge the health of the cells under dehydration. The data collecting programme PamWin-3 was used to record fluorescence levels of dehydrated cyanobacterial mats. The PamWin-3 software calculates the minimum fluorescence intensity of dark adopted mats (Fo), maximum fluorescence intensity of dark adopted mats (Fm), maximum electron transport rate (ETR<sub>max</sub>), maximum photosynthetic quantum yield of the PSII (Fv/Fm), effective photochemical quantum yield [Y(II)], quantum yield of non-regulated energy dissipation [Y(NO)], quantum yield of regulated energy dissipation [Y(NPQ)], and non-photochemical fluorescence quenching (NPQ). To prevent any energy-dependent quenching, dehydrated cyanobacterial mats were left in the dark for 30 min before observations and actinic light (AC) intensity progressively from 3 to 1469 μmol photons m<sup>−2</sup>s<sup>−1</sup> in order to analyze quantum yield measurements (Bag et al., 2020).

## Visualization of (exopolysaccharides) EPS

For accurate imaging, Alcian blue dye was used to stain the acidic mucopolysaccharides released by cyanobacterial species. A solution of 3% (w/w) acetic acid and 0.33% (w/w) alcian blue (Chroma-Gesellschaft, Kongen, Germany) was used to stain cyanobacterial mats (Tamaru et al., 2005). The stained mats were washed with DDW to remove excess dye, then it was observed under a light microscope.

## Biochemical composition analysis in dehydrated mats

### Quantification of photosynthetic pigment

For the estimation of lipid-soluble pigments like chlorophyll-*a* (Chl-*a*), carotenoids, and scytonemin, 20 mg of cyanobacterial mats was subjected to 80% acetone, employing the method of Tandeau de Marsac and Houmard (1988) with slight modifications. The mixture was kept at 4°C overnight for the complete extraction of the pigment in the acetone. Furthermore, the amount of chlorophyll and other compounds was determined by measuring the optical density (OD) at different wave lengths, such as 665 nm for Chl-*a*, 461 nm for carotenoids, and 384 nm for scytonemin, and the absorbance at 750 nm was subtracted to account for light scattering (Hirschberg and Chamovitz, 1994). The remaining cell pellets were mixed with DDW and used for the extraction of water-soluble phycobiliproteins using the freeze-thaw method (Bennett and Bogorad, 1973). The supernatant was collected by centrifugation, and the OD of different phycobiliproteins was determined spectrophotometrically at 562, 615, and 652 for phycocyanin (PC), phycoerythrin (PE), and allophycocyanin (APC), respectively. All the pigments were evaluated using the following the standard formulas:

$$\text{Chl} - a (\mu\text{g/mg}) = (A_{665\text{nm}} - A_{750\text{nm}}) \times 13.9$$

$$\text{Carotenoids} (\mu\text{g/mg})$$

$$= [(A_{461\text{nm}} - A_{750\text{nm}}) - 0.046 \times (A_{665\text{nm}} - A_{750\text{nm}})] \times 4$$

$$\text{Scytonemin} (\mu\text{g/mg})$$

$$= (1.04 A_{384\text{nm}} - 0.79 A_{663\text{nm}} - 0.27 A_{490\text{nm}}) \times V$$

$$\text{PE} (\mu\text{g/mg}) = \{A_{562} - (2.41 - \text{PC}) - (0.849 - \text{APC})\} / 9.62$$

$$\text{PC} (\mu\text{g/mg}) = (A_{615} - 0.474 \times A_{652}) / 5.34$$

$$\text{APC} (\mu\text{g/mg}) = (A_{652} - 0.208 \times A_{615}) / 5.09$$

### Quantification of protein, carbohydrate, and lipid

The total protein content of the dehydrated cyanobacterial mats was quantified using the traditional colorimetric method followed by the standard protocol of Lowry et al. (1951). In brief, 10 mg cyanobacterial mats were first treated with 1 ml of reagent-A (0.1 N

NaOH) and kept in a water bath for 30 min. The mixture was then agitated with 2 ml of reagent-B (2M Na<sub>2</sub>CO<sub>3</sub> and 0.5 M CuSO<sub>4</sub>·5H<sub>2</sub>O in 1M sodium potassium tartrate) for 30 min at room temperature. Then, a further 0.5 ml of 1N folin-ciocalteu reagent (FCR) was mixed and stored for 20 min at room temperature. The development of a blue color confirmed the presence of protein, and their concentration was measured by taking the optical density at 650 nm. During protein estimation, bovine serum albumin (BSA) was used to prepare the standard curve.

Total carbohydrate was quantified using the anthrone method (Loewus, 1952). In brief, 10 mg cyanobacterial mats of each treatment were agitated with 1 ml of 1N NaOH and stored for 25 min in the boiling water bath. The mixture was crushed using a mortar and pestle to obtain a crude homogenate, which was centrifuged at 3158 g for 10 min. Further, 100 μL of each supernatant was used to evaluate the total amount of carbohydrate. The anthrone reagent was prepared in 200 mL of chilled 95% H<sub>2</sub>SO<sub>4</sub> by dissolving 400 mg anthrone. Then, 1 mL of the sample (100 μL cyanobacterial supernatant + 900 μL DDW) was mixed with 4 mL of freshly prepared anthrone reagent and incubated at room temperature for 15 min. The reaction mixture was placed in the preheated water bath for 15 min, and instant ice cooling was conducted for 5 min to arrest the reaction. The absorbance of each sample was measured at 625 nm (Dubois et al., 1956). A standard curve of glucose was prepared and used for the quantification of the carbohydrate content in dehydrated mats.

The total lipid content was extracted from 50 mg of dried cyanobacterial mat using a slightly modified version of Bligh and Dyer's protocol (Bligh and Dyer, 1959). The water, methanol, and chloroform mixture were used in a 2:1:2 ratio for the extraction of total lipids from dehydrated samples. Cyanobacterial mats were mixed with the above-mentioned solution and vortexed for 10 min. The mixture was sonicated for 5 min with 30 seconds on and 30 seconds off pulse, at a frequency of 20 kHz. The whole slurry was centrifuged at 12633 g for 15 min, and the lower organic phase was transferred into a previously weighed tube and evaporated at 40°C using the SpeedVac vacuum concentrator. The total lipid content in the mats was calculated using the following equation:

$$\% \text{ Lipid content} = \text{lipid weight (mg)} \times 100 / \text{dried mat weight (mg)}$$

### Quantification of osmoprotectant

Trehalose content in dehydrated mats was measured according to the protocol of Lillie and Pringle (1980). In brief, 20 mg of dried mats was mixed with 1 ml of 0.5 M trichloroacetic acid and stored for 1 h at room temperature. Then, the mixture was crushed and centrifuged at 12633 g for 15 min. The subsequent procedure was similar to carbohydrate quantification. The turbidity of the supernatant was recorded at 625 nm, and its amount was expressed as μ mole/mg DW using the trehalose calibration curve.

Proline contents were measured following the approach of Bates et al. (1973). With the aid of a mortar and pestle and 3% (w/v)

sulfosalicylic acid, 20 mg of dried mats was homogenized and left at room temperature for 24 h. The homogenate was centrifuged for 20 min at 12633 g and the collected supernatant was then treated with acetic acid and ninhydrin. The process was stopped by submerging the tubes in freezing water after the mixture had been boiling for two hours.

Toluene was used for the final extraction of proline ( $\mu$  mole/mg DW) and also as a reference; an equal amount of toluene was taken, agitated with cooled solution, and kept for layer separation. Lower pink toluene solution was collected in a separate test tube, and the OD was measured at 520 nm.

### Quantification of stress biomarkers

MDA was quantified using 2-Thiobarbituric acid (TBA) and indicated as equivalent to lipid peroxidation (Heath and Packer, 1968). In a 5% trichloroacetic acid (TCA) solution, cyanobacterial mats were homogenized using a mortar and pestle. Centrifuging homogenate mixes took place for 10 min at 12633 g. After being heated to boiling temperature for 20 min, 1 ml of the supernatant was combined with 1 ml of 0.65 M TBA (i.e., TBA produced in a 20 M TCA solution). The mixture was centrifuged at 12633 g for 10 min after cooling in ice-cold water. At 450, 532, and 600 nm, measurements of the supernatant's absorbance were made. The following equation (Chokshi et al., 2015) was used to calculate the MDA concentration:

$$\begin{aligned} \text{MDA } (\mu \text{ mol/mg DW}) \\ = [6.45 \times (A_{532\text{nm}} - A_{600\text{nm}})] - [0.56 \\ \times A_{450\text{nm}}] / \text{dry weight (mg)} \end{aligned}$$

Cyanobacterial mats were crushed in a 0.1 M TCA solution to determine the amount of  $\text{H}_2\text{O}_2$ . Then, 0.5 ml of supernatant was added to the reaction mixture, which contained 0.5 ml of 0.1 M phosphate buffer saline (pH 7.0) and 1 ml of 1 M, KI solution. Further absorbance was taken at 390 nm and the amount of  $\text{H}_2\text{O}_2$  was shown as  $\mu$  mol/mg DW (Velikova et al., 2000).

### Quantification of non-enzymatic antioxidants

To evaluate the total flavonoid (TFC) and phenolic content (TPC), the samples were crushed in the 90% acetone solution. The TFC of dehydrated mats was measured using aluminum chloride ( $\text{AlCl}_3$ ) (Ordóñez et al., 2006), and 1 ml of the extract was further mixed with 1 ml of 2 M  $\text{AlCl}_3$ ; the solution was gently agitated and stored for 2 hours at room temperature. The colour of the mixture was changed and then the OD of the samples were measured at 420 nm. TFC was expressed as  $\mu$ g quercetin (QE)/mg DW.

The TPC of dehydrated mats was measured colorimetrically using the FCR following the standard protocol of Singleton et al. (1999). A total of 0.5 ml supernatant, 1 ml of 2 M  $\text{Na}_2\text{CO}_3$ , and 0.5 ml of 1N FCR were mixed and maintained 5 ml final volume using DDW; the mixture was then heated until blue color developed. The mixtures were allowed to cool at room temperature before measuring absorbance at 760 nm. TPC was expressed in  $\mu$ g gallic acid equivalent (GAE)/mg DW.

### Vital staining of cells with Fluorescein Diacetate (FDA) and Propidium Iodide (PI)

For the determination of the effect of dehydration treatment on the viability of cells, we used the fluorescence microscopy technique with vital staining dyes, i.e., FDA and PI. FDA is a non-fluorescent, uncharged, lipid-soluble dye that is hydrolyzed to fluorescein by non-specific intracellular esterases after uptake and stains live cells (Tamaru et al., 2005).

Since dead and damaged cells lack an unbroken cell membrane, PI, a red fluorescent cell viability dye, can only enter damaged or dead cells (Deligeorgiev et al., 2009). Once inside, it intercalates between the two to bind to DNA. The FDA stock solution was made by combining 3 mg of FDA with 1 ml of cold acetone and storing it at  $-20^\circ\text{C}$ , while the PI stock solution was made by combining 1 mg of PI with 1 ml of 8X phosphate-buffered saline (PBS) and storing it at  $4^\circ\text{C}$ . Using an FDA excitation filter at 480 nm and a 585 nm emission filter at the green channel, and a PI excitation filter at 493 nm and a 636 nm emission filter at the red channel, it was possible to see the live-dead cells (Tamaru et al., 2005).

### Extraction of metabolites

Metabolites were extracted from control and 96 h DD mats using HPLC-grade methanol (Thanh Doan et al., 2000). Methanol-filled flasks with mats were chilled overnight at  $4^\circ\text{C}$  then further centrifuged at 10,000 g for 25 minutes, and supernatants were collected separately. Then, the supernatants were dried through evaporation and redissolved in methanol of HRMS grade.

UHPLC-HRMS analysis of extracts was carried out using an Orbitrap Eclipse Tribrid Mass Spectrometer USA, from the Central Discovery Centre (CDC), Banaras Hindu University BHU, Varanasi, Uttar Pradesh, India. UHPLC was used to separate small molecules chromatographically (COMPOUND DISCOVERER 3.3.2.31). Here, a three-solvent system was used as the mobile phase: Solvent A was water with 0.1% formic acid; Solvent B was 100% acetonitrile with 0.1% formic acid; and Solvent C was 100% methanol with 0.1% formic acid. The metabolites were separated using a GOLD C18 selectivity HPLC column (inner diameter 2.1 mm, length 100 mm and particle size 1.9  $\mu\text{m}$ ). The injection volume was 5  $\mu\text{l}$ , the run time was 30 min., and the flow rate was 0.3 ml/min. The column outlet was connected to a mass spectrometer via H-ESI (electrospray ionization). Both negative and positive modes of H-ESI were used to ionize the compounds that were channelized using Orbitrap. To identify the likely compounds present in the extract, the MS spectra for the analyzed samples were compared to those from the Predicted Compositions, mzCloud Search, ChemSpider Search, and MassList Search databases.

### Statistical analysis

All the data are presented as the mean of three replicates, and to assess the significant difference, data were statistically analyzed using a one-way analysis of variance (ANOVA) with a significance level of  $p < 0.05$  (SPSS 16.3 statistics version, Chicago, IL, USA).



## Results and discussions

### Isolation, identification, and growth behavior of cyanobacterial isolate

To confirm the identity of cyanobacterial isolates, light and brightfield microscopy (Figures 1A, B) was used first, followed by morphological and molecular characterization to further confirm the identity of the isolates.

The presence of a filamentous body with moniliform vegetative cells interrupted with pale yellow intercalary heterocysts and a dome-shaped terminal cell indicated that isolated cyanobacteria are a *Nostoc* species (Desikachary, 1959; Celis-Pla et al., 2021; Usmonkulova et al., 2022). Furthermore, SEM was used to confirm the morphology of isolated cyanobacteria, and all of the present micrographs showed similarities in shape, size, and surface morphology with the previously reported *Nostoc* (Komárek, 2013; Tiwari et al., 2019) (Figures 1C, D).

The molecular identification of the cyanobacterial strain was found using 16S rRNA gene sequencing. The maximum likelihood phylogenetic analyses (Figure 2) of 16S rRNA showed a similarity of 99% with the closest species, *Nostoc calcicola*. Furthermore, the gene sequence was deposited in the NCBI gene bank database with Gene-Bank Accession No. OP453348. However, the best growing circumstances were discovered to be at 14:10 h light-dark, with a photoperiod of 55  $\mu\text{mol m}^{-2}\text{s}^{-1}$  light intensity and a temperature of 25°C.

### Effect of dehydration on morphological changes and EPS production

The EPS of cyanobacteria is unique in its constituents, i.e., its protein, nucleic acid, and lipid content (Costa et al., 2018). EPS has the ability to retain water, thus protecting the photosynthetic apparatus by slowing the rate of desiccation (Raanan et al., 2016;

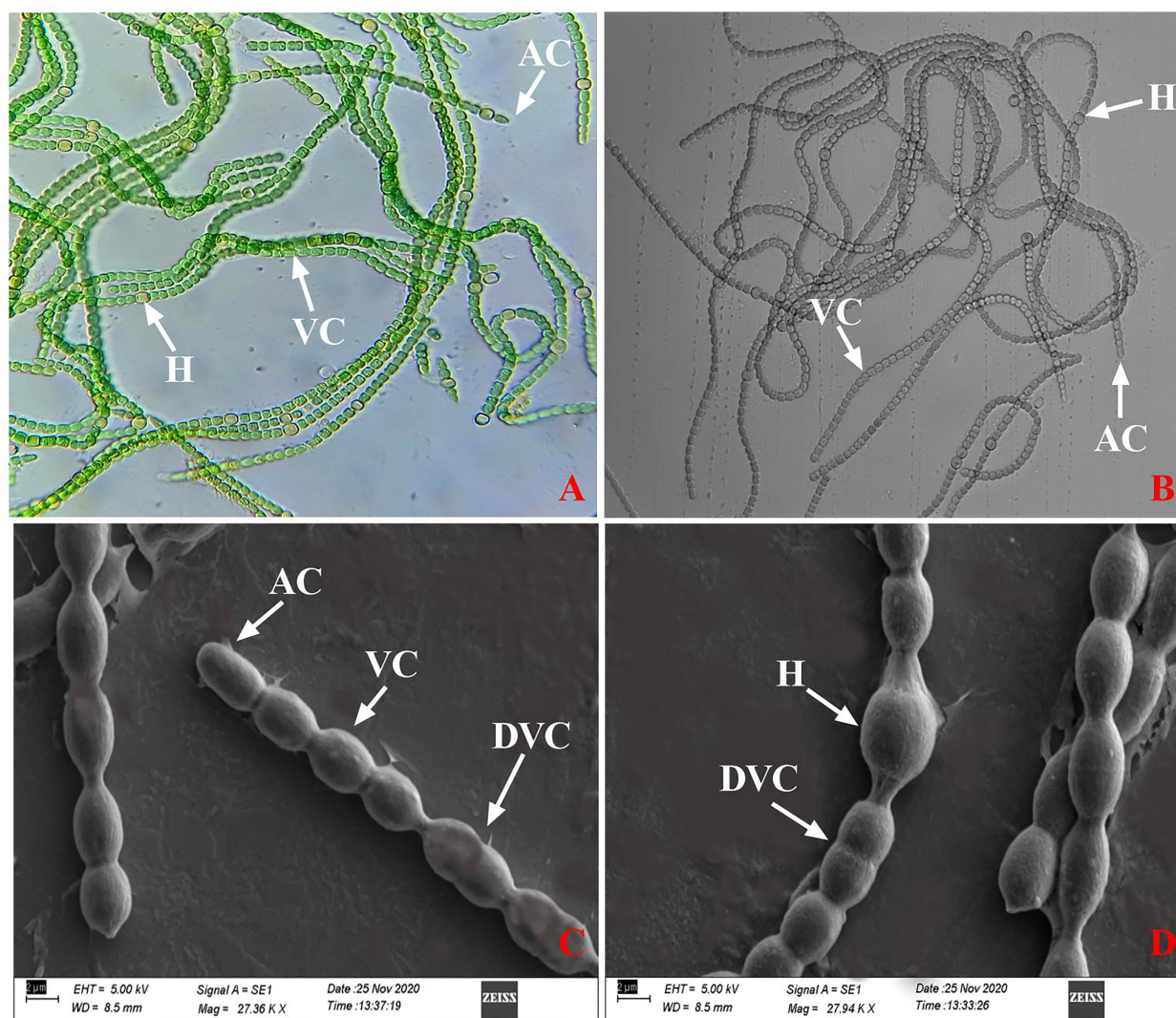
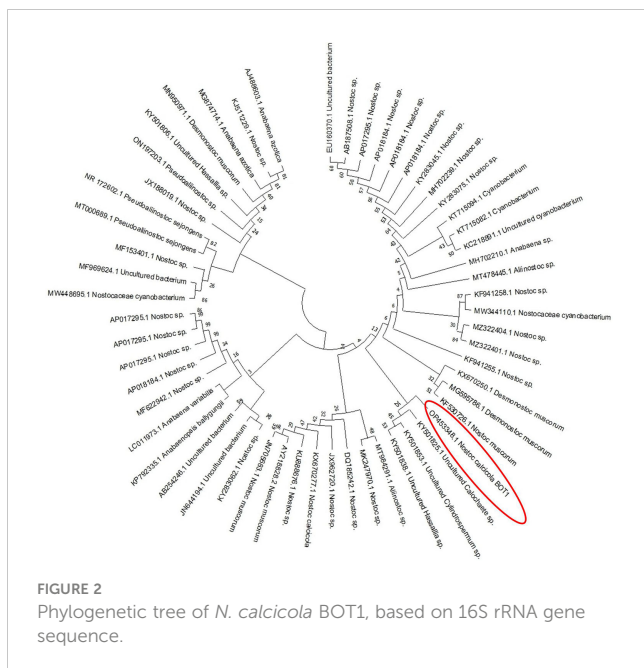


FIGURE 1

(A, B) Light and brightfield microscopic image and (C, D) SEM image of *N. calcicola* BOT1. Were, AC: apical cell, H: heterocyst, VC: vegetative cell, DVC: dividing vegetative cell.



Benard et al., 2019). Since EPS is cohesive, it can shield soil from water and wind erosion, preserve the fertility of soil, and increase water retention (Faist et al., 2017). In the study, dehydration causes morphological changes and affects EPS secretion around the filaments in *N. calcicola* BOT1 during dehydration (Figure 3). The released EPS was stained using alcian blue dye, and it reached its maximum in the control and in 6 h AD and DD dehydrated mats. This experiment was done initially with cyanobacterial filaments, which were not wet beforehand. All microphotographs were taken at the same magnification. With an increase in dehydration duration, there was a rapid decrease in EPS production.

The filament length and width of cells and EPS secretion varied with the change in the duration of dehydration in both AD and DD mats (Figure 3). This result demonstrated that *N. calcicola* BOT1 filaments became shorter and more compact under dehydration conditions in both AD and DD mats and also formed a compact

mat by aggregating their filaments. A similar observation was also reported by Feng et al. (2012) in *Nostoc flagelliforme*. This capability of *N. calcicola* BOT1 makes it suitable for biocrust formation.

## Effect of dehydration on photosynthetic efficiency

In semi-arid and dry environments, where cyanobacteria are frequently subjected to periods of desiccation, water availability is a significant factor impacting cyanobacterial growth (Chaves et al., 2003). Numerous metabolic functions, including photosynthesis, are adversely impacted by desiccation stress. For instance, a lack of water harms the fundamental structure, which prevents the uptake of carbon and harms the photosynthetic machinery of photosynthetic organisms (Golldack et al., 2011).

The highest quantum yield of PSII is indicated by Fv/Fm (Kitajima and Butler, 1975). However, with the RWC dropping from 60 to 80% as a result of dehydration, Fv/Fm decreased quickly. Cyanobacteria were classified as sensitive, semi-tolerant, and desiccation-tolerant by Raanan et al. (2016) based on measurements of oxygen evolution rate and Fv/Fm in response to light stress. Due to the existence of EPS, which serves as an exterior barrier against desiccation in *Nostoc* sp., they believed that *Nostoc* sp. came under the desiccation-tolerant group (Shirkey et al., 2000).

All oxygenic photosynthetic organisms have been extensively studied using ChlF, a delicate mirror of photosynthesis (Housman et al., 2006; Baker and Oxborough, 2004; Baker, 2008). Fv/Fm can offer a quick and easy technique to determine whether or not cyanobacterial colonies were subjected to stressful conditions (Henriques, 2009). When *N. calcicola* BOT1 cells were dehydrated for various amounts of time (6–96 hours) Fv/Fm, Fo, Fm, YII, and ETRmax significantly ( $p < 0.05$ ) decreased, while NPQ, Y(NO), and Y(NPQ) increased, in comparison to the control (Figure 4).

This implies a significant impact of dehydration on the photosynthetic activity of the cyanobacterial isolate *N. calcicola* BOT1. The minimum Fv/Fm was found in 96 h AD and DD mats, which was  $(0.0040 \pm 0.004)$  and  $(0.0043 \pm 0.004)$ , respectively.

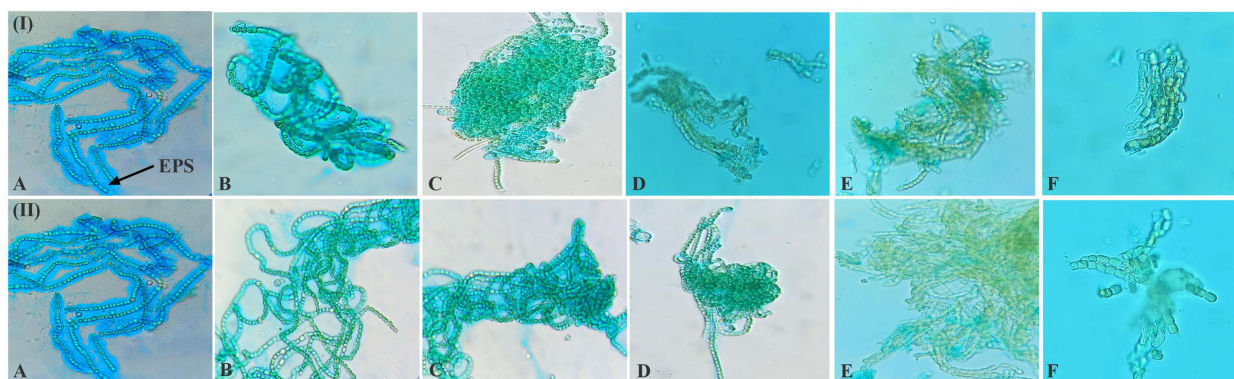


FIGURE 3  
Light microscopic photographs (at 20X magnification) of *N. calcicola* BOT1 at different durations of dehydration treatment. Mucopolypeptide-binding with alcian blue (non-fluorescence dye) was used to stain cyanobacterial mats. (I) air-dried mats and (II) desiccator-dried mats in which, (A) indicates control, and (B–F) denote dehydration treatments for 6, 12, 24, 48, and 96 hours, respectively.



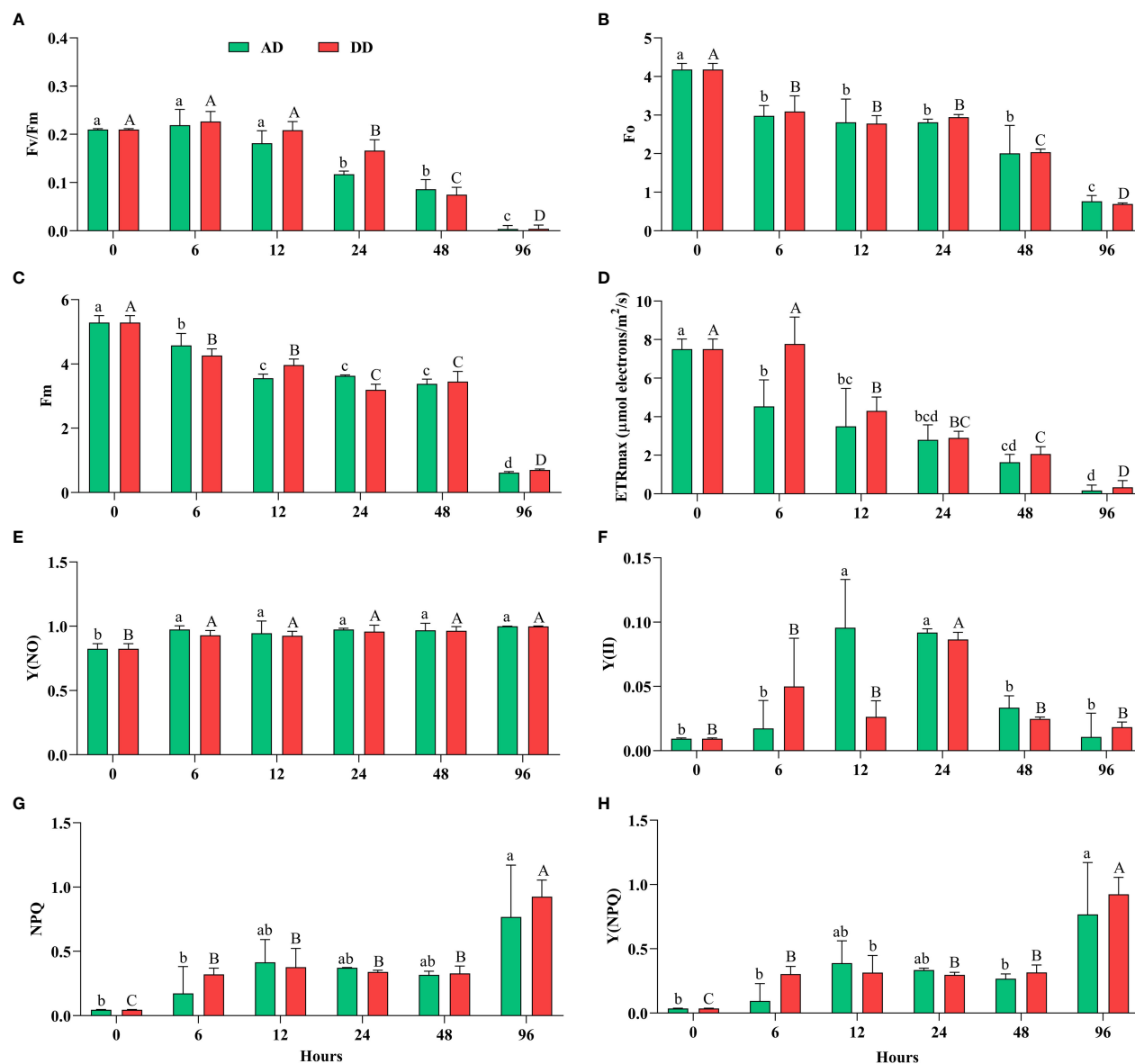


FIGURE 4

Effect of different durations of dehydration on the photosynthetic efficiency of *N. calicicola* BOT1. Different superscript alphabet letters on the values indicated a significant difference ( $p < 0.05$ ) between the mats of different durations of dehydration treatments. (A). (Fv/Fm) is the maximum photosynthetic quantum yield of PS II, (B). (Fo) is the minimum fluorescence, (C). (Fm) maximum fluorescence, (D). (ETRmax) maximum electron transfer rate, (E). [Y(NO)] non-regulated energy dissipation quantum yield of PS II, (F). (YII) amount of energy used in photochemistry by PS II, (G). (NPQ) non-photochemical fluorescence quenching, and (H). Y(NPQ) regulated energy dissipation quantum yield of PS II. The error bars on the histograms indicate the standard error of the mean values of three biological replicates.

During Fv/Fm evaluation, cyanobacteria cells were subjected to subsequent dehydration for 6 to 96 h; there was a significant maximum drop in 96 h compared to the control, 52.5 fold in AD and 48.8 fold in DD mats (Figure 4A). In this study, Fv/Fm significantly decreased in both AD and DD after 12 h of dehydration treatment (Figure 4A).

Our results indicate that Fv/Fm was maintained during 0–12 h of dehydration treatment under both AD and DD conditions; however, this reduced when the RWC decreased below 60%. Data for *N. calicicola* BOT1 (Figure 4), however, indicate a fast decline of Fv/Fm

values at the RWCs below 60%, suggesting a sensitivity of *N. calicicola* BOT1 primary photosynthetic processes to desiccation (Alonso, 2018). This behavior simply depended on the degree of dryness and was unaffected by the drying rate. Disregarding the potential for dried, stabilized Chl-*a* to absorb red light during the PAM test, the observed decrease in Fv/Fm, which did not approach zero even after 96 hours of dehydration, may conceivably reflect a very minimal but continuing function of the photosynthetic apparatus.

In 96 h dehydrated mats, Fo and Fm were significantly ( $p < 0.05$ ) lower than the controls; they were  $(0.766 \pm 0.086)$  and  $(0.616 \pm$

0.019) in AD, and  $(0.693 \pm 0.018)$  and  $(0.700 \pm 0.019)$  in DD mats, respectively (Figures 4B, C). The decreased  $F_o$  (5.45 and 6.03 fold) and  $F_m$  (8.58 and 7.55 fold) in AD and DD mats indicated that both PSI and PSII light-harvesting complexes and the reaction center were inactive. These ratios, according to Heber et al. (2007), are an indication of variations in the degree of photoprotection, which ought to be greater in severely dehydrated cyanobacterial mats than in mildly dehydrated ones. Only very modest residual charge separation levels were seen in AD and DD mats at the end of the dehydration under the circumstances of our experiment. In desiccated mats, the  $F_o$  values were considerably low ( $P < 0.05$ ), indicating higher levels of light energy dissipation in cyanobacterial mats that had completely dried out.

ETRmax followed the same pattern as  $F_v/F_m$  and decreased gradually up to 46.8 fold in AD and 22.7 fold in DD mats after 96 h of dehydration (Figure 4D). It is believed that this stoppage of electron transport is an acclimatory reaction to desiccation (Fukuda et al., 2008). Dehydration significantly decreased the ETRmax, which suggests a decrease in the PSII reaction center, as seen by the light curve. The change from cyclic to sparse linear electron flow is what causes the reduced ETRmax. This conversion of electron flux protects the PSII from excessive activation energy of electrons (Fukuda et al., 2008).

Furthermore, NPQ and Y(NPQ) (Figures 4G, H) increased more than the control at 96 h in both AD and DD mats,  $(0.767 \pm 0.232)$ ,  $(0.768 \pm 0.232)$ , and  $(0.925 \pm 0.074)$ ,  $(0.924 \pm 0.075)$ , i.e., 17.0, 21.3, 20.5, and 25.6 fold, respectively. The rise in the nonphotochemical quenching (NPQ) value provided additional proof of physiological stress (Deng et al., 2014). By dispersing the extra energy as heat, NPQ prevents damage to the photosynthetic reaction center (White et al., 2011). Carotenoid conversion into photo-protective pigments under stress is correlated with a high NPQ value (Boussiba, 2000).

The decrease in  $F_o$  and  $F_m$  and the increase in NPQ and Y (NPQ) after 96 hours of dehydration suggest an enhancement in energy via the xanthophyll cycle (García-Plazaola et al., 2007; Jahns and Holzwarth, 2012). Y(NO) increased significantly in all the treatments, but there was an insignificant difference found in AD and DD mats (Figure 4E), and it was  $(0.999 \pm 0.000)$  and  $(0.997 \pm 0.002)$ , i.e., 1.21 and 1.20 fold, respectively. As previously mentioned, an increase in Y(NPQ) denotes an effort to release excess energy, whereas an increase in Y(NO) denotes excess energy fluxes that are out of control and may result in photodamage to *N. calicicola* BOT1 (Kramer et al., 2004). Severe water stress caused a decrease in Y(II) and an increase in Y(NO), which indicates that dehydration stress increased the fraction of non-reducing and “closed” PS II reaction centers. However, when the internal water content reached 60–40%, Y(II) increased, but increasing the duration of dehydration reduced the Y(II) value (Deng et al., 2014). The lower Y(II) values from the 48–96 h dehydration treatments suggest that water content below a certain point has a greater impact on PS II activity. The quenching parameter Y(NO) increased as dehydration treatment increased. According to Pfündel et al. (2008), a rise in Y (NO) shows an enhancement in the proportion of “closed” PSII centers and PSII’s inability to defend itself from photodamage. In this

experiment, Y (NPQ) was significantly affected by the dehydration treatment. NPQ, which depends on the presence of carotenoids, protects PS II against stress-related damage. Dehydration treatment reduced carotenoids content after 48 hours in both AD and DD mats (Table 1), indicating that NPQ was not protecting PS II from dehydration-induced photoinhibition by regulating energy dissipation Y(NPQ) (Deng et al., 2014).

In our investigation, it was shown through the rise in NPQ, Y (NO), and Y(NPQ) (Figures 4E–H) in AD and DD mats at 96 h of dehydration compared to the control that the extra energy surpassed the cyanobacteria’s capacity for regulation and could not be properly dissipated, particularly under extreme stress. It might indicate irreversible cell dehydration and impaired metabolism (Kramer et al., 2004; Radermacher et al., 2019).

## Effect of dehydration on pigment

A crucial marker of the oxygenic photoautotrophic nature of cyanobacteria is the presence of photosynthetic pigments, Chl-*a*, and phycobiliproteins. The effect of dehydration stress on the different pigment concentration monitored in *N. calicicola* BOT1 which is represented in Table 1. Osmotic stress caused by decreasing water content reduced pigment concentrations. Reduced photosynthetic pigment content could be a sign of oxidative stress caused by decreasing water content and reduced RuBisCo activity because of poor water content that encourages pigment deterioration (Hounslow et al., 2021). Chl-*a* content decreased with increasing dehydration treatment duration. A significant change in Chl-*a* content was observed in 96 h AD  $(2.042 \pm 0.000 \mu\text{g}/\text{mg DW})$  and DD  $(2.202 \pm 0.000 \mu\text{g}/\text{mg DW})$  dehydrated mats, which was 1.37 and 1.279 fold less than the control, respectively. Scytonemin content and carotenoid levels both increase concurrently with dehydration treatment duration. Scytonemin concentration was at its maximum in 96 h AD  $(5.12 \pm 0.000 \mu\text{g}/\text{mg DW})$  and DD  $(0.615 \pm 0.000 \mu\text{g}/\text{mg DW})$  samples, which was 5.12 and 6.15 fold higher than the control. Carotenoids levels in 48-hour AD and DD samples were  $(3.366 \pm 0.001 \mu\text{g}/\text{mg DW})$  and  $(3.414 \pm 0.001 \mu\text{g}/\text{mg DW})$ , respectively, which was 1.17 and 1.19 fold higher than the control sample.

Free radicals and singlet oxygen are quenched, protecting cells from reactive oxygen damage under dehydration stress, which is thought to be the cause of the rise in carotenoids (Tamura and Ishikita, 2020). Carotenoids serve as antioxidants in addition to harvesting light in the blue-green spectrum, and under various stress circumstances, their concentration rises along with a corresponding decline in Chl-*a* (Stamatidis et al., 2014; Zakar et al., 2017). Carotenoids regulate how much energy is transferred from the phycobilisome to the PSII reaction center (Kirilovsky, 2007). Zeaxanthin, a type of carotenoid, is crucial for photosynthetic organisms to respond quickly to stress. It has been thoroughly demonstrated that zeaxanthin binding to the PSII antenna system aids in the dissipation of extra chlorophyll-excited states and the scavenging of oxygen radicals (Ballottari et al., 2014; Tian et al., 2017).

TABLE 1 Effects of different durations of dehydration treatment on photosynthetic pigments of *N. calicicola* BOT1.

| Duration of treatment | Chlorophyll- <i>a</i> (µg/mg DW) |                           | Carotenoids (µg/mg DW)   |                          | Scytonemin (µg/mg DW)      |                          | Chl- <i>a</i> /Caro ratio (µg/mg DW)       |                           | Chl- <i>a</i> /Scyt ratio (µg/mg DW) |                           |
|-----------------------|----------------------------------|---------------------------|--------------------------|--------------------------|----------------------------|--------------------------|--|---------------------------|--------------------------------------|---------------------------|
|                       | AD                               | DD                        | AD                       | DD                       | AD                         | DD                       | AD   | DD                        | AD                                   | DD                        |
| 0                     | 2.81 ± 0.00 <sup>a</sup>         | 2.81 ± 0.00 <sup>A</sup>  | 2.85 ± 0.00 <sup>d</sup> | 2.85 ± 0.00 <sup>E</sup> | 0.10 ± 0.00 <sup>e</sup>   | 0.10 ± 0.00 <sup>D</sup> | 0.98 ± 0.00 <sup>a</sup>                   | 0.98 ± 0.00 <sup>A</sup>  | 28.18 ± 0.67 <sup>a</sup>            | 28.18 ± 0.67 <sup>A</sup> |
| 6                     | 2.47 ± 0.23 <sup>ab</sup>        | 2.75 ± 0.08 <sup>A</sup>  | 2.71 ± 0.00 <sup>e</sup> | 2.26 ± 0.00 <sup>F</sup> | 0.25 ± 0.01 <sup>d</sup>   | 0.30 ± 0.03 <sup>C</sup> | 0.76 ± 0.00 <sup>c</sup>                   | 0.83 ± 0.00 <sup>C</sup>  | 3.07 ± 0.00 <sup>d</sup>             | 3.30 ± 0.00 <sup>C</sup>  |
| 12                    | 2.46 ± 0.05 <sup>ab</sup>        | 2.53 ± 0.16 <sup>AB</sup> | 2.05 ± 0.00 <sup>f</sup> | 3.34 ± 0.00 <sup>B</sup> | 0.43 ± 0.00 <sup>b</sup>   | 0.49 ± 0.01 <sup>B</sup> | 0.90 ± 0.00 <sup>b</sup>                   | 0.80 ± 0.00 <sup>D</sup>  | 4.25 ± 0.00 <sup>d</sup>             | 4.58 ± 0.02 <sup>BC</sup> |
| 24                    | 2.20 ± 0.05 <sup>b</sup>         | 2.23 ± 0.03 <sup>B</sup>  | 3.11 ± 0.00 <sup>b</sup> | 3.00 ± 0.00 <sup>D</sup> | 0.39 ± 0.01 <sup>c</sup>   | 0.46 ± 0.00 <sup>B</sup> | 0.73 ± 0.00 <sup>d</sup>                   | 0.86 ± 0.00 <sup>B</sup>  | 8.72 ± 0.02 <sup>b</sup>             | 5.64 ± 0.00 <sup>B</sup>  |
| 48                    | 2.15 ± 0.03 <sup>b</sup>         | 2.27 ± 0.05 <sup>B</sup>  | 3.36 ± 0.00 <sup>a</sup> | 3.41 ± 0.00 <sup>A</sup> | 0.43 ± 0.00 <sup>b</sup>   | 0.51 ± 0.00 <sup>B</sup> | 0.70 ± 0.00 <sup>e</sup>                   | 0.78 ± 0.00 <sup>E</sup>  | 5.49 ± 0.00 <sup>c</sup>             | 5.19 ± 0.01 <sup>B</sup>  |
| 96                    | 2.04 ± 0.00 <sup>b</sup>         | 2.20 ± 0.00 <sup>B</sup>  | 2.93 ± 0.00 <sup>c</sup> | 3.28 ± 0.00 <sup>C</sup> | 0.51 ± 0.00 <sup>a</sup>   | 0.61 ± 0.00 <sup>A</sup> | 0.69 ± 0.00 <sup>f</sup>                   | 0.67 ± 0.00 <sup>F</sup>  | 3.98 ± 0.00 <sup>d</sup>             | 3.57 ± 0.00 <sup>CD</sup> |
| Phycobiliproteins     |                                  |                           |                          |                          |                            |                          |  |                           |                                      |                           |
|                       | Phycocyanin (µg/mg DW)           |                           | Phycoerythrin (µg/mg DW) |                          | Allophycocyanin (µg/mg DW) |                          | Total phycobiliproteins (TPBPs) (µg/mg DW) |                           | TPBP/Chl- <i>a</i> (µg/mg DW)        |                           |
|                       | AD                               | DD                        | AD                       | DD                       | AD                         | DD                       | AD   | DD                        | AD                                   | DD                        |
| 0                     | 7.02 ± 0.01 <sup>a</sup>         | 7.02 ± 0.01 <sup>A</sup>  | 1.59 ± 0.01 <sup>a</sup> | 1.59 ± 0.01 <sup>A</sup> | 3.96 ± 0.03 <sup>a</sup>   | 3.96 ± 0.03 <sup>A</sup> | 12.58 ± 0.08 <sup>a</sup>                  | 12.58 ± 0.08 <sup>A</sup> | 4.46 ± 0.01 <sup>a</sup>             | 4.46 ± 0.01 <sup>A</sup>  |
| 6                     | 6.73 ± 0.16 <sup>b</sup>         | 7.01 ± 0.58 <sup>A</sup>  | 1.11 ± 0.01 <sup>b</sup> | 1.17 ± 0.09 <sup>B</sup> | 2.86 ± 0.01 <sup>b</sup>   | 3.97 ± 0.00 <sup>A</sup> | 10.71 ± 0.17 <sup>b</sup>                  | 12.16 ± 0.52 <sup>A</sup> | 4.39 ± 0.38 <sup>a</sup>             | 4.43 ± 0.34 <sup>A</sup>  |
| 12                    | 5.18 ± 0.01 <sup>c</sup>         | 5.73 ± 0.11 <sup>B</sup>  | 0.83 ± 0.01 <sup>c</sup> | 0.85 ± 0.02 <sup>C</sup> | 2.87 ± 0.01 <sup>b</sup>   | 2.40 ± 0.00 <sup>B</sup> | 8.90 ± 0.01 <sup>c</sup>                   | 8.99 ± 0.11 <sup>B</sup>  | 3.61 ± 0.08 <sup>b</sup>             | 3.57 ± 0.20 <sup>B</sup>  |
| 24                    | 5.04 ± 0.02 <sup>c</sup>         | 4.16 ± 0.13 <sup>C</sup>  | 0.71 ± 0.03 <sup>d</sup> | 0.82 ± 0.05 <sup>C</sup> | 2.23 ± 0.05 <sup>d</sup>   | 2.15 ± 0.02 <sup>C</sup> | 7.99 ± 0.05 <sup>d</sup>                   | 7.14 ± 0.10 <sup>C</sup>  | 3.63 ± 0.07 <sup>b</sup>             | 3.20 ± 0.07 <sup>BC</sup> |
| 48                    | 3.44 ± 0.02 <sup>e</sup>         | 2.92 ± 0.09 <sup>D</sup>  | 0.43 ± 0.05 <sup>e</sup> | 0.77 ± 0.01 <sup>C</sup> | 2.42 ± 0.05 <sup>c</sup>   | 2.09 ± 0.03 <sup>C</sup> | 6.29 ± 0.04 <sup>e</sup>                   | 5.79 ± 0.09 <sup>D</sup>  | 2.92 ± 0.06 <sup>bc</sup>            | 2.54 ± 0.04 <sup>CD</sup> |
| 96                    | 3.94 ± 0.05 <sup>d</sup>         | 2.83 ± 0.02 <sup>D</sup>  | 0.40 ± 0.04 <sup>e</sup> | 0.40 ± 0.02 <sup>D</sup> | 1.18 ± 0.04 <sup>e</sup>   | 1.27 ± 0.08 <sup>D</sup> | 5.53 ± 0.10 <sup>f</sup>                   | 4.51 ± 0.08 <sup>E</sup>  | 2.70 ± 0.05 <sup>c</sup>             | 2.04 ± 0.03 <sup>D</sup>  |

Chl-*a*: Chlorophyll-*a*, Caro: Carotenoids, Scyt: Scytonemin.

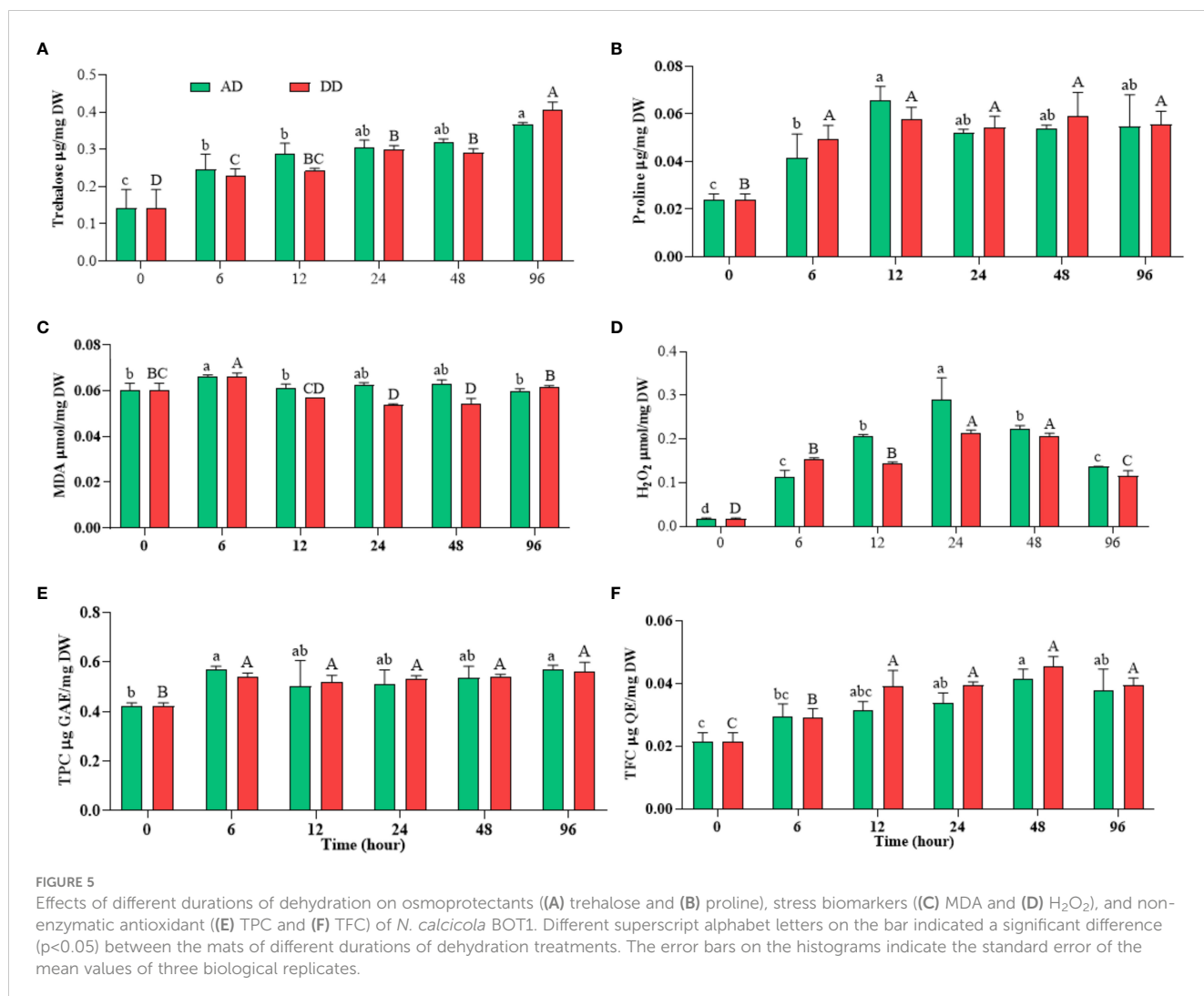
Different letters indicate a significant difference ( $p < 0.05$ ) between the mats of different durations of dehydration treatments. The data given here is the mean of three biological replicates with standard error.

The Chl-*a*/carotenoids ratio decreased significantly with increasing dehydration and reached its minimum in 96 h AD and DD mats, which was ( $0.695 \pm 0.000 \mu\text{g/mg DW}$ ) and ( $0.670 \pm 0.000 \mu\text{g/mg DW}$ ), respectively. This result is very similar to Tammam et al. (2011). The Chl-*a*/scytonemin ratio was very similar to the Chl-*a*/carotenoids ratio; both decreased during subsequent dehydration treatment compared to the control.

So, a change in the Chl-*a*/carotenoids ratio serves as a helpful physiological measure that may be utilized to evaluate how the stressor affects ROS levels (Zakar et al., 2017). Low Chl-*a*/carotenoids ratios during dehydration stress (Table 1) indicated that dehydrated mats had significant ROS levels, which were validated by MDA and H<sub>2</sub>O<sub>2</sub> measurements (Figure 5).

Phycobiliproteins are characteristic-colored pigments found in cyanobacteria and red algae. They act as the light-harvesting complex of PSII during photosynthesis. The PC ( $7.027 \pm 0.015 \mu\text{g/mg DW}$ )

and PE ( $7.958 \pm 0.079 \mu\text{g/mg DW}$ ) content were highest in the control compared to dehydration durations. PC decreased significantly ( $p < 0.05$ ) in 96 h AD and DD mats, which were ( $3.942 \pm 0.054 \mu\text{g/mg DW}$ ) and ( $2.837 \pm 0.024 \mu\text{g/mg DW}$ ), respectively, i.e., 1.78 and 2.47 fold lower than the control (Table 1). PE has a similar transcription pattern to PC, which is ( $2.044 \pm 0.126 \mu\text{g/mg DW}$ ) and ( $2.009 \pm 0.081 \mu\text{g/mg DW}$ ), i.e., 3.89 and 3.96 fold lower than the control in 96 h AD and DD mats, respectively. APC was 3.36, 3.11 fold lower in 96 h AD and DD mats than the control. Our results indicate that total phycobiliproteins (TPBP) were at their maximum in the control ( $18.954 \pm 0.111 \mu\text{g/mg DW}$ ), but their content decreased significantly ( $p < 0.05$ ) in AD and DD mats at 96 h of dehydration treatment. The TPBP/Chl-*a* ratio exhibited the same trend as TPBP and decreased significantly in AD and DD mats after 6, 12, 24, 48, and 96 hours of dehydration treatment (Table 1). The



results indicate that severe dehydration reduces their synthesis and promotes degradation under conditions of water stress.

## Dehydration-dependent accumulation of protein, carbohydrate, and lipid contents

Primary metabolites like carbohydrates, proteins, and lipids are extensively synthesized and utilized during the growth phase. Protein content is the marker of growth and its concentration decreased significantly ( $p < 0.05$ ) during dehydration treatment (Figure 6A). Protein content was highest in the control, at ( $0.592 \pm 0.017 \mu\text{g}/\text{mg DW}$ ), and was at its minimum in 96 h dehydrated mats, at ( $0.449 \pm 0.011 \mu\text{g}/\text{mg DW}$ ) in AD mats and ( $0.457 \pm 0.014 \mu\text{g}/\text{mg DW}$ ) in DD mats.

The dried mats from AD and DD, which were 1.31 and 1.29 fold less than the control, did not show a significant difference. Notably, high TPBP contents directly correlated with high protein accumulation under control conditions, while TPBP contents accumulated at the lowest levels in 96 h AD and DD mats. Similar results were also obtained in several microalgae under abiotic stress (Fal et al., 2022). Autophagy, degradation, and downregulation of genes may be the primary causes of decreased protein and pigment

content in dehydrated cells (Pancha et al., 2015; Chokshi et al., 2017). The reduction in protein content was very similar, with photosynthetic efficiency and different pigment content.

Under dehydration stress, carbohydrate content increased significantly ( $p < 0.05$ ) and its use by cells during prolonged stress conditions was shown (Figure 6B). Carbohydrate quantitatively increased depending on the stress levels of cells. Dehydration treatment provided the highest level of support for carbohydrate accumulation compared to the control, in *N. calicicola* BOT1. (Figure 6B). It was significantly ( $p < 0.05$ ) increased in 96 h AD and DD mats, at ( $1.611 \pm 0.025 \mu\text{g}/\text{mg DW}$ ) and ( $1.574 \pm 0.040 \mu\text{g}/\text{mg DW}$ ), i.e., 1.67 and 1.64 fold greater than the control. Under prolonged stress conditions, cyanobacteria utilized stored carbohydrates as osmoprotectants, like sucrose, trehalose, etc., to ensure homeostasis, maintain osmotic status, and promote adaptability to stress conditions (Tietel et al., 2020).

Abiotic stresses induce the accumulation of lipids in cells, which stabilize the plasma membrane during stressful conditions. Several previous reports have also suggested that lipid content increased during stress conditions due to the conversion of carbohydrates to lipids by several metabolic pathways (Hounslow et al., 2021; Jin et al., 2021). Lipid accumulation during dehydration was measured



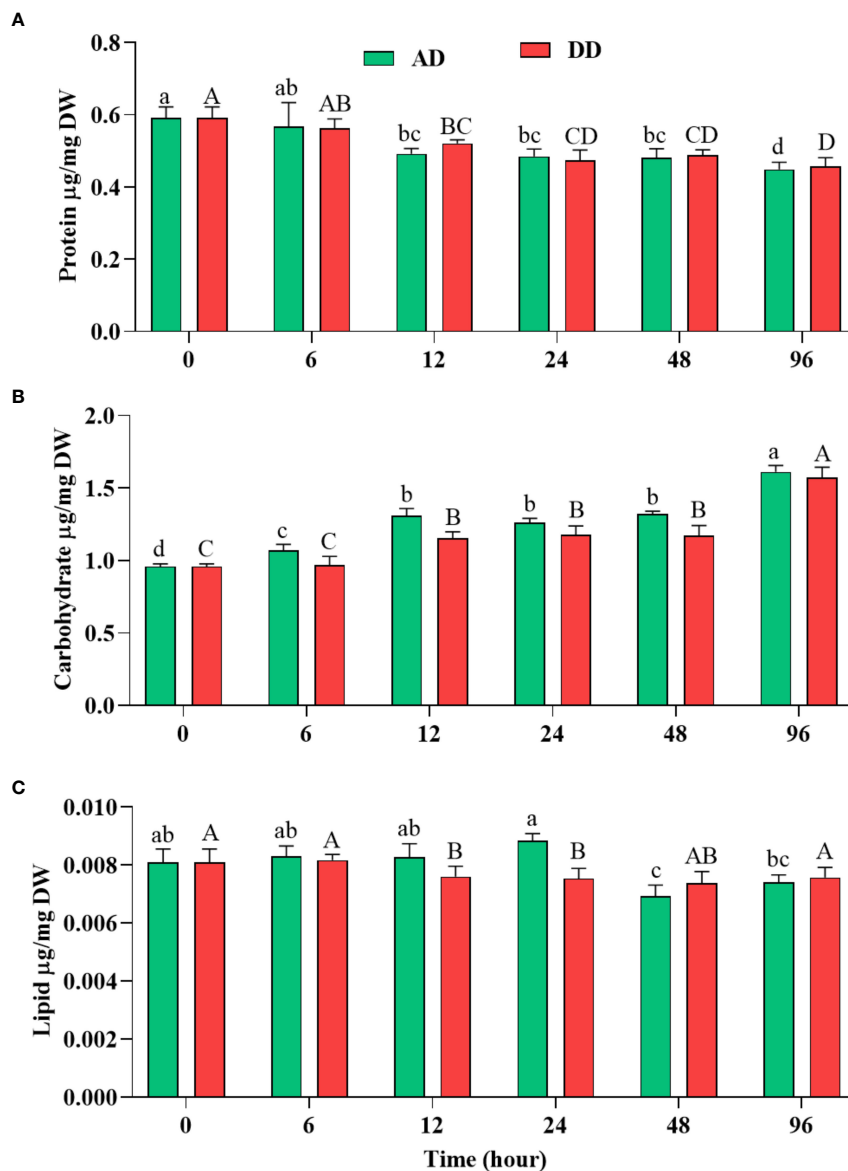


FIGURE 6

Effect of different duration of dehydration on different biochemicals of *N. calicicola* BOT1. Different superscript alphabet letters on the bar indicate a significant difference ( $p < 0.05$ ) between the mats of different durations of dehydration treatments. (A) protein, (B) carbohydrate, and (C) lipid. The error bars on the histograms indicate the standard error of the mean values of three biological replicates.

using the gravimetric method (Feng et al., 2013), which showed a similar percentage of lipid content in all the treatments, at ( $0.0076 \pm 0.000 \mu\text{g}/\text{mg DW}$ ) and ( $0.0075 \pm 0.000 \mu\text{g}/\text{mg DW}$ ), which were decreased by 1.21 and 1.24 fold in 12 and 24 h DD mats, respectively compared to the control (Figure 6C). Our findings suggest that there was no role for lipids in the survival of *N. calicicola* BOT1 under dehydration stress.

## Accumulation of osmoprotectants in response to dehydration

Under the conditions of water scarcity, generally, sugars provide stability of proteins, membranes, and whole cells, but in cases of

acute water loss, only disaccharides trehalose and sucrose have the ability to provide protection (Potts, 1994). Desiccation appears to be the catalyst for trehalose buildup as the concentration rises rapidly when the water content falls below a certain level (Yoshida and Sakamoto, 2009). The rate of trehalose generation is greater than the rate of hydrolysis, and it has been hypothesized that the trehalase enzyme is crucial in the accumulation of trehalose. This is accomplished through the particular inactivation of trehalase in situations of water stress, which are characterized by elevated concentrations of cellular solutes (Yoshida and Sakamoto, 2009). In untreated *N. calicicola* BOT1, it was ( $0.142 \pm 0.028 \mu\text{mole}/\text{mg DW}$ ), while with the increased duration of dehydration, its concentration increased and vice versa, reaching its maximum in 96 h AD and DD mats, at ( $0.366 \pm 0.003 \mu\text{mole}/\text{mg DW}$ ) and

( $0.0407 \pm 0.011 \mu \text{ mole/mg DW}$ ), respectively (Figure 5A). The trehalose concentration of 96 h AD and DD mats was enhanced 2.577 and 2.86 fold compared to untreated mats, which showed a dehydration response.

In line with these findings, natural *N. commune* colonies do not exhibit trehalose buildup in response to desiccation (Sakamoto et al., 2009), indicating that the control of trehalose metabolism may differ in these *Nostoc* species. Trehalose concentration in *N. calcicola* BOT1 was higher in the dehydrated mats compared to the control, but it is still sensitive to desiccation; this study is also comparable to Sakamoto et al. (2009).

Since most stress proteins are water-soluble, they aid in the process of stress tolerance by keeping cellular structures hydrated. Dehydration stress also enhances proline synthesis. Proline is an essential amino acid that performs a number of functions, including preserving the cytosolic pH, acting as a compatible solute, scavenging ROS, and acting as a chaperone molecule to preserve the integrity of protein structure (Fal et al., 2022). Our results show that *N. calcicola* BOT1 had significantly ( $p < 0.05$ ) more proline than the control (Figure 5B). Proline accumulation in 12 h AD and DD mats was ( $0.065 \pm 0.003 \mu \text{ mole/mg DW}$ ) and ( $0.057 \pm 0.002 \mu \text{ mole/mg DW}$ ), which was 2.74 and 2.40 fold greater than the control. Sarker et al. (2018) found similar results in *Amaranthus tricolor* under drought stress. The levels of proline rose during drought stress, while soluble protein decreased under stress conditions (Abid et al., 2018; Barnawal et al., 2019). Glycine, betaine, and proline increased the turgor potential within cells, which enable cyanobacteria to adapt against desiccation stress by maintaining the integrity of cellular structures, scavenging ROS, and protecting the transcriptional and translational machinery of cyanobacteria (Hussain Wani et al., 2013). Additionally, proline inhibits the denaturation of enzymes, elevates the thermo-tolerance of enzymes, and acts as a buffer for cellular redox potential (Berard et al., 2015; Ngumbi and Kloepper, 2016).

## Dehydration effect on stress biomarkers

Stresses aggravate the generation of ROS viz- singlet oxygen hydroxyl radical, superoxide, and hydrogen peroxide and cause oxidative damage in cells (Sharma et al., 2013). The estimation of MDA content is used as a lipid peroxidation marker in studies related to oxidative stress. ROS may interact with macro- and micro-molecules, obstructing cellular processes. ROS are regarded as highly reactive molecules, even though they are considered crucial components of aerobic life due to their direct or indirect role in stress adaptation and the regulation of plant development from germination to senescence (Morales and Munné-Bosch, 2019). Different organelles, such as mitochondria and chloroplasts, serve as both the source and the initial target of ROS generated under drought stress (Farooq et al., 2009). ROS are highly reactive and quickly oxidize other target molecules, which leads to lipid peroxidation among other biochemical reactions. ROS production and lipid peroxidation are both fundamental aspects of aerobic life and essential traits of photosynthetic organisms. Therefore, both nonenzymatic and enzymatic lipid peroxidation

processes may lead to the formation of MDA and other lipid peroxidation products in plants (Weber et al., 2004; Farmer and Mueller, 2013). MDA is a main constituent of lipid peroxidation, which is caused by free radicals oxidizing polyunsaturated fatty acids. In *N. calcicola* BOT1, MDA contents were significantly increased in AD and DD mats at 6 h of dehydration; they were ( $0.0663 \pm 0.000 \mu \text{ mol/mg DW}$ ) and ( $0.0659 \pm 0.000 \mu \text{ mol/mg DW}$ ), i.e., 1.09 and 1.09 fold higher than the control, respectively. Beyond increasing the duration of dehydration, decreased MDA content was found in the cells of DD mats, while there was no significant change in AD mats (Figure 5C). Our obtained result also correlates with the findings of Christou et al. (2013), who studied strawberries. In contrast, increasing the duration of dehydration increased the  $\text{H}_2\text{O}_2$  content, and it reached its maximum at 24 h of dehydration treatment in both AD and DD samples, at ( $0.289 \pm 0.029 \mu \text{ mol/mg DW}$ ) and ( $0.2146 \pm 0.003 \mu \text{ mol/mg DW}$ ), i.e., 17 and 12.5 fold higher than the control (Figure 5D).  $\text{H}_2\text{O}_2$  concentration decreased in further dehydration treatment compared to 24 h treatments. In the current study, high  $\text{H}_2\text{O}_2$  buildup in *N. calcicola* BOT1 at 24 h of dehydration may have amplified the Haber-Weiss reaction, causing the generation of hydroxyl radicals, which in turn caused severe lipid peroxidation in cell organelles and plasma membrane destruction (Mittler, 2002). ROS generation may cause changes in microalgal metabolism like decreased  $\text{CO}_2$  fixation, nutrient uptake, photoreduction, and damage to the reaction center (Fal et al., 2022). In contrast, the production of  $\text{H}_2\text{O}_2$  is essential for the synthesis of plant hormones like brassinosteroids, jasmonates, and abscisic acid, which improve plant, algae, and cyanobacterial stress tolerance (Zhou et al., 2014; Qu et al., 2021). The regulation of various physiological and biochemical processes related to plant growth and stress tolerance depends on signaling molecules, like jasmonates, and their derivatives (Kazan, 2015). Several cyanobacteria, including *Anabaena*, *Cylindrospermum*, *Calothrix*, *Nostoc*, *Spirulina*, *Synechococcus* sp., and *Scytonema* have been found to synthesize and produce jasmonate in previous studies (Ueda et al., 1991; Tsavkelova et al., 2006).

The depleted ROS level after 24 h of treatment may be due to the suppression of ROS production and the enhancement of anti-oxidative enzymes, total carotenoid, TPC, TFC, and proline, which inhibit the  $\text{H}_2\text{O}_2$ , and MDA content. This suggests that the *N. calcicola* BOT1 was under extreme stress to repair the damage brought on by dehydration stress (Bieker and Zentgraf, 2013). In our study, compatible solutes like carotenoid, proline, TPC, and TFC were enhanced under dehydration conditions from 6 to 96 h to reduce MDA and  $\text{H}_2\text{O}_2$  accumulation. Additionally, the substantial negative connection between MDA,  $\text{H}_2\text{O}_2$ , pigments, and protein suggests that oxidative stress brought on by dehydration-induced MDA and  $\text{H}_2\text{O}_2$  generation may be one of the factors inhibiting pigment production in *N. calcicola* BOT1.

## Dehydration effect on non-enzymatic assay

The TFC and TPC are potent ROS scavengers that maintain the integrity of the membrane and insulate cells against oxidative stress

(Mukherjee et al., 2020; Fal et al., 2022). In this investigation, *N. calicicola* BOT1 showed a significant ( $p < 0.05$ ) rise in TFC and TPC in dehydrated mats (Figures 5E, F). The TFC in isolated *N. calicicola* BOT1 was at its maximum in 48 h dehydrated mats of AD and DD (Figure 5E), at  $(0.041 \pm 0.001 \mu\text{g QE/mg DW})$  and  $(0.045 \pm 0.001 \mu\text{g QE/mg DW})$ , i.e., 1.9 and 2.1-fold greater than the control. TPC was always greater in dehydrated mats compared to the control (Figure 5F). TPC was at its maximum in 6 h AD and DD mats, at  $(0.567 \pm 0.009 \mu\text{g GAE/mg DW})$  and  $(0.538 \pm 0.009 \mu\text{g GAE/mg DW})$ , which was 1.34 and 1.27-fold greater than the control. A previous study also found that *Chlamydomonas reinhardtii* and *Acutodesmus dimorphus* significantly increased their TFC and TPC levels under stress conditions (Chokshi et al., 2017). Reddy et al. (2004) also reported an ameliorated response of TFC and TPC under drought stress in higher plants.

## Vital staining by dual fluorescence dye

Fluorescence-based live-dead assays of the cells during dehydration treatments are presented in Figure 7. The green and red fluorescence intensity distributions in live-dead filaments were stained with FDA and PI. PI is a nuclear-binding dye; damaged or dead cells allow the entry of PI inside the cell, while a live cell does not (Deligeorgiev et al., 2009). In contrast, FDA is taken up by cells, which results in the conversion of non-fluorescent to fluorescent green metabolite fluorescein and stains the live or viable cell (Gumbo et al., 2014). Fluorescence microscopic images confirmed that dehydration acts in a dose-dependent manner, i.e., with a gradual increase in the duration of the dehydration treatment, dead cells increased (Figure 7). The results indicate that decreased water content increased the live-dead cell ratio. Fluorescence microscopy also showed morphological changes in the filaments and their compactness. Microphotographs showed a positive correlation with photosynthetic efficiency, pigment composition, and ROS production

in cells. PI and FDA fluorescent staining were used by Yewalkar et al. (2019) for the determination of live-dead status under a photobioreactor for *Chlorella pyrenoidosa*, *Synechococcus* 7002, *Scenedesmus dimorphus*, and *Synechococcus elongatus* 7942. The dual-staining technique was also used by Fan et al. (2013) to detect the viability of *Microcystic* sp. after exposure to ultrasonic radiation.

## Metabolites profiling through UHPLC-HRMS

Utilizing UHPLC-HRMS, the metabolite profiles of *N. calicicola* BOT1 control and 96 h DD mats were examined. The base peak chromatograms of the control and 96 h DD mats were obtained via negative and positive ion mode, and the extracted ion chromatograms (EICs) for some of the significant identified compounds are shown in Figures 8A, B. Compounds were identified based on precise mass measurements, elemental composition, and analysis of the fragmentation pattern generated through MS2 sign. The names of the detected compounds, their chemical formulas, Annot. DeltaMass (ppm), computed molecular weights, m/z values, retention times, Log2 fold change (indicating up and down-regulated metabolites), and peak areas are listed in Table 2 and Supplementary Table 1, respectively. According to Log2 fold change, the majority of the chemicals were elevated throughout the 96 h desiccator dehydrating mat treatment.

Metabolite changes during dehydration included nucleotide derivatives, amino acids, carbohydrates, antioxidants, polyamines, lipids, and some defense compounds. The metabolomics analyses in the control and dehydrated mats revealed several significant compounds, which are listed below (Table 2; Supplementary Table 1). The 96-hour dehydrated mats metabolic profile was different from that of the control. The more prevalent metabolites were amino acids followed by peptides, nucleotides, lipids, and secondary metabolites.

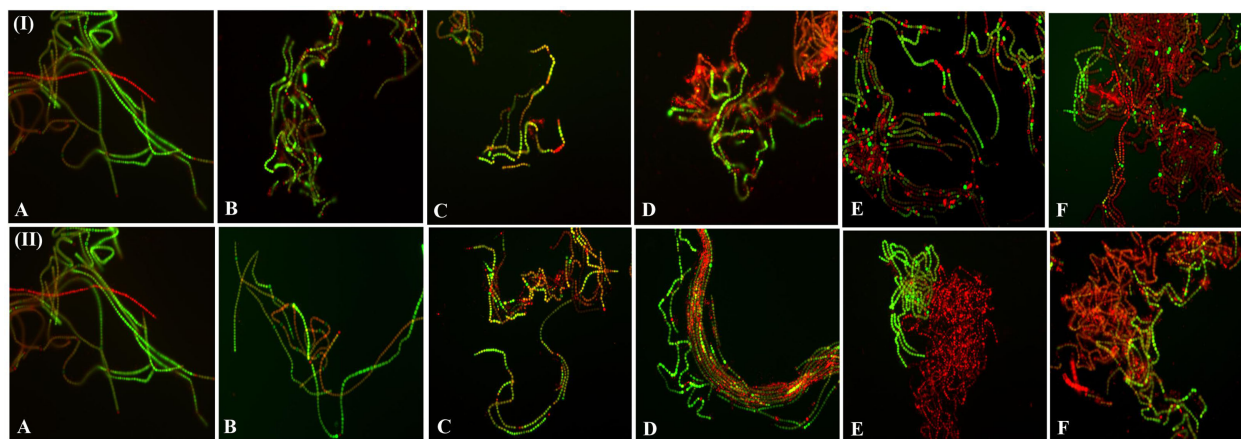


FIGURE 7

Fluorescence microscopic photographs (at 20X magnification) of *N. calicicola* BOT1 at different durations of dehydration treatment. Cyanobacterial mats were stained with FDA and PI. Live cells were stained with FDA and fluorescent green, while dead cells were stained with PI, fluorescent red, and yellow. (I) air-dried mats and (II) desiccator-dried mats in which (A) indicates control, and (B–F), denote dehydration treatments for 6, 12, 24, 48, and 96 hours, respectively.

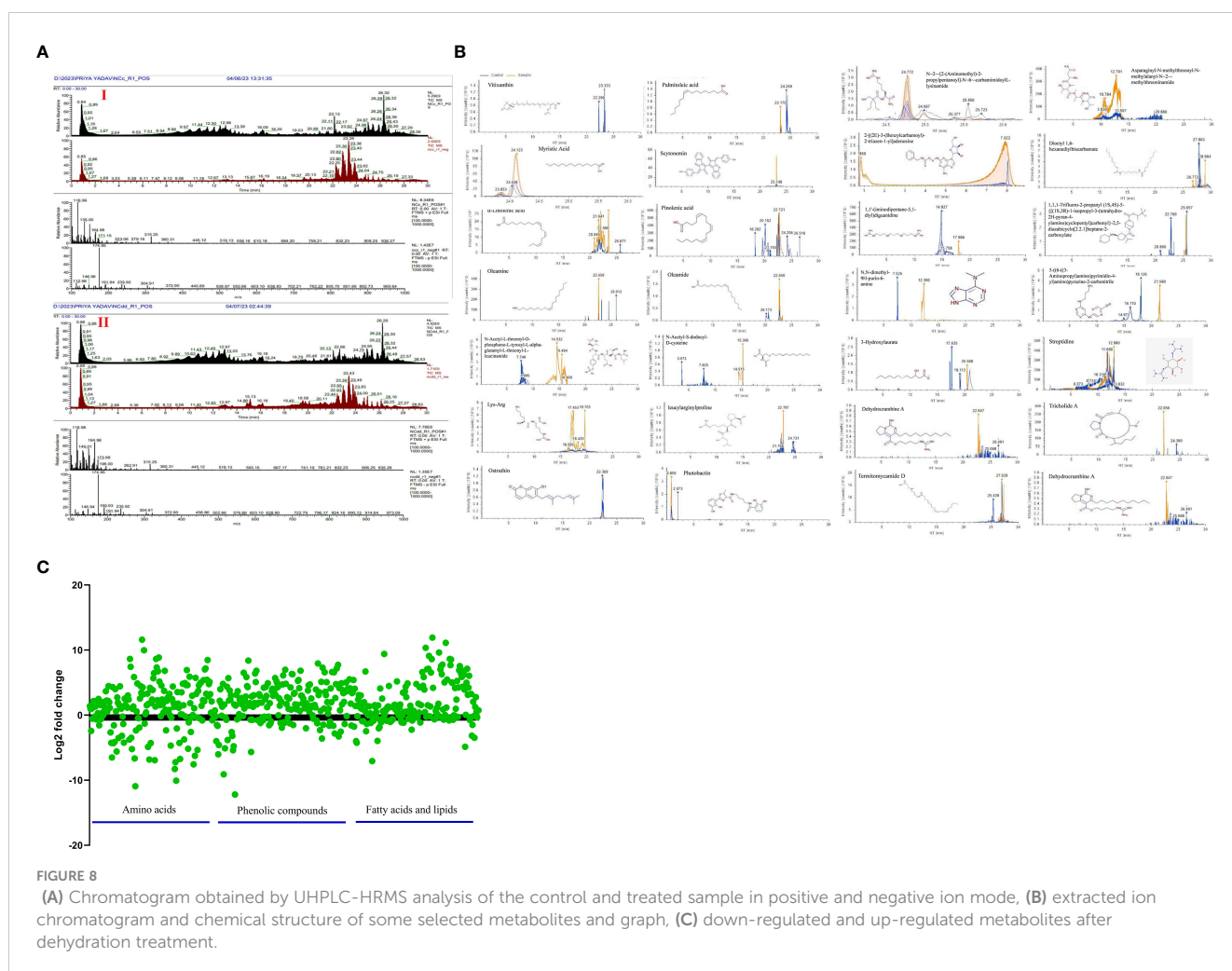


FIGURE 8

(A) Chromatogram obtained by UHPLC-HRMS analysis of the control and treated sample in positive and negative ion mode, (B) extracted ion chromatogram and chemical structure of some selected metabolites and graph, (C) down-regulated and up-regulated metabolites after dehydration treatment.

While under dehydration stress, the amino acids, peptides, and nucleotide metabolites were overrepresented (Yobi et al., 2013). Several plants have been shown to accumulate more amino acids when exposed to drought stress (Bowne et al., 2012; Silvente et al., 2012; Hochberg et al., 2013; Rahman et al., 2017). Some unknown metabolites were more prevalent under dehydration stress than they were under hydrated conditions, indicating that they may play a part in desiccation tolerance. Dehydration causes the metabolism to shift in favor of producing carbohydrate, antioxidant, and nitrogen remobilization (Oliver et al., 2011). While fully hydrated mats contain large amounts of alanine and glycine (Khan et al., 2019), amino acids such as lysine, threonine, glutamine, aspartate, glutamate, arginine, asparagine, N-5~-(Diaminomethylene)-L-ornithylglycinamide, leucylarginylproline N-Acetyl-S-dodecyl-D-cysteine, Fluoro[bis(2-methyl-2-propenyl)]2-propyn-1-ylsilane, N-Acetyl-L-threonyl-O-phosphono-L-tyrosyl-L-alpha-glutamyl-L-threonyl-L-leucinamide, (E)-N~6~-(1-Aminoethylidene)-N-2H-tetrazol-5-yl-L-lysineamide are prominent in dehydrated mats. Martinelli et al. (2007) and Oliver et al. (2011) observed the accumulation of arginine, asparagine, glutamine, glutamate, and quinate during desiccation in *Sporobolus stapfianus*. According to Hoekstra et al. (2001), alterations in lipid compositions are crucial for desiccation tolerance because maintaining membrane integrity

is crucial for dehydration tolerance. Under dehydration stress, a number of fatty acids, including oleic acid, palmitoleic acid, myristic acid, linolenic acid, pinolenic acid, oleamine, and oleamide, are overrepresented in order to preserve the integrity of the membrane. Periodic desiccation also promotes the synthesis of scytonemin in *Chroococcidiopsis* sp. (Fleming and Castenholz, 2007), which may be another protective mechanism for survival under dehydration stress. 3-Hydroxylaurate is a medium-chain fatty acid anion and a 3-hydroxy fatty acid anion. A polycyclic guanidine alkaloid called dehydrocrambine A prevents HIV-1 fusion (Chang et al., 2003). Ostruthin, Tricholide A, Termitomycamide D, and Streptidine show prominent antimicrobial, antibacterial, cytotoxic, and antimycobacterial activity (Schinkovitz et al., 2003; Choi et al., 2010; Bertin et al., 2017).

## Cyanobacteria's mechanisms of adaptation to dehydration stress and their function in reducing drought stress on plants

The variety of cyanobacterial species is a primary constituent of biocrust, which can withstand desiccation, extremely high or low temperatures, salinity, and pH (Singh and Jha, 2016). Acclimation



TABLE 2 List of major compounds identified by UHPLC-HRMS analysis through negative and positive ion mode, showing chemical formula, Annot.

| Metabolites  | Formula  | Annot. DeltaMass (ppm) | Calc. MW  | m/z       | RT [min] | Log2 Fold Change: (Treated)/(Control) | Area (Max.) |
|--|--|------------------------|-----------|-----------|----------|---------------------------------------|-------------|
| Vitixanthin  | C <sub>33</sub> H <sub>42</sub> O <sub>6</sub>                               | 4.99                   | 534.3008  | 533.2936  | 23.34    | 1.67                                  | 5730511.16  |
| Palmitoleic acid   | C <sub>16</sub> H <sub>30</sub> O <sub>2</sub>                               | 0.36                   | 254.2247  | 571.91    | 23.173   | 0.312                                 | 1912670.34  |
| Myristic Acid  | C <sub>14</sub> H <sub>28</sub> O <sub>2</sub>                               | 0.36                   | 228.209   | 182.81    | 24.205   | 1.023                                 | 13944229.86 |
| Scytonemin   | C <sub>36</sub> H <sub>20</sub> N <sub>2</sub> O <sub>4</sub>                | 0.24                   | 544.1424  | 451.21    | 23.165   | .07                                   | 30145757.4  |
| α-Linolenic acid   | C <sub>18</sub> H <sub>30</sub> O <sub>2</sub>                               | 0.39                   | 278.2247  | 416.29    | 22.465   | 0.173                                 | 4545133.92  |
| Pinolenic acid   | C <sub>18</sub> H <sub>30</sub> O <sub>2</sub>                               | -0.6                   | 278.2244  | 461.52    | 22.667   | .99                                   | 3517728.04  |
| Oleamine   | C <sub>18</sub> H <sub>37</sub> N  | 0.3                    | 267.2927  | 142.87    | 22.661   | .07                                   | 1742349.93  |
| Oleamide   | C <sub>18</sub> H <sub>35</sub> NO   | 0.23                   | 281.2719  | 526.72    | 22.704   | .21                                   | 5638042.91  |
| N-Acetyl-L-threonyl-O-phosphono-L-tyrosyl-L-alpha-glutamyl-L-threonyl-L-leucinamide  | C <sub>30</sub> H <sub>47</sub> N <sub>6</sub> O <sub>14</sub> P             | 1.22                   | 746.2897  | 374.1521  | 15.49    | 8.64                                  | 28081785.5  |
| N-Acetyl-S-dodecyl-D-cysteine  | C <sub>17</sub> H <sub>33</sub> NO <sub>3</sub> S                            | -0.33                  | 331.218   | 252.02    | 15.333   | 1.09                                  | 1261055.12  |
| Lys-Arg  | C <sub>12</sub> H <sub>26</sub> N <sub>6</sub> O <sub>3</sub>                | 1.47                   | 302.2071  | 303.2141  | 20.151   | 1.69                                  | 12302196.3  |
| leucylarginylproline   | C <sub>17</sub> H <sub>32</sub> N <sub>6</sub> O <sub>4</sub>                | -4.95                  | 384.2466  | 383.2393  | 22.792   | 1.76                                  | 4200668.53  |
| N~2~- [2-(Aminomethyl)-2- propylpentanoyl]-N~6~- carbamimidoyl-L-lysineamide   | C <sub>9</sub> H <sub>18</sub> N <sub>8</sub> O                              | 2.74                   | 254.1611  | 255.1684  | 9.085    | 3.99                                  | 72178533.1  |
| Asparaginyl-N-methylthreonyl-methylalanyl-N~2~- methylthreoninamide  | C <sub>18</sub> H <sub>34</sub> N <sub>6</sub> O <sub>7</sub>                | 3.1                    | 446.2503  | 445.2432  | 10.59    | 4.43                                  | 8267989.56  |
| 2-[(2E)-3-(Benzylcarbamoyl)-2-triazene-1-yl]adenosine  | C <sub>18</sub> H <sub>21</sub> N <sub>9</sub> O <sub>5</sub>                | 0.19                   | 443.1667  | 442.1594  | 7.914    | 4.31                                  | 137634103   |
| Diocetyl 1,6-hexanediylbiscarbamate  | C <sub>24</sub> H <sub>48</sub> N <sub>2</sub> O <sub>4</sub>                | 2                      | 428.3623  | 429.3696  | 28.145   | 2.78                                  | 26242646.6  |
| 1,1'-(iminodipentane-5,1-diyl)diguandine   | C <sub>12</sub> H <sub>29</sub> N <sub>7</sub>                               | 2.22                   | 271.2491  | 272.2563  | 26.05    | 6.29                                  | 19082853.1  |
| 1,1,1-Trifluoro-2-propanyl (1S,4S)-5-[[[(1S,3R)-1-isopropyl-3-(tetrahydro-2H-pyran-4-ylamino) cyclopentyl]carbonyl]-2,5-diazabicyclo[2.2.1]heptane-2-carboxylate | C <sub>23</sub> H <sub>36</sub> F <sub>3</sub> N <sub>3</sub> O <sub>4</sub> | 1.26                   | 475.2664  | 476.2737  | 25.501   | 5.86                                  | 13290558.3  |
| N,N-dimethyl-9H-purin-6-amine  | C <sub>7</sub> H <sub>9</sub> N <sub>5</sub>                                 | 0.54                   | 163.0859  | 164.0932  | 12.4     | 7.43                                  | 49764270.2  |
| 5-((6-((3-Aminopropyl)amino)pyrimidin-4-yl)amino) pyrazine-2-carbonitrile  | C <sub>12</sub> H <sub>14</sub> N <sub>8</sub>                               | 2.43                   | 270.1348  | 271.1421  | 21.43    | 5.4                                   | 11391203.4  |
| 3-Hydroxylaurate   | C <sub>12</sub> H <sub>23</sub> O <sub>3</sub>                               | 4.85                   | 215.1658  | 216.173   | 20.492   | 4.06                                  | 28678283.4  |
| Photobactin  | C <sub>22</sub> H <sub>25</sub> N <sub>3</sub> O <sub>7</sub>                | -3.61                  | 443.16765 | 478.13786 | 0.866    | 2.13                                  | 22725890.45 |
| Streptidine  | C <sub>8</sub> H <sub>18</sub> N <sub>6</sub> O <sub>4</sub>                 | 4.23                   | 262.1401  | 261.1328  | 12.186   | 2.41                                  | 8162339.66  |
| Dehydrocrambine A  | C <sub>24</sub> H <sub>42</sub> N <sub>6</sub> O <sub>2</sub>                | -2.15                  | 446.336   | 447.343   | 22.841   | 3.56                                  | 4273424.71  |
| Tricholide A   | C <sub>24</sub> H <sub>41</sub> NO <sub>4</sub>                              | -4.82                  | 407.3016  | 406.2938  | 22.064   | 3.53                                  | 721042.996  |
| Ostruthin  | C <sub>19</sub> H <sub>22</sub> O <sub>3</sub>                               | 4.84                   | 298.1583  | 297.1511  | 22.101   | 2.31                                  | 399576947   |
| Termitomycamide D  | C <sub>24</sub> H <sub>44</sub> N <sub>2</sub> O <sub>3</sub>                | 1.82                   | 408.3359  | 409.3434  | 27.009   | 6.16                                  | 146232397   |

DeltaMass (ppm), cal. MW (calculated molecular weight), m/z value, RT (Retention Time), Log2 fold change, and peak area of control and 96 h DD mats in negative and positive ion mode.

strategies employed by cyanobacteria to survive under dehydration stress, including the synthesis and production of EPS, maintenance of ion channels, up-regulation of the DNA repair system, chaperone recruitment to maintain protein and enzyme integrity, synthesis of various compatible solutes, and oxidative stress protection system (Figure 9A), were used to adapt to low levels of available water (Nelson et al., 2021; Yadav et al., 2021; Yadav et al., 2022b).

Compatible solutes like water stress proteins (WspA), sucrose, trehalose, glycine betaine, and proline inhibit protein denaturation and unfolding, stabilize macromolecules, and protect against osmotic imbalance under low water potential (Dabralowski and Isayenkov 2022; Potts, 1999). Several cyanobacterial genera discharge EPS into the environment, which enhances soil stability, water retention, and crusting (Rossi and De Philippis, 2015; Rossi et al., 2017). The EPS

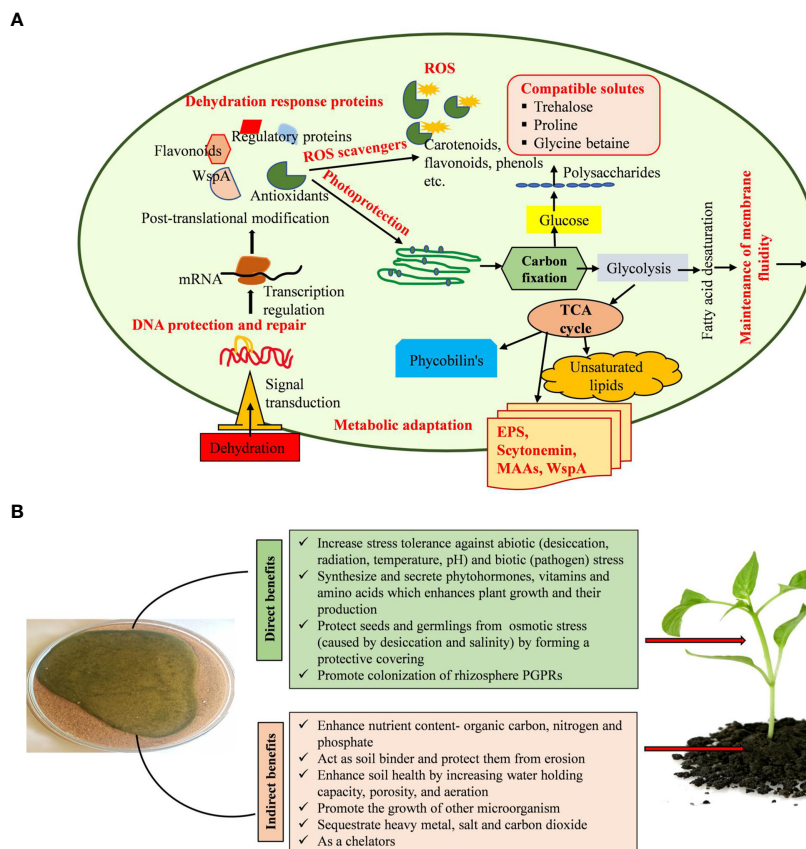


FIGURE 9

(A, B). Mechanisms used by cyanobacteria in alleviating dehydration stress and plant growth promotion.

produced by cyanobacteria is composed of numerous components and serves a variety of functions throughout its life cycle, including symbiosis and predation protection. EPS also protects the cell from various types of stresses like ultraviolet radiation, temperature, desiccation, and salinity stress (Adhikary and Sahu, 1998; Potts, 2004; Van Hijum et al., 2006). EPS bears the features of chelating metal ions and buffering  $H_2O_2$  (Hao et al., 2013; Gao et al., 2015; Zhang et al., 2013; Wang et al., 2014). WspA protein, glycan, mycosporine-like amino acids (MAAs), and scytonemin constitute the majority of the EPS matrix (Wright et al., 2005; Liu et al., 2017). EPS absorbs dew, vapor, and fog for the physiological repair of the cells (Agam and Berliner, 2006; Rao et al., 2009). In addition, serving as a barrier against desiccation, the presence of several functional groups, such as carboxyl, carbonyl, sulfate, and hydroxyl, in cyanobacteria's EPS allows it to accumulate heavy metals (Pereira et al., 2011). It was discovered that the polysaccharides secreted by *Dunaliella salina* activate the jasmonic acid pathway, a metabolic system involved in plants' response against stress, lowering the damages caused by salt stress in tomato cultures (El Arroussi et al., 2018). Similarly, seaweed extracts from *Fucus spiralis* and *Ulva rigida* were applied to bean plants to promote growth and increase their resistance to drought (Mansori et al., 2015).

EPS can absorb and hold water, generating a gelatinous coating around the cell and managing water intake and water loss due to its

hydrophobic and hydrophilic properties (Adhikary and Sahu, 1998; Caiola et al., 1996). Additionally, it supplies organic carbon and nitrogen, solubilizes and mobilizes phosphorus, boosts water retention, and synthesizes and secretes certain phytohormones, all of which have the ability to promote the germination and growth of desert plants (Figure 9B) (Song et al., 2017). The resulting biocrust will have an impact on the emergence and establishment of new plants in arid and semi-arid places (Muñoz-Rojas et al., 2018; Parsons, 2012; Xu et al., 2013). The EPS released by cyanobacteria has a major role in the protection of cells from salinity and desiccation by developing an outer buffer zone (Pointing and Belnap, 2012; Rossi et al., 2017; Chittapun et al., 2018). Cyanobacteria enhance the general functionality of higher plants, promoting their growth, and encourage the formation of antioxidant chemicals, which increases the plants' endurance in stress situations. The application of cyanobacteria as a biostimulant for crops under conditions of high or low temperatures, drought, and salt stress has proved successful (El Arroussi et al., 2018; Haggag et al., 2018). Cyanobacteria promote the growth of other bacteria, residing in the rhizosphere of plants (Badri et al., 2009; Noumavo et al., 2016). By defending plants from phytopathogens and synthesizing substances including hydrogen cyanide, antibiotics, and induced systemic resistance, these bacteria indirectly promote plant growth (Glick, 2014; Olanrewaju et al., 2017). It may be possible to promote plant development in challenging environmental conditions using

phytohormones produced by cyanobacteria (Kaushal and Wani, 2016). These phytohormones help plants cope with abiotic challenges and increase their chances of survival (Fahad et al., 2015; Vurukonda et al., 2016). Many phytohormones, including cytokinins, auxins, gibberellins, jasmonates, abscisic acid, and ethylene, either stimulate shoot development or control growth-inhibitory plant processes, including senescence, abscission, and dormancy, regulating plant growth activities (Liu et al., 2012; Ahmed and Hasnain, 2014). Through all these activities, cyanobacteria promote the development and growth of plants in semi-arid and arid areas.

## Conclusion

The aquatic halotolerant cyanobacterium *N. calcicola* BOT1 was found to be tolerant to moderate desiccation but sensitive to extreme dehydration despite its formation of microscopic colonies with extracellular polysaccharides. In response to dehydration, *N. calcicola* BOT1 accumulated trehalose and proline. Although trehalose deposition is often associated with excessive desiccation tolerance, it has previously been thought to be significant to desiccation tolerance. Understanding the alterations that occur in dehydrated cells is necessary to comprehend the process of dehydration tolerance. It may be possible to determine the most plausible causes for why some cells are sensitive to desiccation while others are not through further research aimed at understanding the mechanism underlying desiccation tolerance. These studies also offer the intriguing potential for biocrust development and the biofertilizer potential of cyanobacteria in semi-arid and arid areas. We were able to recognize the metabolites in dehydrated mats and detect metabolic alterations brought on by dehydration stress attributable to an improved HRMS technique. The study also highlights the functions of lipids, fatty acids, amino acids, and phenolic substances in the biochemical and physiological adjustment of *N. calcicola* BOT1 to dehydration stress. The morphological, physiological, and biochemical changes that occur during acclimation raise the possibility that these particular biomolecules have a significant impact on desiccation tolerance.

## Data availability statement

The datasets presented in this study can be found in online repositories. The names of the repository/repositories and accession number(s) can be found in the article/Supplementary Material.

## Author contributions

PY and RKG: Designed study, Methodology, Writing Original Draft, Visualization; RPS: Validation, Investigation, Resources, Writing- Review, Data curation; HAA: Investigation, Writing-

Original Draft, Review and editing; AAH: Investigation, Writing- Original Draft, Review and editing; GS: Investigation, Writing- Original Draft, Review and editing; AK: Investigation, Writing- Original Draft, Review and editing; RKG: Writing-Review and editing, Supervision. All authors contributed to the article and approved the submitted version.

## Funding

Researchers supporting project number (RSP2023R479) King Saud University, Riyadh, Saudi Arabia.

## Acknowledgments

The authors are grateful to the Central Instrumentation Laboratory, Department of Botany, BHU Varanasi, India. Prof. N.V. Chalapathi Rao, Department of Geology, BHU, for SEM Facility. Interdisciplinary School of Life Science for Fluorescence Microscopy Facility, BHU, DST-FIST, and IoE of BHU India, for providing the instrument facilities during the experiment and to the Department of Science and Technology (DST), India, and the Sophisticated Analytical and Technical Help Institute, Banaras Hindu University (SATHI-BHU) for providing a “High-Resolution Mass Spectrometry” facility. Finally, the authors (PY and RPS) also thank CSIR-UGC New Delhi for their financial support in the form of JRF and SRF.

## Conflict of interest

The authors declare that the research was conducted in the absence of any commercial or financial relationships that could be construed as a potential conflict of interest.

## Publisher's note

All claims expressed in this article are solely those of the authors and do not necessarily represent those of their affiliated organizations, or those of the publisher, the editors and the reviewers. Any product that may be evaluated in this article, or claim that may be made by its manufacturer, is not guaranteed or endorsed by the publisher.

## Supplementary material

The Supplementary Material for this article can be found online at: <https://www.frontiersin.org/articles/10.3389/fpls.2023.1147390/full#supplementary-material>

## References

- Abd-Alla, M. H., Mahmoud, A. L. E., and Issa, A. A. (1994). Cyanobacterial biofertilizer improved growth of wheat. *Phyton* 34, 11–18.
- Abid, M., Ali, S., Qi, L. K., Zahoor, R., Tian, Z., Jiang, D., et al. (2018). Physiological and biochemical changes during drought and recovery periods at tillering and jointing stages in wheat (*Triticum aestivum* L.). *Sci. Rep.* 8, 4615. doi: 10.1038/s41598-018-21441-7
- Adhikary, S. P., and Sahu, J. K. (1998). UV Protecting pigment of the terrestrial cyanobacterium *Lyngbya birchmannii*. *J. Plant Physiol.* 153, 770–773. doi: 10.1016/S0176-1617(98)80233-2
- Agam, N., and Berliner, P. R. (2006). Dew formation and water vapor adsorption in semi-arid environments—a review. *J. Arid. Environ.* 65, 572–590. doi: 10.1016/j.jaridenv.2005.09.004
- Ahmed, A., and Hasnain, S. (2014). Auxins as one of the factors of plant growth improvement by plant growth promoting rhizobacteria. *Pol. J. Microbiol.* 63, 261–266. doi: 10.33073/PJM-2014-035
- Alonso, M. C. (2018). Changes in chlorophyll fluorescence parameters during desiccation and osmotic stress of *Hassallia antarctica* culture. *Czech Polar Rep.* 8, 198–207. doi: 10.5817/CPR2018-2-16
- Badri, D. V., Weir, T. L., van der Lelie, D., and Vivanco, J. M. (2009). Rhizosphere chemical dialogues: plant–microbe interactions. *Curr. Opin. Biotechnol.* 20, 642–650. doi: 10.1016/j.copbio.2009.09.014
- Bag, P., Chukhutsina, V., Zhang, Z., Paul, S., Ivanov, A. G., Shutova, T., et al. (2020). Direct energy transfer from photosystem II to photosystem I confers winter sustainability in Scots pine. *Nat. Commun.* 11, 6388. doi: 10.1038/s41467-020-20137-9
- Baker, N. R. (2008). Chlorophyll fluorescence: a probe of photosynthesis *in vivo*. *Annu. Rev. Plant Biol.* 59, 89. doi: 10.1146/annurev.arplant.59.032607.092759
- Baker, N. R., and Oxborough, K. (2004). “Chlorophyll fluorescence as a probe of photosynthetic productivity,” in *Chlorophyll fluorescence: a signature of photosynthesis. Adv. photosynthesis and respiration*, vol. 19. Ed. G. Papageorgiou C (The Netherlands: Springer), 65–82.
- Ballottari, M., Alcocer, M. J., D’Andrea, C., Viola, D., Ahn, T. K., Petrozza, A., et al. (2014). Regulation of photosystem I light harvesting by zeaxanthin. *Proc. Natl. Acad. Sci. U. S. A.* 111, E2431–E2438. doi: 10.1073/pnas.1404377111
- Barnawal, D., Singh, R., and Singh, R. P. (2019). Role of plant growth promoting rhizobacteria in drought tolerance: regulating growth hormones and osmolytes. *In PGPR amelioration Sustain. Agric.*, 107–128. doi: 10.1016/B978-0-12-815879-1.00006-9
- Bates, L. S., Waldren, R. P., and Teare, I. D. (1973). Rapid determination of free proline for water-stress studies. *Plant Soil* 39, 205–207. doi: 10.1007/BF00018060
- Becerra-Absalón, I., Muñoz-Martin, M. A., Montejano, G., and Mateo, P. (2019). Differences in the cyanobacterial community composition of biocrusts from the drylands of central Mexico: are there endemic species? *Front. Microbiol.* 10. doi: 10.3389/fmicb.2019.00937
- Belnaj, J., Weber, B., and Büdel, B. (2016). “Biological soil crusts as an organizing principle in drylands,” in *Biological soil crusts: an organizing principle in drylands* (Cham: Springer), 3–13. doi: 10.1007/978-3-319-30214-0
- Benard, P., Zarebanadkouki, M., Brax, M., Kaltenbach, R., Jerjen, I., Marone, F., et al. (2019). Microhydrological niches in soils: how mucilage and EPS alter the biophysical properties of the rhizosphere and other biological hotspots. *Vadose Zone J.* 18, 1–10. doi: 10.2136/vzj2018.12.0211
- Bennett, A., and Bogorad, L. (1973). Complimentary chromatic adaptation in a filamentous blue-green alga. *J. Cell Biol.* 58, 419. doi: 10.1083/jcb.58.2.419
- Berard, A., Sassi, M. B., Kaisermann, A., and Renault, P. (2015). Soil microbial community responses to heat wave components: drought and high temperature. *Clim. Res.* 66, 243–264. doi: 10.3354/cr01343
- Bertin, M. J., Roduit, A. F., Sun, J., Alves, G. E., Via, C. W., Gonzalez, M. A., et al. (2017). Tricholides a and b and unarmycin d: new hybrid PKS-NRPS macrocycles isolated from an environmental collection of trichodesmium thiebautii. *Mar. Drugs* 15, 206. doi: 10.3390/md15070206
- Bieker, S., and Zentgraf, U. (2013). “Plant senescence and nitrogen mobilization and signaling,” in *Senescence and senescence-related disorders*, vol. 16. Eds. Z. Wang and H. Inuzuka (Croatia: INTECH), 53–83. doi: 10.5772/54392
- Bligh, E. G., and Dyer, W. J. (1959). A rapid method of total lipid extraction and purification. *Can. J. Biochem. Physiol.* 37, 911–917. doi: 10.1139/o59-099
- Boussiba, S. (2000). Carotenogenesis in the green alga *Haematococcus pluvialis*: cellular physiology and stress response. *Physiol. Plantarum* 108, 111–117. doi: 10.1034/j.1399-3054.2000.108002111.x
- Bowne, J. B., Erwin, T. A., Juttner, J., Schnurbusch, T., Langridge, P., Bacic, A., et al. (2012). Drought responses of leaf tissues from wheat cultivars of differing drought tolerance at the metabolite level. *Mol. Plant* 5, 418–429. doi: 10.1093/mp/sss114
- Büdel, B., Dulić, T., Darienko, T., Rybalka, N., and Friedl, T. (2016). “Cyanobacteria and algae of biological soil crusts,” in *Biological soil crusts: an organizing principle in drylands* (Cham: Springer), 55–80.
- Caiola, M. G., Billi, D., and Friedmann, E. I. (1996). Effect of desiccation on envelopes of the cyanobacterium *Chroococcidiopsis* sp. (Chroococcales). *Eur. J. Phycol.* 3, 197–105. doi: 10.1080/09670269600651251a
- Castenholz, R. W. (1992). Species usage, concept, and evolution in the cyanobacteria (blue-green algae). *J. Phycol.* 28, 737–745. doi: 10.1111/j.0022-3646.1992.00737.x
- Celis-Pla, P. S., Rearte, T. A., Neori, A., Masojidek, J., Bonomi-Barufi, J., Álvarez-Gómez, F., et al. (2021). A new approach for cultivating the cyanobacterium *Nostoc calcicola* (MACC-612) to produce biomass and bioactive compounds using a thin-layer raceway pond. *Algal Res.* 59, 102421. doi: 10.1016/j.algal.2021.102421
- Chamizo, S., Adessi, A., Mugnai, G., Simiani, A., and De Philippis, R. (2019). Soil type and cyanobacteria species influence the macromolecular and chemical characteristics of the polysaccharidic matrix in induced biocrusts. *Microb. Ecol.* 78, 482–493. doi: 10.1007/s00248-018-1305-y
- Chang, L., Whittaker, N. F., and Bewley, C. A. (2003). Crambesicidin 826 and dehydrocrambine a: new polycyclic guanidine alkaloids from the marine sponge *Monanchora* sp. that inhibit HIV-1 fusion. *J. Nat. Prod.* 66, 1490–1494. doi: 10.1021/np030256t
- Chaves, M. M., Maroco, J. P., and Pereira, J. S. (2003). Understanding plant responses to drought—from genes to the whole plant. *Funct. Plant Biol.* 30, 239–264. doi: 10.1071/fp02076
- Chittapun, S., Limbipichai, S., Amnuaysin, N., Boonkerd, R., and Charoensook, M. (2018). Effects of using cyanobacteria and fertilizer on growth and yield of rice, pathum thani I: a pot experiment. *J. Appl. Psychol.* 30, 79–85. doi: 10.1007/s10811-017-1138-y
- Choi, J. H., Maeda, K., Nagai, K., Harada, E., Kawade, M., Hirai, H., et al. (2010). Termitomycamides a to e, fatty acid amides isolated from the mushroom *Termitomyces titanicus*, suppress endoplasmic reticulum stress. *Org. Lett.* 12, 5012–5015. doi: 10.1021/ol102186p
- Chokshi, K., Pancha, I., Ghosh, A., and Mishra, S. (2017). Salinity induced oxidative stress alters the physiological responses and improves the biofuel potential of green microalgae *Acutodesmus dimorphus*. *Bioresour. Technol.* 244, 1376–1383. doi: 10.1016/j.biortech.2017.05.003
- Chokshi, K., Pancha, I., Trivedi, K., George, B., Maurya, R., Ghosh, A., et al. (2015). Biofuel potential of the newly isolated microalgae *Acutodesmus dimorphus* under temperature induced oxidative stress conditions. *Bioresour. Technol.* 180, 162–171. doi: 10.1016/j.biortech.2014.12.102
- Christou, A., Manganaris, G. A., Papadopoulos, I., and Fotopoulos, V. (2013). Hydrogen sulfide induces systemic tolerance to salinity and non-ionic osmotic stress in strawberry plants through modification of reactive species biosynthesis and transcriptional regulation of multiple defense pathways. *J. Exp. Bot.* 64, 1953–1966. doi: 10.1093/jxb/ert055
- Chua, M., Erickson, T. E., Merritt, D. J., Chilton, A. M., Ooi, M. K., and Muñoz-Rojas, M. (2020). Bio-priming seeds with cyanobacteria: effects on native plant growth and soil properties. *Restor. Ecol.* 28, S168–S176. doi: 10.1111/rec.13040
- Colica, G., Li, H., Rossi, F., Li, D., Liu, Y., and De Philippis, R. (2014). Microbial secreted exopolysaccharides affect the hydrological behavior of induced biological soil crusts in desert sandy soils. *Soil Biol. Biochem.* 68, 62–70. doi: 10.1016/j.soilbio.2013.09.017
- Costa, O. Y. A., Raaijmakers, J. M., and Kuramae, E. E. (2018). Microbial extracellular polymeric substances: ecological function and impact on soil aggregation. *Front. Microbiol.* 9, 1636. doi: 10.3389/fmicb.2018.01636
- Dabravolski, S. A., and Isayenkov, S. V. (2022). Metabolites facilitating adaptation of desert cyanobacteria to extremely arid environments. *Plants* 11, 3225. doi: 10.3390/plants11233225
- Deinlein, U., Stephan, A. B., Horie, T., Luo, W., Xu, G., and Schroeder, J. I. (2014). Plant salt-tolerance mechanisms. *Trends Plant Sci.* 19, 371–379. doi: 10.1016/j.tplants.2014.02.001
- Deligeorgiev, T. G., Kaloyanova, S., and Vaquero, J. J. (2009). Intercalating cyanine dyes for nucleic acid detection. *Recent Pat. Mater. Sci.* 2, 1–26. doi: 10.2174/1874465610902010001
- Deng, C., Pan, X., Wang, S., and Zhang, D. (2014). Cu<sup>2+</sup> inhibits photosystem II activities but enhances photosystem I quantum yield of *Microcystis aeruginosa*. *Biol. Trace Elem. Res.* 160, 268–275. doi: 10.1007/s12011-014-0039-z
- Desikachary, T. V. (1959). ICAR monograph on algae. *India Council Agric. Research New* 1-686, 72s. doi: 10.1038/189343a0
- Dojani, S., Kauff, F., Weber, B., and Büdel, B. (2014). Genotypic and phenotypic diversity of cyanobacteria in biological soil crusts of the succulent karoo and nama karoo of southern Africa. *Micro. eco.* 67, 286–301. doi: 10.1007/s00248-013-0301-5
- Dubois, M., Guilles, K. A., Hamilton, J. K., Rebers, P. A., and Smith, F. (1956). Calorimetric method for the determination of sugars and related substances. *Analyt. Chem.* 18, 350–356. doi: 10.1021/ac60111a017
- Ebi, K. L., and Loladze, I. (2019). Elevated atmospheric CO<sub>2</sub> concentrations and climate change will affect our food's quality and quantity. *Lancet Planet. Health* 3, e283–e284. doi: 10.1016/S2542-5196(19)30108-1
- El Arroussi, H., Benhima, R., Elbaouchi, A., Sijilmassi, B., El Mernissi, N., Aafsar, A., et al. (2018). *Dunalilla salina* exopolysaccharides: a promising biostimulant for salt stress tolerance in tomato (*Solanum lycopersicum*). *Environ. Boil. Psychol.* 30, 2929–2941. doi: 10.1007/s10811-017-1382-1



- Fahad, S., Hussain, S., Bano, A., Saud, S., Hassan, S., Shan, D., et al. (2015). Potential role of phytohormones and plant growth-promoting rhizobacteria in abiotic stresses: consequences for changing environment. *Environ. Sci. Pollut. Res.* 22, 4907–4921. doi: 10.1007/s11356-014-3754-2
- Faist, A. M., Herrick, J. E., Belnap, J., Van Zee, J. W., and Barger, N. N. (2017). Biological soil crust and disturbance controls on surface hydrology in a semi-arid ecosystem. *Ecosphere* 8, e01691. doi: 10.1002/ecs2.1691
- Fal, S., Aasfar, A., Rabie, R., Smouni, A., and Arroussi, H. E. (2022). Salt induced oxidative stress alters physiological, biochemical and metabolomic responses of green microalga *Chlamydomonas reinhardtii*. *Heliyon* 8, e08811. doi: 10.1016/j.heliyon.2022.e08811
- Fan, G., Liu, D., and Lin, Q. (2013). Fluorescein diacetate and propidium iodide FDA-PI double staining detect the viability of microcystis sp. after ultrasonic irradiation. *J. Food Agric. Environ.* 11, 2419–2421.
- Farmer, E. E., and Mueller, M. J. (2013). ROS-mediated lipid peroxidation and RES-activated signaling. *Annu. Rev. Plant Biol.* 64, 429–424. doi: 10.1146/annurev-arplant-050312-120132
- Farooq, M., Wahid, A., Kobayashi, N., Fujita, D., and Basra, S. M. A. (2009). Plant drought stress: effects, mechanisms and management. *Agron. Sustain. Dev.* 29, 185–212. doi: 10.1051/agro:2008021
- Feng, G. D., Zhang, F., Cheng, L. H., Xu, X. H., Zhang, L., and Chen, H. L. (2013). Evaluation of FT-IR and Nile red methods for microalgal lipid characterization and biomass composition determination. *Bioresour. Technol.* 128, 107–112. doi: 10.1016/j.biortech.2012.09.123
- Feng, Y. N., Zhang, Z. C., Feng, J. L., and Qiu, B. S. (2012). Effects of UV-B radiation and periodic desiccation on the morphogenesis of the edible terrestrial cyanobacterium *Nostoc flagelliforme*. *Appl. Environ. Microbiol.* 78, 7075–7081. doi: 10.1128/AEM.01427-12
- Fleming, E. D., and Castenholz, R. W. (2007). Effects of periodic desiccation on the synthesis of the UV-screening compound, scytonemin, in cyanobacteria. *Environ. Microbiol.* 9, 1448–1455. doi: 10.1111/j.1462-2920.2007.01261.x
- Fukuda, S., Yamakawa, R., Hirai, M., Kashino, Y., Koike, H., and Satoh, K. (2008). Mechanisms to avoid photoinhibition in a desiccation-tolerant cyanobacterium, *Nostoc commune*. *Plant Cell Physiol.* 49, 488–492. doi: 10.1093/pcp/pcn018
- Gao, L., Pan, X., Zhang, D., Mu, S., Lee, D. J., and Halik, U. (2015). Extracellular polymeric substances buffer against the biocidal effect of H<sub>2</sub>O<sub>2</sub> on the bloom-forming cyanobacterium *Microcystis aeruginosa*. *Water Res.* 69, 51–58. doi: 10.1016/j.watres.2014.10.060
- Garcia-Plazaola, J. I., Matsubara, S., and Osmond, C. B. (2007). The lutein epoxide cycle in higher plants: its relationships to other xanthophyll cycles and possible functions. *Funct. Plant Biol.* 34, 759–773. doi: 10.1071/FP07095
- Garlapati, D., Chandrasekaran, M., Devanesan, A., Mathimani, T., and Pugazhendhi, A. (2019). Role of cyanobacteria in agricultural and industrial sectors: an outlook on economically important byproducts. *Appl. Microbiol. Biotechnol.* 103, 4709–4721. doi: 10.1007/s00253-019-09811-1
- Glick, B. R. (2014). Bacteria with ACC deaminase can promote plant growth and help to feed the world. *Microbiol. Res.* 169, 30–39. doi: 10.1016/j.micres.2013.09.009
- Goldack, D., Lüking, L., and Yang, O. (2011). Plant tolerance to drought and salinity: stress regulating transcription factors and their functional significance in the cellular transcriptional network. *Plant Cell Rep.* 30, 1383–1391. doi: 10.1007/s00299-011-1068-0
- Gr, S., Yadav, R. K., Chatrath, A., Gerard, M., Tripathi, K., Govindsamy, V., et al. (2021). Perspectives on the potential application of cyanobacteria in the alleviation of drought and salinity stress in crop plants. *J. Appl. Phycol.* 33, 3761–3778. doi: 10.1007/s10811-021-02570-5
- Guindon, S., and Gascuel, O. (2003). A simple, fast, and accurate algorithm to estimate large phylogenies by maximum likelihood. *Syst. Biol.* 52, 696–704. doi: 10.1080/10635150390235520
- Gumbo, J. R., Cloete, T. E., van Zyl, G. J. J., and Sommerville, J. E. M. (2014). The viability assessment of microcystis aeruginosa cells after co-culturing with bacillus mycoides B16 using flow cytometry. *Phys. Chem. Earth Parts A/B/C.* 72–75, 24–33. doi: 10.1016/j.pce.2014.09.004
- Haggag, W., Hoballah, M., and Ali, R. (2018). Applications of nano biotechnological microalgae product for improve wheat productivity in semai aird areas. *Int. J. Agric. Technol.* 14, 675–692.
- Hao, L., Li, J., Kappler, A., and Obst, M. (2013). Mapping of heavy metal ion sorption to cell-extracellular polymeric substance-mineral aggregates by using metal-selective fluorescent probes and confocal laser scanning microscopy. *Appl. Environ. Microbiol.* 79, 6524–6534. doi: 10.1128/AEM.02454-13
- Heath, R. L., and Packer, L. (1968). Photoperoxidation in isolated chloroplasts: i. kinetics and stoichiometry of fatty acid peroxidation. *Arch. Biochem. Biophys.* 125, 189–198. doi: 10.1016/0003-9861(68)90654-1
- Heber, D., Seeram, N. P., Wyatt, H., Henning, S. M., Zhang, Y., Ogdan, L. G., et al. (2007). Safety and antioxidant activity of a pomegranate ellagitannin-enriched polyphenol dietary supplement in overweight individuals with increased waist size. *J. Agric. Food Chem.* 55, 10050–10054. doi: 10.1021/jf071689v
- Henriques, F. S. (2009). Leaf chlorophyll fluorescence: background and fundamentals for plant biologists. *Bot. Rev.* 75, 249–270. doi: 10.1007/s12229-009-9035-y
- Hirschberg, J., and Chamovitz, D. (1994). “Carotenoids in cyanobacteria,” in *The molecular biology of cyanobacteria* (Dordrecht: Springer), 559–579.
- Hochberg, U., Degu, A., Toubiana, D., Gendler, T., Nikolski, Z., Rachmilevitch, S., et al. (2013). Metabolite profiling and network analysis reveal coordinated changes in grapevine water stress response. *BMC Plant Biol.* 13, 1–16. doi: 10.1186/1471-2229-13-184
- Hoekstra, F. A., Golovina, E. A., and Buitink, J. (2001). Mechanisms of plant desiccation tolerance. *Trends Plant Sci.* 6, 431–438. doi: 10.1016/S1360-1385(01)02052-0
- Hounslow, E., Evans, C. A., Pandhal, J., Sydney, T., Couto, N., Pham, T. K., et al. (2021). Quantitative proteomic comparison of salt stress in *Chlamydomonas reinhardtii* and the snow alga *Chlamydomonas nivalis* reveals mechanisms for salt-triggered fatty acid accumulation via reallocation of carbon resources. *Biotechnol. Biofuels* 14, 1–25. doi: 10.1186/s13068-021-01970-6
- Housman, D. C., Powers, H. H., Collins, A. D., and Belnap, J. (2006). Carbon and nitrogen fixation differ between successional stages of biological soil crusts in the Colorado plateau and chihuahuan desert. *J. Arid. Environ.* 66, 620–634. doi: 10.1016/j.jaridenv.2005.11.014
- Hussain Wani, S., Brajendra Singh, N., Haribhushan, A., and Iqbal Mir, J. (2013). Compatible solute engineering in plants for abiotic stress tolerance-role of glycine betaine. *Curr. Genomics* 14, 157–165. doi: 10.2174/1389202911314030001
- Jahn, P., and Holzwarth, A. R. (2012). The role of the xanthophyll cycle and of lutein in photoprotection of photosystem II. *Biochim. Biophys. Acta* 1817, 182–193. doi: 10.1016/j.bbabi.2011.04.012
- Jin, C., Yu, B., Qian, S., Liu, Q., and Zhou, X. (2021). Impact of combined monochromatic light on the biocomponent productivity of *Dunaliella salina*. *J. Renew. Sus. Energ.* 13, 023101. doi: 10.1063/5.0041330
- Kadirova, G. K., Andreevich, K. A., Adrian, L., and Bakhtiyor, R. (2012a). Functioning of salt tolerant anabaena variabilis and nostoc calcicola strains in salt stress, destructors of hexachlorocyclohexane (HCH) in saline conditions. *Nat. Resour. Environ.* 2, 63. doi: 10.5539/enr.v2n1p63
- Kadirova, G. K., and Shakhov, Z. S. (2012b). Identification of nitrogen-fixing and salt-resistant cyanobacteria *Nostoc calcicola* isolated from the rhizosphere of cotton in Uzbekistan. *Environ. Sci. Indian J.* 7, 305. doi: 10.5539/enr.v2n1p63
- Kaushal, M., and Wani, S. P. (2016). Rhizobacterial-plant interactions: strategies ensuring plant growth promotion under drought and salinity stress. *Agric. Ecosyst. Environ.* 231, 68–78. doi: 10.1016/j.agee.2016.06.031
- Kazan, K. (2015). Diverse roles of jasmonates and ethylene in abiotic stress tolerance. *Trends Plant Sci.* 20, 219–229. doi: 10.1016/j.tplants.2015.02.001
- Khan, N., Bano, A., Rahman, M. A., Rathinasabapathi, B., and Babar, M. A. (2019). UPLC-HRMS-based untargeted metabolic profiling reveals changes in chickpea (*Cicer arietinum*) metabolome following long-term drought stress. *Plant Cell Environ.* 42, 115–132. doi: 10.1111/pce.13195
- Kirilovsky, D. (2007). Photoprotection in cyanobacteria: the orange carotenoid protein (OCP)-related non-photochemical-quenching mechanism. *Photosynth. Res.* 93, 7–16. doi: 10.1007/s11120-007-9168-y
- Kitajima, M., and Butler, W. L. (1975). Quenching of chlorophyll fluorescence and primary photochemistry in chloroplasts by dibromothymoquinone. *Biochim. Biophys. Acta* 376, 105–111. doi: 10.1016/0005-2728(75)90209-1
- Komárek, J. (2013). “Cyanoprokaryota. part 3: heterocytous genera,” in *Freshwater flora of central Europe*. Eds. B. Büdel, G. Gärtner, L. Krienitz and M. Schägerl (Berlin Heidelberg: Springer-Verlag), p. 1–1130.
- Kramer, D. M., Johnson, G., Kiirats, O., and Edwards, G. E. (2004). New fluorescence parameters for the determination of QA redox state and excitation energy fluxes. *Photosyn. Res.* 79, 209–218. doi: 10.1023/b:pres.0000015391.99477.0d
- Kuraganti, G., Edla, S., and Pallaval, V. B. (2020). Cyanobacteria as biofertilizers: current research, commercial aspects, and future challenges. *Adv. Plant Microbiome Sustain. Agric.*, 259–278. doi: 10.1007/978-981-15-3204-7\_11
- Lan, S., Wu, L., Zhang, D., and Hu, C. (2013). Assessing level of development and successional stages in biological soil crusts with biological indicators. *Microb. Ecol.* 66, 394–403. doi: 10.1007/s00248-013-0191-6
- Lillie, S. H., and Pringle, J. R. (1980). Reserve carbohydrate metabolism in saccharomyces cerevisiae: responses to nutrient limitation. *J. Bacteriol.* 143, 1384–1394. doi: 10.1128/jb.143.3.1384-1394.1980
- Liu, W., Cui, L., Xu, H., Zhu, Z., and Gao, X. (2017). Flexibility-rigidity coordination of the dense exopolysaccharide matrix in terrestrial cyanobacteria acclimated to periodic desiccation. *Appl. Environ. Microb.* 83, e01619–e01617. doi: 10.1128/AEM.01619-17
- Liu, H., Li, X., Xiao, J., and Wang, S. (2012). A convenient method for simultaneous quantification of multiple phytohormones and metabolites: application in study of rice-bacterium interaction. *Plant Methods* 8, 1–12. doi: 10.1186/1746-4811-8-2
- Loewus, F. A. (1952). Improvement in anthrone method for determination of carbohydrates. *Anal. Chem.* 24, 219–219. doi: 10.1021/ac60061a050
- Lowry, O. H., Rosenbrough, N. J., Farr, A. L., and Randall, R. J. (1951). Protein measurement with the folin phenol reagent. *J. Biol. Chem.* 193, 265–275. doi: 10.1016/S0021-9258(19)52451-6
- Mansori, M., Chernane, H., Latique, S., Benaliat, A., Hssissou, D., and El Kaoua, M. (2015). Seaweed extract effect on water deficit and antioxidative mechanisms in bean

plants (*Phaseolus vulgaris* L.). *J. Appl. Psychol.* 27, 1689–1698. doi: 10.1007/s10811-014-0455-7

Martinelli, T., Whittaker, A., Bochicchio, A., Vazzana, C., Suzuki, A., and Masclaux Daubresse, C. (2007). Amino acid pattern and glutamate metabolism during dehydration stress in the ‘resurrection’ plant *Sporobolus stapfianus*: a comparison between desiccation-sensitive and desiccation tolerant leaves. *J. Exp. Bot.* 58, 3037–3046. doi: 10.1093/jxb/erm161

Mittler, R. (2002). Oxidative stress, antioxidants and stress tolerance. *Trends Plant Sci.* 7, 405–410. doi: 10.1016/S1360-1385(02)02312-9

Morales, M., and Munné-Bosch, S. (2019). Malondialdehyde: facts and artifacts. *Plant physiol.* 180, 1246–1250. doi: 10.1104/pp.19.00405

Mugnai, G., Rossi, F., Felde, V. J. M. N. L., Colesie, C., Büdel, B., Peth, S., et al. (2018). The potential of the cyanobacterium *leptolyngbya ohadii* as inoculum for stabilizing bare sandy substrates. *Soil Biol. Biochem.* 127, 318–328. doi: 10.1016/j.soilbio.2018.08.007

Mukherjee, P., Gorain, P. C., Paul, I., Bose, R., Bhadoria, P. B. S., and Pal, R. (2020). Investigation on the effects of nitrate and salinity stress on the antioxidant properties of green algae with special reference to the use of processed biomass as potent fish feed ingredient. *Aquac. Int.* 28, 211–234. doi: 10.1007/s10499-019-00455-6

Muñoz-Rojas, M., Chilton, A., Liyanage, G. S., Erickson, T. E., Merritt, D. J., Neilan, B. A., et al. (2018). Effects of indigenous soil cyanobacteria on seed germination and seedling growth of arid species used in restoration. *Plant Soil* 429, 91–100. doi: 10.1007/s11104-018-3607-8

Nelson, C., Giraldo-Silva, A., and Garcia-Pichel, F. (2021). A symbiotic nutrient exchange within the cyanosphere microbiome of the biocrust cyanobacterium, *Microcoleus vaginatus*. *ISME J.* 15, 282–292. doi: 10.1038/s41396-020-00781-1

Ngumbi, E., and Kloepper, J. (2016). Bacterial-mediated drought tolerance: current and future prospects. *Appl. Soil Ecol.* 105, 109–125. doi: 10.1016/j.apsoil.2016.04.009

Noumavo, P. A., Agbodjato, N. A., Baba-Moussa, F., Adjanohoun, A., and Baba-Moussa, L. (2016). Plant growth promoting rhizobacteria: beneficial effects for healthy and sustainable agriculture. *Afr. J. Biotechnol.* 15, 1452–1463. doi: 10.5897/AJB2016.15397

Nübel, U., Garcia-Pichel, F., and Muyzer, G. (1997). PCR primers to amplify 16S rRNA genes from cyanobacteria. *Appl. Environ. Microbiol.* 63, 3327–3332. doi: 10.1128/aem.63.8.3327-3332.1997

Ogawa, T., Misumi, M., and Sonoike, K. (2017). Estimation of photosynthesis in cyanobacteria by pulse -amplitude modulation chlorophyll fluorescence: problems and solutions. *Photosynth Res.* 133, 63–673. doi: 10.1007/s11120-017-0367-x

Olanrewaju, O. S., Glick, B. R., and Babalola, O. O. (2017). Mechanisms of action of plant growth promoting bacteria. *World J. Microbiol. Biotechnol.* 33, 197. doi: 10.1007/s11274-017-2364-9

Oliver, M. J., Guo, L., Alexander, D., Ryals, J., Wone, B., and Cushman, J. (2011). A sister group metabolomic contrast using untargeted global metabolomic analysis delineates the biochemical regulation underlying desiccation tolerance in *Sporobolus stapfianus*. *Plant Cell* 23, 1231–1248. doi: 10.1105/tpc.110.082800

Ordóñez, A. A. L., Gomez, J. D., and Vattuone, M. A. (2006). Antioxidant activities of sechium edule (Jacq.) Swartz extracts. *Food Chem.* 97, 452–458. doi: 10.1016/j.foodchem.2005.05.024

Pancha, I., Chokshi, K., Maurya, R., Trivedi, K., Patidar, S. K., Ghosh, A., et al. (2015). Salinity induced oxidative stress enhanced biofuel production potential of microalgae *scenedesmus* sp. CCNM 1077. *Bioresour. Technol.* 189, 341–348. doi: 10.1016/j.biortech.2015.04.017

Park, C. H., Li, X. R., Zhao, Y., Jia, R. L., and Hur, J. S. (2017). Rapid development of cyanobacterial crust in the field for combating desertification. *PLoS One* 12, e0179903. doi: 10.1371/journal.pone.0179903

Parsons, R. F. (2012). Incidence and ecology of very fast germination. *Seed Sci. Res.* 2, 161–167. doi: 10.1017/S0960258512000037

Pereira, S., Micheletti, E., Zille, A., Santos, A., Moradas-Ferreira, P., Tamagnini, P., et al. (2011). Using extracellular polymeric substances (EPS)-producing cyanobacteria for the bioremediation of heavy metals: do cations compete for the EPS functional groups and also accumulate inside the cell? *Microbiology* 157, 451–458. doi: 10.1099/mic.0.041038-0

Pfändel, E., Klughammer, C., and Schreiber, U. (2008). Monitoring the effects of reduced PS II antenna size on quantum yields of photosystems I and II using the dual-PAM-100 measuring system. *PAM Appl. Notes* 1, 21–24.

Pointing, S. B., and Belnap, J. (2012). Microbial colonization and controls in dryland systems. *Nat. Rev. Microbiol.* 10, 551–562. doi: 10.1038/nrmicro2831

Potts, M. (1994). Desiccation tolerance of prokaryotes. *microbiol. storage. Soil Biol. Biochem.* 23, 313–322. doi: 10.1128/mr.58.4.755-805.1994

Potts, M. (1999). Mechanisms of desiccation tolerance in cyanobacteria. *Eur. J. Phycol.* 34, 319–328. doi: 10.1080/09670269910001736382

Potts, M. (2004). Nudist colonies: a revealing glimpse of cyanobacterial extracellular polysaccharide. *J. Phycol.* 40, 1–3. doi: 10.1046/j.1529-8817.2004.40101.x

Qu, R. Y., He, B., Yang, J. F., Lin, H. Y., Yang, W. C., Wu, Q. Y., et al. (2021). Where are the new herbicides? *Pest Manage. Sci.* 77, 2620–2625. doi: 10.1002/ps.6285

Raanan, H., Oren, N., Treves, H., Keren, N., Ohad, I., Berkowicz, S. M., et al. (2016). Towards clarifying what distinguishes cyanobacteria able to resurrect after desiccation from those that cannot: the photosynthetic aspect. *Biochim. Biophys. Acta (BBA)-Bioenergetics* 1857, 715–722. doi: 10.1016/j.bbabo.2016.02.007

Radermacher, A. L., du Toit, S. F., and Farrant, J. M. (2019). Desiccation-driven senescence in the resurrection plant *Xerophyta schlechteri* (Baker) NL menezes: comparison of anatomical, ultrastructural, and metabolic responses between senescent and non-senescent tissues. *Front. Plant Sci.* 10. doi: 10.3389/fpls.2019.01396

Rahman, M. A., Akond, M., Babar, M. A., Beecher, C., Erickson, J., Thomason, K., et al. (2017). LC-HRMS based non-targeted metabolomic profiling of wheat (*Triticum aestivum* L.) under post-anthesis drought stress. *Am. J. Plant Sci.* 8, 3024–3061. doi: 10.4236/ajps.2017.812205

Rao, B., Liu, Y., Wang, W., Hu, C., Dunhai, L., and Lan, S. (2009). Influence of dew on biomass and photosystem II activity of cyanobacterial crusts in the hopq desert, northwest China. *Soil Biol. Biochem.* 41, 2387–2393. doi: 10.1016/j.soilbio.2009.06.005

Reddy, A. R., Chaitanya, K. V., and Vivekanandan, M. (2004). Drought-induced responses of photosynthesis and antioxidant metabolism in higher plants. *J. Plant Physiol.* 161, 1189–1202. doi: 10.1016/j.jplph.2004.01.013

Rippka, R., Deruelles, J., Waterbury, J. B., Herdman, M., and Stanier, R. Y. (1979). Generic assignments, strain histories and properties of pure cultures of cyanobacteria. *Microbiology* 111, 1–61. doi: 10.1099/00221287-111-1-1

Roncero-Ramos, B., Muñoz-Martin, M.Á., Chamizo, S., Fernández-Valbuena, L., Mendoza, D., Perona, E., et al. (2019). Polyphasic evaluation of key cyanobacteria in biocrusts from the most arid region in Europe. *Peer J.* 7, e6169. doi: 10.7717/peerj.6169

Rossi, F., and De Philippis, R. (2015). Role of cyanobacterial exopolysaccharides in phototrophic biofilms and in complex microbial mats. *Life* 5, 1218–1238. doi: 10.3390/life5021218

Rossi, F., Li, H., Liu, Y., and De Philippis, R. (2017). Cyanobacterial inoculation (cyanobacterisation): perspectives for the development of a standardized multifunctional technology for soil fertilization and desertification reversal. *Earth Sci. Rev.* 171, 28–43. doi: 10.1016/j.earscirev.2017.05.006

Sadiq, I. M., Dalai, S., Chandrasekaran, N., and Mukherjee, A. (2011). Ecotoxicity study of titania (TiO<sub>2</sub>) NPs on two microalgae species: *Scenedesmus* sp. and *Chlorella* sp. *Ecotoxicol. Environ. Saf.* 74, 1180–1187. doi: 10.1016/j.ecoenv.2011.03.006

Sakamoto, T., Yoshida, T., Arima, H., Hatanaka, Y., Takani, Y., and Tamaru, Y. (2009). Accumulation of trehalose in response to desiccation and salt stress in the terrestrial cyanobacterium *Nostoc commune*. *Phycol. Res.* 57, 66–73. doi: 10.1111/j.1440-1835.2008.00522.x

Sarker, U., Islam, M. T., Rabbani, M. G., and Oba, S. (2018). Phenotypic divergence in vegetable amaranth for total antioxidant capacity, antioxidant profile, dietary fiber, nutritional and agronomic traits. *Acta Agric. Scand. B. Soil. Plant Sci.* 68, 67–76. doi: 10.1080/09604710.2017.1367029

Schinkovitz, A., Gibbons, S., Stavri, M., Cocksedge, M. J., and Bucar, F. (2003). Ostruthin: an antimycobacterial coumarin from the roots of *Peucedanum ostruthium*. *Planta Med.* 69, 369–371. doi: 10.1055/s-2003-38876

Sharma, S., Lin, W., Villamor, J. G., and Verslues, P. E. (2013). Divergent low water potential response in *Arabidopsis thaliana* accessions *Landsberg erecta* and *Shahdara*. *Plant Cell Environ.* 36, 994–1008. doi: 10.1111/pce.12032A

Shirkey, B., Kovarcik, D. P., Wright, D. J., Wilmoth, G., Prickett, T. F., Helm, R. F., et al. (2000). Active fe-containing superoxide dismutase and abundant sodF mRNA in *nostoc commune* (cyanobacteria) after years of desiccation. *J. Bacteriol.* 182, 189–197. doi: 10.1128/JB.182.1.189-197.2000

Silvente, S., Sobolev, A. P., and Lara, M. (2012). Metabolite adjustments in drought tolerant and sensitive soybean genotypes in response to water stress. *PLoS One* 7, e38554. doi: 10.1371/journal.pone.0038554

Singh, R. P., and Jha, P. N. (2016). Alleviation of salinity-induced damage on wheat plant by an ACC deaminase-producing halophilic bacterium *Serratia* sp. SL-12 isolated from a salt lake. *Symbiosis* 69, 101–111. doi: 10.1007/s13199-016-0387-x

Singh, V., Pandey, K. D., Mesapogu, S., and Singh, D. V. (2015). Influence of NaCl on photosynthesis and nitrogen metabolism of cyanobacterium *Nostoc calcicola*. *Appl. Biochem. Microbiol.* 51, 720–725. doi: 10.1134/S0003683815060149

Singh, P., Singh, S. S., Aboal, M., and Mishra, A. K. (2015). Decoding cyanobacterial phylogeny and molecular evolution using an eponymic approach. *Protoplasma* 252, 519–535. doi: 10.1007/s00709-014-0699-8

Singleton, V. L., Orthofer, R., and Lamuela-Raventós, R. M. (1999). “Analysis of total phenols and other oxidation substrates and antioxidants by means of folin-ciocalteu reagent,” in *Methods in enzymology*. (Academic Press), 299, 152–178. doi: 10.1016/S0076-6879(99)99017-1

Song, G., Li, X., and Hui, R. (2017). Effect of biological soil crusts on seed germination and growth of an exotic and two native plant species in an arid ecosystem. *PLoS One* 12, e0185839. doi: 10.1371/journal.pone.0185839

Stamatakis, K., Tsimilli-Michael, M., and Papageorgiou, G. C. (2014). On the question of the light-harvesting role of β-carotene in photosystem II and photosystem I core complexes. *Plant Physiol. Biochem.* 81, 121–127. doi: 10.1016/j.plaphy.2014.01.014

Tamaru, Y., Takani, Y., Yoshida, T., and Sakamoto, T. (2005). Crucial role of extracellular polysaccharides in desiccation and freezing tolerance in the terrestrial

- cyanobacterium *Nostoc commune*. *Appl. Environ. Microbiol.* 71, 7327–7333. doi: 10.1128/AEM.71.11.7327-7333.2005
- Tammam, A. A., Fakhry, E. M., and El-Sheekh, M. (2011). Effect of salt stress on antioxidant system and the metabolism of the reactive oxygen species in *Dunaliella salina* and *Dunaliella tertiolecta*. *Afr. J. Biotechnol.* 10, 3795–3808.
- Tamura, H., and Ishikita, H. (2020). Quenching of singlet oxygen by carotenoids via ultrafast superexchange dynamics. *J. Phys. Chem. A* 124, 5081–5088. doi: 10.1021/acs.jpca.0c02228
- Tandeau de Marsac, N., and Houmard, J. (1988). Complementary chromatic adaptation: physiological conditions and action spectra. *Method Enzymol.* 167, 318–328. doi: 10.1111/j.1574-6941.2011.01114.x
- Tashyreva, D., and Elster, J. (2016). Annual cycles of two cyanobacterial mat communities in hydro-terrestrial habitats of the high Arctic. *Microb. Ecol.* 71, 887–900. doi: 10.1007/s00248-016-0732-x
- Thanh Doan, N., Rickards, R. W., Rothschild, J. M., and Smith, G. D. (2000). Allelopathic actions of the alkaloid 12-epi-hapalindole e isonitrile and calothrixin a from cyanobacteria of the genera *Fischerella* and *Calothrix*. *J. Appl. Phycol.* 12, 409–416. doi: 10.1023/A%3A1008170007044
- Thapar, R., Srivastava, A. K., Bhargava, P., Mishra, Y., and Rai, L. C. (2008). Impact of different abiotic stresses on growth, photosynthetic electron transport chain, nutrient uptake and enzyme activities of Cu-acclimated *Anabaena doliolum*. *J. Plant Physiol.* 165, 306–316. doi: 10.1016/j.jplph.2007.05.002
- Tian, L., Xu, P., Chukhutsina, V. U., Holzwarth, A. R., and Croce, R. (2017). Zeaxanthin-dependent nonphotochemical quenching does not occur in photosystem I in the higher plant *Arabidopsis thaliana*. *Proc. Natl. Acad. Sci. U. S. A.* 114, 4828–4832. doi: 10.1073/pnas.1621051114
- Tietel, Z., Wikoff, W. R., Kind, T., Ma, Y., and Fiehn, O. (2020). Hyperosmotic stress in *Chlamydomonas* induces metabolomic changes in biosynthesis of complex lipids. *Eur. J. Phycol.* 55, 11–29. doi: 10.1007/s12649-022-01712-1
- Tillett, D., and Neilan, B. A. (2000). Xanthogenate nucleic acid isolation from cultured and environmental cyanobacteria. *J. Phycol.* 36, 251–258. doi: 10.1046/j.1529-8817.2000.99079.x
- Tiwari, O. N., Mondal, A., Bhunia, B., Kanti Bandyopadhyay, T., Jaladi, P., Oinam, G., et al. (2019). Purification, characterization and biotechnological potential of new exopolysaccharide polymers produced by cyanobacterium *Anabaena* sp. CCC 745. *Polymer* 178, 121695. doi: 10.1016/j.polymer.2019.121695
- Tsavkelova, E. A., Klimova, S. Y., Cherdynseva, T. A., and Netrusov, A. I. (2006). Hormones and hormone-like substances of microorganisms: a review. *Appl. Biochem. Microbiol.* 42, 229–235. doi: 10.1134/S000368380603001X
- Ueda, J., Miyamoto, K., Aoki, M., Hirata, T., Sato, T., and Momotani, Y. (1991). Identification of jasmonic acid in *Chlorella* and *Spirulina*. bulletin of the university of Osaka prefecture. *Ser. B Agric. Biol.* 43, 103–108. doi: 10.24729/00009274
- Usmonkulova, A., Shonakhunov, T., and Kadirova, G. (2022). Activity of nitrogen-fixing cyanobacteria under salinity and heavy metals stress. *Pharm. Negat. Results* 13, 355. doi: 10.47750/pnr.2022.13.03.055
- Van Hijum, S. A., Kralj, S., Ozimek, L. K., Dijkhuizen, L., and van Geel-Schutten, I. G. (2006). Structure-function relationships of glucanase and fructanase enzymes from lactic acid bacteria. *Microbiol. Mol. Biol. Rev.* 70, 157–176. doi: 10.1128/MMBR.70.1.157-176.2006
- Velikova, V., Yordanov, I., and Adreva, A. (2000). Some antioxidant systems in acid rain treated bean plants; protective role of exogenous polyamines. *Plant Sci.* 151, 59–66. doi: 10.1016/S0168-9452(99)00197-1
- Vurukonda, S. S. K. P., Vardharajula, S., Shrivastava, M., and SkZ, A. (2016). Enhancement of drought stress tolerance in crops by plant growth promoting rhizobacteria. *Microbiol. Res.* 184, 13–24. doi: 10.1016/j.micres.2015.12.003
- Wang, J., Li, Q., Li, M. M., Chen, T. H., Zhou, Y. F., and Yue, Z. B. (2014). Competitive adsorption of heavy metal by extracellular polymeric substances (EPS) extracted from sulfate reducing bacteria. *Bioresour. Technol.* 163, 374–376.
- Weber, H., Chételat, A., Reymond, P., and Farmer, E. E. (2004). Selective and powerful stress gene expression in *Arabidopsis* in response to malondialdehyde. *Plant J.* 37, 877–888. doi: 10.1111/j.1365-313X.2003.02013.x
- White, S., Anandraj, A., and Bux, F. (2011). PAM fluorometry as a tool to assess microalgal nutrient stress and monitor cellular neutral lipids. *Bioresour. Technol.* 102, 1675–1682. doi: 10.1016/j.biortech.2010.09.097
- Wigley, T. M. L., and Jones, P. D. (1985). Influences of precipitation changes and direct CO<sub>2</sub> effects on streamflow. *Nature* 314, 149–152. doi: 10.1038/314149A0
- WMO (2021). Climate change indicators and impacts worsened in 2020. *Press Release Number: 19042021* 12 (4), 24–27. doi: 10.1109/MPULS.2021.3094253
- Wright, D. J., Smith, S. C., Joardar, V., Scherer, S., Jervis, J., Warren, A., et al. (2005). UV Irradiation and desiccation modulate the three-dimensional extracellular matrix of *Nostoc commune* (Cyanobacteria). *J. Biol. Chem.* 280, 40271–40281. doi: 10.1074/jbc.M505961200
- Xu, Y., Rossi, F., Colica, G., Deng, S., De Philippis, R., and Chen, L. (2013). Use of cyanobacterial polysaccharides to promote shrub performances in desert soils: a potential approach for the restoration of desertified areas. *Biol. Fertil. Soils* 49, 143–152. doi: 10.1007/s00374-012-0707-0
- Yadav, P., Singh, R. P., and Gupta, R. K. (2022a). Role of cyanobacteria in germination and growth of paddy seedlings. *Int. J. Phytol. Res.* 2, 11–18.
- Yadav, P., Singh, R. P., Rana, S., Joshi, D., Kumar, D., Bhardwaj, N., et al. (2022b). Mechanisms of stress tolerance in cyanobacteria under extreme conditions. *Stresses* 2, 531–549. doi: 10.3390/stresses2040036
- Yadav, R. K., Tripathi, K., Varghese, E., and Abraham, G. (2021). Physiological and proteomic studies of the cyanobacterium *Anabaena* sp. acclimated to desiccation stress. *Curr. Microbiol.* 78, 2429–2439. doi: 10.1007/s00284-021-02504-x
- Yang, J., Kloepper, J. W., and Ryu, C. M. (2009). Rhizosphere bacteria help plants tolerate abiotic stress. *Trends Plant Sci.* 14, 1–4. doi: 10.1016/j.tplants.2008.10.004
- Yewalkar, S., Wu, T., Kuan, D., Wang, H., Li, D., Johnson, A., et al. (2019). Applicability of differential fluorescein diacetate and propidium iodide fluorescence staining for monitoring algal growth and viability. *W.D.S.E.* 1, 199–206.
- Yobi, A., Wone, B. W. M., Xu, W., Alexander, D. C., Guo, L., Ryals, J. A., et al. (2013). Metabolic profiling in *Selaginella lepidophylla* at various hydration states provides new insights into the mechanistic basis of desiccation tolerance. *Mol. Plant* 6, 369–385. doi: 10.1093/mp/sss155
- Yoshida, T., and Sakamoto, T. (2009). Water-stress induced trehalose accumulation and control of trehalase in the cyanobacterium *Nostoc punctiforme* IAM m-15. *J. Gen. Appl. Microbiol.* 55, 135–145. doi: 10.2323/jgam.55.135
- Zakar, T., Herman, E., Vajravel, S., Kovacs, L., Knoppová, J., Komenda, J., et al. (2017). Lipid and carotenoid cooperation-driven adaptation to light and temperature stress in *Synechocystis* sp. PCC6803. *Biochim. Biophys. Acta Bioenerg.* 1858, 337–350. doi: 10.1016/j.bbabi.2017.02.002
- Zakhia, F., Jungblut, A. D., Taton, A., Vincent, W. F., and Wilmotte, A. (2008). “Cyanobacteria in cold ecosystems,” in *Psychrophiles: from biodiversity to biotechnology* (Berlin, Heidelberg: Springer), 121–135.
- Zhang, H. L., Fang, W., Wang, Y. P., Sheng, G. P., Zeng, R. J., Li, W. W., et al. (2013). Phosphorus removal in an enhanced biological phosphorus removal process: roles of extracellular polymeric substances. *Environ. Sci. Technol.* 47, 11482–11489. doi: 10.1021/es403227p
- Zhou, J., Wang, J., Li, X., Xia, X. J., Zhou, Y. H., Shi, K., et al. (2014). H<sub>2</sub>O<sub>2</sub> mediates the crosstalk of brassinosteroid and abscisic acid in tomato responses to heat and oxidative stresses. *J. Exp. Bot.* 65, 4371–4383. doi: 10.1093/jxb/eru217





## OPEN ACCESS

## EDITED BY

Milan Skalicky,  
Czech University of Life Sciences Prague,  
Czechia

## REVIEWED BY

Ramazan Beyaz,  
Ahi Evran University, Türkiye  
Neftali Ochoa-Alejo,  
Centro de Investigación y de Estudios  
Avanzados del Instituto Politécnico  
Nacional, Mexico  
Hakime Oloumi,  
Graduate University of Advanced  
Technology, Iran  
Hamidreza Balouchi,  
Yasouj University, Iran

## \*CORRESPONDENCE

Zhiqing Ma

✉ zhiqingma@163.com;

✉ mazhiqing2000@gmail.com

Jun Wang

✉ 850340659qq.com

RECEIVED 01 February 2023

ACCEPTED 04 September 2023

PUBLISHED 27 September 2023

## CITATION

Lu X, Wu Q, Nie K, Wu H, Chen G, Wang J  
and Ma Z (2023) Exogenous phthalanilic  
acid induces resistance to drought stress in  
pepper seedlings (*Capsicum annuum* L.).  
*Front. Plant Sci.* 14:1156276.  
doi: 10.3389/fpls.2023.1156276

## COPYRIGHT

© 2023 Lu, Wu, Nie, Wu, Chen, Wang and  
Ma. This is an open-access article distributed  
under the terms of the [Creative Commons  
Attribution License \(CC BY\)](#). The use,  
distribution or reproduction in other  
forums is permitted, provided the original  
author(s) and the copyright owner(s) are  
credited and that the original publication in  
this journal is cited, in accordance with  
accepted academic practice. No use,  
distribution or reproduction is permitted  
which does not comply with these terms.

# Exogenous phthalanilic acid induces resistance to drought stress in pepper seedlings (*Capsicum annuum* L.)

Xiaopeng Lu<sup>1</sup>, Qiong Wu<sup>1</sup>, Keyi Nie<sup>1</sup>, Hua Wu<sup>1,2</sup>,  
Guangyou Chen<sup>1,2</sup>, Jun Wang<sup>3\*</sup> and Zhiqing Ma<sup>1,2\*</sup>

<sup>1</sup>College of Plant Protection, Northwest A & F University, Yangling, China, <sup>2</sup>Provincial Center for Bio-Pesticide Engineering, Yangling, Shaanxi, China, <sup>3</sup>Institute of Water Conservancy and Soil Fertilizer, Xinjiang Academy of Agricultural Sciences/Northwest Oasis Water-saving Agriculture Key Laboratory, Ministry of Agriculture and Rural Affairs, Shihezi, Xinjiang, China

Drought stress (DS) is one of the main abiotic negative factors for plants. Phthalanilic acid (PPA), as a plant growth regulator, can promote the growth and development of crops. In order to evaluate the ideal application concentration and frequency of PPA-induced drought resistance in pepper (*Capsicum annuum*) seedlings, the concentration of PPA was 133.3 mg·L<sup>-1</sup>; 200.0 mg·L<sup>-1</sup>; 266.7 mg·L<sup>-1</sup>, and some key indicators were investigated, including leaf wilting index (LWI), relative water content (RWC), and malondialdehyde (MDA). We found that the LWI and RWC in the PPA-applied pepper leaves under light drought stress (LDS) and moderate drought stress (MDS) were all elevated, while MDA contents were decreased. To better understand how PPA makes pepper drought resistant, we examined the photosynthetic characteristics, growth parameters, antioxidant activities, and osmotic substances in pepper seedlings treated twice with PPA at a concentration of 133.3 mg·L<sup>-1</sup> under LDS, MDS, and severe drought stress (SDS). Results showed that PPA increased the chlorophyll, plant height, stem diameter, root-shoot ratio, and seedling index of pepper leaves under LDS, MDS, and SDS. The net photosynthetic rate (Pn), stomatal conductance (Gs), intercellular CO<sub>2</sub> concentration (Ci), transpiration rates (Tr), and water-use efficiency (WUE) in the PPA-treated pepper leaves under LDS and MDS were improved, while their stomatal limitation (Ls) were reduced. PPA also boosted the activities of enzymatic antioxidants (superoxide dismutase, catalase, and peroxidase), as well as enhanced the accumulation of osmotic substances such as soluble sugar, soluble protein, and free proline in pepper leaves under LDS, MDS, and SDS. Thus, PPA can alleviate the growth inhibition and damage to pepper seedlings caused by DS, and the PPA-mediated efficacy may be associated with the improvement in PPA-mediated antioxidant activities, Pn, and accumulation of osmotic substances.

## KEYWORDS

malondialdehyde, photosynthesis, chlorophyll, soluble sugar, soluble protein, proline



# 1 Introduction

Plants are susceptible to various abiotic factors throughout their life cycle, including salinity, drought, high and low temperature, heavy metal, hypoxia, and high wind stresses (Etesami, 2018). Drought stress (DS) is considered to be among the most critical and devastating abiotic stresses (Grillakis, 2019). The physiological and biochemical processes of plants, such as photosynthesis, respiration, secondary metabolites, and enzyme activities, are severely suppressed under DS (Okunlola et al., 2017), resulting in a reduction in yield (Hussain et al., 2018; Leng and Hall, 2019). Especially in recent years, global climate change has exacerbated the frequency and severity of DS (Harrison et al., 2014; Liu et al., 2019). Meanwhile, it has been reported that the world's population is expected to reach approximately 9.8 billion by 2050 (Mphande et al., 2020). Therefore, it is necessary to investigate approaches to overcome the yield losses brought on by DS in order to avoid a global food shortage as food demand rises.

Irrigation can mitigate the negative impact of drought stress on crops, but this measure is difficult to implement in most cases due to water resource constraints (Leng and Hall, 2019). The application of exogenous compounds is a common practice to stimulate the drought resistance of crops, such as plant growth regulators (PGR) (Chen et al., 2018), nutrients (Etesami and Jeong, 2018; Shehzad et al., 2020), and phytohormones or analogues (Anjum et al., 2016). For example, PGRs, such as spermidine (Li et al., 2018), and 24-epibrassinolide (EBL) etc. (Shahzad et al., 2018), are a potent tool for sustainably mitigating drought stress in many plants. Phytohormones or analogues are also a promising practical strategy to enhance crop drought resistance, such as brassinolide (Anjum et al., 2011), brassinosteroids (Krishna et al., 2017), jasmonic acid (Farhangi-Abriz and Ghassemi-Golezani, 2019), methyl jasmonate (Anjum et al., 2016), salicylic acid (Sharma et al., 2018), cytokinin (Egamberdieva et al., 2017), melatonin (Sharma et al., 2020), and gibberellin (Gaion et al., 2018).

Phthalanilic acid [2- (phenyl carbamoyl) benzoic acid], also known as N-phenyl-phthalamic acid (PPA), is a PGR developed by the Neviki Research Institute of Hungary in 1982 (Zhao et al., 2014). It can improve the stigma vitality, pollination, setting fruit, and yield of many fruit trees without causing any phytotoxicity (Racsko, 2004; Khadivi-Khub and Nosrati, 2013). Our previous investigations showed that PPA significantly increased the yield of pepper (*Capsicum annuum*) fruits as well as enhanced the stress resistance of pepper plants in field conditions (Zhang et al., 2017; Wu et al., 2018; Zhang et al., 2018), especially in the typical arid and semi-arid regions of northwest China, where drought often occurs due to the frequent shortage of water resources (Yang et al., 2018). Thus, we believed that PPA may stimulate resistance to DS in peppers, thereby reducing the negative effects of DS on peppers. However, the role of PPA in mitigating DS-induced damage is only partially understood and merits further investigation.

In general, the plants in response to drought stress cause changes in several important markers, including malondialdehyde (MDA), proline, and the activity of antioxidant enzymes such as superoxide dismutase (SOD), catalase (CAT), and peroxidase (POD) (Beyaz, 2019; Beyaz, 2022). These markers are often used as the basis for drought stress studies of pepper (Kim et al., 2022). Therefore, to elucidate the

drought-resistance effect of PPA on pepper (*C. annuum*) seedlings, the content of these markers was measured in this study. Besides, this work also made in-depth studies on other characteristics of pepper, such as the leaf wilting index, relative water content, photosynthetic characteristics, growth parameters, and osmotic substances.

# 2 Materials and methods

## 2.1 Plant material and chemicals

Pepper (*C. annuum*, Shijihong) seeds were obtained from the Horticulture College of Northwest A & F University. PPA 20% soluble liquid (SL) was provided by Shaanxi Sunger Road Bioscience Co., Ltd. Trichloroacetic acid, coomassie brilliant blue G-250, thiobarbituric acid, and other reagents were provided by Aladdin™ (Shanghai, China).

## 2.2 Experimental design

The pepper seeds were sown in the plug trays with 32 holes (the top diameter of 6 cm, the bottom diameter of 3.0 cm, and 5.5 cm depth) filled with the nutritive soil (garden soil: compost: humus = 1:1:1, v/v/v). The trays were then placed in a temperature-controlled climatic chamber (L:D = 12:12 h, RH = 60%-70%, T = 25 ± 5 °C) to continue cultivation. At the five-leaf stage, the pepper seedlings were treated with PPA (133.3 mg·L<sup>-1</sup>; 200.0 mg·L<sup>-1</sup>; 266.7 mg·L<sup>-1</sup>) at 8:00 - 9:00 am by using a small manual sprayer. Water was applied as a control. The number of PPA treatments was also thought to be a factor. PPA was sprayed again at a two-day interval. Then, the pepper seedlings were transplanted to new trays. To control soil moisture in the new trays, the nutritive soil was dried to a constant weight in an oven at 105 °C for 8 h, and then mixed with different proportions of water (mass ratio). In this experiment, four drought conditions were set according to the soil relative water (SRW) content, including (1) the normal group representing that the SRW content was maintained between 70% and 80%, (2) the light drought stress (LDS) group (SRW: 50% ~ 60%), (3) the moderate drought stress (MDS) group (SRW: 40%~50%), and (4) the severe drought stress (SDS) group (SRW: 30% ~ 40%). The leaf wilting index, relative water content, and malondialdehyde content of pepper seedlings under LDS and MDS for 15 days were measured to evaluate the ideal application concentration and frequency of PPA.

To further clarify the mechanism of PPA causing drought resistance in pepper, the morphological indicators, photosynthetic parameters, antioxidant activities, and osmotic substances of pepper seedlings treated twice with PPA at a concentration of 133.3 mg·L<sup>-1</sup> were further measured on days 1, 3, 7, 11, 15 (LDS and MDS) or on days 1, 3, 5, 7, 10 (SDS). Each drought condition was repeated three times, and each repetition contained 30 pepper seedlings.

## 2.3 Morphological indicators of pepper seedlings

The plant height and stem diameter were measured five times using a ruler and vernier caliper, respectively (Xiong et al., 2016).

The pepper seedlings were washed with deionized water and dried naturally to determine the dry weight of the whole plant, including the dry weight of underground and above-ground parts. Each treatment was repeated three times, and five pepper seedlings were randomly selected from each repetition. The root-shoot ratio, seedling index, and leaf wilting index were calculated according to the following formulas:

$$\text{Root-shoot ratio (RSR)} = \text{DUW} / \text{DAW}$$

$$\text{Seedling index (SI)} = (\text{SD} / \text{PH} + \text{DUW} / \text{DAW}) \times \text{DWW}$$

$$\text{Leaf wilting index (LWI)} = (1 - \text{NWL} / \text{NTL}) \times 100 \%$$

Where DWW, DUW, and DAW represent the dry weight of the whole plant (g), the dry weight of underground parts (g), and the dry weight of above-ground parts (g), respectively. SD and PH are stem diameter (cm) and plant height (cm), respectively. NWL and NTL represent the number of wilted leaves and the number of total leaves, respectively.

## 2.4 Relative water content

Relative water content was measured according to the method of Liang et al. (2018). Five leaves were randomly collected from each plant, and the fresh weight (FW) of the leaves was recorded. The leaves were immersed in distilled water for 24 h to further measure the turgid weight (TW). Finally, the leaves placed in an oven were roasted at 105 °C for 30 min, and then dried at 80 °C to a constant weight, and the dry weight (DW) was determined.

$$\text{Relative water content (RWC)} = (\text{FW} - \text{DW}) / (\text{TW} - \text{DW}) \times 100 \%$$

## 2.5 Chlorophyll content

Chlorophyll content was determined according to the method of Min et al. (2019), with some modifications. Ten fresh leaves were collected from each plot and washed as test samples. The samples (0.3 g) were then ground to homogenate in a mortar with quartz sand, calcium carbonate powder, and 5.0 ml of pure acetone. The extracting reaction was performed by adding 5.0 mL of 80% (w/v) acetone to the homogenate for 10 min under dark conditions. The extraction solution was centrifuged using the Centrifuge 5424 (Eppendorf AG, Germany) at 20,000 g for 30 min at 4 °C. Supernatant was collected, and its absorbance was recorded by the UV3310 spectrophotometer (Hitachi, Japan) at 663 nm and 645 nm, respectively. There were three replicates for each treatment. The chlorophyll content (chlorophyll *a* and chlorophyll *b*) was calculated using the equation of Min et al. (2019). The results are expressed on a dry weight basis (mg·g<sup>-1</sup> FW).

## 2.6 Photosynthetic parameters

The photosynthetic parameters, including net photosynthesis rate (Pn), transpiration rate (Tr), stomatal conductance (Gs),

intercellular CO<sub>2</sub> concentration (Ci), and atmospheric CO<sub>2</sub> concentration (Ca), were measured using a portable photosynthesis instrument (PP-Systems, MA, USA) on a sunny day between 9:00 and 11:00 a.m. The light intensity was set to 100.0 μmol·m<sup>-2</sup>·s<sup>-1</sup>. The flow rate of the air with 60%–70% relative humidity was maintained at 500.0 μmol·s<sup>-1</sup>. The leaf temperature was 25 ± 1.5 °C, and the CO<sub>2</sub> concentration was set at 400 μmol·mol<sup>-1</sup>. The instantaneous water-use efficiency (WUE) was calculated as Pn/Tr. Stomatal limitation (Ls) was calculated as Ls = 1 - Ci/Ca. Among them, the fully expanded uppermost leaf (from the top of the main stem) of each plant was selected for the photosynthetic parameter's measurement. Each treatment was repeated three times, and five plants were randomly selected from each repetition.

## 2.7 Malondialdehyde content

Malondialdehyde (MDA) content was measured as described by Goñi et al. (2018) with minor modifications. Briefly, the sample of fresh leaf (1.0 g) was ground to homogenate. The homogenate added 10.0 mL of 20% (w/v) trichloroacetic acid (TCA) was centrifuged at 10,000 g for 10 min at 4 °C. Supernatant (2.0 mL) was incubated with 2.0 mL of thiobarbituric acid (0.5%, w/v) at 95 °C for 15 min. After centrifugation again, the absorbance of the supernatant was recorded at 450 nm, 532 nm, and 600 nm. The MDA content was calculated according to the following equations,

$$\begin{aligned} \text{MDA (nmol MDA} \cdot \text{g}^{-1} \text{FW)} \\ = [(\text{OD}_{532} - \text{OD}_{600}) \times 6.452 - 0.559 \times \text{OD}_{450}] \times \text{VE} / (\text{VEM} \\ \times \text{W}) \end{aligned}$$

Where VE means the total volume of the extraction solution (mL); VEM is the total volume of the extraction solution for measurement (mL); W represents the fresh weight of the sample (g).

## 2.8 Free proline content

The procedure of Bates et al. (1973) with some modifications was used for the measurement of free proline. Briefly, leaves (0.5 g) were homogenized in 10.0 mL of 3% (w/v) sulfosalicylic acid. The homogenate was centrifuged at 15,000 × g for 30 min at 4 °C. Then, its supernatant (2.0 mL) was mixed with acidic ninhydrin (2.0 mL) and acetic acid (2.0 mL) and boiled for 40 min. After cooling at room temperature, the mixture was extracted with toluene (4.0 mL), and the absorbance of the toluene extract was read at 520 nm. The free proline content was calculated by the standard curve method and expressed as mg·g<sup>-1</sup> FW.

## 2.9 Extraction and determination of antioxidant enzymes

Antioxidant enzyme activities, including superoxide dismutase (SOD), catalase (CAT), and peroxidase (POD), were determined following the protocol of Shehzad et al. (2020) and expressed as U·g<sup>-1</sup>

FW. Firstly, leaves (0.5 g) were fully homogenized with 2.0 mL of pre-cooled phosphate buffer (50 mM, pH 7.8) and 7.0 mL of 1.0% (w/w) polyvinylpyrrolidone. The homogenate was then centrifuged at  $8,000 \times g$  for 15 min at 4 °C to collect supernatant for enzyme analysis. The absorbance was monitored every 20 s by a UV-3310 spectrophotometer (Hitachi, Japan) at 240 nm wavelength. The CAT activity was evaluated by measuring the decomposition of  $H_2O_2$ . The POD activity was assessed by monitoring the absorbance at 470 nm using guaiacol. To assay the SOD activity, the absorbance was measured at 570 nm after 20 min of chromogenic reaction. All enzymes' activities were expressed as units  $U \cdot g^{-1} \cdot FW$ .

## 2.10 Soluble sugar content

Soluble sugars were determined according to the method described by Du et al. (2020). The fresh leaves (0.5 g) were extracted in the boiling water bath for 30 min. Its remaining residue was extracted twice more, and the extraction solutions were combined in a volumetric flask (100.0 mL). Then, the test tube with extraction solution (0.5 mL) added cocktail consisting of 0.5 mL of anthrone-ethyl acetate reagent, 5.0 mL of concentrated sulfuric acid, and distilled water (1.5 mL). After shaking, the test tube was immediately put into the boiling water bath for 10 min. After cooling, absorbance was determined three times by the UV-3310 spectrophotometer (Hitachi, Japan) at 620 nm wavelength. The soluble sugar content was calculated by a standard curve (glucose) and expressed as  $mg \cdot g^{-1} \cdot FW$ .

## 2.11 Soluble protein content

Soluble protein was measured using the UV-3310 spectrophotometer (Hitachi, Japan) at 595 nm. Briefly, leaves (0.5 g) were ground to homogenate with 5.0 mL of distilled water, and then the homogenate was centrifuged at  $12,000 \times g$  for 20 min at 4 °C. Supernatant (1.0 mL) was collected and added to 5.0 mL of Coomassie Brilliant Blue G-250 solution in the test tube at 30 °C for 30 min for the soluble protein determination. The absorbance of the reaction solution was measured with a spectrophotometer at 595 nm. Bovine serum albumin was used as a standard to quantitatively analyze the content of soluble protein, which was expressed as  $mg \cdot g^{-1} \cdot FW$  (Zou et al., 2017).

## 2.12 Statistical analysis

All data were analyzed with the SPSS 20.0 statistics package (Ver. 22.0, IBM, USA). A one-way analysis of variance (ANOVA) followed by Duncan's multiple range test ( $P < 0.05$ ) was used to assess the differences between means. All graphics were drawn using Origin version 8.1.

## 3 Results

### 3.1 Effect of PPA on the LWI, RWC and MDA of pepper seedlings under DS

The effects of PPA on pepper plants under LDS or MDS situations are shown in Tables 1, 2. The pepper leaves under LDS did not become wilted, so the LWI value did not exist. Compared with the control, the LWI values were increased in the PPA-treated pepper seedlings under MDS, especially with the notable increase rate of 23.38% on the  $133.3 \text{ mg} \cdot L^{-1}$  of PPA treatment (sprayed twice). The PPA also raised the RWC of pepper leaves. Notably, in comparison with the control, RWC in the pepper leaves treated with PPA ( $133.3 \text{ mg} \cdot L^{-1}$ ) twice was significantly ( $P < 0.05$ ) increased by 21.47% and 9.32% under LDS and MDS, respectively. MDA content in the PPA-treated pepper leaves under drought decreased in comparison with the control. In particular, PPA that was applied two times at a concentration of  $133.3 \text{ mg} \cdot L^{-1}$  observably ( $P < 0.05$ ) reduced the MDA content by 44.42% and 42.30% under LDS and MDS, respectively. According to the changes in LWI, RWC, and MDA, the PPA-pretreated pepper seedlings had preferable resistance to DS. Therefore, the effects of PPA-induced resistance to DS were further researched in pepper seedlings.

### 3.2 Effect of PPA on morphological indices of pepper seedlings under DS

The PPA-pretreated pepper seedlings exhibited obvious advantages over water-pretreated pepper seedlings in plant height, root-shoot ratio, and seedling index under three drought conditions (Table 3). Among them, the seedling index increased by 20.54%

TABLE 1 Effect of PPA on pepper (*C. annuum*) seedlings under light drought stress.

| Treatment † | Concentration ( $mg \cdot L^{-1}$ ) | Number of applications | RWC (%)            | MDA content ( $mmol \cdot g^{-1} \cdot FW$ ) |
|-------------|-------------------------------------|------------------------|--------------------|--|
| Control     | —                                   | —                      | $73.95 \pm 1.43d$  | $9.41 \pm 0.65a$                             |
| PPA         | 133.3                               | 1                      | $82.15 \pm 1.14b$  | $6.02 \pm 0.53c$                             |
|             |                                     | 2                      | $89.83 \pm 1.45a$  | $5.23 \pm 0.23d$                             |
|             | 200.0                               | 1                      | $81.72 \pm 1.23b$  | $5.40 \pm 0.35cd$                            |
|             |                                     | 2                      | $77.95 \pm 1.14c$  | $5.93 \pm 0.48cd$                            |
|             | 266.7                               | 1                      | $76.04 \pm 0.54c$  | $6.50 \pm 0.23c$                             |
|             |                                     | 2                      | $75.78 \pm 0.90cd$ | $8.40 \pm 0.25b$                             |

† PPA is an abbreviation of phthalanilic acid.

Data are the average of three replications ( $n = 3$ ) and represented as mean  $\pm$  standard deviation. Values followed by different small letters in the same column are significantly different at  $P < 0.05$ . RWC represents the relative water content of pepper leaves. MDA is the malondialdehyde content in pepper leaves.

TABLE 2 Effect of PPA on pepper (*C. annuum*) seedlings under moderate drought stress.

| Treatment † | Concentration (mg·L <sup>-1</sup> ) | Number of applications | LWI (%)        | RWC (%)       | MDA content (mmol·g <sup>-1</sup> FW) |
|-------------|-------------------------------------|------------------------|----------------|---------------|---------------------------------------|
| Control     | —                                   | —                      | 61.11 ± 4.62bc | 62.22 ± 1.59d | 13.97 ± 0.83a                         |
| PPA         | 133.3                               | 1                      | 74.14 ± 3.18a  | 73.69 ± 1.19b | 11.01 ± 0.86b                         |
|             |                                     | 2                      | 75.40 ± 4.87a  | 68.02 ± 2.19c | 8.06 ± 0.23c                          |
|             | 200.0                               | 1                      | 68.26 ± 2.75ab | 68.27 ± 1.33c | 10.64 ± 0.95b                         |
|             |                                     | 2                      | 69.56 ± 2.55ab | 77.40 ± 1.52a | 11.50 ± 0.96b                         |
|             | 266.7                               | 1                      | 67.26 ± 2.85b  | 66.68 ± 1.19c | 10.98 ± 0.25b                         |
|             |                                     | 2                      | 63.49 ± 3.50b  | 65.99 ± 1.43c | 11.34 ± 1.13b                         |

† PPA is an abbreviation of phthalanilic acid.

Data are the average of three replications (n = 3) and represented as mean ± standard deviation. Values followed by different small letters in the same column are significantly different at P < 0.05. LWI means the leaf wilting index of pepper leaves.

(LDS), 21.29% (MDS), and 23.20% (SDS), respectively. The stem diameter was increased by 1.18 times under SDS. However, the stem diameter was not affected by PPA under LDS or MDS.

### 3.3 Effect of PPA on photosynthetic parameters of pepper seedlings under DS

As illustrated in Figure 1, the exogenous application of PPA improved the net photosynthetic rate (Pn), transpiration rates (Tr), stomatal conductance (Gs), intercellular CO<sub>2</sub> concentration (Ci), and water-use efficiency (WUE) on the pepper seedling leaves under LDS but reduced the values of stomatal limitation (Ls). Among them, the PPA-treated pepper seedlings showed remarkable (P < 0.05) increases in Pn (38.65% - 61.04%), Ci (27.43% - 38.81%), and WUE (20.61% - 33.63%) during the LDS period over control. The Gs values were significantly (P < 0.05) higher than those of the control, with the increase rates ranging from 33.12% to 51.69% by day 11, but there were no significant changes for the Gs value on day 15. The Ls values were markedly (P < 0.05) lower than those of control by a range of 12.53% to 17.66%, except on the 7<sup>th</sup> day. The

transpiration rates (Tr) were significantly (P < 0.05) improved by 17.59% (on day 1) and 21.23% (on day 3) over control under LDS (Figure 1).

Similarly, PPA enhanced the Pn, Ci, and WUE on the pepper leaves under MDS, with marked (P < 0.05) increase rates of 17.23% - 36.94% (from day 1 to day 15), 13.43% - 28.53% (from day 3 to day 15), and 17.44% - 33.92% (from day 3 to 15) in comparison with control (Figure 2); and the Gs value was observably (P < 0.05) improved by 19.32% on day 1. PPA also raised the Tr values of pepper leaves during the MDS period; especially compared with the control, the Tr values were observably (P < 0.05) increased by 28.81% (on day 1) and 15.19% (on day 3) (Figure 2). However, the values of Ls were decreased by PPA under MDS for 15 days, with a notable (P < 0.05) reduction of 15.82% (on day 11) over control (Figure 2).

The chlorophyll contents of PPA-treated peppers were higher than those of non PPA-treated peppers under SDS, with significant (P < 0.05) increases ranging from 19.69% (on day 5) to 22.22% (on day 10) (Figure 3A). PPA had significant effects on chlorophyll contents within the MDS period, with the increase rate ranging between 18.68% and 38.78% (Figure 3B). As shown in Figure 3C, in

TABLE 3 Effect of PPA on morphological indicators of pepper (*C. annuum*) seedlings under drought stress.

| Treatment †             | Plant height (cm) | Stem diameter (cm) | Root-shoot ratio | Seedling index |
|-------------------------|-------------------|--------------------|------------------|----------------|
| Light drought stress    |                   |                    |                  |                |
| Control                 | 13.492 ± 0.128    | 2.103 ± 0.033      | 0.230 ± 0.010    | 0.370 ± 0.021  |
| PPA                     | 13.958 ± 0.170*   | 2.145 ± 0.015      | 0.243 ± 0.010*   | 0.446 ± 0.017* |
| Moderate drought stress |                   |                    |                  |                |
| Control                 | 13.258 ± 0.138    | 0.208 ± 0.030      | 0.181 ± 0.007    | 0.310 ± 0.009  |
| PPA                     | 13.667 ± 0.092*   | 0.212 ± 0.018      | 0.212 ± 0.09*    | 0.376 ± 0.013* |
| Severe drought stress   |                   |                    |                  |                |
| Control                 | 13.285 ± 0.104    | 1.735 ± 0.036      | 0.094 ± 0.008    | 0.250 ± 0.012  |
| PPA                     | 14.158 ± 0.325*   | 2.043 ± 0.048*     | 0.106 ± 0.009    | 0.308 ± 0.014* |

† PPA was twice applied to pepper seedlings at a concentration of 133.3 mg·L<sup>-1</sup> before drought stress.

The data are presented as the mean value ± standard deviation (n = 3), and asterisk denotes significant difference to corresponding control at P < 0.05.



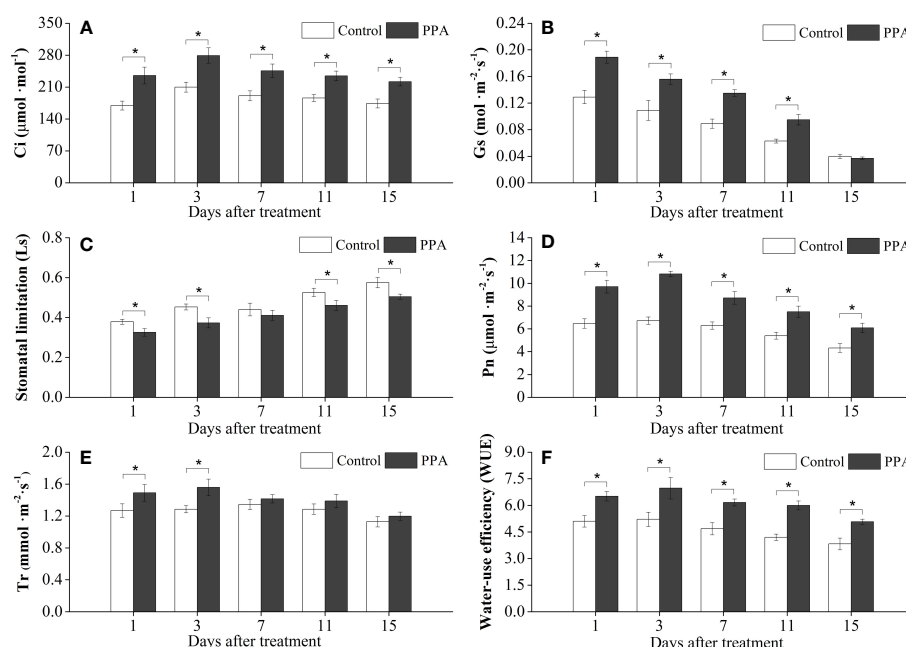


FIGURE 1

Effects of PPA on the intercellular  $\text{CO}_2$  concentration ( $C_i$ ; A), stomatal conductance ( $G_s$ ; B), stomatal limitation (Ls; C), net photosynthesis rate ( $P_n$ ; D), transpiration rates ( $Tr$ ; E), and water-use efficiency (WUE; F) of pepper (*Capsicum annuum*) leaves under light drought stress (LDS). LDS means that pepper seedlings were maintained the SRW content of 50% - 60%. Control means that pepper seedlings were treated with water before drought stress and maintained the soil relative water (SRW) content of 70% - 80%. Bars represent means  $\pm$  SD of three replications, and asterisk denotes significant difference to corresponding control at  $P < 0.05$ . Phthalanilic acid (PPA) was twice applied to pepper seedlings at a concentration of  $133.3 \text{ mg} \cdot \text{L}^{-1}$  before drought stress. The same as Figures 2–6.

comparison with the control, the chlorophyll contents in PPA-applied pepper leaves were obviously ( $P < 0.05$ ) increased by between 13.30% and 39.20% under the LDS situation for 15 days.

### 3.4 Effect of PPA on antioxidant enzyme activities in pepper seedlings under DS

Exogenous PPA application enhanced the activities of antioxidative enzymes (SOD, CAT, and POD) in pepper leaves under DS (Figures 4, 5). POD activities were markedly ( $P < 0.05$ ) improved 13.50% - 39.25% (from day 1 to day 7) by PPA under SDS in comparison with control (Figure 4A). PPA also obviously ( $P < 0.05$ ) enhanced the POD activities during the 15 days by 21.26% - 58.30% under MDS (Figure 4B), and 28.64% - 65.78% under LDS (Figure 4C), respectively. Furthermore, PPA significantly ( $P < 0.05$ ) elevated SOD activities under LDS (with increase rates of 16.50% on day 1), MDS (increasing by 26.40% on day 1 and 17.39% on day 11), and SDS (going up 21.43% to 36.64% from day 1 to day 10), respectively (Figures 4D–F). Interestingly, CAT activities in the pepper leaves treated with PPA were also higher ( $P < 0.05$ ) than those of the control, which were increased by 13.91% - 48.13% and 20.05% - 36.08% during LDS and SDS periods, respectively (Figures 5D, F). During the MDS period, the CAT activities were significantly ( $P < 0.05$ ) increased by 16.44% to 62.32% (from day 3 to day 11) (Figure 5E).

### 3.5 Effect of PPA on free proline in pepper seedlings under DS

Compared with the control, exogenous PPA significantly ( $P < 0.05$ ) boosted the free proline content in the pepper leaves under LDS, MDS, and SDS by 44.61% - 72.92%, 25.53% - 68.06% and 28.80% - 69.77%, respectively (Figures 5A–C).

### 3.6 Effects of PPA on soluble sugar and soluble protein in the pepper seedlings under DS

As shown in Figure 6, PPA was associated with increases in soluble sugar and soluble protein in the pepper seedlings under drought conditions. In comparison with the control, the contents of soluble sugar were notably ( $P < 0.05$ ) enhanced by 21.57% - 50.22% (LDS), 28.49% - 36.13% (MDS), and 20.51% - 41.98% (SDS) throughout the drought stress period (Figures 6A–C). Analogously, the soluble protein contents were observably ( $P < 0.05$ ) increased by 20.13% - 44.63% over control during the SDS period except on day 10 (Figure 6D). Within the LDS and MDS periods, the soluble protein contents in the PPA-treated pepper leaves were significantly ( $P < 0.05$ ) increased by 33.46% - 58.74% and 27.20% - 70.85%, respectively (Figures 6E, F).

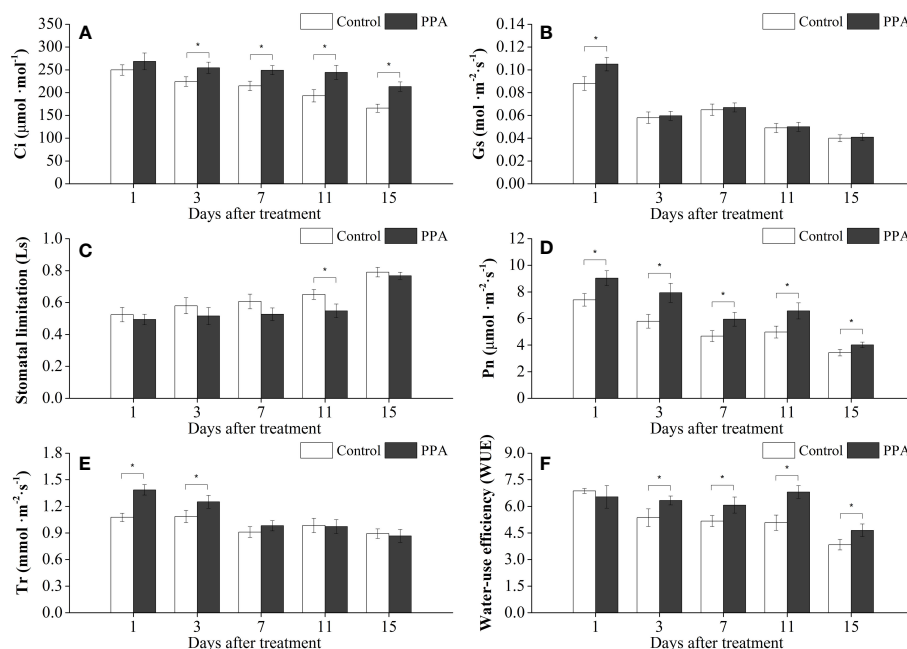


FIGURE 2

Effects of PPA on the Ci (A), Gs (B), Ls (C), Pn (D), Tr (E), WUE (F) of pepper (*C. annuum*) leaves under moderate drought stress (MDS). MDS represents that pepper seedlings were kept the SRW content of 40% - 50%. Asterisk denotes significant difference to corresponding control at  $P < 0.05$ .

## 4 Discussion

PPA plays an important role in alleviating plant growth inhibition and damage caused by DS. In general, the leaf wilting index (LWI) directly reflects the wilting degree of leaves, and its value is positively related to the tolerance of crops for DS (Wang et al., 2015). RWC represents the tissue moisture of crops, and its reduction means that the crops have suffered drought (Malika et al., 2019). In addition, MDA is the final product of membrane lipid peroxidation caused by ROS and acts as a signal of cell membrane damage (Gao et al., 2020). In this work, pepper seedlings were pretreated with PPA and then placed in DS, and it was found that LWI and RWC values were significantly raised, while the MDA content was markedly decreased, indicating that PPA could induce resistance to DS in pepper seedlings.

Obviously, the effect of PPA can be confirmed by improving the morphology of pepper. Normally, once plants are placed under DS, their most intuitive influence is morphological damage (Gupta et al., 2014). In this work, we found that exogenous PPA treatment promoted the plant height, root-shoot ratio, and seedling index of pepper plants under LDS, MDS, and SDS, especially the seedling index, which was significantly increased by PPA. These results are in accord with the effect of other PGRs on the growth of drought-stressed plants. For instance, exogenous spermidine increased the root-shoot ratio of maize (*Zea mays*) seedlings under DS (Li et al., 2018). It has been reported that 50%-80% of Pn-related leaf photoassimilates are required to meet the requirements of plant non-photosynthetic organs (Ahmadi Lahijani et al., 2018). The Pn of pepper leaves under DS was also enhanced

by PPA. Therefore, the increase in PPA-mediated seedling index indicated that PPA might promote the transport of photoassimilates to the whole plant. Similarly, PPA could promote the transport of more photoassimilates to the underground part of plants, resulting in an increase in the root-shoot ratio. The underground part of plants plays a key role in absorbing water from the soil to maintain balance between transpiration and hydration (Li et al., 2018). Interestingly, in this work, the RWC of pepper leaves treated with PPA was significantly increased under drought conditions, which may be associated with the PPA-induced increase in root-shoot ratio, which also makes the plants more adaptable to drought. However, this inference needs to be further studied from a molecular perspective.

The reason why PPA improves the tolerance of plants to drought may be associated with the improvement of PPA-mediated antioxidant activity, Pn and osmotic substance accumulation. Firstly, when plants are subjected to drought, reactive oxidative species (ROS) are increased in plants (Min et al., 2019), including singlet oxygen, superoxide anion, hydrogen peroxide, and hydroxyl radicals (Etesami and Jeong, 2018), leading to membrane disruption, enzyme dysfunction, and protein oxidation and aggregation (Wang et al., 2019). The strategy for plants to resist or repair damage caused by ROS can be achieved by promoting the activity of enzymatic antioxidants (such as SOD, POD, and CAT, etc.) or non-enzymatic antioxidants (carotenoids, non-protein amino acids, and phenolic compounds, among others) (Chavoushi et al., 2019). Of course, free proline is a non-enzyme scavenger for free radicals, which can protect membranes and various macromolecules like enzymes and proteins (Xiao et al.,

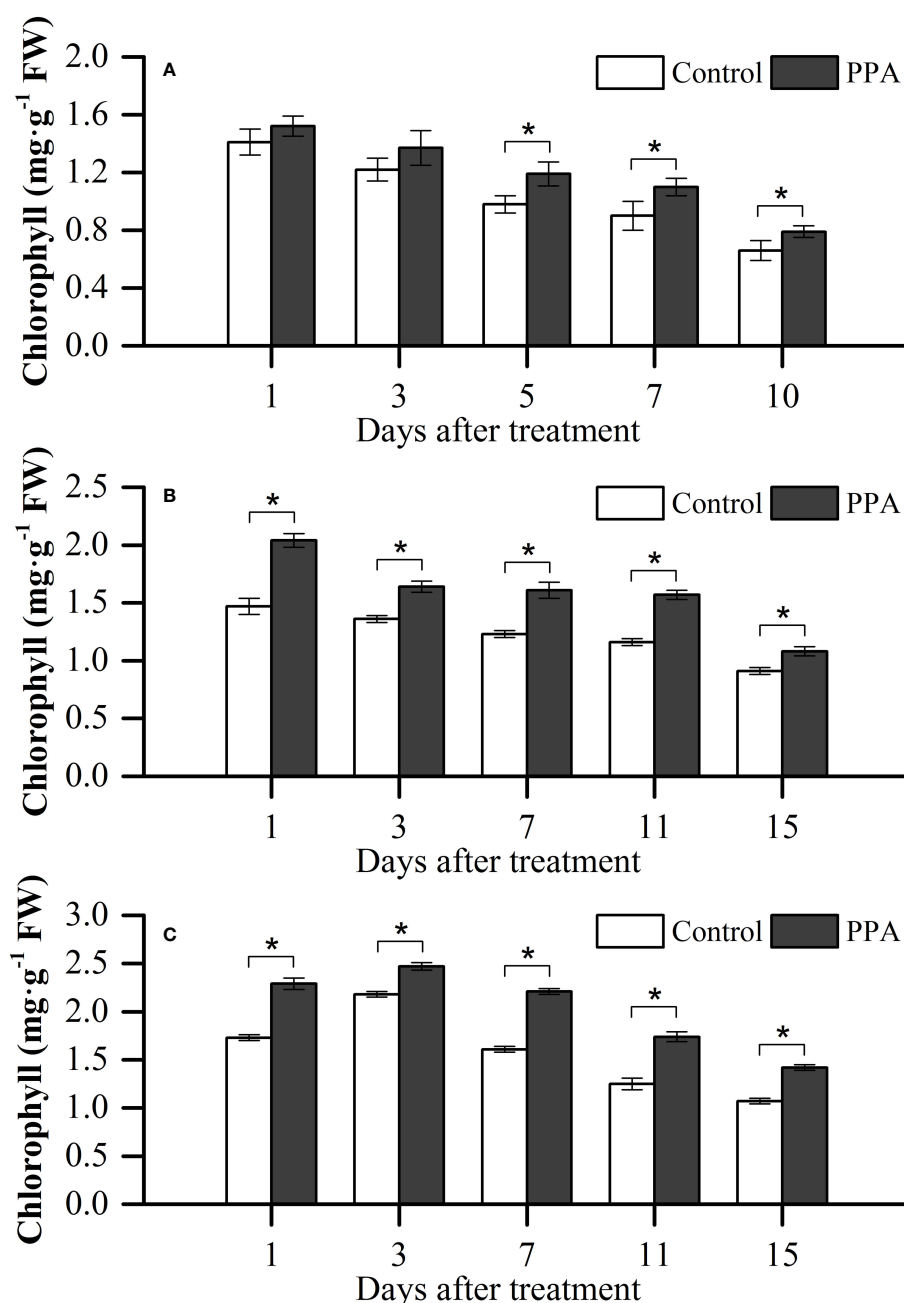


FIGURE 3

Effect of PPA on the chlorophyll of pepper (*C. annuum*) leaves under severe drought stress (SDS; **A**), moderate drought stress (MDS; **B**), and light drought stress (LDS; **C**). Among them, SDS symbolizes that pepper seedlings were provided the SRW content of 30% - 40%. Asterisk denotes significant difference to corresponding control at  $P < 0.05$ .

2008). Our research revealed that PPA promoted the content of free proline and the activities of CAT, POD, and SOD in pepper leaves under LDS, MDS, and SDS, leading to the reduction of ROS. At the same time, we observed that the MDA content of pepper leaves subjected to PPA treatment was decreased, which also verifies that ROS in drought-stressed pepper was reduced. Therefore, the enhancement of tolerance to drought in PPA-treated pepper seedlings may be linked to the activation of enzymatic and non-enzymatic antioxidant systems by PPA.

Secondly, stomata close during drought periods to limit water loss by evapotranspiration, which directly causes the reduction of  $G_s$ , further decreases the  $C_i$ ,  $T_r$ , and  $P_n$ , and then affects the  $L_s$  and WUE in plants (Bhusal et al., 2019). At present, the judgment of the decline in the photosynthetic rate of plant leaves depends on the trends of  $L_s$  and  $C_i$ . In other words, the stomatal factor seems to mainly limit the photosynthetic rate with the decrease of  $C_i$  and the increase of  $L_s$ ; in contrast, non-stomatal factors chiefly limit the inhibition of the photosynthetic rate as  $C_i$  increases and  $L_s$

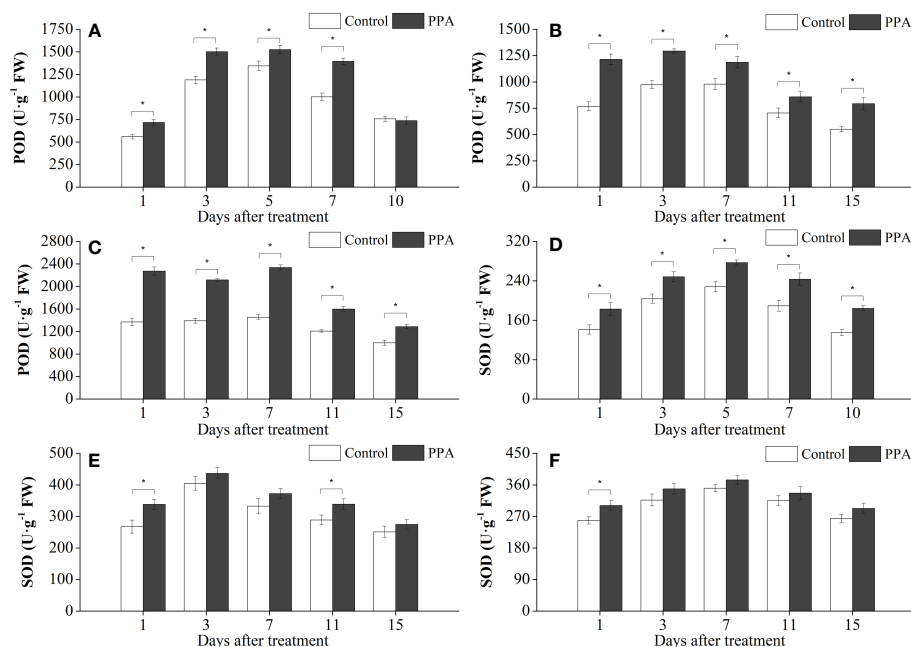


FIGURE 4

Effect of PPA on POD (A, SDS; B, MDS; C, LDS) and SOD (D, SDS; E, MDS; F, LDS) in pepper (*C. annuum*) leaves under drought stress. Asterisk denotes significant difference to corresponding control at  $P < 0.05$ .

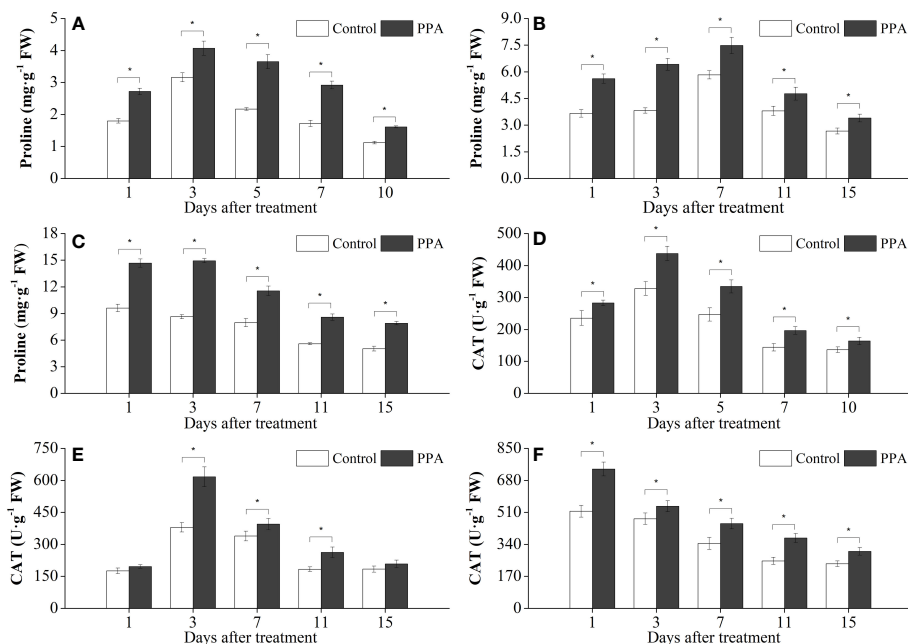


FIGURE 5

Effects of PPA on proline (A, SDS; B, MDS; C, LDS) and CAT (D, SDS; E, MDS; F, LDS) in pepper (*C. annuum*) leaves under drought stress. Asterisk denotes significant difference to corresponding control at  $P < 0.05$ .

decreases (Mantlana et al., 2008). In the present study, PPA improved  $C_i$  in pepper leaves under LDS and MDS but reduced the values of  $L_s$ . Undoubtedly,  $C_i$  in untreated pepper leaves under LDS and MDS may be reduced; on the contrary,  $L_s$  may be increased. Based on the tendency of changes in  $C_i$  and  $L_s$ , we

speculated that the photosynthetic rate of the pepper leaves facing drought was primarily controlled by stomatal factors. Fortunately,  $P_n$  in PPA-treated pepper leaves under LDS and MDS was significantly enhanced, attributing to the PPA-mediated increase in  $C_i$  and  $Tr$ , especially the PPA-mediated increase in  $G_s$ . Besides,



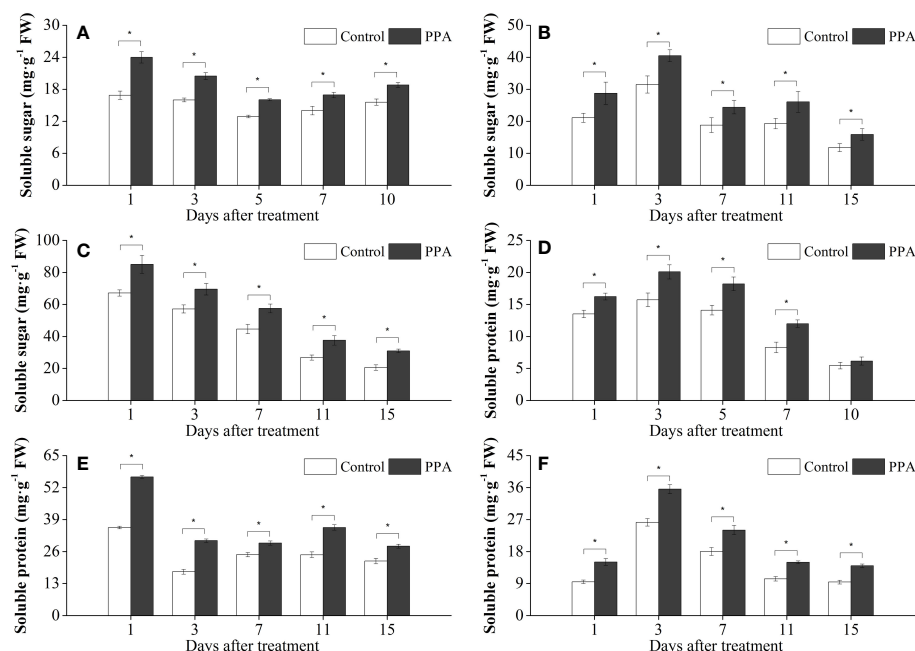


FIGURE 6

Effects of PPA on soluble sugar (A, SDS; B, MDS; C, LDS) and soluble protein (D, SDS; E, MDS; F, LDS) in pepper (*C. annuum*) leaves under drought stress. Asterisk denotes significant difference to corresponding control at  $P < 0.05$ .

chlorophyll plays a central role in the photosynthetic light reactions, whose degradation is associated with the production of reactive oxygen in the leaves caused by droughts (Liang et al., 2018). In this study, the chlorophyll content in PPA-applied pepper leaves increased under three different degrees of drought. Meanwhile, the CAT, POD, and SOD activities in pepper leaves under LDS and MDS were improved by PPA. Thus, PPA-mediated enhancement of Pn in pepper leaves under LDS and MDS may also be related to the elimination of ROS and the protection of chlorophyll. In addition, PPA improved the WUE of pepper leaves under LDS and MDS, indicating that drought-stressed pepper seedlings modified the hydraulic structure of leaves due to the intervention of PPA, which results in the formation of efficient water use mechanisms and high Pn. In this work, the LWI of pepper leaves treated with PPA was significantly higher under DS, indicating that most of the leaves that suffered drought remained apparently normal. These results demonstrated that PPA-applied pepper plants can maintain more favorable photosynthesis, respiration, and transpiration compared to untreated pepper plants under drought.

Thirdly, the accumulation of osmotic substances such as soluble sugar, soluble protein, and proline is one of the adaptive solutions for plants under DS (Chavoushi et al., 2020). These osmolytes play an important role in holding the moisture inside tissues as well as absorbing water from the external environment, thereby ultimately maintaining the normal physiological and biochemical activity of the cells (Cheng et al., 2018). This work showed that the application

of PPA was closely associated with increases in soluble sugar, soluble protein, and proline in pepper leaves under drought conditions. Especially the accumulation of these three osmotic substances was obviously increased in the pepper leaves under SDS conditions, this is similar to the results of Gao et al. (2020), which means that plants need more water to overcome the damage caused by DS. Correspondingly, this statement has been corroborated; that is, this study revealed that the RWC of pepper leaves treated with PPA was significantly improved. Thus, PPA can better maintain the water required for drought-stressed pepper seedlings by promoting the accumulation of osmotic substances.

PPA has excellent application value in field agricultural production. This study found that PPA can clearly alleviate the growth inhibition and damage to pepper seedlings caused by drought. Applying PPA ( $133.3 \text{ mg} \cdot \text{L}^{-1}$ ) to crops twice can produce preferable efficacy. In addition, three years of field trials have shown that PPA ( $133.3 \text{ mg} \cdot \text{L}^{-1}$ ) can also increase the yield of pepper fruits (Zhang et al., 2017; Wu et al., 2018; Lu et al., 2023). Therefore, PPA exerts a variety of beneficial effects in field applications.

## 5 Conclusion

Exogenous PPA can induce DS resistance in pepper seedlings, reducing the damage that DS causes to peppers. A dosage of  $133.3 \text{ mg} \cdot \text{L}^{-1}$  of PPA applied twice can considerably increase the drought

resistance of peppers. The PPA-mediated efficacy may be linked to the improvement of multiple physiological processes, including antioxidant activities, photosynthesis, and the accumulation of osmotic substances. PPA can help peppers adapt to drought and is worthy of widespread use in pepper production.

## Data availability statement

The original contributions presented in the study are included in the article/supplementary material. Further inquiries can be directed to the corresponding authors.

## Author contributions

XL: Conceptualization, Methodology, Data curation, Software, Writing - original draft, Writing-review & editing. QW: Conceptualization, Investigation, Data curation. KN: Investigation. HW: Data curation, Validation. GC: Writing-review & editing, Funding acquisition. JW: Writing-review & editing, Funding acquisition. ZM: Funding acquisition, Project administration, Data curation, Validation, Supervision. All authors contributed to the article and approved the submitted version.

## References

- Ahmadi Lahijani, M. J., Kafi, M., Nezami, A., Nabati, J., Mehrjerdi, M. Z., Shahkoomahally, S., et al. (2018). Variations in assimilation rate, photoassimilate translocation, and cellular fine structure of potato cultivars (*Solanum tuberosum* L.) exposed to elevated CO<sub>2</sub>. *Plant Physiol. Bioch.* 130, 303–313. doi: 10.1016/j.plaphy.2018.07.019
- Anjum, S. A., Tanveer, M., Hussain, S., Tung, S. A., Samad, R. A., Wang, L., et al. (2016). Exogenously applied methyl jasmonate improves the drought tolerance in wheat imposed at early and late developmental stages. *Acta Physiol. Plant* 38, 1–11. doi: 10.1007/s11738-015-2047-9
- Anjum, S. A., Wang, L. C., Farooq, M., Hussain, M., Xue, L. L., and Zou, C. M. (2011). Brassinolide application improves the drought tolerance in maize through modulation of enzymatic antioxidants and leaf gas exchange. *J. Agron. Crop Sci.* 197, 177–185. doi: 10.1111/j.1439-037X.2010.00459.x
- Bates, L., Waldren, R., and Teare, I. (1973). Rapid determination of free proline for water stress studies. *Plant Soil* 39, 205–207. doi: 10.1007/BF00018060
- Beyaz, R. (2019). Biochemical responses of sainfoin shoot and root tissues to drought stress in *in vitro* culture. *Legume Res.* 42, 173–177. doi: 10.18805/LR-460
- Beyaz, R. (2022). Morphological and biochemical changes in shoot and root organs of common vetch (*Vicia sativa* L.) after exposure to drought stress. *Scienceasia* 48, 51–56. doi: 10.2306/scienceasia1513-1874.2022.010
- Bhusal, N., Han, S., and Yoon, T. (2019). Impact of drought stress on photosynthetic response, leaf water potential, and stem sap flow in two cultivars of bi-leader apple trees (*Malus × domestica* Borkh.). *Sci. Hortic.* 246, 535–543. doi: 10.1016/j.scienta.2018.11.021
- Chavoushi, M., Najafi, F., Salimi, A., and Angaji, S. A. (2019). Improvement in drought stress tolerance of safflower during vegetative growth by exogenous application of salicylic acid and sodium nitroprusside. *Ind. Crop Prod.* 134, 168–176. doi: 10.1016/j.indcrop.2019.03.071
- Chavoushi, M., Najafi, F., Salimi, A., and Angaji, S. A. (2020). Effect of salicylic acid and sodium nitroprusside on growth parameters, photosynthetic pigments and secondary metabolites of safflower under drought stress. *Sci. Hortic.* 259, 108823. doi: 10.1016/j.scienta.2019.108823
- Chen, Z., Wang, Z., Yang, Y., Li, M., and Xu, B. (2018). Absciscic acid and brassinolide combined application synergistically enhance drought tolerance and photosynthesis of tall fescue under water stress. *Sci. Hortic.* 228, 1–9. doi: 10.1016/j.scienta.2017.10.004
- Cheng, L., Han, M., Yang, L. M., Yang, L., Sun, Z., and Zhang, T. (2018). Changes in the physiological characteristics and baicalin biosynthesis metabolism of *Scutellaria baicalensis* Georgi under drought stress. *Ind. Crop Prod.* 122, 473–482. doi: 10.1016/j.indcrop.2018.06.030
- Du, Y. L., Zhao, Q., Chen, L. R., Yao, X. D., Zhang, W., Zhang, B., et al. (2020). Effect of drought stress on sugar metabolism in leaves and roots of soybean seedlings. *Plant Physiol. Bioch.* 146, 1–12. doi: 10.1016/j.plaphy.2019.11.003
- Egamberdieva, D., Wirth, S. J., Alqarawi, A. A., AbdAllah, E. F., and Hashem, A. (2017). Phytohormones and beneficial microbes: essential components for plants to balance stress and fitness. *Front. Microbiol.* 8, 2104. doi: 10.3389/fmicb.2017.02104
- Etesami, H. (2018). Can interaction between silicon and plant growth promoting rhizobacteria benefit in alleviating abiotic and biotic stresses in crop plants? *Agr. Ecosyst. Environ.* 253, 98–112. doi: 10.1016/j.agee.2017.11.007
- Etesami, H., and Jeong, B. R. (2018). Silicon (Si): Review and future prospects on the action mechanisms in alleviating biotic and abiotic stresses in plants. *Ecotox. Environ. Safe.* 147, 881–896. doi: 10.1016/j.ecoenv.2017.09.063
- Farhangi-Abri, S., and Ghassemi-Golezani, K. (2019). Jasmonates: Mechanisms and functions in abiotic stress tolerance of plants. *Biocatal. Agr. Biotechnol.* 20, 101210. doi: 10.1016/j.bcab.2019.101210
- Gaion, L. A., Monteiro, C. C., Cruz, F. J. R., Rossatto, D. R., López-Díaz, I., Carrera, E., et al. (2018). Constitutive gibberellin response in grafted tomato modulates root-to-shoot signaling under drought stress. *J. Plant Physiol.* 221, 11–21. doi: 10.1016/j.jplph.2017.12.003
- Gao, S., Wang, Y., Yu, S., Huang, Y., Liu, H., Chen, W., et al. (2020). Effects of drought stress on growth, physiology and secondary metabolites of two *Adonis* species in northeast China. *Sci. Hortic.* 259, 108795. doi: 10.1016/j.scienta.2019.108795
- Goñi, O., Quille, P., and O'Connell, S. (2018). *Ascophyllum nodosum* extract biostimulants and their role in enhancing tolerance to drought stress in tomato plants. *Plant Physiol. Bioch.* 126, 63–73. doi: 10.1016/j.plaphy.2018.02.024
- Grillakis, M. G. (2019). Increase in severe and extreme soil moisture droughts for Europe under climate change. *Sci. Total Environ.* 660, 1245–1255. doi: 10.1016/j.scitotenv.2019.01.001
- Gupta, N., Thind, S. K., and Bains, N. S. (2014). Glycine betaine application modifies biochemical attributes of osmotic adjustment in drought stressed wheat. *Plant Growth Regul.* 72, 221–228. doi: 10.1007/s10725-013-9853-0
- Harrison, M. T., Tardieu, F., Dong, Z. S., Messina, C. D., and Hammer, G. L. (2014). Characterizing drought stress and trait influence on maize yield under current and future conditions. *Global Change Biol.* 20, 867–878. doi: 10.1111/gcb.12381

## Funding

This work was supported by the Agricultural Science and Technology Innovation Project of Xinjiang Production and Construction Corps (Grant Number: NCG202204) and the Shaanxi Provincial Key Research and Development Program (Grant Number: 2019ZDLNY03-04 and 2021NY03-122).

## Conflict of interest

The authors declare that the research was conducted in the absence of any commercial or financial relationships that could be construed as a potential conflict of interest.

## Publisher's note

All claims expressed in this article are solely those of the authors and do not necessarily represent those of their affiliated organizations, or those of the publisher, the editors and the reviewers. Any product that may be evaluated in this article, or claim that may be made by its manufacturer, is not guaranteed or endorsed by the publisher.

- Hussain, M., Farooq, S., Hasan, W., Ul-Allah, S., Tanveer, M., Farooq, M., et al. (2018). Drought stress in sunflower: physiological effects and its management through breeding and agronomic alternatives. *Agric. Water Manage.* 201, 152–166. doi: 10.1016/j.agwat.2018.01.028
- Khadivi-Khub, A., and Nosrati, Z. (2013). Study of n-phenyl-phthalamic acid effects on fruit setting and fruit quality of sweet, sour and duke cherries. *Acta Agr. Serbica.* 17, 3–9.
- Kim, S. T., Yoo, S., Weon, H., Song, J., and Sang, M. K. (2022). *Bacillus butanolivorans* KJ40 contributes alleviation of drought stress in pepper plants by modulating antioxidant and polyphenolic compounds. *Sci. Hortic.* 301, 111111. doi: 10.1016/j.scienta.2022.111111
- Krishna, P., Prasad, B. D., and Rahman, T. (2017). Brassinosteroid action in plant abiotic stress tolerance. *Methods Mol. Biol.* 1564, 193. doi: 10.1007/978-1-4939-6813-8\_16
- Leng, G., and Hall, J. (2019). Crop yield sensitivity of global major agricultural countries to droughts and the projected changes in the future. *Sci. Total Environ.* 654, 811–821. doi: 10.1016/j.scitotenv.2018.10.434
- Li, L. J., Gu, W. R., Li, J., Li, C. F., Xie, T. L., Qu, D. Y., et al. (2018). Exogenously applied spermidine alleviates photosynthetic inhibition under drought stress in maize (*Zea mays* L.) seedlings associated with changes in endogenous polyamines and phytohormones. *Plant Physiol. Bioch.* 129, 35–55. doi: 10.1016/j.plaphy.2018.05.017
- Liang, B., Ma, C. Q., Zhang, Z. J., Wei, Z. W., Gao, T. T., Zhao, Q., et al. (2018). Long-term exogenous application of melatonin improves nutrient uptake fluxes in apple plants under moderate drought stress. *Environ. Exp. Bot.* 155, 650–661. doi: 10.1016/j.envexpbot.2018.08.016
- Liu, W., Sun, F., Sun, S., Guo, L., Wang, H., and Cui, H. (2019). Multi-scale assessment of eco-hydrological resilience to drought in China over the last three decades. *Sci. Total Environ.* 672, 201–211. doi: 10.1016/j.scitotenv.2019.03.408
- Lu, X., Jiang, L., Li, Z., Wu, H., and Ma, Z. (2023). Analysis of endogenous hormones in different organs reveals the critical role of phthalanilic acid in the yield and quality of pepper (*Capsicum annuum*) fruits. *Sci. Hortic.* 319, 112148. doi: 10.1016/j.scienta.2023.112148
- Malika, L. Y., Deshabandu, K. S. H. T., De Costa, W. A. J. M., Ekanayake, S., Herath, S., and Weerakoon, W. M. W. (2019). Physiological traits determining tolerance to intermittent drought in the *Capsicum annuum* complex. *Sci. Hortic.* 246, 21–33. doi: 10.1016/j.scienta.2018.10.047
- Mantlana, K., Arneth, A., Veenendaal, E., Wohland, P., Wolski, P., Kolle, O., et al. (2008). Photosynthetic properties of C-4 plants growing in an African savanna/wetland mosaic. *J. Exp. Bot.* 59, 3941–3952. doi: 10.1093/jxb/ern237
- Min, Z., Li, R. Y., Chen, L., Zhang, Y., Li, Z. Y., Liu, M., et al. (2019). Alleviation of drought stress in grapevine by foliar-applied strigolactones. *Plant Physiol. Bioch.* 135, 99–110. doi: 10.1016/j.plaphy.2018.11.037
- Mphande, W., Kettlewell, P. S., Grove, I. G., and Farrell, A. D. (2020). The potential of antitranspirants in drought management of arable crops: A review. *Agr. Water Manage.* 236, 106143. doi: 10.1016/j.agwat.2020.106143
- Okunlola, G. O., Olatunji, O. A., Akinwale, R. O., Tariq, A., and Adelusi, A. A. (2017). Physiological response of the three most cultivated pepper species (*Capsicum* spp.) in Africa to drought stress imposed at three stages of growth and development. *Sci. Hortic.* 224, 198–205. doi: 10.1016/j.scienta.2017.06.020
- Racsko, J. (2004). Effect of auxin-synergistic preparation and fertilization on fruit setting and fruit quality of apple. *J. Agric. Sci.* 15, 21–25. doi: 10.34101/actaagrar/15/3352
- Shahzad, B., Tanveer, M., Che, Z., Rehman, A., Cheema, S. A., Sharma, A., et al. (2018). Role of 24-epibrassinolide (EBL) in mediating heavy metal and pesticide induced oxidative stress in plants: A review. *Ecotox. Environ. Safe.* 147, 935–944. doi: 10.1016/j.ecoenv.2017.09.066
- Sharma, M., Gupta, S. K., Majumder, B., Maurya, V. K., Deeba, F., Alam, A., et al. (2018). Proteomics unravel the regulating role of salicylic acid in soybean under yield limiting drought stress. *Plant Physiol. Bioch.* 130, 529–541. doi: 10.1016/j.plaphy.2018.08.001
- Sharma, A., Wang, J., Xu, D., Tao, S., Chong, S., Yan, D., et al. (2020). Melatonin regulates the functional components of photosynthesis, antioxidant system, gene expression, and metabolic pathways to induce drought resistance in grafted *Carya cathayensis* plants. *Sci. Total Environ.* 713, 136675. doi: 10.1016/j.scitotenv.2020.136675
- Shehzad, M. A., Nawaz, F., Ahmad, F., Ahmad, N., and Masood, S. (2020). Protective effect of potassium and chitosan supply on growth, physiological processes and antioxidative machinery in sunflower (*Helianthus annuus* L.) under drought stress. *Ecotox. Environ. Safe.* 187, 109841. doi: 10.1016/j.ecoenv.2019.109841
- Wang, X., Gao, Y., Wang, Q., Chen, M., Ye, X., Li, D., et al. (2019). 24-epibrassinolide-alleviated drought stress damage influences antioxidant enzymes and autophagy changes in peach (*Prunus persicae* L.) leaves. *Plant Physiol. Bioch.* 135, 30–40. doi: 10.1016/j.plaphy.2018.11.026
- Wang, L. F., Wu, J., Jing, R. L., Cheng, X. Z., and Wang, S. M. (2015). Drought resistance identification of *Mungbean germplasm* resources at seedlings stage. *Acta Agron. Sin.* 41, 145–153. doi: 10.3724/SP.J.1006.2015.00145
- Wu, Q., Zhang, R., Li, Z. H., Ma, Z. Q., and Zhang, X. (2018). Effect of phthalanilic acid on the endogenous hormone content of leaves and fruit quality and yield of peppers. *Chin. J. Pestic. Sci.* 20, 625–633. doi: 10.16801/j.issn.1008-7303.2018.0080
- Xiao, X., Xu, X., and Yang, F. (2008). Adaptive responses to progressive drought stress in two *Populus cathayana* populations. *Silva Fenn.* 42, 705–719. doi: 10.14214/sf.224
- Xiong, X., Yao, M., Fu, L. L., Ma, Z. Q., and Zhang, X. (2016). The botanical pesticide derived from *Sophora flavescens* for controlling insect pests can also improve growth and development of tomato plants. *Ind. Crop Prod.* 92, 13–18. doi: 10.1016/j.indcrop.2016.07.043
- Yang, P., Xia, J., Zhang, Y., Zhan, C., and Qiao, Y. (2018). Comprehensive assessment of drought risk in the arid region of Northwest China based on the global palmer drought severity index gridded data. *Sci. Total Environ.* 627, 951–962. doi: 10.1016/j.scitotenv.2018.01.234
- Zhang, O., Ma, Q., Liu, N., Ma, Z. Q., and Zhang, X. Z. (2017). Effect of phthalanilic acid on stress resistance and yield of pepper. *Chin. J. Pestic. Sci.* 19, 449–456. doi: 10.16801/j.issn.1008-7303.2017.0059
- Zhang, O., Ma, Q., Liu, N., Ma, Z. Q., and Zhang, X. (2018). Effect of plant growth regulator phthalanilic acid on growth and stress physiology of pepper (*Capsicum annuum* L.). *J. Northwest Sci-Tech. Univ. Agric. For. (Nat. Sci. Ed.)* 46, 81–88. doi: 10.13207/j.cnki.jnwafu.2018.08.011
- Zhao, H. H., Xu, J., Dong, F. S., Liu, X. G., Wu, Y. B., Zhang, J. G., et al. (2014). Determination of phthalanilic acid residue in bean, fruits and vegetables using a modified QuEChERS method and ultra-performance liquid chromatography/tandem mass spectrometry. *Anal. Methods* 6, 4336–4342. doi: 10.1039/c4ay00458b
- Zou, Y. D., Han, Z. Q., Liu, X. D., and Shi, J. C. (2017). Physiology of cold resistance of *Amorpha fruticosa* L. cv. jinye. *Agr. Sci. Tech.* 18, 2286–2290. doi: 10.16175/j.cnki.1009-4229.2017.12.021

# Frontiers in Plant Science

Cultivates the science of plant biology and its applications

The most cited plant science journal, which advances our understanding of plant biology for sustainable food security, functional ecosystems and human health.

## Discover the latest Research Topics

[See more →](#)

### Frontiers

Avenue du Tribunal-Fédéral 34  
1005 Lausanne, Switzerland  
[frontiersin.org](https://frontiersin.org)

### Contact us

+41 (0)21 510 17 00  
[frontiersin.org/about/contact](https://frontiersin.org/about/contact)

